

BEST PRACTICE FOR THE STORAGE OF CO₂ IN SALINE AQUIFERS

**Observations and guidelines from the SACS
and CO2STORE projects**

Edited and compiled by:

**Andy Chadwick, Rob Arts, Christian Bernstone, Franz May,
Sylvain Thibeau & Peter Zweigel**



Derived from projects receiving financial support from the European Union

British Geological Survey
Kingsley Dunham Centre, Keyworth, Nottingham
NG12 5GG

Tel: 0115 936 3100 (switchboard); 0115 936 3143

E-mail: enquiries@bgs.ac.uk

Website: www.bgs.ac.uk

*The British Geological Survey is a component body of
the Natural Environment Research Council.*

Natural Environment Research Council, Polaris
House, North Star Avenue, Swindon SN2 1EU

Tel: 01793 411500

Website: www.nerc.ac.uk

Printed in the UK for the British Geological Survey by
Halstan & Co. Ltd, Amersham.

Best practice for the storage of CO₂ in saline aquifers

*Edited and compiled by**

Andy Chadwick, Rob Arts, Christian Bernstone, Franz May,
Sylvain Thibeau & Peter Zweigel

** For a list of project partners and contributors see over*

Keywords

Best practice, carbon sequestration, carbon dioxide storage, CCS, CO₂ storage, CO₂STORE, SACS, saline aquifer.

Front cover

The Sleipner platform, North Sea.

Bibliographical reference

CHADWICK, R A, ARTS, R, BERNSTONE, C, MAY, F, THIBEAU, S, and ZWEIGEL, P. 2008. Best practice for the storage of CO₂ in saline aquifers. (Keyworth, Nottingham: *British Geological Survey Occasional Publication No. 14.*)

ISBN: 978-0-85272-610-5

© NERC 2008. All rights reserved.
Reproduced with permission of the
CO₂STORE Consortium.

Keyworth, Nottingham British Geological Survey 2008

PROJECT PARTNERS AND CONTRIBUTORS

BGR (Bundesanstalt für Geowissenschaften und Rohstoffe)

Stilleweg 2
D-30655 Hannover
Germany

*Franz May, Robert Meyer, Peer Hoth,
Paul Krull, Christian Müller.*

BGS (British Geological Survey)

Kingsley Dunham Centre
Keyworth
Nottinghamshire
NG12 5GG
United Kingdom

*Keith Bateman, Andy Chadwick, Dave
Evans, Jon Harrington, Sam Holloway,
Steve Horseman, Gary Kirby, Xiang-Yang
Li, Enru Liu, Tony Milodowski, Jonathan
Pearce, Simon Kemp, Chris Rochelle,
Gareth Williams, Paul Williamson.*

BP Exploration Operating Company Ltd

Chertsey Road
Sunbury-on-Thames
Middlesex
TW16 7LN
United Kingdom

Shelagh Baines, John Williams.

BRGM (Bureau de Recherches Géologiques et Minières)

3 Avenue Claude Guillemin
BP 36009
45060 Orléans Cedex 2
France

*Pascal Audigane, Isabelle
Czernichowski-Lauriol, Pierre Durst,
Hubert Fabriol, Irina Gaus,
Christophe Kervevan, Bernard
Sanjuan.*

DONG Energy [formerly represented by Energie E2.]

Teglholmen
A C Meyers Vænge 9
DK-2450 København SV
Denmark

Jørgen Nørklit Jensen.

ExxonMobil International Limited

325A St Catherine's House
2 Kingsway
London
WC2B 6WE
United Kingdom

*Mark Northam, Dave Slater, Dave
Taylor.*

GEUS (De Nationale Geologiske Undersøgelser for Danmark og Grønland)

Øster Voldgade 10
DK-1350 København K
Denmark

*Niels Bech, Torben Bidstrup, Niels
Peter Christensen, Ulrik Gregersen,
Peter Johannessen, Lars Kristensen,
Michael Larsen, Niels Springer,
Thomas Vangkilde-Pedersen.*

Hydro Oil & Energy

N-0240 Oslo
Norway

Lars Ingolf Eide.

IEA Greenhouse Gas R&D Programme

Orchard Business Centre
Stoke Orchard
Cheltenham
Gloucestershire
GL52 7RZ
United Kingdom

John Gale, Angela Manancourt.

IFP (Institute Francais du Petrole)

1 & 4 avenue de Bois-Préau
92852 Rueil Malmaison Cedex
France

*Yann Le Gallo, Pierre Le Thiez,
Bernard Zinszner.*

Industrikraft Midt-Norge

P O Box 496
N-1327 Lysaker
Norway

**NGU (Norges Geologiske
Undersøkelse)**

Leiv Eirikssons vei 39
7040 Trondheim

Reidulv Bøe.

Progressive Energy Ltd

Swan House
Bonds Mill
Stonehouse
Gloucestershire
GL10 3RF
United Kingdom

David Hanstock.

Schlumberger Stavanger Research

Stavanger Oilfield Services Research
Risabergveien 3
P O Box 8013
N-4068 Stavanger
Norway

*Hilde Grude Borgos, Geir Vaaland
Dahl, Kristine Arland Halvorsen,
Magne Lygren, Trygve Randen, Lars
Sonneland, Thorleif Skov.*

SINTEF Petroleum Research AS

S P Andersens vei 15B
NO-7031 Trondheim
Norway

*Per Bergmo, Emmanuel Cause, Erik
Lindeberg, Anne-Elisabeth Lothe,
Severine Pannetier-Lescoffit, Svend
Østmo, Peter Zweigel.*

Statoil

Statoil Research Centre
NO-7005 Trondheim
Norway

*Bjorn Berger, Ola Eiken, Hans Aksel
Haugen, Christian Hermanrud, Tore
Torp, Peter Zweigel (formerly
SINTEF).*

**TNO Built Environment and
Geosciences**

Geological Survey of the Netherlands
Princetonlaan 6
P O Box 80015
3508 TA Utrecht
The Netherlands

*Rob Arts, Bert Van der Meer, Eric
Kreft.*

TOTAL - E&P

Avenue Larribau
64018 Pau Cedex
France

*Sylvain Thibeau, Johann Frangeul,
Rodolphe Bouchard.*

**UK Department of Trade &
Industry (DTI)**

Carbon Abatement Technologies
Programme
1 Victoria Street
London
SW1H 0ET
United Kingdom

*Richard Archer, Pete Edwards, Tim
Dixon.*

Vattenfall AB

Vattenfall Research and Development
AB and Vattenfall Generation Nordic
AB
SE-162 87 Stockholm
Sweden

*Christian Bernstone, Clas Ekström,
Ole Biede (formerly Energie E2), Sara
Eriksson, Rickard Svensson.*

FOREWORD

Funded by the EU, industry and national governments, the SACS, SACS2 and CO2STORE projects have run sequentially from 1998 to 2006, with the aim of developing research into the potential for large-scale storage of CO₂ in underground saline aquifer formations. The earlier projects, SACS and SACS2, focussed specifically on scientific aspects of the Sleipner CO₂ injection operation. CO2STORE continued the work on Sleipner, but widened its scope to four new case studies selecting and characterising potential storage sites in Europe, in both offshore and onshore settings. As well as establishing protocols for conventional geological, geochemical and geophysical characterisation and monitoring, significant effort was put into evaluating requirements for the more holistic discipline of site risk assessment.

Many of the research results from the SACS and CO2STORE projects are published in the scientific literature but in a somewhat fragmented form. This report consolidates some of the key findings into a manual of observations and recommendations relevant to underground saline aquifer storage, aiming to provide technically robust guidelines for effective and safe storage of CO₂ in a range of geological settings. This will set the scene for companies, regulatory authorities, non-governmental organisations, and ultimately, the interested general public, in evaluating possible new CO₂ storage projects in Europe and elsewhere.

The document is framed around a seven-stage template for site development, from initial project inception to eventual site closure, outlined below.

1. statement of storage aims and benefits
2. site screening, ranking and selection
3. site characterisation
4. site design and planning consent
5. site construction
6. site operations
7. site closure

Each project stage is assigned a separate chapter. The document is based mainly on our experiences with a limited number of case studies and, when considering its applicability to other potential storage sites, it is important to bear in mind that the Earth's subsurface is an extremely variable natural system with properties that are highly site specific. Thus, the importance of some of the issues and procedures highlighted in this manual will vary from site to site and, as new potential sites and storage concepts are investigated, new issues may arise that were not considered here. Nevertheless, a wide range of geological, environmental and planning issues are addressed, and the document forms a sound basis for establishing recommended procedures for the planning and setting up of a potential CO₂ storage operation.

The SACS and CO2STORE partners comprise: Statoil, BP, ExxonMobil, Hydro (formerly Norsk Hydro), Total, Energi-E2, Vattenfall, DONG, UK Department of Trade and Industry, BGR (Bundesanstalt für Geowissenschaften und Rohstoffe), BGS (British Geological Survey), BRGM (Bureau de Recherches Géologiques et Minières), GEUS (Geological Survey of Denmark), IFP (Institut Français du

Petrole), PEL (Progressive Energy Ltd), TNO-NITG (Netherlands Institute of Applied Geoscience – National Geological Survey), NGU (Norwegian Geological Survey), SSR (Schlumberger Stavanger Research), SINTEF (SINTEF Petroleum Research) and IEAGHG.

The funding of the EU, industry partners and national governments is gratefully acknowledged. We also thank the operators of the Sleipner licence, Statoil, ExxonMobil, Hydro and Total for their co-operation and provision of data.

CONTENTS

1 Introduction	1
1.1 Introduction to the case studies	2
<i>Sleipner (offshore Norway)</i>	2
<i>Kalundborg (onshore/offshore Denmark)</i>	3
<i>Mid Norway (offshore Norway)</i>	4
<i>Schwarze Pumpe (onshore Germany)</i>	5
<i>Valleys (offshore UK)</i>	7
2 Statement of storage aims and benefits	9
2.1 Emissions reduction targets	9
2.2 Local environmental impacts	13
3 Site screening, ranking and selection	15
3.1 Storage capacity	15
3.2 Basic reservoir properties	30
3.3 Basic overburden properties	50
3.4 Basic reservoir flow simulations	53
3.5 Safety assessment of prospective CO ₂ storage sites	65
3.6 Conflicts of use	70
3.7 Costs	75
4 Site characterisation	80
4.1 Geological characterisation of the site	80
4.2 Predictive flow modelling	118
4.3 Geochemical assessment	134
4.4 Geomechanical assessment	151
4.5 Characterisation phase risk assessment	152
4.6 Monitoring programme design	168
4.7 Transport	177
5 Site design and planning consent	183
5.1 Design	183
5.2 Planning consent	183
6 Site construction	188
7 Operations	189
7.1 Operation and maintenance of pipeline and injection facilities	189
7.2 Monitoring	190
7.3 Flow simulations history-matched to monitoring data	221
7.4 Laboratory experiments on wellbore materials	237
8 Closure	240
8.1 Closure application	240
8.2 Criteria for safe site closure	241
8.3 Transfer of liability from operator to national authority	245
8.4 Post-closure issues	247
References	249
SACS AND CO₂STORE Bibliography	259

1 INTRODUCTION

Funded by the EU, industry and national governments, the SACS, SACS2 and CO2STORE projects have run sequentially from 1998 to the present day, with the aim of developing research into the potential for large-scale storage of CO₂ in underground saline aquifer formations. The earlier projects, SACS and SACS2, focused specifically on scientific aspects of the Sleipner CO₂ injection operation. CO2STORE continued the work on Sleipner, but widened its scope to a number of new case studies selecting and characterising potential storage sites in Europe, in both offshore and onshore settings (Figure 1.1). As well as establishing protocols for conventional geological, geochemical and geophysical characterisation and monitoring, significant effort was put into evaluating requirements for site risk assessments.



Figure 1.1 The CO2STORE case studies.

Many of the research results from the SACS and CO2STORE projects are published in the scientific literature but in a somewhat disseminated form. This report aims to consolidate some of the key findings into a manual of observations and recommendations relevant to underground saline aquifer storage. The work builds upon and complements earlier best practice manuals from the SACS/SACS2 and GEO-SEQ projects (SACS, 2003; GEO-SEQ, 2004), and aims to provide technically robust guidelines for effective and safe CO₂ storage in a range of geological settings. This will set the scene for companies, regulatory authorities, non-governmental organisations (NGOs), and ultimately the interested general public, in evaluating possible new CO₂ storage projects in Europe and elsewhere.

The document is based mainly on our experiences with a limited number of case studies and, when considering its applicability to other potential storage sites, it is important to bear in mind that the Earth's subsurface is an extremely variable natural system with properties that are highly site specific. Thus, the importance of some of

the issues and procedures highlighted in this manual will vary from site to site and, as new potential sites and storage concepts are investigated, new issues may arise that were not considered here. Nevertheless, a wide range of geological, environmental and planning issues are addressed, and the document forms a sound basis for establishing recommended procedures for the planning and setting up of a potential CO₂ storage operation.

The document is framed around a seven-stage template for site development, from initial project inception to eventual site closure, outlined below.

1. statement of storage aims and benefits
2. site screening, ranking and selection
3. site characterisation
4. site design and planning consent
5. site construction
6. site operations
7. site closure

Each project stage is assigned a separate chapter in the document. Some chapters, for example that dealing with site characterisation, incorporate data from all of the case studies, whereas others, such as the one dealing with site operations, have information only from Sleipner. Site construction is outwith the remit of this document and no views are expressed here.

1.1 Introduction to the case studies

Sleipner (offshore Norway)

The carbon dioxide injection at the Sleipner field in the North Sea, operated by Statoil and the Sleipner partners, is the world's first industrial scale CO₂ injection project designed specifically as a greenhouse gas mitigation measure.

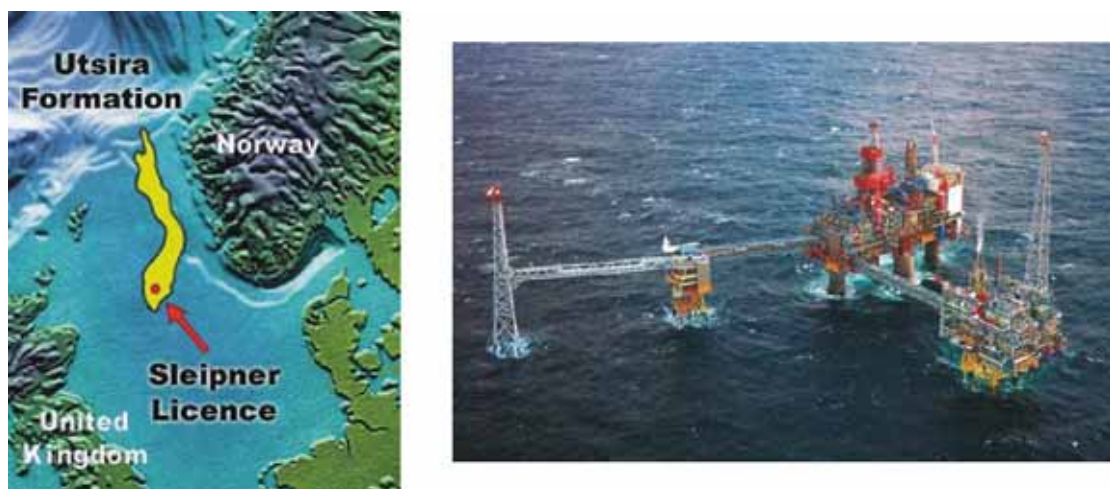


Figure 1.2 The Sleipner injection operation showing the extent of the Utsira Sand reservoir (yellow) and platform infrastructure.

CO₂ separated from natural gas is being injected into the Utsira Sand (Figure 1.2), a major saline aquifer of late Cenozoic age. Injection is via a deviated well, near-horizontal at the injection point (Figure 1.3). The injection point lies some 3 km from the platform at a depth of 1012 m below sea level, about 200 m below the reservoir top. Injection started in 1996, with, by mid 2006, more than 8 million tonnes (Mt) of CO₂ in the reservoir.

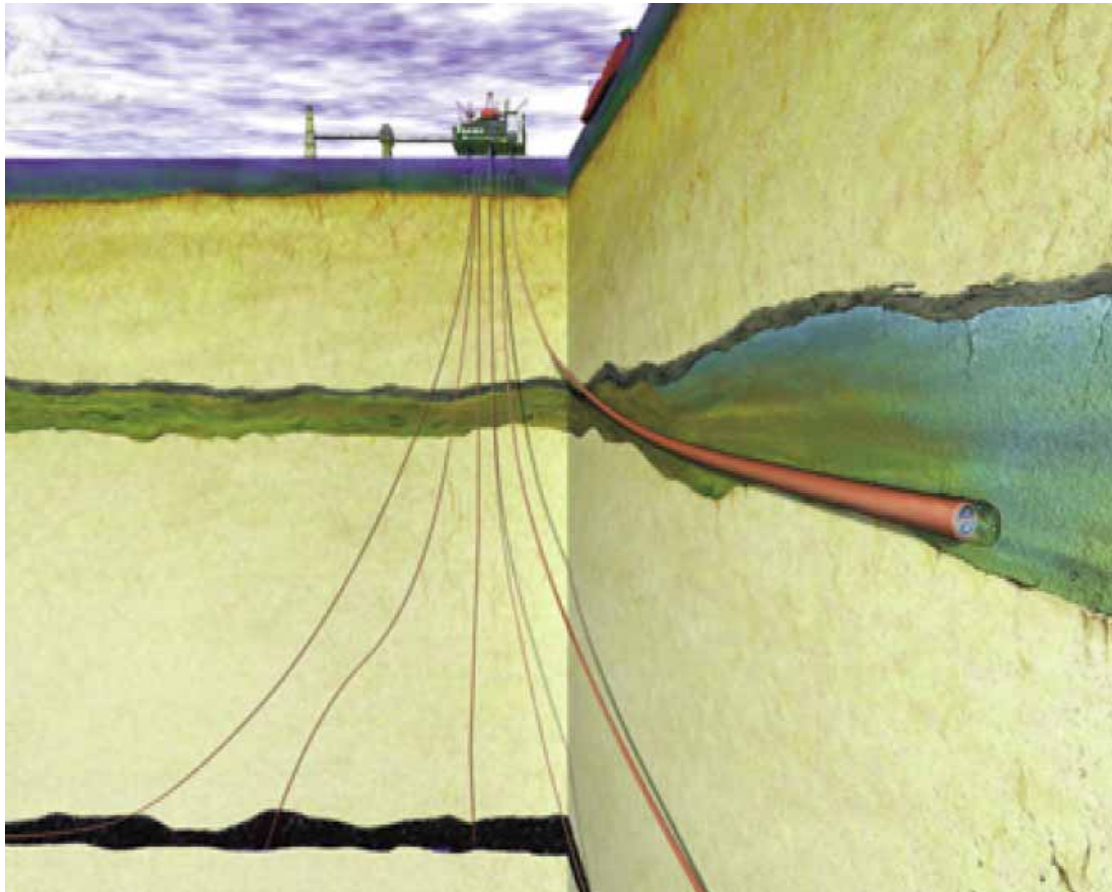


Figure 1.3 Sleipner well cartoon showing deviated wellbore trajectory to the storage reservoir.

Kalundborg (onshore/offshore Denmark)

This Danish case study is centred on the possible future capture and underground storage of CO₂ from two sources: the coal-fired powerplant Asnaesvaerket owned by Energie E2, and the Statoil refinery, both located in the city of Kalundborg (Figure 1.4).

The potential storage site comprises a large gentle anticline covering an area of about 160 km², some 15 km north-east of Kalundborg. The Gassum Formation, a Triassic sandstone, forms the target reservoir at a depth of about 1500 m.



Figure 1.4 Aerial view of the Kulundborg coal-fired powerplant (background) and the Statoil refinery (foreground).

Mid Norway (offshore Norway)

Plans for a combined heat and power plant (CHP) in Skogn in the inner part of Trondheimsfjorden include options to capture approximately 2 Mt of CO₂ per year from the flue gas stream. At Tjeldbergodden in mid Norway, a methanol plant currently emits about 0.45 Mt of CO₂ per year. There are plans to build an additional methanol plant with a similar CO₂ emission, and a gas-fired power plant which would emit about 2.1 Mt of CO₂ per year.

Three potential offshore sites for underground storage of CO₂ have been investigated, the small Beitstadfjord Basin of the Trondheimfjord, the Frohavet Basin, and the Froan Basin of the Trøndelag Platform (Figure 1.5).

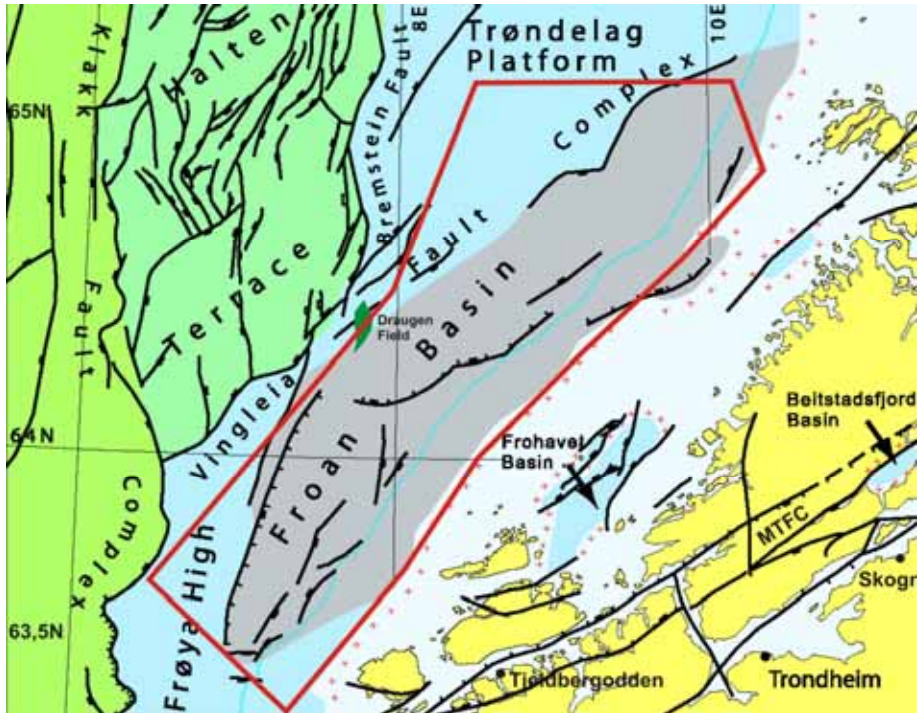


Figure 1.5 Outline geological structure map showing the three mid-Norway potential storage sites (modified from Blystad et al., 1995).

Schwarze Pumpe (onshore Germany)

The Schwarze Pumpe power station (Figure 1.6) is located in the Niederauslitz region south-east of Berlin.



Figure 1.6 Schwarze Pumpe power station.

Operated by Vattenfall, it comprises two 900 MW blocks fuelled by lignite, together emitting around 10 Mt of CO₂ per year, which is in the mid-range of lignite-fuelled power plants operated by Vattenfall in north-east Germany (Figure 1.7).

The case study has identified and characterised deep saline aquifers of regional extent in the North-east German Basin with a number of potential storage sites. The Schweinrich structure, identified as most promising for storing the total lifetime emissions of the plant, forms an elongated anticline covering around 100 km² with Triassic and Jurassic reservoir formations at a depth of about 1500 m.

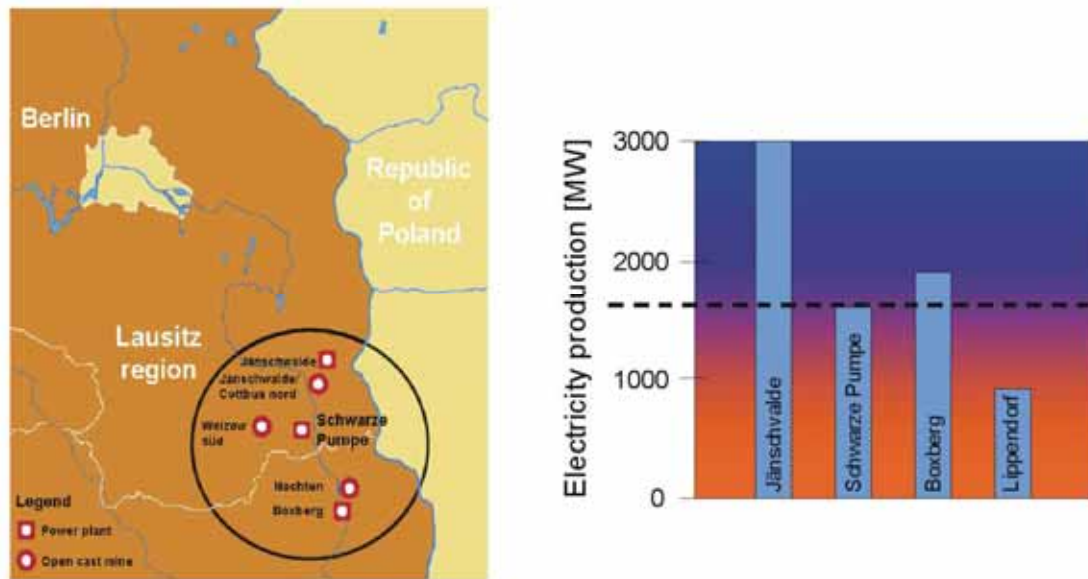


Figure 1.7 Location of Schwarze Pumpe and power generation figures for it and neighbouring power stations.

Vattenfall are currently building a 30 MW pilot-scale power plant at Schwarze Pumpe (Figure 1.8), expected to be operational by 2008. Even though the CO₂ captured in the pilot plant will have suitable properties to be transported and stored, the principle aim of the pilot is to validate and improve technology around capturing carbon dioxide. Amounts of this gas produced from the pilot plant will, at full-load operation, be about 60 kt per year, compared to the 10 Mt per year produced currently at Schwarze Pumpe. CO₂ volumes that will need to be handled from high-range point sources are large, with a project scale significantly bigger than any of the current worldwide CO₂-storage projects that are in operation today. For example, the annual CO₂ amounts stored at Sleipner, In Salah (Algeria), and Weyburn (Canada) are in the range about 1 to about 2 Mt.

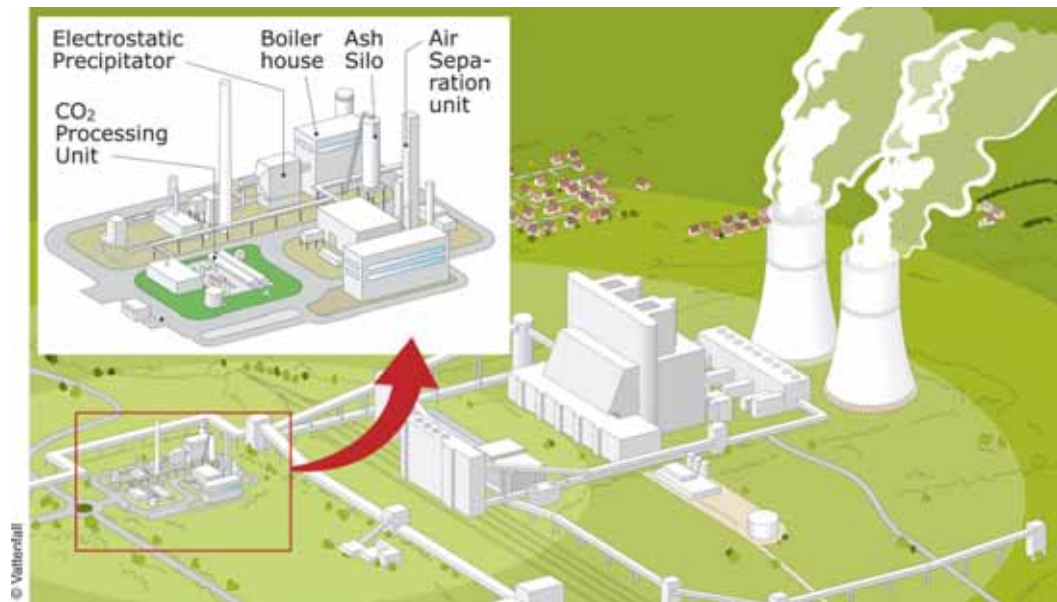


Figure 1.8 A sketch of the planned 30 MW oxy-fuel power plant, at the Schwarze Pumpe industrial site.

Valleys (offshore UK)

Progressive Energy Ltd, a specialist energy project company, is developing plans to build a 450 MW coal gasification combined cycle (CGCC/IGCC) power station in South Wales (Figure 1.9). The power station will be fed with a mixture of local anthracitic coal and petcoke. The Progressive Energy design produces a synthetic gas, rich in CO₂ and hydrogen, from which the CO₂ can be removed very cheaply at the pre-combustion stage.



Figure 1.9 Artist's impression of the proposed IGCC Valleys power plant in South Wales.

CO₂ emissions are expected to be around 2 Mt per year. A number of offshore sites for underground storage of the CO₂ have been evaluated in CO2STORE. The favoured site lies offshore, in a sandy aquifer of Cenozoic age, some 120 km from the plant, beneath the Irish Sea in the St George's Channel Basin.

Hydrogen produced by the gasification process can either be converted to electricity in the power plant or used to supply the anticipated growing market in fuel cells. Markets for fuel cells could increase rapidly in the transport or stationary small-scale CHP sectors.

2 STATEMENT OF STORAGE AIMS AND BENEFITS

The European Commission forecast in 1996 that the renewable energy share of total EU consumption was to increase from 4.6% in 1990 to 8–9% in 2010–2015. This means that fossil fuel would still have to provide about 70–80% of the rising total energy consumption, the remainder to be provided by nuclear energy. Overall energy consumption would increase by some 18–20%. Decisions have been taken by parliaments in Germany and Sweden to cease expansion of nuclear power and, in the longer-term, to phase it out completely. This implies that fossil fuels will have to cover a larger percentage of the increasing energy needs if standards of living are to be maintained.

Whilst considerable effort should be directed towards reducing CO₂ emissions through fuel efficiency measures and fuel switching, these measures can only achieve a fraction of the emission reductions required and will not be sufficient to meet even the modest demands of the Kyoto Protocol. Other viable means of reducing CO₂ emissions, such as CO₂ capture and geological storage, will have to be utilised if Europe is not to face a serious shortage of environmentally acceptable energy sources.

It is essential to bring the potential major benefits of geological CO₂ storage to the notice of potential end-users, policy advisers and the public, and to establish a safe, technically feasible, socially acceptable, CO₂ mitigation option for widespread deployment. The SACS and CO₂STORE projects have monitored and modelled industrial-scale CO₂ injection at Sleipner for a number of years. Methodologies and techniques developed have been notably successful and the short-term feasibility and safety of the operation have been amply demonstrated. The Sleipner operation has proved to be a golden opportunity to establish the terms of reference for future CO₂ injection schemes. The CO₂STORE project has moved the knowledge base further by evaluating potential CO₂ reservoirs other than the Utsira Sand, with the aim of broadening understanding of a wider range of storage possibilities.

2.1 Emissions reduction targets

A key initial project step is to define the primary objective of the proposed storage project in terms of emissions reduction and timescale of storage. It is important that emphasis should be placed on the key strategic benefits to be accrued by CO₂ storage, which is not a normal ‘for-profits’ industrial operation, but rather a fundamental strategy to protect the planet.

The objective of underground storage is to contain CO₂ for a long enough period of time to mitigate global warming. In a well-selected storage site, retention times may well be indefinite, but as a minimum requirement, recent work indicates that average storage times should be in the order of a few thousand years or more (Lindeberg, 2003), or that annual leakage rates from an average storage site should be less than about 0.01% of the injected CO₂ (Hepple and Benson, 2002; IPCC, 2005).

2.1.1 Observations from the CO2STORE case studies

Sleipner

The Sleipner fields in the Norwegian sector of the North Sea are covered by production licences operated by Statoil, with licence partners ExxonMobil, Hydro and Total. The main reserves are gas/condensate in the Sleipner East and Sleipner West fields. According to official Norwegian government sources, the Sleipner West Field originally contained 202 GSm³ of rich gas, with a CO₂ content between 4 and 9.5%. In order to deliver Sleipner West natural gas directly into the European gas distribution network, the CO₂ content has to be reduced below 2.5%. To meet this specification, CO₂ is removed from the natural gas by an amine stripping process on the Sleipner platform. Normally, the separated CO₂ would be vented to the atmosphere, but by storing it underground, CO₂ emissions will be reduced by up to 20 Mt over the projected twenty years of the project. An increase of 3% in total Norwegian CO₂ emissions over the period will thereby be avoided. Emission of CO₂ from offshore installations of the petroleum industry in Norway is charged by an emission tax, which, for natural gas production, currently amounts to 325 Norwegian Kroner/tonne of CO₂. The Sleipner licence owners avoided this tax by underground storage. The costs for the compressor and for the injection well were offset by saved tax within the first few years of injection.

Statoil reports the amount of CO₂ emitted and the amount injected every year to the Norwegian Pollution Control Authority. The injected CO₂ is taken as having been removed from the atmosphere and is not reported in the emission inventory. When the injection operation has to stop for maintenance etc, Statoil have to pay a CO₂ tax for the consequent emissions. These emissions are reported to the Norwegian Petroleum Directorate and are reported in the national emissions inventory (Hoem, 2005). A detailed account of Sleipner emissions and emissions avoided is given in Hoem (2005) and is summarised below:

	1996	1997	1998	1999	2000	2001	2002	2003	2004
CO ₂ injected (kT)	70	665	842	971	933	1009	955	914	750
CO ₂ emissions from injection plant (kT)	0	0	4	9	8	3	8	24	21

Table 2.1 Sleipner emissions inventory, showing approximate amounts of CO₂ injected and also emissions from the injection plant during maintenance periods (adapted from Hoem, 2005).

The reported data covers emissions to the atmosphere (e.g. when the injection system is out of operation), measured by continuous metering of the gas (accurate to 5%). The reported amounts of CO₂ that are injected into the Utsira Sand are based on continuous metering of the gas stream by orifice meter (accurate to 3%). So far, no migration from the primary storage reservoir has been detected.

Kalundborg

Danish power plants are among the world's most energy efficient, burning mainly coal, with, in recent years some natural gas, and to a minor extent, biomass. The Kalundborg case study addresses the potential future capture and underground storage of CO₂ from two point sources: the coal-fired power plant Asnæsværket and the adjacent Statoil refinery.

The Asnæs power station is the biggest power plant in Denmark. Besides producing electricity for the grid, the power plant produces district heat for Kalundborg and process steam for neighbouring industry. It was commissioned from 1959 to 1981 with an installed capacity of 1057 MW of electricity and 602 MW of heat. Of the original five generating units only three (2, 4 and 5) are still in operation. It is, furthermore, expected that Unit 4 will also be closed down in 2008, leaving only two units in operation with a total installed capacity reduced to 787 MW of electricity and 552 MW of heat. Lately, both Unit 2 and Unit 5 were rehabilitated with an extended operational lifetime of 12–15 years (until 2015–2020). As the remaining lifetime of Unit 5 is limited, this case-study assumes that a new Unit 6 will commence operation within ten years. It is anticipated that the new Unit 6 will be a high-efficiency pulverised coal-fired unit of approximately the same size as the old Unit 5 with regard to fuel input and flue gas rate. Predicted total emissions from the power-plant are in the order of 2.5 Mt per year.

The Statoil refinery in Kalundborg is the largest in Denmark, with a production capacity of 5.5 Mt of hydrocarbon products per year. Heavy oil and condensate from the North Sea are transported to the refinery by ship, and final products are redistributed within Denmark and to countries around the Baltic Sea. In addition to refining hydrocarbon products, the refinery runs a fertiliser plant, also a significant CO₂ emitter. According to the environmental report delivered to the authorities, total CO₂ emissions from the refinery in 2004 were 0.49 Mt. In fact annual emissions have been almost constant around 0.5 Mt for the past few years. Not all of the emitted CO₂ will be available for the capture process, as emission takes place from numerous smaller point sources, with different flue gas compositions, scattered around the refinery. It is anticipated that any CO₂ captured at the refinery will be transported to the nearby power plant and transported together with the CO₂ captured there. Capture and storage will therefore be totally dependent on the realisation of the power plant storage project. The power plant and the refinery have a long history of co-operation and products such as heat and water are exchanged between the production units.

Emission reduction targets are linked to the Kyoto agreement adopted in 1997 and taking force in March 2005. The EU thus aimed at reducing greenhouse gas emissions by 8% relative to base year 1990. The Danish contribution according to the EU's burden-sharing agreement is 21% to be met in the period 2008–2012. The agreement is intended to form the basis for far bigger reductions during the remainder of the 21st century. Short-term national targets are mostly linked to the EU burden-sharing agreement for reaching the Kyoto goals. The EU Emission Trading Scheme (ETS) commenced in January 2005. The ETS system provides for the trading and exchange of CO₂ allowances and thereby sets a market price for CO₂. This system works along the lines of the national systems that have been applied to Danish power plants and industry since January 2005. According to the national system each CO₂ emitter is allowed a specific CO₂ emission based on the record of previous years. The amount is fixed and excess CO₂ emission is taxed. In 2006–2007 the tax is 40 €/tonne rising to 100€/tonne in 2008 onwards. According to the official Danish Energy Agency (DEA) website, the Asnæs power plant received a CO₂ emission allowance of 3.29 Mt in 2005, reducing to 2.47 Mt in 2007. The Statoil Refinery had a 2005 emissions allowance of 0.65 Mt while for 2006 and 2007 the allowance will be 0.49 Mt of CO₂.

Danish annual greenhouse gas emissions are 62 Mt in 2005, of which about 80% are CO₂. The national reduction targets of 21% by 2012 would therefore correspond to a reduction of approximately 12 Mt of CO₂. According to the Danish Energy Agency the current need for reductions is around 6 Mt (DEA 2005) so capture and storage of the CO₂ from Asnæs and the Statoil refinery could provide a significant contribution to this.

Potential underground CO₂ storage may influence the energy policy and plans for future coal-fired power plants of Denmark, depending on the evolution of ETS CO₂ quota prices and possible implementation of emission taxes.

Mid Norway

Plans for a combined heat and power plant (CHP) in Skogn in the inner part of Trondheimsfjorden (mid Norway) include options to capture about 2 Mt of CO₂ per year from the flue gas stream. At Tjeldbergodden in mid Norway, a methanol plant currently emits about 0.45 Mt of CO₂ per year. It is planned to build an additional methanol plant there with similar CO₂ emissions and a gas-fired power plant that would emit about 2.1 Mt of CO₂ per year. The plants will utilise natural gas from Haltenbanken, off mid Norway. The total saline aquifer storage capacity for CO₂ in offshore mid Norway has been estimated at about 30 000 Mt, assuming a storage efficiency of 2% (Bøe et al., 2002). A significant portion of this storage capacity is on the south-eastern part of the Trøndelag Platform (Froan Basin area, east and south of the major hydrocarbon province on the Halten Terrace/Nordland Ridge). CO₂ storage in oil and gas fields on the Halten Terrace will not be possible in the next ten to twenty years (except for enhanced oil recovery) due to probable conflicts with hydrocarbon exploitation. The area of interest has not previously been mapped in detail for the purposes of CO₂ storage, but has the advantage of being closer to onshore CO₂ sources, thereby requiring shorter pipelines. Potential sites assessed here for CO₂ storage are the Beitstadfjord Basin, the Frohavet Basin and the Froan Basin area of the Trøndelag Platform.

In the spring of 2005 Shell and Statoil announced an initiative to evaluate the possibility of an integrated project involving power production at Tjeldbergodden, capture and transport of CO₂ offshore, and use of the captured CO₂ for enhanced oil recovery (EOR) in the Draugen and Heidrun hydrocarbon fields offshore mid Norway. Although not explicitly part of the published initiative, saline aquifers offshore mid Norway may play an important role in this concept. They could potentially be utilised as storage buffers, taking up CO₂ in periods when demand at the hydrocarbon fields is low, for example in periods of maintenance or during water injection periods of water-alternate-gas (WAG) EOR measures. Furthermore, the EOR infrastructure may be utilised for cost-efficient parallel or subsequent CO₂ aquifer storage.

Schwarze Pumpe

The expected future growth of electricity consumption requires significant new generation capacity in Europe from around 2010 (Vattenfall, 2004). CO₂ emissions in Germany in 2003 were about 850 Mt (Figure 2.1). However, in accordance with the Kyoto protocol, the German government intends to reduce annual CO₂ emissions to 770 Mt by 2012. Looking further ahead, the proposed emission target for 2020 is 600 Mt CO₂, a reduction of more than 200 Mt CO₂ per year compared to 2003 levels.

The power industry is expected to contribute around 40% of these reductions—about 80 Mt CO₂ per year. The reduction will be implemented through the European Trading System (ETS), including future new CO₂-free power plants at cost effective levels.

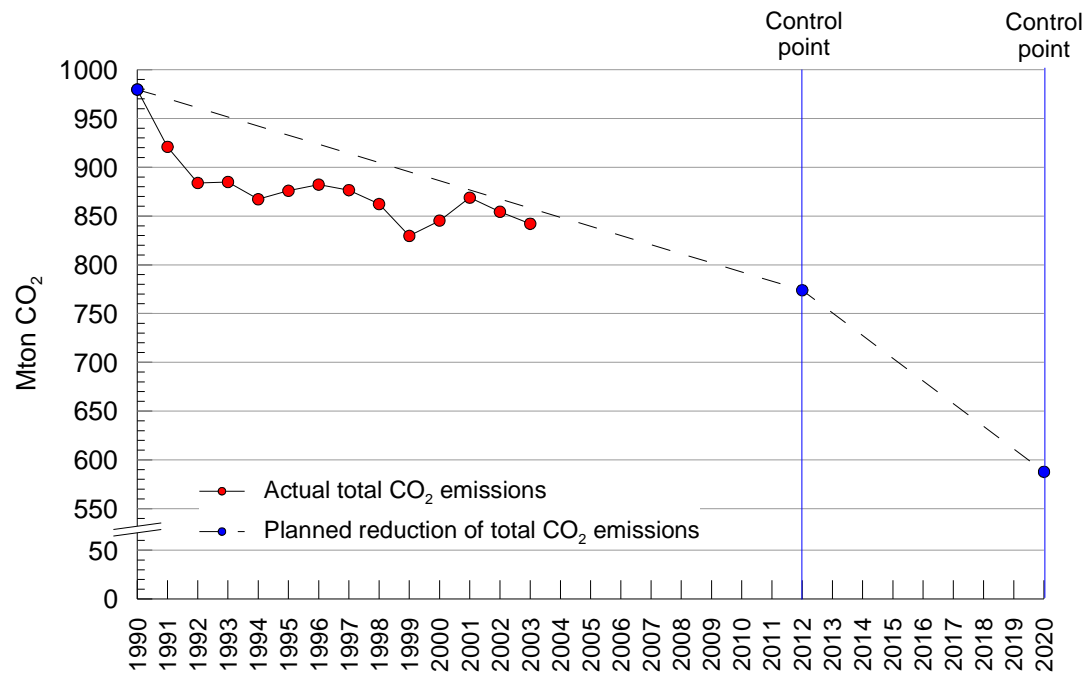


Figure 2.1 Annual CO₂ emissions in Germany, and planned reductions.

The Schwarze Pumpe power station, operated by Vattenfall Europe Generation, is a modern, lignite-fired power plant producing 1600 MW_e, typical of the lignite-fuelled power plants operated by Vattenfall in north-east Germany. The power plant consists of two 900 MW_{th} blocks fuelled by lignite. In total the two blocks emit around 10 Mt of carbon dioxide per year. The cumulative mass of CO₂ expected to be produced during the predicted operational lifetime of the plant will about 400 Mt.

Valleys

The proposed Valleys power plant, to be constructed at Onllwyn in the South Wales Coalfield, comprises a 450 MW IGCC plant, fuelled by a mixture of petcoke and locally mined anthracite. Emissions are likely to comprise up to about 2.45 Mt of CO₂ per year. These would account for some 1.4 % of total UK CO₂ emissions from power generation.

2.2 Local environmental impacts

It is necessary to provide assurance that storage will be undertaken in an environmentally acceptable manner with minimal impacts on marine/terrestrial ecology and groundwater. Before commencing a CO₂ capture and storage project therefore, it is important to consider all aspects of potential environmental impacts that may occur, both during normal operations where the project proceeds according to plan, and also in the case of unforeseen events.

Environmental effects at the surface, or in shallow subsurface layers, relating to normal operations will be minimised through appropriate precautionary measures and safety procedures. Emissions and noise levels will be regulated in the operational permit so that they are kept within acceptable limits. Pipeline routes and the location of the storage site may cause some environmental disturbance and interfere with other interests (land owners, nature protection areas, military training etc.). Impacts on potential deep subsurface ecosystems, in and around the reservoir, may be significant, but may be considered as acceptable from an environmental viewpoint.

The risk of a potential leakage from a CO₂ storage site can be minimised through a combination of thorough site characterisation, the utilisation of safety measures and deployment of suitable monitoring systems. However, it is still important to assess the potential environmental consequences in the event of a leakage. The main environmental consequences relating to leakage from a CO₂ reservoir are:

Possible groundwater pollution from migrating CO₂ will cause a decrease in pH in groundwater aquifers and may cause dissolution and alteration of minerals from rocks and soils that could release elements such as heavy metals, potentially contaminating fresh water supplies.

If surface conditions allow leaking CO₂ to locally accumulate, high concentrations may be attained in depressions and confined spaces, which can be hazardous to humans and other living organisms.

Leakage of CO₂ will impact on the biodiversity of ecosystems.

Leakage types can range between short-term potentially large leakages and long-term more diffuse leakages. Short-term localised leakages are likely to be more readily remediated, since they will occur over a limited area, but may have large impacts due to potentially high concentration levels. Long-term diffuse leakages would be more difficult to detect and remediate, since they can occur over large areas, and may therefore be considered as a more serious concern. Local environmental impacts resulting from a release of CO₂ depend more on the duration time, concentration and the ambient conditions, than on the total amount of CO₂ released. At an organism level, tolerance thresholds relating to increased CO₂ concentrations will vary between species. Because of these differences in sensitivity, a continuum of impacts on ecosystems is more likely than the existence of a well-defined threshold beyond which CO₂ cannot be tolerated.

If precautionary measures are taken to minimise the environmental impacts, capture, transport and storage of CO₂ can be undertaken in an acceptable way with only very minor impacts on the environment. Assurance for this is provided by:

a thorough site selection and characterisation procedure including an assessment of the potential consequences of a CO₂ leakage

guidelines and standards for safe operation

appropriate safety measures and monitoring during and after operation of the site.

3 SITE SCREENING, RANKING AND SELECTION

The screening phase evaluates the practicality of storing CO₂ in an appropriate region by identifying, assessing and comparing possible candidate storage sites. Screening typically utilises existing datasets to produce a ranked list of storage sites based on geological, environmental, economic and logistical considerations. Key geological selection criteria include reservoir depth, thickness, porosity, permeability, seal integrity and salinity (Table 3.1).

	Positive indicators	Cautionary indicators
RESERVOIR EFFICACY		
Static storage capacity	Estimated effective storage capacity much larger than total amount of CO ₂ to be injected	Estimated effective storage capacity similar to total amount of CO ₂ to be injected
Dynamic storage capacity	Predicted injection-induced pressures well below levels likely to induce geomechanical damage to reservoir or caprock	Injection-induced pressures approach geomechanical instability limits
Reservoir properties		
Depth	>1000 m <2500m	< 800 m > 2500 m
Reservoir thickness (net)	> 50 m	< 20 m
Porosity	> 20%	< 10%
Permeability	> 500 mD	< 200 mD
Salinity	> 100 g ⁻¹	< 30 g ⁻¹
Stratigraphy	Uniform	Complex lateral variation and complex connectivity of reservoir facies
CAPROCK EFFICACY		
Lateral continuity	Stratigraphically uniform, small or no faults	Lateral variations, medium to large faults
Thickness	> 100 m	< 20 m
Capillary entry pressure	Much greater than maximum predicted injection-induced pressure increase	Similar to maximum predicted injection-induced pressure increase

Table 3.1 Key geological indicators for storage site suitability.

Given the buoyant nature of CO₂, proven efficacy of the topseal is normally a prerequisite, and, with storage in dipping aquifers, the nature of lateral sealing features is also important (see Section 3.4 on the mid Norway case study). Lateral sealing in reservoirs (compartmentalisation) can help retain CO₂ in the desired storage location, but can also impair injectivity and lead to elevated injection pressures.

3.1 Storage capacity

Assessment of the total regional CO₂ storage capacity of a potential storage formation is required to devise a long-term local, jurisdictional, national or supranational injection strategy, which may involve several operations by a number of different operators. Consequently it is of great interest to policymakers and regulators as well as prospective storage site operators.

3.1.1 Principles of storage

CO₂ storage capacity depends not only on the properties of the reservoir rock itself but also on the nature of its boundaries. Very little CO₂ can be injected into the water-filled porosity of a small reservoir with perfectly sealed non-elastic boundaries, as the only space available will be that created by the compression of the water and rock. For significant storage to be possible, it is necessary for a significant proportion of the native pore fluid to be displaced from the reservoir over the injection period. This may occur either by anthropogenic production of fluids (oil and gas), by deliberate production of formation water, and/or by migration of groundwater into adjacent formations and/or to the ground surface or sea bed. Internal barriers within the reservoir, such as faults, also need to be considered as these may divide it into separate, unconnected or poorly connected compartments.

Four main storage mechanisms for CO₂ operate in reservoir rocks.

Structural and stratigraphical trapping occurs where the migration of free (gas, liquid, fluid) CO₂ in response to its buoyancy and/or pressure gradients within the reservoir is prevented by low permeability barriers (caprocks) such as layers of mudstone or halite.

Residual saturation trapping occurs when capillary forces and adsorption onto the surfaces of mineral grains within the rock matrix immobilise a proportion of the injected CO₂ along its migration path.

Dissolution trapping occurs where injected CO₂ dissolves and becomes trapped within the reservoir brine.

Geochemical trapping occurs when in which dissolved CO₂ reacts with the native pore fluid and/or the minerals making up the rock matrix of the reservoir. CO₂ is incorporated into the reaction products as solid carbonate minerals and aqueous complexes dissolved in the formation water (sometimes called ‘ionic trapping’, because of the often predominant bicarbonate anions).

The timescales on which these processes operate need to be taken into account in CO₂ storage capacity assessment. Storage by mineral reactions that induce carbonate precipitation will play little part in creating additional space during CO₂ injection because they act too slowly. Injection is most likely to take place over the next century or so, when the need to store CO₂ is likely to be greatest, whereas the kinetics of mineral trapping are so slow that they will only have a significant effect over hundreds to thousands of years. In practice, mineral trapping commonly can be ignored as a significant storage mechanism on a hundred-year timescale. Any analysis of the CO₂ storage capacity of formations needs to take account of the three remaining storage mechanisms *and* the boundary constraints.

Availability of storage sites also needs to be considered. Oil and gas fields will not become available until the economic circumstances are right, which may not match CO₂ storage requirements.

Undesirable effects that could occur before the theoretical maximum storage capacity has been achieved might limit the amount of CO₂ that can be stored in a reservoir formation. These include:

an unacceptable rise in reservoir pressure towards caprock capillary entry pressure or fracturing pressure

migration of displaced native pore fluids, CO₂ or entrained substances, to parts of the geosphere or biosphere where they are not acceptable (the oceans, the atmosphere, mines, potable water supplies etc.).

3.1.2 Storage capacity calculation

A lower limit can be placed on the storage capacity of reservoir formations by estimating the volume of their hydrocarbon fields (if present). For scoping calculations, the methodology of Bachu and Shaw (2003) can be followed. This is based on the principle that a proportion of the pore space occupied by the recoverable reserves of a field will become available for CO₂ storage. Appropriate discounts are applied to the total pore volume occupied by the recoverable reserves, to take account of factors such as water invasion that will reduce the storage capacity, then the mass of CO₂ that would fill this pore volume at reservoir conditions is calculated. More detailed calculations can be made for individual fields, using a reservoir model and a numerical reservoir simulator.

The most likely storage capacity of a reservoir formation is more difficult to calculate because in most reservoir rocks it includes, or comprises exclusively, CO₂ stored in the saline water-bearing pore space and/or the saline pore fluids, i.e. aquifer storage capacity. The volumes that can be stored in aquifers depend on many commonly poorly-determined parameters and issues, including:

the pore volume in structural or stratigraphical traps

whether any of the traps will leak

the achievable CO₂ saturation in traps

where there are many small traps, and the percentage of these that can be accessed by a realistic number of wells

the amount of CO₂ that will dissolve into the saline pore fluids

the amount of CO₂ that will be trapped along the CO₂ migration path as a residual saturation

whether local or regional pressurisation of the aquifer due to CO₂ injection will limit its storage capacity

the density of CO₂ and any other gas components.

Therefore, a significant amount of reservoir information, in addition to the extent, thickness and porosity of the formation, is needed to assess aquifer storage capacity in detail. The pore volume in structural traps can be calculated from a structure contour map on the top of the formation. For stratigraphical traps, knowledge of some of the boundaries within the reservoir is also needed. Inferences about the potential for leakage can, in some cases, be made from regional knowledge, interpretation of seismic surveys or geomechanical modelling. Given sufficient data, the achievable CO₂ saturation, dissolution and residual saturation can be assessed using a numerical reservoir simulator, as they are essentially dependent on the injection strategy, the reservoir properties and fluid properties. Interaction between residual saturation and dissolution will be a key storage process, that is, how quickly and much of the residual gas saturation will dissolve. Local or regional pressure constraints might also be assessed using numerical simulation and depend mainly on the reservoir properties and the nature of the boundaries within and surrounding the formation. The density of CO₂-rich gases depends on temperature, pressure, and impurities. As a general rule of thumb, densities of pure CO₂ are in the range 300 to 800 kgm⁻³ (Figure 3.1) at depths greater than about 800 m (about 8 MPa pressure). The specific effects of variable geo-

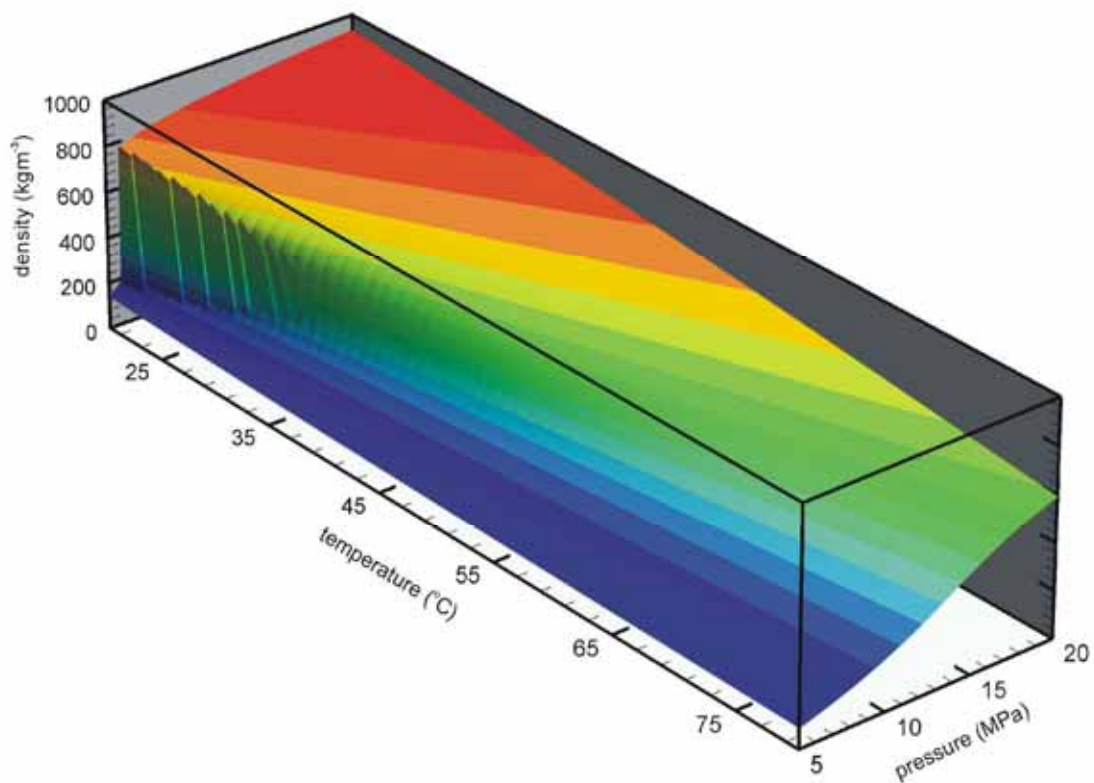


Figure 3.1 Variation of CO₂ density over a range of typical reservoir temperatures and pressures.

thermal gradient and fluid pressure gradient are however quite significant (Figure 3.2) and should be taken into account, particularly when planning shallow storage sites where P,T conditions are close to the critical point for CO₂. If the stored CO₂ is in a dense phase (liquid or supercritical) at reservoir conditions, this dramatically improves storage efficiency compared with storage in the gaseous state.

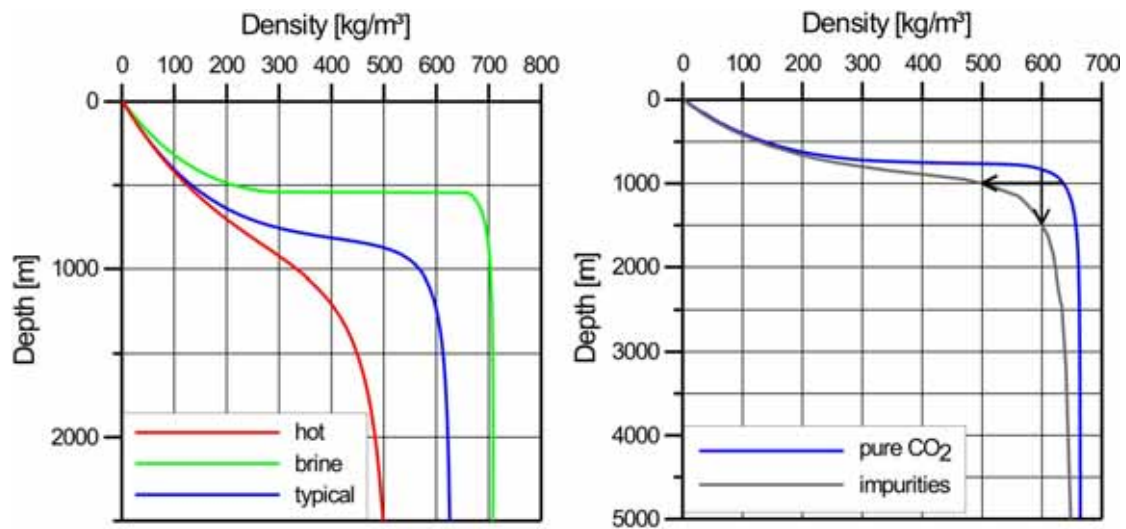


Figure 3.2 CO₂ density variation with depth (left) assuming hydrostatic pressure and typical temperature gradients in sedimentary basins (blue); elevated geothermal gradients (45 °Ckm⁻¹, red) and hydrostatic pressure gradients of highly concentrated brines (12.5 MPakm⁻¹, green). Effect of impurities (right) e.g. 2.75 % O₂ and other components.

Suitable aquifers should:

- contain saline water (e.g. salinity > 100 g l⁻¹) to avoid spoiling potable water resources

- exceed minimum permeabilities and porosities (Table 3.1)

- provide storage at depths of 800 m or more (where CO₂ will be in a dense fluid phase and a long way from the ground surface or sea bed)

- have a minimum thickness (to limit the potential storage areal footprint)

- must be overlain by low permeability caprocks. They should however, have (other) boundaries permeable to the native pore fluids (mainly brine) that will allow the native pore fluids to be displaced (via single-phase flow).

The amount of CO₂ that can be stored in a given saline reservoir formation is termed the capacity factor C (Geo-Seq, 2004). C is the volume fraction of the reservoir volume available for storage, and is defined as the sum of the terms for the free supercritical CO₂ (C^{gas}), and the CO₂ dissolved in the native pore fluid (C^{liq}).

$$C = C^{gas} + C^{liq}$$

$$C^{gas} = \langle \phi \cdot S_g \rangle \quad \text{and} \quad C^{liq} = \langle \phi \cdot S_l \cdot X_l^{CO_2} \cdot \rho_l / \rho_g \rangle$$

where ϕ is porosity, S_g and S_l are the volume fractions of the pore space containing supercritical CO₂ and liquid respectively, $X_l^{CO_2}$ is the mass fraction of CO₂ dissolved in the brine, ρ_g and ρ_l are the densities of the supercritical and liquid phases respectively, and the angle brackets represent averaging over the spatial domain of storage.

Capacity factor can be conceptualised as the product of five parameters: (1) the intrinsic capacity, C_i , controlled by multiphase flow and transport phenomena (the relative permeability to CO_2 and the viscosity ratio between CO_2 and brine); (2) a gravity capacity parameter, C_g , controlled by buoyancy forces; (3) a heterogeneity capacity parameter, C_h , controlled by local geological variability such as sand channels and shale lenses; (4) a structural capacity parameter, C_s , controlled by larger-scale geological structures such as anticlines and fault blocks; and (5) the formation porosity, φ .

In addition to the above, C is also strongly influenced by how much of the native pore fluid can be displaced from the reservoir during injection.

The suitability of reservoirs, based on the above simple criteria, can be derived from regional maps of well-studied areas. However, published maps are already generalised and interpolated, and they typically show average parameter values of uncertain precision; for example, facies variations may not be taken into account properly. Few wells exist in sedimentary basins that are not of economical interest and reservoir properties may be extrapolated from wells regarded to be representative of a wider area with large associated uncertainty. On the other hand, in areas of economical interest, too much well information may be available to realistically be considered in a regional screening exercise. In this case a subset of typical or representative wells, giving unbiased spatial coverage, should be selected.

An expression for storage capacity in a regional aquifer can be defined:

$$Q = A \cdot D \cdot \varphi \cdot \rho_{\text{CO}_2} \cdot h_{\text{st}}$$

where Q is the storage capacity in kg, A is the areal distribution of the aquifer (m^2), D is the cumulative thickness of good reservoir rocks (m), φ is the effective porosity (<1), h_{st} is the storage efficiency (<1) (see section 3.1.3), and ρ_{CO_2} is the density (kgm^{-3}) of pure CO_2 under reservoir conditions.

Deviations of reservoir data from the average values assumed for area, thickness and porosity, will of course lead to errors in calculation of storage capacity. In regional studies uniform values of CO_2 density often have to be assumed, due to the lack of reservoir information, or due to a wide range of pressure and temperature conditions in the investigated area.

In a confined reservoir the storage capacity principally depends on constraining the pressure increase with respect to caprock stability, and can be written:

$$Q = A \cdot D \cdot \varphi \cdot (C_R + C_W) \cdot p \cdot \rho_{\text{CO}_2}$$

where C_R = compressibility of the rock (grain), C_W = Compressibility of water, and p = Permissible pressure increase

3.1.3 Storage efficiency

Storage efficiency is defined as that fraction (by volume) of the reservoir pore space that can be filled by CO_2 (in free or dissolved form). Storage efficiency is not an

intrinsic petrophysical property of reservoir rocks and so it constitutes perhaps the greatest uncertainty in storage estimation. It depends on geological factors such as the structural geometry and stratigraphical heterogeneity of the storage formation, and also on the geotechnical effort undertaken to achieve high gas saturations.

In the case of natural gas storage in aquifers, a bulk gas saturation of more than 50 volume percent may be reached, because it is desirable to keep the valuable methane in a closely confined area. Making use of several injection wells facilitates an efficient and flexible storage operation. According to numerical case studies, less injection effort would result in lower mean saturations.

It is useful to distinguish between **regional storage efficiency**, a parameter used during screening and relating to the total pore volume of a reservoir in a (large) area covering several potential traps and **local storage efficiency**, a parameter normally used during site characterisation/planning and relating to the pore volume in a specific trap or linked trap system.

The calculation of storage capacity for aquifers of large extent depends on another factor; the volumetric fraction of the aquifer that lies within structurally closed traps. In tectonically complex areas there are too many small structures to be identified, delineated and investigated individually, even if detailed structural information is available at all. The volumetric average gas saturation for individual structures or entire aquifers has to be determined by appropriate up-scaling methods that accurately represent the spatial integral of CO₂ saturations throughout the aquifer. In practice this is usually a matter of intuition. Areal fractions of about 2 to 8 % have been calculated in previous regional studies (e.g. May et al., 2005, and Section 3.1.4). If undulations of the top of thick reservoir formations act as traps, volume fractions may be lower if the relief of the top reservoir undulations is much less than the aquifer thickness. For example, the regional storage efficiency of the Utsira Sand is only a very small fraction of the total pore volume of the formation (see Section 3.1.4).

The degree to which complex storage efficiency concepts are utilised at this stage will depend on data availability and the degree of discrimination required to select the preferred site. In many cases it is likely that refined estimates of storage capacity, including simulation of various injection strategies, will not be carried out until the site characterisation stage.

3.1.4 Observations from the CO₂STORE case studies

Sleipner

The site screening process for Sleipner was mainly constrained by potential conflicts of use (see Section 3.6). The relatively modest projected storage amounts (20 Mt), and the large scale of the Utsira reservoir, meant that ultimate storage capacity was not a key site selection issue, nor was the likely small increase in formation pressure. Ultimately the Utsira reservoir was chosen because it had none of the disadvantages of the other alternatives, because of its size and good injection quality, and not least, because of its shallow depth and consequent low well and topside costs. The total storage capacity of the whole Utsira Sand, calculated from the above equation, and

based on the isopach map (Figure 3.3), regional assessments of porosity and shale volume and assuming a storage efficiency of 1.0, is about 3×10^5 Mt.

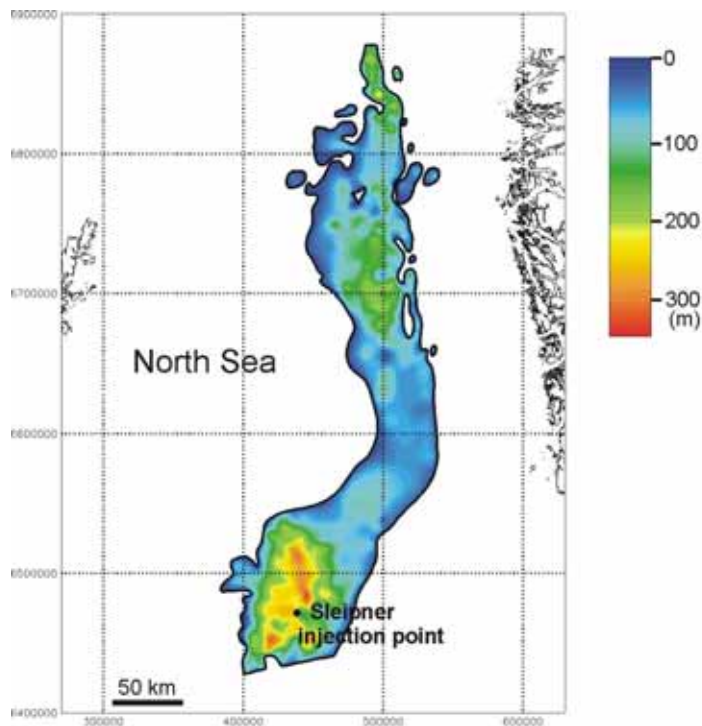


Figure 3.3 Utsira Sand thicknesses.

In practice this is likely to be a serious overestimate, as the storage efficiency (h_{st}) will in reality be much less than 1.0. As described above, effective storage can be defined as the pore volume enclosed within structural and stratigraphical traps, wherein CO_2 can be expected to accumulate in the long-term. The 3D seismic mapping around Sleipner (Zweigel et al., 2000) indicates that only about 0.3% of the available porosity is actually situated within structural closures at the top of the reservoir. Given that CO_2 migrating from a limited number of injection wells is unlikely to encounter all of the small traps, a more realistic estimate of the pore space within accessible closed structures around Sleipner is just 0.11% of the total pore volume. A simple extrapolation of these figures over the entire Utsira Sand gives an approximate storage volume in traps of just 6.6×10^8 m³, some three orders of magnitude less than the total pore volume giving a storage efficiency of just 0.0009.

On the other hand, trapping of CO_2 beneath intra-reservoir mudstones in the Utsira Sand may significantly increase realisable storage volumes. The time-lapse seismic data at Sleipner (Section 7) clearly show how the bulk of the injected CO_2 is currently being trapped as a number of discrete layers beneath thin intra-reservoir mudstones. This has the effect of markedly limiting lateral migration distances in the short term. Simple buoyancy-driven migration simulation assuming a homogeneous sandy reservoir shows that about 4.2 Mt of CO_2 trapped wholly at the top of the reservoir would ultimately migrate 6 km or so from the injection point (Figure 3.4). This compares with the observed 2001 CO_2 plume (4.3 Mt in situ) whose areal extent or

‘footprint’, lay entirely within 1.3 km of the injection point. The intra-reservoir mudstones are, therefore, providing a mechanism for delaying CO₂ dispersal in the short-term (tens of years). This effect would be particularly useful when it is necessary to avoid contamination of nearby working well infrastructure.

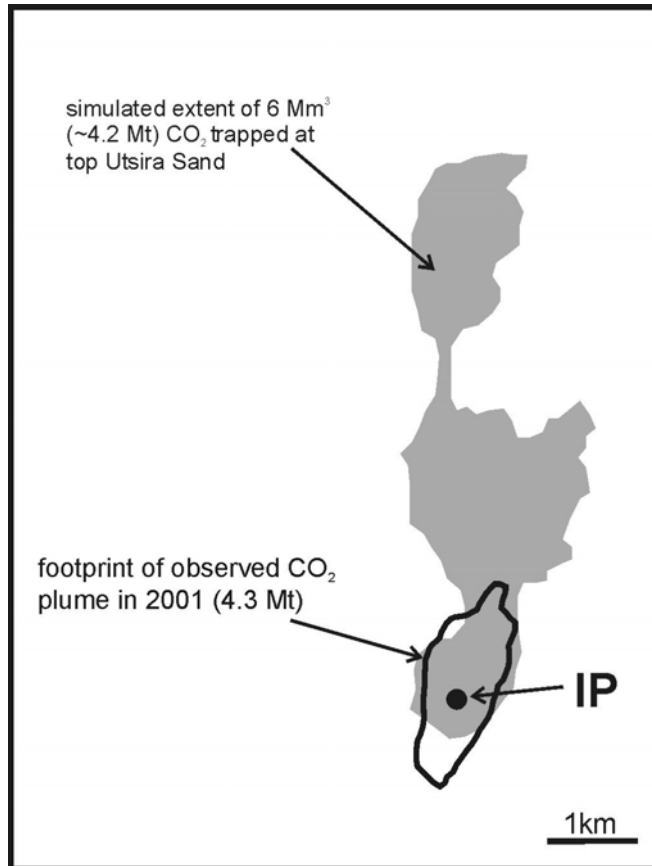


Figure 3.4 Sleipner CO₂ migration footprints: observed and from SEMI modelling.

Kalundborg

An early evaluation of the CO₂ storage capacity in Denmark was presented in Holloway et al. (1996), who concluded that 47 Gt of CO₂ could be stored in the unconfined onshore aquifers of Triassic and Jurassic age based on the assumption that 2% of the entire pore volume of the mapped formations could be filled. The low storage efficiencies were based on reservoir simulations indicating that the CO₂ would spill from the traps before a significant amount of the formation pore space was occupied.

In a refinement of this early study, estimates made in the GESTCO project restricted capacity calculations to structural traps with well-defined spill points. Based on experience from natural gas storage facilities in Denmark, Germany and France it was assumed that 40% of the total pore volume within a trap may be filled with CO₂. This requires that the reservoir behaves as an unconfined aquifer that allows pore fluids to be displaced by CO₂. It is also assumed that CO₂ is stored only as a free phase in the reservoir (dissolution of CO₂ into the formation waters would further increase storage capacity). Based on the above assumptions, the total storage capacity of major Danish structural traps (Figure 3.5) was estimated as about 16 Gt (Christensen and Holloway, 2003).

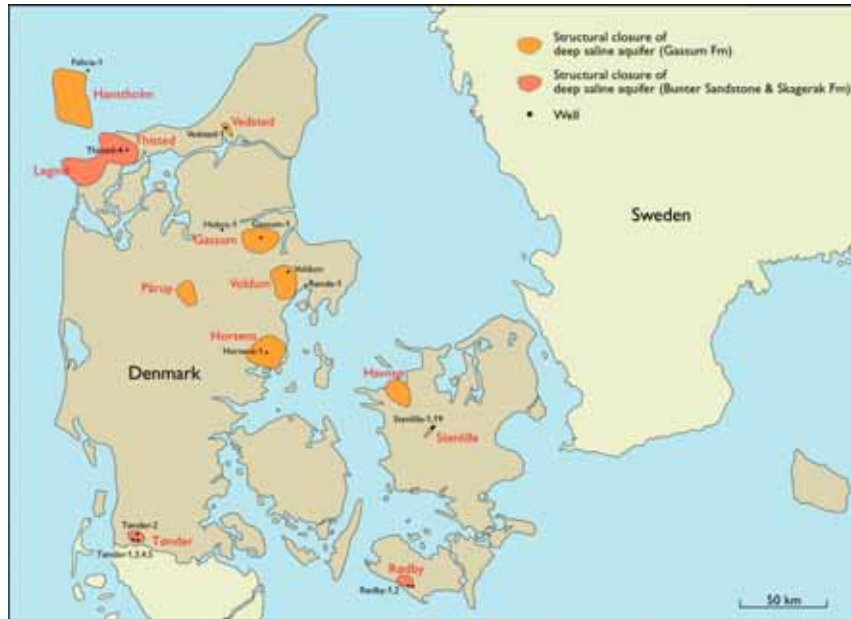


Figure 3.5 Map showing the location of the eleven structural closures mapped in the GESTCO study. Black dots indicate the position of deep exploration wells used in the evaluation of the reservoir formation (from Larsen et al., 2007. Copyright: Geological Survey of Denmark and Greenland).

A selection of these structures is illustrated in Table 3.2. Several reservoir units are present in some of the structures, providing an upside potential for increasing the total storage capacity. The secondary reservoir units are, however, often poorly characterised and their storage volumes have not been calculated, the storage capacities shown referring to the primary Gassum reservoir unit alone.

Structure	Formation	Available from	Area	Top depth msl	Gross thick	Net gross	Net sand	Porosity	Pore volume	Effective storage volume	Reservoir density of CO ₂	Storage capacity
			km ²	m	m		m	%	km ³	%	kg/m ³	Mt CO ₂
Gassum	Gassum	2006	242	1460	130	0.32	53	25	2,517	40	627	631
Hanstholm [‡]	Gassum	2006	603	1000	230	0.40	92	20	11,095	40	620	2752
Havnsø [‡]	Gassum	2006	166	1500	150	0.67	100	22	3,670	40	629	923
Horsens	Gassum	2006	318	1506	94	0.26	24	25	1,943	40	630	490
Pårup [‡]	Gassum	2006	121	1550	130	0.23	30	10	0,362	40	625	90
Stenlille [§]	Gassum	Not available	10	1507	130	0.76	100	25	0,247	40	631	-
Vedsted	Gassum	2006	31	1898	139	0.74	103	20	0,638	40	633	161
Voldum	Gassum	2006	235	1757	128	0.38	30	10	1,143	40	630	288
Total storage capacity (Mt)												5335

[‡] Extrapolated values, [§] Presently a natural gas storage operated by DONG,

Table 3.2 Table listing the key data for seven aquifer structures and the Stenlille gas storage structure in the Upper Triassic–Lower Jurassic Gassum Formation evaluated for future CO₂ storage in Denmark.

For the Kalundborg case study, the Havnsø structure, with an estimated capacity of 900 Mt, was selected as most suitable for more detailed appraisal (see Chapter 4).

Mid Norway

For the mid-Norway case study, three sites, the Beitstadfjord, Frohavet and Froan basins (Figure 1.5) were assessed at the screening stage. A preliminary selection of three basins was based on prior knowledge of an existing sedimentary succession of suitable thickness and an estimate of the available pore volume. The pore volume of the Beitstadfjord Basin was rated as potentially too small, but its location close to a potential CO₂ source (the planned Skogn power plant) increased its attractiveness. In addition, its potential suitability was a topic of national political debate and a proper technical investigation was deemed to be helpful to rationalise the issues.

The relatively short distance to the potential CO₂ sources was an argument during pre-selection of the three basins. Offshore areas with potential for conflict with other industry (particularly hydrocarbon production) were excluded, in spite of proven seal capacity and known trap volumes.

The characterisation of the Froan Basin area of the Trondelag Platform (which was based on seismic data and analogy with the nearby Halten Terrace hydrocarbon fields) did not provide indications for major changes in structure or reservoir property along strike. Accordingly, a narrow segment in the dip direction was selected as representative; storage capacity evaluations were carried out for this segment and then extrapolated to the whole basin.

All three mid-Norway sites are situated within dipping, open aquifers. The fact that they lack structural (or stratigraphical) closure requires that determination of storage capacity be more sophisticated than a simple volume calculation based on reservoir geometry and reservoir properties. Storage capacity estimations for these sites had to employ fluid flow simulations to determine what amounts (rates and total volumes) of CO₂ could be injected while staying below given leakage rates or critical pore pressures.

Schwarze Pumpe (Schweinrich)

The Schweinrich structure is situated beneath the small village of Schweinrich, some 250 km to the northwest of Schwarze Pumpe (Figure 3.6). It was selected from a number of similar salt-related features in northern Germany. Though not the closest potential structure to the power plant, it was deemed most suitable for a number of reasons including high storage capacity (sufficient for 400 Mt of CO₂) and likely good caprock. The site selection process is further described below.

Because no target storage aquifer was identified in advance, regional maps of saline aquifers and associated structural closures deemed suitable for CO₂ storage were compiled over the study area covering a large part of the Northeastern German Basin.

Target areas were mapped, based on thresholds for suitable open aquifers of a minimum 20 m sandstone thickness, minimum 20% porosity, and a depth of more than 1000 m (in order to maintain high CO₂ fluid density). In this case, the underground storage of about 400 Mt of CO₂, at a density of about 700 kgm⁻³ and a storage efficiency of 6%, would require a storage footprint of about 2380 km². Due to this large requirement, which seldom is available in a single trap, a cumulative

sandstone bed thickness of 20 m and porosities of about 20% can be regarded as minimum values for areas with realistic potential for CO₂ storage.

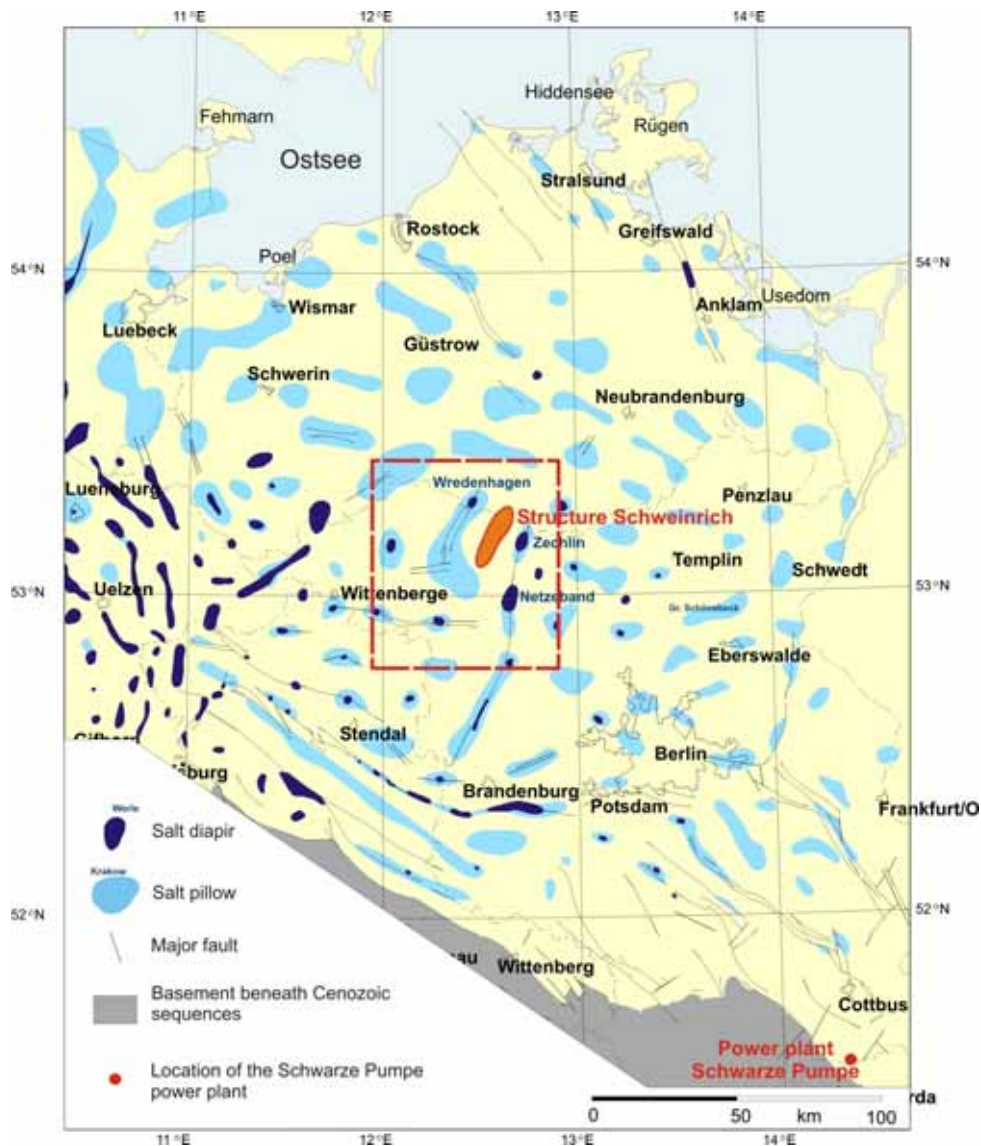


Figure 3.6 Location of Schwarze Pumpe and the Schweinrich structure relative to salt structures and basement topography in the Northeastern German Basin. The area investigated and modelled in detail is marked by the red frame.

Porosities of about 20% or more are also generally required for problem-free injection of fluids into porous strata. A CO₂ density of 700 kgm⁻³ was assumed for all structures, though this value is probably at the higher end of densities that can be expected from the actual formation pressure and temperatures. This uniform value allows a level comparison of different structures and comparisons with calculations in the literature which commonly use a similar density.

Using a geographical information system (GIS), maps of potential storage reservoirs were produced for the Lower Cretaceous, Jurassic (Aalenian, Lias) and Triassic (Rhaetic, Keuper, Schilfsandstein and Buntsandstein). All these formations have units suitable for CO₂ storage in association with good sealing rocks.

An initial GIS base map was produced showing the distribution of reservoir formations in the study area. The first filter applied to the base map was the requirement of a storage reservoir thickness exceeding 20 m. The reduced areas fulfilling this requirement were then input to a second filter requiring a minimum depth requirement of 1000 m. Finally, a third filter was applied, limiting the areas of interest to match the distribution of underlying salt structures.

In this way, a total of 130 salt structures in the study area were investigated, of which 26 were identified as potentially suitable storage sites. Aquifer volumes of the potential structures were calculated from areal distributions based on the deepest closed contour line on 1:200 000-scale maps and thicknesses derived from boreholes. Storage capacities were derived using an estimated storage efficiency of 0.4 (i.e. an average gas saturation of 40 vol.-%), a CO₂ density of 700 kgm⁻³, and the total thickness of good reservoir sandstones derived from wells in the area of the structure. The storage capacity of the evaluated structures varies from 11 to 1192 Mt of CO₂ (Figure 3.7). These estimated capacities should be regarded as upper limits and might be modified after site characterisation, when more detailed information about the aquifers and the structures is available. The selected structures cover about 3 % of the total study area, although smaller structures or less favourable aquifers adjacent to well-suited structures may increase this fraction somewhat (e.g. structures between 600 to 1000 m depth).

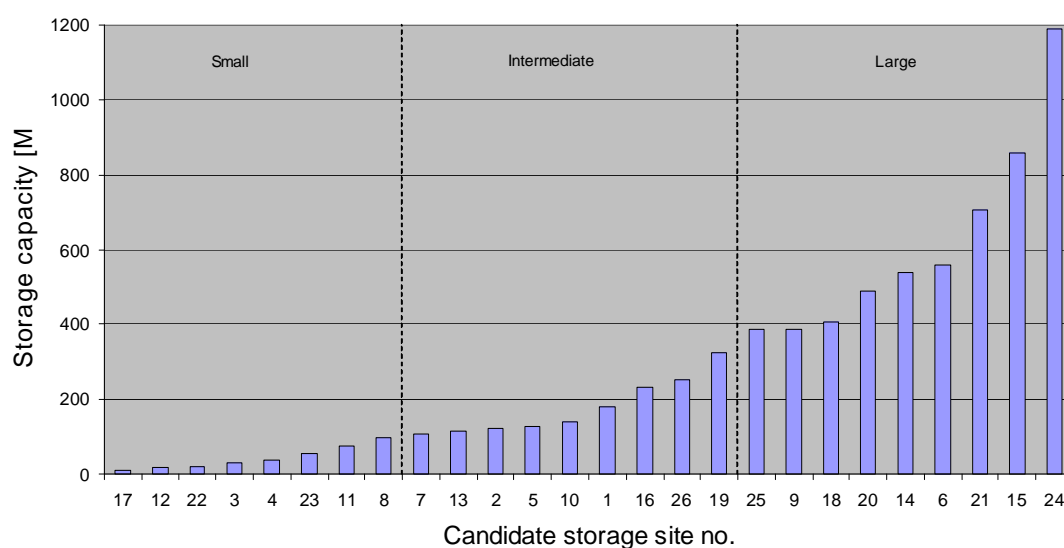


Figure 3.7 Estimated CO₂ storage capacities for candidate sites in the Northeastern German Basin based on a storage efficiency of 0.4, sorted by increasing capacity and subdivided into categories of small (< 100 Mt), intermediate (100 to 400 Mt), and large (> 400 Mt) storage capacity.

For the final site selection, a workshop was held with the overall goal of ranking the potential > 400 Mt storage sites, and to choose one site that was best suited for the continued CO2STORE work. Several potential storage sites were analysed with respect to the following additional criteria, to the extent that information about them was currently available:

protected areas - military, nature resources, lakes and rivers, and ‘Nature 2000’

existing industrial use/rights

landscape picture (pipelines, power plant)

population density

special interest groups.

Areas of cultural interest and recreation were not included due to the lack of sufficiently detailed information.

The final ranking of the potential storage sites was mainly based on their geological properties and on potential conflicts of use, with the Schweinrich structure as first choice (albeit with a qualification regarding the long transport distance from the Schwarze Pumpe power plant). This structure is not affected by nature protection areas or areas that are used by the military (although the military has interest in an adjacent area to the east). Regarding environmental issues this structure is also favoured.

After Schweinrich was selected, a more detailed estimation of storage capacity was carried out, based on a detailed 3D reservoir model. Since no wells have been drilled within the closure, the lithofacies interpretation has been derived from the correlation of nearby wells. The total bulk rock volume above the spill point has been calculated using the geological model. The reservoir is split by a low permeability bed (the Triletes Claystone), which is some tens of metres thick. Since it is not known whether this unit forms a laterally persistent seal within the reservoir, two different geological scenarios have been considered in the calculations.

Scenario A is based on the assumption that the intra-reservoir claystone is somewhat permeable and both reservoir units (Hettangium and Contorta) are hydraulically connected. In scenario B, the Triletes Claystone is assumed to be impermeable to CO₂ and two separate reservoir units are considered. Based on these two assumptions, different spillpoints (at 1500 m and 1700 m depth) are proposed (Figure 3.8).

The total available pore volume calculated for both scenarios ranges between 1800 Mm³ (scenario A) and 3000 Mm³ (scenario B). The considerably higher pore volume in scenario B is due to the additional contribution from the deeper part of the Contorta reservoir. Estimated storage capacities, calculated for an assumed 40% average CO₂ saturation and a CO₂ density of 600 kgm⁻³, range from 430 Mt CO₂ to 720 Mt CO₂ respectively, which should be sufficient, even if the necessary storage efficiency were less than 0.4.

Uncertainty of the calculated total storage capacity is estimated to be within 20 %. Reasons for this uncertainty are the limited availability of geological data and the associated geological interpretation as well as the high variability in lithology and the resulting uncertain correlation of widely spaced wells.

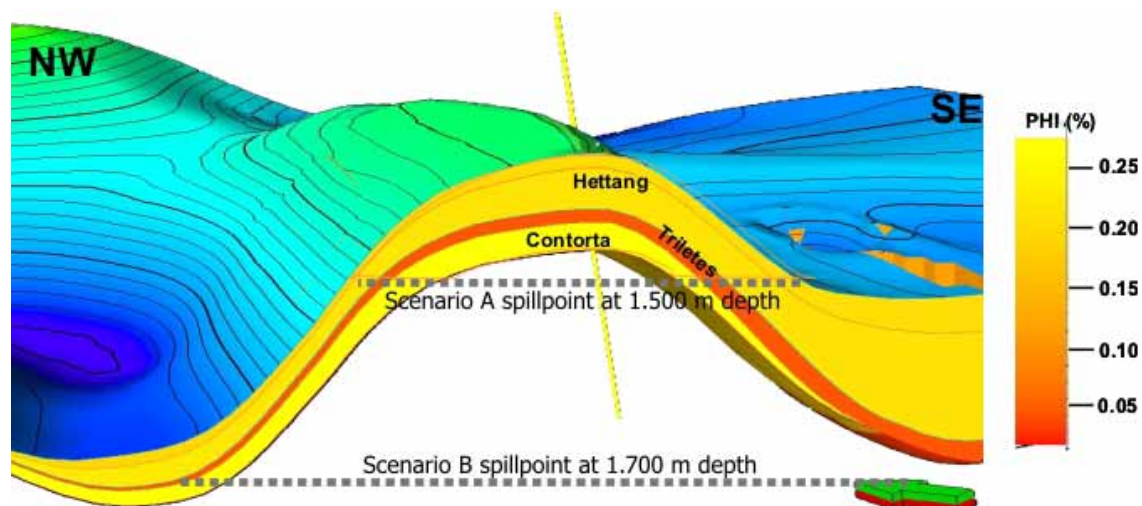


Figure 3.8 Simplified north-west to south-east cross-section through the Schweinrich site, showing reservoir structure and average porosity distribution. Dashed lines indicate the position of the deepest closure contour line (spill point) for scenarios A and B.

The CO₂ storage efficiency is given by the volume of CO₂ under reservoir conditions divided by the maximum available pore volume for storage (van der Meer, 1995). Under Schweinrich reservoir conditions a CO₂ density of 600 kgm⁻³ can be expected and 400 Mt of CO₂ would fill a pore volume of about 0.67 km³. Taking the calculated pore volumes, storage efficiencies of 0.22 to 0.37 would result for the two respective reservoir scenarios.

Reservoir simulations (see Chapter 4) also contribute to the evaluation of the storage potential. Ten injection wells have been proposed in order to inject 10 Mt of CO₂ per year, with a total amount of 400 Mt of CO₂ over 40 years. As a result of the reservoir simulations, it is clear that both the storage capacity and the storage efficiency are controlled by a number of other parameters including peak reservoir pressure. With respect to the Schweinrich case, it is clear that a large, supra-regional aquifer is required for the storage site to accommodate very large volumes of CO₂.

Valleys

No formal capacity assessment was carried out at the screening stage of the Valleys case study. Site selection was based on clear geological indicators without a need for calculation of storage capacities (see below).

3.1.5 Generic findings

Where it is required that large volumes of CO₂ be stored, possibly from multiple injection sites, it is important to assess the storage capacity of potential storage reservoirs. For a number of reasons, storage of CO₂ in saline aquifers is likely to focus on large structural traps. Here storage capacity is quite readily defined, as CO₂ can reasonably be expected to accumulate at high saturations with predictable trapping geometries. Regional flat-lying aquifers pose greater problems because a high percentage of the total pore volume of the reservoir cannot necessarily be utilised, and in consequence, very low storage efficiencies may be encountered. On the other hand,

these may paint an unrealistically pessimistic picture. As shown above for Sleipner, stratigraphical complexity within the reservoir will readily promote alternative ‘fixing’ processes that do not require any form of structural trapping. Intra-reservoir heterogeneity is likely to increase effective storage capacity in the longer term by encouraging dissolution of CO₂ into the groundwater, promoting ‘stratigraphical’ trapping of CO₂ as an immobile residual phase (see Section 4.2) and promoting geochemical reactions leading to chemical ‘fixing’ (see Section 4.3). It is clear, therefore, that the assessment of effective storage capacity in an aquifer requires detailed treatment of reservoir structure, stratigraphy and fluid flow.

To summarise, calculations of storage capacity are inherently uncertain, regardless of the size of the target investigated, due to the limitations of underground data availability and quality. They further include assumptions about the future geotechnical utilisation of the available pore space. Planning of CO₂ capture and storage projects requires reliable predictions including estimates of uncertainty ranges for storage capacity. Such predictions require intensive site characterisation, taking into account local variations of aquifer properties. Reservoir models are used to simulate the effects of different CO₂ injection strategies and to predict storage efficiencies.

In some cases (exemplified by the Valleys case study), formal capacity estimations may not form part of the site selection stage, if other geological indicators are sufficiently diagnostic of the preferred site. However, for high-range CO₂ point sources such as a coal-fired power plant, the capacity assessment is important at an early stage. If large storage capacities are not available, there is no basis for pushing such a project further ahead.

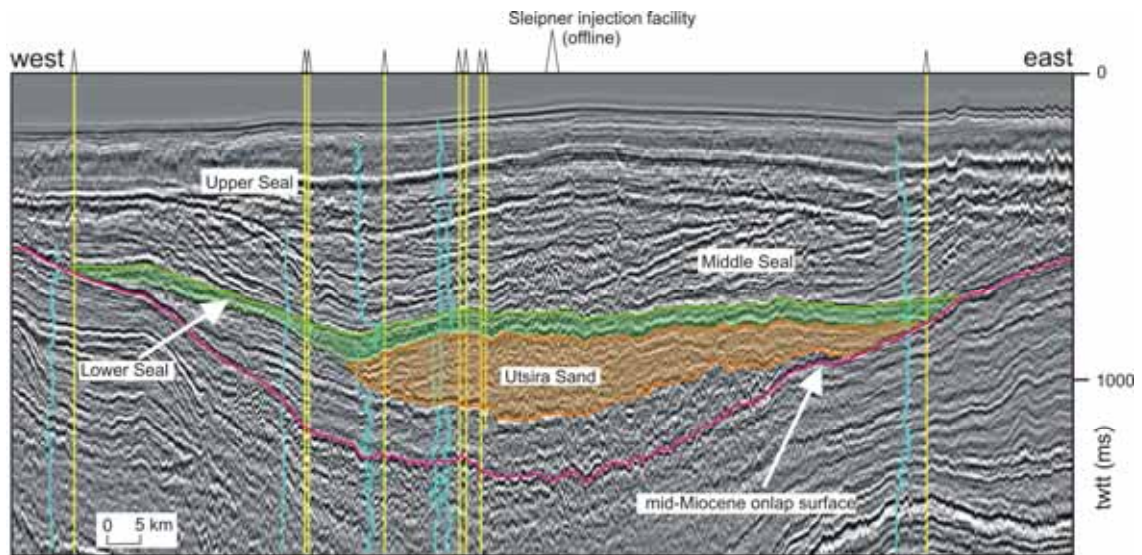
3.2 Basic reservoir properties

A necessary step prior to site selection is to ensure that fundamental reservoir properties (e.g. structural geometry, porosity, fluid flow properties) are consistent with the requirements of the proposed CO₂ injection programme. Reservoir characterisation is a routine procedure in the exploration industry, so discussion here is limited to site-specific findings.

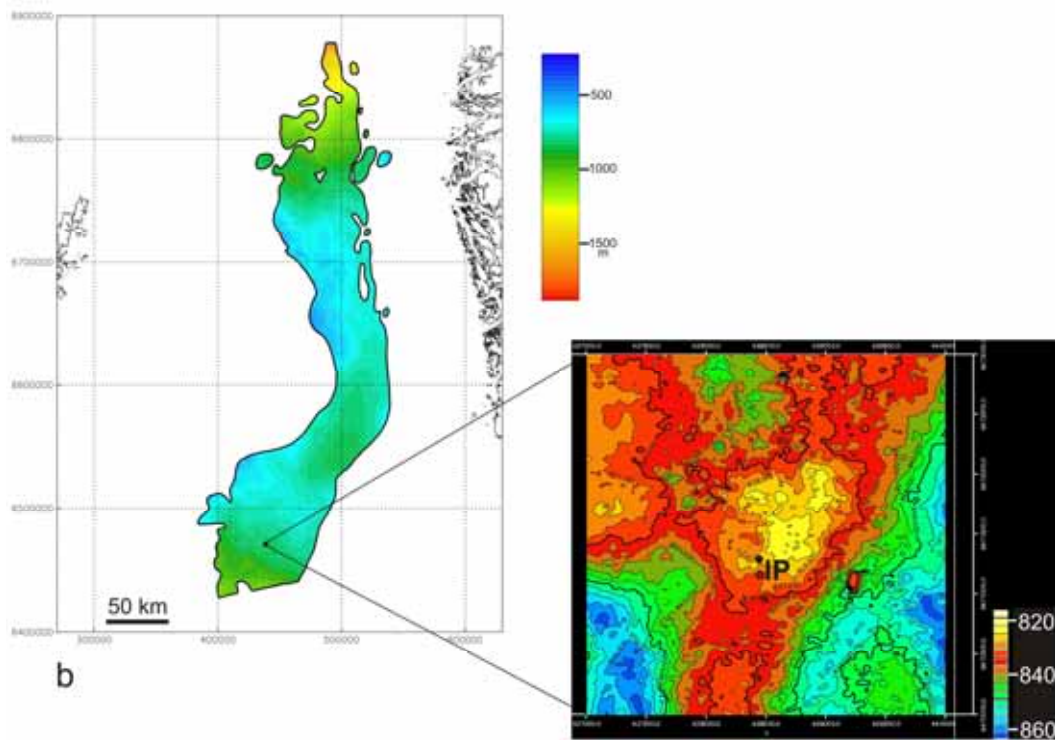
3.2.1 Observations from the CO₂STORE case studies

Sleipner

The Utsira Sand forms the Sleipner reservoir and comprises a basinally restricted deposit of Mio-Pliocene age extending for more than 400 km north to south and between 50 and 100 km east to west (Figure 3.9). Its eastern and western limits are defined by stratigraphical lap-out, to the south-west it passes laterally into finer-grained sediments, and to the north it occupies a narrow, deepening channel. Locally, particularly in the north, depositional patterns are quite complex with some isolated depocentres, and lesser areas of non-deposition within the main depocentre.



a



b

c

Figure 3.9 Sleipner seismic datasets. a) Regional 2D seismic line through the Utsira Sand. b) Depth map of the top of the Utsira Sand based on 2D regional seismic data. c) Detailed contour map of the top of the Utsira Sand reservoir based on 3D seismic data. IP = Injection Point. (2D seismic data reproduced courtesy of WesternGeco).

Regional interpretation was based on 2D seismic and well information (details in Chapter 4), which show the reservoir to be notably uniform on the regional scale. In the immediate vicinity of Sleipner the detailed structure of the Utsira reservoir was mapped with 3D seismic data. A domal trap, north-north-west of the Sleipner platform was initially selected as a potential storage site. Reservoir simulations, which focussed on injectivity and on migration during the planned 20-years injection period, were carried out for this trap. Later, a different trap north-east of the Sleipner platform was identified (Figure 3.10)

based on new 3D seismic data. The generic results from the previous reservoir simulations were then applied to this trap, which was subsequently chosen to become the actual storage site (for more details see Chapter 4).

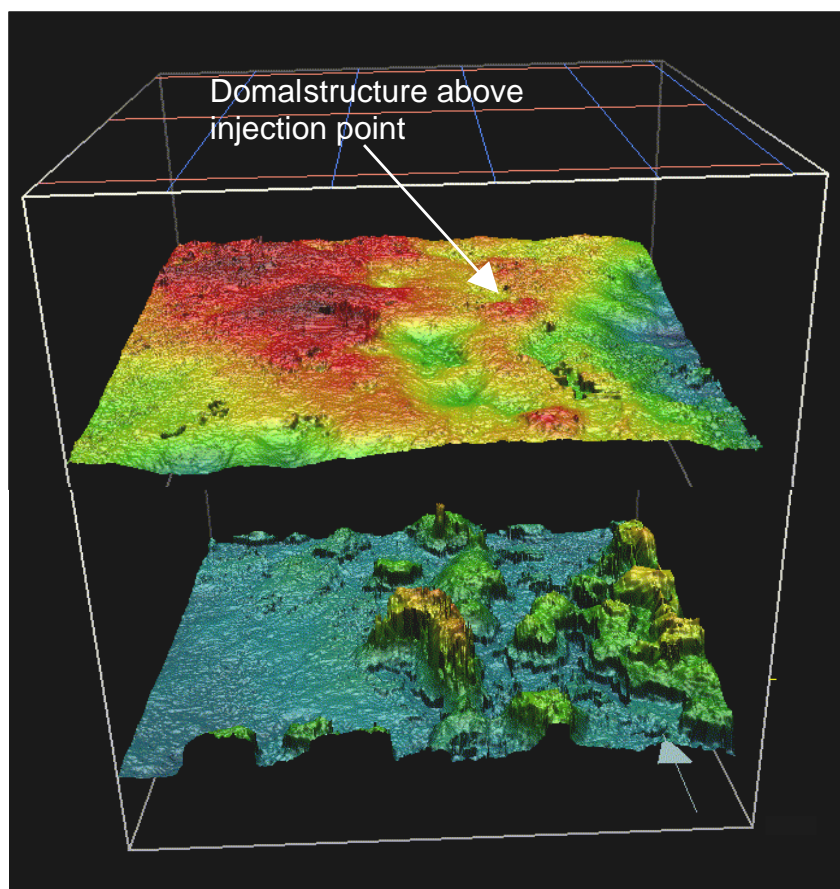


Figure 3.10 Perspective view of the top and base of the Utsira Sand around the injection point, based on 3D seismic. Note domal structure above the injection point.

A basic assessment of reservoir properties was carried out utilising geophysical log data. These showed the reservoir sand to be largely unconsolidated, with excellent porosity and probably with permeability of several Darcies. More detailed characterisation of the reservoir was subsequently carried out by the SACS project (Chapter 4).

This relatively simple screening study has proved to be largely accurate and certainly fit for purpose. Key aspects are that the Utsira Sand reservoir is structurally simple, relatively homogeneous and with a very large pore volume; the relatively small injected amounts therefore do not really test storage capacity uncertainty.

Kalundborg

In the onshore or nearshore Danish area the potential reservoirs are of Mesozoic and late Palaeozoic age. Mapping of these units has been carried out in the search for hydrocarbons and geothermal reservoirs (Michelsen, 1981; Sørensen et al., 1998), and reservoir parameters (lithology, thickness, net/gross, porosity and permeability) have

been summarised. Seal properties and presence of structural closures (traps) were not considered in these earlier studies.

To supplement earlier work, the site screening study focused on four stratigraphical units (Figure 3.11), the Bunter Sandstone and Skagerrak Formations (Triassic), the Gassum Formation (Upper Triassic to Lower Jurassic), the Haldager Sand Formation (Middle Jurassic) and the Frederikshavn Formation (Upper Jurassic to Lower Cretaceous).

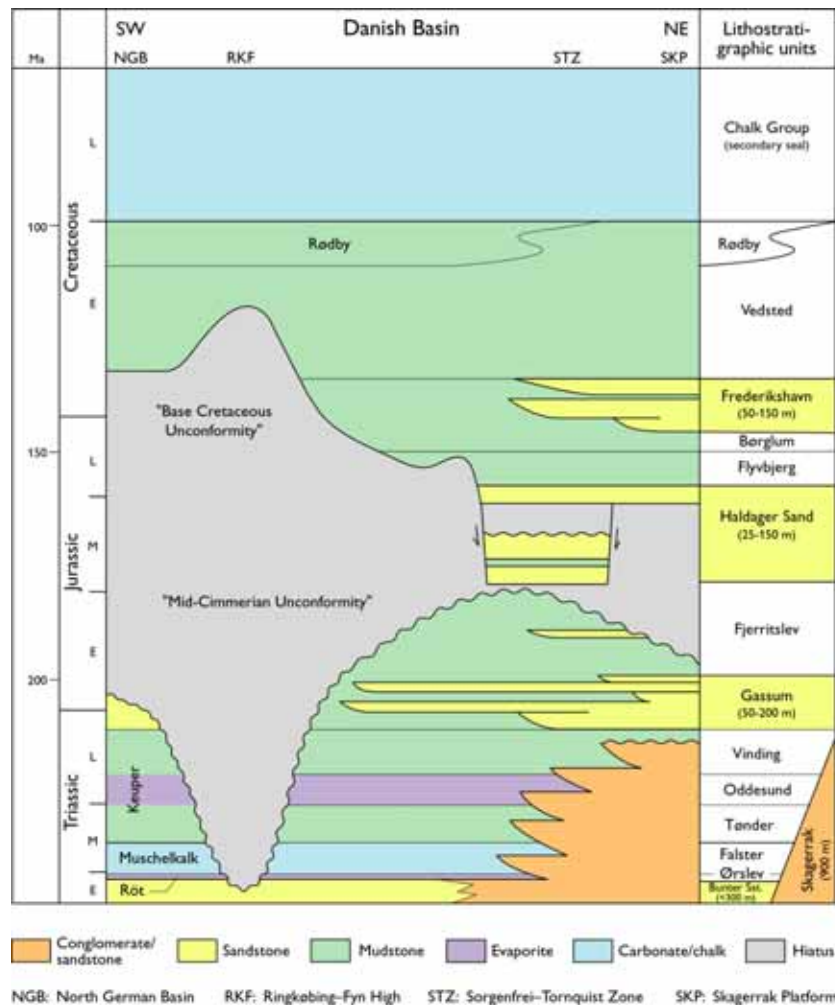


Figure 3.11 Simplified stratigraphy and lithostratigraphy of the sedimentary succession in the Danish Basin (based on Bertelsen, 1980; Michelsen and Clausen, 2002; Michelsen et al., 2003).

Burial depth and reservoir properties make the Gassum Formation the most attractive storage option overall. In addition the reservoir behaviour is well understood as the formation is currently used for natural gas storage by DONG in the Stenlille area. The Gassum Formation is present in the Danish Basin, the North German Basin and on the Ringkøbing-Fyn High in the Lolland Falster area (Figure 3.12). It shows remarkable lateral continuity with thicknesses between 100 and 150 m throughout most of Denmark.

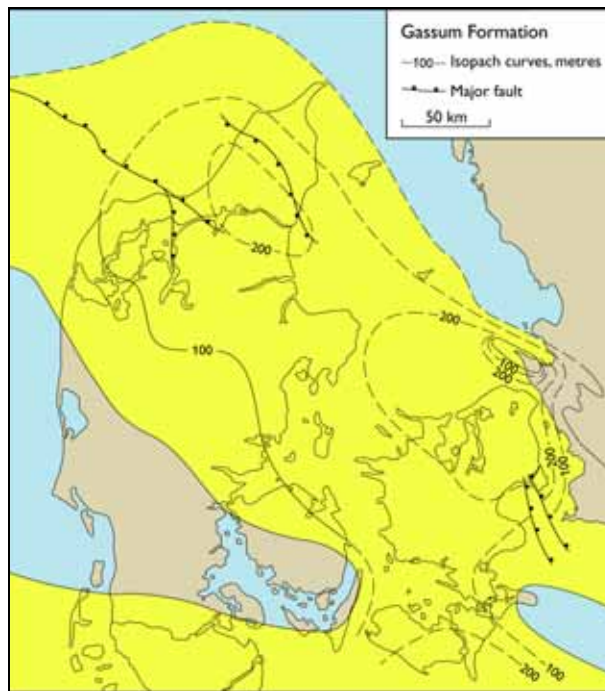


Figure 3.12 Isopach map showing the distribution and formation thickness of the Gassum Formation in the Danish area (from Larsen et al., 2007. Copyright: Geological Survey of Denmark and Greenland).

Lithologically the Gassum Formation consists of stacked shoreface units with excellent reservoir properties separated with thin claystone or heterolithic units (Nielsen et al., 1989; Hamberg and Nielsen, 2000; Nielsen, 2003). Each of these units may act as discrete reservoir compartments and is characterised by a distinct set of porosity/permeability parameters. The porosity and permeability of the Gassum sandstones are known from a number of wells and illustrate the relationship between reservoir properties and depth in the Danish Basin (Figure 3.13). Reservoir properties are generally excellent with porosities in the range 18 to 27% (maximum 36%) and permeabilities up to 2000 mD.

In the vicinity of Asnæs and Kalundborg eight structural traps are evident at Gassum stratigraphic level: Hanstholm, Vedsted, Gassum, Voldum, Pårup, Horsens, Havnsø and Stenlille structures (Figure 3.5, Table 3.2). These structures were mapped from existing seismic 2D surveys. The reservoir, and to some extent, the seal properties were evaluated using data from old exploration wells (well logs, cores) drilled at the structures or nearby.

The structures were selected on the basis of a number of criteria:

The top of the reservoir should be situated deeper than 900 m below the surface.

The reservoir should be situated at depths less than 2500 m in order to ensure that adequate porosity and permeability is preserved (unless well data were present to validate porosity and permeability values at greater depths).

The structure should be of sufficient size (storage capacity ~100 Mt).

An effective topseal (caprock) should be present.

The structure and seal should be unfaulted.

The structure should be within reasonable distance of the CO₂ source.

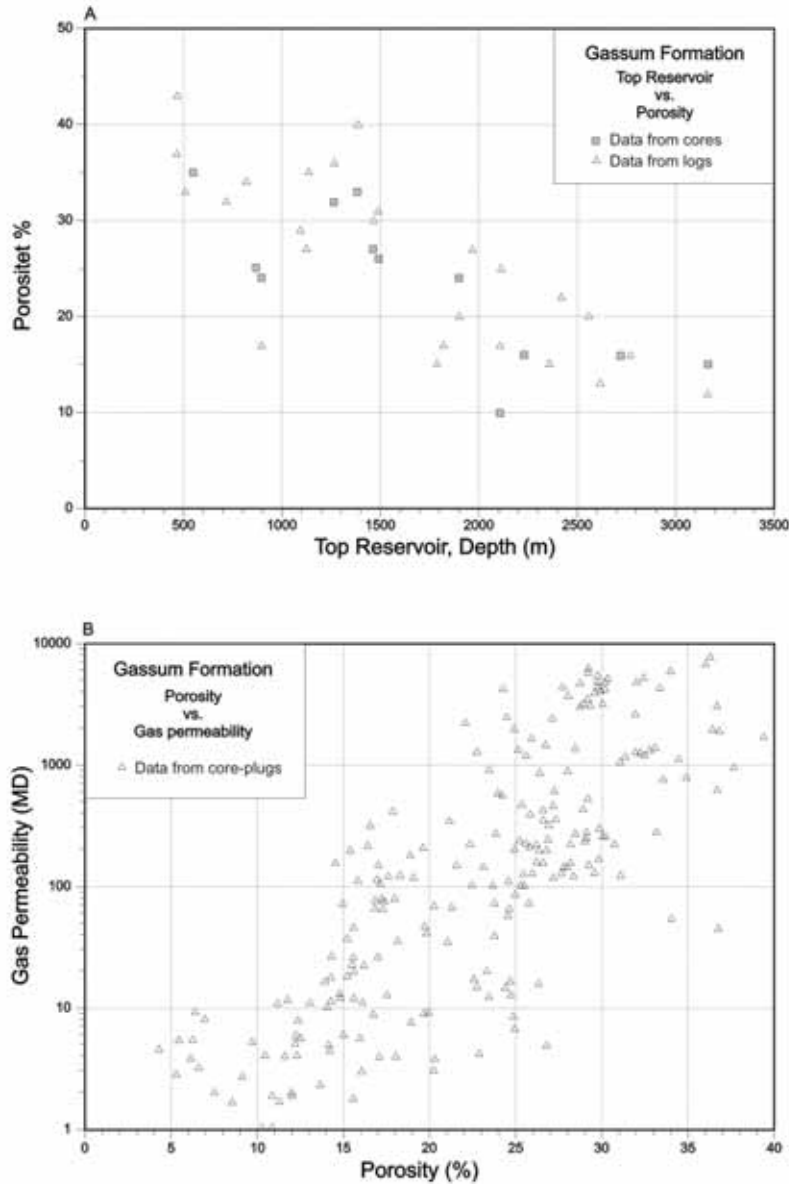


Figure 3.13 Porosity and permeability versus depth for the Upper Triassic–Lower Jurassic Gassum Formation (from Larsen et al. 2007. Copyright: Geological Survey of Denmark and Greenland).

A number of structures were evaluated, but excluded from the final list due to problems of satisfying one or more of the above criteria. These structures may form additional storage sites, but detailed site-specific studies are needed in order to prove their ability to store CO₂. The most common problem was the presence of faults either at the top of domal structures or forming the updip closure of traps. Fault bounded traps do however form an interesting storage type along the Ringkøbing-Fyn-Møn High where domal storage structures are not present.

Storage	Havnsø	Røsnæs
Onshore/offshore	2/3 onshore, 1/3 offshore	Offshore
Reservoir	Gassum Formation	Gassum
Stratigraphy	Late Triassic	Late Triassic
Lithology	Siliciclastic sandstone	Siliciclastic sandstone
Top depth msl	1500 m	1700 m
Gross thickness	150 m	100 m
Net/gross	0.67	0.5
Net sand	100 m	50 m
Porosity	22	20
Permeability	500 mD	200 mD
Pore volume	3 670 km ³	900 km ³
Pressure	150 bar	170 bar
Temperature	~ 50 °C	~ 55 °C
Reservoir density of CO ₂	629 kg/m ³	631 kg/m ³
Seal	Fjerritslev Formation	Fjerritslev Formation
Stratigraphy	Early Jurassic	Early Jurassic
Lithology	Marine mudstone	Marine mudstone
Gross thickness	500 m	500 m
Trap	4-D domal closure	Fault closure (Neogene movement)
Area of closure	166 km ²	90 km ²
Distance to source	15 km	18 km
Effective storage factor	40%	40%
Storage capacity	923 Mt	227 Mt
Comments	Eclipse simulation	

Table 3.3 Attributes of two potential storage sites for the Kalundborg case study.

From the initial screening process, two structures, Havnsø and Røsnæs, were considered as potentially suitable for the Kalundborg case study (Table 3.3). Both are domal closures at Gassum Formation level situated in the Kalundborg area (Figure 3.14). The reservoir unit in both structures comprise shoreface sandstones of the Gassum Formation, with marine mudstones of the Fjerritslev Formation forming the caprock.

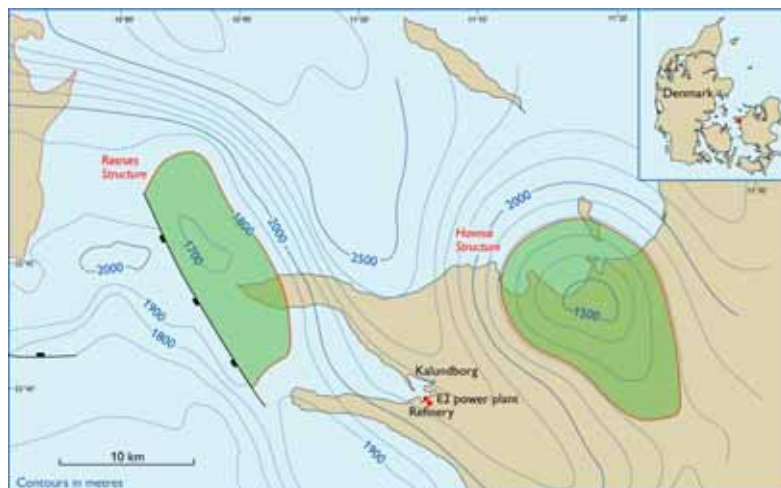


Figure 3.14 Depth structure map of the Havnsø and Røsnæs closures. Both structures are defined in the Upper Triassic to Lower Jurassic Gassum Formation.

Selection of the Havnsø structure for detailed study (Chapter 4) was based on a combination factors:

very large structure

absence of faulting

good quality of reservoir

proximity to the CO₂ sources

analogous to nearby natural gas storage in a similar, but much smaller structure.

Public acceptance factors were not included in the considerations. It is worth mentioning that the Rosnæs structure, being offshore, may have had more straightforward public relations issues, but these were outweighed by likely site performance deficiencies.

Mid Norway

For the mid Norway case study, three distinct sites, the Beitstadsfjord, Frohavet and Froan basins (Figure 1.5) were assessed at the screening stage. Reservoir units at the sites have all been interpreted as sharing some basic similarities. They consist probably of highly porous clastic rocks with good permeability, they are overlain by thick argillaceous sequences forming capillary seals and they have a significant dip but no major closed structures, causing them to either crop out at the sea floor or subcrop beneath thin, unlithified layers of Quaternary strata.

Geological data for the study was scarce, with high uncertainties. Because of this, geological screening was based upon developing a generalised model for each basin, followed by a number of reservoir flow simulations designed to examine the significance and sensitivity of the property uncertainties.

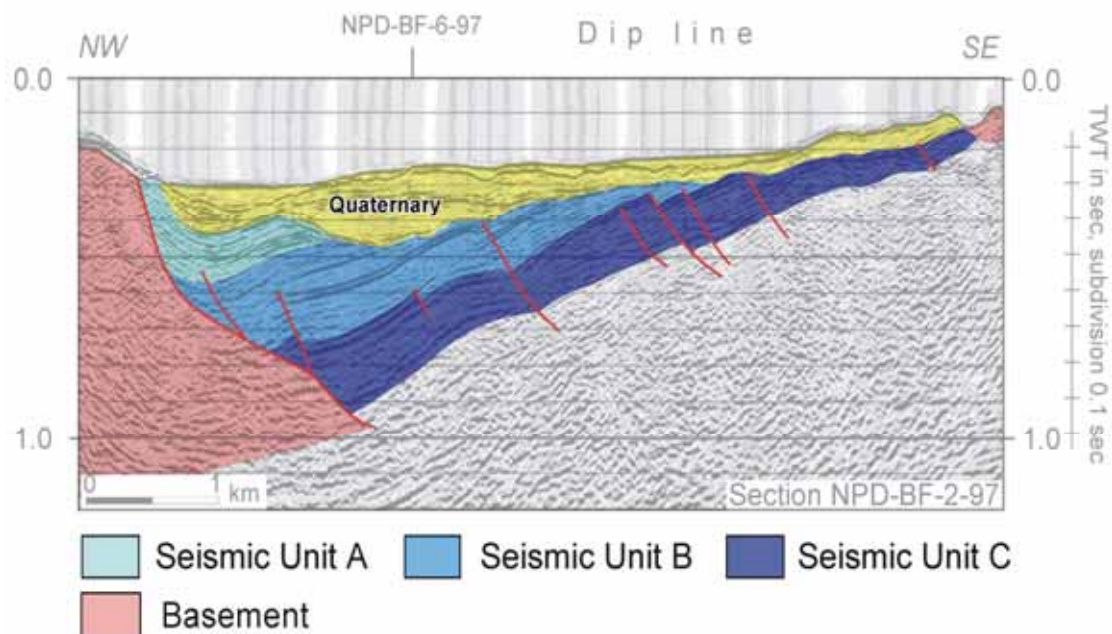


Figure 3.15 Geoseismic section through the Beitstadsfjord Basin. Note major basin-bounding fault (More–Trondelag Fault System) to the north-west (from Sommaruga and Bøe, 2002).

The *Beitstadsfjord Basin* (Figure 1.5) is a small north-east-trending half graben located at the northeastern extremity of the Trondheimfjord in water depths generally more than one hundred metres. It is approximately 14 km long by 6 km wide, surrounded

by Precambrian migmatitic rocks to the north and Lower Palaeozoic metasediments to the south. The basin fill (Figure 3.15) dips to the north-west, against the bounding normal fault, part of the Møre-Trøndlag Fault Complex, which has experienced fault movements from Ordovician to Cenozoic times. Based on seismic character, the dipping succession has been divided into three units A–C, believed to correlate with the Middle Jurassic Ile, Garn, and Melke Formations known from offshore mid-Norway (Sommaruga and Bøe, 2002). However, there is no well control in the Beitstadvjord Basin, so besides seismic character, the age and type of basin fill can only be inferred from loose rock fragments found on nearby shores, including Middle Jurassic sideritic ironstone and sandstones. The sideritic ironstones, show measured porosities of 0.6–2.1% , but these highly cemented samples are considered unrepresentative of the basin sequence as a whole; it is likely that they are preferentially preserved because of their hardness. It is considered that porosities up to 20% should be expected in less well-cemented units.

The Jurassic succession is overlain by Quaternary deposits ranging in thickness from 30 m to approximately 200 m. The succession is dominated by till, but there are also marine and glaciomarine, fine-grained sediments.

The basin is relatively shallow, with a maximum depth of approximately 1.3 km (Polak et al., 2004a) and has been uplifted and significantly eroded. Consequently the basin fill is overcompacted. Organic matter maturation measured on Middle Jurassic sandstone fragments found along the shores of the Beitstadvjord suggests a maximum burial depth of 1.8 to 2.3 km.

With the present poor knowledge of the basin stratigraphy, it was considered inappropriate to include possible fault barriers in a model (Polak et al., 2004a). Thus, for flow modelling purposes, the basin was treated as a simple north-west-dipping homocline without a topseal.

The *Frohavet Basin* lies on the inner part of the Trøndelag Platform (Figure 1.5) in water depths everywhere more than 200 m (Sommaruga and Bøe, 2002). It forms a half-graben, about 60 km long by 15 km wide, with a maximum depth of about 1.6 km (Figure 3.16).

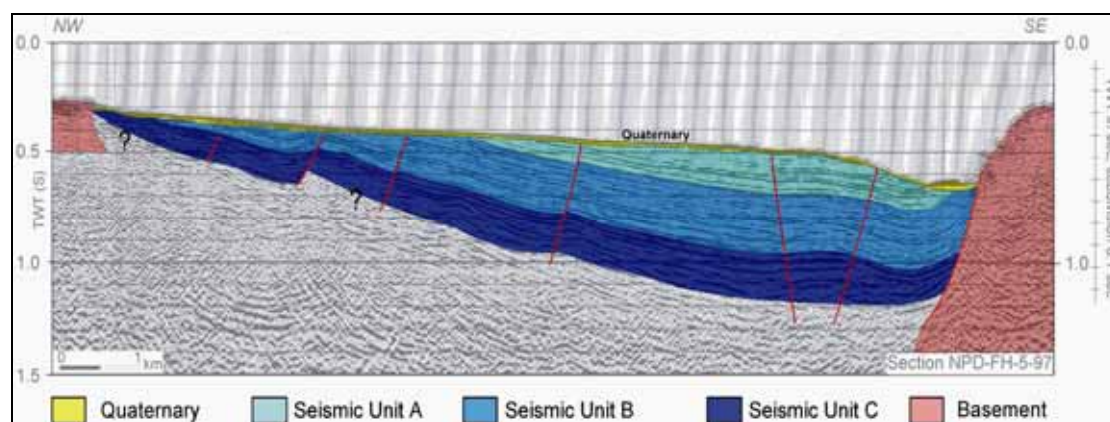


Figure 3.16 Geoseismic section through the Frohavet Basin. Note the basin bounding fault (Tarva Fault) to the south-east (from Sommaruga and Bøe, 2002).

The basin is surrounded by Caledonian plutonic rocks, various gneisses and Devonian sedimentary rocks. The latter, which have suffered very low grade metamorphism and have practically zero porosity and permeability, may also be present beneath the basin floor.

The north-east-trending half-graben dips to the south-east, its sedimentary succession showing stratigraphical thickening towards the bounding faults indicating syndepositional growth. There is no well control, so the age and type of basin fill have been inferred from seismic character and from loose blocks found in beach deposits on the Froan Islands. These were eroded from the Frohavet Basin and deposited by ice streams moving towards the north-west during the final stages of the last glaciation. The erratic blocks comprise various marine and nearshore, fine- to coarse-grained sandstones, conglomerates and mudstones. The blocks frequently contain coal fragments and shells, but in contrast to the Beitstadvjord Basin samples, do not contain freshwater fossils. Biostratigraphical analysis (Kelly, 1988) concluded that the sediments are of Middle Jurassic age.

The same stratigraphical subdivision has been suggested for the Frohavet Basin as for the Beitstadvjord Basin (see above), being divided into Units A–C, that are proposed to be correlative with the Middle Jurassic Melke, Garn and Ile formations known offshore mid Norway. The porosity of the erratic sandstone blocks is poor (generally less than 8%) due to significant cementation (Johansen et al., 1988; Mørk et al., 2003). As with similar rocks in the Beitstadvjord Basin, the preserved blocks are thought to represent highly cemented layers, carbonate concretions in sandstone, and sideritic concretions in mudstone. Mørk et al. (2003) have estimated that the porosity in non-cemented sandstone beds may be 10–20%.

The Frohavet Basin is characterised by a simple geometry, homoclinally dipping to the south-east. Although there are some minor faults, these are not considered to be large enough to generate significant traps (Polak et al., 2004b). With the present poor knowledge of the basin stratigraphy, it appears inappropriate to include possible fault barriers in a model. Thus, for the flow modelling, the basin was treated as a simple south-east-dipping homocline (Polak et al., 2004b). The basin subcrops beneath a very thin cover of Quaternary moraine and clays, which is not considered to be an efficient topseal.

The *Froan Basin area of the Trøndelag Platform* lies offshore of mid Norway (Figure 1.5), covering an area of more than 50 000 km², in variable water depths locally shallower than 200 m, but 400–500 m above glacial troughs. At the shelf edge, in the west, water depths increase rapidly to more than 800 m.

The Trøndelag Platform is covered by relatively flat-lying sedimentary strata and forms one of the major structural elements off central Norway. It includes a number of subsidiary elements including the Nordland Ridge, Frøya High and Froan Basin. A cover sequence of Quaternary, Cenozoic and Cretaceous strata overlie Jurassic deposits that in turn overlie deep basins filled by Triassic and Upper Palaeozoic sedimentary rocks. The pre-Jurassic rocks are arranged in north-east trending, enechelon basins which contain a profound unconformity of probable Middle Permian age that separates an early period of intense block faulting from the tectonically quieter Late Permian and Triassic.

On the Trøndelag Platform, Triassic and older rocks have very low porosities and permeabilities. They are thus probably unsuitable for CO₂ storage and were not further considered in this study. The reservoir rocks with the largest theoretical storage potential are of Early to Middle Jurassic age (Figure 3.17). Formations with an assumed storage potential are the Åre, Tilje, Ile, and Garn formations, separated by the shale-dominated Ror and Not Formations (Bøe et al., 2002). Younger rock units are mostly fine grained and/or glacial tills, and would perhaps act as seals to storage formations.

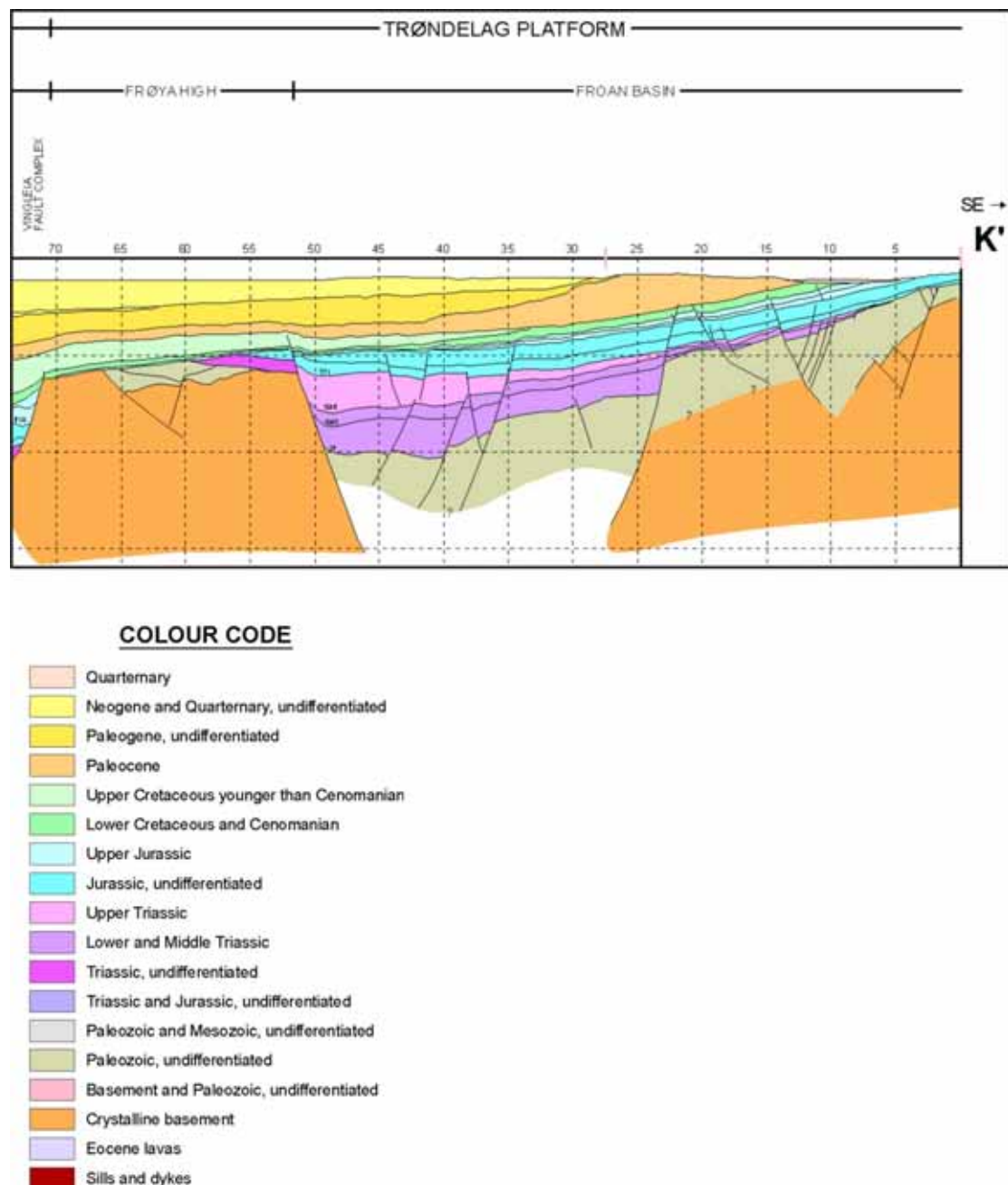


Figure 3.17 Cross-section through the Froan Basin of the Trøndelag Platform (modified from Blystad et al., 1995, reproduced with permission of NPD).

Based on a large number of exploration wells, the thickness of the Tilje Formation alone reaches 450 m (Bøe et al., 2002). Towards the north-east, the succession thins to

around 200 m. From various published descriptions it has been estimated that of the total (gross) reservoir interval thickness on the Trøndelag Platform, the Garn and Tilje Formations constitute around 27% each, while the Ile Formation constitutes about 14%.

The potential Jurassic storage formations are interbedded with the claystone-dominated Ror and Not formations. The Viking Group (Melke and Spekk formations), which lies above the Garn Formation, is dominated by shales and mudstones with minor thin beds of carbonate and scattered sandstone stringers; sandstone is only a significant component in the Draugen Field (Rogn Formation). The Viking Group extends to the basin margin on the eastern part of the Trøndelag Platform where it has been sampled just beneath the sea floor at several locations. The Viking Group is again overlain by thick successions of Cretaceous and Cenozoic fine-grained sedimentary rocks and by Quaternary glacial deposits.

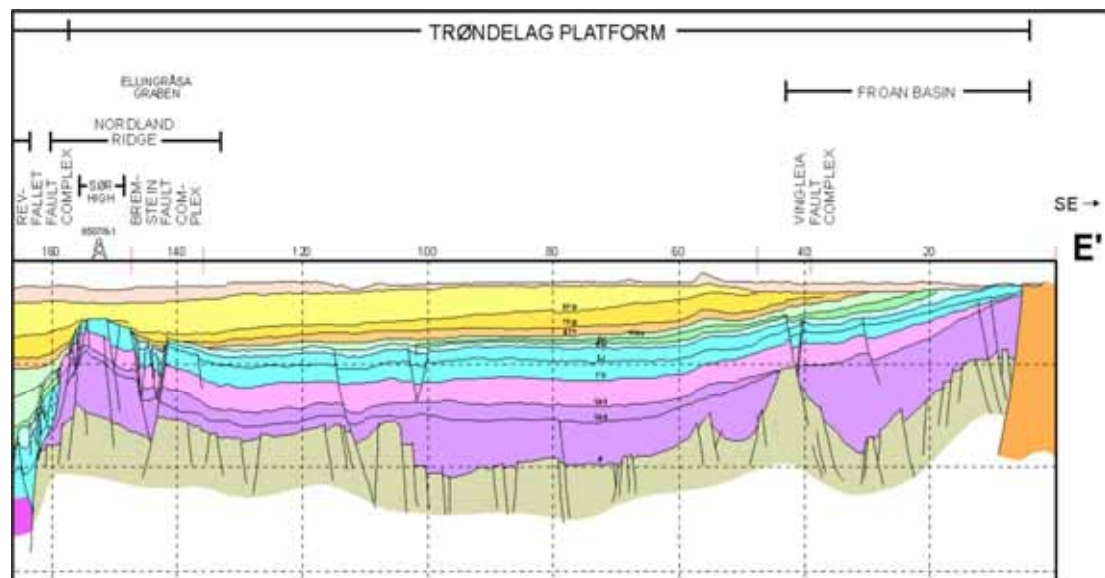


Figure 3.18 Mid Norway Trøndelag regional cross-section through the Trøndelag Platform (modified from Blystad et al., 1995, reproduced with permission of NPD).

The Froan Basin area of the Trøndelag Platform (Figure 3.18) was identified as particularly promising for large-scale CO₂ storage. A large regional grid of seismic data is available (Figure 3.19) comprising several 2D seismic surveys, a selection of which was used for reservoir mapping.

The Froan Basin area is characterised by generally simple structural geometry, homoclinally dipping to the north-west (Figure 3.20), where the Vingleia Fault Complex forms the north-west basin margin. The reservoir interval considered for CO₂ storage is located between two regional seismic reflectors interpreted as Intra Lower Jurassic and Base Upper Jurassic. These reflectors can be traced throughout the investigated area, but are locally offset by a number of normal faults which dip both landward and basinward with displacements mainly less than around 200 m. Seismic mapping shows that the faults do not compartmentalise the area significantly, so even if they were perfectly sealing they would not be expected to create large

structural traps. Thus, for flow modelling purposes, the basin was treated as a simple north-west-dipping homocline, with some minor undulations at its top that cause local trapping (Lundin et al., 2005). The basin subcrops beneath a very thin cover of Quaternary moraine and clays, which is not considered to be an efficient topseal.

Uncertainties, which are largely due to the lack of subsurface information (particularly well data), have been addressed by carrying out several reservoir simulations for each case, covering reasonable ranges of key reservoir parameters (Section 3.4).

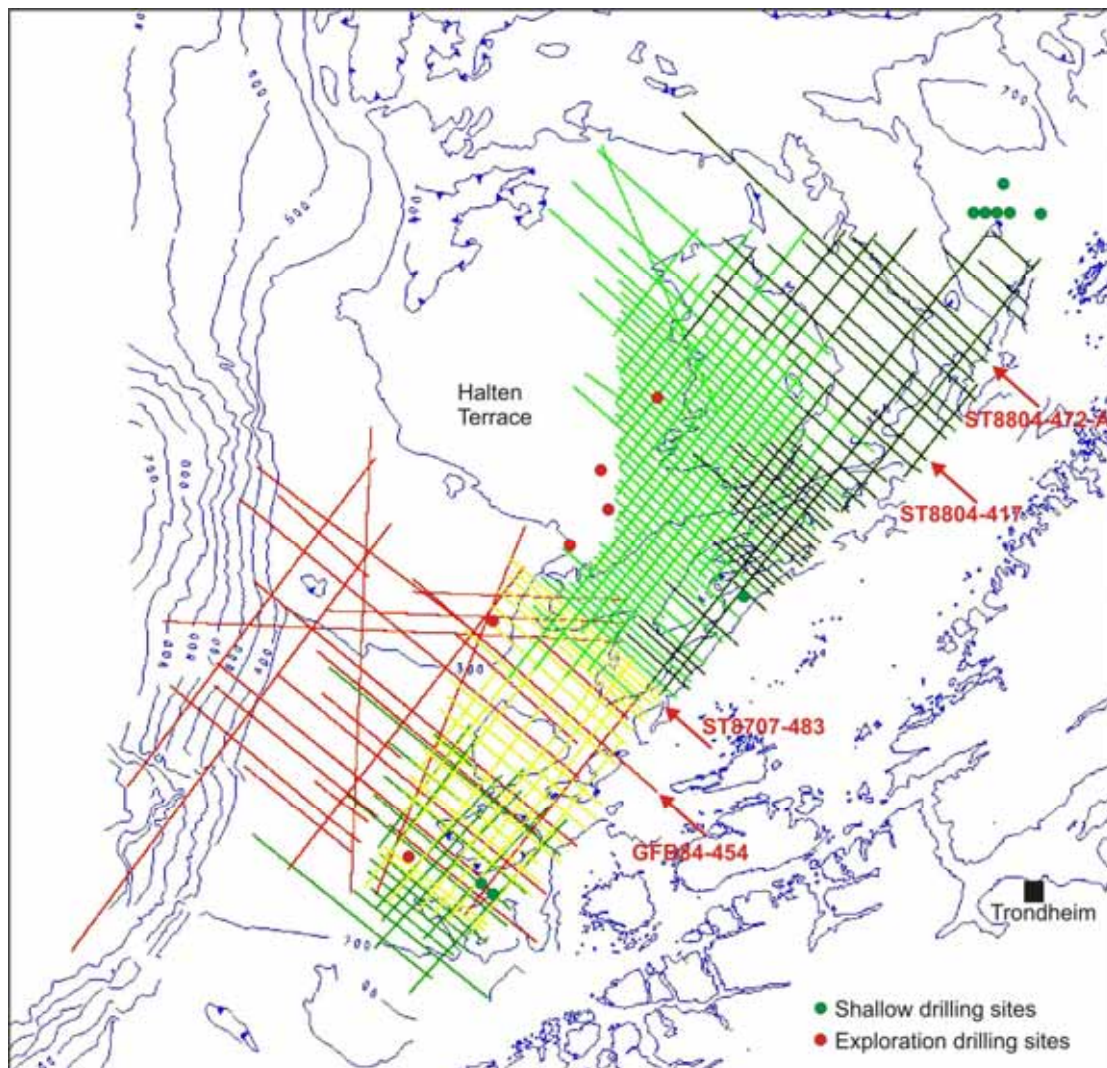


Figure 3.19 Mid Norway 2D seismic coverage on the Trondelag Platform.

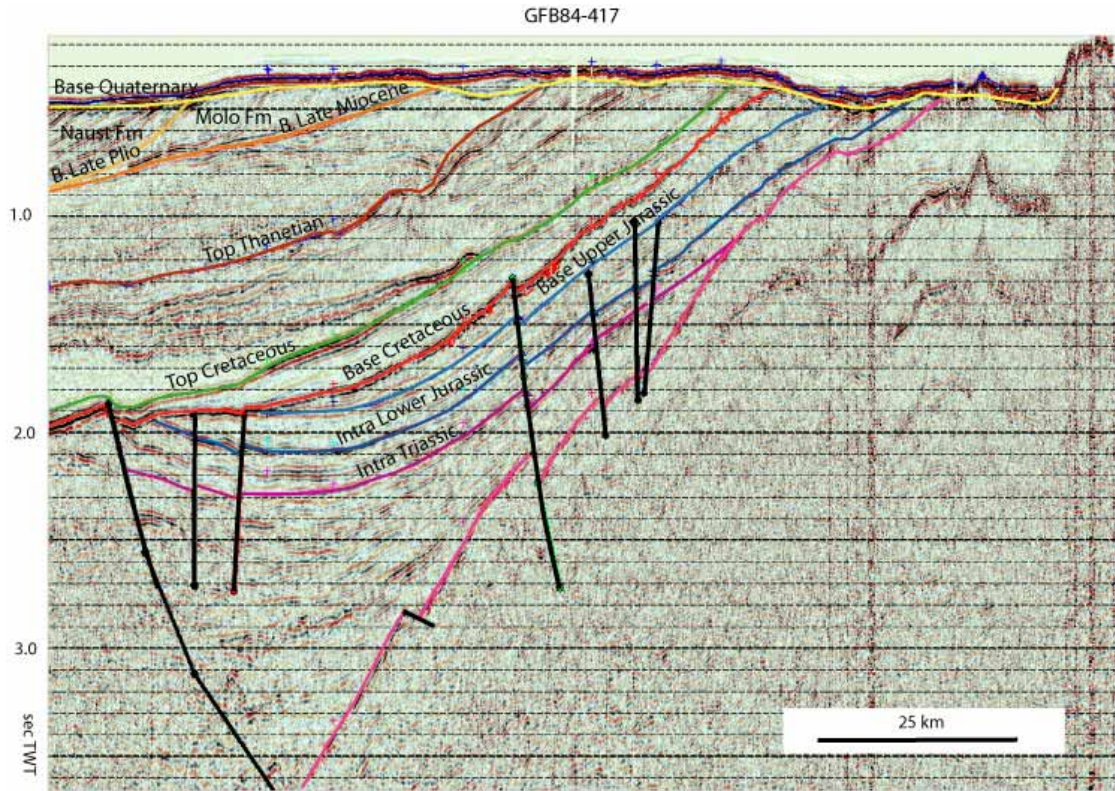


Figure 3.20 Seismic line through the Froan Basin (vertical exaggeration ~20x). Seismic data courtesy of WesternGeco.

More detailed aspects of reservoir characterisation in the Froan Basin area are set out in Chapter 4.

Schwarze Pumpe (Schweinrich)

Within the Schweinrich structure (Figure 3.21) the target horizons for CO₂ storage are two saline aquifers of the Lower Jurassic (Hettangium) and the Upper Triassic (Contorta Beds), situated at more than 1300 m depth. The reservoir sands consist of several layers of predominantly fine- to medium-grained, highly porous sandstones with interbedded silty and clay-rich layers. According to logs from nearby wells, the gross thickness of both reservoir formations ranges between 270 and 380 m within the extent of the Schweinrich structure. The entire reservoir is sealed by Jurassic clay formations several tens of metres thick. The two reservoir units are separated by a major claystone layer (Triletes, uppermost Triassic) some tens of metres thick. Average porosities range between 20 to 33 %, with permeabilities in the range 120 to about 2100 mD. The reservoir sandstones contain minor amounts of CO₂-reactive minerals (< 5 wt-% feldspar, up to 10 wt-% mica and 0 to 2 wt-% carbonates). Several silt and claystone layers are embedded within the reservoir. Within the entire area of investigation, the thickness and lithological composition (sand/shale distribution) of the reservoir formations may vary considerably. The pore-space of the reservoir is filled with saline formation water, whose density ranges from 1.12 to 1.14 kg l⁻¹ (Figure 3.22) with formation temperatures between about 60° and 90° C.

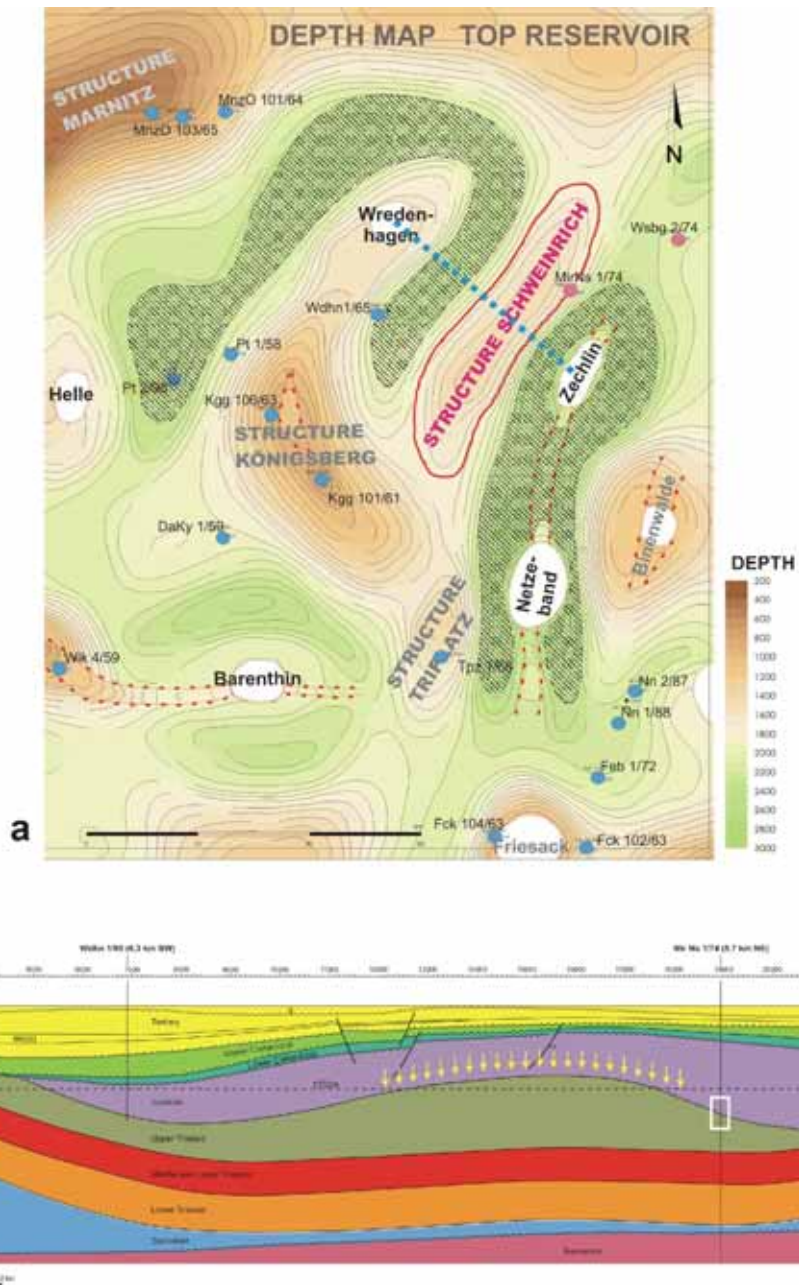


Figure 3.21 The Schweinrich structure. a) Depth contours on top reservoir with spill-contour marked in red. Associated troughs and the position of wells used for site characterisation are shown. White areas indicate positions of salt structures, predominantly diapirs. b) Cross-section (blue dashes) through the storage anticline between two salt diapirs. Yellow arrows indicate the reservoir and storage position. Faults in the reservoir overburden are not definitely confirmed.

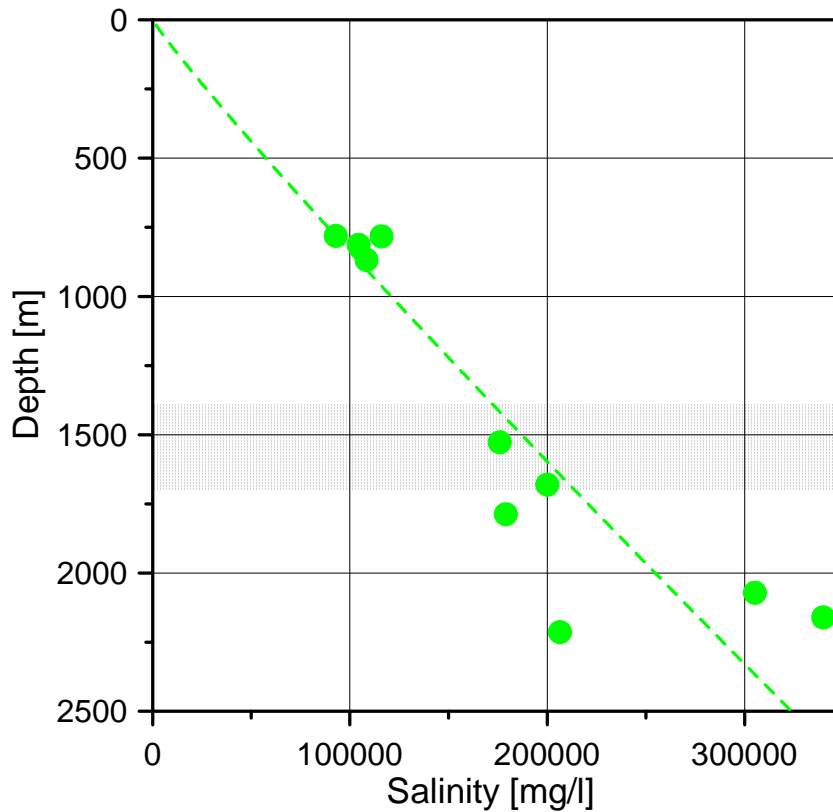


Figure 3.22 Salinity of formation waters in wells from the vicinity of Schweinrich (depth of the Schweinrich reservoir indicated by the stippled band).

Valleys

The first step in the site selection process was to screen neighbouring sedimentary basins for CO₂ storage potential. The goal of the screening process was to identify predictable, laterally continuous, suitably permeable reservoir rocks overlain by potentially good quality caprocks at suitable depth. A by-product of the screening was to narrow the search at an early stage so that costly and time-consuming structural interpretation using seismic data could be confined to potentially prospective areas only.

The screening stage of the Valleys case study took in a large geographical area, up to 200 km from the proposed Valleys powerplant (Figure 3.23). The only onshore basin assessed was the South Wales Coalfield, which underlies and surrounds the proposed power plant site. Offshore areas screened were the Bristol Channel, Celtic Sea and St George's Channel, which lie to the south, south-west and west of South Wales respectively.

Pre-existing published sources were used to establish the reservoir characteristics of the onshore formations in the South Wales Coalfield. Offshore, the overall storage potential of the outer Bristol Channel and St George's Channel basins was assessed using some 5500 line-kilometres of 2D seismic data together with wireline logs, drill cuttings and core samples from wells. BGS reports and in-house knowledge were utilised to augment the basic datasets.

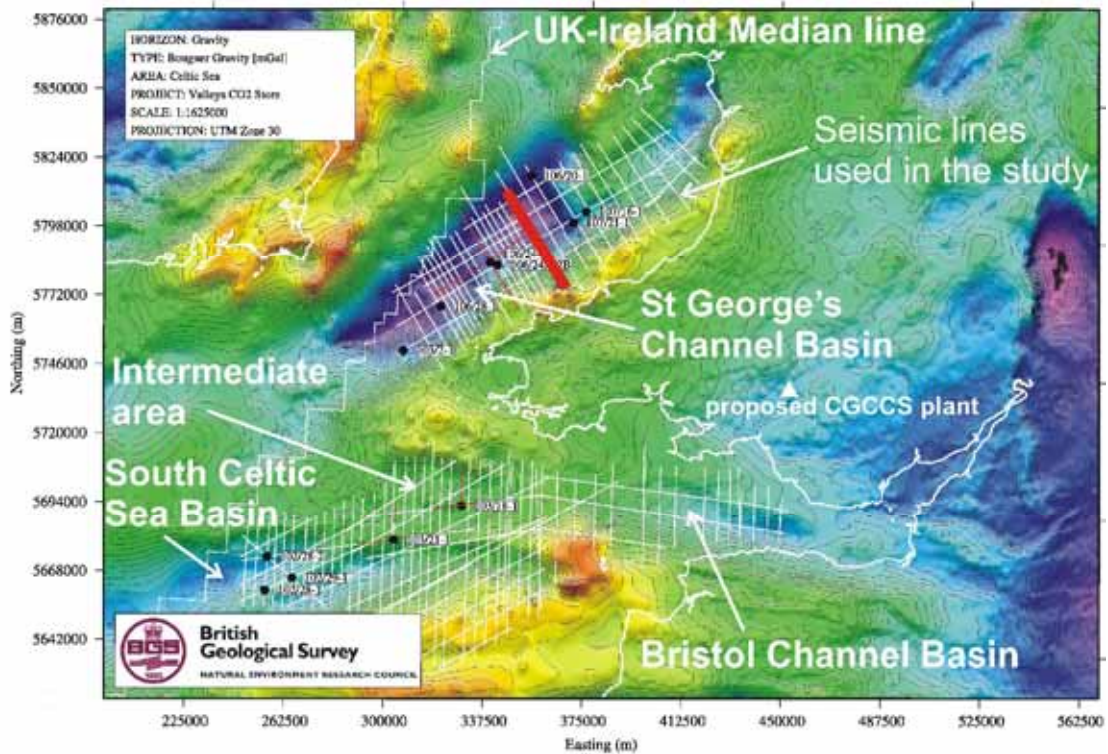


Figure 3.23 Map of the proposed power plant location and surrounding offshore sedimentary basins with regional seismic lines (white). Colour shading denotes Bouguer and free-air gravity field (red = high, purple = low).

When suitable reservoir and caprock occurrences were established, pre-existing small-scale maps (Tappin et al., 1994) were used to establish whether they occurred at a suitable depth. The presence of structural closure was not considered excepting where it could be determined from the pre-existing very small-scale maps, which only show closures of exceptional size. There are only sparsely scattered wells in the offshore area and it was therefore difficult to establish the lateral continuity of thin reservoir sandstones.

Areas closest to the proposed power plant were considered first because these were thought likely to offer the cheapest storage options.

The only potential reservoir rocks *onshore in South Wales* are of Devonian and Carboniferous age. The sandstone formations were rejected as potential storage sites because of their low matrix permeability. The coal seams of the South Wales Coalfield were rejected as potential storage sites due to their low permeability and their potential utilisation as an energy mineral suitable for underground coal gasification in the future.

The *Bristol Channel Basin* lies nearshore, to the south of the proposed power station site (Figure 3.23). It forms a faulted syncline filled with Mesozoic rocks. These are proven from adjacent basins and seismic mapping, but there are no wells within the basin itself, so details of stratigraphy are poorly known. The only potential reservoir formation that would be at sufficient depth for CO₂ storage is the Sherwood Sandstone Group, although it is thought likely to be thin. In the nearest well (onshore to the east), core samples and geophysical logs indicate that the Sherwood Sandstone

has very low permeability, less than 3% porosity and is mainly in a calcrete facies. In the other offshore wells, adjacent to the basin, porosity is less than 6.5% and usually less than 5%.

Good quality Cretaceous sands are found in wells to the south-west of the Bristol Channel, but in the basin itself they are too shallow and are capped by the calcareous Chalk Marl. This was considered to be a relatively poor topseal because it could be subject to adverse CO₂/water/rock reactions.

Interpretation of seismic data in the outer (western) part of the Bristol Channel Basin (Brooks, Trayner and Trimble, 1988) suggests that Mesozoic rocks are heavily faulted and there are no major structural traps at the level of the Sherwood Sandstone Group.

In the light of these various negative indicators, the Bristol Channel Basin was rejected as a suitable storage site.

The *South Celtic Sea Basin* lies to the south-west of Pembrokeshire and the Bristol Channel (Figure 3.23). The Lower Greensand (Early Cretaceous) in wells probably has excellent reservoir properties and is at a suitable depth in the areas to the west and north-west, but it was considered to be too poorly sealed by the (calcareous) Chalk Marl.

Cenozoic strata are present at depths of between 500 and 1000 metres in a relatively small area south-west of Pembrokeshire. These strata are poorly known, but they could not be completely ruled out for consideration as a repository for CO₂.

The *St George's Channel Basin* lies some distance offshore to the north-west of the proposed power-station site (Figure 3.23). Main reservoir units comprise the Sherwood Sandstone, thin Lower Jurassic sandstones, thicker Middle Jurassic sandstones, thin Upper Jurassic sandstones and highly porous Cenozoic sandstones. Structurally, the basin is much deeper than the Bristol Channel and South Celtic Sea basins. There is a significant structural closure visible on even very small-scale maps at base Cenozoic and Middle Jurassic levels around wells 106/24-1 and 106/24a-2b, on the downthrown side of the St George's Fault (Figure 3.24).

The Sherwood Sandstone is deeply buried in the St George's Channel Basin. In well 103/2-1 it contains a net 97.5 m of sandstone averaging 9% porosity, between depths of 2673 and 2885 m. The permeability of this sandstone is not known. However, using an empirical relationship between porosity and horizontal permeability in the Sherwood Sandstone of south-west England (Penn et al., 1987) the average permeability of these sands might be as low as 1.7 mD. In well 106/28-1, the Sherwood Sandstone consists of >89 m of fine to medium grained sandstone, with individual beds 3 to 15 m thick at depths of 2930–3051 m. Its base was not reached. The sandstone is well sorted and friable with either a siliceous cement or argillaceous matrix, and interbedded with slightly silty and sandy mudstone with anhydrite. Preliminary log analysis suggests there is about 35 m of >10% porosity sand in the drilled interval. It was recognised that if areas could be found where the Sherwood Sandstone were at depths of only around 800–1200 m, its porosity might be higher.

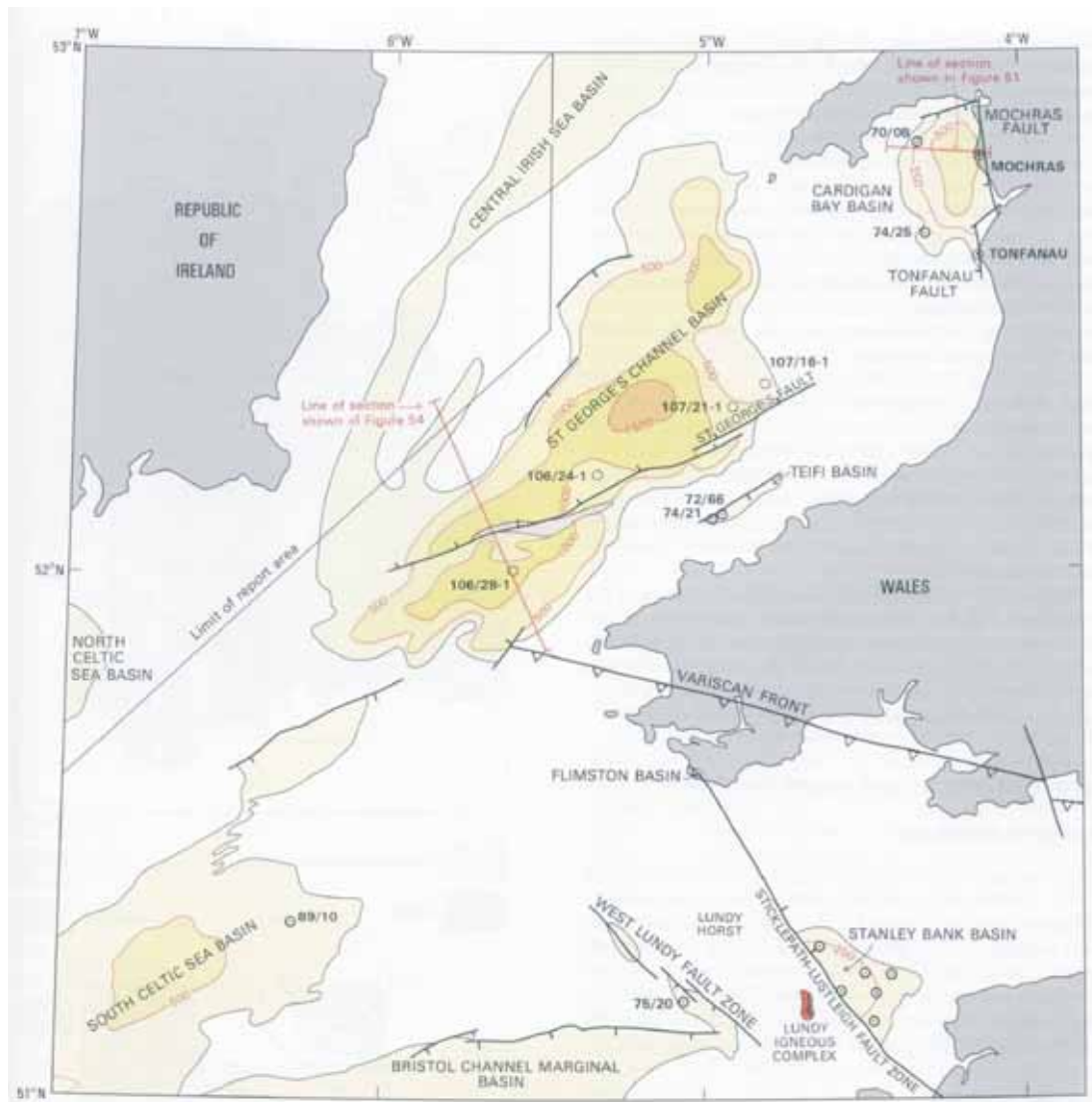


Figure 3.24 Map of depth to base of the Cenozoic succession, offshore South Wales (from Tappin et al. 1994).

Jurassic sandstones occur in all six wells but could not be correlated with confidence between some wells and there is no core or cuttings-based analysis of their porosity and permeability. It was noted that the Dragon gas discovery in the St George's Channel Basin was in a Jurassic sandstone reservoir.

Cenozoic sandstones reach depths of more than 1500 m in the centre of the basin (Figure 3.24). In well 106/24-1 they occur between about 591 m and 753 m below sea level. Log analysis suggests that some of the sands are slightly shaly, but the clean sand beds between 680 and 692 m drilled depth have porosities of around 36–39%. Stratigraphically, the sandstones were considered likely to be sealed by the overlying Cenozoic strata, which, between 241 m and 540 m drilled depth, consist mainly of clay and lignite. Above 241 m the lithology is not known because drill cuttings were not collected. An attraction of the Cenozoic sands was that the mapped structural closure around well 106/24-1 was thought to be sufficiently large for the Valleys storage project if the reservoir were sealed against the St George's Fault.

In summary, the Valleys screening study demonstrated that the South Wales Coalfield and the Bristol Channel Basin did not contain suitable storage reservoirs capped by suitable caprocks at suitable depths.

The Early Cretaceous Lower Greensand has good reservoir characteristics and occurs at appropriate depths in part of the South Celtic Sea Basin, but was sealed by a calcareous formation, the Chalk Marl, which was considered liable to react adversely with CO₂-rich formation waters.

The Sherwood Sandstone, a prolific hydrocarbons reservoir both onshore in the UK and offshore to the north in the East Irish Sea Basin, is present in the St George's Channel and Celtic Sea basins. Its porosity is poor in the wells, but this may be because it is buried to depths of over 2000 m in the wells that penetrate it (and was more deeply buried before the basin was uplifted). It was thought that it could have reservoir potential if large structural closures could be identified at shallower depths.

Jurassic sands occur at suitable depths in the St George's Channel Basin. By analogy with the Dragon gas discovery, which is in thin Jurassic sands close to the UK/Ireland median line in the St George's Channel Basin, these sands are likely to be well sealed. However, there is uncertainty about their permeability and lateral continuity, and thus the volumes of CO₂ that could be injected into or stored within them.

Cenozoic sandstones in the wells in the St George's Channel Basin have good porosity, occur at appropriate depths, and are likely to be sealed by overlying strata. It was judged likely that the sands would have sufficient permeability to allow CO₂ injection at the required rate of 2.4 Mt per year for the lifetime of the power-plant.

It was concluded therefore that the St George's Channel Basin was the most suitable for geological storage of CO₂. The need for further data acquisition was identified, including licensing proprietary 2D seismic, and obtaining core and cuttings samples from the potential reservoirs and some caprocks. Characterisation of the Cenozoic sandstones is described in Chapter 4.

3.2.2 Generic findings

The importance of pre-existing hydrocarbon exploration and production datasets in providing crucial information about the subsurface cannot be overstated. For all of the case studies there would be no seismic data available if the target areas had not already been identified as potential hydrocarbon or geothermal provinces. In particular, without pre-screening seismic datasets, no structural control would be available. Further, there would be fewer wells and little data on subsurface properties. In the mid-Norway case, if porosity and permeability estimates had depended just on the collected boulders, the Beitstadfjord and Frohavet basins would have been considered unsuitable right from the beginning. Their close proximity to the offshore hydrocarbons province enabled a more insightful evaluation to be made.

A key lesson learned from the Valleys case study was that prospects identified in areas with few wells and petroleum discoveries are difficult to develop to the level of confidence required to trigger investment, because of a lack of geological and reservoir engineering

data or nearby gas-tight structures that could be used as analogies. The study also served to emphasise that the balance of risk and reward is currently very different between petroleum exploration and exploration for CO₂ storage sites. In petroleum exploration, the potential high profitability of successful discoveries means that the discovery ratio can be low. In CO₂ storage exploration, potential profitability is likely to be low and, moreover, the real-world integrity of an aquifer storage site may be difficult to test, even when an exploration or potential injection well has been drilled. This is likely to put off investors unless the balance of risk and reward changes.

The Schweinrich case study has demonstrated that large-scale coal-based CO₂-free power plants will require very large storage capacities, but these are indeed available in an aquifer setting. Identified structural closures account for about 3% of the basin area. There is a good basis of existing data in north-east Germany due to former geothermal and hydrocarbon exploration. A good process for the screening phase has been established, but issues remain that must be further investigated in later stages, such as the existence of faults that may compromise reservoir integrity.

3.3 Basic overburden properties

Basic overburden properties to be evaluated at this stage include stratigraphy (and specifically lithology and thickness), and nature of any faulting or fracturing. Favourable overburden properties may include the presence of shallower aquifers that could, through monitoring, give early warning of upward CO₂ migration.

3.3.1 Observations from the CO₂STORE case studies

Sleipner

Prior to CO₂ injection, caprock properties were qualitatively evaluated by means of cuttings and geophysical well logs. The generally argillaceous nature of the caprock, lack of visible faulting, its likely plastic, self-sealing mechanical state, and its considerable thickness (~200 m), together with an additional 500 m of mostly fine-grained overburden, were considered to constitute an effective seal. Indicators of gas migration, such as shallow seismic amplitude anomalies ('brightspots') and sea-bed pockmarks were mapped in an area of several tens of km² based on 3D seismic data. The storage site was located in an area where gas migration indicators are scarce.

Kalundborg

Geological formations in Denmark with sealing properties are lacustrine and marine mudrocks, evaporites and carbonates. The most important sealing rock type in the Danish area is marine mudstone, which is present at several stratigraphical levels. Migration may take place through the caprock due to slow capillary migration, through microfractures or along faults. Detailed site surveys will be needed in order to test the integrity of the seal at future storage sites.

Marine mudstones of the lower Jurassic Fjerritslev Formation form the primary sealing unit for the prospective Gassum reservoir. It is characterised by a relatively uniform succession of marine, slightly calcareous claystones, with varying content of silt and siltstone laminae. Siltstones and fine-grained sandstones are locally present,

most commonly in the north-eastern, marginal areas of the Danish Basin. Deposition took place in a deep offshore to lower shoreface environment (Michelsen, 1975, 1978; Michelsen et al., 2003). The formation is present over most of the Danish Basin with thicknesses up to 1000 m, although this varies significantly due to mid-Jurassic erosion. A criterion of the site screening process, was the requirement that no faults crossing the caprock were identified on seismic lines through the storage site. Minor fractures and faults however cannot be excluded in the screening phase. Due to the widespread occurrence of thick mudstone deposits no specific caprock criteria were formulated in the Kalundborg case.

Mid Norway

By analogy with the nearby offshore hydrocarbon province, the Jurassic potential storage formations are interpreted to be interbedded with the claystone-dominated Ror and Not formations. The Viking Group (Melke and Spekk formations), which lies above the Garn Formation, is totally dominated by shales and mudstones and extends to the basin margin on the eastern part of the Trøndelag Platform where it has been sampled just beneath the sea floor at several locations (Bugge et al., 1984). It might also be present in the Beitstadfjord and Frohavet basins. The Viking Group on the Trøndelag Platform is itself overlain by thick successions of Cretaceous and Cenozoic fine-grained sedimentary rocks and by Quaternary glacial deposits.

The tilted, homoclinal geometry of the reservoirs implies that the caprocks directly overlying the reservoir do not provide a complete topseal for the sites. Rather, they inhibit vertical rise of the injected CO₂ to the sea floor and cause a strong lateral deflection such that the CO₂ has to migrate a considerable distance before it would reach outcrop at sea floor or subcrop below a thin cover of Quaternary sediments. The Quaternary cover, due to its low thickness (and local absence) and its unlithified nature, is not considered to constitute an effective seal.

Schwarze Pumpe (Schweinrich)

At Schweinrich, the direct overburden above the Hettangium/Contorta reservoir is a thick succession of the Lower Jurassic (more than 200 m of claystones, siltstones, sandstones and secondarily, marls), the Middle Jurassic (claystones, siltstones, sandstones and carbonates) and the Upper Jurassic (carbonates, marls and claystones). In some areas (e.g. in the eastern part of the Schweinrich anticline), parts of the Upper Jurassic (Malm) and Lower Cretaceous are missing due to erosion or interruption of sedimentation.

The Lower Cretaceous mainly consists of claystones, marls and glauconitic sandstones. Parts of the Upper Cretaceous and the Lowest Cenozoic (Paleocene) are missing in some areas. In the vicinity of the Schweinrich anticline, preserved parts of the Upper Cretaceous (Turonian, Coniacian and Santonian) are predominantly composed of limestones and marls. In the nearby Trieplatz structure, no Upper Cretaceous sediments have been preserved.

The Cenozoic succession predominantly consists of unconsolidated clay with variable amounts of silt and sand (Eocene and Oligocene) and carboniferous sands (Miocene). The Oligocene Rupel Clay forms the uppermost major barrier separating the saline formation water from the freshwater aquifers within the upper Cenozoic formations and the Pleistocene.

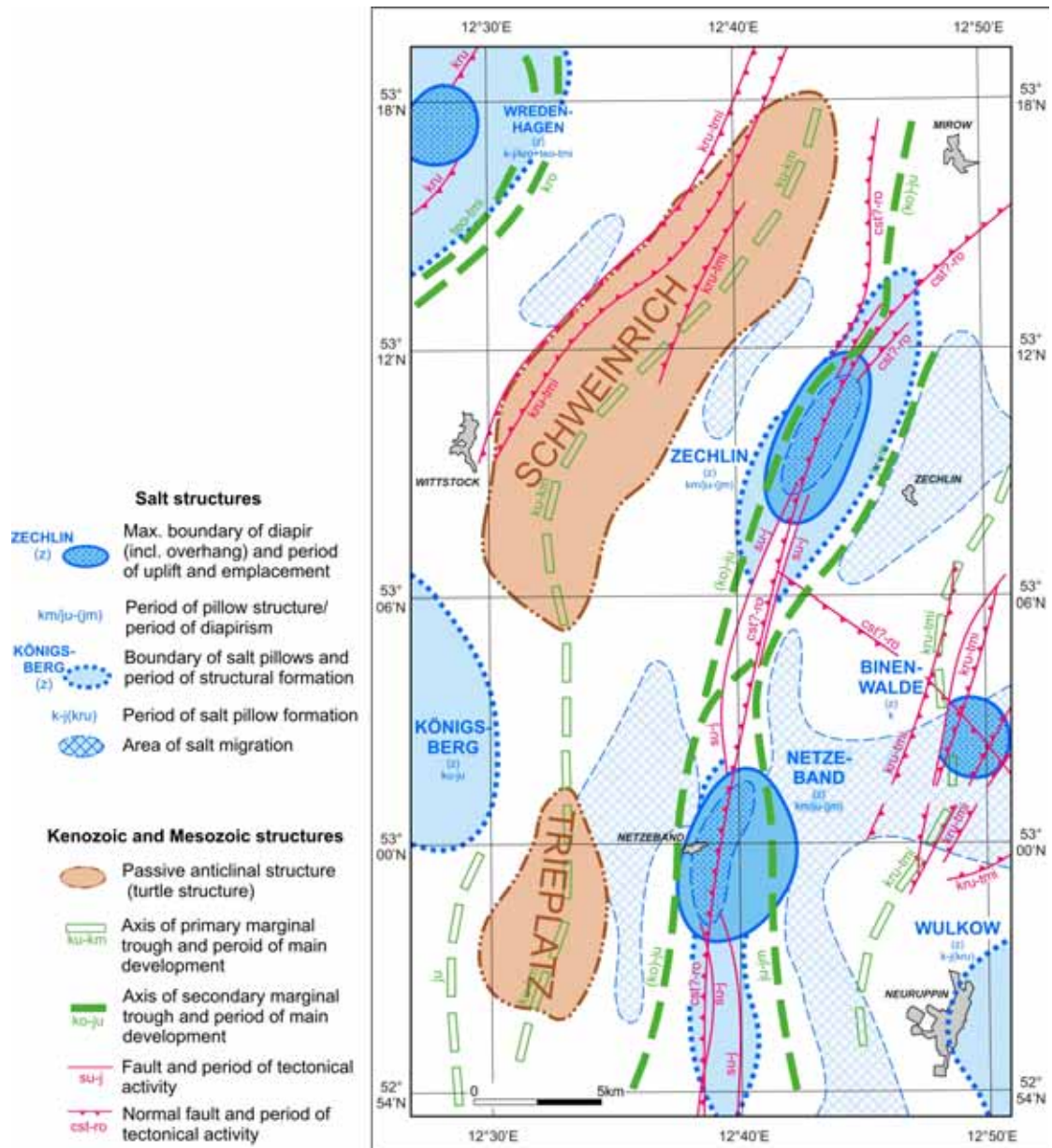


Figure 3.25 Structural geological map of the Schweinrich area showing the position and the period of formation of major structural geological elements (modified after Kockel and Krull, 1995. Reproduced with permission of BGR).

The Pleistocene succession is composed of alternating sands and tills. Thicknesses range from several tens of metres to several hundred metres. The sand layers contain fresh water used for drinking water.

Due to the limited resolution of the available seismic data, only the existence of major structural features in the overburden of the Schweinrich structure (e.g. major faults with a displacement larger than 50 m) is relatively certain. Earlier seismic interpretations reached the conclusion that several normal faults in the Mesozoic and Cenozoic were active during the emplacement of nearby salt diapirs and in the course of relaxation of the former north-west to south-east compressive stresses.

One major feature seen on the seismic data is a group of three north-east trending normal faults, positioned in the central area and on the western flank of the Schweinrich structure (Figures 3.21 and 3.25). These normal faults probably affect the base of the Rupel Clay and penetrate down into the Jurassic with a vertical extent of several hundreds of metres. Within the Upper Cretaceous and down to the upper Jurassic, the lateral extent of the faults is unknown, but probably exceeds 20 km. Within the Cenozoic succession, this graben structure is about 10 to 12 km long. The vertical fault displacements are presumably of several tens of metres up to more than 100 m. At the present state of knowledge, it is not confirmed whether this major graben structure affects the proposed storage system (reservoir and caprock). New modern 3D seismic would be indispensable in clarifying the nature of the lower termination of this fault system. The existence of faults with smaller displacements cannot be verified by the existing data.

With respect to caprock integrity, we do not expect major pathways for fluid migration along the dislocation planes of the identified faults, unless the complete caprock is penetrated by a single fault. The latter, very conservative, assumption is not indicated by the existing seismic data, but nevertheless has been used as a scenario for predictive geochemical modelling, as well as in a fault leakage scenario in the risk assessment (see Sections 4.3 and 4.4). Due to the high confining stresses at depths greater than 1000 m it is expected that possible faults are closed shear-zones filled with sealing debris of the sheared wall rock.

Valleys

The Cenozoic overburden of the preferred Valleys storage site comprises a layer-cake sequence of mudstones, siltstones with minor sandstones and lignite. The dominantly argillaceous lithologies, lack of faulting and low structural dips (which means that most of the caprock succession is not in direct contact with the sea bed), suggest that the overburden should form a satisfactory regional seal. More detailed investigations into overburden properties (including chemical reactivity) are presented in Chapter 4.

3.4 Basic reservoir flow simulations

Flow simulation may or may not form part of the site screening and selection phase, depending on how easily rival sites may be discriminated with more simple criteria. Its utility at this stage is most vividly demonstrated in the mid-Norway case study (Section 3.4.1) where the lack of robust geological control led to the requirement for developing a set of reservoir flow scenarios to examine the effects and consequences of geological uncertainty.

Simulation tools generally comprise industry-based software designed for hydrocarbon systems, adapted or tuned for use with CO₂-water systems. A code comparison study (Pruess, 2003) indicated that in general terms, available modelling codes are capable of simulating satisfactorily many processes associated with CO₂ storage.

3.4.1 Observations from the CO2STORE case studies

Sleipner

At Sleipner a simple initial reservoir simulation was carried out (see Chapter 4) to assess a number of injection-related issues, pertinent at the screening stage, notably injectivity.

Kalundborg

A preliminary simulation model using Eclipse 100 has been made for the Havnsø structure. The calculations are reported in Bech and Larsen (2003) and show that the rock properties in the reservoir would allow CO₂ injection rates of 200 kgs⁻¹ per well, equal to the average emissions of Asnæsværket. The CO₂ may be injected through a single injection well perforated over a length of 500 m. The simulation was run for a period of 30 years (see Chapter 4 for summary).

Mid Norway

Due to the dearth of subsurface geological information, a key step in the mid-Norway screening phase was to run a series of flow simulations on all of the basins to assess their relative suitability for large-scale storage and to evaluate the significance of uncertainties. The three basins share some basic similarities:

Reservoir units probably comprise highly porous clastic rocks with probable good permeability.

Reservoir units are overlain by thick argillaceous sequences that constitute capillary seals.

Reservoirs have gentle dips.

Reservoirs either outcrop at the sea floor or subcrop beneath thin unlithified Quaternary deposits.

Injection was assumed to take place at such depths that the corresponding reservoir pressures and temperatures would cause CO₂ to exist as a dense fluid ('supercritical'), but with a density lower than that of brine. The most likely scenario therefore for injected CO₂ is that it will rise vertically within the storage formation from the injection point to the reservoir top. It will then migrate updip beneath the top seal towards the reservoir subcrop beneath the Quaternary or at the sea floor. CO₂ density would first increase slightly during upward migration until the transition from liquid to gaseous state at around 500 m depth, which causes a rapid density reduction. Further ascent would be accompanied by a continued, gradual density decrease. Key parameters influencing the migration velocity are:

the presence of local traps and their volume

density difference between CO₂ and brine (largely a function of pressure and temperature and, therefore, depth)

reservoir permeability

vertical and horizontal reservoir heterogeneity

relative permeability of the reservoir to CO₂.

Buoyancy-driven updip migration is counteracted by processes that limit the speed of migration and the distance to which the CO₂ front can advance. The major counteracting process is dissolution of CO₂ into formation water in the reservoir unit. However this process is slow, operating over a timescale of hundreds to thousands of years. Brine with dissolved CO₂ will generally have a higher density than surrounding formation waters and will tend to sink within the formation. This allows fresh brine to come in contact with CO₂ and leads to further dissolution. Another beneficial process is trapping of CO₂ in pores as an immobile residual phase. Both dissolution and residual phase trapping are more efficient if CO₂ is spread over a large volume of the pore space in the reservoir.

If formation water, and/or CO₂, can leave the storage reservoir only at very low fluxes (e.g. due to efficient sealing), pore pressure in the reservoir will increase. This may induce hydraulic fracturing of the seal, generating highly efficient pathways for pressure release and potential migration of CO₂ from the reservoir into sea water.

Simulations of the subsurface behaviour of injected CO₂ were carried out for all three basins with the commercial black-oil simulator Eclipse 100 (Polak et al., 2004a, b; Lundin et al., 2005). The base case for the injection scenarios was an annual injection rate of 2 million tonnes of CO₂ for a period of 25 years, corresponding to the output of a typical small power station over its lifetime.

Petrophysical properties of the potential reservoir formations were not known in the studied basins, so had to be inferred from offshore geological analogues. The implicit uncertainty was addressed by simulation of a range of cases with varying reservoir properties (porosity, horizontal reservoir permeability, k_v/k_h ratio, relative permeability, residual gas saturation, fluid saturation dependence on capillary pressure and permeability of the Quaternary seal).

For the *Beitstadfjord Basin* injection was assumed to take place at the maximum possible depth of around 1000 m. At the probable pressure and temperature conditions, CO₂ will have a density of about 800 kgm⁻³ below a depth of about 500 m. The critical pore pressure in the reservoir at which hydraulic fracturing of the thin Quaternary seal is predicted to occur is estimated at 0.36 MPa.

Reservoir simulations were carried out to test if CO₂ injected at a rate of 2 Mt per year would leak from the reservoir or if it would induce pore pressures causing hydraulic fracturing of the seal. The key simulations assume co-injection into the 'Ile' and 'Garn' formations with injection rates per formation being proportional to their calculated pore volume. Reservoir horizontal permeabilities were set at 2000 mD for base-case scenarios.

The simulation results showed that if the Quaternary seal has a permeability of ~0.1 mD or less, it can contain CO₂ initially. However, the pore pressure in the reservoir will increase very rapidly to a level at which the seal will undergo hydraulic fracture. Serious pressure build-up will also occur at higher seal permeabilities, up to around

1000 mD. If the Quaternary seal were to have even higher permeability, pressure would not build-up to critical levels, but leakage rates will be very high, and within 50 years of the start of injection most of the injected CO₂ will have leaked.

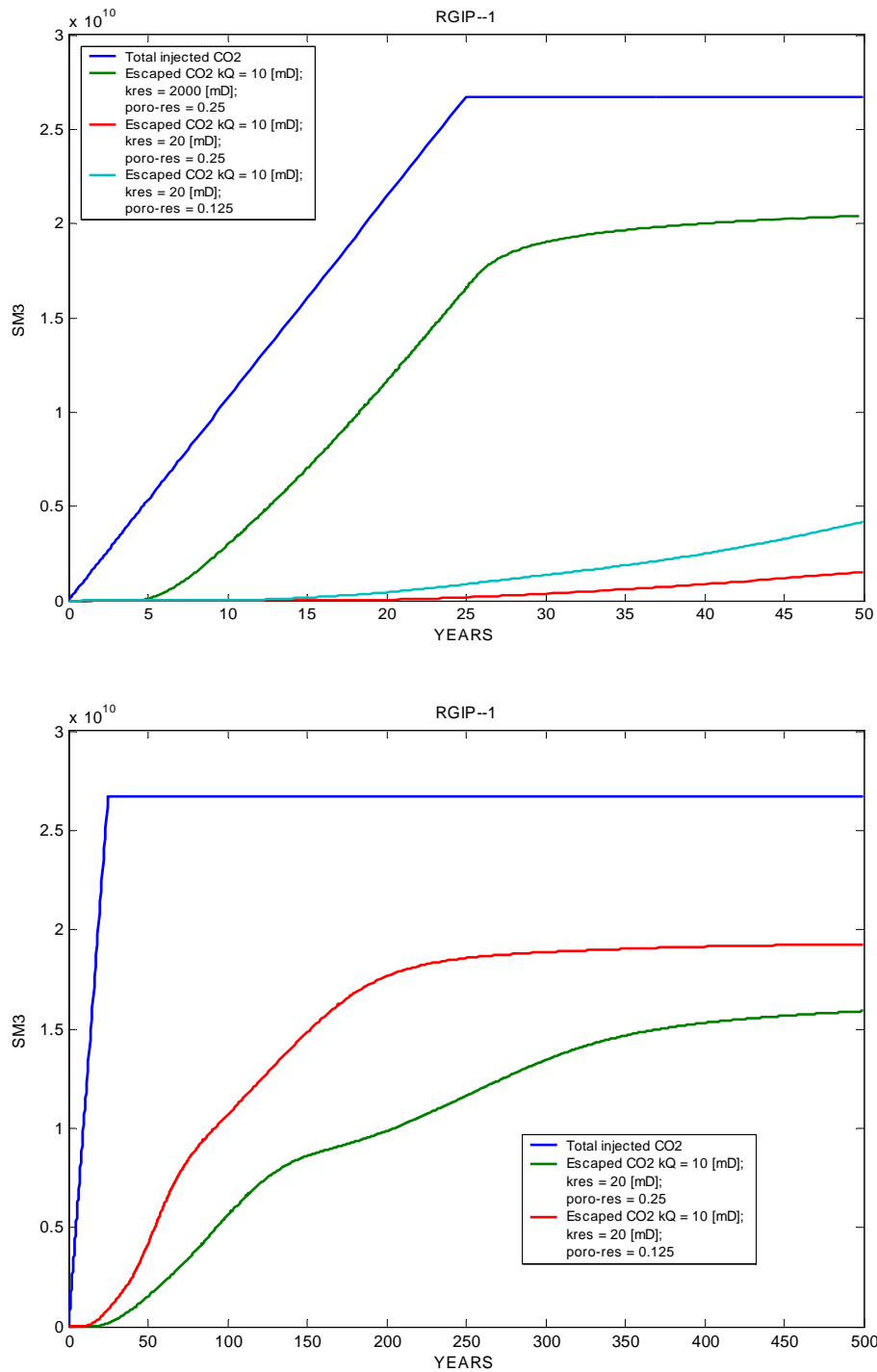


Figure 3.26 Beitstadjfjord Basin. Simulated cumulative volume of CO₂ leaked from the reservoirs for the case of co-injection into the 'Ile' and 'Garn' formations, for three combinations of high seal permeabilities (kQ) with reservoir permeability and net reservoir porosity. The cumulative injected volume of CO₂ is also shown. Upper: first 50 years from injection start. Lower: first 500 years from injection start.

Leakage may be somewhat slower if the reservoir permeability is lower than in the base case, but nevertheless, most of the injected CO₂ will have leaked after 500 years (Figure 3.26). Simulated cases of injection into only one of the two reservoir units yield even less favourable results.

Further simulations with injection rates of only 100 kt per year (about 5% of the emissions of the planned power plant) still indicate unacceptable pressure build-ups in the case of a low-permeability seal and unacceptable leakage rates in the case of a high permeability seal.

The conclusion of the assessment is that the Beitstadvjord Basin is unsuitable for long-term CO₂ storage, even at modest injection rates, the main problem being its very limited storage volume.

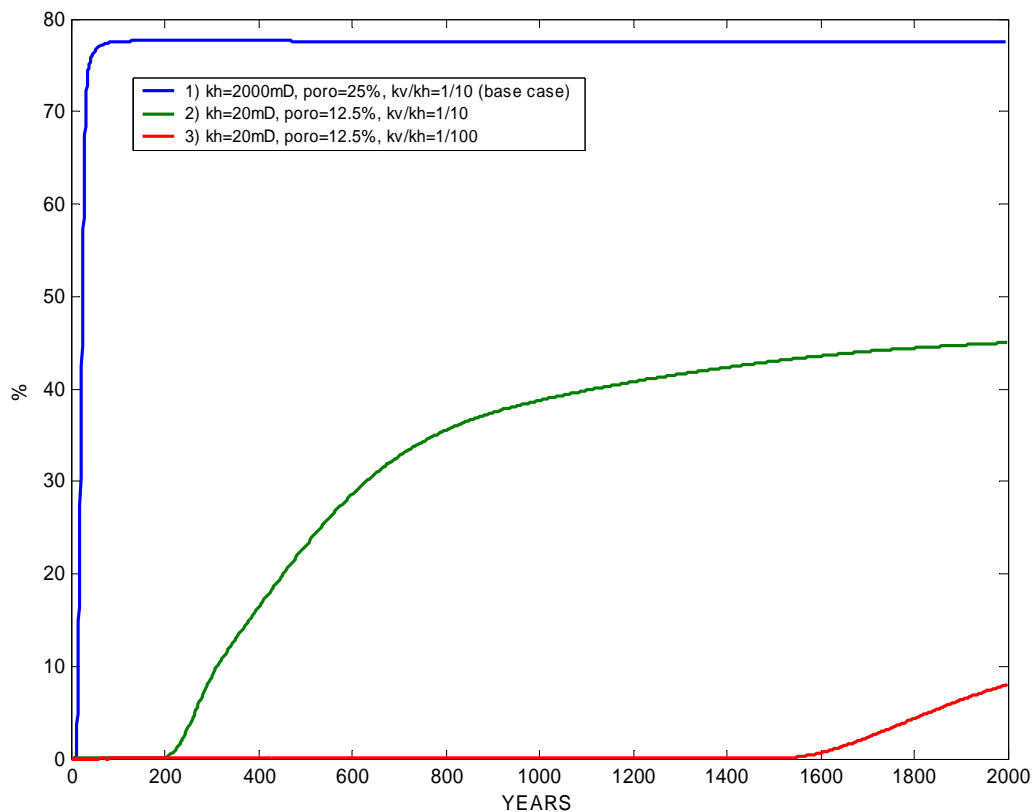


Figure 3.27 Frohavet Basin. Simulated fraction of total injected CO₂ predicted to have leaked from the reservoir; effect of changes to the absolute permeability, porosity and k_v/k_h ratio.

At the probable pressure and temperature conditions in the *Frohavet Basin*, CO₂ will have a density of about 800 kgm⁻³ below a depth of about 450 m. The critical pore pressure in the reservoir at which hydraulic fracturing of the seal is predicted to occur, has been estimated at 1.36 MPa. The critical pore pressure can be equated to the minimum principal stress at the base of the seal, which in turn was estimated as being 85% of the lithostatic pressure. Thus, a greater depth of the base of the seal above the injection site will result in a larger critical pore pressure for hydraulic fracturing. However, such overpressuring is unlikely to occur, because the site is an open system

(the Quaternary is not sealing) and because the accessible pore volume in the basin is sufficiently large.

The simulations assume injection close to the base of the deepest reservoir formation at a depth of about 1400 m. For conservative property scenarios the simulations predict early updip leakage to sea bed with unacceptably high fluxes. With a base-case assumed reservoir permeability of 2000 mD, kv/kh ratio of 0.1, and high relative permeability to gas, migration of the CO₂ front to the sea bed is predicted to take only 10 years after the start of injection with cumulative leakage of around 70–80 % of the injected quantity 50 years after injection start (Figure 3.27). However, if these parameters are moderated, there may be no leakage for several centuries, and leakage rates afterwards may be acceptable, with annual leakage rates at or below 0.01% of the total injected mass of CO₂.

Further work is required to assess the sensitivity of the simulation results to some of the governing parameters, especially to establish which parameter combinations would be reasonable. In addition, simulated trapping as residual gas in pores should be analysed in more detail, because this process may have been overestimated due to up-scaling procedures.

It is concluded that the Frohavet Basin is potentially suitable for long-term CO₂ storage given favourable reservoir properties. Further studies should investigate the likelihood of suitable parameter combinations in more detail before taking the costly step to acquire reservoir data from a well.

At the probable pressure and temperature conditions in the *Froan Basin area of the Trøndelag Platform*, CO₂ will have a density of 600–800 kgm⁻³ below a depth of about 500 m (Lundin et al., 2005). The Garn Formation is locally dissected by faults, but these die out rapidly upwards above the reservoir and should not constitute efficient migration pathways. Beneficially they may define local structural traps. Flow simulations were inherently conservative in that faults were neglected.

For reasons of practicality the Froan Basin–Trøndelag Platform assessment comprised simulations for two scenarios: injection directly beneath a local domal trap and injection at a point with no overlying structural trap, a situation more likely to result in rapid migration towards the subcrop (Figure 3.28). The trap case covered an area of ~2250 km² and the no-trap case an area of ~1450 km². Simulations were restricted to the Garn Formation, with injection at the reservoir base at a depth of about 1900 m, some 60 km (trap case) and 55 km (no-trap case) from its subcrop beneath the Quaternary or at the sea floor. Simulations (Figure 3.29) show that, with or without structural closure immediately above the injection point, the CO₂ plume is contained within 20 km or so of the injection point for 5000 years or more. In both scenarios, almost all of the CO₂ is rapidly trapped in structural closures on the migration path. As the plume migrates slowly up the dip-slope, dissolution progressively reduces the volume of free CO₂ that is left to migrate (Figure 3.30), with around 40% dissolved after 5000 years. CO₂ in solution sinks to the bottom of the reservoir where it will remain ponded in a gravitationally stable state.

In addition to the base case with simulated injection of 2 million tonnes per year over a period of 25 years, cases were also simulated with the same injection rate but with

the injection time extended to 50 years. Reservoir parameters were also varied within likely limits. None of the simulations resulted in any leakage. In all of the simulations CO₂ migrated upwards along the base of the seal towards the Quaternary subcrop or sea bed. In most cases, all of the CO₂ was contained within structural traps, on the migration pathway. Any CO₂ not accumulating in structural traps was dissolved into formation water before reaching the subcrop.

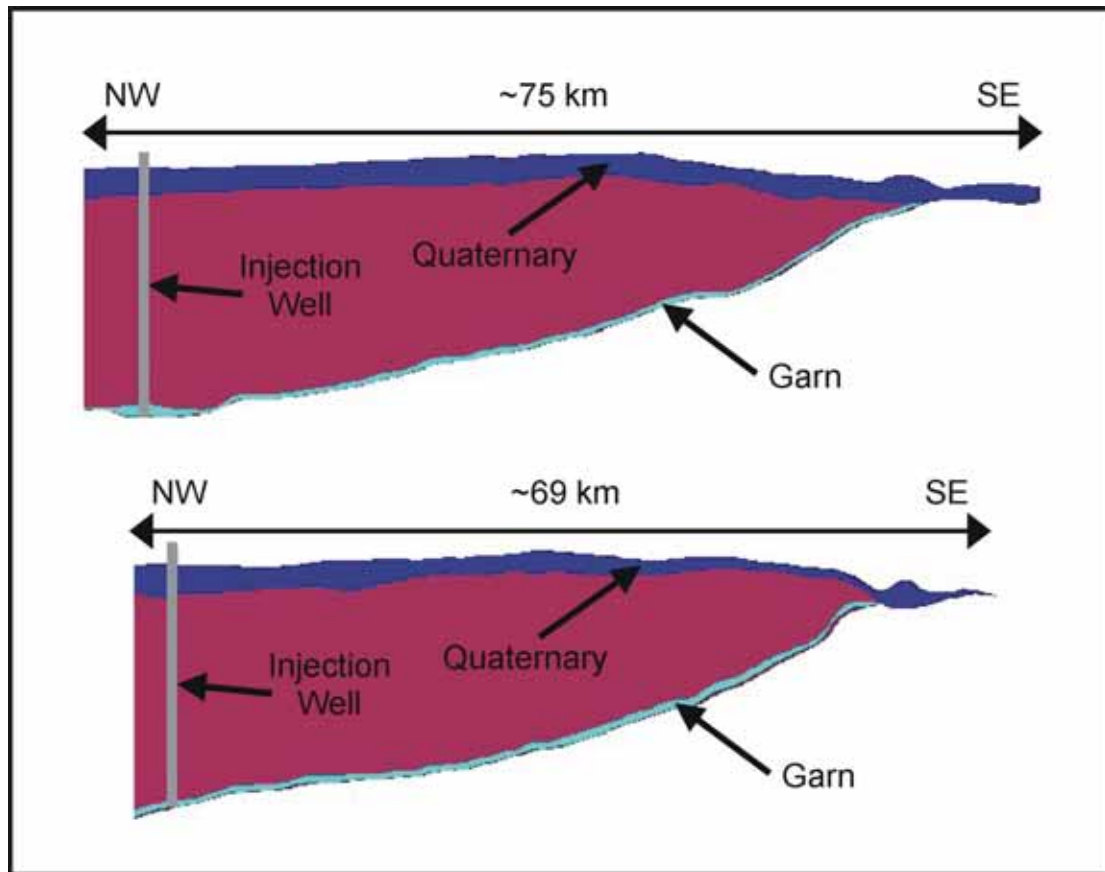


Figure 3.28 Cross-sections through the reservoir model of the Froan Basin showing the case of injection below a structural trap (top) and the case of injection without a structural trap giving shortest time to leakage (bottom). Vertical exaggeration ~10x.

The overall conclusion is that the Froan Basin area of the Trøndelag Platform seems to be suitable for underground long-term CO₂ storage.

The simulations carried out so far utilised only one of three potential reservoir units in only a small part of the Trøndelag Platform. The overall storage potential of the Jurassic formations of the Trøndelag Platform is estimated to be several thousand Mt. This estimate however requires validation of at least one of two assumptions: that sufficient structural traps are present everywhere in the basin, or that CO₂ dissolution occurs sufficiently quickly to inhibit lateral migration of free CO₂. A more detailed study is required to derive a more precise estimate of the storage capacity and to evaluate the seal quality above the reservoir formations.

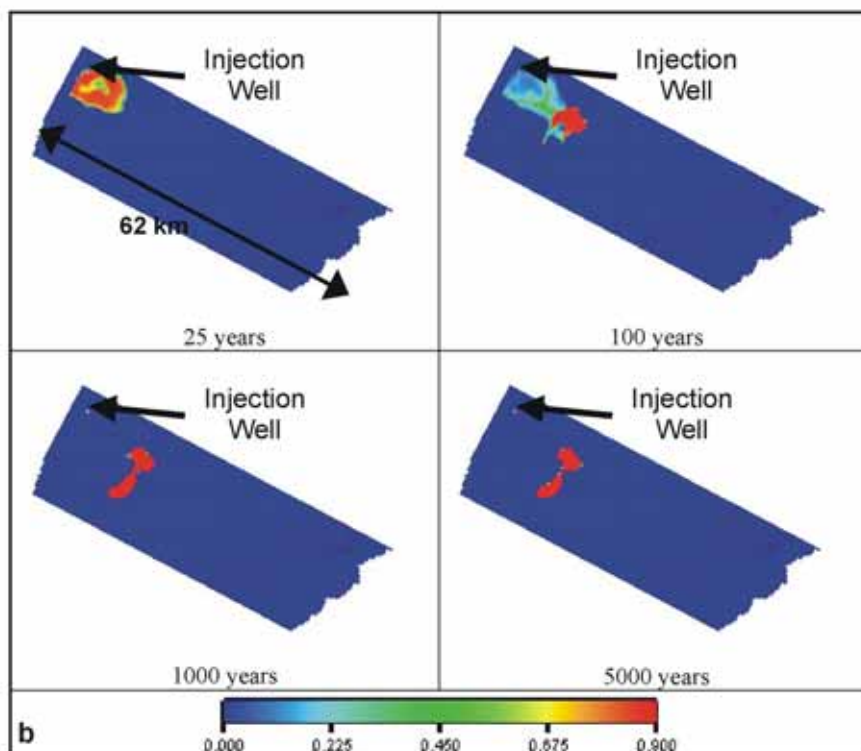
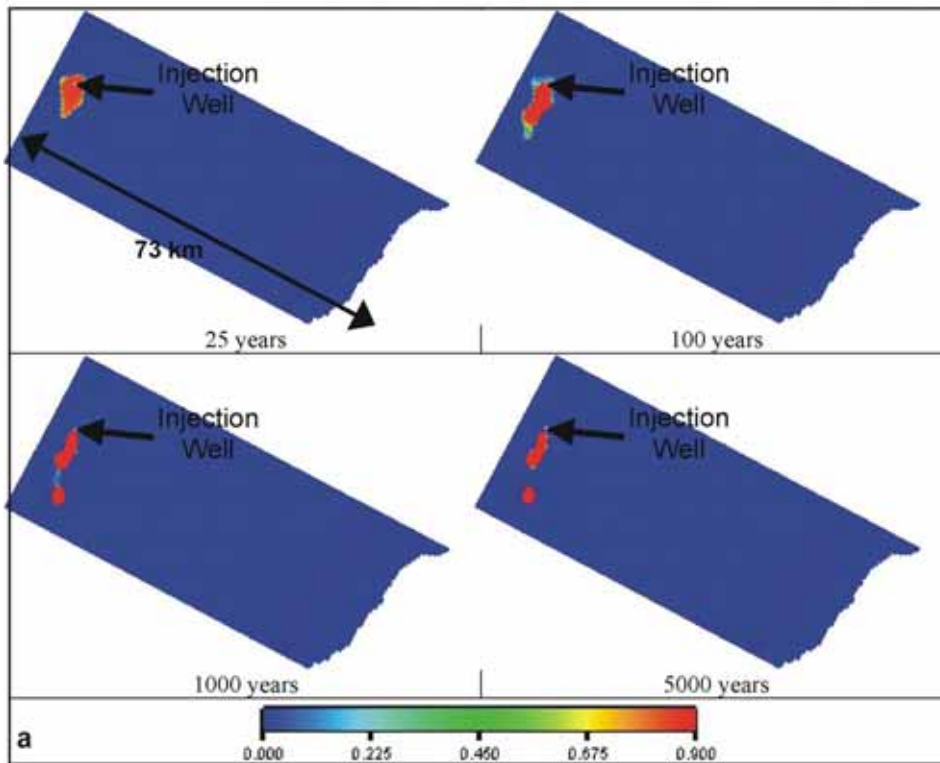


Figure 3.29 Flow simulation models for the Froan Basin area. a) Injection below the trap showing gas saturation at the top of the Garn Formation after 25, 100, 1000 and 5000 years. b) Injection with no primary trap showing gas saturation at the top of the Garn Formation after 25, 100, 1000 and 5000 years.

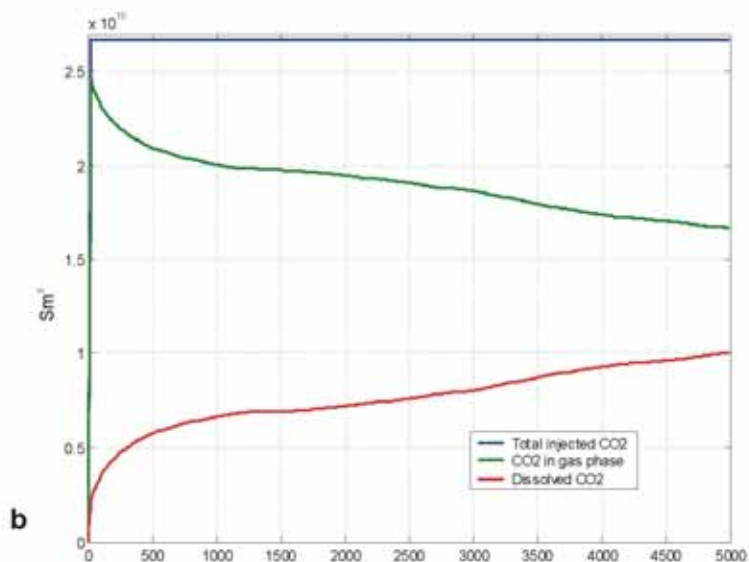
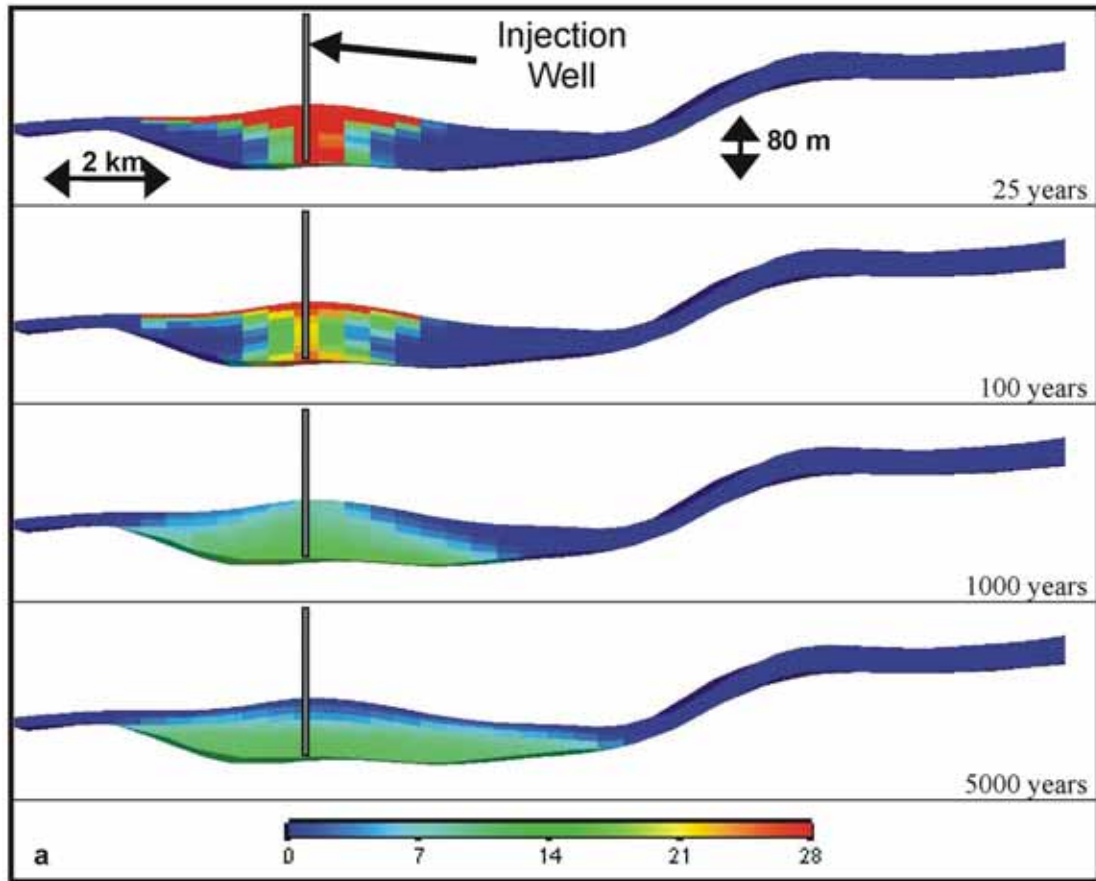


Figure 3.30 Simulations of CO₂ dissolution in the Froan Basin area. a) Dissolved CO₂ (RS = Sm³ gas/m³ liquid) in lower part of the reservoir after 25, 100, 1000 and 5000 years (convection process). Distance from left margin to the subcrop is approximately 66 km. Vertical exaggeration approximately 10x. b) Simulated dissolution of CO₂ in the reservoir.

The effects of pressure increase have not been assessed in detail. A distribution of pressure increase due to injected CO₂ over large parts of the basin is likely, which will keep the overall increase small. Injection at high rates at several places in the basin may however lead to pressure increases, which should be studied in a comprehensive model for the whole basin.

In summary, the screening study shows a clear preference for the Froan Basin area on the Trøndelag Platform. Simulations indicate that none of the tested combinations of parameters is likely to cause leakage of CO₂. Accordingly, storage at this site would probably fulfil relevant criteria to qualify for long-term CO₂ storage. For the Beitstadfjord Basin, all parameter combinations show that leakage will occur rapidly, and the area can therefore be excluded as a potential storage site. The Frohavet Basin might have a storage potential given a fortuitous combination of reservoir parameters.

The simulations contain several uncertainties which largely relate to the lack of relevant data and to limitations of the simulator software.

Reservoir heterogeneity has not been evaluated for any of the areas. The distribution, interconnectivity and lithological variations of the reservoir sandstones depend on depositional environment. Well data and seismic data (ideally 3D seismic) would be necessary to evaluate reservoir heterogeneity since this strongly influences CO₂ sweep efficiency. Reservoir properties employed in the simulations (porosity, permeability, net-to-gross ratio) are extrapolated from the Haltenbanken area further offshore. Prior to any injection a full site characterisation, incorporating detailed reservoir and caprock characterisation studies would have to be carried out.

Two-phase flow properties of the rocks are very poorly-constrained and for the simulations were just based on previous analyses of other sandstone reservoirs. These properties would have to be determined from samples from the potential storage formations. The choices made for the present simulations suggest that migration rates are generally overestimated, such that likely real migration rates and migration distances would be less than those simulated.

Seal efficacy of the immediate stratigraphic seal has been assumed to be perfect, such that no CO₂ would be able to leak from the storage formation into the overburden. However, this assumption must be confirmed by data from wireline logs and cores prior to injection.

Reservoir temperature influences CO₂ migration in a number of ways. At higher temperature CO₂ has a lower density, which implies less efficient use of available storage pore volume and a stronger buoyancy force driving migration; also viscosity would be reduced, which would result in increased migration rates.

Faults have been identified on seismic lines, but they have not been incorporated into the reservoir simulations. They may have several, partly opposing effects on migration. Sealing faults can constitute traps, thereby both trapping CO₂ and constraining its migration pathways. Non-sealing faults in contrast could enable migration from the storage formation into overburden formations from which CO₂ may potentially escape if suitable migration pathways exist. In the Frohavet Basin, faults typically extend throughout the sedimentary succession all the way to the base

of the very thin Quaternary cover. In the case of non-sealing faults this implies that CO₂ might leak along fault planes directly into the ocean. On the Trøndelag Platform, the situation is quite different. There, the faults that cut through the Jurassic storage formations typically terminate upwards at the base of the Cretaceous or in the Lower Cretaceous fine-grained formations. In the case of non-sealing faults, CO₂ could leak upwards to a Lower Cretaceous level, but there it would stop in the thick succession of fine-grained Cretaceous and Cenozoic rocks. The effects of faults should be thoroughly evaluated through detailed mapping (ideally 3D seismic) and fault seal evaluation (clay smear or fault-gouge ratio determinations).

CO₂ dissolution processes and the variation of CO₂ density as a function of pressure and temperature have been treated in a simplified way due to the limitations of the reservoir simulator Eclipse 100.

In addition to physical trapping in structural traps, and to trapping by dissolution, some CO₂ is likely to be trapped as residual gas due to hysteretic flow processes. This trapping mechanism has only been included in a few simulations. In general, residual gas trapping would reduce CO₂ migration and would thus contribute to the safety of the storage site. The amount of CO₂ trapped as residual gas depends strongly on the pore volume that becomes saturated during migration. A longer migration distance towards a potential leak (such as for the Froan Basin case) would imply a greater degree of residual gas trapping.

Generic study of dipping aquifers

As a consequence of the mid-Norway case study, a generic study was initiated to investigate the effect of some key reservoir parameters on the efficiency of open, dipping aquifers for long-term underground CO₂ storage by calculating leakage profiles (Akervoll et al., 2006). The study used a generic aquifer model whose dimensions and base case parameters were based on the most promising mid-Norway storage case, the Trøndelag Platform. Base-case models incorporated residual gas trapping, with results showing that leakage to the seawater should only occur for very high horizontal permeabilities of more than 3500 mD (Figure 3.31). Even for the extreme cases, simulated annual leakage rates are below an annual leakage threshold value of 0.01% of the stored mass: simulated cumulative leakage 5000 years after injection was only just above 2% of the total injected mass for the most extreme permeability (5000 mD).

Some parameters additional to horizontal permeability are likely to affect the balance between retaining processes (such as viscosity, residual gas trapping, dissolution) and driving processes (such as buoyancy forces and aquifer flow). So far only a few of these have been studied in the generic simulation model. The non-realistic, extreme assumption of zero residual gas trapping (non-hysteretic two-phase flow) results in much more leakage than the base case, but simulations still indicate that around 70% of the injected mass should remain in the reservoir after 5000 years even for the most extreme permeability of 5000 mD (Figure 3.31).

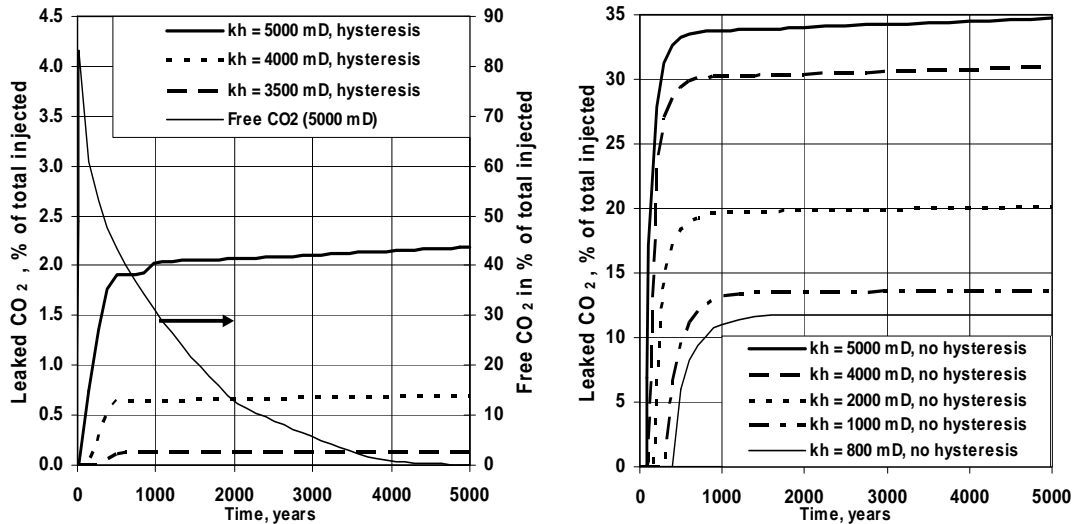


Figure 3.31 Leakage hysteresis: Cumulative escape profiles from open, dipping aquifers with varying horizontal permeability (k_h) at 1.4 % dip (from Akervoll et al., 2006). Only for $k_h > 3500$ mD significant escape could be observed (left). The importance of residual gas trapping is illustrated by simulations of the same cases, but excluding any residual CO_2 by imbibition due to hysteresis (right).

The effect of the dip of the trap was also studied. As expected, steeper dips result in earlier leakage, greater leakage rates and more cumulative leakage. However, for a dip of 2.8° (twice as steep as the base case), no leakage occurred for horizontal permeabilities less than 2700 mD.

The effect of migration distance was not explicitly evaluated by Akervoll et al. (2006), but it can qualitatively be assessed from their results. Sufficient minimum migration distance is of key importance to achieve low or zero leakage rates. The efficiency of both dissolution of CO_2 into formation water and residual gas trapping requires that the migrating CO_2 contacts as large water volumes as possible. This can best be achieved by a long minimum migration path towards the spill point (~ 75 km for the simulated case).

Schwarze Pumpe (Schweinrich)

No reservoir simulation was carried out at the site screening stage.

Valleys

No reservoir simulation was carried out at the site screening stage.

3.4.2 Generic findings

Typical traps for underground CO_2 storage are similar to those containing oil and gas, in that a buoyant fluid is kept in place by a seal that partly or completely inhibits migration of the fluid out of the trap. A different type of storage site, such as has been evaluated for the mid-Norway case study, involves open, dipping aquifers. The seals above these aquifers are dipping and may be incomplete; they would inhibit direct vertical migration of the injected CO_2 and deflect the migration path to near horizontal course, but they would not hold the CO_2 permanently in situ. Ultimately

the CO₂ would likely reach a non-sealed part of the reservoir and escape into the ocean and the atmosphere if it were not kept within the reservoir by counteracting processes. Suitable counteracting processes that have an effect at the relevant timescales (hundreds to thousands of years) are dissolution into formation water and residual gas trapping due to relative permeability hysteresis. In conclusion, open, dipping aquifers may provide effective CO₂ storage options, given reasonable reservoir parameters (particularly horizontal permeability) and adequate distances between the injection well and the leakage point. Even with open aquifers however, pressure is a key limit on injectivity for small reservoirs.

3.5 Safety assessment of prospective CO₂ storage sites

In order to evaluate the health, safety and environmental (HSE) effects and identify weak links in a geological CO₂ storage system, there is a need to perform safety assessment studies to identify and rank the main containment risks. Several such studies have been performed or are underway by various research groups worldwide (e.g. Chalaturnyk et al., 2004; Saripalli, 2002 and Wildenborg et al., 2005).

3.5.1 Risk and risk criteria

A risk relates to the consequences of potential sources of harm, so-called hazards, and the likelihood of the same. It is defined as a function of the probability of an event that causes harm and its consequence (ISO/IEC 2002). A function often used is the following:

$$\text{Risk} = \text{probability of hazard} \times \text{consequence of hazard (impact)}$$

Risk criteria are used as a reference by which the significance of risk is assessed. Examples of often-used criteria are associated costs, concerns of stakeholders, environmental aspects and legal considerations.

3.5.2 Health, safety and environmental risks with CO₂ storage

The risks associated with storage of CO₂ relate to many areas, such as system integrity, HSE effects (including climate change), economic risks, and risks related to public perception and trust. In this specific section, the focus is on HSE-related risks.

HSE risks fall into two main categories: local and global risks. This division is based on the fact that CO₂ constitutes a hazard both at a global level when considering global warming, and at a local level when considering hazards to, for example, humans, fauna and flora that may be found nearby to a CO₂ storage site. Figure 3.32 summarises the HSE risks associated with geological storage of CO₂.

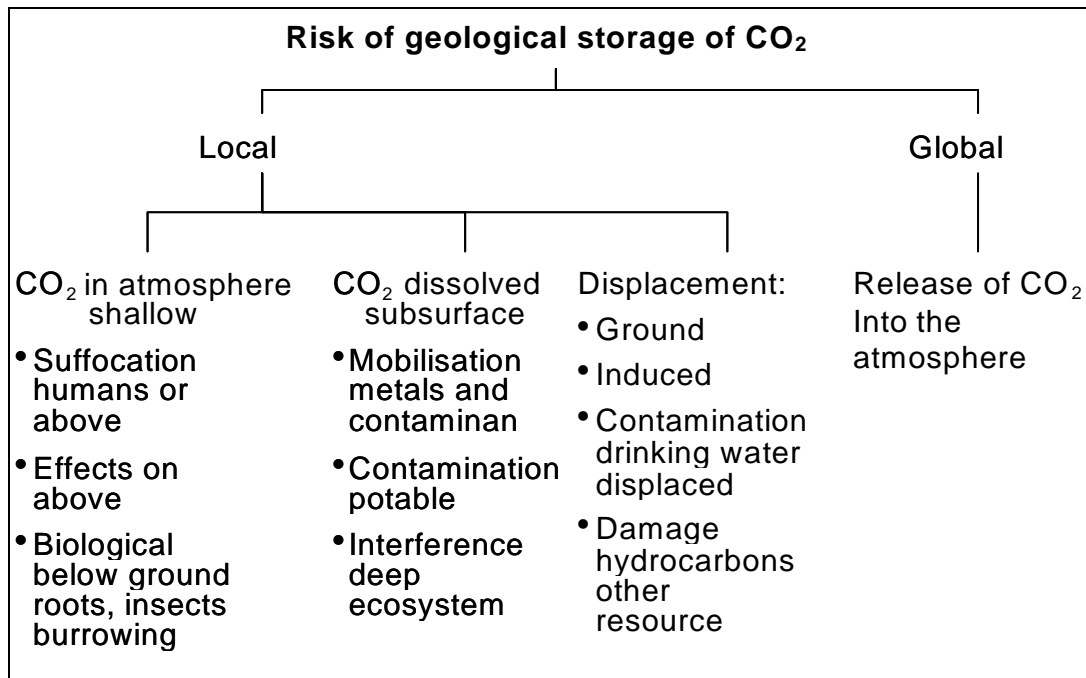


Figure 3.32 HSE risks associated with geological storage of CO₂ (based on Wilson et al., 2003).

3.5.3 Local HSE risks

The main local HSE risk of concern to humans is elevated CO₂ concentrations in air. Even if CO₂ is non-toxic, it can be dangerous to life at concentrations above 10% by volume causing unconsciousness, change of blood pH and failure of respiratory muscles. Such concentrations can arise through sudden leaks from well blowouts. However, even slow leaks from deep CO₂ reservoirs may cause serious events if the CO₂ is confined in the near subsurface and then suddenly released or were to accumulate in a confined space like a cellar (Benson et al., 2002).

Slow leaks of CO₂ are known to have detrimental effects on burrowing fauna and flora. This is because surface air is far better mixed than air in soils, which means that hazardous concentrations in the ground may result from CO₂ fluxes far smaller than those required to produce harm to above-ground organisms (Benson et al., 2002; Saripalli, 2002).

3.5.4 Global HSE risks

The global HSE risks are related to release of CO₂ back to the atmosphere. Predicting the global impact on climate change due to a release of CO₂ depends on the quantity, duration and timing of the release (Wilson et al., 2003).

3.5.5 Offshore and onshore issues

In terms of potential risks it is useful to distinguish between onshore and offshore storage settings. Unwanted effects may have more severe consequences in densely

populated areas and in environmentally sensitive locations than in sparsely utilised rural areas or offshore. Risks resulting from rapid processes (e.g. blow-outs) leave less time to react than risks resulting from slow processes (e.g. surface tilting), where effects accumulate over time.

3.5.5.1 Offshore

Slow leakages of CO₂ from a storage reservoir beneath the ocean would not generally pose an immediate threat to humans. In the open ocean, released CO₂ will be partly dissolved in the water column, and any remaining CO₂ escaping to the atmosphere will be mixed with air and rapidly diluted. For people on ships and offshore installations, the situation might possibly be different if they were located directly above the leakage site. The risk that a ship might conceivably sink in a large rising gas bubble has not been assessed. In general however, from studies of natural analogues in the NASCENT project (www.bgs.ac.uk/nascent/), it is evident that leaking CO₂ from the subsurface constitutes only a small threat to human beings. A prerequisite for it to cause suffocation is that it accumulates in topographic depressions or in subsurface rooms, which is not the case offshore. Wind action would cause rapid mixing and dilution in the atmosphere.

Leakage from offshore pipelines, wells, and reservoirs could adversely affect a larger area because of the dissolution and acidification of the surrounding seawater. They should be modelled with regard to possible CO₂ concentrations in the pelagic and surface zones and biological effects assessed thereafter. Such modeling was not carried out in CO₂STORE.

3.5.5.2 Onshore

The risks of CO₂ leakage during separation, transport and injection are well known and subject to health and safety regulations. Special care should nevertheless be taken because of the large quantities of CO₂ that have to be handled.

The effects of leakage during pipeline transport and injection are usually restricted to the immediate vicinity of the leak, but may pose a threat to people and animals nearby. In the atmosphere, CO₂ concentrations are likely to be diluted rapidly below critical levels due to ground-layer turbulence. This can be observed at natural CO₂ emissions and has also been calculated for a leaking storage scenario (Oldenburg et al., 2003b). In built-up areas there is a risk of CO₂ accumulation in underground rooms of buildings. Even small rates of seepage can lead to hazardous concentrations in badly ventilated rooms.

The possibility of a sudden release of CO₂ (a blow-out) from a subsurface storage site is practically zero. Preventing a blow-out may be achieved by thorough investigations of the storage reservoirs and caprocks prior to storage. Such investigations must include 3D seismic surveys, drilling and reservoir and geomechanical simulations.

Geomechanical risks are not necessarily directly linked to CO₂ leakage. Microseismicity caused by injection could create public concern, even if it does not

cause physical damage. Differential movements along reactivated fault-lines in the caprocks could cause earthquakes. The production of natural gas has triggered earthquakes in Germany up to magnitudes of 2.6 to 2.8 in Germany. In The Netherlands, over the last two decades, a total of about 350 induced tremors has been recorded, with magnitudes (M_L) ranging up to 3.5 (van Eijs et al., 2006, G. Leydecker, personal communication).

Non-seismic displacements of the Earth's surface could also damage built infrastructure, comparable to the effects of subsidence in underground mining areas. Vertical uplift above large reservoirs could affect lake levels and shift streams in lowland areas with low topographic relief.

The risk of initiating a mud diapir in unconsolidated (plastic, water-rich, under-compacted) reservoir and overburden strata, possibly including the entire reservoir, because of the buoyancy of stored CO_2 has not yet been investigated.

Migration of CO_2 could occur along faults in the caprocks, either undetected, or known faults that have been wrongly thought to be sealing, or that have become transmissive because of mechanical reactivation or elevated reservoir pressures. Undetected pathways in the caprocks (e.g. sand injection features), poorly defined spill-points, and (supposedly sealed) wells are other potential conduits for CO_2 to escape from the storage reservoir.

CO_2 storage will, at least temporarily, before a possible complete dissolution of the gas in the surrounding formation water, lead to the displacement of formation brines that could reach shallow freshwater environments, soils or discharge at the surface. Both CO_2 and brines could poison shallow aquifers. This risk can be amplified by the dissolution and mobilisation of heavy minerals from the surrounding rock.

In carbonate aquifers carbonate dissolution along localised fluid (water and CO_2) paths (such as a shattered bore-hole environment or fractures) could create larger voids that might create sinkholes at the surface. Rapid ascent of water in larger fault zones accelerated by rising and expanding gas-bubbles could cause vigorous eruptions and surface craters in soil and incompetent rocks. Similarly, in fine-clastic unconsolidated rocks, suspensions could form and cause mud-volcanism and mud-flows. These effects would, however, be areally restricted.

Foundations of buildings might be damaged by seepage of carbonated groundwater in shallow unconsolidated sediments and soils, which could create considerable problems if CO_2 were to be stored (and leak) underneath, for example, historical city centres, other heritage objects, or archaeological sites.

Undetected accumulations of CO_2 -supersaturated water or gaseous CO_2 in shallow traps might be a risk for future drilling.

Long-term risks might result from the gravitational sinking of dense CO_2 saturated brines; if they come into contact with salt formations this could lead to a degassing of the formation water and the ascent of CO_2 outside of the original closed storage structure.

Storage in aquifers with up-dip connections to the shallow surface (open aquifers) is considered to be more risky than storage in closed reservoirs. Neotectonically active or volcanic areas should be avoided. Besides caprock damage, rapid pressure and temperature changes due to heating, stress, or displacement could affect CO₂ density and solubility, creating the risk of uncontrolled, rapid migration and escape of stored CO₂.

3.5.6 Observations from the CO₂STORE case studies

Kalundborg

Generalised risks were assessed when comparing the Havnsø and the Rosnæs structures (Table 3.4).

Economic/Risk evaluation	Havnsø	Røsnæs
3-D seismic	High costs	Low costs
Drilling	Low costs	Medium costs
Transport	Onshore pipeline	Offshore pipeline
Monitoring	Wells	Seismic
Permission requirements	National and local authorities	OSPAR/ National and local authorities
Risk project	High seismic costs	Fault sealing capacity
Risk humans	Low	None
Risk environment	Low	Low

Table 3.4 Economic and risk evaluation for the Havnsø and the Rosnæs structures.

Most of the perceived risk variations are related directly to whether the structures are in an onshore or offshore setting.

Mid Norway

Flow simulations show that, for the Trøndelag Platform, it is very unlikely that CO₂ would reach the seabed within 5000 years, after which leakage might occur at a low rate. In the Frohavet Basin, the situation is less clear. In the case of favourable parameter combinations, it might be possible to store CO₂ for thousands of years without leakage. However, more simulations, well data, and 3D seismic data are needed to evaluate this. The most critical parameter for the Frohavet Basin is probably whether faults are sealing or not. Sealing faults might increase storage capacities while non-sealing faults might cause leakage of CO₂ into the sea water.

For both the Frohavet Basin and the Trøndelag Platform, any CO₂ that does leak would enter the sea. As water depths are generally less than 200 m, gaseous CO₂ would probably rise rapidly to the surface (and atmosphere) in the form of bubbles. For the Frohavet Basin, leakage from non-sealing faults or subcropping storage formations could theoretically occur about 10 km from the nearest islands. On the Trøndelag Platform, leakage from subcropping storage formations could theoretically occur as close as 15 km from the nearest islands, but only after 5000 years. This implies that there is no potential direct hazard to humans.

Schwarze Pumpe (Schweinrich)

No safety assessment was carried out during the screening phase.

Valleys

No safety assessment was carried out during the screening phase.

3.6 Conflicts of use

3.6.1 Contamination of other resources

Saline water from deep aquifers is used for table water (artificial mineral water) production, in spas, as a source of base material for chemical industry and for geothermal energy production. Though little use is made of these resources currently, they are protected by mining law in some EU states. Additionally, in Germany and other countries, brines legally are classified as groundwater and protected by the federal water law.

Deep aquifers with high porosity suitable for CO₂ storage would also be potentially suitable for geothermal energy production. At average geothermal gradients (e.g. ~30 Ckm⁻¹) aquifers suitable for geothermal utilisation would lie at depths of 1500 m or more (Schulz & Röhling, 2000), while the minimum depth of aquifers for CO₂ storage would be about 800 m, according to the anticipated CO₂ density gradients. Thus, both activities aim for aquifers of high porosity in a partly overlapping depth range, which holds some potential for conflict. Quantitative comparisons of these two options for a given storage area are needed.

Brines often contain elevated trace element concentrations. It is at least feasible that such brines might become a resource, e.g. lead, zinc, nickel, or other metals that might become important for future technologies.

Strategic reserves of natural gas have been stored in aquifers for several decades, particularly in France and Germany (for example at Berlin, Buchholz, Kalle and Ketzin). The down-dip catchment area of such storage facilities cannot be used for storing CO₂, which might possibly migrate into the gas storage structures.

Brines and salty mineral waters are used in health spas across much of Europe and commonly are protected by local or national regulations. In Germany, the federal states have agreed upon criteria for the establishment of protection zones around health spas (Baumann et al., 1998), these include protection of their catchment areas. Thus, the deeper saline aquifers in the vicinity of such spas could be excluded from potential CO₂ storage.

Restrictions on underground exploration or drilling may exist in sedimentary basins with hydrocarbon prospectivity. Licence areas are published and updated by national authorities. Restrictions may also be valid for aquifers in the overburden of deeper hydrocarbon reservoirs.

3.6.2 Surface installations and pipeline routes

Storage activities on the land surface will generally conflict with land use, albeit temporarily. Pipelines, injection and monitoring wells and surface installations may not be allowed within groundwater protection zones, protected natural reserves, and waste deposits. It may also be difficult to obtain permissions from property owners in urban, military, and industrial areas to build or operate surface infrastructure. Considerable parts of the land surface will not be available or difficult to use in densely populated areas and in rural areas as well. Building may be costly there. Application, permission and contract processes may take several years for new pipeline projects. Permissions may be bound to additional ecologic compensation measures. Activities in areas of ecological importance are affected by a range of restrictions or a preferential use has been declared for these areas. Taking a German example, Lower Saxony may be an important region for future aquifer storage of CO₂, but ecologically important areas cover much of the state (Figure 3.33).

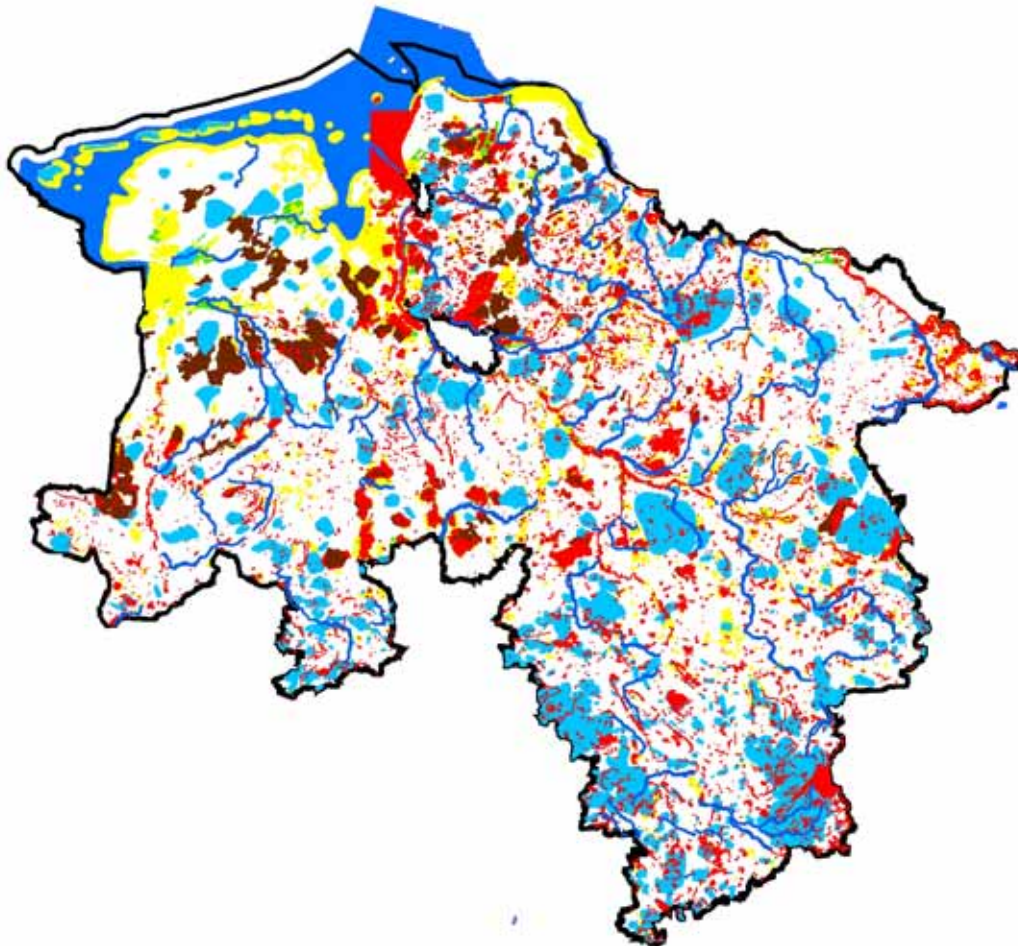


Figure 3.33 Areas of ecological importance in Lower Saxony: biotopes (red), groundwater protection areas (light blue), protected streams and adjoining valley meadows, lakes and coastal waters (dark blue), wet grass lands (green), peat bogs (brown), bird's resting and breeding areas (yellow). Data source: Geo-Daten-Server der niedersächsischen Umweltverwaltung.

3.6.3 Observations from the CO2STORE case studies

Sleipner

Site screening at Sleipner included several alternatives to the Utsira Sand reservoir (Baklid et al., 1996). These were mostly rejected on the basis of incompatibility of objectives or direct conflicts of use.

Storage options are listed below:

use of CO₂ for EOR in nearby oilfields (problem: mismatch between supply and demand rates)

injection into the Sleipner East gas/condensate reservoir (Heimdal Formation) for enhanced gas recovery (problem: potential contamination of originally low-CO₂ gas in this reservoir)

injection into the aquifer part of the Heimdal Formation (problem: potential contamination of originally low-CO₂ gas in this reservoir)

injection into the Skagerrak Formation at about 2500 m depth (problem: close to Sleipner Øst gas/condensate reservoir and therefore potential for contamination)

injection into the Utsira Sand.

For the first alternative the amounts of CO₂ needed in the possible fields did not match the production rate. For the next options the risk of unwanted CO₂ contamination of the produced gas from Sleipner East was considered too high. As a result of this, storage in the Utsira Sand was chosen on the basis of incurring fewest conflicts of use.

Some potential conflicts of use do remain, however. The presence of free CO₂ in the Utsira Sand impairs the quality of seismic at deeper levels. This may compromise exploration, production, and monitoring activities in the footprint area of the CO₂ plume. The Utsira Sand is used in other areas of the North Sea for production of water for injection into hydrocarbon reservoirs. The presence of free or dissolved CO₂ may interfere with such activities and may trigger additional costs, e.g. for corrosion-resistant low-carbon steel for wells and platform equipment.

Kalundborg

The Havnsø structure was selected for the current study on the basis of technical criteria and its immediate suitability for the nearby CO₂ sources. Potential conflicts of interest would include the use of structures for storage of natural gas and other more valuable commodities. A surface conflict of interest may arise in some localities with respect to the monitoring of CO₂ storage sites, in restricted areas such as national parks, bird sanctuaries etc.

Geothermal energy resources have been evaluated for the major Danish towns (Sørensen et al., 1998). The survey included Kalundborg which, with an estimated specific resource of 359 000 TJ, was ranked 7th on a list of 23 potential sites for geothermal energy recovery.

The geothermal potential, however is not considered to be of current commercial interest due to the fact that excess heat is produced from the coal-fired powerplant. Potential conflicts will nevertheless lie in possible future plans for geothermal energy systems after powerplant closure.

The Havnsø structure was evaluated as a natural gas storage reservoir in 1973, but was disregarded due to its large size. The Danish natural gas company DONG established the Stenlille gas storage facility (Table 3.2) 45 km south-east of Havnsø using the same reservoir formation. The pore-volume of the Stenlille structure is estimated at 0.247 km³ compared with 3.67 km³ at Havnsø. It is considered unlikely therefore that Havnsø will be considered for gas storage in the future.

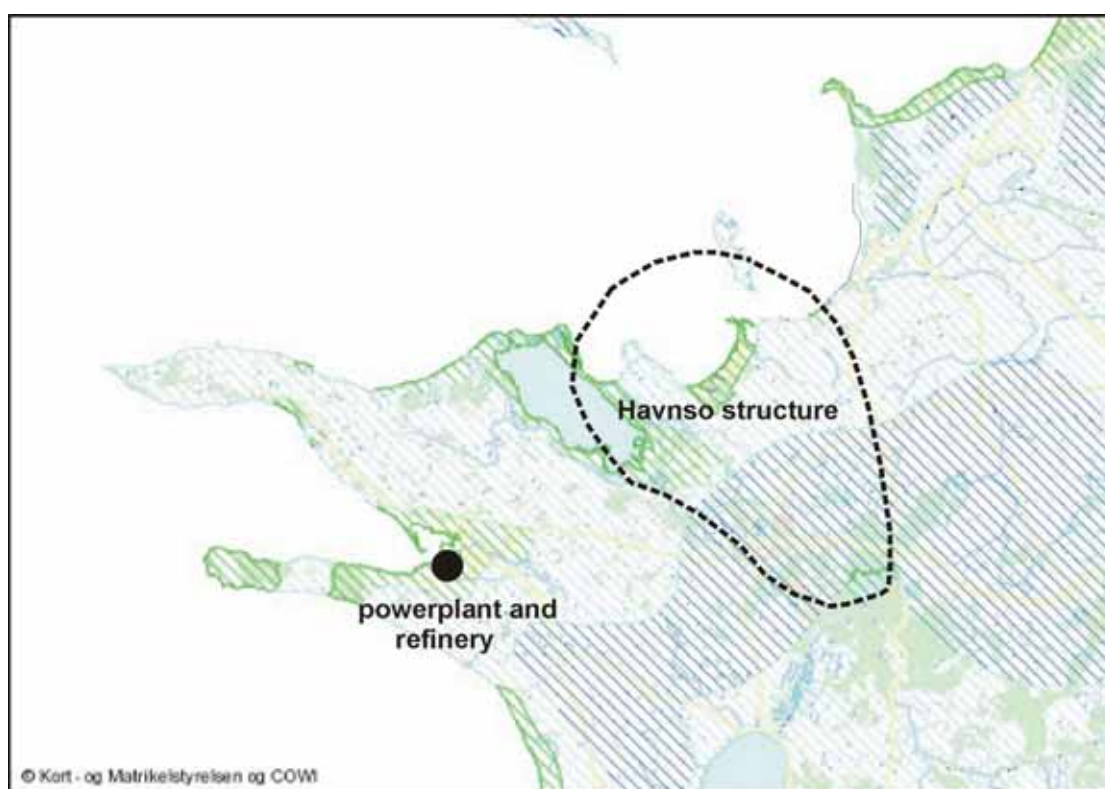


Figure 3.34 Classification of the areas around Kalundborg concerning their importance for drinking water resources. Dark blue hatches: important drinking water resources; light green hatches: drinking water resources; dark green hatches: limited drinking water resources. Incorporating data from www.Vestsjællandsamt.dk and information © Kort & Matrikelstyrelsen (182).

Several of the structures that form potential CO₂ storage sites in Denmark have been evaluated and drilled for hydrocarbon exploration. However there are, at the time of writing, no hydrocarbon discoveries in the more easterly structures, due to a likely lack of mature source rocks. Although petroleum exploration through history has presented unexpected discoveries, the Havnsø structure is assumed to hold only saline water.

No conflict is expected with drinking water production, which utilises Quaternary sandstone aquifers at depths down to a few hundred metres (Figure 3.34).

The Havnsø caprock is assumed to form an effective capillary seal, and escape of CO₂ along faults is not considered likely. Diffusive transport of CO₂ through the caprock

and overburden has been modelled by Bech and Larsen (2005), who show that it will take more than 1 million years for the CO₂ to reach the surface.

Drinking water may, however, be contaminated if CO₂ were to escape along linings of injection or observation wells. Well integrity therefore requires special attention in the storage project (Larsen et al., 2006).

Mid Norway

The selection of the three basins included in the screening study, took potential conflicts with the hydrocarbon industry into account. The three basins are not likely to contain hydrocarbons in commercial quantities.

Schwarze Pumpe (Schweinrich)

Potential conflicts of use were considered in the site selection procedure using the GIS approach (Figure 3.35).

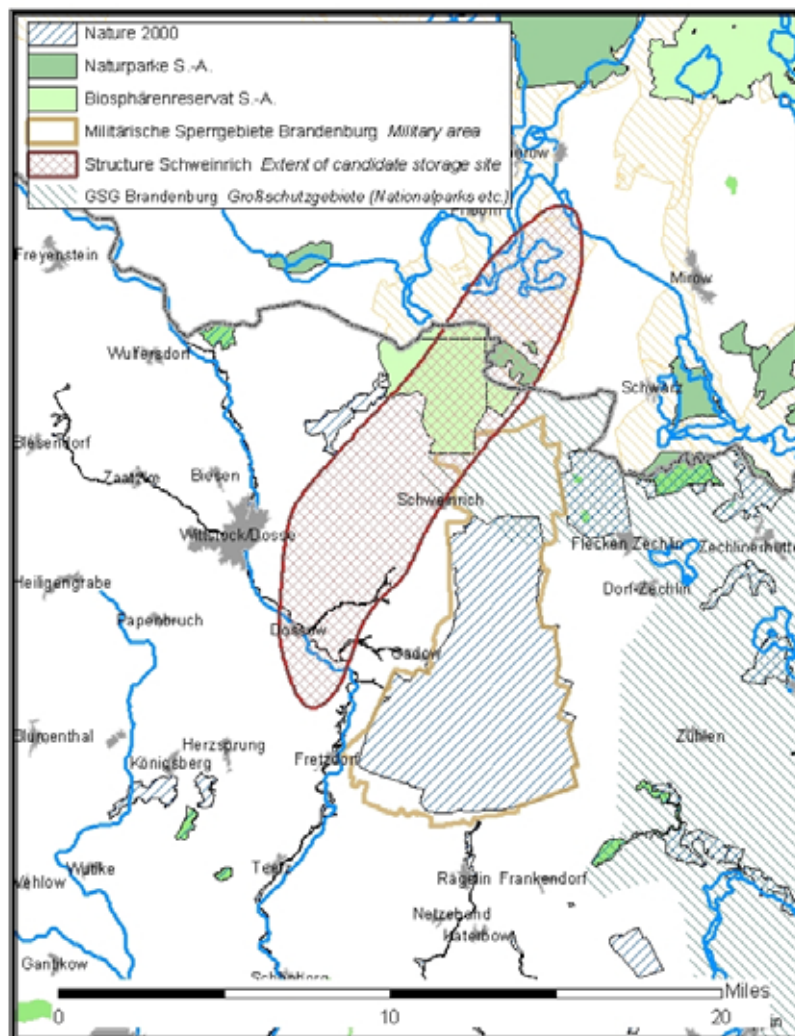


Figure 3.35 The Schweinrich structure and its relationship to protected areas (several types of nature reserve and national parks) and land used by the military.

Even given the large area of the Schweinrich storage footprint, it is not seriously overlapped by nature protection areas or land used by the military.

Valleys

The screening process did not explicitly take potential conflicts into account. The preferred Cenozoic site in the St George's Channel Basin is not currently likely to encounter conflicts with the hydrocarbon industry.

3.7 Costs

In most cases main project costs will relate to capture of CO₂ at the power plant, with transport and storage contributing a relatively small percentage.

When modelling the economics of the storage system the different cost factors are brought together in a discounted cash flow calculation. The assumptions made in this calculation can have a major impact on the results. These include the level of the discount rate, the lifetime of the project and the economic model used. Published studies normally use three methodologies to account for the timing of costs and of emission abatement (Freund and Davison, 2002):

Costs are discounted to the present and related to total emission reduction over the project lifetime (net present cost).

Costs are discounted throughout the project lifetime and to the time when the CO₂ abatement takes place (levelised costs).

Costs and abatement are discounted to the present (net present value).

Other factors that may or may not be included in the cost calculations are inflation, taxation, insurance, fees, working capital etc.

3.7.1 Observations from the CO₂STORE case studies

Sleipner

For the Sleipner case, capture costs are part of the natural gas production process because CO₂ must be separated from the produced natural gas to fulfill customer requirements. Costs for underground storage can be divided into the following categories (Torp and Brown, 2004):

costs for CO₂ compressor train and gas turbine drive: 79 M€

operation costs for compressors, including CO₂ tax on exhaust: 7 M€ per year

costs for CO₂ injection well: 15 M€

preparation cost: 2 M€.

Costs for pre-injection site studies have not been documented. However, they are probably negligible in comparison to the cost items listed above. In addition, site characterisation and monitoring were carried out as part of an extensive research programme (SACS and CO2STORE projects). Costs for acquisition, processing and interpretation of a 3D monitoring survey will vary strongly as a function of seismic acquisition market conditions. A current estimate for the seismic monitoring costs, assuming ‘standard’ (non-research) type interpretation and no mobilisation costs for the seismic vessel, is approximately 0.7 M€ per survey. Coring of reservoir material (SACS) and caprock material (CO2STORE) cost 0.9 M€ and 0.5 M€, respectively (Torp and Brown, 2004).

Kalundborg

The economics of the Kalundborg case were evaluated as part of the GESTCO project (Hendriks and Egberts, 2003), with the assumption that 6 Mt per year of CO₂ would be stored.

Calculations using the GESTCO decision-support system (DSS) showed that total costs would amount to 32€ per tonne of CO₂ avoided. The capture costs (using retrofitting on the existing power units) would amount to about 22 € per tonne, contributing some 67% of the total costs.

As part of CO2STORE, Jakobsen (2005) made a new economic evaluation using a modified version of the GESTCO DSS. Jakobsen used a benchmark scenario and compared the net present value of the system as a function of a number of variables (Table 3.5).

	Net Present Value		
	Benchmark scenario	5 000 production hours/year. Minor efficiency improvements	6 000 production hours/year. Major efficiency improvements and Falling
Fixed quota price 5 euro per tonnes CO ₂	-2.91	-3.18	-2.67
Quota price 10 euro, increasing 1% per year	-2.62	-2.75	-2.15
Quota price 13 euro, increasing 5% per year	-2.02	-1.88	-1.11

Table 3.5 Kalundborg scenario showing net present value (billion Euro). Data from Jakobsen (2005).

The study concluded that high capture costs in the region of 40 € per tonne of captured CO₂ would make the Kalundborg scenario uneconomic. Most studies have reported current costs of 40–50 € per tonne of captured CO₂, but foresee a reduction in capture costs to about 20 € per tonne at some point in the future. For the economic calculations, capture costs of 15 to 40 € per tonne of CO₂ were used (Figure 3.36).

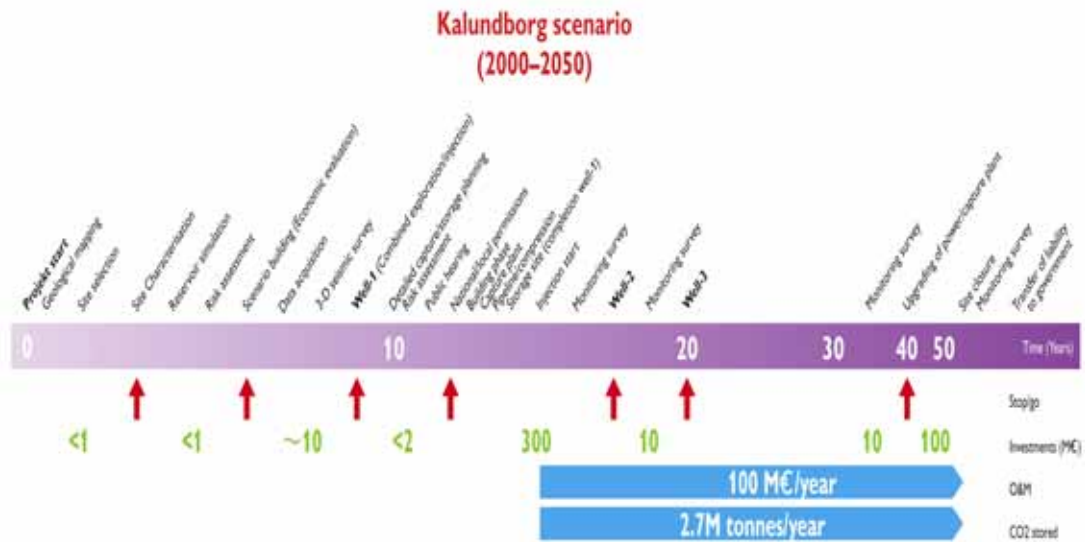


Figure 3.36 Timeline showing the Kalundborg scenario (2000–2050) and the expected investments.

Mid Norway

Cost calculations were not carried out for the mid Norway case study.

Schwarze Pumpe (Schweinrich)

The total costs were calculated as a yearly amortisation of the investment plus the yearly operation and maintenance costs divided by the yearly amount injected CO₂:

$$Cost = \frac{K \cdot \frac{r}{1 - (1+r)^{-n}} + O}{I}$$

- K = Capital investment costs
- O = Operation and maintenance + post operation costs
- r = Discount rate. In this study a general rate of 7% is used.
- n = Depreciation time. In this study a general time of 25 years is used.
- I = Injected amount of CO₂.

Using the model, the yearly amortisation for the capital investment for pipeline and CO₂ storage is calculated at 32.8 M€. Adding the operation and maintenance costs gives a total cost per year of 45 M€. At an injection rate of 10 Mt per year, the total cost per tonne is approximately 4.50 €/tonne. The cost distribution between capital investment and operational costs is shown in Figure 3.37.

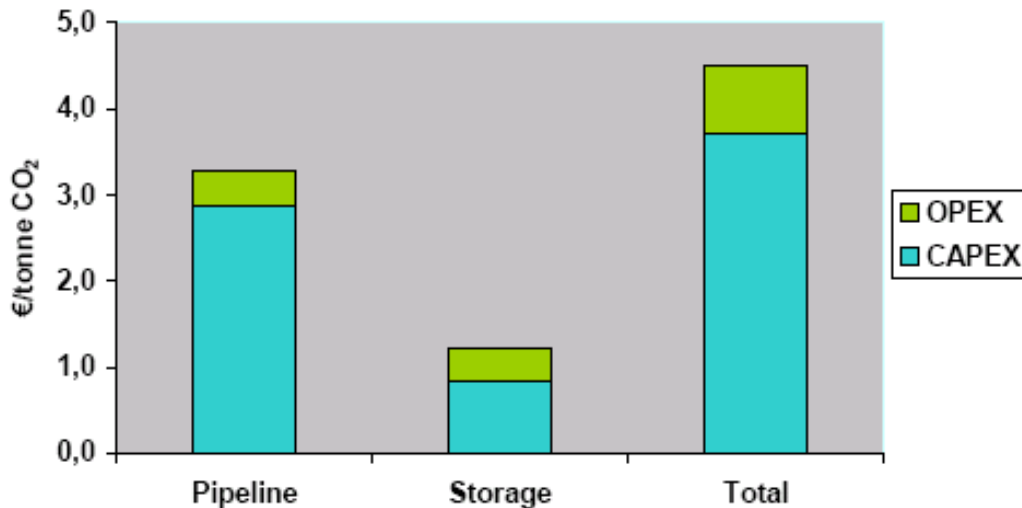


Figure 3.37 Distribution of costs for the Schwarze Pumpe (Schweinrich) case study.

Valleys

For the Valleys case study (UK DTI, 2006) detailed information of mass flow rates has been gathered from a mass balance model. Using this, project costings have been developed for two scenarios:

a ‘capture-ready’ IGCC plant designed for subsequent low cost CO₂ capture of the type envisaged for the Valleys Energy project

a ‘CO₂ capture’ IGCC plant that captures around 85% of the CO₂ emissions.

Moving from the ‘capture-ready’ to ‘CO₂ capture’ plant involves additional capital cost for CO₂ capture and compression equipment. It also involves significant energy penalties associated with solvent recirculation, provision of alternative diluent to the gas turbine for NO_x control, and compression of the captured CO₂ to 11 MPa (110 bar).

A financial model was established to achieve a 10% real pre-tax project return for the ‘capture ready’ case. The cost of CO₂ capture and compression was assessed as the CO₂ price which was required to restore a real pre-tax project return of 10%. This price for capture and compression of 2.45 Mt per year of CO₂ was assessed at around 10 Euros/tonne. This low price can only be achieved through adopting an initial commercial design of IGCC that seeks to minimise the subsequent modifications required for CO₂ capture.

The CO₂ would be captured pre-combustion, using a physical solvent process. The pipeline would be constructed of carbon steel and would consist of an onshore leg of around 90 km and an offshore leg of around 45 km. Pipeline capital costs were assessed at between 50 and 70 M Euros. Annual pipeline operation and maintenance costs were assessed as 3% of the capital cost, at around 1.8 M Euros per year.

Using this capture price, together with the assessed cost of the CO₂ pipeline and injection facilities, a project finance model was developed to take account of the projected project costs and revenues.

Unlike use of CO₂ for enhanced oil recovery, currently the EU Emissions Trading Scheme provides the only fiscal benefit that is potentially available to a CO₂ storage project such as this. It was assumed that the project would be eligible for credits associated with the net atmospheric CO₂ reductions which would be achieved through capture and storage. This takes account of the CO₂ emissions associated with the capture and storage process. On this basis it was assessed that some 2 Mt per year of the 2.45 Mt per year that was captured, would be available for EUETS credits.

On this basis, the price of EUETS credits required to establish a 10% real project return for the whole capture, compression, transport and storage project was assessed. An EUETS price of just under 20 Euros/tonne was required. This is comparable to the price of EUETS credits for much of the financial year 2005, though this subsequently slumped dramatically. Consequently, the Valleys capture and storage project has the prospect of commercial viability under favourable EUETS market conditions..

3.7.2 Generic findings

Irrespective of project specifics, a current financial barrier to CO₂ capture and storage at the present time is the lack of a long-term bankable framework for achieving EU emissions trading benefits. There is no certainty that the current scheme, which started in 2005, will be extended beyond the end of the first Kyoto compliance period in 2012. Provision of a scheme which provides certain long-term financial benefits, over a 15 to 20 year period, will be an essential prerequisite to enabling the long term investments that are associated with carbon capture and storage to be made.

4 SITE CHARACTERISATION

In the site characterisation phase, a complete investigation of one or more selected CO₂ storage sites is performed. The aim is to refine storage capacity estimates, and thereby confirm capacity requirements, and to provide the geological information necessary to show that, as far as can be discerned prior to injection, the site will perform effectively and safely. In the event that more than one site is initially selected, it is envisaged that a single preferred site would be identified during this process.

The main deliverable comprises the material necessary to make an application for permission to store CO₂ to the relevant authorities. This consists of a full techno-economical evaluation of the project including site characterisation, risk assessment and short/medium/long term monitoring plan and remediation strategy.

Key investigations are outlined below:

4.1 Geological characterisation of the site

Satisfactory geological characterisation of the storage reservoir and its overburden is an essential step in the site storage process. It should produce information on reservoir structure, stratigraphy and physical properties. The key datasets for a robust characterisation of reservoir and overburden are:

- a regular grid of 2D seismic data over sufficient area to characterise broad reservoir structure and extents

- a high quality 3D seismic volume over the injection site and adjacent area, tuned if possible for satisfactory resolution of both reservoir and overburden

- sufficient well data to permit characterisation of reservoir and overburden properties.

The aim is to confirm and refine the earlier screening studies and, more specifically, to provide basic data for the predictive fluid flow and geochemical simulations (Sections 4.2 and 4.3), the risk assessment (Section 4.4) and monitoring programme design (Section 4.5). Data is required at a variety of scales and densities, with seismic and well data the key to establishing structure and stratigraphy at both regional and storage site scales. Reservoir properties can best be determined by an analysis of seismic and well log data augmented by rock material (core and cuttings).

After selection of one or more sites, more detailed capacity calculations are needed. Geological models of the reservoir have to be constructed as the basis for reservoir volume calculations. Porosity values obtained from logs and core samples can be assigned to the geological models in order to calculate the integral pore volume. Pressure and temperature information estimated for the reservoir or measured in wells in individual compartments of it can be used in the calculation of the density of the CO₂-rich phase. The geological models can be used in reservoir simulation models to explore the effects of uncertainty via different CO₂ injection strategies (number of

wells, spacing, orientation, injection intervals and rates) and to predict sweep efficiencies. Efficient storage strategies should be developed in order to avoid wasting of underground storage structures and to avoid conflicts with other options of future use, e.g. geothermal energy utilisation.

With geomechanically suitable caprocks, the pressure of the injected CO₂ may significantly exceed the initial formation pressure, which would increase the effective storage capacity. Depending on the hydraulic communication of the storage structure with the surrounding aquifer, pressure build up may be insignificant, or may be larger and persist for millennia.

The volume of formation water and rock that can be displaced or compressed is usually unknown. Conceptually, closed (finite volume, closed boundaries) and open (laterally unconfined, infinite volume) structures can be distinguished (Chapter 3). In the first case CO₂ can be stored by compression of the rock matrix and the formation water and by dissolution within the water only, while in the second case formation water can be displaced by CO₂. In practice CO₂ injection is a dynamic process however, with a transient pressure build up around the injection wells. After injection, a period of further expansion of the CO₂ phase, pressure relaxation, and dissolution in formation water follows. In large open aquifers pressure relaxation is fast due to the rapid displacement of formation water (in the case of the Utsira Sand reservoir at Sleipner no significant pressure build-up has been observed). In closed aquifers pressure relaxation resulting predominantly from dissolution is slow. Thus, the volumes that can be displaced and compressed during the injection time determine the storage capacity within an aquifer structure. In order to establish the effective extent of a structure, knowledge of the hydraulic conductivity of faults in the vicinity of an injection site is required. This information can be derived from well tests. Variations of the effective aquifer radius in reservoir simulations can be used to study its impact on storage capacity.

4.1.1 Reservoir structure

It is necessary to characterise the reservoir structure on both local and regional scales to elucidate CO₂ migration patterns and bulk storage potential. Studies should include, as a minimum, structure mapping of depth to top reservoir, reservoir thickness and reservoir structural compartmentalisation.

A key step in characterising a potential storage reservoir is to estimate the extent of the likely storage footprint. Dependent on the geological setting, the storage footprint will be controlled by several parameters such as the existence, or otherwise, of a structural trap, the amount of CO₂ to be injected, likely migration paths and migration velocity of free (gaseous, liquid or supercritical) and dissolved CO₂, and resulting pressure increases due to the injection.

Dependent on the overall reservoir structural setting, the likely lateral and vertical spread of the CO₂ needs to be estimated or predicted. In general, we can distinguish between two basic storage geometries:

The **structural closure** (anticlinal trap), whereby free CO₂ is held buoyantly within a distinct subsurface volume, spatially limited by impermeable rocks surrounding the top of the CO₂ accumulation. A key advantage of the structural trap is that migration of free CO₂ *within the reservoir* is tightly constrained and likely to be of limited lateral extent. This is helpful both for estimation of storage capacity and also in risk analysis. The main disadvantage of the structural trap is the possibility, depending on trap geometry and reservoir thickness, of building up a tall, closed vertical column of stored CO₂. This will develop large buoyancy forces on the overlying caprock (Figure 4.1), challenging its capillary and structural integrity. A secondary drawback is the fact that the gas-water contact is limited to a quite small contact area, thereby restricting CO₂ dissolution processes.

In the case of storage in a structural closure, the geometry not only of the anticlinal trap has to be assessed, but also its downdip flanks and marginal downwarps where dissolved CO₂ (denser than saline formation waters) will ultimately migrate in the longer term (see Section 4.2.1).

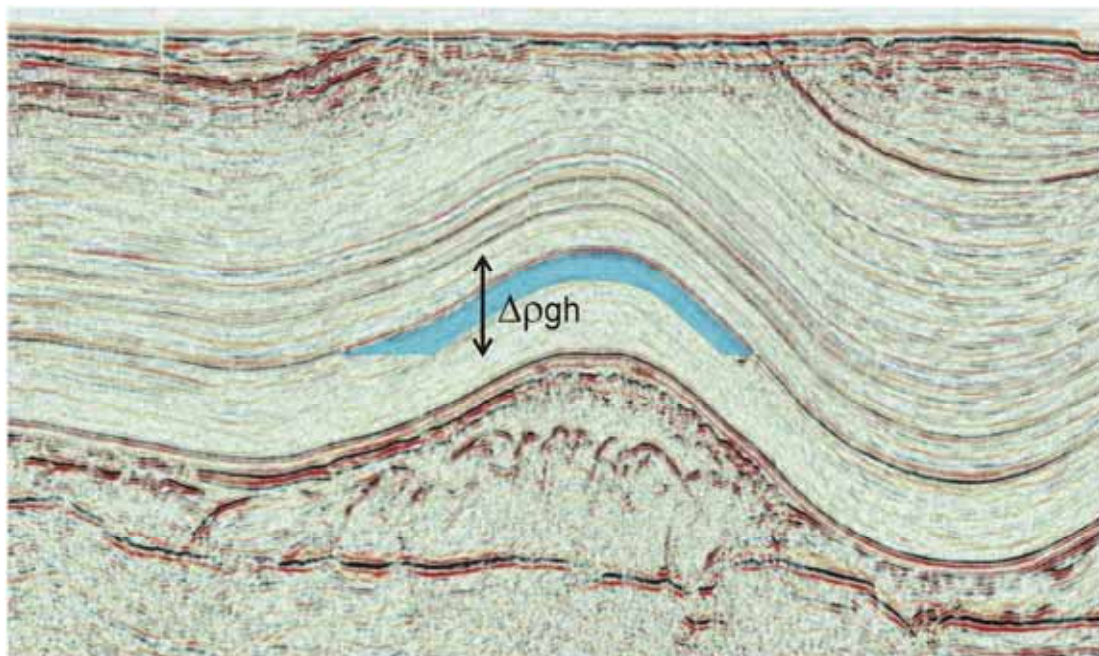


Figure 4.1 Buoyancy forces acting on the crest of the structural closure (seismic data courtesy of WesternGeco).

The so-called **open aquifer** occurs where CO₂ may spread laterally, largely unhindered, provided there are no lateral flow boundaries (compartmentalisation) within the reservoir. Injected CO₂ will initially migrate upwards driven by buoyancy until it reaches reservoir seals beneath which it can spread laterally. Accordingly, a large contact area with surrounding formation waters is created which facilitates the CO₂ dissolution processes, a very beneficial storage process (Section 4.2). A major disadvantage of a large storage footprint is that it requires a large area to be mapped in detail to identify potential leakage pathways (particularly faults, but also high-permeability sediment stringers in the immediate overburden, or shallow gas occurrences as indicators for previous or ongoing leakage), and also to be monitored.

4.1.1.1 Observations from the CO2STORE case studies

Sleipner

Geological characterisation prior to CO₂ injection focussed on the identification of structural traps and on the quantification of parameters relevant for injectivity. The top of the Utsira Sand was initially mapped on 2D seismic data and early 3D seismic data (from 1982). This map showed a large domal trap north-north-west of the Sleipner A platform which was preliminarily chosen as the potential storage site and which constituted the case for initial reservoir simulations (see Section 4.2.1). The Sleipner A Platform is situated above the margin of this trap and migration of injected CO₂ to the location of the production wells in the long term could therefore not be excluded. A 3D seismic survey acquired in 1994 revealed domal traps north-east of the Sleipner A platform. Mapping of the top of the Utsira reservoir showed the presence of a structural depression between these traps and the location of Sleipner A wells, thus providing a barrier to buoyancy-driven CO₂ migration. One of these traps was subsequently chosen as the injection site (see Section 4.2.1).

The main Sleipner geological characterisation is based on interpretations carried out during the operations phase, but is more appropriately presented here.

Detailed assessment of reservoir structure was based on the interpretation of a regional grid of 2D seismic profiles (~ 16 000 line km) together with a 3D seismic volume (~ 770 km²) around the injection point, the latter covering the area of predicted future CO₂ plume migration (Figure 3.9). Some 130 wells penetrated the reservoir unit (with around 30 wells within 20 km of the injection site), with interpreted stratigraphy, geophysical logs, and core material (reservoir and caprock), drill cuttings (reservoir and caprock) and three reservoir pressure measurements (two from Sleipner and one from the Brage field, around 250 km to the north). It is noted that the core material was actually acquired, on behalf of the SACS and CO2STORE projects, during the operations phase.

The 2D seismic and well data were used for regional reservoir mapping. The top reservoir surface generally varies quite smoothly in the depth range 550 to 1500 m, and is around 800–900 m near Sleipner (Figure 3.9). The reservoir sand forms two main depocentres, one in the south, around Sleipner, where thicknesses locally exceed 300 m, and another some 200 km to the north with thicknesses approaching 200 m. Spatial resolution of the reservoir topography is severely limited by the grid spacing of the 2D seismic data, typically 5 to 10 km.

Around the injection point itself, some 770 km² of 3D seismic data were interpreted, with special attention given to accurate analysis of top reservoir stratigraphy and topography and the identification of small faults that may influence CO₂ migration. Within the 3D volume, the top of the Utsira Sand dips generally to the south, but in detail it is gently undulatory with small domes and valleys. The Sleipner CO₂ injection point is located beneath a small domal feature which rises about 12 m above the surrounding area (Figure 3.10). The base of the Utsira Sand is structurally more complex, and is characterised by the presence of numerous mounds, interpreted as mud diapirs. Mud diapirism is associated with local, predominantly reverse, faulting that cuts the base of the Utsira Sand, but does not appear to affect the upper parts of the reservoir or its caprock (Zweigle et al., 2004).

The presence of a >5 m thick mudstone layer close to the top of the Utsira Sand (see more below) yielded an additional seismic reflector close to the reservoir top and allowed for a detailed interpretation of the geometry of the reservoir top. This revealed the existence of a channel in the uppermost leaf of the Utsira Sand, which was predicted to influence fluid flow at the reservoir top, a prediction which was confirmed later by the time-lapse seismic (Chapter 7).

The 2D and 3D seismic surveys constituted the key datasets, essential for delineating the reservoir limits, structure and stratigraphical correlation. The regional seismic datasets were proprietary, so the SACS project had no control over acquisition and processing parameters. The 2D data quality was variable, ranging from moderate early 1980s data to very good late 1980s data. Even the older datasets were mostly adequate for mapping the reservoir structure and extents. The later datasets enabled more accurate assessment of stratigraphical relationships both within the reservoir itself and also at the reservoir–topseal interface.

Kalundborg

The apex of the Havnsø structure is situated beneath the small harbour town of Havnsø, approximately 15 km northeast of Kalundborg (Figure 4.2).

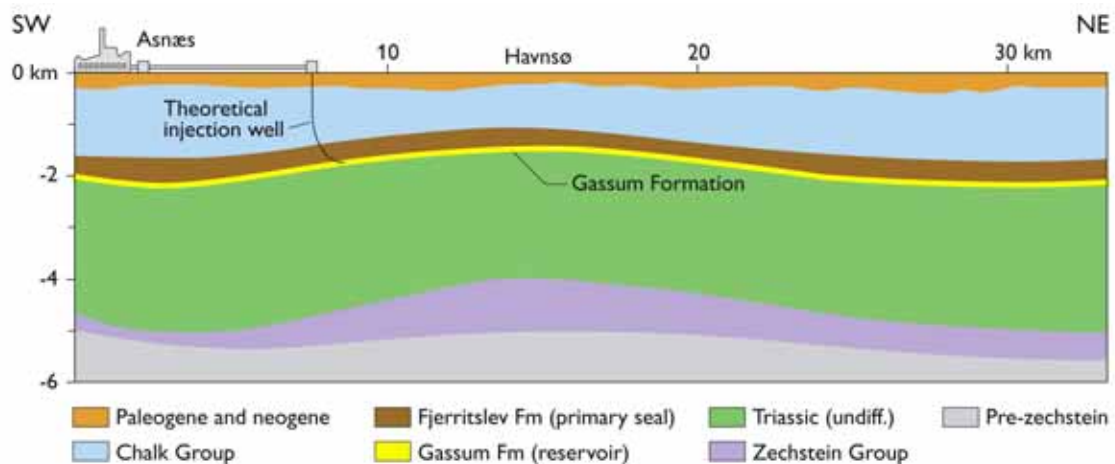


Figure 4.2 Schematic geological cross-section through the Havnsø structure.

About one third of the structure is situated offshore, with its structural culmination located beneath the land. The structure was evaluated for possible natural gas storage in the 1980s, but was rejected in favour of the Stenlille structure. The depth to the top point of the reservoir is ~ 1500 m and the closure is estimated to cover an area of ~ 166 km². The spill-point is situated in the south-eastern part of the structure at approximately 1850 m depth (Figure 3.14). The size of the structure makes it attractive for CO₂ storage, not only from the local point sources but also from industrial sources in the Copenhagen area (some 85 km away).

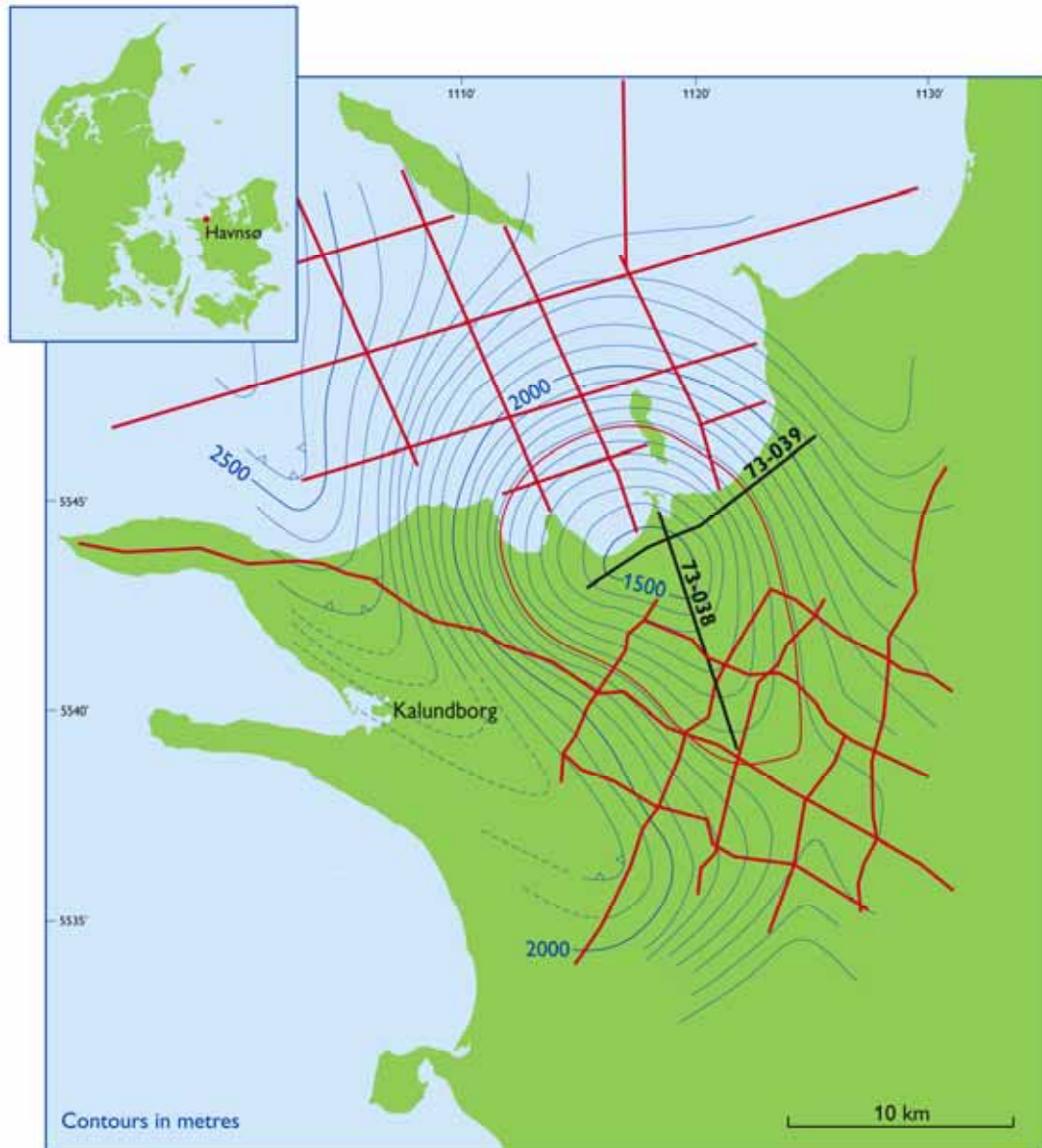


Figure 4.3 Seismic line map around the Havnsø structure (sample line shown in Figure 4.4).

The structure was identified on old, rather low-quality 2D seismic lines (Figures 4.3 and 4.4). At present no structural map has been published and the interpretation is based on GEUS internal work.

The Havnsø structure has not yet been drilled and the aquifer data are extrapolated from the Stenlille-1, Stenlille-19 and Horsens-1 wells (see below). Palaeogeographical models suggest that the reservoir quality of the sandstones decreases offshore towards the north-west relative to the Stenlille structure where the formation is well-known. The Gassum Formation has been described in detail elsewhere (Nielsen et al., 1989; Hamberg and Nielsen, 2000; Nielsen, 2003).

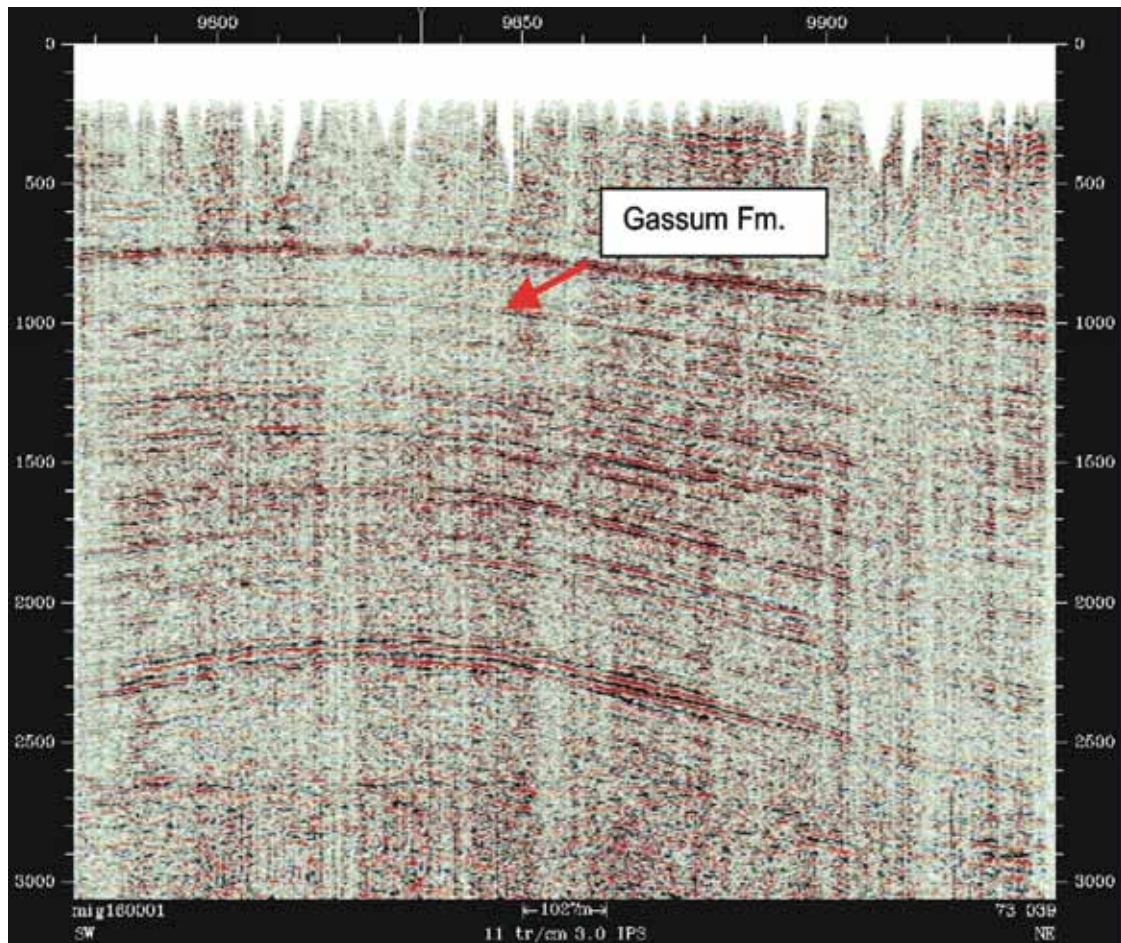


Figure 4.4 South-west to north-east seismic line (two-way time display) crossing the top of the Havnsø structure (from Larsen et al. 2007., Copyright: Geological Survey of Denmark and Greenland).

Mid Norway

No detailed characterisation of reservoir structure was carried out for the mid Norway case study. Details of the outline characterisation carried out for the Screening Phase are given in Chapter 3.

Schwarze Pumpe (Schweinrich)

No new data were acquired for the Schweinrich case study, assessment of the reservoir structure utilising only existing information.

At Schweinrich the footprint of the storage site can be split into two distinct components (Figure 4.5). The area occupied by free CO₂ is defined by the spill point contour on the structural closure, amounting to some 120 km². The total extent of long-term CO₂ migration in the dissolved state is much larger, comprising the downdip synclines flanking the primary storage site. It is clear however that surface risks associated with CO₂ storage in the dissolved state are extremely low since it is not subject to buoyancy-driven upward migration (see Section 4.5). Subsurface conflicts of use may need however to consider this type of long-term scenario.

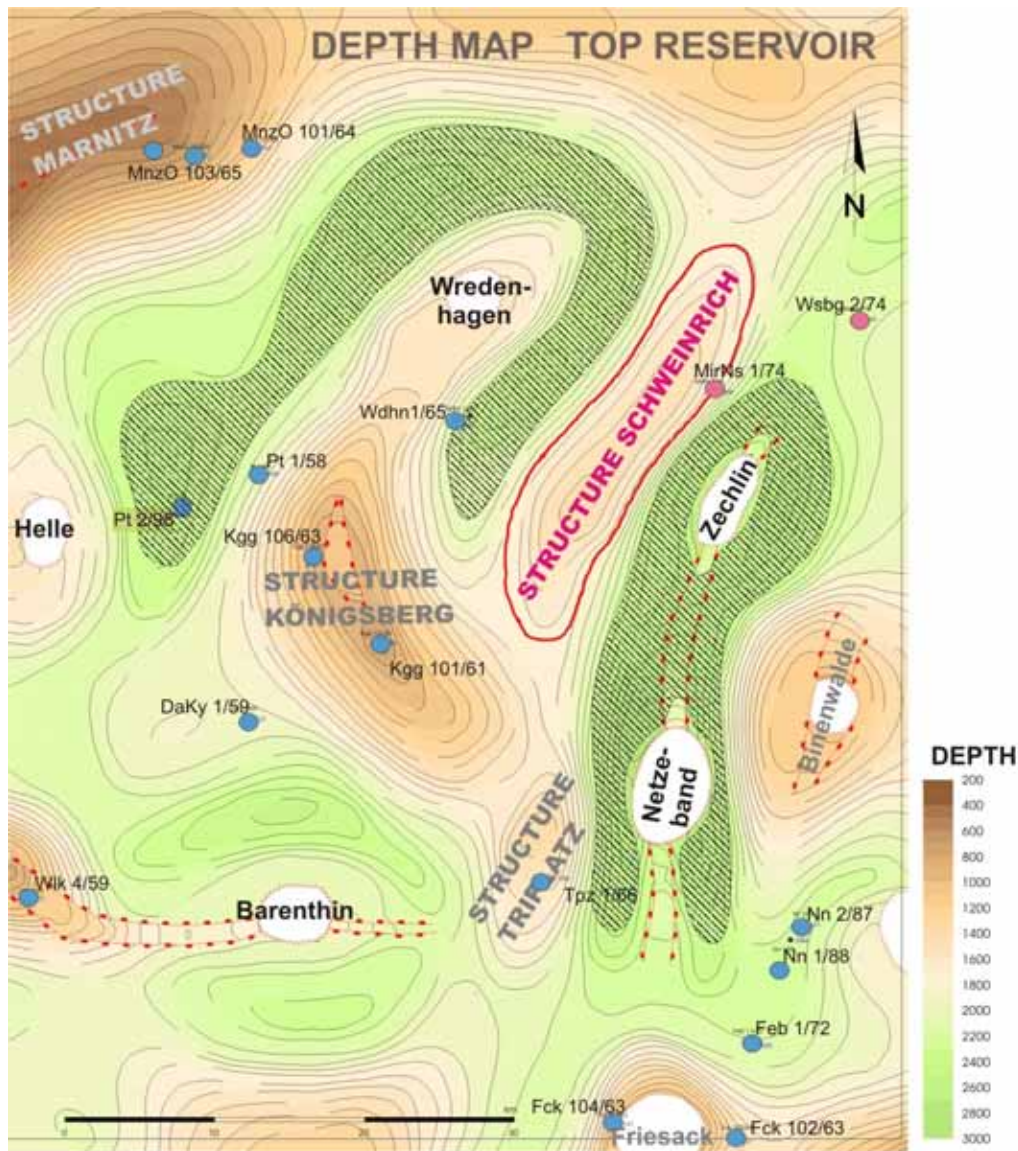


Figure 4.5 Depth map of the Schweinrich structure and the surrounding areas included in the site characterisation. Note that the final ‘footprint’ of dissolved CO₂ (hatched areas denote long-term resting-place of dense CO₂-saturated formation waters) is much more extensive than the structural closure, where the free CO₂ has been initially injected.

Valleys

The most suitable storage site for the Valleys project lies offshore in the St George’s Channel Basin some 110 km north-west of the proposed power-station site. Geological characterisation (Evans et al., 2004) was based on about 1700 km of 2D seismic data and six exploration wells. The datasets were sufficient to provide a good understanding of the overall basin structural and stratigraphical architecture (Figure 4.6), but were not able to provide sufficient detail of reservoir geology. Three main potential reservoir units were assessed: the Permo-Triassic Sherwood Sandstone Group, a series of thin Jurassic sandstones and a Cenozoic fluvio-deltaic sandstone sequence. Poor well coverage was a key limiting factor: Jurassic sand continuity could not be proven and promising sites in the Permo-Triassic on the south-east flank of the basin have been set aside for the time being due to lack of well information.

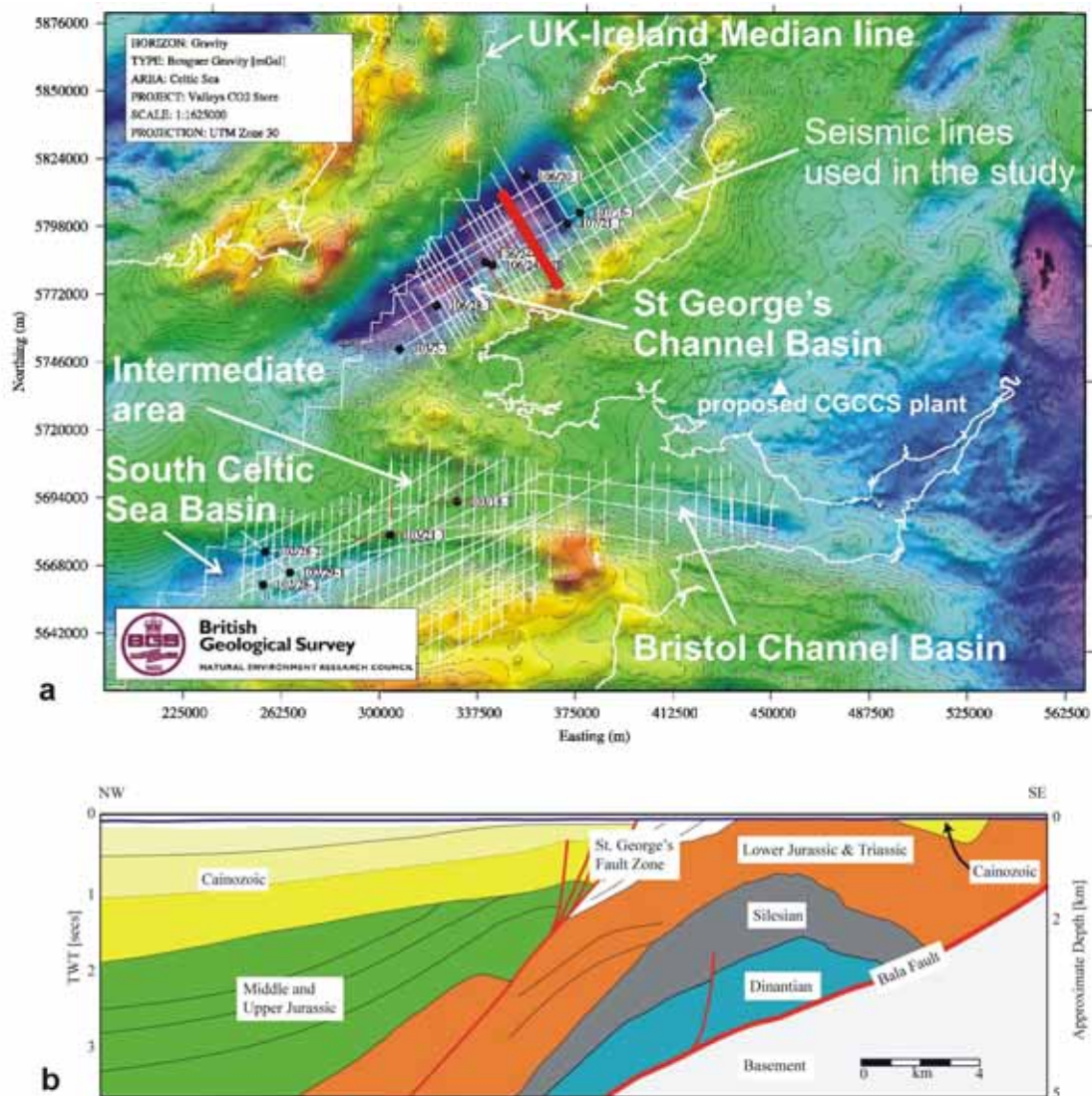


Figure 4.6 St Georges Channel Basin overview a) 2D seismic coverage b) cross-section through the basin (red line on map).

The Cenozoic sandstones were chosen as the preferred storage site because their relatively simple structural configuration allowed reasonable seismic control on reservoir geology despite the limited well information (see below).

4.1.1.2 Generic findings

The 2D and 3D seismic data generally constitute key datasets, essential for delineating reservoir limits, structure and stratigraphical correlation. Because regional reservoir mapping is relatively insensitive to data quality, cheaper, older datasets may offer good value for money. The same would not apply however to 3D data around the injection point. Careful assessment of data and requirements is recommended prior to purchase or acquisition.

At Sleipner, the large number of wells was useful for delineating regional structure, and was essential for mapping reservoir properties (see below). In general terms however, it is considered that a lesser amount of well data, perhaps only 20% of the

available dataset (albeit evenly distributed), would have been adequate for the purposes of the regional reservoir characterisation. In contrast, a reduction in the amount of the seismic data, depending on location, could have significantly reduced the confidence of the regional reservoir mapping. A proportionately similar reduction in well data would not have had such a seriously detrimental effect on the regional mapping, but would have adversely affected confidence in reservoir characterisation and storage estimates, particularly around the injection point.

As free CO₂ is buoyant in most storage situations, it will tend to rise to the top of the repository reservoir. Assessment of the depth to the top of the reservoir is therefore a basic prerequisite of CO₂ storage. It allows a first order estimate of short-term storage capacity, and permits likely migration pathways and extents to be assessed. The accuracy to which structure needs be resolved however, depends on the structural form of the reservoir into which the CO₂ is injected. If injection is into a large domal structure with closure of several tens of metres or more, CO₂ migration trends are likely to be well constrained and small uncertainties in reservoir geometry are not significant. If, on the other hand, the injection is into a reservoir with gentle dips and only minor topography at its top (as at Sleipner), very detailed depth mapping is required. This will permit accurate definition of the structure of the top surface to allow the prediction of the overall migration direction and evaluation of the location and volume of any structurally defined traps along the migration paths. Detailed subsurface structural mapping requires a 3D seismic survey around the injection site. In the case of very low structural relief it is essential to produce an accurate depth map. This requires sufficient velocity control from nearby boreholes to minimise uncertainties in depth conversion. The Sleipner case provides a good example. The top of the reservoir above the injection point is gently undulating but relatively flat. Uncertainty of just a few metres in regional depth trends (requiring less than 1% error in depth conversion) will radically alter the modelled migration direction (see below). This has impacts not only on assessing the long-term safety case, but also, from a practical point of view, the design of future monitoring surveys.

It is important to identify and map any faults in the reservoir and caprock, and to make some assessment of fault sealing capacity (e.g. by empirical fault gouge shale ratio estimation), so as to be able to detect and assess possible reservoir compartmentalisation and/or the potential for fault-related migration. Reservoir structural compartmentalisation could lead to a rapid increase in formation pressures with time as fluid flow between compartments is inhibited and is a key input to reservoir flow models. Fair quality 2D seismic should be sufficient to identify the presence of larger faults, but accurate mapping of fault networks and linkages requires 3D data coverage. In particular, robust mapping of small localised areas of faulting, such as commonly occur on structural crests, requires 3D seismic coverage with adequate resolution.

Disadvantages of closed structures relate to the tall, confined columns of CO₂ that may develop, particularly if the reservoir unit itself is quite thin, with high resulting buoyancy forces. In such cases, particular attention must be paid to the capillary sealing efficacy of the caprock and to its geomechanical stability.

4.1.2 Reservoir properties

Once the general architecture of the storage system is established, data gathered from wells are essential to determine the most relevant properties of the reservoir. Lithological and petrophysical data have to be derived from wells drilled at or near the storage location.

It is essential to assess the lateral and vertical stratigraphical and fluid flow properties of the reservoir, as these control the evolution of the CO₂ plume. As above, the presence of stratigraphical reservoir compartmentalisation is a key input to reservoir flow models. Facies interpretations (homogeneity, possible structural compartmentalisation) and the sand/shale ratio control the number of required injection wells, the injectivity and the overall reservoir performance. A systematic joint/fault analysis from core examinations (e.g. RQD index) can provide useful information to assess general hydraulic parameters in some reservoirs.

Detailed geochemical and mineralogical analysis is essential to predict likely reactions between dissolved and gaseous CO₂, the host rock, and saline fluids within the reservoir. For the reservoir, the amount of CO₂ reactive minerals is relevant to predicting possible changes in porosity and permeability and also the potential of the reservoir to fix CO₂ more-or-less permanently as precipitated minerals (Section 4.3).

4.1.2.1 Observations from the CO2STORE case studies

Sleipner

The main analysis of stratigraphy and reservoir properties of the Utsira Sand, with emphasis on the Sleipner area, was carried out in the operations phase, but is more appropriately reported here.

Structural mapping of the reservoir prior to injection has been summarised above. Prior to submission of the field development plan ('Plan for utvikling og drift'; PUD), a brief petrophysical study of the Utsira reservoir, based on wire-line logs from six wells in the Sleipner area, was carried out to yield key parameters for reservoir simulations (Section 4.2.1). Both net-to-gross ratio and porosity for several reservoir zones within the Utsira Sand were determined. Permeability was estimated from experience with other rocks of similarly high porosity.

Internally the Utsira Sand comprises stacked overlapping 'leaves' or 'mounds' of very low relief, interpreted as individual fan-lobes and commonly separated by thin intra-reservoir mudstone horizons. It is interpreted as a composite lowstand fan, deposited by mass flows in a marine environment with water depths of 100 m or more.

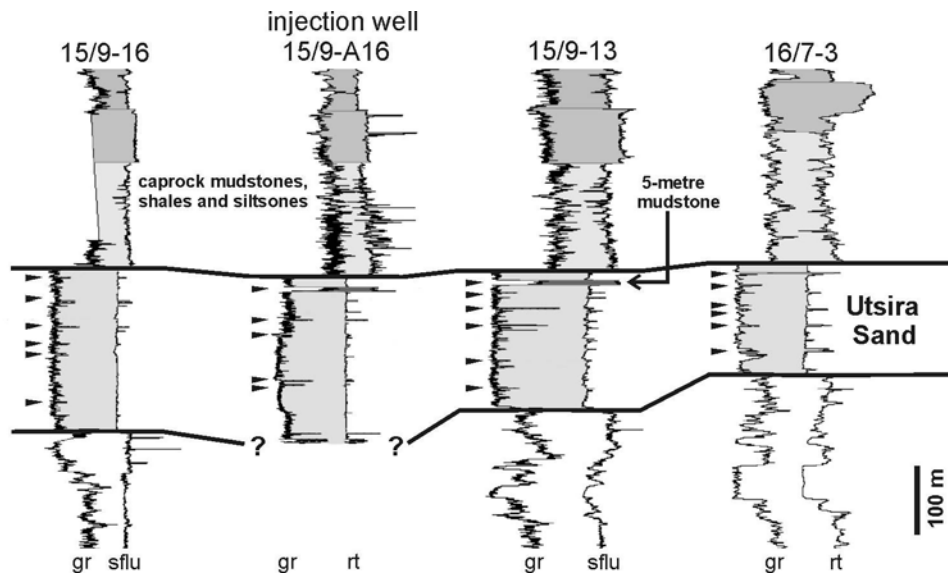


Figure 4.7 Geophysical logs from wells around the Sleipner injection site. The Utsira Sand has much lower gamma-ray (gr) signature than the caprock succession. Gamma-ray peaks within the reservoir sand (main peaks arrowed), are interpreted as thin beds of mudstone. Note the injection well is strongly deviated so the drilled sequence will differ from that at the plume location, especially with respect to the number and position of the mudstone beds.

On geophysical logs the reservoir characteristically shows a sharp top and base (Figure 4.7), with the proportion of clean sand in the reservoir unit varying generally between 0.7 and 1.0. The shale fraction mostly comprises a number of thin silty mudstone beds (typically about 1m thick), which show as peaks on the gamma-ray, sonic and neutron density logs, and also on some induction and resistivity logs. In the Sleipner area, a thicker mudstone (here termed the ‘five metre mudstone’ though it is estimated at 6 to 7 m thick around the injection point) separates the uppermost leaf of the sand from the main reservoir beneath. The mudstone layers constitute important permeability barriers within the reservoir sand, and have proved to have a significant effect on CO₂ migration through, and entrapment within, the reservoir. Notwithstanding this, the five-metre mudstone was expected to be effectively tight for free CO₂, an expectation which the time-lapse seismic analysis has proved to be wrong. The structural and stratigraphical detail which the geophysical data have revealed around the injection point is essential to understanding and predicting the long-term behaviour of the CO₂ plume (Section 4.2).

Macroscopic and microscopic analysis of core and cuttings samples of the Utsira Sand show a largely uncemented fine-grained sand (Figure 4.8), with medium and occasional coarse grains (Figure 4.9). The grains are predominantly angular to sub-angular and consist primarily of quartz with some feldspar and shell fragments and minor sheet silicates (Table 4.1). Porosity estimates of the core, based on microscopy, range generally from 27% to 31%, locally up to 42%. Laboratory experiments on the core give porosities from 35–42.5%. These results are broadly consistent with regional porosity estimates, based on geophysical logs, which are quite uniform, in the range 35 to 40% over much of the reservoir.

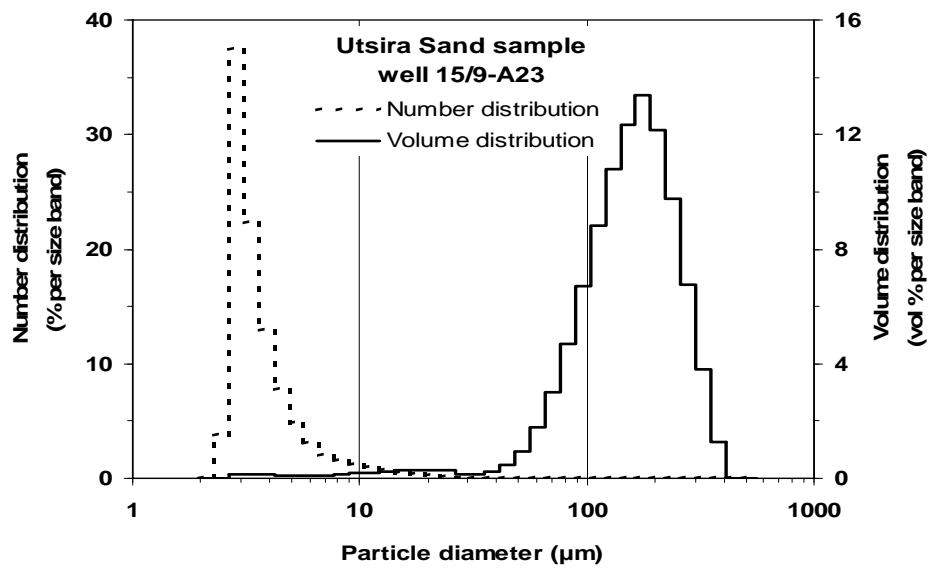


Figure 4.8 Grain size distribution in the Utsira Sand (from core material).

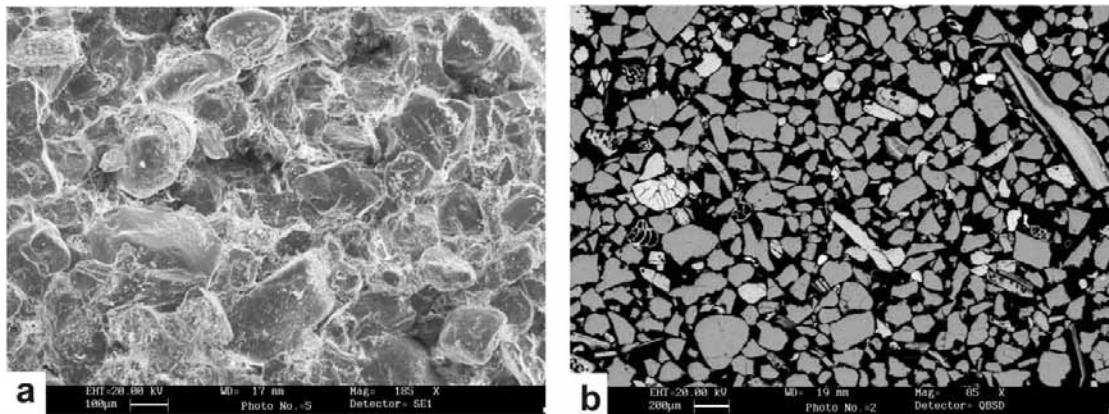


Figure 4.9 SEM images of the Utsira Sand a) reflected light b) transmitted light (pore-spaces are black).

In addition to the physical properties of the reservoir, its mineralogical and chemical properties are essential for robust geochemical modelling (Section 4.3). Detailed mineralogy of the Utsira Sand was obtained by XRD analysis (Table 4.1).

grain size	porosity	permeability	sand/shale ratio	% mineral					
				quartz	calcite	K-feldspar	albite	aragonite	mica and others
fine (medium)	35 - 40 % (27 - 42 %)	1 - 3 Darcy	0.7 - 1.0 (0.5 - 1.0)	75	3	13	3	3	3

Table 4.1 Utsira Sand properties.

Kalundborg

Lithologically the aquifer is expected to be roughly similar to that described for the Gassum Formation at the Stenlille gas storage facility, where the basal part comprises a thick, relatively coarse-grained sandstone unit (Figure 4.10).

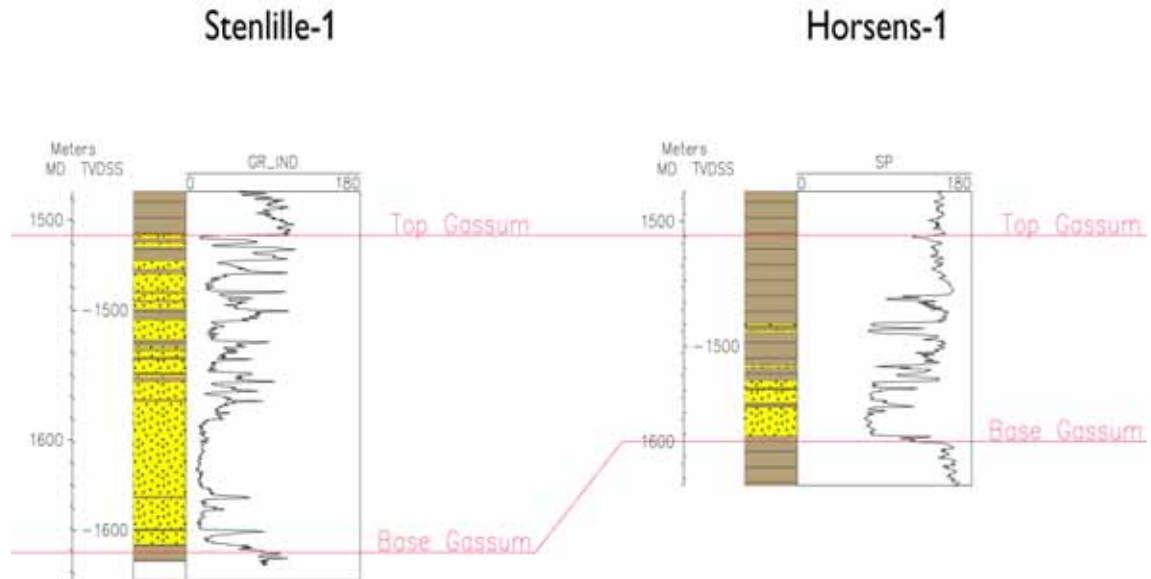


Figure 4.10 Petrophysical well logs of the Stenlille-1 and Horsens-1 wells showing the interpreted sand/shale ratios and lateral variability of the primary reservoir unit. The top and base of the reservoir is based on interpretations given in Nielsen and Japsen (1991).

Compartment no.	Reservoir model layer(s)	% of total pore volume	Pore volume (m ³)	Storage capacity (tons)
1	1	5.7	0.21x10 ⁹ m ³	48x10 ⁶ tons
2	2	1.3	0.05x10 ⁹ m ³	11x10 ⁶ tons
3	3 – 7	14.9	0.55x10 ⁹ m ³	126x10 ⁶ tons
4	8	1.2	0.04x10 ⁹ m ³	10x10 ⁶ tons
5	9 - 15	76.9	2.85x10 ⁹ m ³	651x10 ⁶ tons
Total reservoir	1 - 15	100.0	3.70x10⁹ m³	846x10⁶ tons

Table 4.2 Definition, pore volume and estimated storage capacity of the five reservoir compartments in the Havnsø structure.

This unit is overlain by four sequences containing fine-grained sandstones and mudstones (Nielsen et al., 1989) (Table 4.3).

Wells	Stratigraphical units with possible reservoirs				Reservoirs					
			Depth Interval MDm	Gross reservoir thickness (m)	Sand cut off value	Net reservoir thickness (m)	Sand / gross ratio	Porosity (%)	Permeability (mD)	Temp (°C)
Horsens-1		Lower Cretaceous undifferentiated	1111–1168	57						
	Gassum Fm	Gassum Fm	1449–1543	94	90 API SP	25	0.26	S–31, C–25	G–500	
Stenlille-1		Lower Cretaceous undifferentiated	1158–1205	47	GR=56	1	0.02			
	Gassum Fm	Lower Jurassic 2; TS 10–TS 11	1326–1398	72	GR=56	9	0.13			
		Lower Jurassic 1; TS 7–TS 10	1398–1465	67	GR=56	6	0.09			
		Gassum Fm; Base Gassum – TS 7	1465–1609	144	GR=56	110	0.76	20–25		60–70

Table 4.3 Reservoir data from wells closest to Havnsø. Porosity values are given by S: porosity based on FDC log, C: porosity measured on core. The permeability values are given by G: air permeability measure on core (based on Michelsen, 1981).

Porosity varies between the different reservoir units but an average of 22% has been applied for the storage calculations. The permeability of the Havnsø structure is uncertain, but is estimated to be comparable to the values seen in Stenlille where the Gassum Formation occurring at similar depth has an average permeability around 500 mD, suitable for obtaining high injection rates of CO₂.

Based on the reservoir information from the Stenlille natural gas storage site, and the north-westwards facies changes of the Gassum Formation, the gross thickness is estimated to be 150 m with a net/gross of 0.67 leading to approximately 100 m of net sand. No information exists on the actual reservoir pressure and temperature, so hydrostatic pressure and regional temperature gradients have been applied in the storage calculations. The structure is calculated to hold a maximum of 1028 Mt of CO₂. A more detailed model for the reservoir is presented by Bech and Larsen (2003, 2005).

Mid Norway

More detailed analysis of the Froan Basin succession, though carried out as part of the Screening Phase (Bøe et al., 2005), is more appropriately included here within reservoir characterisation.

No deep well information is available from the Froan Basin itself, so reservoir properties can only be estimated from regional considerations (Figure 4.11). On the Trøndelag Platform, Triassic and older rocks have very low porosities and permeabilities (Bugge et al., 1984). They are thus probably unsuitable for CO₂ storage and have not been further considered in this study.

A description of the Mesozoic and Cenozoic lithostratigraphic succession offshore mid Norway was provided by Dalland et al. (1988). The reservoir rocks with the largest theoretical storage potential are of Early to Mid Jurassic age (Figure 4.11). Younger rock units are mostly fine-grained and/or glacial tills. They are thus considered as potential seals to the Jurassic sandy formations. On the south-eastern Trøndelag Platform, the formations with assumed storage potential are the Jurassic Åre, Tilje, Ile, and Garn formations, separated by the shale-dominated Ror and Not formations.

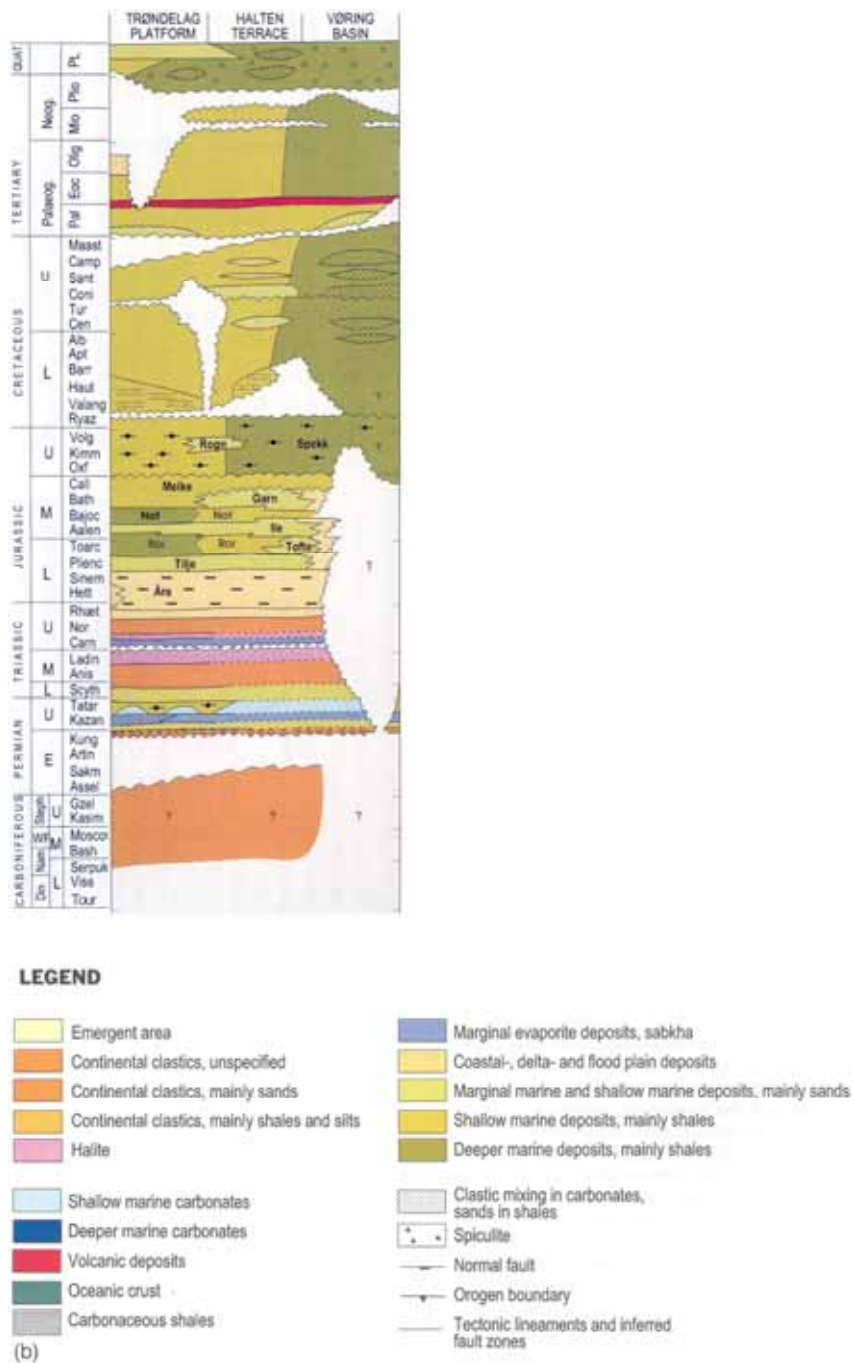


Figure 4.11 Stratigraphy of the Trøndelag Platform (modified from Brekke et al., 2001 Elsevier).

The only stratigraphical wells that have penetrated Jurassic sequences in the Froan Basin area are those belonging to a shallow sampling program along the southeastern margin of the Trøndelag Platform (Bugge et al., 1984). Samples were collected with electric rock core drilling and vibrocore, which limited the core lengths to 5.5 m and 6 m respectively. A large number of exploration wells have drilled the Jurassic successions on the Haltenbanken Terrace however (Dalland et al. 1988). Potential CO₂ storage units are summarised below.

The Tilje Formation comprises fine to coarse-grained sandstones interbedded with shales and siltstones. The sandstones are commonly moderately sorted, have high clay content, and most beds are bioturbated. Shale clasts and coaly plant remains are common. Pure shale beds are rare; most of the finer grained interbeds are silty or sandy. The shallow sampling data close to the coast indicates time equivalent deposits dominated by coarse-grained clastics. The formation was deposited in nearshore marine to intertidal environments characterised by a gradual transition to continental environments eastwards (Bugge et al., 1984).

The Ile Formation comprises fine to medium and occasionally coarse-grained sandstones with varying sorting are interbedded with thinly laminated siltstones and shales. Mica-rich intervals are common. Thin carbonate-cemented stringers occur, particularly in the lower parts of the unit. The formation represents various tidal-influenced delta or coastline settings. Sandstone-dominated successions of similar age have been located by sea-bottom sampling and shallow drilling on the eastern part of the Trøndelag Platform (Bugge et al., 1984).

The Garn formation consists of medium to coarse-grained, moderately to well-sorted sandstones. Mica-rich zones are present. The sandstone is occasionally carbonate-cemented. The Garn Formation may represent progradations of braided delta lobes. Delta top and delta front facies with active fluvial and wave-influenced processes are recognised. Time-equivalent deposits have been mapped in the Frohavet and Beitstadvjord Basins further east (Sommaruga and Bøe, 2002).

Aquifer parameters for the Tilje, Ile and Garn formations in Haltenbanken (Table 4.4) are assumed to be representative also for the Jurassic deposits in the Froan Basin.

Formation	Aquifer thickness (m)	Porosity at 2000 m depth	Porosity at 3000 m depth	Permeability at 2000 m depth (mD)	Permeability at 3000 m depth (mD)	Net/ Gross at 2000 m depth	Net/ Gross at 3000 m depth
Garn	50	30%	20%	5000	1000	1	0.9
Ile	50	28%	21%	5000	650	0.85	0.65
Tilje	100	25%	20%	1000	500	0.85	0.65

Table 4.4 Properties of potential reservoir units, mid Norway (primary sources referenced in Lundin et al., 2005).

Schwarze Pumpe (Schweinrich)

No new datasets were acquired for the Schweinrich site characterisation, assessment of reservoir properties being limited to existing information.

The Schweinrich storage reservoir comprises two Mesozoic saline aquifers, the Rhaetic and the Liassic. The two reservoirs are separated by a major argillaceous unit more than 10 m thick. With respect to CO₂ storage, both reservoirs are assumed to be hydraulically connected. Within the extent of the structural closure the combined thickness of the two reservoir units ranges between 270 and 380 m. The entire reservoir is overlain by thick Jurassic clay formations several tens of metres thick.

Sample Nr	Cap rock	Reservoir	Well	Depth [m]	Stratigraphy and lithology
1		X	Mir 1/74	1899,6	Contorta, sandstone, massive, homogenous, very well sorted, carbonate-free, grey, crumbly, minor cemented.
2		X	Mir 1/74	1898,3	Contorta, sandstone, massive, well sorted, uniform cross beddings, carbonate-free, crumbly, minor cemented, micas, bleached yellowish-grey.
3		X	Mir 1/74	1707,9	Hettangium, sandstone, massive, well sorted, thin interbeddings/cross beddings of silt, micas and plant detritus, carbonate-free, phacoidal structures, grey, hard.
4		X	Mir 1/74	1663,9	Hettangium, sandstone, massive, homogenous, well sorted, cross beddings, carbonate-free, reddish-grey, hard.
5		X	Mir 1/74	1662,7	Hettangium, sandstone, massive, homogenous, well sorted, cross beddings, fine laminations with silt and plat detritus, carbonate-free, grey, hard.
6	X		W sbg 2/74	2047,8	Sinemur, claystone, carbonate-free, fine laminated, homogenous, red-brown, tight, hard, argillite.
7	X		W sbg 2/74	2040,7	Sinemur, claystone, slight carbonatic, fine laminated, homogenous, red-brown, greenish grey, tight, hard, argillite.
8	X		W sbg 2/74	2030,2	Sinemur, claystone, carbonate-free, fine laminated, homogenous, dark grey, tight, argillite.
9	X		W sbg 2/74	2019,7	Sinemur, claystone - marl, carbonatic, laminated, dark grey to light grey, reddish brown, tight, hard, harnish, argillite.
10	x		W sbg 2/74	2015,7	Sinemur, claystone, carbonatic, fine laminated, dark grey to light grey, tight, hard, argillite.

Table 4.5 Lithological description of samples taken from wells MirNs 1/74 (reservoir sandstones) and Wsbg 2/74 (caprock claystones).

Both reservoirs were deposited in a shallow marine to lacustrine setting. Thick sandstone sequences are repeatedly intercalated with silt and shale layers. The overall sand-shale distribution has been determined from geophysical well logs (gamma ray and spontaneous potential).

Regional epirogenic movements, combined with sea-level changes and the syn-sedimentary uplift and emplacement of several salt structures (diapirs and pillows) strongly influenced the sedimentary facies and the sand-shale ratio. Parts of the reservoir were deposited within the peripheral trough during the uplift of a diapir with consequently higher thicknesses and enhanced shale contents.

Lithological, geochemical and mineralogical analyses (Tables 4.5, 4.6 and 4.7) confirm a quartz-rich sandstone with up to 8 % feldspars and low contents of clay- and heavy minerals (mostly illite and pyrite). In thin section the reservoir sands are seen to be poorly cemented with carbonates (ankerite, siderite and dolomite). Variable amounts of diagenetically formed quartz overgrowths can also be seen (Figure 4.12).

Sample	SiO ₂	TiO ₂	Al ₂ O ₃	Fe ₂ O ₃	MnO	MgO	CaO	Na ₂ O	K ₂ O
Sandstone 1	93,8	0,363	1,75	0,25	0,006	0,02	0,123	0,78	0,73
Sandstone 2	94,23	0,187	1,82	0,29	0,005	0,06	0,095	0,77	0,77
Sandstone 3	88,12	0,602	4,32	2,06	0,06	0,28	0,112	0,4	0,82
Sandstone 4	97,36	0,085	0,91	0,21	0,002	<0.01	0,062	0,09	0,39
Sandstone 5	96,34	0,176	1,28	0,34	0,005	0,03	0,068	0,12	0,39

Sample	P ₂ O ₅	SO ₃	F	Ba	Cr	Cu	Ni	Pb	Rb	Sr	Th	V	Zn
Sandstone 1	0,018	0,04	<0.05	270	77	<10	8	<4	22	42	8	17	4
Sandstone 2	0,014	0,02	<0.05	405	35	<10	8	5	24	41	6	17	3
Sandstone 3	0,025	0,01	<0.05	191	77	<10	12	<4	29	30	9	23	10
Sandstone 4	0,008	<0.01	<0.05	90	30	<10	4	5	16	15	5	6	6
Sandstone 5	0,01	0,03	<0.05	98	51	<10	5	5	16	15	<5	<5	8

Table 4.6 Geochemical composition of the reservoir sandstones (Hettangium and Contorta). Main components are quartz and feldspars.

Sample	Quartz	Illite	Kaolinite	Albite	K-Feldspar	Calcite	Dolomite Ankerite	Siderite
Sandstone 1	85-90	<i>n. p.</i>	<i>n. p.</i>	4	4-5	<i>n. p.</i>	<i>n. p.</i>	<i>n. p.</i>
Sandstone 2	90	<i>n. p.</i>	<i>n. p.</i>	3	5	<i>n. p.</i>	<i>n. p.</i>	<i>n. p.</i>
Sandstone 3	80	10	3	1-2	1	<i>n. p.</i>	<i>n. p.</i>	2
Sandstone 4	95	<i>n. p.</i>	<i>n. p.</i>	<i>n. p.</i>	3	<i>n. p.</i>	<i>n. p.</i>	<i>n. p.</i>
Sandstone 5	95	<i>n. p.</i>	<i>n. p.</i>	< 1	2	<i>n. p.</i>	<i>n. p.</i>	<i>n. p.</i>

Sample	Rutil & Anatase	Fe-Oxhydroxide	Halite	TC	TOC	TIC	CaCO ₃ [%], (calc.)	Density [g/cm ³]
Sandstone 1	< 0.5	< 0.5	1	0,03	0,03	0,00	<i>n. p.</i>	2,702
Sandstone 2	« 0.5	< 0.5	1	0,04	0,04	0,00	<i>n. p.</i>	2,748
Sandstone 3	0,5	« 0.5	<i>n. p.</i>	0,49	0,21	0,28	2,3	2,699
Sandstone 4	<i>n. p.</i>	« 0.5	<i>n. p.</i>	0,15	0,13	0,02	0,2	2,706
Sandstone 5	<i>n. p.</i>	0,5	<i>n. p.</i>	0,17	0,16	0,01	0,1	2,699

Table 4.7 Mineral composition and chemical characteristics of the reservoir sandstones (Hettangium and Contorta). XRD analysis in weight%. TC = total carbon, TOC = total organic carbon, TIC = total inorganic carbon, *n. p.* = not proven.

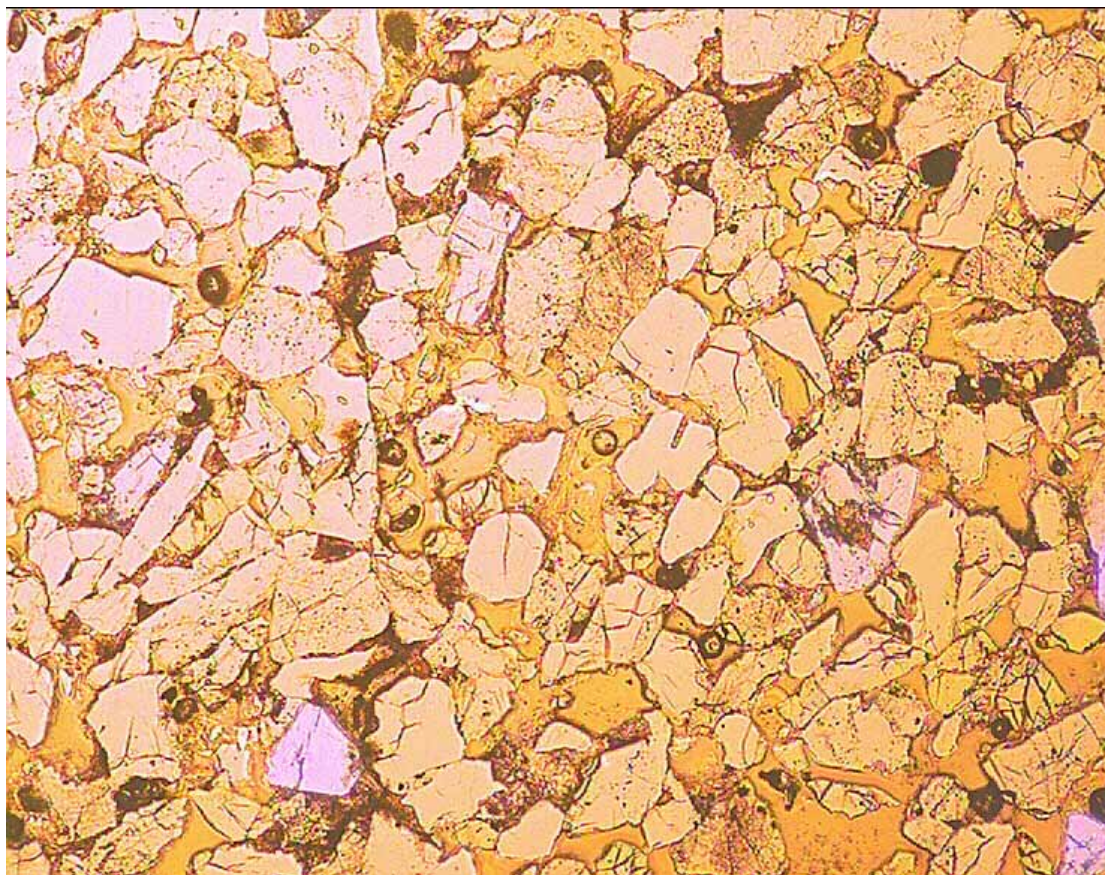


Figure 4.12 Thin section of a highly porous, well sorted and grain supported Liassic sandstone from the Schweinrich reservoir.

Valleys

As discussed above, the basal Cenozoic section was selected as the most promising storage reservoir. More than 1500 m of Cenozoic rocks are preserved in a large faulted syncline cut by the east-north-east trending St Georges Fault (Figure 3.24). Well 106/24-1 encountered a basal Cenozoic succession some 160 m thick (Figure 4.13), of which 63 m were sandstones, giving a net-to-gross ratio of 0.39. Subordinate clays and lignites are present and log characteristics suggest the presence of upward fining and coarsening sandstone units deposited in fluvial environments. The sandy succession is likely to be sealed by the overlying Cenozoic strata, the lower 300 m of which comprise mainly of clay and lignite.

Petrographical and mineralogical analysis of reservoir samples was carried out utilising SEM and XRD methods (Kemp and Bouch, 2004), and compositional data were incorporated into geochemical modelling studies (Section 4.3). Porosity estimates derived from the sonic and density logs suggest that some individual sand bodies within the target storage succession have porosities as high as 40 % (Figure 4.13).

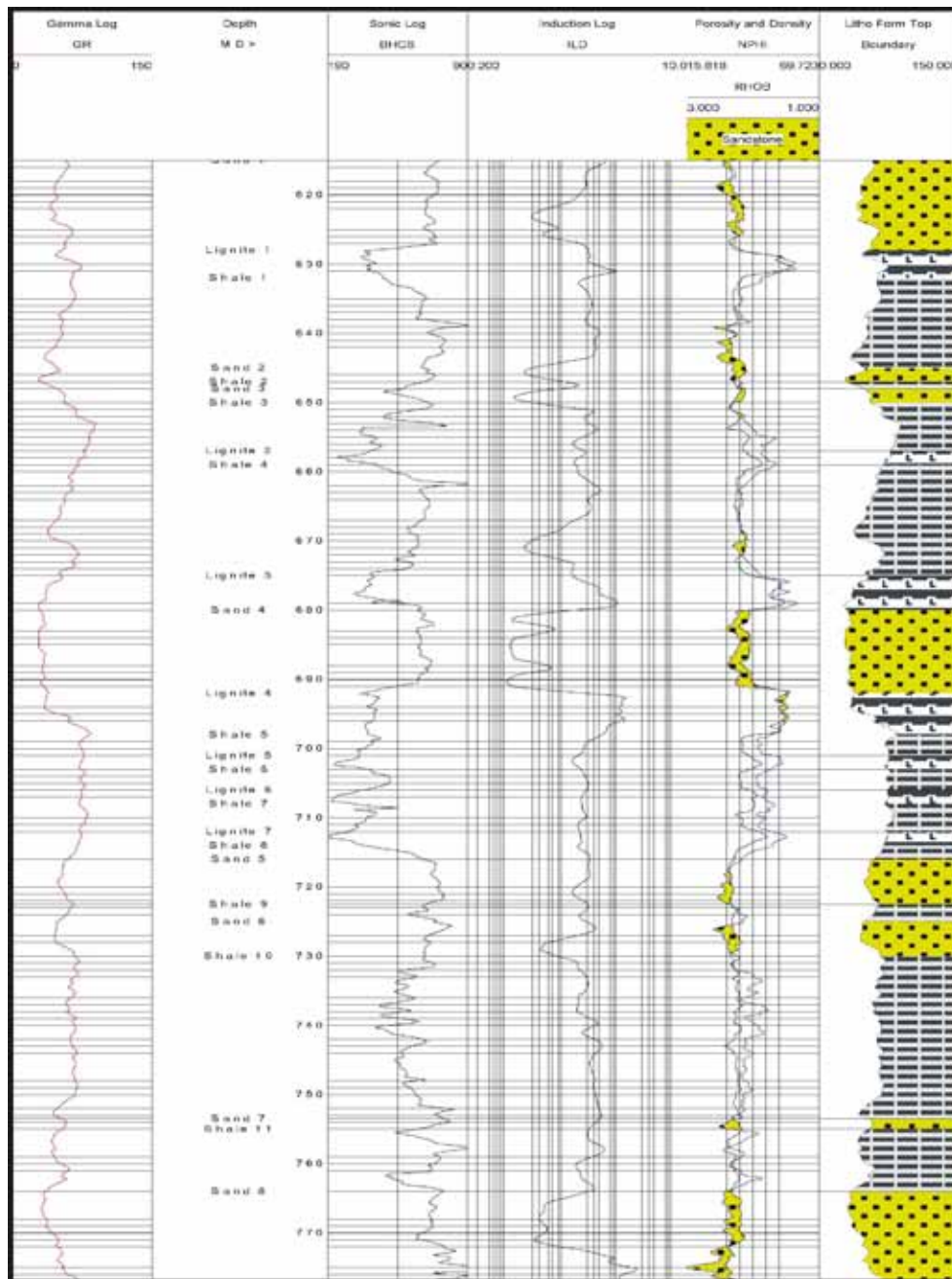


Figure 4.13 The basal Cenozoic sandstone sequence encountered in well 106/24-1 from the St George's Channel Basin.

The sandy unit is mappable on the seismic over an area of about 180 km², with good general continuity. Taking a net/gross ratio of 0.39 and an average porosity of about 20%, the estimated pore volume of the sand at depths greater than 800 m is approximately 10⁹ m³, equivalent to around 600 Mt of supercritical CO₂.

The area downdip and to the north of wells 106/24-1 and 106/24-A2B (Figure 4.14) represents the best prospect for a CO₂ storage site in basal Cenozoic sands. Here a north-west-trending saddle divides the main basin into two depocentres. A north-east to south-west seismic section along the saddle shows a broad synformal geometry, the target sand rising, over a distance of several kilometres, from the saddle at a depth of just over 1000 m to less than 600 m adjacent to the St George's Fault (Figure 4.14).

Around well 106/24-1 there is three-way dip closure against the fault. The fault has been intruded by salt along much of its length to form a salt wall, which enhances sealing potential along the fault plane (Section 4.3).

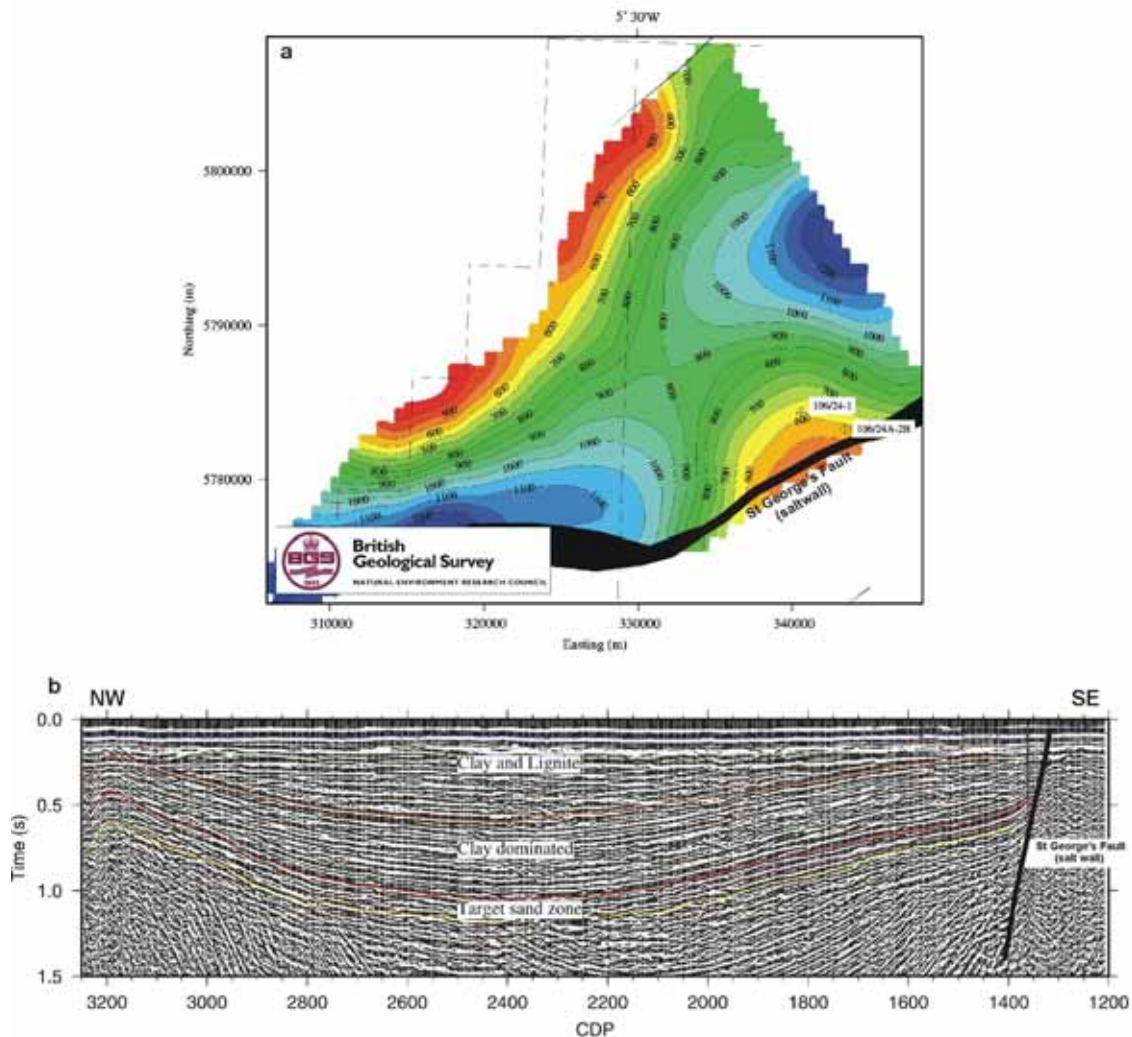


Figure 4.14 a) Depth map of the top of the Cenozoic sand succession. b) Seismic line showing closure against the St George's Fault corresponding to the salt wall. Seismic data courtesy of WesternGeco.

The well coverage is too sparse and the seismic resolution insufficient to map the continuity of individual sand bodies in three dimensions. Two models of reservoir lithology were developed. The simpler model incorporated a reservoir interval comprising 13 layers of alternating sheet sand and mudstone, with thicknesses and vertical distributions taken from well 106/24-1. The second, more complex model used a stochastic distribution of fluvial sandstone bodies within mudstones and local coaly horizons (Figure 4.15). The model was constrained to fit the sandstone geometries present in the two available exploration wells (106/24A-2B and 106/24-1) and is considered to be the most realistic reservoir model that could be generated from the available data. Both models were considered in the reservoir flow simulations.

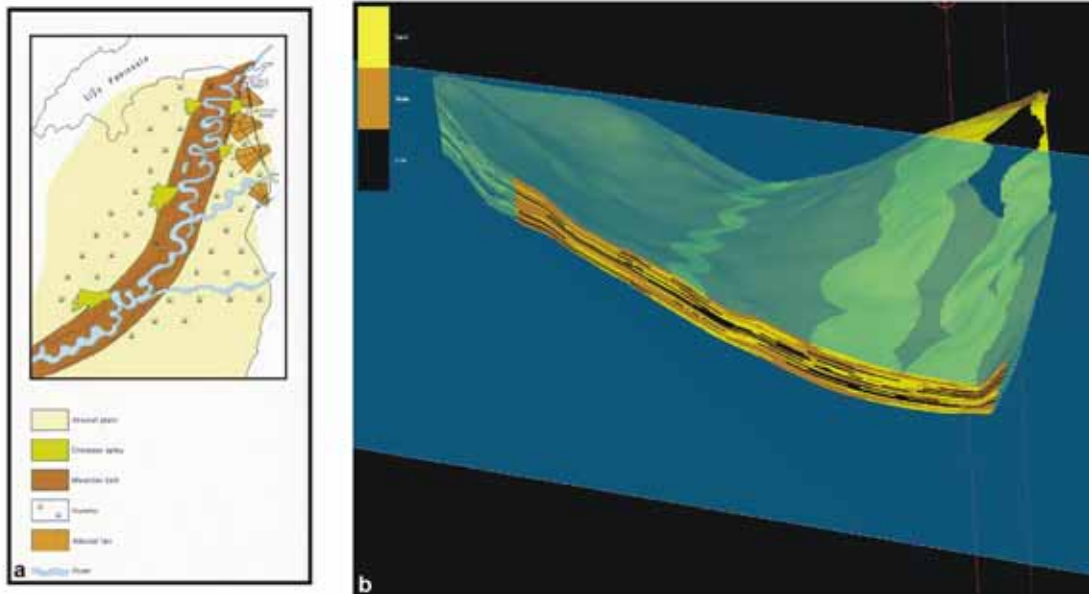


Figure 4.15 Reservoir model of the Cenozoic sands, St. George's Channel Basin. a) Schematic early Cenozoic palaeogeography of the reservoir. b) Stochastic sand-mudstone-coal reservoir model based on assumption of fluvial facies.

4.1.2.2 Generic findings

Knowledge of reservoir properties, such as porosity and permeability, is required to quantify potential storage capacity and likely migration paths and rates. To determine these properties, the importance of having core material from the reservoir close to the injection point cannot be overemphasised. Core and cuttings material from additional wells will further improve characterisation, particularly if vertical and lateral reservoir inhomogeneity is suspected. It should be noted that, taken in isolation, cuttings samples of reservoir sand, particularly unconsolidated lithologies such as the Utsira, are likely to be unrepresentative of the formation as a whole. It is far better to have one or more cores, augmented by an evenly distributed selection of well logs to obtain reliable reservoir properties. Reservoir material sampled from the likely CO₂ migration pathways, e.g. the top of the reservoir, are of particular importance.

Analysis of the reservoir core should be prioritised according to the requirements of the reservoir (transport and reaction-transport) modellers, but is likely to include:

- sedimentology, petrography, fabric
 - optical microscopy (optical porosity)
 - SEM (scanning electron microscopy)

- mineralogy
 - XRD (x-ray diffraction)
 - particle-size analysis

- petrophysical / rock physics properties
 - absolute and relative permeability
 - porosity

mechanical and thermal properties
acoustic/elastic properties

reservoir-water-CO₂ chemical properties (cf Sections 4.3.1.1 and 4.3.1.2)
pore water analysis
dissolution/precipitation reactions.

In order to extrapolate effectively from the coring point(s) it is necessary to have geophysical log data, suitable for physical property determination, from wells at least as far from the injection point as the predicted CO₂ migration. Wherever possible, outcrop information should be incorporated into the characterisation process. Outcrop correlatives or analogues are valuable in understanding the nature of medium- and small-scale spatial variation in reservoir properties, and geostatistical or stochastic methods of 3D reservoir model building may be useful.

The amount of information needed to characterise the reservoir varies with type. The Utsira Sand forms a large-scale sand body, which in spite of its interspersed thin mudstones, has a rather simple internal geometry. Thus, in practical terms the fairly sparse cover of wells appears sufficient to characterise the reservoir adequately in terms of both of broad stratigraphy and also predicted fluid flow behaviour in the CO₂ plume (Section 4.2).

Even here, though, considerable variation of porosity and sand–shale ratio are evident, of considerable significance when calculating the regional reservoir storage capacity. For the SACS project physical properties were mapped in 2D (x, y, value) across the entire reservoir unit. In other reservoirs, physical properties may vary more significantly and information from more wells is required to define the variability and to assess whether it is systematic or random. In some cases a full 3D reservoir property model (x, y, z, value) may be deemed necessary. To this end, an understanding of the environment of deposition of the reservoir is important as this will provide models for the likely distribution of different lithologies and therefore lateral variations away from any borehole provings. Depositional assessment relies both on the interpretation of borehole data (cores, cuttings, logs) and on seismic (sequence) stratigraphic analysis. The latter may, in addition, provide specific details on the presence and geometry of internal migration barriers (e.g. shaly units on clinoforms in deltaic successions). The effect of internal flow barriers (either dipping or horizontal) on CO₂ migration could be substantial in altering the migration path from the injection point to the top of the reservoir.

In the Valleys case the reservoir is much more complex. Here knowledge of the depositional system is key to establishing a sedimentary facies model, which can then be expressed as a stochastic 3D distribution of reservoir and non-reservoir strata (Figure 4.15). In the Valleys case, well information is sparse, but even if there were more wells (for example at a spacing frequency comparable to that at Sleipner), a true picture of the 3D sand configuration would be very difficult to develop. Targetted stratigraphical test drilling prior to injection seems to be a pre-requisite in this type of situation.

4.1.3 Overburden and caprock properties

The whole geological succession overlying the reservoir can, for convenience, be termed the overburden and, forming the lower part of this, the sealing formation directly overlying the reservoir, can be termed the caprock. Robust evaluation of the extent, nature and sealing capacity of the reservoir overburden is perhaps the key purely geological element in assessing and establishing the long-term safety case for a CO₂ repository. Particularly for the case of CO₂ storage on land, knowledge of additional reservoirs and sealing formations in the overburden is of great importance in developing a multibarrier/multireservoir system of storage. The presence in the overburden of porous reservoir strata is of considerable interest as it affords the possibility of providing early warning of CO₂ accumulation at shallower depths, via seismically imaged ‘brightspots’, changes in groundwater chemistry or even changes in gravity values (see Section 4.6).

With respect to the long-term integrity of the caprock, detailed sensitivity analysis is required. Most suitable caprock is composed of mineralogically homogeneous, thick layers of unfaulted clays, claystones or mudstones. Capillary entry pressures should be well in excess of any likely pressure increase due to the injection process or to the buoyancy-driven accumulation of CO₂. Lithologically the caprock should not be unduly rich in carbonates since, in case of dissolution of carbonate rich layers such as marls, its sealing capacity might be significantly reduced, with local development of new migration pathways for CO₂ into overburden rocks (Section 4.3). Accordingly, careful laboratory evaluation, via a core testing programme, of capillary entry and breakthrough pressure, as well as a representative, preferably quantitative analysis of mineralogical and geochemical composition is recommended.

Microfractures may be present in the caprock due to compaction-induced hydraulic fracturing. Such microfractures may substantially improve cross-bedding permeability and may thus impair seal efficacy.

It should always be borne in mind that core measurements relate to specific localities, and extrapolation of favourable results should be based on additional information such as cuttings analysis or geophysical logs from other wells, to establish regional caprock suitability. Analysis of cuttings may give information on grain and pore size distribution, specific surface area, mineralogy and TOC (total organic carbon) that bear close relation to flow and capillary properties of the caprock.

If the integrity of the caprock cannot be robustly demonstrated, the consequences of likely migration scenarios (e.g. leaking fault or leaking seal) should be analysed as part of the site risk analysis (Section 4.5).

A number of techniques have been developed to examine the transport characteristics (e.g. intrinsic permeability, capillary entry pressure, relative permeability, dilatancy and pathway flow) of natural and synthetic materials. The choice of test methodology depends on the type of material under investigation and the parameters required for a particular study. The main laboratory and field techniques are based on simple principles where the injection permeant is held at a constant pressure, injected at a constant flow rate or increased to an elevated pressure and then allowed to decay. A

laboratory or field study can often employ one or more of these techniques to fully quantify the transport characteristics of a particular material or formation.

4.1.3.1 Laboratory permeability testing

Accurate characterisation of very low permeability caprock strata requires extremely careful and rigorous laboratory procedures because of the very low flow rates involved.

In **constant pressure gas testing**, the injection pressure of the permeant is raised in a series of steps until gas entry occurs. Subsequent steps in gas pressure are used to define the gas permeability function. In **constant flow rate tests**, the gas permeant is pumped into the upstream reservoir of the injection system, gradually raising its pressure until it overcomes the resistance for flow within the laboratory specimen. Once gas movement within a specimen occurs, flow rate into the injection system can be varied to examine the transport characteristics of the material, thereby defining the permeability function. In **pressure decay tests**, the gas pressure is increased rapidly to a value exceeding that of sum of capillary entry and porewater pressures, so that gas flow begins at the start of the test. Pressure in the injection system is then allowed to decay with time. The shape and asymptote of the pressure decay curve can be analysed to yield both permeability and capillary pressure data. The **pore-pressure oscillation technique** (Kranz et al., 1990; Fischer, 1992; Fischer and Paterson, 1992) relies on the generation of a sinusoidally varying pressure pulse in the upstream pore fluid reservoir by means of a computer-controlled servosystem. Transference of this pressure wave through a porous sample results in amplitude attenuation and phase shift when measured in the downstream reservoir, from which specimen permeability can be calculated. Tests can be conducted with different upstream pressure amplitudes, typically 1 MPa, and with varying periods, usually between 100 and 2000 seconds.

Constant pressure and **constant flow rate** tests result in a progressive dewatering of the material as gas pressure and gas saturation increases (i.e. a drainage response). In contrast, pressure decay tests result in a progressive reduction in gas saturation as gas pressure decreases (i.e. an imbibition response). The hysteresis between these two types of behaviour and the time dependency of some of the processes under investigation may result in a range of values depending on the test methodology selected. A comparative study of the different testing techniques has yet to be undertaken. However, given the unique physico-chemical properties of mudrocks and diversity and complexity of their behaviour, a rigorous and complete appraisal may take considerable time.

By altering the axial load and/or the confining pressure, laboratory tests provide a means to examine changes in transport properties during deformation. This allows transport properties to be mapped onto mechanical frameworks, such as the critical state model. The laboratory allows researchers to isolate the environmental parameters, such as pore pressure, confining pressure, axial stress, temperature, pore fluid chemistry etc, to fully describe the effect of each.

Selection of test methodology and subsequent design of the experimental programme should be appropriate for the formation under investigation in order to provide data suitable for the purposes of the study. In designing a test programme, care should be taken to minimise perturbations (both chemical and physical) to the material under examination, for example, caused by installation of field equipment or sampling and specimen manufacture. When determining intrinsic permeability in chemically reactive formations such as clays, mudrocks and shales, drill fluids and aqueous permeants should be matched, where appropriate, to the properties of the interstitial fluid. Laboratory and field tests should be performed under representative conditions, with the test procedure carefully designed to prevent an induced material response that is non-representative of the natural behaviour.

4.1.3.2 Observations from the CO₂STORE case studies

Sleipner

The overburden succession overlying the Utsira reservoir is several hundred metres thick, and can be divided into three main units (Figure 3.9). The Lower Seal forms a fine-grained basin-restricted unit some 50 to 100 m thick. Above this, the Middle Seal mostly comprises prograding sediment wedges of Pliocene age, dominantly muddy or silty in the basin centre, but coarsening into a sandier facies both upwards and towards the basin margins. The Upper Seal is of Quaternary age, mostly glacio-marine clays and glacial tills.

Seismic stratigraphy plays a key role in mapping caprock efficacy by enabling potentially sandy units, such as prograding foreset strata to be mapped. Seismic amplitude anomalies, or ‘bright-spots’, are also evident in the caprock succession. These indicate localised occurrences of sandy strata, probably gas-filled, and perhaps indicative of conduits for gas migration. Particularly at the top of the Middle Seal, the seismic amplitude anomalies are located in topographic highs, an observation consistent with their being due to accumulations of buoyant gas. Amplitude anomalies in the Lower Seal are scattered. They have circular to oval shapes in map view with diameters of approximately 1 km and show no clear relationship to reflection topography. In contrast, the few mapped amplitude anomalies at the top of the Utsira Sand are predominantly localised in structural traps. However, their occurrence does not always conform completely to trap geometry, which may be partly an effect of uncertainties in time-depth conversion. In general, seismic amplitude anomalies are almost completely absent in the predicted footprint area of the CO₂. This absence may be an indicator of poor sealing performance, but may equally well be explained by a lack of inflow of gas into the traps of the predicted footprint area.

The Lower Seal forms the primary sealing unit (the caprock), extending well beyond the area currently occupied by CO₂, and beyond the predicted final migration footprint. Cuttings samples from wells in the vicinity of Sleipner comprise dominantly grey clay silts or silty clays. Most are massive, although some show a weak sedimentary fabric (Figure 4.16a,b). XRD analysis typically reveals quartz, undifferentiated mica, kaolinite, K-feldspar, calcite, smectite, albite, chlorite, pyrite and gypsum together with traces of drilling mud contamination (Figure 4.16c, Table 4.8). The clay particle-size fraction is generally dominated by illite with minor kaolinite and traces of chlorite and smectite.

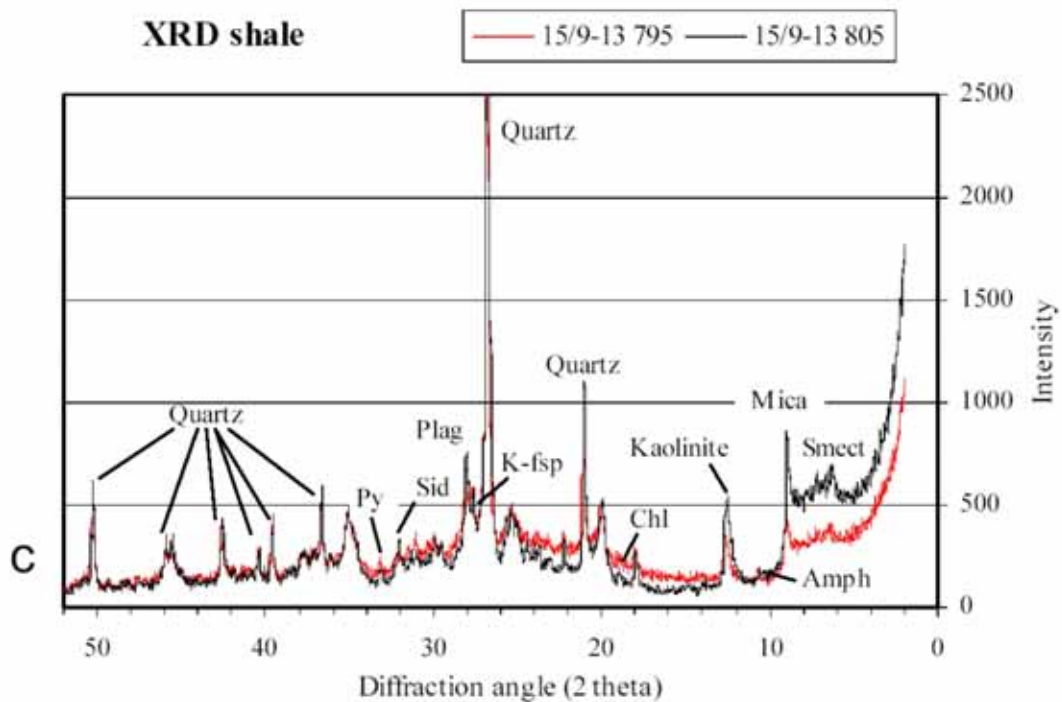
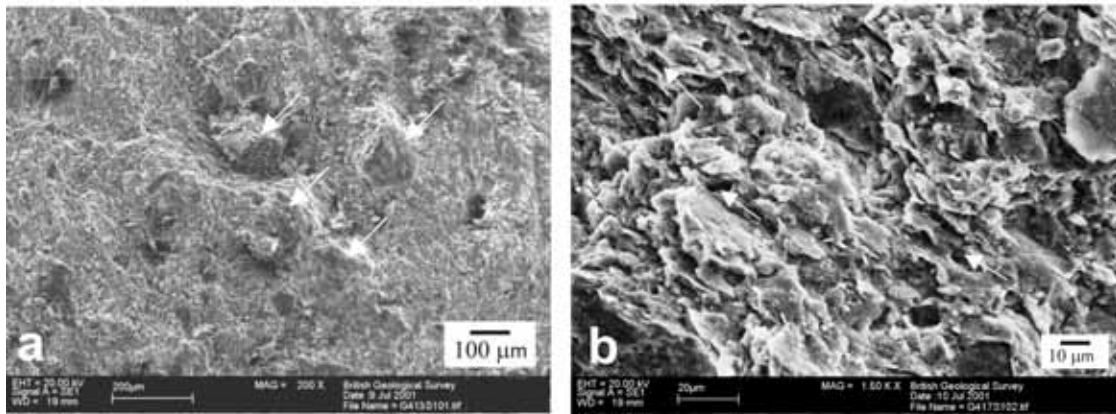


Figure 4.16 Cuttings material from the Utsira caprock. a) SEM image of massive mudrock with a number of rounded, fine-grained quartz grains (arrowed). b) High magnification detail of laminated mudrock showing tightly packed platelets with preferred orientation. Micropores (arrowed) are a few microns in diameter and appear to be poorly connected. c) X-ray diffraction (XRD) traces from two samples.

The cuttings samples are classified as non-organic mudshales and mudstones according to the Krushin classification (Krushin, 1997). Although the presence of small quantities of smectite may invalidate its predictions, XRD-determined quartz contents suggest displacement pore throat diameters in the range 14 to 40 nm (Kemp et al., 2001).

sand (>63 µm)	silt (2 - 63 µm)	clay (<2 µm)	% mineral													CEC meq/100g	TOC (%)
			quartz	k-spar	alb	calc	mica	kaol	smect	chlor	pyr	gyp	hal	syv	bar		
0 - 5%	40 - 60%	45 - 55%	30	5	2	3	30	14	3	1	1	1	2	1	5	6.0 - 20.2	0.68 - 1.28

Table 4.8 Utsira caprock properties from cuttings.

From Lindeberg (1997), it is possible to relate the displacement pore throat radius (r in m) to the required pressure difference (Δp in Pa) for CO_2 to enter a water-wet shale pore where σ (in Nm^{-1}) is the surface tension between water and CO_2 :

$$\Delta p = \frac{2\sigma}{r}$$

Assuming the surface tension of supercritical CO_2 to be around $20 \times 10^{-3} \text{ Nm}^{-1}$ (this is reasonable for CO_2 close to its critical point), measured pore throat diameters are consistent with capillary entry pressures to supercritical CO_2 of between 2 and 5.5 MPa. In addition, the predominant clay fabric with limited grain support resembles type 'A' or type 'B' seals (Sneider et al., 1997), stated to be capable of supporting a column of 35 API oil greater than 150 m in height. Empirically, therefore, the caprock cuttings samples indicate the presence of an effective seal at Sleipner, with capillary entry of CO_2 unlikely to occur.

The seismic, geophysical log and cuttings data enable many caprock properties to be characterised and mapped on a broad scale. Specific knowledge of mechanical and transport properties, however, requires core material and a detailed testing programme.

A caprock core (Figure 4.17) was acquired at Sleipner in 2002, from the Lower Seal unit (Figure 3.9), around 20–25 m above the Utsira Sand reservoir. The core material is typically a grey to dark grey silty mudstone, uncemented and plastic, and generally homogeneous with only weak indications of bedding. It contains occasional mica flakes, individual rock grains up to three millimetres in diameter and a few shell fragments. XRD-determined quartz contents suggest displacement pore throat diameters in the range 2.2 to 21 nm (Kemp et al., 2002), similar values to those of the cuttings samples from other wells, and suggesting capillary entry pressures to supercritical CO_2 of between 3.4 and 37 MPa .

The core has been subjected to a number of testing procedures including geomechanics (Pillitteri et al., 2003), transport testing with nitrogen and supercritical CO_2 (Springer et al., 2005), and long-term gas transport testing with nitrogen (Harrington et al., 2006; Harrington et al. in press).



Figure 4.17 Photograph of the Utsira caprock core.

Long-term hydraulic and gas transport testing on the caprock core at reservoir P,T conditions using nitrogen (Figure 4.18), indicates porosities in the range 32% to 38%, directional intrinsic permeabilities in the range 4 to $10 \times 10^{-19} \text{ m}^2$ and a capillary entry pressure to nitrogen of around 3 MPa.

A second parallel study on the Utsira caprock core (Figure 4.19, Springer et al., 2005) conducted at 5.6 MPa effective confining stress and 37 °C showed a normal in situ porosity of ~35%. The test was started by applying a constant CO₂ upstream pore pressure of 10.3 MPa and then lowering the downstream pore pressure stepwise (Figure 4.19 purple curve). A differential pressure is thereby generated across the sample that eventually overcomes the capillary forces and drives supercritical CO₂ into the sample upstream end. This was observed at 8.6 MPa downstream pore pressure where the slope 'b' of the injected upstream volume curve (Figure 4.19 green curve) deviates significantly from the previous stable plateau level. Further lowering of the downstream pressure accelerates the upstream injection of CO₂ accordingly.

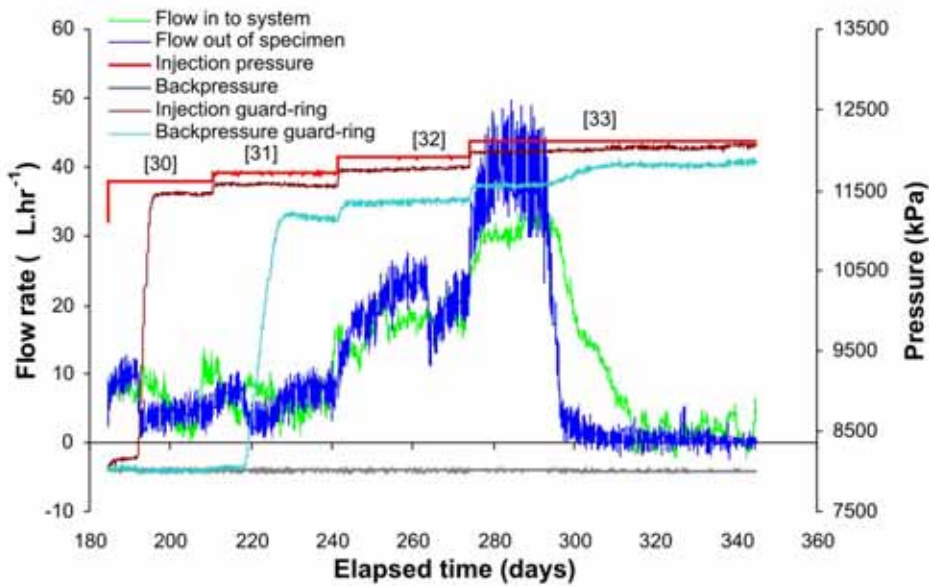
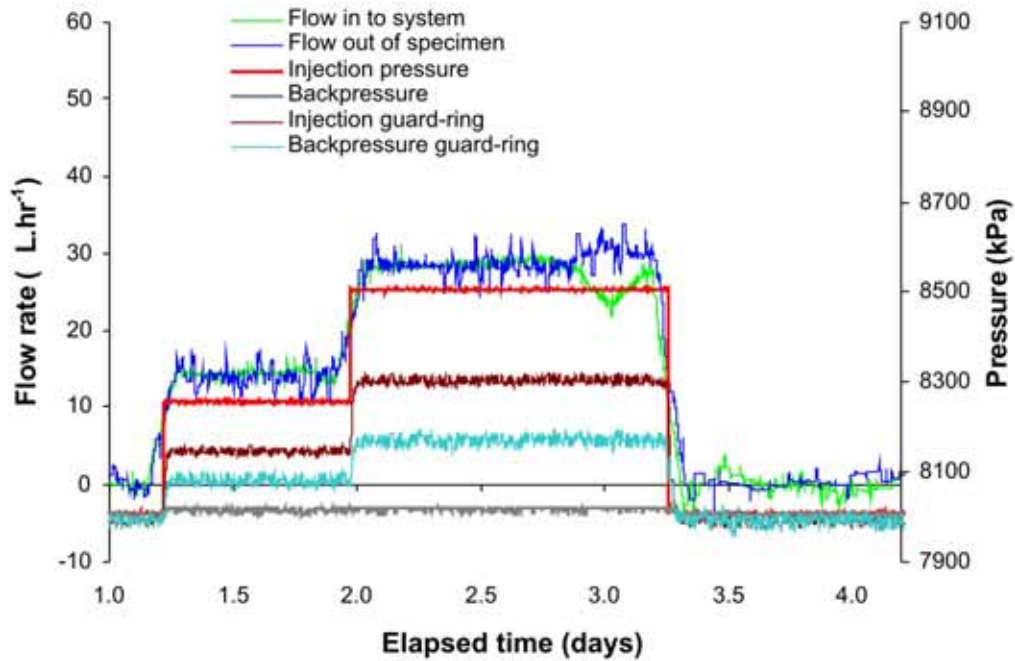


Figure 4.18 Long term fluid transport testing of Sleipner caprock: a) hydraulic testing b) gas (N₂) transport testing.

The vertical intrinsic liquid permeability was observed to be in the range $7.5\text{--}15 \times 10^{-19} \text{ m}^2$, slightly higher than in the study by Harrington et al. (2004) presumably due to a lower clay content in the samples used in the second study. Effective stress varied in some experiments to account for changes in overburden within the Sleipner area and to examine the effect of additional compaction of the weakly-consolidated mudstone. Capillary entry pressure was 3–3.5 MPa to both nitrogen and gaseous CO₂, and ~ 1.7 MPa to supercritical CO₂ (Figure 4.19). Increasing compaction had a significant effect on permeability and capillary entry pressure.

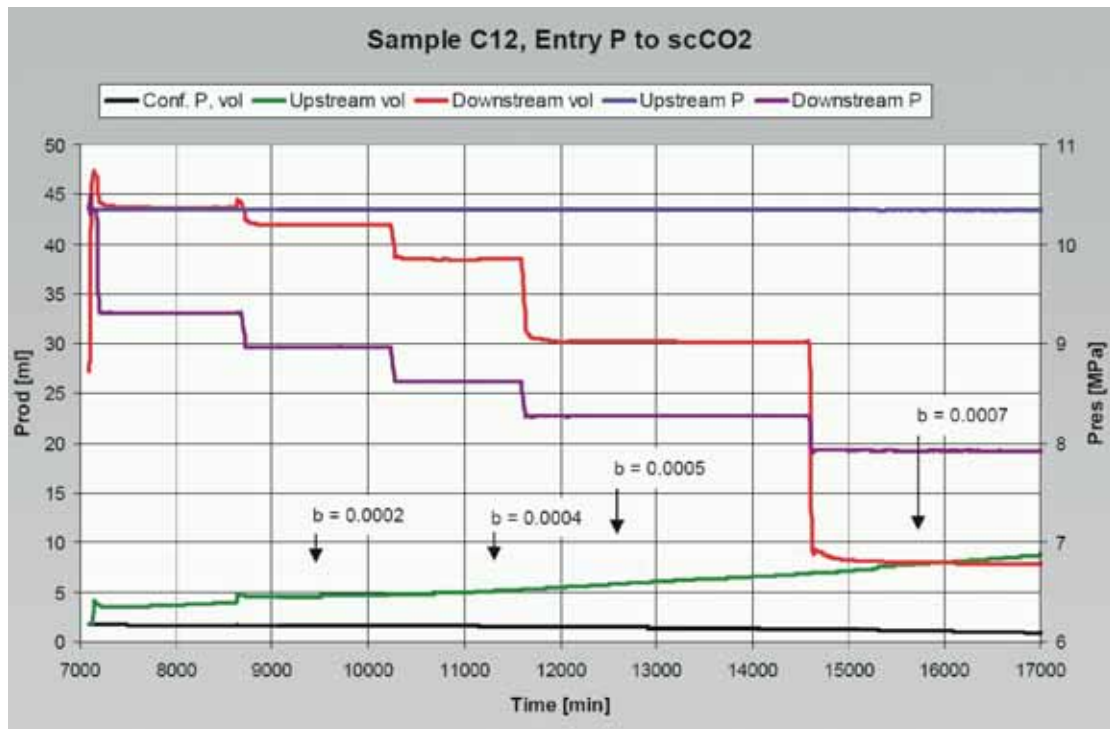


Figure 4.19 Evolution diagram for Sleipner caprock sample during supercritical CO₂ entry pressure test. Effective confining stress 5.6 MPa, initial pore pressure in the upstream and downstream end of the sample 10.3 MPa to make sure that CO₂ remains in its supercritical state even during a significant pressure drop.

The gas transport testing indicates that the Sleipner caprock has acceptable sealing capacity, capable of holding a supercritical CO₂ column of least 100 m and perhaps up to 400 m, depending on the density of the CO₂. This is significantly in excess of buoyancy pressures likely to be encountered in the Utsira Sand, where maximum confined column heights are generally < 10 m.

At Sleipner geomechanical effects are likely to be small, as predicted injection pressures are considered unlikely to induce either dilation of incipient fractures or microseismicity (Fabriol, 2001; Zweigel and Heill, 2003).

Kalundborg

The Havnsø structure is sealed by a thick package of marine mudstones of the Fjerritslev Formation (Figure 4.2). Laboratory experiments and full-scale testing at the Stenlille natural gas storage facility suggests that the mudstones form a tight seal. The integrity of the caprocks with respect to CO₂ however, has not been tested in the laboratory. Geochemical modelling of caprock–CO₂ reactions were performed as part of the CO₂STORE project and are presented below (Section 4.3.3.4).

Mid Norway

No deep well information is available from the Froan Basin. Further west on the Trøndelag Platform, the Cretaceous succession provides a good topseal to the proposed Jurassic storage units. Prior to drilling a well, seal properties could be extrapolated from the Haltenbanken province to the west and from shallow nearshore wells to the east. Extrapolating these data with the help of depositional models and

simulations can be done. This work can then be refined with data from a dedicated exploration test well.

Schwarze Pumpe (Schweinrich)

No new investigations were carried out for the Schweinrich structure. The assessment of the overburden and caprock properties was therefore limited to the extent that existing information were available.

The overburden of the Schweinrich reservoir comprises a thick Jurassic and Lower Cretaceous succession, overlain by Upper Cretaceous and Cenozoic strata. In some areas (e.g. Königsberg and at the eastern part of the Schweinrich anticline), parts of the Lower Jurassic to Lower Cretaceous succession are missing due to erosion or interruption of sedimentation. Parts of the Upper Cretaceous and the Paleocene are also missing in some areas, such as the nearby Trieplatz structure where the entire Upper Cretaceous is absent.

Immediately above the proposed storage reservoir is a thick sequence of Lower Jurassic rocks comprising claystones, siltstones, sandstones and marls. The first sealing unit is a Liassic (Sinemurian to Toarcian) claystone sequence several hundred metres thick. The dominant lithology is a carbonate-free to carbonate-poor claystone, interstratified by several siltstone layers and marls. Depending on the geological position, this succession is characterised by local stratigraphical gaps due to erosion and lack of sedimentation. Due to variable subsidence relative to local salt accumulation and diapirism, their thickness varies strongly within a few kilometres.

The Sinemurian succession predominantly comprises claystones, locally interbedded with siltstones. Carbonaceous sandstones locally occur in the lower parts. In the vicinity of Schweinrich thicknesses range between 25 m at the Königsberg structure and up to more than 150 m at the passive anticlinal Trieplatz structure. The Pliensbachian is dominantly claystone, interbedded with marls, siltstones and locally thick sandstones of several decametres thickness. Around Schweinrich thicknesses range from 130 m to 260 m. The Toarcian is composed of interbedded claystones, siltstones and sandstones, usually carbonate-free or with minor amounts of carbonate. Thicknesses range between 130 m and 180 m near to Schweinrich, but in the Königsberg area the Toarcian is locally absent due to interrupted sedimentation or erosion.

The Lower Jurassic succession is by Middle Jurassic claystones, siltstones, sandstones and carbonates and Upper Jurassic carbonates, marls and claystones.

The Lower Cretaceous mainly consists of claystones, marls and glauconitic sandstones. In the vicinity of Schweinrich, preserved parts of the Upper Cretaceous (Turonian, Coniacian and Santonian) are predominantly composed of limestones and marls.

The Cenozoic succession predominantly consists of unconsolidated clay with variable amounts of silt and sand (Eocene and Oligocene) and carbonaceous sands (Miocene). The Eocene clays form a major seal unit composed of several hundred metres of unconsolidated, mostly carbonate-free to slightly calcareous clay, interbedded with silt and sand layers. The Oligocene Rupel Clay is a thick, unconsolidated clay

sequence, forming the uppermost seal and separating saline formation water from fresh water in the shallow subsurface. It is lithologically homogeneous, quite thick (several tens of metres), and is of regional extent.

Within the area of investigation, the base of the Rupel Clay lies between 150 m to 750 m depth (bsl). On the Schweinrich structure the base of the Cenozoic clay sequence lies at depths of about 400 m bsl, with the base of the Rupel Clay at about 200 m depth. On the north-western flank of the Schweinrich structure, the base of the Rupel clay plunges down to more than 650 m below sea. In this area, the Rupel Clay is characterised by a strongly reduced thickness (down to about 15 m locally). However, across the area no interruption of the Cenozoic clay succession is evident. Only salt diapirs are known to pierce the regionally extensive Rupel Clay.

Pleistocene tills and sand bodies form the uppermost seals and aquifers. The Pleistocene was deposited within deepened erosive, north-east trending channels, formed by hydroglacial erosion and is composed of interbedded sands and tills. Thicknesses range from several tens of centimetres to several hundred metres. The sand layers contain fresh water used for drinking water.

The reservoir topseal is a claystone sequence several tens of metres thick. A number of siltstone and sandstone layers as well as marls are also present. Mineral components determined using XRD are illite/mixed layers (30 to 50 %) and kaolinite (5 to 25 %) with minor amounts of quartz, plagioclase and K-feldspar. The analysed claystone samples contain variable amounts of carbonate minerals, mostly siderite, dolomite/ankerite and calcite. The claystone typically is carbonate-free or contains less than 5% carbonates (calcite and siderite), only one marl sample contains about 50% carbonate (calcite + siderite + ankerite/dolomite).

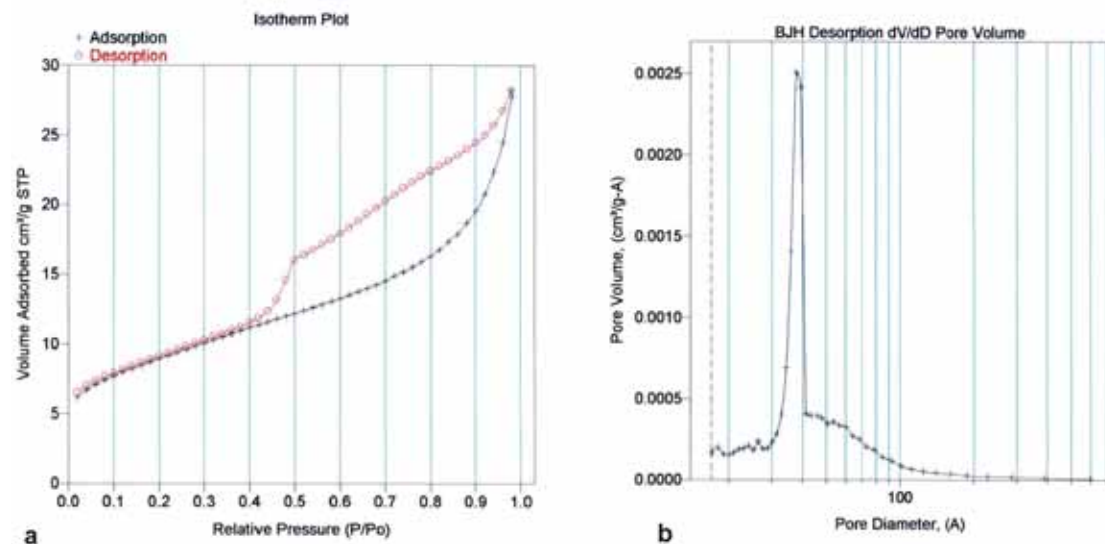


Figure 4.20 BET measurements from a claystone sample from the Schweinrich caprock: (a) pore volume and (b) pore diameters.

Grain-size analysis indicates that the clay and fine silt fraction contains up to 70 weight-percent of all mineralogical components. Pore volume analysis (Figure 4.20) using the BET (measured via nutrient absorption) indicates average pore diameters ranging between 10 and 100 Å (1 to 10 nm). This is somewhat smaller than the Utsira

caprock samples (see above). Porosity values range between 9.1 and 10.4 volume percent, again lower than for the Utsira caprock samples.

Geochemical and mineralogical characteristics of the Lower Jurassic caprock samples are given below (Tables 4.9 and 4.10).

Sample	Quartz	Illite & mixed layer clays	Chlorite	Kaolinite	Plagioclase	K-Feldspar	Calcite
Claystone 6	10	50	5	20-25	7	1	n. p.
Claystone 7	10	45-50	5	20	6	4	n. p.
Claystone 8	20	30-35	9	25-30	4	3	n. p.
Claystone 9	10	15	5	5	5	6	11
Claystone 10	15-20	50	5	5-10	8	5	3

Sample	Dolomite & Ankerite	Siderite	Hematite	Rutile & Anatase	TC	TOC	TIC	CaCO ₃ [%]: TIC calculated
Claystone 6	n. p.	n. p.	5	1	0.23	0.19	0.04	0.3
Claystone 7	n. p.	3	4	1	0.75	0.13	0.62	5.2
Claystone 8	n. p.	n. p.	2	1	1.11	1.08	0.03	0.3
Claystone 9	15	26	n. p.	0,5	5.41	0.19	5.22	44
Claystone 10	n. p.	2	2	1	1.09	0.21	0.88	7.3

Sample	Density [g/cm ³]	BET surface area	Porosity* [vol.-%]	< 2 µm	2 - 6.3 µm	6.3 - 20 µm	> 20 µm
Claystone 6	2.524	31	9.14	50.5	37.2	11.9	0.4
Claystone 7	2.517	35	10.39	45.5	31.3	18.6	4.6
Claystone 8	2.476	27	7.45	31.5	27.3	27.7	13.5
Claystone 9	2.815	25	7.26	45.8	24.6	25.4	4.1
Claystone 10	2.477	40	10.23	57.0	20.9	14.5	7.6

Table 4.9 Mineral composition (weight%) and petrophysical properties of the Sinemurian caprock samples. The claystones predominantly consists of kaolinite, illite + mixed layers and quartz. CO₂-sensitive minerals are feldspars (orthoclase and plagioclase) and Fe-bearing minerals, predominantly carbonates and chlorite. (Data derived from well Ug Wsbg 2/74). TC = total carbon, TOC = total organic carbon, TIC = total inorganic carbon. * Average pore diameter = 50 Å (range 10 to 100 Å), measured via the BET method.

Sample	SiO ₂	TiO ₂	Al ₂ O ₃	Fe ₂ O ₃	MnO	MgO	CaO	Na ₂ O	K ₂ O
Claystone 6	47.96	1.10	25.89	8.17	0.027	1.62	0.3	1.06	3.01
Claystone 7	49.11	0.99	22.47	9.18	0.086	2.1	0.77	1	3.1
Claystone 8	54.67	1.21	23.84	4.35	0.025	1.36	0.13	0.85	2.46
Claystone 9	27.26	0.51	10.98	19.07	0.29	4.32	10.66	0.71	1.58
Claystone 10	52.25	0.95	19.76	5.8	0.072	2.71	2.56	1.08	3.43

Sample	P ₂ O ₅	SO ₃	F	Ba	Cr	Cu	Ni	Pb	Rb	Sr	Th	V	Zn	Zr
Claystone 6	0.13	0.02	0.1	307	129	23	70	21	125	205	15	171	46	180
Claystone 7	0,13	0,03	0,07	305	120	18	57	14	123	197	11	136	56	178
Claystone 8	0.07	0.14	<0.05	318	133	22	61	40	104	125	18	160	76	229
Claystone 9	1.68	0.29	0.2	146	63	11	34	<4	61	156	<5	80	47	96
Claystone 10	0.12	0.1	<0.05	297	112	34	66	10	140	147	9	137	52	184

Table 4.10 Chemical composition of the Sinemurian caprock samples. XRF analysis; main elements in weight%; trace elements in mg / kg.

As above, Lindeberg (1997) relates the displacement pore throat radius (r in m) to the required pressure difference (Δp in Pa) for CO₂ to enter a water wet shale pore where σ (in Nm⁻¹) is the surface tension between water and CO₂:

$$\Delta p = \frac{2\sigma}{r}$$

Assuming the surface tension of supercritical CO₂ to be around 20 x 10⁻³ Nm⁻¹ (reasonable for CO₂ close to its critical point) and a range of displacement pore throat radii from 1 to 10 nm, capillary entry pressures in the range 4 to 40 MPa are predicted (higher values for CO₂ surface tension would result in still higher capillary entry pressures).

The density difference between CO₂ and water at reservoir conditions is likely to be around 500–600 kgm⁻³. This will create a buoyancy pressure of about 0.0055 MPa per metre of CO₂ column. Therefore, the predicted capillary entry pressures suggest that the Schweinrich seal is capable of trapping a confined CO₂ column ranging in height from around 730 m to 7300 m in hydrostatic conditions. This exceeds the maximum possible CO₂ column heights at Schweinrich.

Valleys

Analysis of caprock was limited to cuttings samples from scattered wells (Kemp and Bouch, 2004). Caprock lithology was determined using the following procedure:

Cuttings were ground to about 125 μ m, soaked in deionised water for 10 mins and dried at 55°C. Clay and sand fractions were separated using standard techniques (sieving, Stokes Law). Bulk mineralogy was determined using X-ray diffraction

(XRD). Polished thin sections were examined by scanning electron microscope (SEM), and image analysis software, to determine pore volumes and pore size distributions.

Caprock samples comprise kaolinitic mudstones, which locally contain siderite crystals and nodules within the mudstone fragments. Whole-rock XRD analyses identified mica, quartz and kaolin with minor K-feldspar, siderite, halite, calcite and barite. Clay mineral assemblages comprise varying amounts of smectite with illite, kaolinite and chlorite.

Geochemical modelling of caprock–CO₂ interactions was carried in CO2STORE and is summarised in Section 4.3.5.5

4.1.3.3 Generic findings

Determination of the extent of the caprock will rely on a regional spread of boreholes and on grids of 2D and 3D seismic data. Sample material should be available in the form of cuttings (for wide regional coverage) and core (for specific property testing) in sufficient quantity to undertake a detailed suite of analytical tests. The core material should ideally be in a location above the likely CO₂ migration pathway or from a demonstrably analogous position. Geophysical well logs should also be utilised to extrapolate sample parameters across the whole caprock volume.

Analysis of the caprock core should be prioritised according to the requirements of the geomechanical and reservoir (transport and reaction-transport) modellers, but is likely to include:

- Sedimentology, petrography, fabric

 - SEM (scanning electron microscopy)

 - X-ray screening

 - N₂BET

- Mineralogy

 - XRD (x-ray diffraction)

 - particle-size analysis

 - CEC (cation exchange capacity)

 - TOC (total organic carbon)

- Petrophysical and rock physics properties

 - Mohr-Coulomb behaviour

 - Young's modulus

 - drained bulk modulus

 - cam-clay parameters

 - time-dependent creep

 - Poisson's ratio

 - acoustic velocity

 - capillary entry pressure

 - permeability

 - caprock-water-CO₂ chemical properties (cf Sections 4.3.1.1 and 4.3.1.3)

- pore water analysis
- chemical reactions
- physical reactions (dehydration)

In the absence of core material, drill cuttings (preferably augmented by sidewall core material) are suitable for a limited range of analytical techniques such as petrography, SEM and XRD. Results from cuttings analysis can be used to assess sealing capacity in a qualitative manner, by comparison with samples from proven oil/gasfield caprocks, or semi-quantitatively such as by the Krushin grain-size method (Krushin, 1997). The discrepancy noted at Sleipner between capillary entrance pressures derived from core and empirical values derived from cuttings may just reflect limitations of the latter method. On the other hand it does highlight the important consideration that core samples are from a single point and may well not be representative of the caprock volume as a whole. Thus, in addition to establishing physical properties at a number of point locations (wells) it is necessary to evaluate the bulk properties of the caprock and any structures that may affect it (particularly in the vicinity of the predicted CO₂ migration paths).

Caprocks consist typically of sediments from distal depositional environments, which are characterised by relatively uniform conditions over large areas. Caprock lithology, fluid-flow and geomechanical properties are therefore likely to vary much less than those of the reservoir rocks. Consequently, extrapolation of lithology-related caprock properties from a small number of wells over a large potential footprint area (typically some tens to a few hundred square kilometres) can be better constrained than extrapolation of reservoir properties. However, relevant caprock properties due to deformation (faults, joints) cannot easily be extrapolated but require detailed local assessment covering the whole footprint area.

The regional seismic stratigraphy of the caprock should be discernible from 2D seismic data, as would major faults that cut it. Smaller structural features for example 'polygonal' type minor faults that characterise some shale sequences, generally require 3D seismic data for their proper identification. Very small structures, fractures and joints are beneath the limit of seismic resolution.

Assessment of the presence of microfractures in the subsurface is challenging because mechanical deformation and depressurisation during coring may induce microfractures in core samples that are difficult to distinguish from those that formed in situ. Consequently, careful coring and preservation of cores is a prerequisite for successful microfracture assessment. Core analysis can be aided by numerical simulation, supported by experimental studies, of coring-induced damage and of the pore pressure evolution during compaction. Further, high-resolution well-logs (e.g. FMS) may reveal the presence of microfractures in the borehole walls.

Injection-induced pressure changes could lead to compromise of the caprock seal and possible geomechanical consequences should be assessed prior to injection commencing. Two main effects should be considered: fracture dilation due to increased pore pressures and induced seismic slip due either to raised pore pressures or a reduction in normal stress due to buoyancy forces exerted by the CO₂ plume. Fracture orientations that are likely to be conducive to fluid flow or susceptible to

seismic slip can be determined relative to the principal stress axes if the in situ stress is known.

The inability of a caprock succession to provide a long-term seal for the underlying reservoir may be revealed by indicators of hydrocarbon migration into and through the caprock. Seismic amplitude anomalies and gas shows in the caprock may signify the presence of shallow gas. Pockmarks and vents at the seafloor are indicators for gas migration from the underground into the sea water. However, gas within the caprock may have formed biogenically in situ, and does not necessarily imply migration from below. The nature and source of shallow gas needs therefore to be addressed if indicators of its presence have been detected. The degree of correlation between seismically imaged gas migration indicators and mapped faults is clearly of potential importance in evaluating fault-related leakage.

4.2 Predictive flow modelling

Flow modelling is a key element in the characterisation phase of a CO₂ storage project, providing quantitative predictions of reservoir behaviour and, via multiple realisations, parameter sensitivity to uncertainty. Generically it serves to demonstrate that we understand the basic reservoir system processes. More specifically it can be used to refine capacity estimates, to evaluate the likely lateral spread of CO₂ in the future (essential for designing effective monitoring programmes) and to examine putative leakage scenarios (for site risk assessment). Preliminary long-term modelling can also be carried out to support the overall site safety case.

The main data requirement at this stage is some form of 3D geological model, attributed with reservoir and overburden parameters. Reservoir parameters should be based on core measurements if possible, supplemented by geophysical logs to gain more robust areal coverage. Key modelling parameters include:

reservoir

- temperature
- pressure
- porosity
- permeability
- relative permeability curves
- capillary pressure curves

caprock

- permeability
- capillary entry pressures

fluids

- CO₂ composition, presence of impurities and physical properties
- salinity
- phase behaviour.

4.2.1 Observations from the CO2STORE case studies

Sleipner

Pre-injection reservoir flow simulations were carried out with a modified black oil simulator in two stages. The first stage was carried out prior to the submission of the field development plan ('plan for utbygging og drift', PUD) and its key results were included in the PUD. The model had simple radial geometry with a horizontal top and was run for a simulated injection interval of 20 years. The main aim of the first stage modelling was to test injectivity of CO₂ into the storage formation. Permeability was set to 2 Darcy and porosity was set to 35%. The main result was that injectivity should be good and that pressure increase should be minimal if the active aquifer has a large enough extent (radius of 16 km or more). It was predicted that CO₂ would move into local domes and would dissolve into formation water in the long term.

A second set of pre-injection simulations was carried during the final stages of the preparation of the PUD but their results were not included in the PUD. These simulations had three main aims: (a) to predict injectivity, (b) to identify the potential for injection-induced overpressure, and (c) to find out if injected CO₂ may reach production wells which it may corrode. The simulations were carried out for a large domal trap north-north-west of the Sleipner A platform (see Section 4.1.1.1) for an injection period of 20 years and an annual injection rate of approximately 1.16 Mt per year (base case) and used the following reservoir data:

Reservoir pressure:	8–10 MPa
Reservoir temperature:	27 °C (base case), alternative 40 °C
Permeability:	K _h = 5 Darcy; K _v = 2.5 Darcy
Porosity:	31–41%
Net sand:	80–98%

The results of this study indicated that:

The CO₂ should be injected near the bottom of the formation to minimise areal distribution and maximise the dissolution in formation water.

The maximum extent of CO₂ after 20 years of injection would reach a radius of about 3 km around the injection site, which was located at 2.5 km distance from the Sleipner A platform. Most simulations, however, yielded a maximum areal extent of the plume of only around 2 km radius.

There were no major differences in areal distribution between free and dissolved CO₂.

Up to 18% of the CO₂ injected was dissolved in the formation water.

There was a risk that CO₂ ultimately may approach the Sleipner A platform such that gas production wells may be reached and corroded. Uncertainty of the geometry of the almost horizontal reservoir top was so large that CO₂ potentially could reach these wells in the near-term. Protection of the upper parts of the gas producers by use of high-grade steel was therefore recommended. The recommendation has been followed for all production wells on Sleipner.

Later, in about 1994, a new location for the storage site was chosen, based on newer seismic data (see Section 4.1.1.1). No reservoir simulations seem to have been carried out for this new site prior to injection. However, the general findings of the previous simulations were deemed to be valid for this new site as well, due to the homogeneity of the Utsira Sand and the structural similarities of the traps. The main advantage of the new site, that is the presence of a depression between it and the location of Sleipner A wells, could be qualitatively assessed without the need for additional reservoir simulations.

Subsequent to the pre-injection modelling, further, more-detailed flow simulations were carried out within the SACS project as part of the site characterisation work. This was carried out synchronously with the ongoing injection operation. Much of this is described in Chapter 7. Discussion is limited here to simple buoyancy-migration modelling.

The simplest type of flow simulation utilised at Sleipner was to assess the likely plume extent (or footprint). This assumed that migration is driven solely by buoyancy and takes place instantaneously, neglecting processes such as two-phase flow, dissolution, residual phase trapping and chemical reactions. The secondary hydrocarbon migration modelling tool SEMI was used (Zweigel et al., 2000), its output effectively showing the ultimate ‘maximum extent’ distribution of a given amount of CO₂ according to a simple ‘static ponding’ mechanism.

Two main SEMI migration models have been constructed (Figure 4.21), taking an injected CO₂ volume of 30 Mm³ (approximating the planned final injected mass of 20 Mt).

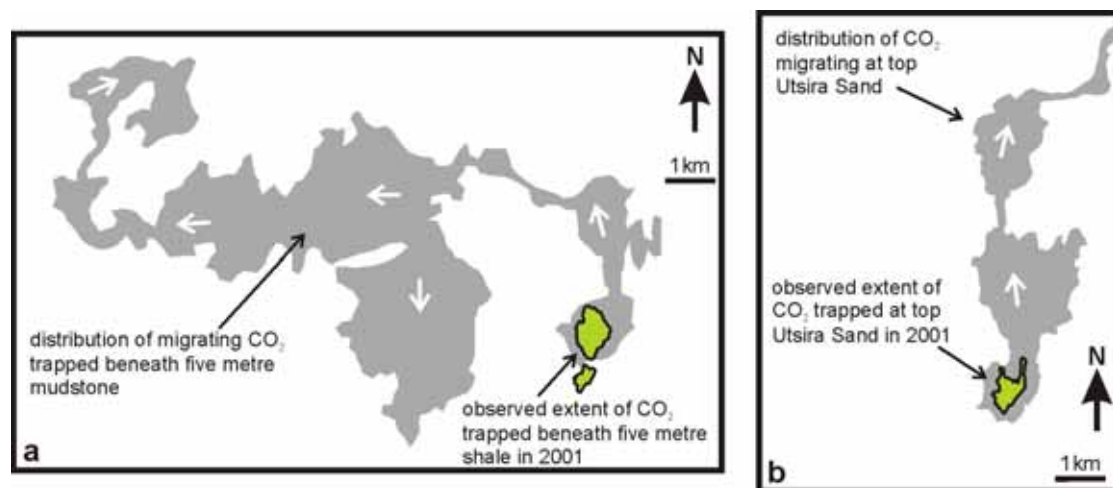


Figure 4.21 SEMI migration models of predicted (grey) and observed (green) migration paths for CO₂: a) beneath five metre mudstone b) beneath the Utsira topseal.

The first model assumed that the ‘five-metre mudstone’ (Figure 4.7) forms an effective long-term trapping horizon. Migration simulation predicts that CO₂ would migrate generally in a westerly direction, to reach a maximum distance from the injection site of about 12 km (Figure 4.21). Observations from the 2001 seismic data

indicate that CO₂ currently trapped beneath the mudstone broadly follows the predicted distribution. An ‘anomalous’ small outlier of CO₂ to the south of the predicted closure seems principally to be due to complexity of vertical feeder pathways within the plume itself. Because the mudstone topography is very subdued, however, results are very sensitive to the accuracy of the depth mapping. Changes of dip angle, and errors in the small depth differences between different potential spill points, emphasise the need for precision in the depth conversion.

An alternative scenario is that the CO₂ migrates directly to the top of the Utsira Sand whose topography controls its subsequent lateral spread (Figure 4.21). Because the top reservoir has a slight dip discordance with the underlying five-metre mudstone, the simulation gives quite different results. Migration is northwards, then north-eastwards, until, with 7.4 Mm³ injected, the CO₂ front moves out of the area of 3D seismic data coverage. A subsequent migration simulation study based on a dense grid of 2D seismic lines east of the injection site (Hamborg et al., 2003) showed that north-eastward moving CO₂ is likely to be trapped in a large domal trap (with a capacity >75 Mm³ of CO₂) immediately outside the area covered by 3D seismic, that is about 10 km from the injection site. In combination with additional traps along a hypothetical continued migration route, trapping space for about 100 Mm³ of CO₂ has been identified within 25 km of the injection site to the north-east.

Observations from the 2001 seismic data support the migration simulation, showing the general northward transport with recent alignment along a north-trending linear channel (Section 7.2).

In the medium term, the bulk transport direction of CO₂ depends on how much CO₂ will be trapped beneath the five-metre mudstone compared with how much is trapped beneath the top of the Utsira Sand. As yet this cannot be determined with the current monitoring datasets. The time-lapse seismic data indicate that the five-metre mudstone was breached by CO₂ as early as 1999. Nevertheless the CO₂ layer beneath it had grown considerably by 2001, and may well continue to do so during much of the injection phase. On cessation of injection however it is expected that most of the CO₂ will drain to the top of the Utsira Sand, with lateral migration beneath intra-reservoir flow barriers becoming less important with time.

Kalundborg

The Havnsø reservoir is divided into five compartments, which means that it would be necessary to inject the CO₂ at five different locations to exploit fully the available total storage volume, estimated at 846 Mt. However, the largest of the five compartments accounts for some 77% of the total storage volume. This corresponds to 651 Mt of CO₂, sufficient to hold 100 years’ worth of the emissions from both Asnæsværket and the Statoil refinery (together about 6 Mt per year).

A preliminary simulation model using Eclipse 100 has been made for the Havnsø structure. Details are reported in Bech (2003) and show that the rock properties in the reservoir would allow injection of 200 kgs⁻¹ of CO₂, equal to the average daily emission rates of Asnæsværket.

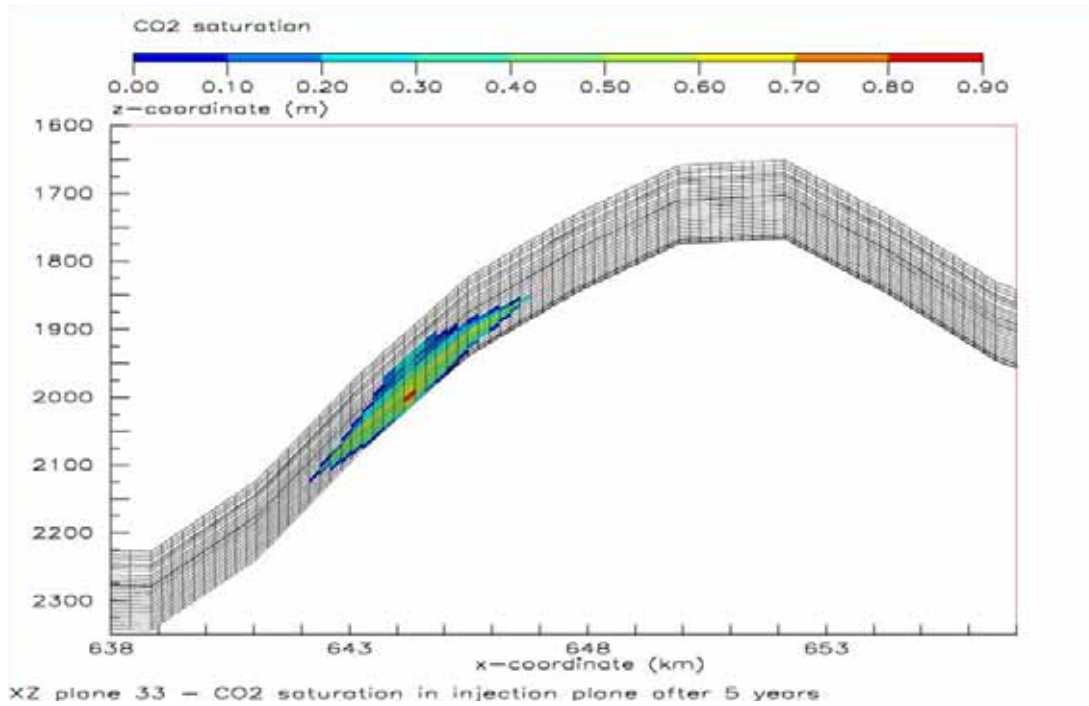


Figure 4.22 Vertical distribution (in the injection plane) of CO₂ saturation in the Havnsø structure after five years of injection. The injection rate was 200 kg^s⁻¹ or 6 Mtyr⁻¹ in 100 years.

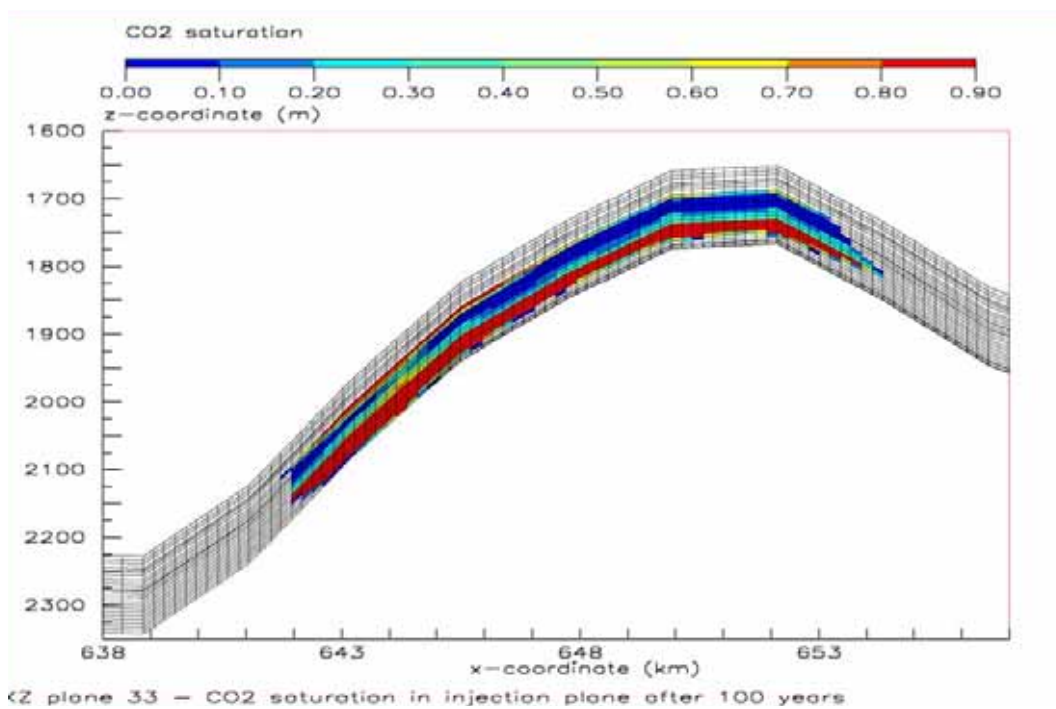


Figure 4.23 Vertical distribution (in the injection plane) of CO₂ saturation in the Havnsø structure after 100 years of injection. The injection rate was 200 kg^s⁻¹ or 6 Mtyr⁻¹ for 100 years.

The CO₂ may be injected through a single injection well 8 km long perforated over a length of 500 m. Maximum permissible injection pressures of 30 MPa would be

reached, but only during the first few days. Figures 4.22 and 4.23 show the flow model and the predicted distribution of CO₂ after 5 and 100 years, respectively. The injected CO₂ migrates to the top of the reservoir compartment while partly dissolving in the formation water. Irrespective of caprock capillary trapping, CO₂ which has not reacted to form carbonate minerals will eventually move out of the reservoir by molecular diffusion, but this process would be on the million year timescale.

Mid Norway

No flow simulations have been carried out as part of a detailed site characterisation exercise. The scoping flow simulations carried out for the screening phase (Section 3.4) suggest that the Trøndelag Platform is likely to be suitable for safe, long-term subsurface CO₂ storage and that the Frohavet Basin may also be suitable (given favourable reservoir properties).

Reservoir properties are presently unknown due to the lack of well data or subsurface samples and simulations were of necessity based on simplified subsurface models with reservoir parameters from the nearby Haltenbanken hydrocarbon province (Polak et al., 2004a,b; Lundin et al., 2005).

The storage concept relies on injection being far enough from the subcrop of the storage formations for CO₂ to be immobilised within the reservoir long before reaching the subcrop. This is critically dependent on reservoir properties so, prior to injection, the suitability of any storage concept needs to be assessed in much more detail. Local geological and reservoir property data from dedicated wells are an indispensable part of such an assessment. More sophisticated simulations should include more detailed reservoir models with internal heterogeneity (representing the depositional environment) and an adequate upscaling procedure. They should be carried out with a simulator handling compositional and PVT effects in a realistic way, and including hysteretic flow effects.

Schwarze Pumpe (Schweinrich)

Two different reservoir flow simulations have been carried out to assess site performance at Schweinrich. The first one simulates the CO₂ injection and reservoir performance during the 40 years of site operation. The second simulation focusses on long-term CO₂ dissolution into the formation waters and migration within the reservoir. There are many uncertainties in the data used to build the model, and results from the reservoir flow simulations should be taken as indicative only. Going beyond the CO₂STORE case study, much more effort would be needed to establish a high-quality geological model of the Schweinrich structure.

The following issues have been addressed:

The capacity of the structure to accommodate the required 400 Mt of CO₂.

Prediction of the spatiotemporal spread of CO₂ during the operational phase (40 years injection period).

Long-term prediction of CO₂ dissolution and migration of CO₂-saturated formation water (10 000 years period).

Due to the likely reservoir properties and associated injectivity issues, spatially dispersed injection and perforation is required. Flow simulations were carried out with ten injection wells arranged around the flanks of the storage anticline (Figure 4.24).

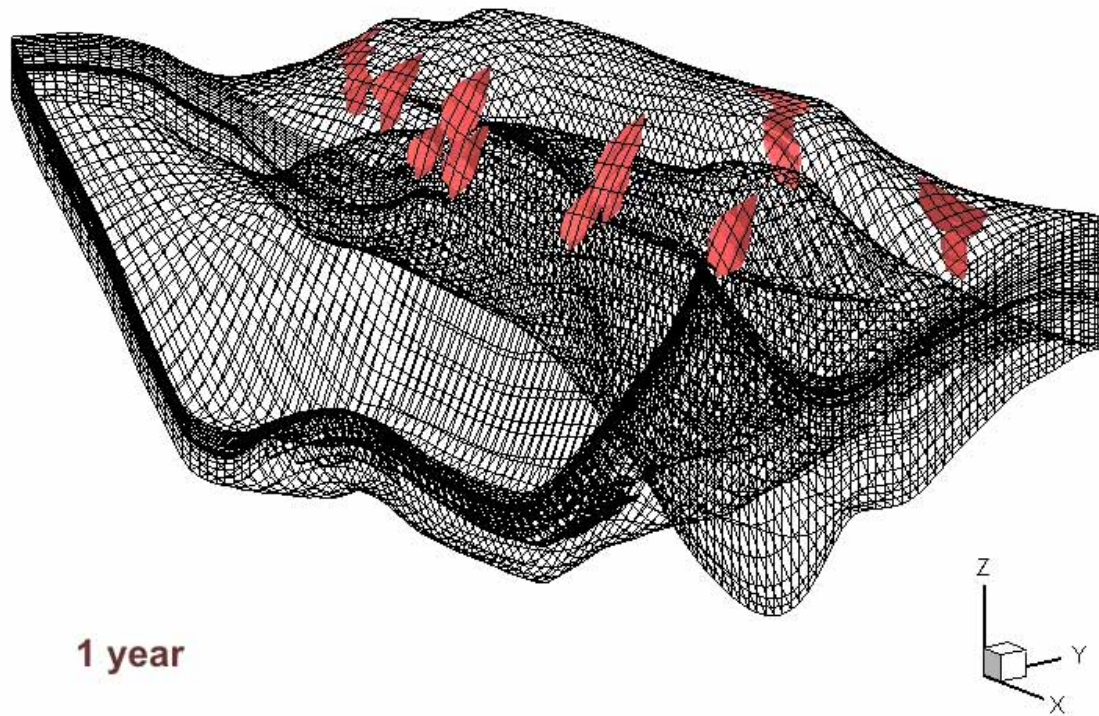


Figure 4.24 Schweinrich 1 year flow simulation showing CO₂ migrating from the 10 injection wells arranged around the flank of the storage anticline.

Each well injected 1 Mt of CO₂ per year over a total injection period of forty years. The simulations show gradual coalescence of the ten individual CO₂ plumes over the forty-year injection period, and progressive migration of free CO₂ to the top of the structural closure (Figure 4.25).

Much longer-term simulations on timescales of a thousand years or more (Figure 4.26) show progressive dissolution of CO₂ into the formation waters. The denser CO₂-bearing brines sink gradually down the flanks of the storage anticline such that after 10 000 years or so, a significant amount of dissolved CO₂ resides in a stable state in the flanking synclines.

Because of the very large volumes of CO₂ involved, there is a potential issue concerning injection-induced pressure changes in reservoir. Pressure increase due to the additional volume of injected CO₂ depends strongly on the ability of the entire storage system to take up formation water displaced from the injection plume and the reservoir. This depends both on far-field fluid leakage and also on the compressibility of the formation water, which is controlled by physico-chemical parameters like salinity and viscosity (Obdam et al., 2003).

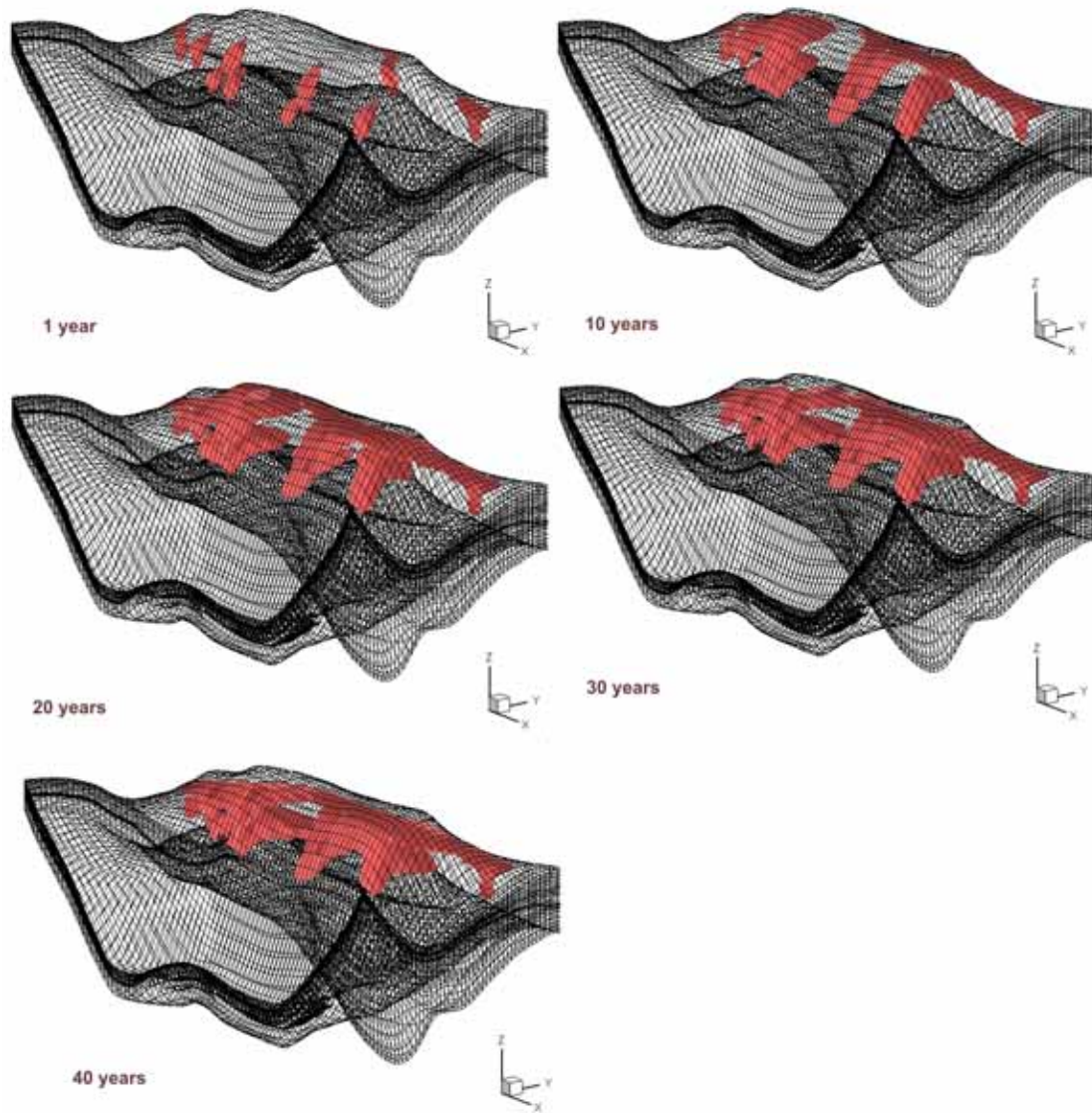


Figure 4.25 Migration of 400 Mt of CO₂ injected into the Schweinrich structure during the 40 years injection phase. The initial injection of CO₂ via ten injection wells positioned at the flank of the structure is visualised with the subsequent buoyancy-driven migration into the crest of the structure due to the buoyancy. The spatial differentiation of both reservoir formations is also visible.

The effective hydrodynamic extent of the reservoir units around Schweinrich is unknown, so the far-field boundary was conservatively set as a no-flow interface. A simple assessment of possible pressure changes was then made by running a number of flow simulations with a reservoir model of variable size (Figure 4.27). This was originally set at 60 x 75 km (the storage structure itself is about 30 x 10 km) but induced pressure increases were very large. The model storage reservoir was then increased by stepwise lateral extensions of the boundary elements (by 15 km, 25 km and 50 km) i.e. moving the no-flow boundaries away from the injection wells. This provided additional amounts of compressible pore water to help accommodate the large volume of injected CO₂.

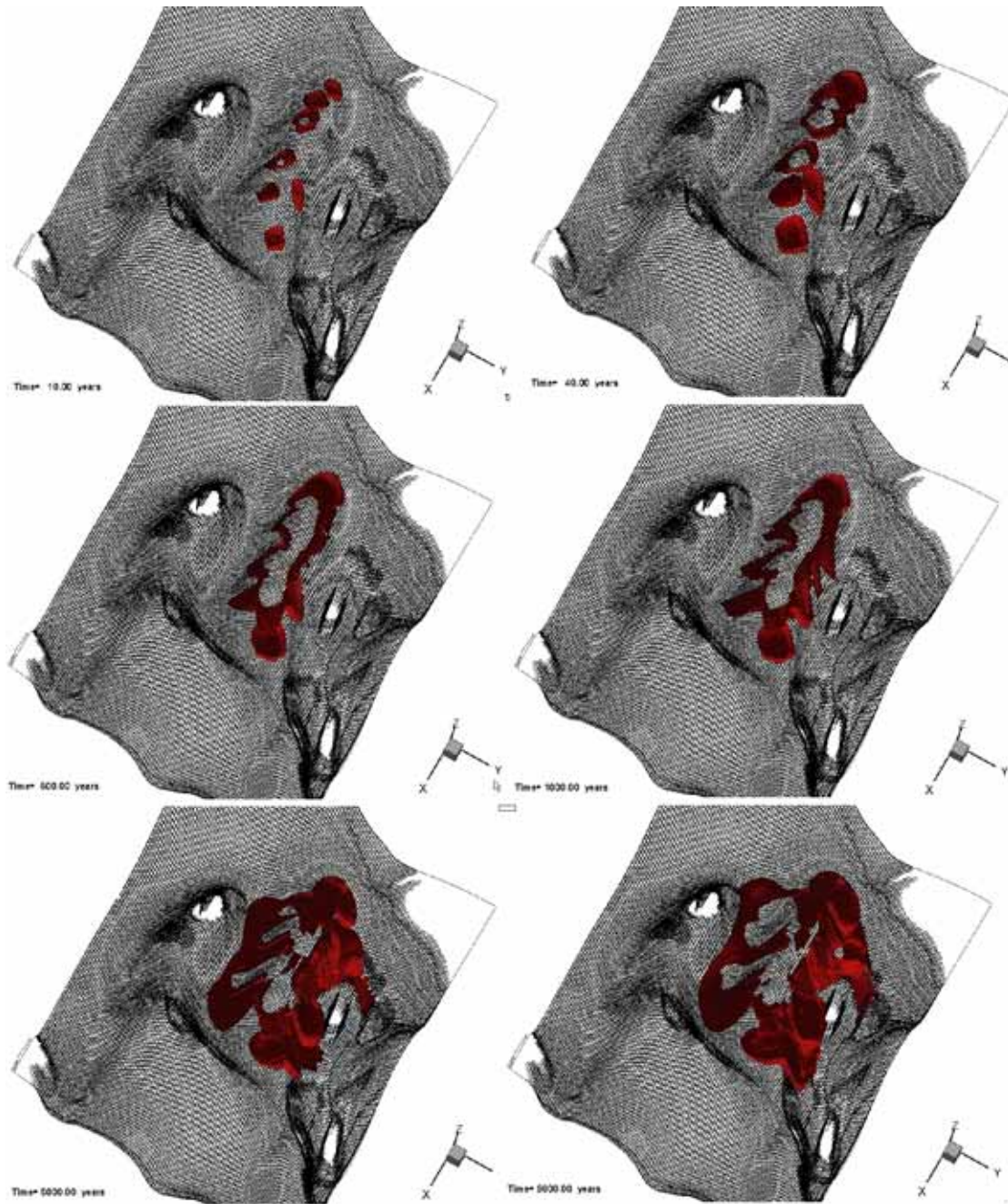


Figure 4.26 Schweinrich long term simulation: Simulated migration of CO₂-saturated formation water over 10 000 years. Note the great portion of dissolved CO₂ (red) leaving the structural trap. Accordingly, the total area affected by dissolved CO₂ is much larger than the anticlinal structure itself.

Extending the reservoir limits by 50 km reduced the average pressure increase to about 1 MPa, a relatively low figure thought to be compatible with maintaining integrity of the caprock. Extending the reservoir limits by smaller amounts however resulted in much larger average pressure increases, up to 10 MPa in the case of a 15 km extension. It is clear that for the Schweinrich structure, simulated pressure distributions are very responsive to the injected CO₂ volume for a large area surrounding the storage structure and average reservoir pressure increase falls sharply as effective reservoir volume increases. It is notable that even for the largest model, where the average pressure increase over the entire model areas was only 1 MPa, the

local pressure increase calculated for the middle of the structure between the injection wells, was much higher (Figure 4.28).

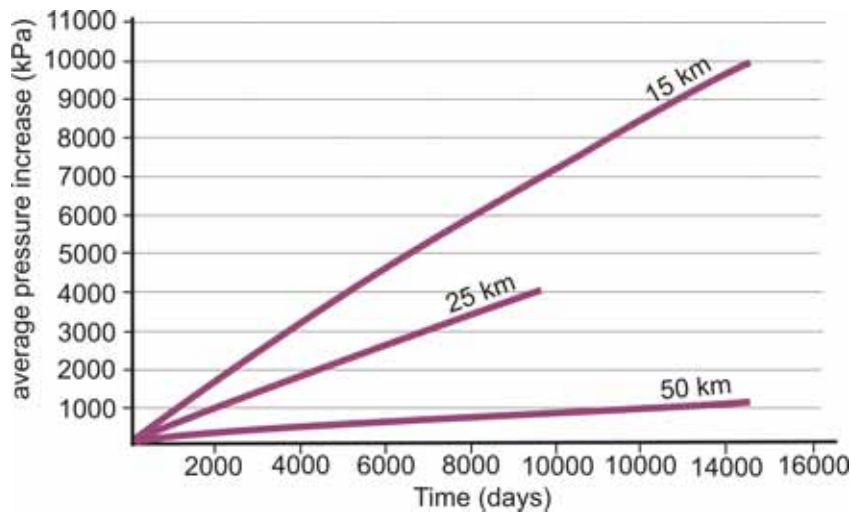


Figure 4.27 Time dependent evolution of the average formation pressure increase at Schweinrich calculated for different model lateral extensions.

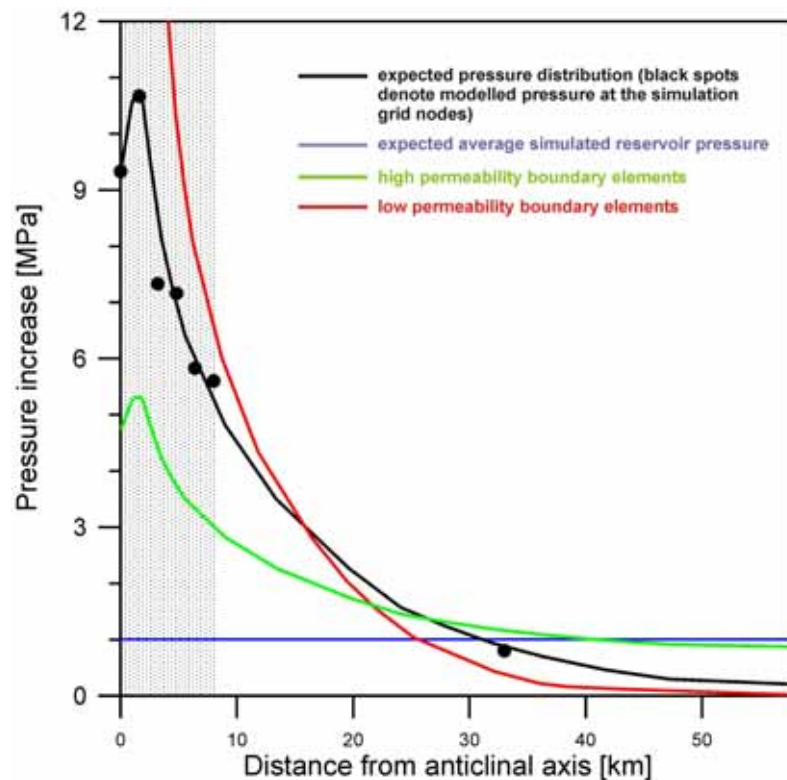


Figure 4.28 Schematic illustration of the pressure distribution in the aquifer (50 km extension to limits) surrounding the storage site. The shaded area represents the volume of the reservoir model, while the blank area is equal to the size of the boundary elements in the numerical model. The maximum pressure after 40 years of injection occurs on the flanks of the anticline where the injection wells are positioned, and is very sensitive to aquifer permeability.

It is clear from this study that fluid pressures depend strongly on the nature of flow compartmentalisation within the reservoir. If laterally extensive flow barriers are present within kilometres or a few tens of kilometres of the injection site pressures may rise above the capillary entry pressure of the caprock (Section 4.1). As a consequence the number of wells, their spacing and injection rates may have to be modified compared to the simulated scenario.

Valleys

Flow simulations for the Valleys site were based on two proposed reservoir models based on available well information and, in the case of the second model, an assumed sedimentary architecture. Model 1 comprised a simple layer-cake reservoir with 13 layers of alternating sheet sand and mudstone. This was considered to be the ‘best-case’ scenario for ease of CO₂ injection and storage capacity, and the ‘worst-case’ scenario for rapid migration of CO₂ to the containment risk at the St George’s Fault.

Model 2 (Figure 4.15) assumed a stochastic distribution of fluvial sandstone bodies within the reservoir unit, constrained to fit sandstone occurrences in the two available exploration wells (106/24A-2B and 106/24-1). This model is considered a more realistic portrayal of reservoir heterogeneity. It represents an improved scenario for retardation of migration of CO₂ to the St George’s Fault, but a significantly worse case for pore fluid pressure increase in the reservoir sand.

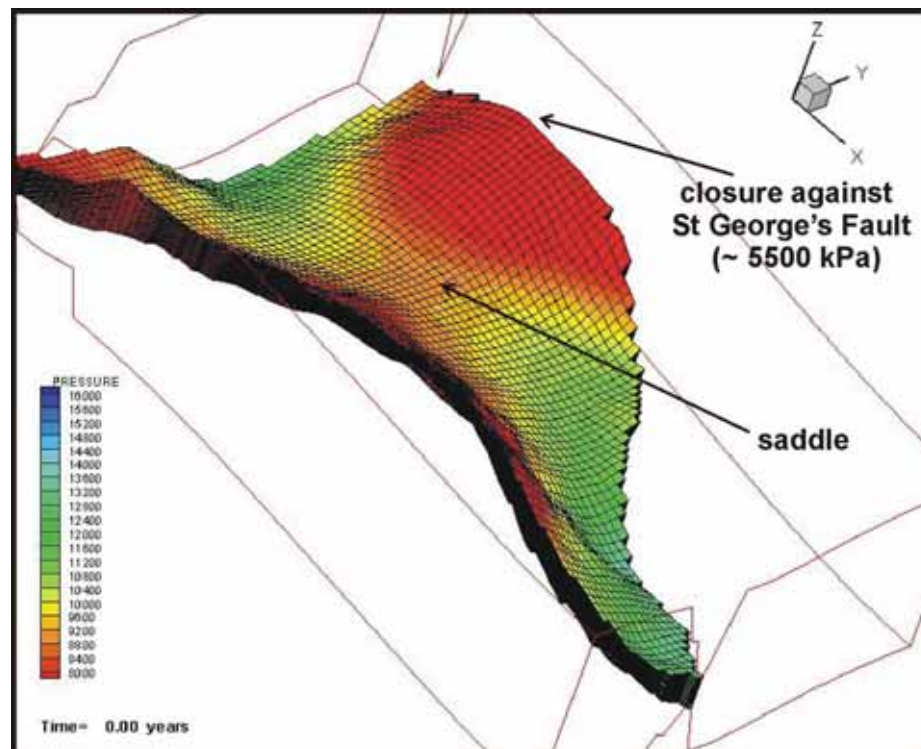


Figure 4.29 Valleys flow simulation: initial pressure conditions.

The reservoir models were input to the SIMED reservoir flow simulator. Zero-flow boundaries were assumed to be present at all edges of the full model which corresponds to the mapped extent of the reservoir unit. This may be realistic in that

the reservoir sands may well shale out laterally. On the other hand it is likely to be pessimistic in terms of pressure build-up in the model. Initial pore fluid pressures were assumed to be hydrostatic, around 5.5 MPa at the top of the storage structure (Figure 4.29). The sand bodies were assigned a permeability of 1000 mD, and other reservoir lithologies a permeability of 10mD. The simulations injected 2.3 Mt of CO₂ per year, over a period of 20 years, through three vertical wells located on the western flank of the storage structure. In each simulation the numerical model was run for a 10 000-year period. In the first two simulations CO₂ was considered to remain wholly in the free phase but the third simulation incorporated the effects of CO₂ dissolution.

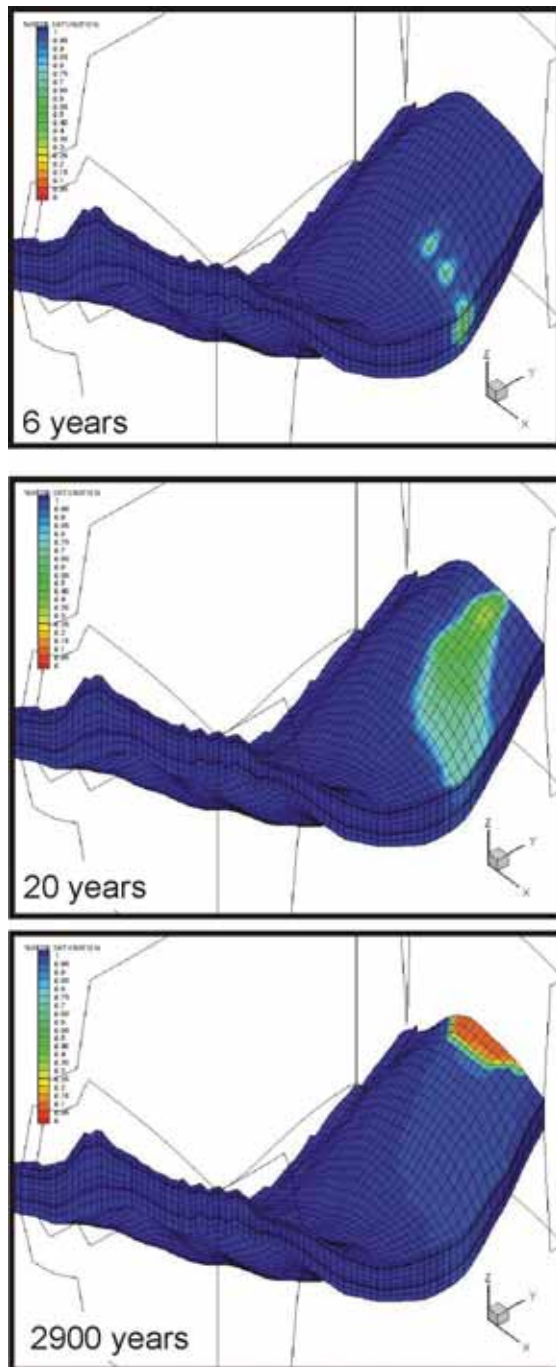


Figure 4.30 Valleys flow simulation Model 1: free CO₂ saturation.

The simulation for Model 1 (Figure 4.30) shows CO₂ to be still concentrated around the injection points after six years, migrating updip to reach St George's Fault after 20 years. After 2900 years the CO₂ distribution is stable, accumulating at the top of the fault-bounded closed structure.

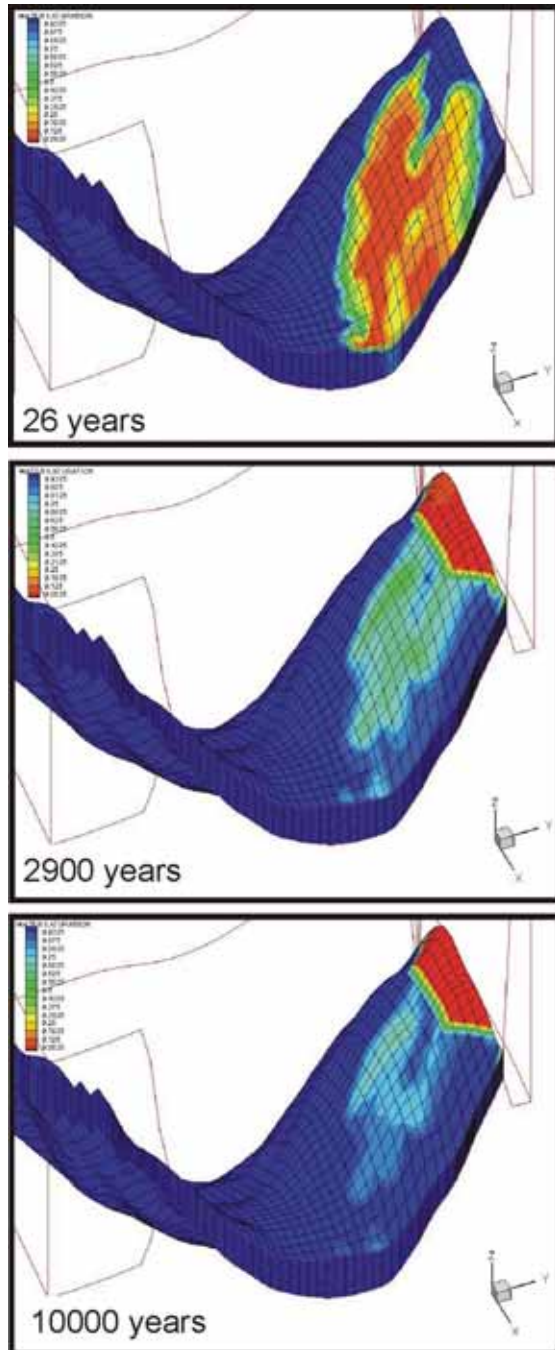


Figure 4.31 Valleys flow simulation Model 2: free CO₂ saturation.

The simulation for Model 2 (Figure 4.31) shows the CO₂ reaching the fault within 30 years, somewhat slower than for the simple layer-cake model, but subsequently taking much longer to stabilise at the top of the structure. In fact significant amounts of CO₂ remain in the downdip part of the aquifer even after 10 000 years.

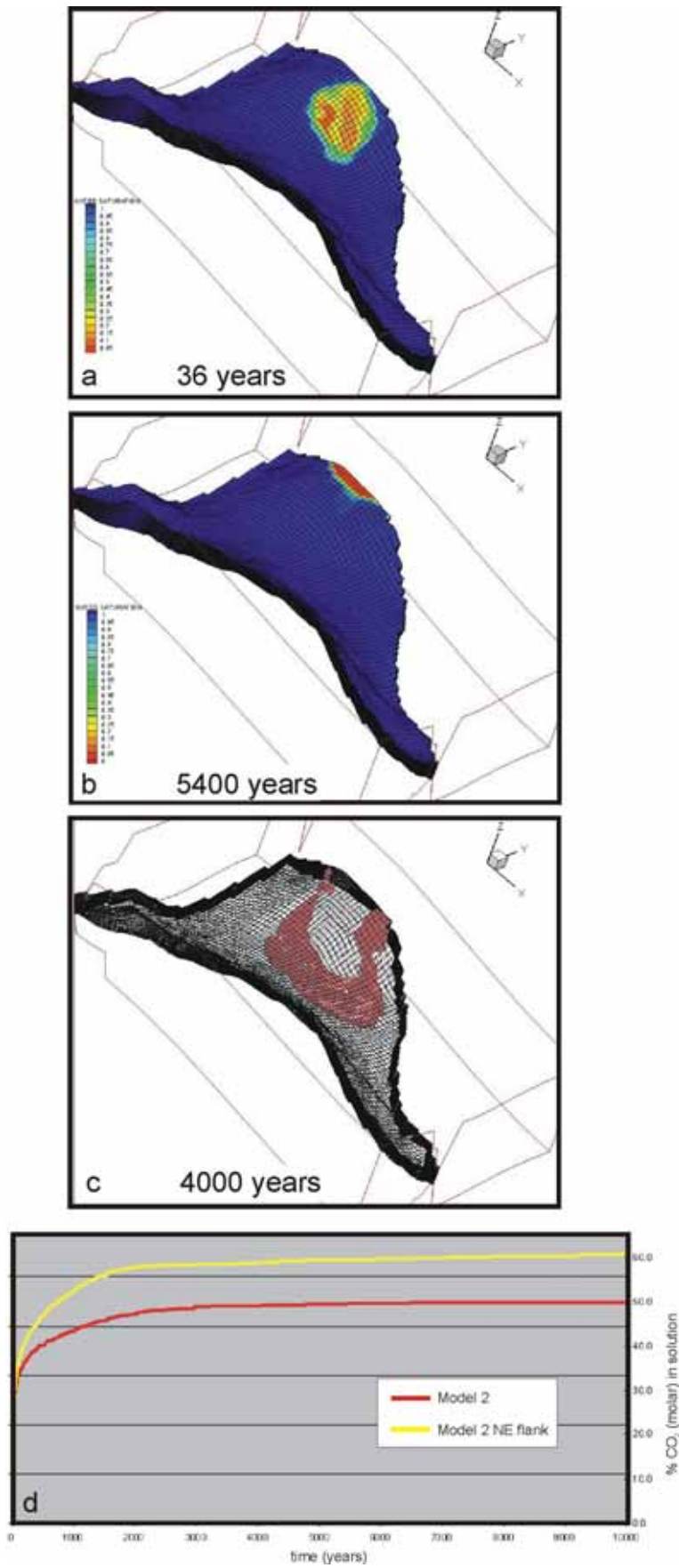


Figure 4.32 Valleys flow simulation Model 2 with dissolution: a) free CO₂ saturation b) free CO₂ saturation c) dissolved CO₂ d) evolution of dissolved CO₂ for initial and revised injection points.

The Model 2 flow simulation was repeated, but allowing CO₂ to dissolve into the aquifer waters. Undissolved free CO₂ reaches St George's Fault after about 36 years and stabilises at the top of the structure between 5000 and 6000 years after injection (Figure 4.32a,b). However, the amount of CO₂ accumulating next to the fault is considerably lower than in the previous simulations because a significant proportion of the CO₂ dissolves as it moves updip through the reservoir. The denser, CO₂-saturated brine forms a fringe around the diminishing plume of free CO₂ (Figure 4.32c) and starts to sink downwards in the reservoir move from 200–300 years onward. Approximately 50% CO₂ would be in solution after 2500 years (Figure 4.32d).

The second simulation with Model 2 reservoir properties investigated the effect of moving the injection wells to the north-east flank of the storage structure. Other parameters, including dissolution, were unchanged. CO₂ took slightly longer to reach St George's Fault (approximately 60 years as opposed to 36 years) and stabilised at almost the same time (5600 years as opposed to 5400 years). However, the amount of dissolved CO₂ is further increased, reaching around 60% in 2500 years (Figure 4.32d).

The effects of residual CO₂ remaining trapped as an immobile phase along the CO₂ migration path were not investigated. As discussed in Chapter 3, this process is potentially important in storing CO₂ within dipping reservoirs, especially in heterogeneous reservoir units. The third simulation run indicates that CO₂ injection ceases well before CO₂ reaches the fault, so residual CO₂ saturation might have a significant effect on the volume of CO₂ reaching the fault. It is recommended that this process should be investigated further in future studies.

Turning to pressure effects, in Model 1 (layer-cake sheet-sand reservoir distribution), pore fluid pressure near the top of the structure reaches a maximum of approximately 8.3 MPa after 20 years injection (Figure 4.33). In the Model 2 (fluvial sand reservoir) simulation without CO₂ dissolution, pore fluid pressure reaches a maximum of about 11 MPa after 20 years. The pore fluid pressure in Model 2 reaches a higher value because it contains less reservoir sand. If however the effects of CO₂ dissolution are taken into account, pressure increase is limited to a maximum of approximately 9 MPa after 20 years injection, because dissolved CO₂ occupies less space within the reservoir than free CO₂. As dissolution continues, on a timescale of hundreds of years (Figure 4.32d), pressure will decrease in proportion, as more CO₂ enters the aqueous phase.

Reservoir leak-off pressure has been estimated empirically to be around 1.35 times the reservoir pressure at depths less than 1000 m, so in all simulations the pore fluid pressure after 20 years exceeds the likely leak-off pressure and the seal may be breached, especially as the leak-off pressure in any damage zone adjacent to the St George's Fault is likely to be lower than in the overburden. However it should be stressed that the simulated pore fluid pressures are a function of the volume of reservoir sand in the models and the nature of the model boundaries.

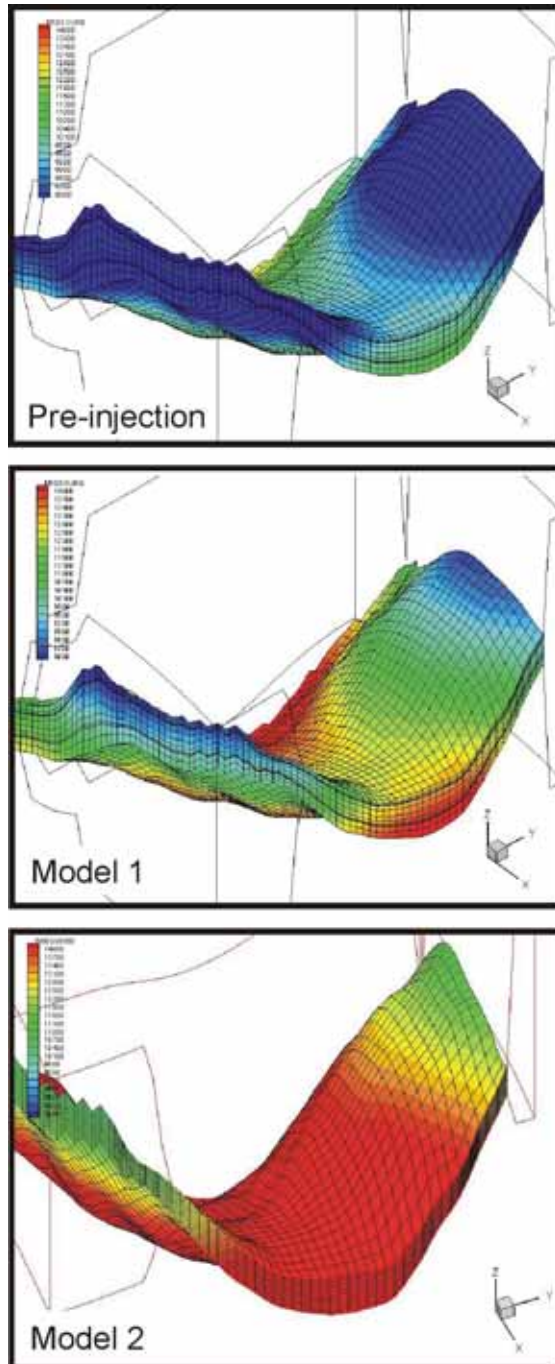


Figure 4.33 Valleys flow simulation pressures prior to injection and at 20 years for models 1 and 2 (assuming no dissolution).

It is stressed that the actual (as opposed to modelled) volume of reservoir sand is not known, and could be significantly larger than in the models. Moreover, in reality, the pore pressures would probably not reach the calculated values because formation water would partially bleed off (via single-phase flow) through the predominantly mudstone strata above and below the reservoir interval. The zero-flow barriers on the model therefore are quite pessimistic with respect to the predicted pressure increase.

4.2.2 Generic findings

At the site characterisation stage, flow modelling is likely to be rather rudimentary, since key controlling parameters on the scale of the CO₂ plume do not become constrained until the monitor data are acquired. Nevertheless, full ‘dynamic’ flow simulations should be considered a mandatory component of the site characterisation phase. They are required to constrain or validate injectivity, storage capacity, plume migration extent and likely reservoir pressures (see below).

A useful modelling tool at this stage is the simple buoyant ‘ponding’ simulator, exemplified by the SEMI software used at Sleipner. The main point of this type of modelling is to assess the maximum likely lateral extent of plume migration, principally to ensure no unexpected conflicts will arise (e.g. CO₂ impacting on well infrastructure, interfering with adjacent injection plumes), but also to assess the requirements for future monitoring.

There is a potential generic issue associated with the injection of such large amounts (400 Mt) of CO₂ into a single anticlinal aquifer structure. A key parameter is the effective size of the aquifer (dependent on flow barriers), which dictates how easily the native formation waters can be displaced and ultimately how much formation pressure will be increased. It is clearly of the utmost importance that the nature of flow compartmentalisation within the storage reservoir is properly addressed in the simulation.

4.3 Geochemical assessment

While it is assumed that dry CO₂ in a dense phase is chemically inert, once it dissolves in water it will form carbonic acid. This will acidify the formation water and potentially attack and alter many types of rock when coming in contact with them. This can occur in the reservoir where it is injected, in the overlying caprock(s), in fractures present in the caprock and/or in the reservoir and at the wellbores. These chemical interactions might change the physical characteristics of parts of the storage site and thus potentially enhance CO₂ migration towards the surface. The assessment of the geochemical impact is therefore an important aspect in assessing the safety of a CO₂ storage site.

The degree of reactivity between CO₂, porewater and minerals will influence the long-term storage potential of the reservoir. For example, instead of free CO₂ being trapped as a buoyant, mobile phase (physical trapping), reaction with formation water could trap the CO₂ as a dissolved phase (solubility trapping). Dissociation of the dissolved CO₂ will lead to the transformation of dissolved CO₂ into bicarbonate ions (ionic trapping) inducing a lowering of the pH in the formation water. Reaction of certain non-carbonate calcium-, iron-, or magnesium-rich minerals could even trap the CO₂ as a solid carbonate precipitate (mineral trapping), essentially immobilising the CO₂ for geological time periods (Bachu et al., 1994). Depending on the nature and scale of the chemical reactions, the reservoir-CO₂ interactions may have significant consequences on the CO₂ storage capacity, the injection process, and long-term safety, stability and environmental aspects (Rochelle et al., 2004; Czernichowski et al., 1996).

In order to assess possible geochemical impacts at a storage site in the most reliable way, four steps have to be undertaken:

Baseline geochemical conditions at the storage site must be characterised properly **before the injection starts (Step 1)**, leading to **the assessment of the initial geochemical status (Step 2)**. This requires a phase of data acquisition that differs from the usual practice in hydrocarbon operations, and consists of:

- geochemical characterisation of the caprock, reservoir and fracture fillings (if appropriate)

- characterisation of the formation waters

- measurement of the pressure and temperature conditions

- establishing the gas composition and chemical properties of the CO₂ to be injected.

In the third step, a geochemical model of the water and rock system must be constructed, both for the CO₂ injection reservoir and the caprock, aiding **the assessment of the short-term geochemical reactions**. It is based on the initial characterisation of the rock and formation water, and should be constrained by laboratory experiments. These experiments will determine how the water and rock will respond to CO₂ injection, and provide input to better constrain the geochemical model, by determining some of the unknown geochemical parameters of the model (types of reactions, reaction rates and reactive surfaces). Results from these experiments are used to inform and calibrate the predictive geochemical modelling (at least over shorter timescales).

Finally in the fourth and last step, **long term predictive modelling** of the geochemical interactions has to be carried out. This is the only way to assess the geochemical impact of the injected CO₂ over hundreds to thousands of years. It can predict the effects of CO₂ formation porewaters, and the consequent changes in fluid chemistry and host rock mineralogy over the long term. However, output from simulations is crucially dependent on which reactions are taken into account and their underpinning chemical data (i.e. the simulations cannot predict phases or reactions which are not included within the database of the model). The outputs are also dependant on the reliability of the conceptual model chosen (which requires a good expertise in geochemical processes). The amount of uncertainty can be reduced by performing a detailed sensitivity analysis on critical parameters. Computer processing demands might put a limit on the number and complexity of simulations that can be performed however. Further reductions in uncertainty can be made through comparison with observations from laboratory experiments (however, only on the short term), field monitoring at other CO₂ injection sites and knowledge derived from geochemical reactions observed at natural CO₂ analogue sites. The latter can be particularly useful, but care should be taken not to misunderstand or over-interpret the observations from these very complex natural systems.

While the first step (baseline characterisation) is described for both the caprock and the reservoir, the next steps are discussed separately in the sections focussing on

reservoir and and caprock reactivity. An additional section is added with respect to interactions in faults since in it is extremely difficult to collate data regarding their geochemical characteristics and to design specific experiments while modelling has to be performed on a very generic level.

4.3.1 Geochemical baseline characterisation of the storage site

A good geochemical understanding of the system will require knowledge of the 'baseline' conditions of mineralogy and fluid chemistry prior to CO₂ injection. It is important therefore, that a programme of sample acquisition be implemented prior to CO₂ injection operations. Baseline geochemistry can be best determined by analysis of suitably preserved borehole core material and porewaters. This should aim to produce data on the chemical make-up of reservoir and caprock formations prior to any CO₂ injection.

A knowledge of the chemical make-up of the reservoir and its properties is required to quantify possible chemical reactions, and their reaction rates, leading to an estimation of the storage capacity and potential changes in porosity and permeability. Acquiring knowledge on the sealing capacity of the caprock is perhaps the key element in assessing and establishing the long-term safety case for CO₂ containment. Two aspects are important here; the natural seal (i.e. caprock), and the man-made seal around breaches in the caprock (i.e. boreholes). Caprock core material should be available in sufficient quantities to undertake a detailed suite of analytical tests. Ideally, samples of borehole cement should also be available for testing and analysis. Also for the reservoir seal, knowledge on the chemical make-up and its transport properties are required to quantify possible chemical reactions and their rates leading in this case to an estimation of the overall sealing efficiency. To determine these properties, a minimum prerequisite is to have core material from the caprock above where the CO₂ is to be stored. Core and cuttings material from additional wells will further improve characterisation, particularly if vertical and lateral caprock inhomogeneity is suspected.

It is recommended that data be collected as outlined in the following.

4.3.1.1 Caprock and reservoir mineralogical composition

Analysis should include mineralogical and chemical characterisation of solid phases, identification of detrital and authigenic phases and their specific surface areas. Special attention should be paid to the identification of the exact composition of the clay and feldspars present, since these minerals are likely to contribute to the mineral trapping of CO₂ on the long term. Recommended analytical tools include optical microscopy, SEM (scanning electron microscopy), XRD (X-ray diffraction), electron microprobe analysis, particle-size analysis and BET (specific surface measurements).

4.3.1.2 Reservoir porewater sampling

Water can be collected either down-hole or at the surface. For all surface sampling, water flowrate and gas-water ratio as well as non-conservative parameters (e.g. temperature, conductivity, pH, Eh, alkalinity) must be measured on site. This is because samples taken at the surface are prone to chemical modifications (mainly degassing, but also possibly cooling and mineral precipitation). Also, producing formation water may lead to mixing of water from various reservoir units, and indirect calculations are needed to assess fluid chemistry at depth. Suitably preserved samples of gas and water can then be analysed subsequently for their compositions in the laboratory.

Down-hole water sampling enables the retrieval of pressurised samples, but care has to be taken to avoid pollution of the water sample from the drilling fluids. Although in ideal circumstances such down-hole samples would be preferable, their recovery requires specific tools and know-how, is costly, and is generally not common practice.

These two techniques assume that water is mobile in the injection site, which may not be the case (especially when injecting water in a depleted hydrocarbon reservoir). In such cases, alternative techniques have to be tried, possibly involving similar approaches to those used to evaluate the composition of caprock pore water.

4.3.1.3 Caprock pore-water analysis

It is much more difficult to get a water sample from a caprock, as the water mobility is extremely low. The following two core-based techniques are available.

First, caprock pore waters can be extracted from core material. However the water sample obtained is not representative of in situ conditions at depth and additional information on gas:water ratios and gas content has to be obtained, ideally from the same well. Moreover porewaters extracted from core material are often contaminated by drilling fluids and corrections have to be made to assess the actual fluid chemistry.

Second, caprock pore-water chemistry can be reconstructed from residual salt analysis whereby formation water salts are collected from a water percolation test in a core plug.

Several residual salt analysis methods can be mentioned:

Elemental residual salt analysis, to establish the water chemistry from shaly samples.

Water salinity from plugs cut in hydrocarbon bearing intervals.

Sr-residual salt analysis, based on the analysis of the isotopic composition of Strontium ($^{87}\text{Sr}/^{86}\text{Sr}$).

This is also an indirect method that must be implemented with care.

4.3.1.4 Laboratory data to be acquired to assess the water chemistry

The minimum range of parameters to be analysed are:

cations (e.g. Li, Na, K, Mg, Ca, Sr, Ba, Mn, total Fe, Al, Si, total S, and others as necessary)

anions (e.g. HCO_3^- , Br^- , Cl^- , SO_4^{2-} , and others as necessary)

pH with corresponding temperature

alkalinity

total inorganic carbon (TIC)

total organic carbon (TOC).

4.3.1.5 Prevailing pressure and temperature conditions in the reservoir and caprock and their physical properties

Pressure and temperature conditions have an important impact on the type of geochemical reactions that will occur, as well as on their reaction rates, and should be measured with great care. Also the presence of temperature and/or pressure gradients should be established. Physical parameters of the reservoir and caprock that are needed to perform coupled flow and transport models are porosity, absolute and relative permeabilities and capillary entry pressure as well as diffusion rates in the case of caprock characterisation.

4.3.1.6 Characterisation of the CO_2 to be injected

The presence of other substances together with CO_2 when it is injected (e.g. H_2S) may have an important impact on the geochemical interactions in the reservoir as well as on its phase behaviour. It is therefore necessary to establish the exact composition of the CO_2 stream (as well as its anticipated temperature) that will be injected and acquire the necessary data to establish its phase behaviour. The impact of certain impurities can currently be assessed using existing models, but this very much depends on the type of impurities.

4.3.1.7 Observations from the CO2STORE case studies

Sleipner

Baseline geochemical characterisation at Sleipner was able to draw on only limited geochemical information and samples from the Utsira Sand and its caprock. These included a single (partial) analysis of Utsira formation water from the Oseberg Field (approximately 200 km north of Sleipner) and a 7-m core of Utsira Sand from the Sleipner field (preserved frozen).

The core sample allowed for detailed mineralogical analyses and determination of transport properties. However, it was heavily contaminated by drilling fluids, and no reliable formation water sample could be obtained. Although there is a single analysis of Utsira porewater from the Oseberg field, it is of limited use due to the absence of Al and Si measurements. An additional sample taken at the surface from the Brage Field (also about 200 km north of Sleipner) was obtained (but without information on the gas phase) and was analysed for a range of elements including Al and Si. However, the sample was unpreserved (unfiltered and un-acidified) and so the resulting Al and Si data are probably best described as being 'uncertain'. Despite this lack of information and samples, a reasonable assessment of baseline conditions within the Utsira Sand was made by combining information from the Sleipner, Oseberg and Brage hydrocarbon fields, and through numerical modelling and the performance of blank laboratory experiments.

During the SACS and CO2STORE projects a core was obtained from the Nordland Shale caprock a few kilometres from the injection point. The core was analysed for its physical and geochemical properties. These parameters were subsequently used for the experimental work and the long-term coupled modelling. Unfortunately it was not possible to determine a realistic composition of the pore water present in the caprock because of significant contamination by drilling fluid.

4.3.2 Reservoir reactivity

The reactivity of dissolved CO₂ in the reservoir will act as an open system from a geochemical point of view, meaning that dissolved CO₂ is likely to be in excess and will not limit the reactivity. The dissolution of CO₂ will cause a significant drop in the pH of the pore water and where this occurs dissolution of carbonates is likely to take place relatively rapidly. This might cause a local increase in porosity (especially around the injection well). In the longer term, slower reacting minerals (aluminosilicates) will dominate the geochemical interactions depending on the mineralogy of the host rock. When sparse and slow reacting aluminosilicates are being dissolved and only a minor amount of cations is liberated due to CO₂ interactions, small amounts of the dissolved CO₂ will become trapped as carbonates (mineral trapping). In this case carbonate dissolution might be dominant even over long timescales. However when the mineralogy of the host rock is such that substantial amounts of host rock aluminosilicates can be altered, substantial carbonate precipitation can occur, thereby trapping large amounts of dissolved CO₂. In this case mineral trapping can become significant and might locally decrease the porosity of the reservoir in the long term. The interaction between flow and geochemical reactions requires a coupled modelling approach taking into account the geometry of the reservoir as well as the flow of the phases involved (dense phase CO₂, brine, oil, gas) and the geochemical reactions. These types of models are also crucial for calculating the time evolution of CO₂ dissolved in the pore water over time, since in most reservoirs solubility trapping is expected to dominate over mineral trapping.

4.3.2.1 Assessment of initial geochemical status

If a full and detailed analysis of the reservoir formation water is not available, then it may be possible to use geochemical modelling to estimate the missing data. This requires mineralogical analysis of reservoir rock samples. Minerals present in the host rock can be selected to fix the missing concentration data (e.g. by equilibrating with chalcedony or quartz in case Si concentrations were not measured, and with kaolinite in case Al concentrations were not measured) or where pH measurements seem unreliable. Furthermore an initial analysis should be made with respect to the minerals that should be included in the geochemical models taking into account temperature and pressure conditions as well as detailed mineralogical analysis and SEM imaging if possible. Thermodynamic and kinetic data with respect to these minerals should be selected with care. In this step, pre-dimensioning modelling can also be performed to get preliminary insights into the potential reactivity of the caprock when in contact with pore water modified by the dissolution of CO₂.

4.3.2.2 Short-term geochemical interactions

Shorter-term geochemical reactions (measured in timescales of minutes to several months) lend themselves well to investigation through laboratory experiments. Indeed, it is relatively straightforward to design and build experimental systems that can reproduce in situ conditions that might be found in the top few kilometres of the Earth's crust. The complexity of the experiments undertaken will depend upon the specifics of the study or the storage site in question, and what data are required. As a minimum requirement however, simple 'batch' experiments should be performed. These would react samples of the reservoir rock with a representative pore-water composition \pm CO₂, under representative in-situ pressure and temperature conditions. Conducting experiments in pairs (i.e. with and without CO₂) allows purely CO₂-induced reactions to be discriminated from possible experimentally induced 'artefacts'. Periodic sampling of the fluid phase(s) can be used to follow reaction progress in real time, whilst mineralogical analysis of the solid phases at the end of the experiments can provide detailed information on which minerals dissolved or precipitated during the experiments. Although laboratory experiments will only tend to investigate time periods of months to a very few years, they are very important in that they can provide the detailed and well-constrained data against which predictive computer models can be checked. Modelling simple batch experiments using equilibrium geochemical codes is relatively straightforward, and the drivers for mineral dissolution and precipitation can be followed by tracking parameters such as the saturation state of individual minerals.

Experiments reacting samples of the Utsira Sand over timescales up to two years show relatively little reaction (Rochelle et al., 2002). Most of the reaction when CO₂ was added to the experiment was associated with dissolution of carbonate minerals (both detrital carbonates and shell fragments), and re-equilibration appears to be more-or-less complete within about two months under in-situ temperature and pressure (assumed to be 37°C, 8 MPa). Conversely, silicate mineral reactions were still ongoing after two years of reaction (the maximum duration of the laboratory experiments).

The rates of fluid-rock reaction can be relatively slow, and so it may take several months (or longer) for significant fluid-rock reaction to occur. Grinding of the rock sample can provide increased surface over which reactions can occur. However, care must be taken not to expose unrepresentative mineral surfaces (e.g. the reaction of an intact piece of sandstone where all the quartz grains are coated with a thin layer of iron oxides, will be very different to a disaggregated sample of the same material where the oxide coating has been abraded away). Although raising the temperature of the experiments can increase the rates of reactions (i.e. in an attempt to compress many years of reaction into a few weeks), applying unrealistically high temperatures can also favour unrepresentative reactions. These might result in the precipitation of 'unexpected' secondary minerals (e.g. the precipitation of Ca as an aluminosilicate phase at high temperatures rather than as calcite).

In order that geochemical computer codes can model accurately short-term reactions involving real rocks (be they in experiments or deep underground), it is necessary to have certain basic kinetic data as well as thermodynamic data. Although various databases of the latter exist, kinetic data are scarcer. It may be necessary therefore, to undertake short-term experiments on specific single minerals to derive kinetic parameters that are not available in the literature. Such parameters are particularly important when considering far from equilibrium conditions, such as when a plume of CO₂-rich water passes through a rock for the first time. With appropriate kinetic data therefore, it should be possible to model not just the end point of a particular experiment for example, but also how long it will take for the experiment to get there.

Although simple 'batch' experiments can be used to identify the types, rates and magnitudes of CO₂-water-rock reactions, they can not simulate the complex interplay between kinetically-controlled dissolution/precipitation reactions and fluid migration through rocks. Simulating this complexity is necessary in order to make accurate predictions about the future evolution of real CO₂ storage schemes. For example, the precipitation of secondary minerals may be relatively slow compared to the dissolution of primary phases. As a consequence, CO₂-rich water flowing through a rock may produce a series of reaction fronts that migrate over time. These are likely to be associated with changes in porosity, and so will affect fluid flow. Although various reaction-transport codes have been developed, they tend to produce somewhat idealised models. Laboratory experiments involving CO₂-water-rock reactions under flowing conditions can provide the well-constrained and detailed data that are needed to refine preliminary models. For example, a model may predict a series of narrow and discrete reaction fronts after a certain time period. However, experimental observations could reveal reaction fronts that are more gradual and 'smeared out'. Complex flow experiments can also show that rates of mineral reaction (or reactive mineral surface areas) can be very much lower than literature values (e.g. Bateman et al., 2005).

4.3.2.3 Long-term predictive modelling

Long-term predictive modelling, calibrated if possible by laboratory data, is key to understanding the possible future geochemical effects of CO₂ storage. 1D geochemical modelling was utilised on two of the CO₂STORE case studies to explore geochemical interactions. Recent developments in coupled reaction-transport

modelling tools have enabled 2D and 3D reaction-transport modelling to be carried out for the Sleipner case.

4.3.2.4 Observations from the CO2STORE case studies

Sleipner

1D reaction transport modelling was carried out early in the CO2STORE project (Gaus, 2005). More sophisticated 2D and 3D reaction transport modelling was carried out as part of the operations phase and is described in Chapter 7.

Kalundborg

It was decided to focus the modelling on the role of the low permeability clay layers in the reservoir and the potential impact of a difference between the temperature of the injected CO₂ and the reservoir temperature. Full details are given in Durst and Gaus (2005).

In the first scenario the reservoir is assumed to contain shale layers with very low vertical permeability that act as local capillary seals. 1D modelling of the diffusion of CO₂ in the shale, and in the reservoir above, was performed to assess potential porosity changes as well as the time needed for the CO₂ to break through a shale layer.

A second scenario assumed that CO₂ loaded brine was allowed to flow through some weak zone of the shale and 1D modelling was aimed to determine if the geochemical reactions are likely to prohibit the flow or to enhance it.

A third scenario assessed the impact on geochemical interactions of injected CO₂ having a different temperature to the reservoir temperature. 1D model simulating a near well environment was set up for the whole injection period and a sensitivity analysis with respect to the injection temperature carried out (in the range 30°C–90°C).

The studies all concluded that dissolution and precipitation will occur as a result of the acidity of dissolved CO₂. However the geochemical reactions are not expected to cause severe damage to the caprock lithologies within the reservoir.

Schwarze Pumpe (Schweinrich)

The modelling work performed on the reservoir concerns the storage capacity, so only the composition of the dominant reservoir rock, the sandstone, has been taken into account (Table 4.11).

Mineral	Weight%	Porosity	Amount per fluid volume (mol/l)	Reactive surface per fluid vol. (m ² /l)
Quartz	90	28%	107.73	14.663
Albite	5		1.373	0.082493
K-Feldspar	5		1.293	0.084393

Table 4.11 Reservoir rock properties used for the simulations.

The formation water approximates to a 190 g^l Na-Cl brine (Table 4.12). Four sample analyses were used for determining the formation water composition. Samples were taken from the bottom of the Wredenhagen well (2403 m depth) at the top of the Upper Triassic formation in the same unit as the reservoir, about 7 km north-east of the planned injection zone. Average values of the four samples have been taken for the simulation. Silica and aluminium content were not analysed, and have been calculated at equilibrium with chalcedony and kaolinite at 60° C.

Temp °C	pH	Na ⁺ mol/kg _{H2O}	K ⁺ mol/kg _{H2O}	Ca ⁺⁺ mol/kg _{H2O}	Mg ⁺⁺ mol/kg _{H2O}	Sr ⁺⁺ mol/kg _{H2O}	Fe ⁺⁺ mol/kg _{H2O}	Al ⁺⁺⁺ mol/kg _{H2O}
60	4.6	3.27	1.16·10 ⁻²	7.57·10 ⁻²	3.13·10 ⁻²	1.48·10 ⁻³	6.40·10 ⁻⁴	1.50·10 ⁻⁸
Density g/l		Cl ⁻ mol/kg _{H2O}	SO ₄ ⁻⁻ mol/kg _{H2O}	Br ⁻ mol/kg _{H2O}	Alk eq/kg _{H2O}			SiO ₂ mol/kg _{H2O}
1.13		3.48	7.63·10 ⁻³	2.01·10 ⁻³	1.35·10 ⁻³			3.37·10 ⁻⁴

Table 4.12 Average composition of the reservoir brine used for simulations.

Thermodynamic simulations have been performed with the PHREEQC software together with the LLNL thermodynamic database. In order to estimate the maximum amount of CO₂ that can be trapped in mineral form, two simulations have been performed.

In the first simulation, a volume of the reservoir rock (minerals + CO₂ saturated brine) is allowed to react over time as a closed system, representing the evolution in a portion of the reservoir where no more CO₂ is available.

In the second, a constant pressure (20 MPa) of CO₂ is applied, meaning that if mineral trapping occurs, more CO₂ can be dissolved in the brine. This second case represents the evolution near the supercritical CO₂ plume.

The most important chemical reactions which occur according to the simulations are: CO₂ dissolution, aqueous CO₂ dissociation, albite and K-feldspar dissolution and dawsonite precipitation. The results of those simulations for 10 000 years are shown in Figure 4.34.

In both cases, some mineral trapping is predicted to occur due to dawsonite precipitation. This process, after 10 000 years, could absorb up to 2.4 kg of CO₂ per cubic metre of reservoir in the closed system case and 3.3 kg per cubic metre of reservoir with constant supercritical CO₂ availability. In the latter case, precipitation of dawsonite allows the dissolution of an equivalent content of supercritical CO₂ in the brine, raising the total amount of CO₂ stored in a volume unit from 8.2 to 11.5 kg per cubic metre.

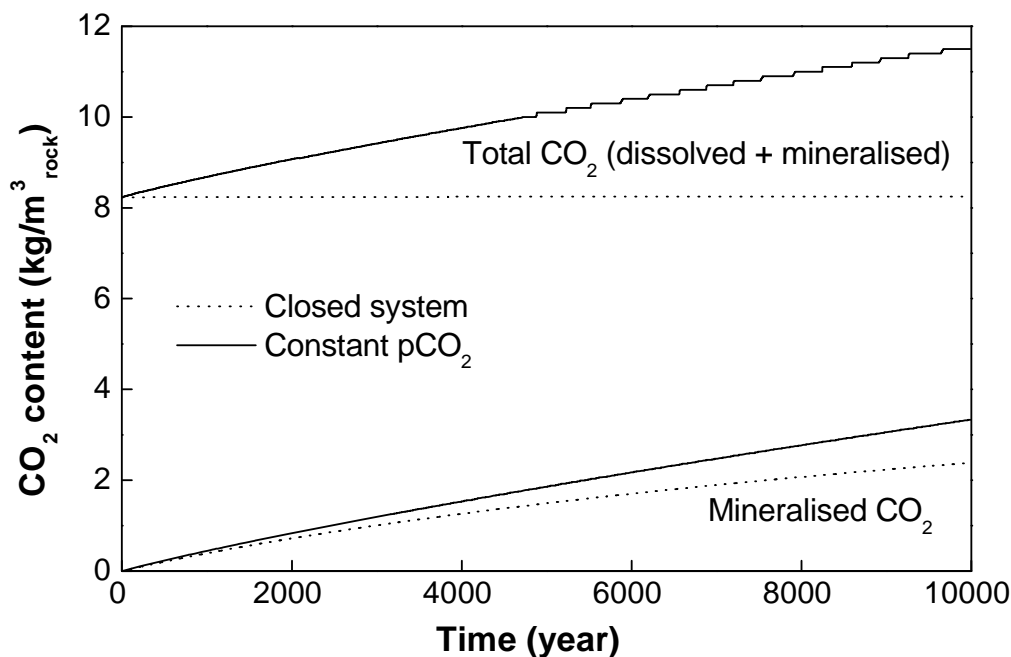


Figure 4.34 Evolution of CO₂ content (dissolved and mineralised) in the Schweinrich reservoir during reaction between CO₂- rich brine and reservoir minerals.

4.3.3. Caprock reactivity

Under the assumption that at a properly selected storage site free CO₂ will be unable to effect capillary penetration into the caprock, then CO₂ will only be able to enter the caprock by diffusion when dissolved in the brine. Diffusion is a very slow process and even on long timescales only the lower section of the caprock is likely to be exposed to CO₂-saturated formation waters. It is however, important to assess the potential geochemical impact in this section since one cannot exclude the possibility that caprock integrity will be affected in a significant way (for better or for worse).

Chemical reactions in the caprock will be limited by the amount of CO₂ available, and are likely to behave as a closed system from a geochemical point of view. Since the availability of CO₂ is small due to the slowness of the diffusion process, CO₂ will be consumed completely due to geochemical interactions which will further retard the movement of the diffusion front. While carbonate dissolution is likely to be limited to a very thin section at the base of the caprock, potentially inducing a slight increase in porosity, higher in the caprock aluminosilicates are likely to dominate the geochemical interactions, leading to minor changes in porosity depending on the specific caprock mineralogy.

4.3.3.1 Assessment of the initial geochemical status

As was the case for the reservoir, caprock data need to be integrated into a coherent dataset, especially with respect to the composition of the caprock formation water, since establishing pore-water composition in low permeability caprocks is particularly difficult. The same procedure should be followed as described in the case of the reservoir rock (Section 4.3.2.1).

4.3.3.2 Short-term geochemical interactions

The laboratory investigation of short-term CO₂–water–caprock reactions has very many similarities with the approach used for reservoir rocks (see earlier). Pairs of simple batch experiments can be used with powdered caprock samples to follow reaction progress in real time, whilst mineralogical analysis of the solid phases at the end of the experiments can provide detailed information on which minerals dissolved or precipitated during the experiments. Again, monomineralic experiments can be undertaken to ascertain specific kinetic data needed to parameterise predictive computer codes. As for the reservoir-rock experiments, care must be taken not to induce unrepresentative reactions. This is particularly important with samples of clay-rich caprocks, which may be more sensitive to changes in temperature for example.

A difference between caprock and reservoir-rock experiments is evident with flowing experiments. These are relatively straightforward for reservoir rocks, and can produce useful data. However, they are more problematical for caprocks as they have (by definition) very low permeabilities. Samples from relatively long (e.g. 12 month) duration experiments studying CO₂ flow/diffusion through a sample of caprock could be analysed for mineralogical changes. However, the degree of reaction may be relatively minor and hard to investigate if only a little CO₂ has passed into the caprock sample. More appropriate to the study of short-term interactions would be the simulation of CO₂-saturated water moving along a fracture in a caprock.

4.3.3.3 Long-term geochemical modelling

Long-term diffusion modelling has been performed for three sites within the CO₂STORE project. Diffusion was assumed to be the dominant transport process in the caprock, occurring mainly in a vertical upward direction, allowing the use of simpler conceptual models including only one dimension. In the reservoir, where density induced flow is anticipated, realistic coupled models require at least two dimensions.

All modelling results were comparable, indicating that major caprock deterioration due to diffusion of CO₂ into the caprock is unlikely, under the condition that no free (supercritical) CO₂ enters into the caprock.

4.3.3.4 Observations from the CO2STORE case studies

Sleipner

An experimental study of caprock reactivity was carried out in CO2STORE (Rochelle et al., 2006), based on techniques developed in previous CO₂ projects (e.g. Holloway, 1996; Czernichowski-Lauriol et al., 1996), and during the SACS project (Rochelle et al., 2002 a,b). Use of similar techniques will hopefully allow for better inter-comparison between the various studies.

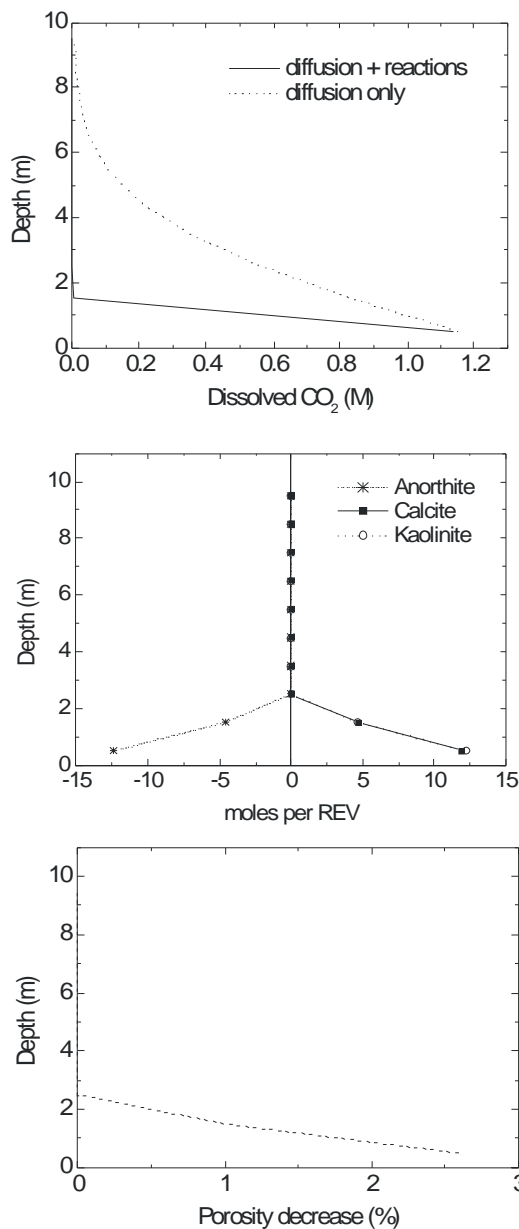


Figure 4.35 Impact of dissolved CO₂ in the Utsira caprock after 3000 years for the most reactive case. a) Diffusion of dissolved CO₂ into the caprock b) Dissolution (-) and precipitation (+) of minerals per representative elementary volume (REV= rock containing 1 litre of brine = 55kg). c) Porosity changes.

The experiments utilised actual caprock core material from the Sleipner field, together with synthetic formation waters based upon measured compositions. The

experimental conditions chosen for the investigation were representative of in situ conditions within the caprock (30°C, 8 MPa). Experiments were pressurised with either nitrogen or carbon dioxide, the former providing a ‘non-reacting’ reference point from which to compare the more reactive CO₂ experiments.

Caprock experiments involved crushed Utsira mudstone, and ran for up to 15 months. Those without CO₂ showed little or no reaction, indicating that the synthetic Utsira porewater used in the experiments was a reasonable approximation for the actual in situ porewater composition. However, the experiments involving high-pressure CO₂ were dominated by carbonate mineral dissolution. It is estimated that over two thirds of the calcite in the mudstone caprock was dissolved in the experiments. No precipitation of Ca/Mg/Fe carbonates or dawsonite reaction products was detected.

A full description of the Sleipner geochemical modelling study in CO₂STORE is given in Gaus et al. (2005). Diffusion is allowed to take place within the shale caprock with dissolved CO₂ moving upwards from the storage reservoir towards the sea bed. In the absence of CO₂ reactivity, this is an extremely slow process that does not significantly adversely affect geological storage efficacy. As such, it is important to confirm that any CO₂ reactivity does not accelerate CO₂ migration towards the sea bed and to make sure that no significant mineralogical and petrophysical changes take place that could lead to two-phase flow (capillary entry) into the caprock. Upward diffusion into the caprock was modelled using 1D reactive transport software (PHREEQC V2.6) combining reaction kinetics and diffusive transport. The main results are summarised in (Figure 4.35). Depending on the reactivity of the caprock, vertical diffusion of CO₂ will tend to be retarded by the chemical reactions. Calculated porosity changes are small and limited to the lower few metres of the caprock. A slight decrease in porosity is predicted which would tend to slightly improve caprock sealing capability. This is caused by the predicted alteration of plagioclase into calcite and dawsonite (as well as chalcedony and kaolinite). Only in the case that Ca-rich plagioclase is present will this reaction and subsequent porosity decrease be significant. At the very base of the caprock some carbonate dissolution is expected to occur.

Kalundborg

Long-term diffusion modelling of CO₂ loaded brine was performed using a 1D coupled model taking into account the caprock mineralogy in order to assess the potential porosity changes at the base of the caprock (Durst and Gaus, 2005). Modelling results show the rate of CO₂ diffusion through the caprock (Figure 4.36). After 4500 years, significant amounts of CO₂ have entered the first 15 m of the caprock. The study concluded that dissolution and precipitation will occur as a result of the acidity of dissolved CO₂. However geochemical reactions are not expected to cause severe damage to the caprock.

Valleys

Geochemical modelling was carried out for the Cenozoic caprock, on top of the structural closure, and for the Mercia Mudstone caprock that seals the Bunter Sandstone reservoir (Gaus, 2005). The same modelling approach was used as for Sleipner (see above).

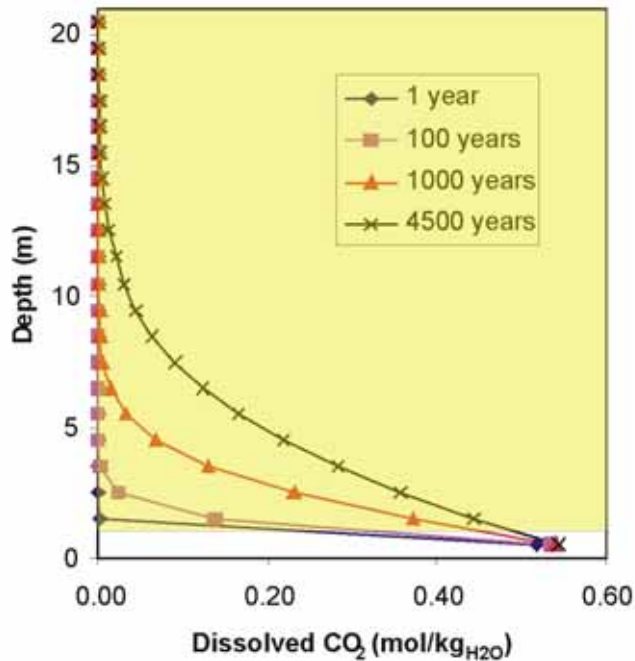


Figure 4.36 Evolution of the dissolved CO₂ concentration in the caprock at Kalundborg (yellow shading) during 4500 years of diffusion (from Durst and Gaus, 2005).

In the case of the Cenozoic caprock, geochemical interactions are predicted to occur at the base of the caprock and are the result of carbonate dissolution buffering the acidity of the CO₂- loaded brine. Modelling suggests this reactivity would be limited to the first metre of the caprock. Due to the lack of relatively rapidly reacting aluminosilicates, which can react as cation donor minerals, very little reactivity is predicted higher up in the caprock. Porosity changes due to the geochemical interactions are limited to the base of the caprock resulting in an absolute porosity increase of no more than 1%. In the case of the Mercia Mudstone caprock, calculation times are extremely long and the modelling was only carried out for a total duration of 60 simulated years. However, model results for this short period are very similar to that of the Cenozoic caprock, and there seems to be no reason to expect its behaviour to be significantly different.

4.3.4 Chemical reactions within faults and fractures

In the event that faults or fractures cut or contact the reservoir and/or its caprock, any potential geochemical interactions in these features have to be assessed. Geochemical reactivity will only be significant if CO₂ (either free phase or dissolved in formation brine) is able to flow through the fracture. If the fracture were initially sealed (which is perhaps most likely), flow would probably require a pressure-induced event to create a leakage path.

When assessing potential reactions in fractures it is of crucial importance to have information on the nature of any fracture-filling material and its mineralogy. Certain minerals might remain relatively unchanged when in contact with large amounts of CO₂ (such as shown below in the case of evaporites), while other mineral assemblages

(such as carbonates) could react quickly when in contact with CO₂ in the fracture. The latter case could risk widening the fracture and increasing the leakage rate.

Within CO2STORE, generic modelling has been carried out to assess geochemical interactions in fractures for the Valleys and Schweinrich case studies.

4.3.4.1 Observations from the CO2STORE case studies

Valleys

Geochemical modelling of the partly mineralised St George's Fault was carried out assuming that the fault (which contacts both the reservoir and caprock) is filled with evaporites (Gaus, 2005). The objective was to assess if geochemical reactions would risk enlarging the fracture and thereby enhance leakage. It was assumed that dissolved CO₂ in brine is transported along the fracture through leakage, prior to any geochemical interactions taking place.

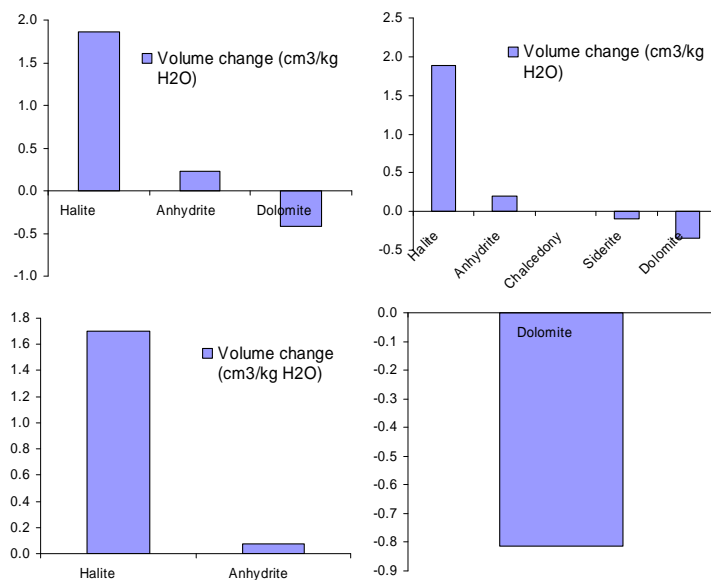


Figure 4.37 Predicted mineralogical change when CO₂ charged water comes into contact with evaporites in the St Georges Fault, modelled for four different evaporite compositions.

Batch modelling was performed to assess the geochemical interactions in a closed system using the local equilibrium hypothesis. Since detail on the exact composition of the fracture filling is not available, a sensitivity analysis was carried out with respect to the composition of the evaporites, assuming different representative mineralogical make-ups (Figure 4.37). Assuming that the fault is filled with evaporitic minerals, preliminary modelling for different evaporite compositions (state examples), indicates that the presence of CO₂-rich formation water will not lead to dissolution of the fracture filling. On the contrary, it is possible that minor precipitation would occur, leading to mineralogical volume increase and to possible sealing of leakage pathways. Only in the extreme case where dolomite makes up the bulk of the evaporite minerals would dissolution become important. However, such an evaporite composition is deemed to be very unlikely.

Schwarze Pumpe (Schweinrich)

No new datasets were obtained for the Schweinrich structure. The assessment of chemical reactions within faults and fractures was therefore limited to a generic modelling study with properties based on existing information.

Faults may be present in the lowest caprock unit at Schweinrich and it is possible that these cross-cut the entire caprock succession. Although one can assume that the faults and fractures are not generally open, it is conceivable that certain (e.g. induced) tectonic events could cause fracture reactivation or dilation and that injected CO₂ enters the fracture. The objective of the modelling was to assess the reactivity of such a non-filled fracture and the potential impact on CO₂ leakage caused by fracture widening or fracture closure.

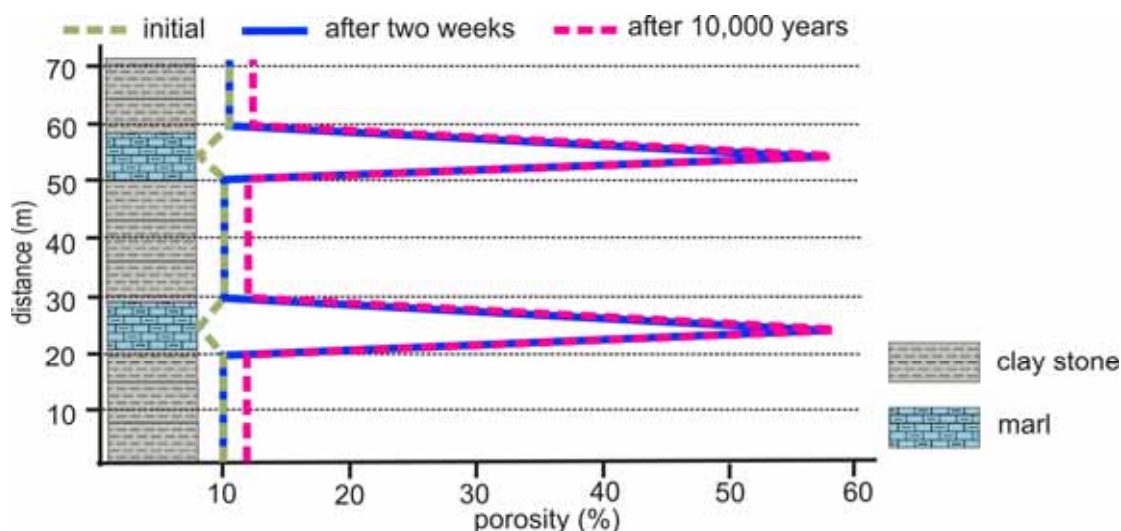


Figure 4.38 Evolution of porosity along a vertical fracture in the caprock at Schweinrich.

The geochemical impact of a large amount of CO₂-rich brine escaping the reservoir through a putative reactivated fracture in the caprock was simulated via 1D reactive-transport modelling including reaction kinetics of all minerals in the caprock at different levels (Durst and Gaus, 2005). The results show that some of the fracture walls will not undergo any significant geochemical reaction. However, the caprock claystones are interbedded with carbonate layers that will undergo significant mineral dissolution (Figure 4.38), with possible effects on caprock integrity.

4.3.5 Generic findings

The SACS and CO₂STORE projects have assessed the chemical impacts of CO₂ injection on the Utsira reservoir at Sleipner, and various caprocks and reservoirs from a number of case studies, via long-term geochemical modelling and laboratory experiments. The main results are summarised below:

The Utsira Sand is most likely to be only slightly reactive due to its mineralogy and low temperature (very slow reaction rates).

Two complementary reservoir modelling strategies were developed to focus either on the effect of the silicates or on the spatial localisation of the reactivity.

Any reactivity in the caprock induced by diffusing CO₂ is expected to be minor.

Reactivity of mineral-filled faults depends on the nature of the mineral fill. Reactions favouring both increased and decreased fault permeability can occur. Severe reactivity of carbonate-rich fault-wall rocks, can lead to potential geomechanical instability of the fault-walls.

It is clear that both laboratory and modelling methods have limitations and that large uncertainties are involved, especially in the assessment of kinetic rates and reactive surfaces. Laboratory experiments tend to see only relatively fast reactions (especially when executed at low temperatures), but long-term geological storage is likely to be dominated by slower reactions (e.g. feldspar alteration). Long-term forward geochemical modelling on the other hand can incorporate large uncertainties (which may easily span orders of magnitude) associated with parameter selection and over-parameterisation, but it is hindered by the fact that long-term calibration of the models is not possible. Studying natural systems that have trapped CO₂ for geological timescales provides valuable opportunities to further constrain these predictive models for two important reasons. Firstly, because natural analogues provide the only way to evaluate geochemical interactions occurring on geological timescales (they are in effect ‘natural, large-scale experiments’). Secondly, this geochemical evidence can then verify long-term predicted behaviour, by matching results from simulations to the observed interactions to demonstrate that these models are able to predict CO₂ fluid–rock interactions. However, natural analogues are not always straightforward because of their complex geological histories, and they must be interpreted with caution,

Advancing our understanding of water–rock–CO₂ geochemical reactions will require close integration of laboratory, analogue and modelling studies. A key part of this will be the provision of detailed quantitative data to underpin the modelling and the construction of more complex models that can take account of a wider range of processes. Only through the repeated testing of models against laboratory data or observations of natural systems will we demonstrate a high degree of confidence in our understanding of the geochemical reactions caused by the underground storage of CO₂.

4.4 Geomechanical assessment

Relatively little work on geomechanical aspects of underground storage has been carried out in the SACS or CO₂STORE projects, significant work being restricted to the Sleipner case study.

4.4.1 Observations from the CO₂STORE case studies

Sleipner

At Sleipner a number of desk studies (geomechanical and microseismicity) were carried out as part of the SACS project (e.g. Zweigel and Heil, 2003; Fabriol, 2001). They all

concluded that geomechanical processes would not be an issue given the likely small reservoir pressure changes and the in situ stress regime which is characterised by low deviatoric stress.

4.5 Characterisation phase risk assessment

Within CO2STORE, formal risk assessment, to a greater or lesser extent, followed the features events and processes (FEP) and scenario methodology.

4.5.1 Working steps of the FEP method

The risk assessment is based on simulations of different scenarios built up from FEPs. The main steps in the assessment are:

establishing risk assessment criteria

description of the geological system by investigation and screening of all features, events and processes (FEPs) that are relevant to the long-term safety, so called FEP analysis

scenario selection and analysis based on the FEP analysis

system model development

qualitative and quantitative consequence analysis.

4.5.2 Evaluation of consequences versus environmental criteria

In the evaluation of consequences versus environmental criteria, the criteria must correspond to amounts or concentrations that are measurable, and acceptable levels and limit values must therefore be determined.

Environmental criteria should be established for both global and local conditions. Predicting the global impact on climate change due to a release of CO₂ depends on the quantity, time and timing of the release. This is difficult to define since so many factors are variable and affect the storage time frame, such as duration of the use of fossil fuels, the coming and going of possible ice ages, natural CO₂ fluctuations in the future and the scale of geological time frames. This issue is often discussed but there is no international consensus (for the Schweinrich study a time frame of 1000 years has been used).

When establishing local criteria, it must be decided how to use site-specific and generic criteria. It would be preferable to use generic criteria so that projects can be compared, but it is likely that they have to be combined with local criteria that reflect conditions at the site. Ideally the same standards and requirements would be used and accepted worldwide.

In order to determine site-specific criteria, it will be necessary to know local baseline conditions, such as groundwater chemistry and ecosystem composition. When determining environmental criteria for groundwater and surface water for example, it is hard to find a single independent parameter to measure. The sensitivity of the system depends on many factors, such as buffering capacity, pH and the presence of metals that can leach into the water if the pH decreases. Other site-specific information that can be used is average wind speed and direction, topography, sensitivity of ecosystems in the area and population.

For CO₂ concentrations in air, it may be possible to use generic standards. Regulations exist for work environment conditions and the effects of exposure to elevated CO₂ concentrations on humans are well documented.

Another issue when establishing environmental criteria is what consequences the criteria should be based upon. Examples of levels are a No Observed Effects Limit (NOEL value), a limit above which no environmental benefits can be determined or a level where reversible or temporary harm to individuals or ecosystems can be detected. Environmental quality standards (EQS) are set as the total maximum concentration/dose from different sources to an ecosystem, and are not given as limit values or emission limits that relate to single activities. EQS already exist in the EU regulations, e.g. for SO₂ and NO_x in the air. In the field of natural gas storage, most regulations and standards relate more to operational procedures than environmental and ecosystem effects.

The authorities are responsible for setting requirements, environmental criteria and limit values. Since CCS is a new concept, input from industry and other stakeholders will be important in the development and determination of acceptable levels and limits that can be used when performing a risk analysis and assessing potential consequences of leakage. It is desirable that there is a consensus in the development of environmental criteria in the field of CCS.

There are presently no established risk criteria for CO₂ storage, a situation that requires future R&D.

4.5.3 Observations from the CO₂STORE case studies

Sleipner

No formal risk assessment for Sleipner was carried out in CO₂STORE.

Kalundborg

In order to address properly the risks related to underground storage of CO₂ the Kalundborg case study (Figure 4.39) used the Quintessa database of features, events and processes (FEPs).

www.quintessa.org/consultancy/index.html?co2GeoStorage.html

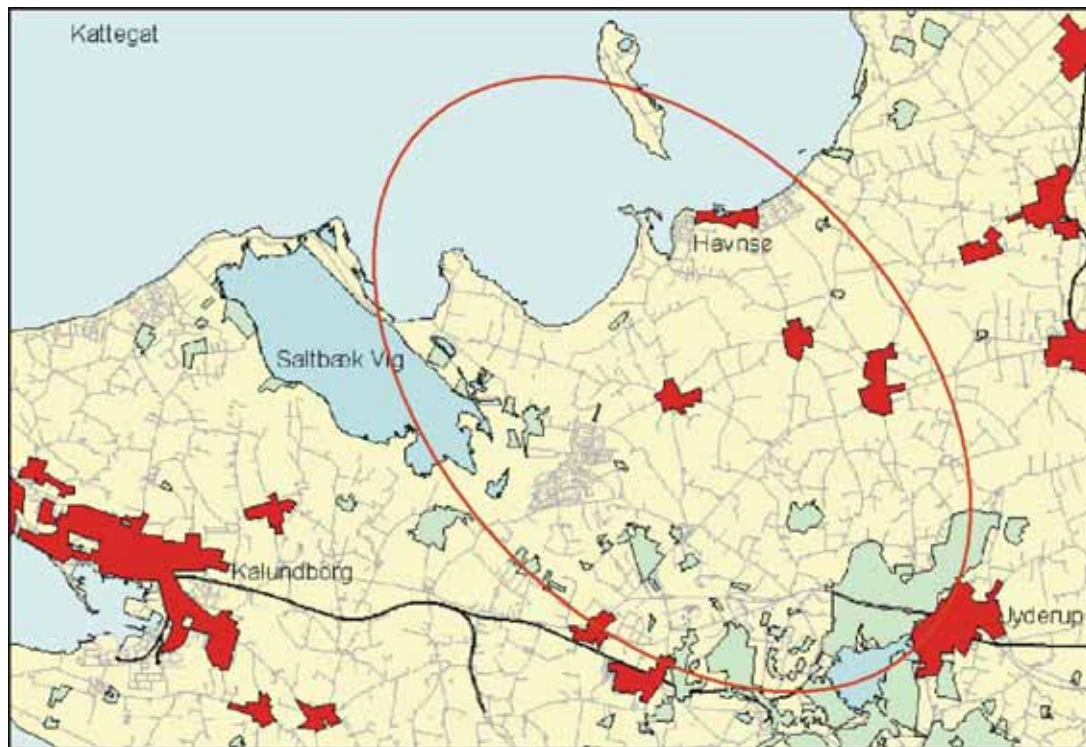


Figure 4.39 The areal extent of the Havnsø structure shown relative to towns (red), forest (green) and open land (light yellow). Infrastructure (roads) and isolated buildings are shown in grey (from Larsen et al. 2007. Copyright: Geological Survey of Denmark and Greenland).

The risk assessment involved analysis of all relevant FEPs, identification of the most important FEPs, and development of some geological scenarios incorporating the major FEPs that could be modelled using numerical reservoir simulation. All FEPs that might affect the underground storage of CO₂ in the Havnsø aquifer are listed in the Kalundborg case report (Larsen et al., 2006). Individual FEPs are categorised and risks identified based on their perceived applicability to the current target reservoir. The most important FEPs resulting from the auditing are summarised below.

geological features

overpressuring – reservoir characteristics

effects of pressurisation of reservoir on caprock

undetected features, faults at top of reservoir

long-term fate of CO₂

reversibility–fingering leading to CO₂ escaping the trap

impact on society and humans

public opposition to the storage project

impacts on humans — health effects of CO₂.

In addition to the risk assessment performed through the Quintessa database a number of other project risks should be considered (Table 4.13). These are risks that would put the project on hold and could ultimately lead to exclusion of the storage site. Several of the risks listed are related to project costs.

Risk assessment		
Risk	Mitigation	Issues
Geological	Seal 3D seismic	Feasibility Permitting Cost
	Analogue Drilling wells and testing	Access to gas injection project data Feasibility Permitting Cost
	Capacity Monitoring of aquifer	Seal integrity during injection
Reservoir	Drilling coring and testing	
Low level leaks	Monitoring of soil/water	Management of a monitoring project Feasibility, locations
Monitoring	4D seismic	Feasibility Permitting Cost
	Monitoring wells	Feasibility Permitting Cost location
Injectivity	Testing Analogue data	
Well leak	Good drilling practise	

Table 4.13 Summary of project risks at Kalundborg.

Mid Norway

No formal risk assessment was carried out for the mid-Norway case. The possibility of various leakage scenarios were tested by flow simulations as part of the site screening phase (Section 3).

Schwarze Pumpe (Schweinrich)

For the assessment of the Schweinrich storage structure, a modified performance assessment (PA) methodology was used. As stated previously, no new information was acquired for the Schweinrich structure so there are many uncertainties in the data that build up the geological model. Consequently the results from the PA should be taken as indicative only. Going beyond the case-study approach of the CO₂STORE project, much further effort would be needed to establish a high-quality geological model of the Schweinrich structure, and thus better data support for the PA.

A PA is a system analysis that predicts the performance of a specified system followed by a comparison of the results against system performance indicators. If the

indicator is a health safety and environmental (HSE) effect, the PA is termed a safety assessment (like this study). As a risk is a function of probability and consequence of a hazard, a PA or a safety assessment becomes a risk assessment if the performance indicator includes a probability factor.

In the Schweinrich study, the PA method comprised the following steps:

- definition of the assessment basis
- FEP analysis
- safety scenario formation
- development of dedicated models for probabilistic simulation of safety scenarios
- safety evaluation against HSE effects.

The method uses computer models to perform long-term probabilistic simulations of identified safety scenarios. This in turn requires powerful models that are acceptably representative of reality, and provide a systematic approach for identifying scenarios that affect site safety. The latter uses a comprehensive evaluation method called FEP analysis.

The FEP analysis was performed using databases developed in earlier CO₂ safety assessment studies (Wildenborg et al., 2005; Maul et al., 2004).

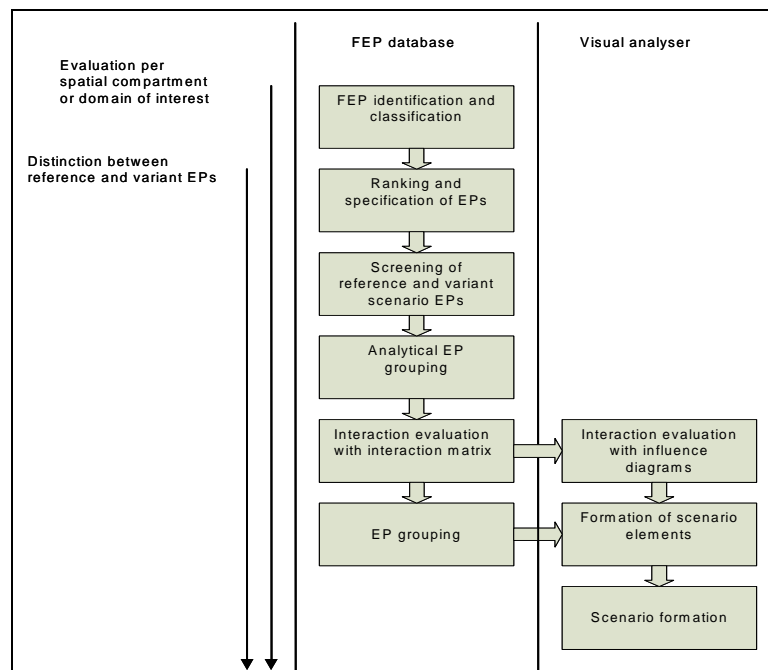


Figure 4.40 Main steps in used FEP analysis methodology. Based on the analysis process in Wildenborg et al. (2005).

The databases are used as selection tool for early screening of relevant FEPs. The main steps in the FEP analysis are illustrated in (Figure 4.40). The main tools that support the process are the FEP database and the visual analyser. The FEP database holds FEPs that may have a potential effect on the safety of the storage system. The latest version of the database contains a total number of 657 FEPs (Table 4.5), extracted from various sources.

F, E or P	Description	Number
F	All (static) factors and parameters describing the storage facility	233
E	Future occurrences, i.e. future changes to features (F) and future alteration of processes (P)	284
P	All surface and subsurface processes that describe the current and future physical, chemical and biological dynamical aspects of the storage facility	140
Total		657

Table 4.14 Numbers of features (F), events (E) and processes (P) in the database.

All FEPs in the database have a complete set of identification and classification attributes (Figure 4.41). These attributes have been assigned generically, and could be used to filter case-specific FEPs with respect to the assessment basis (Figure 4.42).

Figure 4.41 Example of generic FEP attributes in the FEP database.

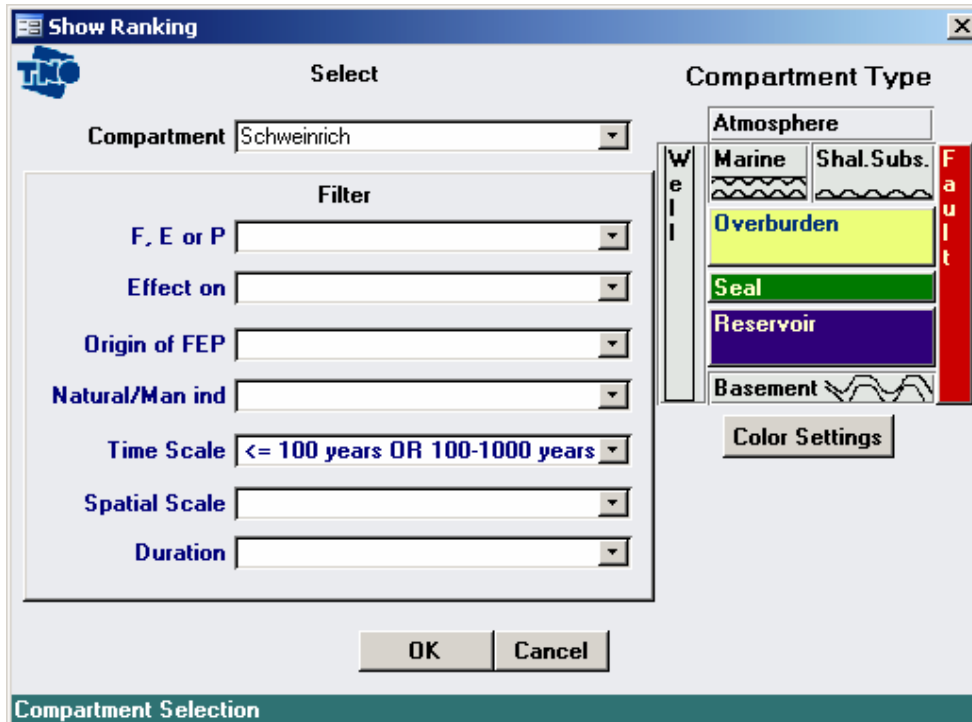


Figure 4.42 Example of FEP identification with the aid of filters in the FEP database.

The spatial domain for a risk analysis can be defined as a number of conceptual compartments (Figure 4.43). For simplicity, a subset of compartments was selected for the Schweinrich case study.

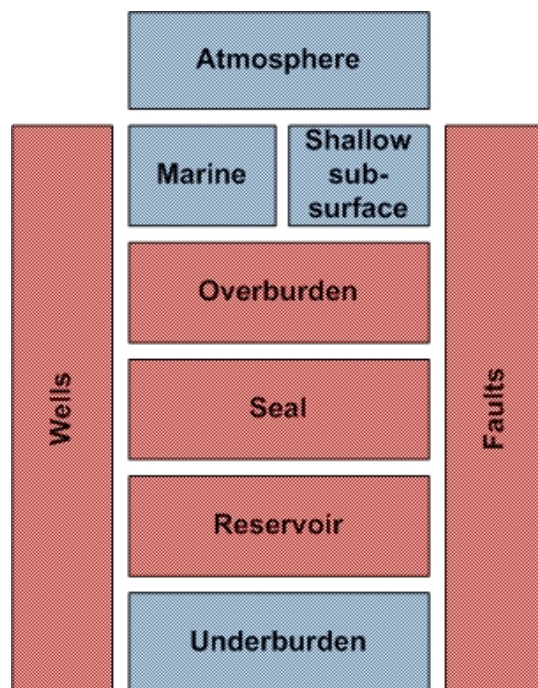


Figure 4.43 Different compartments of the spatial domain. Compartments used in the Schweinrich safety assessment marked in red.

Case specific FEPs for the Schweinrich case were identified according to the following criteria:

FEPs should have a timescale of occurrence less than 1000 years.

FEPs should lie within the spatial domains of reservoir, seal, overburden and fault.

FEPs in the spatial domains shallow subsurface, ocean, atmosphere and underburden are omitted.

FEPs with respect to well integrity and engineering are not evaluated. These FEPs could not be evaluated since the design and completion of future injection wells is unknown. FEPs defined in the SAMCARDS project are considered to also apply here.

The case specific FEPs were evaluated with respect to the assessment basis. A distinction was made between features as static factors, and events and processes (EPs) as dynamic factors. For each individual EP the following aspects were evaluated:

specifications of how the EP is interpreted, e.g. its relation to safety

semi-quantitative probability that an EP will occur

potential impact if the EP occurs.

Finally EP grouping was carried out, the objective being to group EPs that have common characteristics. Criteria for EP groups can be based on the information that is available in the FEP database like (Wildenborg et al., 2005):

common parameters (distinct features such as permeability, rock strength, etc)

process types (mechanical, chemical, thermal, hydraulic, biological)

effect type (on matrix, fluid, stored CO₂, indirect)

timescale of EP occurrence (in 100 years, in 1000 years or in 10000 years)

duration scale of EP while occurring (hours, days, centuries and longer)

spatial scale (metres, km, tens of km, basin scale).

In general terms, EPs for the Schweinrich case can be divided into geochemical EPs acting on long timescales (about 1000 years), and into geomechanical EPs valid for both short and long timescales of occurrence and duration. Two EP groups were identified: a leaking fault EP group and a leaking seal EP group (Figure 4.44). The geomechanical EPs all relate to the leaking fault EP group. The geochemical EPs relate to both the leaking fault and the leaking seal EP group.

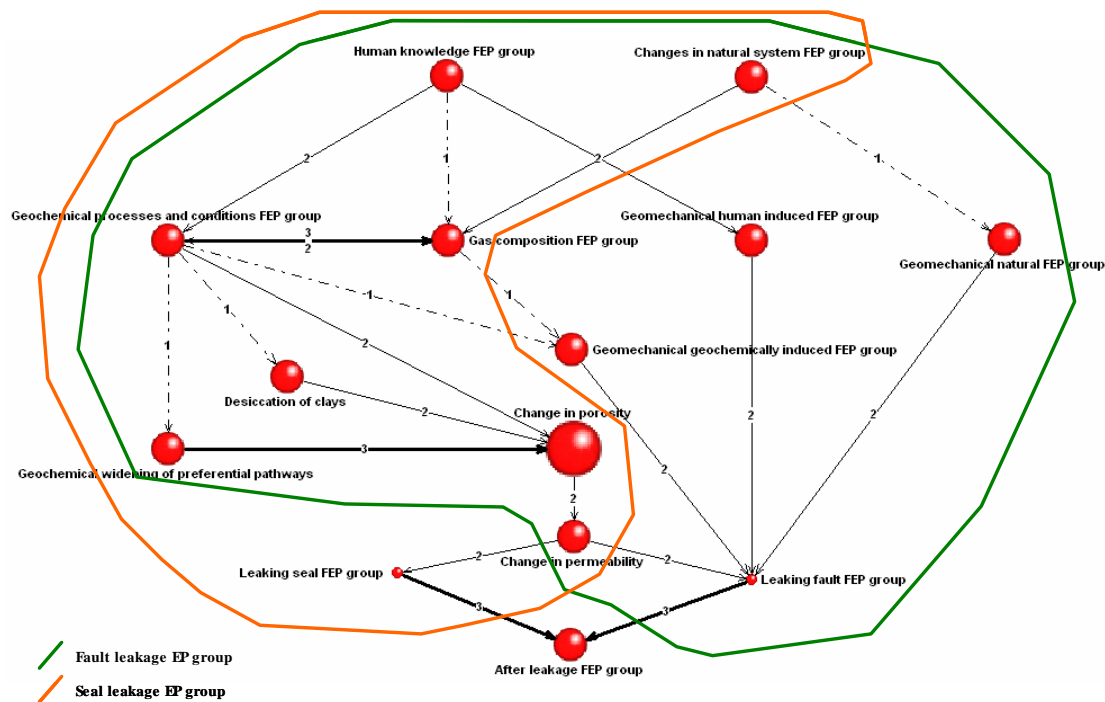


Figure 4.44 Influence diagram with scenario defining EP groups. Green line marks the fault leakage group and orange line marks the seal leakage group.

In practice, a safety assessment will have several limitations, e.g. due to the intended use of the assessment (for this case a feasibility study), limited resources (available input data, model limitations etc), perceived regulatory requirements etc. The following limitations are applicable to this study.

Time frame: The time frame for the FEP analysis was set to 1000 years. Hazards that may occur as consequence of the identified safety factors were evaluated for 10 000 years, i.e. the simulation period was 10 000 years.

Spatial domain of the investigated storage system (Figure 4.43): The reservoir, seal, overburden, faults and wells compartments were evaluated. The shallow subsurface, ocean (not relevant for structure Schweinrich), atmosphere and underburden compartments were excluded. This selection process is related to the available input data and limitations in the model, e.g. the model code utilised cannot analyse the HSE effects in the shallow subsurface. Furthermore, as design specifications of the injection wells have not yet been set, the events and processes that may affect the performance for such wells were taken from the SAMCARDS study (Wildenborg et al., 2005).

Probability of occurrence of evaluated scenarios: No attempt to quantify the probability of occurrence of the evaluated scenarios has been made. Instead, it was assumed that the scenarios will definitely occur, i.e. the probability of occurrence of the CO₂ leakage scenarios is set to 1. It is important to reiterate therefore that these evaluated scenarios represent worst cases.

Input data: The study has used input data that were gained from former geological surveys of the area, e.g. from hydrocarbon explorations performed between 1950 and 1990 and from surveys of geothermal potential in the 1980s. Thus, no dedicated input data acquisition at the site has been performed.

Model limitations: All models are simplifications of the real world. Thus, several assumptions and simplifications are used in the development of the models and the subsequent probabilistic simulations of the leakage scenarios. All simplifications are described and explained in Svensson et al. (2005). No attempts have been made to validate the simplified leakage processes of the models, e.g. by validation against the leakage process of natural analogues.

Based on the FEP analysis and the scenario formation, the following ‘what if?’ scenarios were identified for simulation:

Reference scenario: No failure of the containment zone occurs.

Leaking seal scenario: It is here assumed that the seal will fail by geochemical processes, whereby CO₂ enhances the permeability of the caprock and migrates into the overburden (the probability of failure is set to 1).

Leaking well scenario: It is here assumed that the sealing capacity of an existing old well will fail, followed by transport of CO₂ along the well trajectory (the probability of failure is set to 1). N.B. in reality, there are no existing old wells at the Schweinrich site so this model is hypothetical.

Leaking fault scenario: It is here assumed that there is a fault through the caprock, and that the sealing capacity of the fault will fail, followed by CO₂ escape from the containment zone along the fault (the probability of failure is set to 1).

Model software developed in the SAMCARDS project was used for the simulation of four scenarios. The available model codes were the 2D radial and the 3D orthogonal SIMED II flow models including software shells for probabilistic input and output.

In the Schweinrich case, the scenarios present hypothetical future flow and fate of CO₂ in the next 10 000 years. The potential impact of each scenario was expressed as the maximum concentration and flux of CO₂ in the pore system in the shallowest overburden unit, Pleistocene sediments (which form the topmost subsurface layer in the simulation models). No outcome was simulated regarding groundwater deterioration and mobilisation of heavy metals, since no modelling of the flow and fate of CO₂ in the unsaturated zone was conducted. In case of uncertainty on input parameters that were not varied stochastically, the worst-case scenario values were generally selected. Outcome distributions are consequently biased towards the worst-case scenarios.

The 2D radial flow model was used to represent the reference scenario, the seal leakage scenario (Figure 4.45) and the well leakage scenario (Figure 4.46). The 3D orthogonal model was used to represent the fault leakage scenario (Figure 4.47). The amount of injected CO₂, its lateral spread in time and the reservoir pressure were calibrated to the fine-scaled 3D SIMED II model over the injection period of 40 years.

This deterministic model represented the injection of CO₂ on the flanks of the Schweinrich structure by 10 injection wells (Figure 4.24). In this model, the accumulation of CO₂ was mainly in the topmost reservoir layer (Figure 4.25).

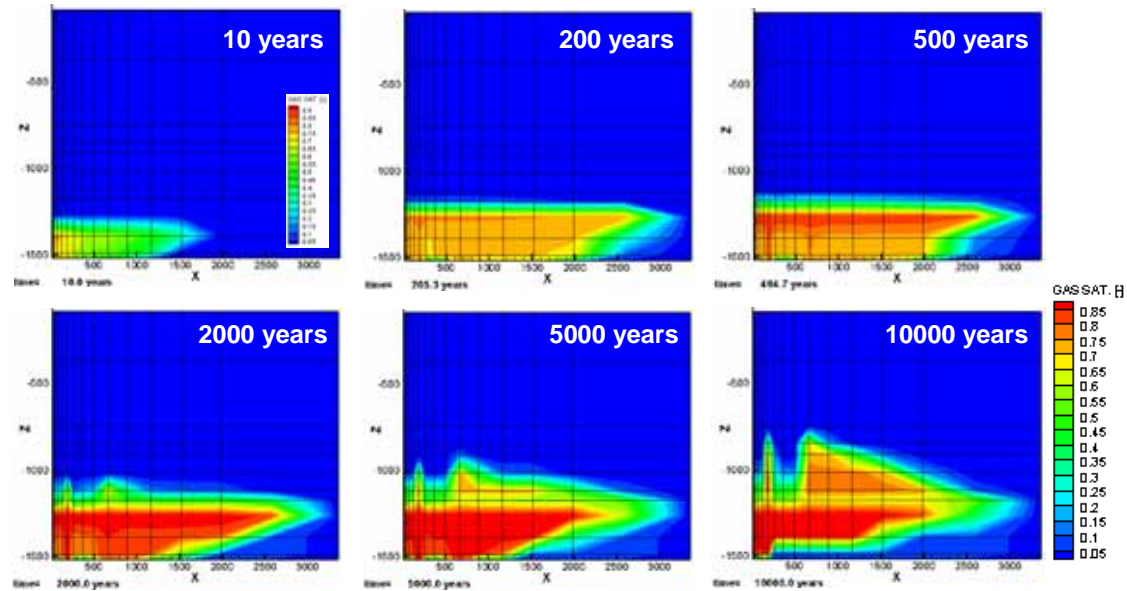


Figure 4.45 Simulated CO₂ saturations from the hypothetical leaking seal scenario (probability of occurrence is set to 1).

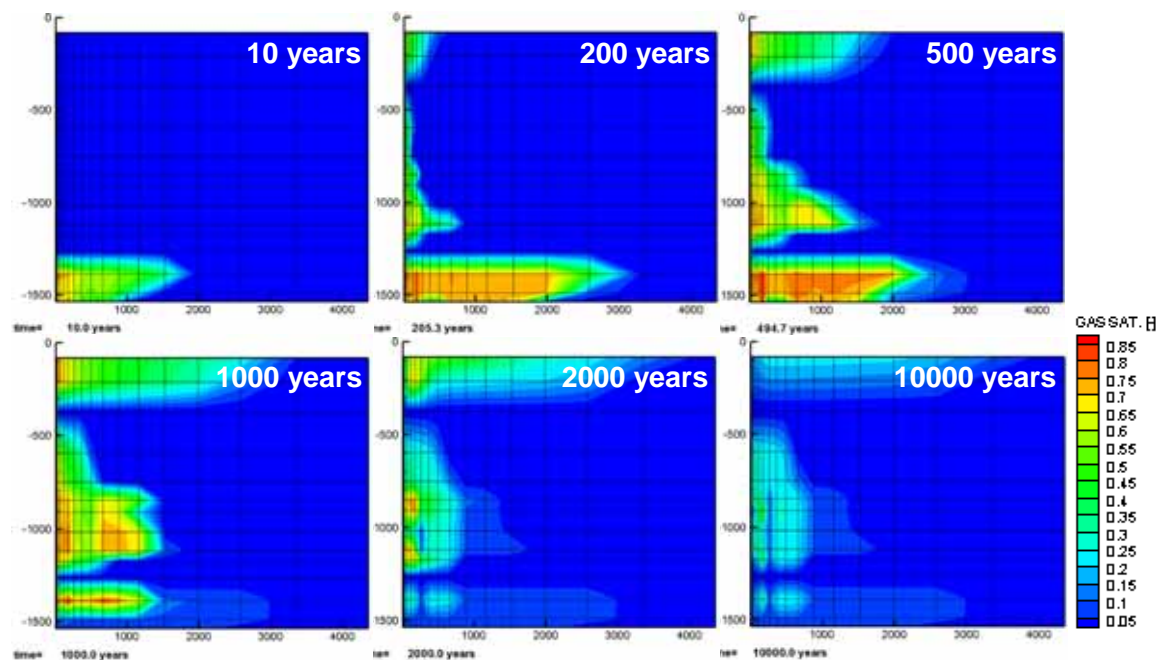


Figure 4.46 Simulated CO₂ saturations from the hypothetical leaking well scenario (probability of occurrence is set to 1).

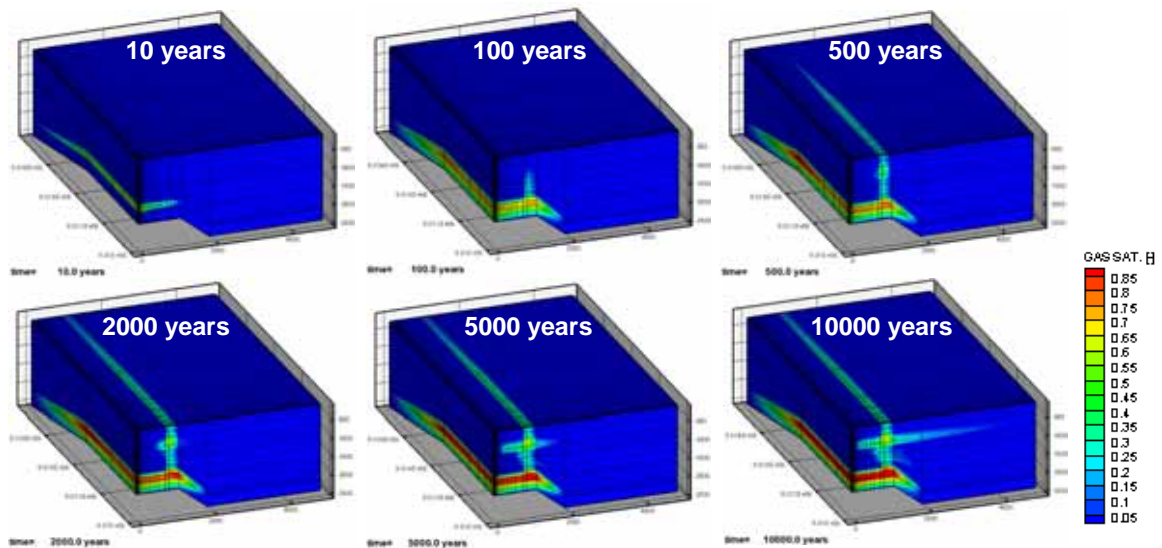


Figure 4.47 Simulated CO₂ saturations from the hypothetical leaking fault scenario (probability of occurrence is set to 1).

Compromises with respect to the run time of the SIMED II models were necessary in order to run the required large number of simulations for each scenario in a reasonable real time period. Hence, the representation of the stochastic models was strongly simplified. Variation of input parameters, such as porosity and permeability should compensate for the model simplifications and related uncertainty. The bandwidths of input parameters were constrained by values from related studies (Hildenbrand et al., 2004; Schlömer et al., 1997).

Each ‘what if?’ scenario was evaluated with 1000 model runs with varying stochastic parameters. Based on the results from these, the following conclusions can be drawn concerning the safety of the evaluated hypothetical scenarios.

Reference scenario: No CO₂ reaches the uppermost overburden sediments after 10 000 years. Hence, the reference scenario does not pose a safety factor with respect to CO₂ release at surface.

Leaking seal scenario: Although the CO₂ passes through the seal in this scenario, the velocity of upward migration of CO₂ is fairly small. Thus, no CO₂ reaches the uppermost overburden and so it does not pose a safety factor.

Leaking well scenario: This scenario is the easily the most significant in terms of modelled CO₂ fluxes and CO₂ concentrations in the shallow overburden. The probability that such a scenario will be valid depends on the existence of an old well, designed for a purpose other than CO₂ storage, penetrating through the caprock. It is likely that the use of the SAMCARDS FEP analysis, including the model representation and parameters for stochastic simulation is not valid for wells specifically designed for CO₂ injection, where CO₂ resistant cement and casing would be used. The critical safety factor in the leaking well scenario is the magnitude of the increase of the (vertical) permeability in the well zone, which would be improved by using a proper cement type. However, the best way to

avoid the leaking well scenario is to design the injection wells in such a way that the scenario cannot occur, for example by designing the wells so that the caprock is not penetrated and that the wells enter the anticlinal structure from below the spill point. This can be done by the use of directionally drilled deviated wells that inject the CO₂ at the flanks of the reservoir.

Leaking fault scenario: This scenario indicates moderate CO₂ fluxes and CO₂ concentrations in the shallow overburden. Modelled maximum surface fluxes are comparable to observed leakage rates from natural CO₂ accumulations in Europe and Australia. The maximum concentrations may lead to adverse effects in groundwater and freshwater ecosystems. The critical safety factor is the vertical permeability of the fault zone.

It is important to stress that the probability of these scenarios actually occurring has not been assessed. They represent hypothetical ‘worst-case’ situations that may well have a very low probability. This particular case study indicates that a more detailed study of structural aspects would be a high priority.

Valleys

For the Valleys case study an outline risk assessment was carried out, comprising a compilation of FEPs associated with storage in the basal Cenozoic sandstone reservoir. From a containment risk perspective, the key features of the site are listed below:

The reservoir consists of relatively thin fluvial sands, individual sands in well 106/24-1 are up to 17 m thick and the total thickness of sand in the reservoir interval is 63 m. The distribution of these sands in three dimensions is unknown.

At the top of the proposed storage structure the seal consists of more than about 500 m of mudstones and silty mudstones, which include some lignite beds. The sealing properties of these strata is not known, but the permeability can reasonably be assumed to be low.

The integrity of the storage site relies on an effective seal along the St George’s Fault.

The risk assessment was based on the Quintessa FEP database. It analysed all relevant FEPs, identified the most important of these, and developed some geological scenarios incorporating the major FEPs that could be modelled using numerical reservoir simulation.

A summary of those FEPs that might affect the underground storage of CO₂ in the St George’s Channel Basin are listed below (Tables 4.15 and 4.16).

FEP Category	FEP Class	Response
0. The assessment basis	0.1 Purpose of the assessment	Assess risks of underground storage of CO ₂ emitted from the proposed Valleys power plant in the St Georges Channel Basin.
	0.2 Endpoints of interest	Constrained to considering the degree of containment within the subsurface, i.e. amount, location and timing of any leakage not impacts
	0.3 Spatial domain of interest	Part of the St George's Channel and the subsurface.
	0.4 Timescales of interest	10,000 years
	0.5 Sequestration assumptions	The amount of CO ₂ stored will be the lifetime emissions from the proposed Valleys Power Plant (2.3 million tonnes CO ₂ per year for a nominal lifetime of 20 years). The CO ₂ will be stored in reservoir rocks beneath the UK sector of the St George's Channel. The reservoir comprises sands in the lower part of the Cainozoic succession. The trapping mechanism for the Cainozoic prospect will be a combination of stratigraphic pinchout, dissolution of CO ₂ into the native pore fluid, residual saturation along the CO ₂ migration path and structural closure against the St George's fault. The cap rock will be overlying Cainozoic strata consisting primarily of mudstones and silty mudstones, including some lignite beds.
	0.6 Future human action assumptions	It is assumed that the injection wells will be sealed and abandoned after the injection period according to prevailing regulations and subsequently the site will be closed by agreement between the regulator and operator. Thereafter human actions will be limited to monitoring, remediation if necessary and (possibly) drilling through the storage reservoir.
	0.7 Legal and regulatory framework	Any CO ₂ storage offshore would have to be legal under the OSPAR and London Conventions. These bodies are currently (March 2006) considering the status of offshore underground CO ₂ storage. Assuming that these bodies agree that CO ₂ storage under these circumstances is legal, it would be subject to regulation by national or supranational bodies, presumably the UK government. No UK or supranational legal and regulatory framework exists at present for CO ₂ storage offshore. It is assumed that after site closure has been agreed, liability will be with the State.
	0.8 Model and data issues	Data coverage is sparse. 2D seismic data and 8 wells with well logs, drill cuttings and core samples are available. The reservoir will be represented as a generic fluvial sandstone reservoir in geological and numerical models. The geological model will be prepared using Petrel software. The numerical simulation will use Simed software.

Table 4.15 FEPs used for forming the assessment basis for risk assessment in the Cenozoic sandstones of the St George's Channel Basin.

FEP Category	FEP Class	FEP	Response
2. CO ₂ Storage		2.1.10 Overpressuring	This is a risk if the reservoir sand distribution is unfavourable, 4.1.4 below. Sensitivity studies on reservoir distribution and boundaries required.
		2.2.4 Reversibility	In the event of overpressuring or unintended migration (e.g. along St George's Fault), the injection wells could be opened up and allowed to flow and return the reservoir to its initial pressure. Given that a high proportion of the CO ₂ would be above the level of the well perforations it is unlikely that much of the CO ₂ would be recovered.
		2.2.5 Remedial actions	See 2.2.4. Leakage via the St George's Fault probably could not be remediated
3. CO ₂ properties, interactions and transport		3.2.5 Mechanical processes and conditions	Increased pore fluid pressure may adversely affect seal and permeability of St George's Fault, which is unknown
		3.3.1 Advection of free CO ₂	Assessed using numerical reservoir simulation. CO ₂ reaches St George's Fault within 100 years in all cases studied
		3.3.1.1 Fault valving	Not known what overpressures (if any) are necessary to make the fault permeable
4. Geosphere	4.1 Geology	4.1.4 Reservoir geometry	'Typical fluvial' reservoir geometry used in (Petrel) reservoir model. Not known how well this reflects the actual reservoir sand distribution. Not known whether any exploration/injection wells would efficiently penetrate reservoir sand.
		4.1.11 Fractures and Faults	St George's Fault closes the storage structure and is considered to be the largest risk
5. Boreholes	5.1 Drilling and completion	5.2.2 Seal Failure	Risk of poor cement bond to likely poorly lithified overlying strata.
		5.2.3 Blowouts	Risk of blowout outside casing as overlying strata ? poorly lithified. Needs further investigation and pressure tolerances to be set. Risk could not be assessed adequately.

Table 4.16 FEPs representing significant issues for CO₂ storage in the Cenozoic sandstones of the St George's Channel Basin.

Individual FEPs were categorised as a major, minor or unknown risk (not considered important in the site characterisation process) based on their perceived applicability to the current target reservoir. The most important FEPs are summarised below:

Leakage of CO₂ through the St George's Fault. The flow simulations indicate that CO₂ is likely to reach the St George's Fault within about 60 years of injection. Amounts trapped against the fault may exceed 40 to 50% of the injected total CO₂, depending on the amount of dissolution and location of the injection wells. Amounts may however be considerably decreased by residual phase trapping within the reservoir. The fault seal cannot be determined without drilling test injection and monitoring wells. The potential for leakage through the St George's Fault is thus a critical unknown. If significant leakage did occur, it would be difficult to remediate and could necessitate the abandonment of the CO₂ storage project.

Overpressure. CO₂ trapped at the top of the reservoir is likely to cause a significant departure from the hydrostatic pressure gradient. This might adversely affect the integrity of the caprock through fracturing and/or dissolution. Pressure distribution in the reservoir through time was again simulated using numerical modeling.

Reservoir heterogeneity. The reservoir sands are probably of fluvial origin and might therefore exhibit significant spatial variation. The main sand units are seen to thin between exploration wells 106/24-1 and 106/24A-2B drilled in the potential storage structure. A heterogeneous reservoir would make it difficult to target injection wells and utilise the maximum storage capacity of the target structure. This uncertainty was incorporated into the reservoir models used in the flow simulations using a stochastic distribution of sand bodies based on standard fluvial facies models.

Leakage from a well. If the strata above the reservoir are poorly consolidated (as expected) it may be difficult to get a robust cement bond between well casing and the surrounding rock. This could allow CO₂ to escape from wells previously drilled in the storage structure. It might also allow CO₂ to escape from the injection wells, although drilling a horizontal injection well (generally below the CO₂ plume) would minimise the risk of gas escape.

4.5.4 Generic conclusions

A safety assessment will have several limitations that could bias the results. As a rule, all limitations should be recognised and the reasons for them explained (NEA Working Group 1997). Generic limitations for FEP/scenario-based risk assessments are listed below:

Time frame of evaluation: The time frame for evaluation is an issue that often is discussed and is not widely agreed. Therefore, arbitrary values were used in the safety assessment of Schweinrich. In the FEP analysis, a time frame of 1000 years was used. In the subsequent simulations, hazards that may occur as consequence of the identified safety factors were evaluated for 10 000 years, i.e. the simulation period was 10 000 years.

The FEP assessment methodology is useful but still has gaps in knowledge. This concerns many aspects, e.g. safety and risk terminology, usage of FEP database, scenario evaluation, assessment criteria, modelling tools and so on.

Regarding FEP methodology, there is some discussion as to whether a 'bottom-up' or 'top-down' approach is best. Bottom-up involves identifying every conceivable FEP and then building scenarios from these. This is time-consuming, and risks missing key scenarios through 'participant exhaustion' and time limitations. Top-down involves identifying a limited number of key risk scenarios and developing a limited FEP listing from these. This risks missing important FEPs, and, by inference, important potential scenarios. Overall, the top-down approach is favoured, but irrespective of

the approach, it is important that the link between FEPs and scenarios should be fully documented.

An important issue connected with FEP/scenario risk analysis is that worst-case processes tend to be emphasised irrespective of how (un)likely they are to actually occur. Thus, leakage scenarios tend to get highlighted and qualifying uncertainties and assumptions ignored. Care is therefore necessary in presenting scenario results to an external audience.

Overall, quantitative assessment of the probability of any particular scenario occurring is very difficult, particularly for scenarios involving geological FEPs (e.g. fault leakage, caprock failure etc). An alternative to quantitative risk analysis may be to set out a storage plan, based on robust site characterisation, identify site-specific containment risks (and uncertainties), and design a monitoring and remediation strategy capable of dealing with these should they occur.

4.6 Monitoring programme design

Developing an optimal site monitoring programme depends principally on the objectives of the monitoring; the main ones are summarised below :

- direct imaging (and if possible, quantification) of CO₂ in the storage reservoir (including the verification and calibration of predictive models)

- detection of migration of CO₂ from the primary reservoir

- detection of migration of CO₂ through the overburden to shallower depths

- detection and/or measurement of CO₂ at the surface or in the atmosphere or water column.

The monitoring programme should be designed to provide sufficient information to enable site remediation in the case of unforeseen events (e.g. risk scenarios) and also to enable a satisfactory site closure strategy by demonstrating that the site is performing according to predictions and is likely to continue to do so into the future.

Proper design of an effective site monitoring programme can be viewed as a three step process.

- Review all available proven and potential monitoring technologies.

- Select which particular techniques are required to achieve the required objectives.

- Design appropriate field deployment parameters to achieve effective monitoring.

This final step will in all likelihood require significant modelling work, including a comprehensive sensitivity analysis.

In addition to the overall objectives, monitoring-tool selection depends on a number of site-specific factors including surface conditions (onshore/offshore, rural, urban, flat, mountainous etc), site geology (reservoir depth, type etc). The IEAGHG website hosts an interactive tool for the design of CO₂ monitoring programmes available at: www.co2captureandstorage.info/co2monitoringtool/

The tool allows the user to input basic storage site parameters (location / land use, reservoir depth, reservoir type, injection quantity), and up to ten monitoring aims:

- CO₂ plume imaging
- topseal integrity
- CO₂ migration in the overburden
- quantification of in situ CO₂
- reservoir storage efficiency
- calibration of flow simulations
- leakage at the surface
- induced seismicity
- well integrity
- public confidence.

The tool then calculates applicability scores for specific monitoring technologies according to the selected aims. Filters, corresponding to ‘basic’ or ‘additional’ monitoring schemes can then be applied. The ‘basic’ filter returns tools that could be routinely employed to adequately verify that injection and storage were behaving as expected, providing assurance on plume location, top-seal integrity, well integrity, migration in the overburden, surface leakage and calibration of predictive models. The ‘additional’ filter returns tools that provide additional complementary information, address specific scientific issues, or tools that may be required in the event that observed site behaviour were to deviate from that predicted.

In all cases, a key aspect of monitoring programme design is to plan appropriate baseline surveys, prior to the commencement of CO₂ injection. These are necessary to establish datasets against which operational monitoring data can be compared.

A large portfolio of potential site monitoring technologies exists (Figure 4.48), though many of these have not yet been tested on real CO₂ storage sites. They can be split broadly into ‘deep’ focussed techniques and ‘shallow’ focussed techniques, or can be categorised more finely into objective-related aims, such as plume location, fine-scale processes etc.

<div style="display: flex; justify-content: space-between; align-items: flex-start;"> <div style="display: flex; flex-direction: column; gap: 5px;"> <div style="display: flex; align-items: center;"> Onshore only </div> <div style="display: flex; align-items: center;"> Offshore only </div> <div style="display: flex; align-items: center;"> Onshore & Offshore </div> </div> <div style="display: flex; flex-direction: column; gap: 5px;"> <div style="display: flex; align-items: center;"> Primary use </div> <div style="display: flex; align-items: center;"> Secondary use </div> </div> </div>									
			Deep	Shallow	Plume location/ migration	Fine scale processes	Leakage	Quantification	
Seismic	Acoustic imaging	3D/4D surface seismic	Onshore & Offshore	Primary	Secondary	Primary	Secondary	Primary	
		Time lapse 2D surface seismic	Onshore & Offshore	Primary	Secondary	Primary	Secondary	Primary	
		Multicomponent seismic	Onshore & Offshore	Primary	Secondary	Primary	Secondary	Primary	
		Boomer / Sparker	Offshore only	Primary	Secondary	Primary	Secondary	Primary	
		High resolution acoustic imaging	Offshore only	Primary	Secondary	Primary	Secondary	Primary	
	Well based	Microseismic monitoring	Onshore & Offshore	Primary	Secondary	Primary	Secondary	Primary	
		4D cross-hole seismic	Onshore & Offshore	Primary	Secondary	Primary	Secondary	Primary	
		4D VSP	Onshore & Offshore	Primary	Secondary	Primary	Secondary	Primary	
Sonar Bathymetry		Sidescan sonar	Offshore only	Primary	Secondary	Primary	Secondary	Primary	
		Multi beam echo sounding	Offshore only	Primary	Secondary	Primary	Secondary	Primary	
Gravimetry		Time lapse surface gravimetry	Onshore & Offshore	Primary	Secondary	Primary	Secondary	Primary	
		Time lapse well gravimetry	Onshore & Offshore	Primary	Secondary	Primary	Secondary	Primary	
Electric / Electro - magnetic		Surface EM	Onshore only	Primary	Secondary	Primary	Secondary	Primary	
		Seabottom EM	Offshore only	Primary	Secondary	Primary	Secondary	Primary	
		Cross-hole EM	Onshore & Offshore	Primary	Secondary	Primary	Secondary	Primary	
		Permanent borehole EM	Onshore & Offshore	Primary	Secondary	Primary	Secondary	Primary	
		Cross-hole ERT	Onshore & Offshore	Primary	Secondary	Primary	Secondary	Primary	
		ESP	Onshore only	Primary	Secondary	Primary	Secondary	Primary	
Geochemical	Fluids	Down hole / Springs		Primary	Secondary	Primary	Secondary	Primary	
			Down hole / Springs	Primary	Secondary	Primary	Secondary	Primary	
			Down hole / Springs	Primary	Secondary	Primary	Secondary	Primary	
	Gasses	Marine	Seawater chemistry	Offshore only	Primary	Secondary	Primary	Secondary	Primary
			Bubble stream chemistry	Offshore only	Primary	Secondary	Primary	Secondary	Primary
		Atmosphere	Short closed path (NDIRs & IR)	Onshore & Offshore	Primary	Secondary	Primary	Secondary	Primary
			Short open path (IR diode lasers)	Onshore & Offshore	Primary	Secondary	Primary	Secondary	Primary
			Long open path (IR diode lasers)	Onshore & Offshore	Primary	Secondary	Primary	Secondary	Primary
			Eddy covariance	Onshore & Offshore	Primary	Secondary	Primary	Secondary	Primary
		Soil gas	Gas flux	Onshore only	Primary	Secondary	Primary	Secondary	Primary
Gas concentrations	Onshore only		Primary	Secondary	Primary	Secondary	Primary		
Ecosystems		Ecosystems studies	Onshore & Offshore	Primary	Secondary	Primary	Secondary	Primary	
Remote sensing		Airborne hyperspectral imaging	Onshore only	Primary	Secondary	Primary	Secondary	Primary	
		Satellite interferometry	Onshore only	Primary	Secondary	Primary	Secondary	Primary	
		Airborne EM	Onshore & Offshore	Primary	Secondary	Primary	Secondary	Primary	
Others		Geophysical logs	Onshore & Offshore	Primary	Secondary	Primary	Secondary	Primary	
		Pressure / temperature	Onshore & Offshore	Primary	Secondary	Primary	Secondary	Primary	
		Tiltmeters	Onshore & Offshore	Primary	Secondary	Primary	Secondary	Primary	

Figure 4.48 A selection of potential monitoring tools for CO₂ storage.

A number of monitoring methods used or evaluated for possible use in the SACS and CO2STORE projects are outlined below.

4.6.1 Deep-focussed methods

The main purpose of deep monitoring systems is to monitor amounts and movement of CO₂ within the storage reservoir, and migration into its immediate surroundings. From this, predictive models of site performance can be calibrated, tested and adjusted as necessary. A secondary objective of deep monitoring systems would be to give early warning of CO₂ migration to shallower depths in the overburden. Deep monitoring techniques can be run both from the surface, as in the case of surface seismic and gravity techniques, or in wells; either the injection well, other adjacent wells or a specifically designed monitoring well.

4.6.1.1 4D surface seismic

The 4D time-lapse seismic is likely to prove the key subsurface monitoring tool in many storage scenarios. Excellent results have already been achieved at Sleipner (see Section 7.3) and also at the Weyburn operation in Canada (Wilson and Monea, 2004). Sleipner in particular is very well-suited to seismic monitoring due to very favourable acoustic properties of the relatively shallow, unconsolidated reservoir. Other storage sites will be less suitable and it is important to carry out pre-monitoring assessment of the technique to ensure that results will produced what is required in terms of plume imaging, quantification, leakage detection etc. Work by the Geodisc group in Australia (McKenna et al., 2003) has shown that reservoirs will generally show significantly impaired seismic response with increasing depth of burial.

The quantitative interpretation of time-lapse seismic monitoring relies on a sufficiently accurate knowledge of the fluid substitution impact on seismic velocity in the reservoir. The theoretical basis of this quantification is the well-known Gassmann (1951) model which relates the elastic moduli of the fluid saturated rock (bulk modulus: K_{sat} and shear modulus: μ_{sat}) to the moduli of the dry rock (bulk modulus: K_{dry} and shear modulus μ_{dry}), to the saturating fluid bulk modulus (K_f), to the porosity (ϕ) and to the bulk modulus of the rock forming mineral (K_g). Knowledge of fluid mixing scales (patchy vs uniform) is also the key to accurate seismic quantification.

Other seismic techniques such as cross-well seismic data and vertical seismic profiles (VSPs) can provide important ancillary information at a higher resolutions, which is very useful for calibrating the surface seismic and constraining quantitative modelling. Downhole techniques are particularly useful in deep storage reservoirs where the efficacy of surface seismic can be severely curtailed.

4.6.1.2 Multicomponent seismic

Multicomponent seismic methods can be used to record shear (S) waves as well as compressional (P) waves. On land, three polarised shear-wave sources, together with

3-component geophones, can be used to produce 9-component (full-wave) data. Offshore, 4C sea-bottom instruments (3 component geophones plus a hydrophone), utilise P to S mode conversions to record PS (P-downgoing, S-upgoing) datasets. Multicomponent datasets contain inherently more information than conventional data. Firstly, S-waves propagate exclusively through the rock matrix and are relatively unaffected (other than by pressure) by the nature of the pore fluid. This allows S-waves to image through volumes containing anomalous fluids (e.g. CO₂ bubbles), more effectively than P-waves, and makes S-wave acoustic properties more uniquely diagnostic of lithology and fluid pressure. Secondly, S-waves interrogate azimuthal subsurface properties, so the polarised waveform may exhibit birefringence due to velocity anisotropy. This can be used to measure azimuthal anisotropy in rock properties (due to structural fabric, or fractures) or lateral variations in effective stress (fluid pressure).

Potential benefits of multicomponent seismic include:

- lithological discrimination

- fluid discrimination and saturation mapping

- fracture anisotropy and stress state characterisation

- improved imaging

- structural imaging through gas/CO₂ cloud

- physical properties

- V_p/V_s ratio.

4.6.1.3 Microseismic monitoring

The measurement of microseismicity using downhole and/or surface sensors, depends on the CO₂ injection inducing microseismic events. Thus, if a cause and effect link can be established between the appearance of microseismicity and the increase in pore pressure in the reservoir due to the flow of CO₂, then, theoretically, a real-time picture can be developed of the movement of CO₂ at certain specific points. It is also possible to characterise zones of weakness in the reservoir (or its caprock), where pre-existing fractures or joints move in brittle shear and therefore constitute preferential flow paths. In general, the technique is likely to be of most use in low permeability reservoirs where a significant pressure increase is likely to accompany injection.

4.6.1.4 Surface microgravimetric monitoring

Gravimetry measures the gravitational acceleration due to mass distributions within the Earth to detect variations in subsurface rock or fluid density. Although of much lower spatial resolution than the seismic method, surface gravimetry offers some important complementary adjuncts to time-lapse seismic monitoring. Firstly, it can

provide independent verification of the change in subsurface mass during injection via Gauss's theorem. This potentially important capability may enable estimates to be made of the amount of CO₂ going into dissolution, a significant uncertainty in efforts to quantify free CO₂ in the reservoir (dissolved CO₂ is effectively invisible on seismic data). Secondly, deployed periodically, gravimetry could be used as an 'early warning system' to detect the accumulation of CO₂ in shallow overburden traps where it is likely to be in the low density gaseous phase with a correspondingly strong gravity signature.

The possibility of monitoring injected CO₂ with repeated gravity measurements is strongly dependent on CO₂ density and subsurface distribution. Thick, laterally restricted plumes of CO₂ will give a much higher peak signal than the same amount of CO₂ spread thinly across a wide area.

Offshore, sea-floor measurements are required to obtain sufficient accuracy, and costs are high. Onshore, data acquisition is a lot less expensive, as no vessel is required, and it is onshore gravity monitoring may have the greatest potential benefit. Because of its cheapness, land gravimetry could be used to 'interpolate' between more widely-spaced (in time) seismic surveys to provide a cost-effective monitoring strategy.

4.6.1.5 Well-based monitoring

Deep-focussed monitoring surveys can be run both from the surface, as in the case of surface seismic and gravity techniques, or in wells; either the injection well, other adjacent wells or a specifically designed monitoring well. The latter provides the most accurate means of assessing CO₂ distributions in the reservoir, in terms of saturation and fluid pressure. The zone of analysis is however restricted to a near 1D profile around the well itself. A basic prerequisite of well monitoring systems is that they are deployed both in the reservoir and also in the overburden, particularly within any overlying aquifers where changes in fluid chemistry should be readily detectable.

4.6.1.6 Observations from the CO₂STORE case studies

Sleipner

Sleipner is the only CO₂STORE case study where extensive work has been carried out on the design and feasibility of deep-focussed monitoring methods. This is summarised below in respect of the tools described above.

The baseline surface seismic survey at Sleipner covers an area of some 24 km x 33 km. It was acquired in 1994, for the purposes of imaging the deeper gas reservoirs. So, whilst it does cover the injection site and its immediate environs, simple migration simulations (Figure 4.21) suggest that CO₂ may migrate out of the baseline seismic cube when more than about 5 Mt of CO₂ become trapped at the reservoir top (Zweigel et al., 2000; Hamborg et al., 2003). Significant uncertainty is attached to the migration estimates as very minor errors in depth mapping can radically alter spill points on the gently undulating reservoir topseal. Nevertheless, a crucial element of the seismic monitoring programme will be to carefully track CO₂ migration beneath the caprock

and to ensure that suitable 'baseline' 3D coverage to the east of the current baseline cube is acquired prior to CO₂ reaching the unsurveyed area.

Prior to acquiring the first repeat survey, a seismic sensitivity analysis was carried out (Lindeberg et al., 1999). Simple reservoir simulations, allied to Gassmann calculations were used as the input to elastic seismic modelling. This indicated that the response from the predicted CO₂ accumulations would be readily visible on surface seismic data, as was subsequently confirmed in the Operations Phase (Chapter 7).

A feasibility study for multicomponent (MC) seismic techniques at Sleipner (Liu et al., 2001) indicated that MC benefits are maximised in a fractured (or otherwise anisotropic) reservoir, particularly when the CO₂ injection is accompanied by a significant increase (e.g. 5–10 MPa) in formation pressure. Neither of these conditions is satisfied at Sleipner, so full benefits cannot be realised. Cost is also a drawback, most severely with offshore data where a permanent sea-bed monitoring system is probably the cheapest option. Land 3D MC data is typically 1.3 (3C) to 2.3 (9C) times as expensive as 3D P-wave data. Offshore however, a typical 3D PS dataset may be between 5 and 10 times as expensive as a conventional 3D survey.

To support the Sleipner seismic monitoring work an experimental programme was carried out to test the validity of the Gassmann model on both consolidated and unconsolidated sandstone samples at reservoir conditions. In addition, a software module was developed to compute the properties of CO₂–methane mixtures (Mougin, 2002).

A reliable method was developed for the laboratory verification of the Gassmann formula and rock physics parameters by measurement on consolidated samples (Mougin et al., 2002). The method is based on the substitution by fluids of various compressibilities. To preserve the properties of the clay fraction in the sandstone, diphasic saturation states have been used. The room dry sample was first saturated with brine. The brine was then displaced by viscous oil (non-miscible viscous displacement), and then the viscous oil was displaced by hydrocarbon liquids of varying bulk modulus (kerosene, hexane, pentane, etc). The P and S wave velocity measurements were performed at a range of pore and confining pressures (up to 70 MPa). In general experimental results supported the Gassmann formula, particularly on well-cemented sandstone samples. Experimental difficulties in applying the method to loose sandstone were considerable. Similar difficulties are encountered for any petrophysical measurement; permeability, capillary pressure etc, but they are more pronounced for petroacoustics (a careful preservation of the initial rock microstructure is needed). Nevertheless some results were obtained (Figure 4.49), indicating a Gassmann-type response for Bulk Modulus (derived from V_p), but with considerable scatter on the shear modulus (derived from V_s).

At the beginning of the SACS project it was expected that the methane content of the injected CO₂ could be up to several percent, due to the relative inefficiency of washing process (actually the methane content is generally lower than 1%). To address this, a tool was developed to compute CO₂–methane mixture properties for the Sleipner case (Mougin et al., 2002). The tool utilises the SBWR (1995) equation (a modification by Soave of the 1940 Benedict-Webb-Rubin equation) to compute

density and compressibility (isothermal and isoentropic) values for a wide range of P, T conditions for mixtures with CO₂ concentration greater than 95% molar.

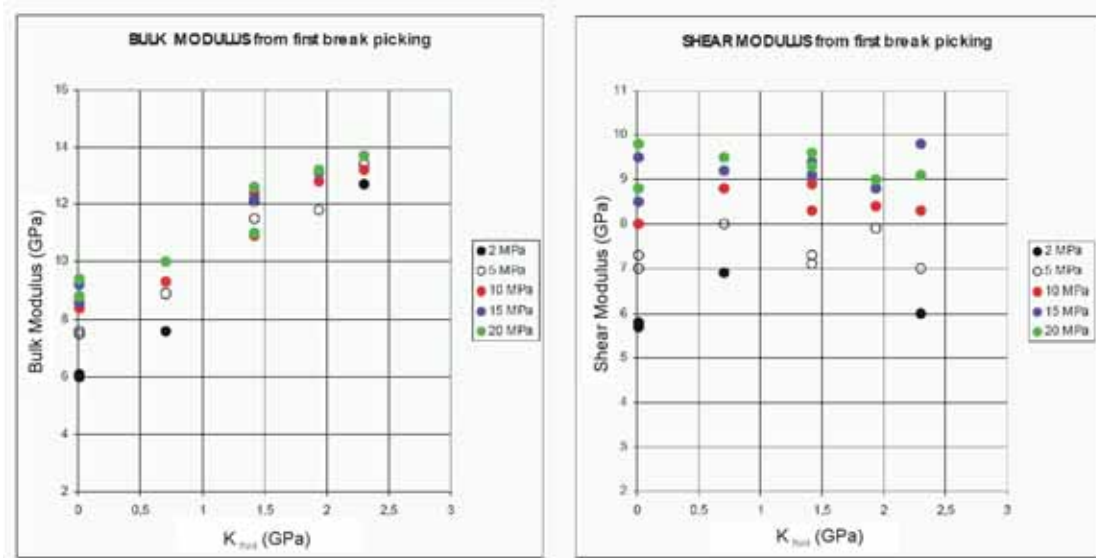


Figure 4.49 Gassmann experiments on loose sandstone carried out for the SACS2 project.

A feasibility study for microseismic monitoring was carried out at Sleipner (Fabriol, 2001). From a practical point of view, microseismicity appears mainly in low permeability reservoir rocks and when injection pressures are relatively high (several tens of MPa). Given the porosity values at Sleipner, microseismicity is unlikely to appear in the Utsira Sand except perhaps in the intra-reservoir mudstones or in the overlying mudstone caprock (Fabriol, 2001). This latter case could be the most interesting to monitor as it could reveal the presence of any leakage into the caprock. However, it remains to be proven that microseismicity actually does exist at Sleipner. This and lack of surrounding adjacent wellbores precludes installation of a monitoring system at this time.

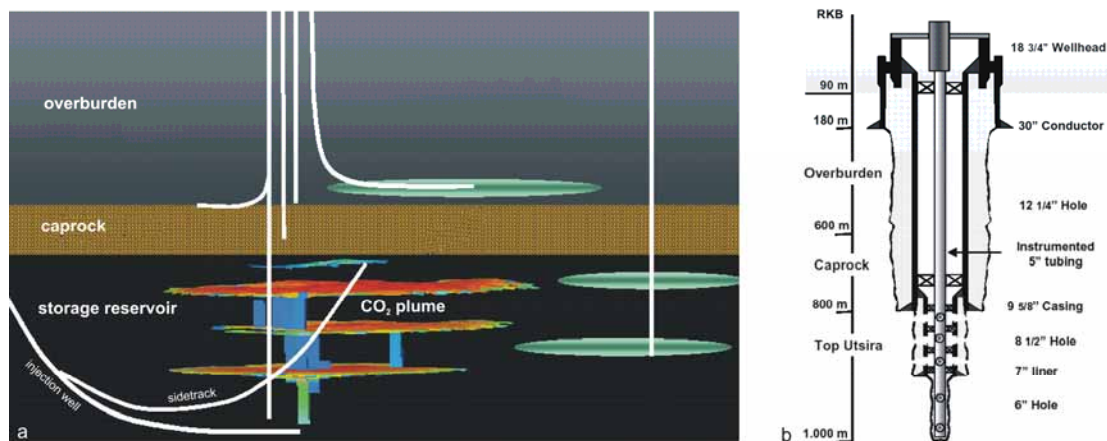


Figure 4.50 Design options for putative monitoring wells at Sleipner.

The microgravimetric method was not evaluated in detail at Sleipner until the Operations phase. Once the first seismic monitoring dataset was available it was possible to develop a realistic initial model for sensitivity analysis (Section 7.2).

A feasibility study to determine the benefits of a monitoring well was carried out for Sleipner (Carlsen et al., 2001) who provided a schematic view of possible well monitoring options the Sleipner injection operation (Figure 4.50). The high cost of such an undertaking has so far precluded this monitoring option however.

4.6.2 Shallow-focussed methods

Shallow monitoring systems (Figure 4.48) aim to detect and measure CO₂ that has migrated into the shallow overburden, into the soil or sea bed and, ultimately, leaked into the seawater or atmosphere. The quantity of CO₂ leaving the geosphere and entering the ocean or atmosphere will likely be needed for accounting in the European ETS. Shallow monitoring includes those methods that detect and measure CO₂ in the subsurface (e.g. potable aquifers, soil, sub-seabed) and those that actually measure CO₂ in the seawater column or atmosphere. In addition, some specialised techniques may be needed to monitor the impacts of leakage, should it occur, on local ecosystems. It should be emphasised however, that careful site selection, predictive modelling and monitoring should prevent any chance of leakage to the ocean or atmosphere occurring.

Baseline surveys, determining conditions prior to injection are an essential part of most monitoring strategies. Leaks may not necessarily occur above the storage site but will be strongly dependant on the local geological structure, for example they may result from migration up gently dipping sandstone beds and thus may appear many kilometres from the storage site. Baseline surveys should take account of these possibilities. Leaks may also not necessarily occur for hundreds of years if the leakage path is long, but thereafter could be highly significant. There is, therefore, a need to use surface monitoring in combination with site characterisation, modelling, risk assessment, subsurface monitoring and history matching to validate the effectiveness of a CO₂ storage site.

Until 2006, when sea-bed bathymetry and imaging has been recently deployed at Sleipner, no shallow monitoring tools had been utilised in the SACS and CO₂STORE projects, but a brief resume of generalised approaches is given below.

4.6.2.1 Detection of CO₂ in the atmosphere and/or sea water

Most techniques for the measurement of atmospheric CO₂ rely on the absorption of infrared radiation by CO₂, and range from large, ground-based instruments to small portable tools that can be mounted either on a vehicle or aircraft. However, the recent availability of reliable diode lasers offers great potential in gas detection. These lasers emit a precisely controlled frequency of infrared light, which can be tuned to the absorbance frequency of a single gas. The diode laser technique has the advantages that the instruments can be small, robust and have relatively low power consumption.

CO₂ leaks from underground storage sites may potentially have an important impact on local ecosystems at the surface, shallow subsurface, and within the marine environment that needs to be assessed, and which could provide very useful indicators of leaks. The severity of this impact is likely to depend on the rate of release of the CO₂ and the proportion that goes into solution or is diluted in the atmosphere.

Tools to analyse sea-water samples for CO₂ are well established, but aimed principally at surface sampling. A recent development is the ability to sample sea water at ambient pressure conditions, preventing errors due to degassing.

4.6.2.2 Detection of CO₂ at the surface or in the shallow subsurface

There is a wide range of established onshore techniques for the measurement of CO₂ in spring and well waters, and in the soil, to define baseline conditions and to identify potential migration pathways and potential leakages at surface. Probes or accumulation chambers are placed in a grid configuration over the expected leakage 'footprint', in or on the soil, and samples analysed periodically to determine CO₂ concentrations and flux.

Ecosystems studies also have the potential to indicate leakage sites. However, little is yet known of the effects of CO₂ on either land or marine plants and organisms, and a significant amount of research is needed before this can become a useful technology.

There are several remote sensing techniques that may be applicable to CO₂ monitoring, including airborne hyperspectral imaging, which may pick up changes in vegetation health due to excess amounts of CO₂, and satellite interferometry that may be able to detect subtle ground surface movements that may occur above injection sites. Airborne EM has been used to detect conductivity anomalies associated with hydrogeochemical changes in groundwater caused by pollution plumes. This could potentially be applied to the detection of changes in shallow groundwater conductivity due to the presence of dissolved CO₂, but only has potential application onshore. Airborne IR spectroscopy may be able to detect elevated levels of CO₂ in the atmosphere above a leak, but this has not yet been demonstrated.

4.7 Transport

Truck, railway, ship and pipeline are all feasible alternatives of transporting CO₂. Pipeline (True, 2000) is the best alternative for transportation of large quantities of CO₂ onshore (> 1 Mt/year). Experience from the construction and operation of onshore CO₂ pipelines exists in USA. No offshore CO₂ pipeline is in operation, but Statoil is constructing one for the LNG project at Snøhvit. Experiences of CO₂ transport by trucks, railway and ship are mainly found in the food and brewery industry, with amounts in the range of some 100 000 t/y. CO₂ is today transported at industrial scales by ship. To summarise, pipeline and ship are the two main alternatives for CCS.

4.7.1 Pipeline

4.7.1.1 Pipeline route

Routing issues are the main factors that determine the feasibility of a pipeline project.

Schwarze Pumpe (Schweinrich)

The Schwarze Pumpe/Schweinrich case (a typical onshore storage scenario), requires a pipeline route of considerable length (Figure 4.51).

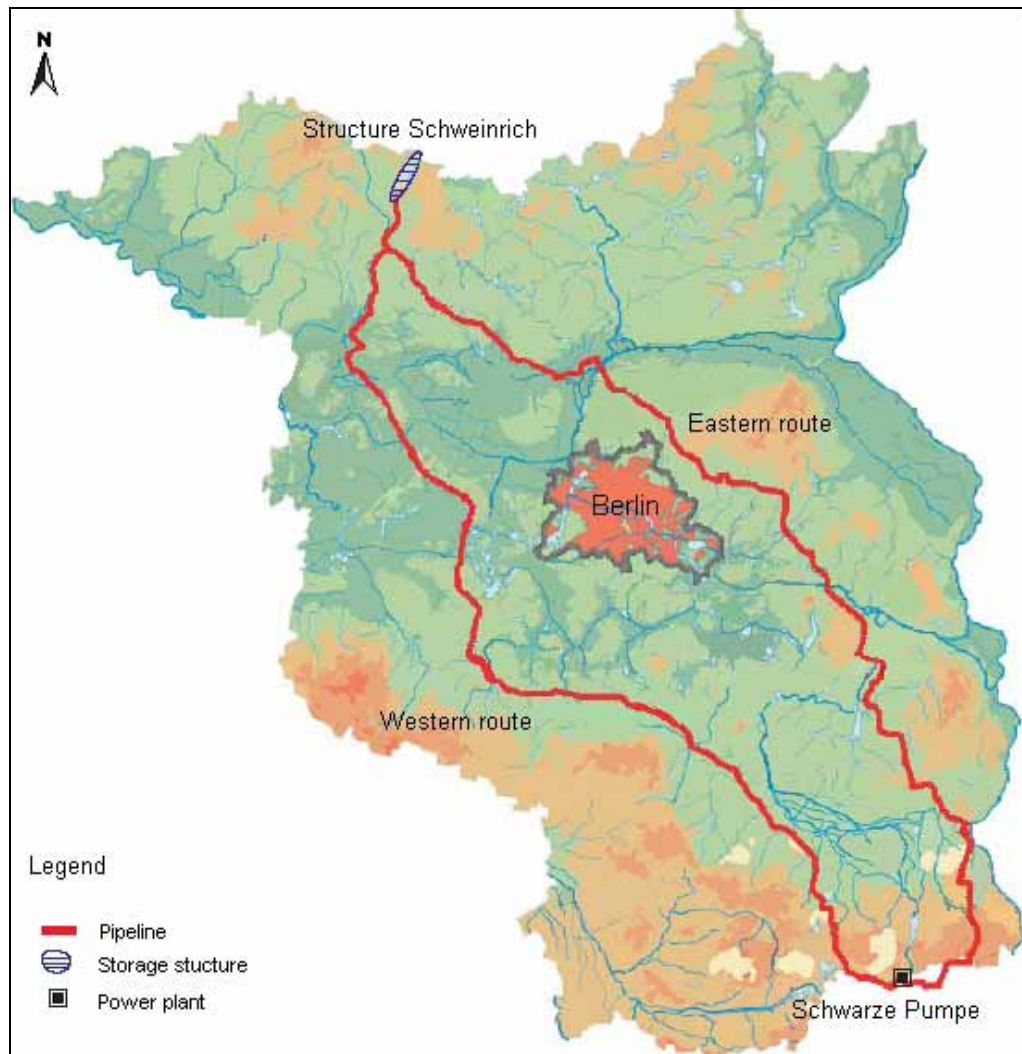


Figure 4.51 Investigated pipeline routes to Schweinrich passing from south-east to north-west through the state of Brandenburg.

The following criteria were used to determine a possible pipeline route.

Extensive use of existing routes: The joint use of existing routes of other media or carrier entities is common practice. This minimises the interference with other interests and results in an integration in the existing regional development and consequently in a route layout with a good chance of success.

Avoidance of residential structures/urban centres as well as surface depressions: The properties of the medium as well as the assumed throughput in case of damage suggest that the pipeline should be constructed with a minimum distance to sensitive features.

Avoidance of higher ground: When crossing high elevations, a loss in pipeline pressure may result in a drop below the minimum system pressure. This would in a worst case require an additional station suitable for increasing the pressure.

Avoidance of nature reserves, closed woodlands etc: Crossing nature reserves is generally a problem (exemptions with conditions under nature protection laws). Woodlands are a problem if the construction requires clearings and replacement of plantations.

Minimisation of the overall length and the number of crossings (streets, railways, bodies of water): This step impacts on the costs of realisation as well as the costs for operation as pressure loss depends on the length of the pipeline.

4.7.1.2 Determination of optimal pipeline diameter

Pipelines suffer from temperature and pressure loss due to factors such as surrounding temperature, frictional loss and elevation. These flow properties are important to simulate in order to determine the optimum pipeline diameter. A sample analysis is here presented for Kalundborg.

Kalundborg

Onshore gas pipelines are often operated at 8 MPa pressure in contrast to offshore (long distance) pipelines which are operated at higher pressure in order to minimise the costs. The dimension of the CO₂ pipeline was adjusted to keep the pressure high enough to keep the CO₂ in the dense fluid phase. The lowest allowable pressure in the pipeline is set to 6 MPa. If pressure drops below this value the CO₂ may revert to a gas phase. This will result in low density and high flow velocities in the pipeline.

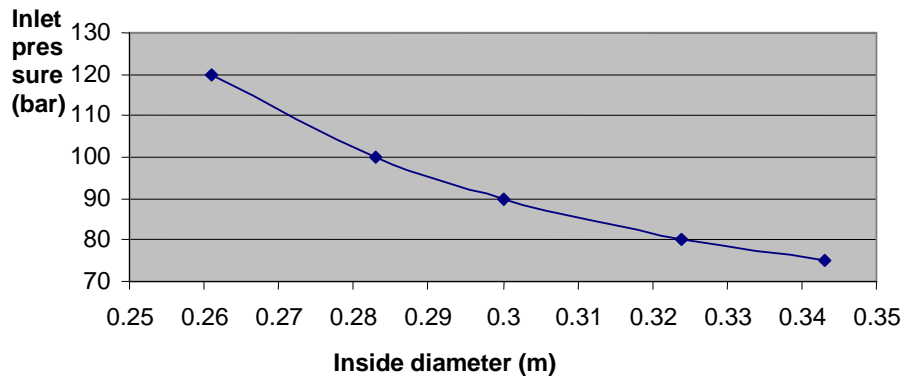


Figure 4.52 Inlet pressure versus dimension for the proposed 15 km long CO₂ pipeline from Kalundborg to the Havnsø structure (6 Mt CO₂ per year, outlet pressure of 60 bars, 6MPa).

Pipe dimensions have been calculated for different inlet pressure (Figure 4.52). The outlet pressure is set to a minimum value of 6 MPa (60 bars). The temperature in the CO₂ and surroundings are set to 10° C in the calculations. The calculations show that an inlet pressure of 8 MPa will require a minimum inner diameter of 0.324 m (12.76”). For the Kalundborg case an inside diameter of 0.33 m (13”) is preferred.

4.7.1.3 Costs

The construction represents the greatest part of the total cost and can be divided into four main categories (True, 2000).

materials: costs for line pipe, pipe coating and cathodic corrosion protection, booster stations, etc

right of way (ROW): Costs for obtaining the ROW and allowing for damages

labour costs

miscellaneous costs of surveying, engineering, supervision, contingencies, administration and overheads, telecommunications equipment, and other remaining costs.

Pipeline transportation costs are site-specific and must be determined on a case-by-case basis. The total cost expressed as cost per tonne of CO₂ depends on the following factors:

length: longer distances result in higher investment costs for all categories listed above

the adjustment between dimension and capacity: greater dimension results in higher investment costs, but also raises the capacity

the adjustment between number of booster stations and capacity: more booster stations results in greater investment costs, but also raises the capacity

interest rate and depreciation time.

Kalundborg

For the Kalundborg case study, technical requirements and costs for a surface pipeline were evaluated. The calculations are based on the transport of a maximum of 6 Mt of CO₂ per year captured at the powerplant site and injected at the south-eastern flank of the Havnsstructure. Transport would be in a specifically designed pipeline with estimated total length of 15 km. It is anticipated that the pipeline would be buried in the Quaternary cover to a minimum depth of 0.9 m. The cost estimate is a ‘best guess’ and no geotechnical analysis has been made concerning the practicality of pipeline route and ground stability.

The calculations are based on a tentative pipeline route chosen to avoid densely populated areas and where possible to follow existing pipelines and high voltage

cables. It is anticipated that the soil types will not present major problems to the pipeline construction. According to normal procedures it is anticipated that the pipeline will be surrounded by a security zone 25 metres wide. This zone will exist on both sides of the pipeline and will be given strict restriction concerning buildings and general use. The cost estimate assumes that the pipeline including the security zone can be constructed without conflicts with existing buildings. The cost estimate is made only on the main pipeline and does not include connection lines from the power plant or the refinery.

The calculation is based on a construction cost of 625–750 € per metre for a 13” (0.330 m) pipeline. The total construction costs for a 15 000 m pipeline will thus amount to 9.4–11.3 million Euros.

The cost evaluation includes:

- gas pipeline, valves and spare parts
- digging of trench and covering of pipeline
- re-establishment of vegetation, road pavement etc
- signal cable and warning strips
- surface markings
- pressure tests
- detailed building project
- building planning and surveillance
- 10% additional costs.

The cost estimate does not include compensation costs to landowners.

Project costs cover the period from draft project to start of detailed building project (e.g. Environmental Impact Assessment (EIA) from the West Zealand County authority).

It is most likely that the capture plant will need an EIA and it is almost certain that the transport- and especially the storage systems will require an EIA. Consequently, it is most likely that the entire CCS system will be evaluated together as one system. The EIA process will include several public hearing phases. As this CCS system would be the first system in Denmark of its kind some public involvement can be expected. It is expected to take about 18 months to get an approval.

Schwarze Pumpe (Schweinrich)

A preliminary estimate of CO₂ transportation and storage costs was presented in Chapter 3.

4.7.2 Ship

It is common practice to lease ships on time charter from shipping companies. When a ship is leased on time-charter basis, all fixed (i.e. capital costs) and day costs (all expenses that can be related to the ship operation and management including spare parts, labour, maintenance and repair) are included in the monthly time charter charge, whilst the travelling costs (all expenses that can be related to the line operating, such as fuel and terminal fees) are taken care of by the leaseholder.

The ship transportation costs are also site-specific and must be determined on a case-by-case basis. Factors contributing to the total transportation cost are:

time-charter cost (depends on ship size)

harbour fees (depends on ship size)

fuel (depends on ship size and time needed for round trip)

time needed for round trip (depends on route length and loading/unloading time)

loading/unloading time (depends on loading/unloading capacity)

number of round trips/year (total time the ship can be in operation divided by the time needed for a round trip)

total capacity per year (depends on ship size and the number of round trips per year).

5 SITE DESIGN AND PLANNING CONSENT

This phase includes design of all facilities in the CO₂ transport/storage infrastructure and planning for the implementation and operation of CO₂ injection. Includes all planning and consenting procedures with the relevant regulatory authorities and various outreach and dissemination initiatives.

5.1 Design

Some design issues are illustrated by the Sleipner case study.

Sleipner

Natural gas from the Sleipner West Field is produced from a well-head platform, through a 12 km long pipeline to the process and treatment platform Sleipner T (itself connected by a bridge to the Sleipner A platform at Sleipner East (Figure 1.2).

CO₂ is removed from the natural gas by an active amine process (Total patent) in one of the processing modules at Sleipner T. Natural gas to be treated passes through two large absorption columns, weighing about 8000 tonnes and standing 35 m high. Energy freed by the amine process runs two generators, yielding six megawatts of power for use on the platform. After the carbon dioxide has been separated it is transferred to the Sleipner A platform for injection. The natural gas is treated in another module and exported via Sleipner A through the pipeline system to continental Europe. The cost of the carbon dioxide module was about NOK 2 billion.

Full details of well design are given in Baklid, Korbøl and Owren (1996). The design capacity was set to 1.7 MSm³ of CO₂ per day and to keep the CO₂ in the dense phase. In the injection area the 7" casing was perforated over a length of 100 m to achieve this capacity. In the early phase of the injection there were some problems due to collapse in the unconsolidated sand. Installing a sand screen restored the well injectivity.

To assure the necessary lifetime of 25 years, 25% Cr duplex (stainless) steel was chosen for the well. The performance of the injection well infrastructure at Sleipner is currently being monitored by tubing head pressure measurement. As the free CO₂ plume is not expected to ever impact on the injection well, it need only perform effectively for the active injection period. More generically, performance of the current well materials (steel, cement) are being tested through a series of geochemical laboratory experiments (Chapter 7).

5.2 Planning consent

5.2.1 National

National planning-consent issues are illustrated with respect to the Sleipner and Kalundborg case studies.

Sleipner

The application to store CO₂ at Sleipner was an integral part of the field development plan for Sleipner Vest ('Plan for utbygging og drift', PUD) from December 1991. In this PUD, five different alternatives for CO₂ storage were listed (see Section 3.6.3), of which storage in the Utsira Sand was presented as the most promising option. Some key properties of the reservoir formation were provided, mostly in qualitative terms (e.g. 'good reservoir properties'). The supporting documentation of the PUD included the set-up and results of reservoir simulations which indicated suitable injectivity and little risk of pressure build-up ('first series' of simulations summarised in Ch. 4.2.1).

The PUD with minor modifications, none of which involved the CO₂ storage plans, was accepted by the Storting (the Norwegian parliament) in December 1992 and subsequently the Oil and Energy Department issued a formal acceptance to the licence partners. The CO₂ storage plans were thus formally accepted by the national authorities.

Kalundborg

When building a CO₂ capture, transportation and storage system (CCS) a number of permits will be required. As CCS will be a new technology in Denmark it is expected that the requirements from the authorities regarding environmental investigations and documentation will be rather stringent.

Regarding permission requirements for the capture plant itself, this will most likely include the following permissions:

- expression from the county whether an environmental impact assessment (EIA) will be necessary or not

- most likely an EIA from the county

- environmental permission from the community

- building permission from the community

- technical approval of some parts of the installations, like erection permissions from the Factories Inspectorate.

When building new, large facilities or plants, the authority must be contacted for an expression of whether an environmental impact assessment (EIA) will be necessary. An EIA is an evaluation of the influence on the overall environment including evaluation of different alternatives. For Asnæs Power Station the authority is West Zealand County. It is most likely that the capture plant will need an EIA and it is almost certain that the transport and especially the storage systems will require an EIA. Consequently, it is most likely that the entire CCS system will be evaluated together as one system.

The EIA process will include several public hearing phases. As this CCS system would be the first system in Denmark of its kind, some public involvement can be expected. It is anticipated that the process would take about 18 months.

The existing environmental permission for the power station given by the local authorities will have to be adjusted to include the capture plant. The local authorities in this case are West Zealand County. The focus of the renewed environmental permission will most likely be on five topics:

use and handling of any chemicals

changes in noise

changes in emissions

waste water

changes in cooling water.

The capture plant will introduce two new chemicals to the power plant: absorbent and inhibitor, and increase the use of cooling water, active carbon as filter material and NaOH for cleaning, besides an increase in use of process steam and electricity. With regard to the environmental permission it is important whether the selected absorbent and inhibitor are listed in Appendix 1 to the Risk Order from the Danish Environment Department. A special detailed risk evaluation has to be performed for any of the chemicals are included in the list. The traditionally used absorbent, Monoethanolamine (MEA) is not included in the list, but other potential novel absorbents may be included.

It is not anticipated that a capture plant will contribute significantly to an increase in noise levels from the power plant.

In the Environmental Permission it is anticipated that there will be requirements with respect to the emissions from the plant. In the Guidelines No. 2, 2002 from the Danish Environment Department, B-values for emission concentrations are given for ethanolamin, MEA. The B-value is set to 0.01 mgm^{-3} . If another absorbent were to be used, it is anticipated that a specific B-value for this absorbent would have to be prepared. For a pilot capture plant, the estimated escape of absorbent through the stack from the absorber and the stripper is 50-200 ppm, equal to the escape in similar industrial facilities. For full-size capture plants this will be a matter requiring careful assessment.

Traditionally, a considerable amount of cooling water is needed for the operation of a capture plant. At present, cooling water for the existing plant is taken from the fjord and from different underground reservoirs. It is anticipated that, as the capture plant will be integrated with the new Unit 6, the amount of cooling water will be considerably reduced.

The capture plant will produce two kinds of by-products in the form of filter material (used active carbon) and disposals from the reclaimers. Both kinds of material can be disposed of normally. In any case, concerns about risks of leakage to the ground and to the groundwater will have to be evaluated and also an assessment of the use of BAT (best available technology) will have to be included.

All buildings established have to be reported to and approved by the local authorities, in this case Kalundborg Community. Obtaining a building permit is a standard procedure and as the plant will be built on an existing power plant site, no special considerations are foreseen. Application for the building permission will take place after the environmental permissions have been obtained but the time needed for obtaining the building permission is anticipated to be negligible.

When planning the surface installation (pipeline, and injection site) special attention should be paid to the national Danish protection laws (Naturbeskyttelsesloven §33) that designate areas of special scientific, environmental or cultural interest. No conflicts, however, are anticipated for the installations planned in the Kalundborg case study.

Certain types of installation have to be approved by the Factories Inspectorate. As long as the rules are fulfilled there is no significant delaying process and no special considerations are anticipated.

5.2.2 International

There is no explicit European legislation that governs offshore geological storage of CO₂. Three international treaties currently govern the disposal of materials in the maritime environment:

1972 London Convention (Convention on the Prevention of Marine Pollution by Dumping of Wastes and Other Matters)

1996 Protocol to the London Convention.

1992 OSPAR Convention (Convention for the Protection of the Marine Environment of the North East Atlantic)

The 1996 protocol came into force in March 2006 and supercedes the 1972 London Convention.

Both the OSPAR Convention and the 1996 protocol provide control of the disposal of matter in 'the subsoil'. The OSPAR convention prohibits 'the introduction by man, directly or indirectly, of substances or energy into the maritime area which results, or is likely to result, in hazards to human health, harm to living resources and marine ecosystems ...' Although deep geological storage is not generally regarded as in 'the subsoil', there is a view that because there is a small but finite possibility of leakage of CO₂ to the marine environment, these treaties could be deemed to apply to geological storage of CO₂.

The OSPAR Convention and the 1996 Protocol do allow geological storage of CO₂ associated with the process of Enhanced Oil Recovery, as both treaties permit 'placement of matter for a purpose other than mere disposal'.

The treaties did not envisage geological storage of CO₂ purely for environmental reasons when drafted, so international agreement, and amendment of the treaties is

required before geological storage of CO₂ arising from an inland European source could be deployed using existing offshore facilities.

Contracting parties to the London Protocol, at their first meeting held in London from 30 October to 3 November 2006, adopted amendments to the 1996 Protocol to the Convention on the Prevention of Marine Pollution by Dumping of Wastes and Other Matter, 1972 (London Convention). The amendments regulate the sequestration of CO₂ streams from CO₂ capture processes in sub-seabed geological formations.

Parties agreed that guidance on the means by which sub-seabed geological sequestration of carbon dioxide can be conducted should be developed as soon as possible. This will, when finalised, form an important part of the regulation of this activity. Arrangements have been made to ensure that this guidance will be considered for adoption at the 2nd Meeting of Contracting Parties in November 2007.

This means that a basis has been created in international environmental law to regulate carbon capture and storage (CCS) in sub-seabed geological formations, for permanent isolation, as part of a suite of measures to tackle the challenge of climate change and ocean acidification, including, first and foremost, the need to further develop low carbon forms of energy. In practice, this option would apply to large point sources of CO₂ emissions, including power plants, steel and cement works.

The applicability of international treaties to CCS is examined with respect to the Kalundborg case study which would involve both offshore and onshore storage.

Kalundborg

In general the OSPAR convention regulates the use of the maritime areas and prevents any disposal of waste. As around one third of the Havnsø structure is situated offshore the OSPAR convention may come into force if a decision for underground storage of CO₂ were to be made. The main conclusion from the Trondheim workshop was that any project should be planned in accordance with national regulations and international agreements. In addition the risks of leakage from an underground storage should be balanced against the affects of atmospheric CO₂ on the marine environment.

The Havnsø structure is situated partly within an EF bird protection and special habitat area and an EU RAMSAR area. These areas are regulated by international laws to prevent damage to bird and animal life. It is anticipated that the underground storage facilities will not be in conflict with these regulations, however, pre-injection site surveys and monitoring surveys e.g. shooting surface seismics may pose a problem. It is recommended that contact is made with the authorities early in the planning phase.

6 SITE CONSTRUCTION

This phase deals with the construction of the following three components:

Pipeline

Injection facilities and distribution system

CO₂ injection well(s)

No specific observations on site construction are available from the SACS or CO2STORE projects.

7 OPERATIONS

This phase is concerned with maintaining site infrastructure and ensuring that the site is performing to expectations. Observations here are restricted to the ongoing Sleipner operation.

7.1 Operation and maintenance of pipeline and injection facilities

7.1.1 Measurement of injected CO₂

A critical storage verification issue is the accurate measurement of injected CO₂. This may, in future projects, be linked to gaining emissions credits, and in any case is essential for the development of robust reservoir simulations.

At Sleipner, surface injection pressure, temperature and injected CO₂ volume are monitored daily, with cumulative figures computed on an ongoing basis (Figure 7.1, Table 7.1).

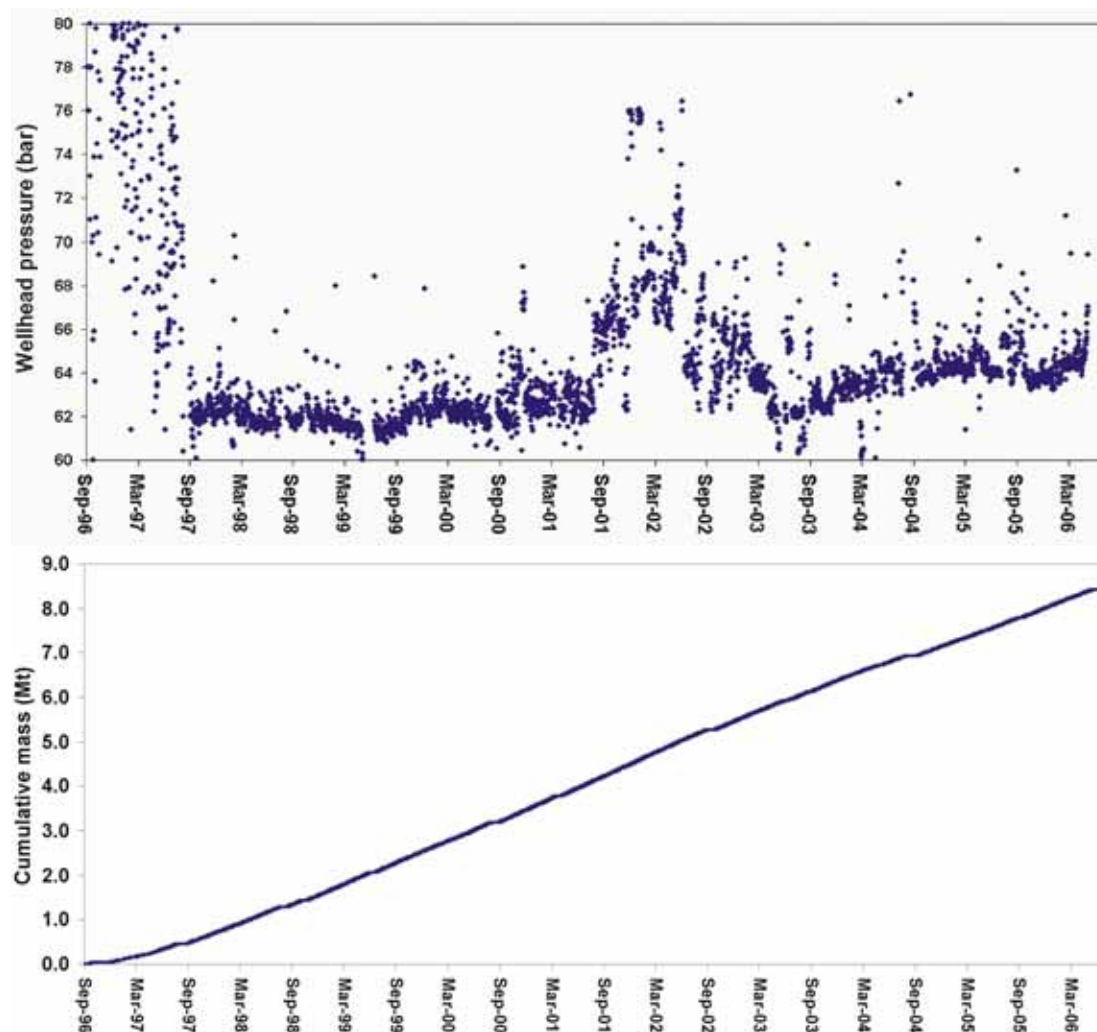


Figure 7.1 Sleipner CO₂ injection history 1996 to 2006, wellhead pressure and injected mass.

Injection well	Date	On-stream (hours)	Average wellhead pressure (bar)	Injected volume (Sm ³)	Injected mass (tonnes)	Cumulative volume (Sm ³)	Cumulative mass (million tonnes)
A16	19-Apr-02	24	66.85	1569599	2945	2588858380	4.8567
A16	20-Apr-02	24	67.53	1605050	3011	2590463430	4.8597
A16	21-Apr-02	24	67.99	1617605	3035	2592081034	4.8627
A16	22-Apr-02	24	67.67	1620188	3039	2593701222	4.8658
A16	23-Apr-02	24	68.05	1631902	3061	2595333124	4.8688
A16	24-Apr-02	24	67.67	1623090	3045	2596956214	4.8719
A16	25-Apr-02	24	67.41	1594772	2992	2598550986	4.8749

Table 7.1 Sample extract from Sleipner daily injection log.

7.2 Monitoring

The monitoring programme at Sleipner is closely linked to the reservoir flow simulation (Section 7.3). Key aims are outlined below:

- to image the distribution and migration of CO₂ within and around the storage reservoir

- to assess the potential for direct quantitative assessment of CO₂ in the subsurface, the Utsira reservoir being particularly suitable for this type of analysis

- to test and calibrate flow simulations of the plume both in the short-term and also for the longer-term prediction of plume behaviour.

7.2.1 Time-lapse surface seismic monitoring

Prior to the onset of CO₂ injection the Sleipner licence group had planned to monitor the subsurface distribution of CO₂ by means of time-lapse seismic. When it became evident that the storage project would be of much wider public interest, this activity became a major part of the SACS project, with a focus extending from basic operational aspects to more research oriented topics.

The baseline survey at Sleipner was acquired in 1994. As discussed in Chapter 4, the acquisition geometry and location of the baseline survey were however focussed on a deeper target than the CO₂ plume. This was not ideal for optimal resolution imaging, but was wholly satisfactory for time-lapse monitoring purposes. Subsequent monitor surveys were acquired in 1999 and 2001 with 2.35 and 4.26 Mt of CO₂ in the reservoir respectively. The acquisition geometry of the time-lapse seismic surveys was a compromise between keeping the same geometry as the base survey and focussing more on the CO₂ plume. Within these constraints the surveys were matched as closely as practicable to the baseline survey through careful control of acquisition and processing parameters (Tables 7.2 and 7.3). Due to cost constraints the repeat surveys covered an area only of some 7 x 3 km, sufficient to cover the predicted extent of the plume at those times.

Survey	SI947	SI996	SI016	SI026	SI04B	SI067	SI06
Date acquired	68-10/9/1994	8.10-10.10.1999	27.9-1.10.2001	26.5-1.6.2002	13.6-13.8.2004	June 2006	June 2006
Vessel	Seisranger	Akademic Nardinov	Geo Diamnd	Geo Diamnd	CGG Alize	Ranfom Explorer	Ocean Seaker
Shooting direction	0.853 degrees	0.853 degrees	0.850 degrees	0.850 degrees	90.00 degrees	0.850 degrees	variable
Source tow depth	6m	6m	6m	6m	6m	6m	3m
Source length	16m	15m	15m	15m	148m	15m	point
Source width	20m	16m	10m	16m	24m	16m	point
No. of subarrays	3	3	2	3	4	3	1
Source x-line sep	50m	50m	50m	50m	na	50m	na
Source volume	3400 in ³	3542 in ³	3390 in ³	3147 in ³	4280 in ³	3600 in ³	160 in ³
No. of sources	2	2	2	2	1	2	1
Shotpoint interval	18.75m	12.5m	12.5m	18.75m	18.75m	18.75m	12.5m
Streamer type	Nessie III	Nessie IV	Nessie IV	Nessie IV	Syntrak	PGSRDH/Teledyne	Fjord HSSQ
No. of cables	5	4	6 (on 4 str preplot)	6	10	8 (on 6 str preplot)	1
Cable separation	100m	100m	100m	100m	37.5m	100m	na
Cable length	300m	300m	1500m (3000m)	360m	450m	360m	1200m
Near offset	195m	165m	150m	130m	77m	130m	29m
Group interval	12.5m	12.5m	12.5m	12.5m	12.5m	12.5m	12.5m
Group length	16.10m	14.86m	14.86m	14.86m	12.5m	12.5m	12.5m
Tow depth	8m	8m	8m	8m	8m	8m	3m
Bin size acq	6.25x25m	6.25x25m	6.25x25m	6.25x25m	6.25x18.75m	6.25x25m	na
Record length	5500ms	4500ms	4500ms	6000ms	6000ms	6000ms	3000ms
Sample interval	2ms	2ms	2ms	2ms	2ms	2ms	1ms
Lowcut filter	3.4Hz/18dBQt	3Hz/18dBQt	3Hz/18dBQt	3Hz/18dBQt	3.4Hz/12dBQt	3Hz/12dBQt	8Hz
Highcut filter	180Hz/70dBQt	180Hz/70dBQt	200Hz/406dBQt	180Hz/72dBQt	206Hz/276dBQt	206Hz/276dBQt	cut

Table 7.2 Some key acquisition parameters for the Sleipner time-lapse seismic (1994, 1999, 2001, 2002, 2004, 2006 and 2006 2D high resolution).

In addition to the dedicated repeat surveys, further datasets were acquired by the Sleipner operators in 2002, 2004 and 2006 (the latter with more than 8 Mt of CO₂ injected). These were not obtained with the specific aim of monitoring the CO₂ plume (for example the 2002 survey does not cover the easternmost portion of the plume in 2001 and 2002), but nevertheless provide very useful additional datasets. The 2004 and 2006 surveys are, at the time of writing, undergoing full time-lapse processing. In addition to the 3D datasets, a number of 2D high resolution lines were also acquired in the summer of 2006. Again, these data are currently being processed.

The dedicated monitor surveys from 1999 and 2001 show good repeatability. The additional surveys shot in 2002 and 2006 also show good repeatability, assisted by the fact that it was acquired in the same azimuth as the earlier datasets. In contrast, the 2004 survey was acquired roughly perpendicular to the earlier datasets and its repeatability characteristics are currently being assessed. The results of this will be of considerable interest in predicting how effectively datasets not specifically acquired for time-lapse purposes can be used for time-lapse analysis.

Survey	ST9407	ST9904	ST0106	ST0206
Select common offset range to process (approx. 240-1740 m)	yes	yes	yes	Yes
Select time-window to process 0-2300 ms	yes	yes	yes	
Deterministic zero phasing using supplied far-field signature	94-signature	99-signature	01-signature	02-signature
Lowcut filter 6 Hz	yes	yes	yes	Yes
Gain t2	yes	yes	yes	Yes
Gun + cable & recording time correction	+ 9.46 ms	-38.6 ms	-38.6 ms	
Tidal correction based on model	yes	yes	yes	Yes
Swell noise attenuation using "Deband", applied in two frequency bands separated at 20 Hz	yes	yes	yes	Yes
Tau-p forward transform, predictive deconvolution with 64 ms gap and 364 ms operator, design window 800-1500 ms tau-p inverse transform	yes	yes	yes	Yes
NMO, k-filter, spatial decim from 12.5m to 25m receiver interval	yes	yes	yes	Yes
sort to 20 offset groups	yes	Resampling from 50 m to 75 m trace spacing	Resampling from 50 m to 75 m trace spacing	Resampling from 50 m to 75 m trace spacing
Swath dependent static correction based on offset group 4 & 5 (500-600 m)	no	yes	yes	yes
Global amplitude scaling	factor 0.8264			
Global frequency amplitude match	no	yes	yes	yes
Phase rotation			-20 degrees	10 degrees
Time shift			-1.3 ms	
50 % bin overlap, Calibrated log stretch DMO, half number of offset groups	yes	yes	yes	yes
unNMO	yes	yes	yes	yes
Xline fx holefilling		yes	yes	yes
New NMO, with velocities slightly adjusted from a previous reprocessing of ST9407	yes	New velocity picking in CO ₂ injection area	Same velocities as 1999	Same velocities as 1999
Front mute, down to 50 ms at 330 m offset, down to 3000 ms at 3162 m offset	yes	yes	yes	yes
3D stack	yes	yes	yes	yes
	selection of common area	selection of common area	selection of common area	
FX interpolation to 12.5 m x 12.5 m grid	yes	yes	yes	yes
Finite difference migration with 100 % interval velocities	yes	yes	yes	yes
Residual frequency, phase and time match to ST9407		yes	yes	yes
Q comp. filter, Q=300	yes	yes	yes	yes
SEGY output	yes	yes	yes	yes

Table 7.3 Some key processing parameters for the Sleipner time-lapse seismic showing the 2003 processing to match the 1994, 1999, 2001 and 2002 surveys.

7.2.1.1 Imaging CO₂ distribution and migration

A key aim of the monitoring programme at Sleipner is to provide robust 3D volumetric imaging of the storage site, such that CO₂ migration both within the reservoir also into adjacent strata, is effectively imaged. Ideally monitoring will show that the CO₂ is being confined wholly within the primary storage reservoir, but, should this not be the case, then it should provide early warning of any migration into the overburden and, in the future, any potential migration towards the sea bed.

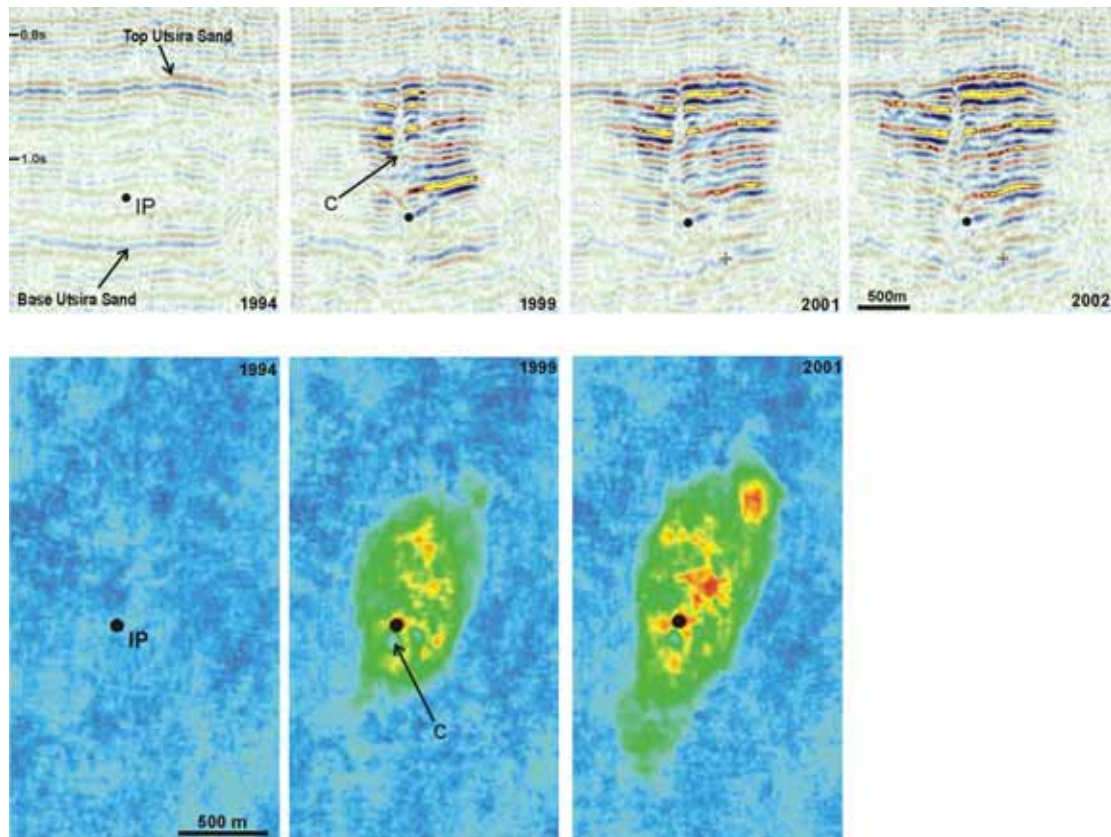


Figure 7.2 Sleipner time-lapse surface seismics 1994 to 2002. Seismic sections (inline) showing progressive development of plume reflectivity (top). Plume in plan view, showing integrated reflectivity (bottom). Note prominent low reflectivity vertical feature interpreted as primary feeder chimney (C).

At Sleipner the time-lapse seismic datasets have proved notably successful in providing striking images of plume morphology and how this has developed through time. It is clear that even for CO₂ in a relatively dense (supercritical) phase, rather than a gaseous state, conventional p-wave surface seismic data can be a successful monitoring tool for CO₂ injected into a saline aquifer (Eiken et al., 2000; Brevik et al., 2000; Arts et al., 2000).

The CO₂ plume is imaged as a number of bright sub-horizontal reflections within the reservoir, growing with time (Figure 7.2). The reflections are interpreted as interference tuning wavelets arising from thin (< 8 m thick) layers of CO₂ trapped beneath the thin intra-reservoir mudstones and the reservoir caprock.

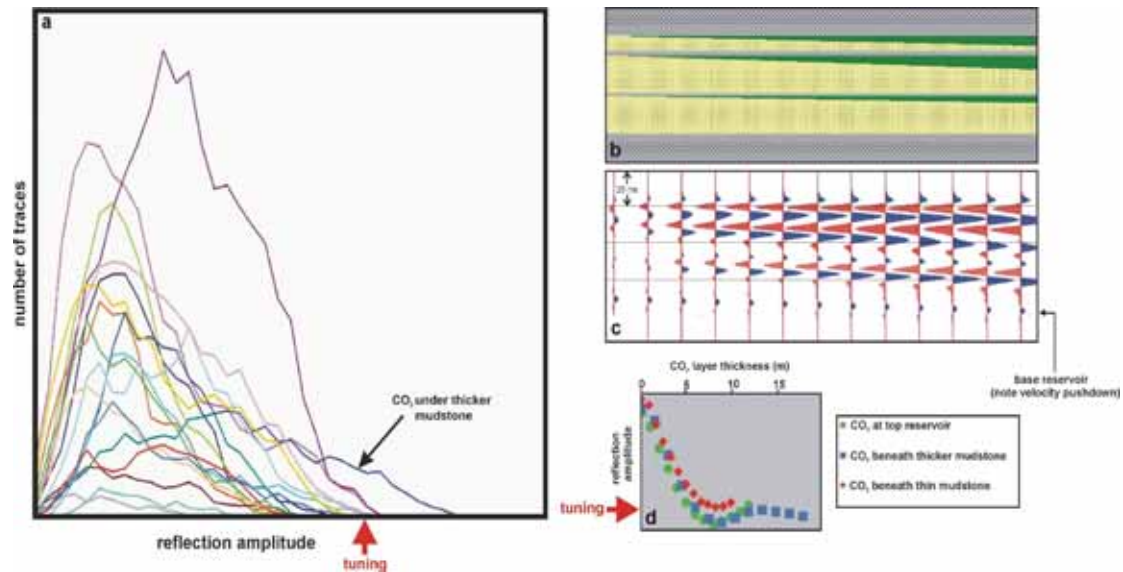


Figure 7.3 Sleipner tuning amplitude plots and synthetics. a) Sleipner time-lapse seismic: reflecton amplitude distribution for the nine interpreted seismic horizons (1999 and 2001) showing likely tuning amplitude. b) Illustrative Utsira reservoir model with mudstones of various thickness overlying rightward thickening layers of CO₂ - saturated sand. c) Seismic response of the above model convolved with a zero-phase wavelet statistically derived from the Sleipner data windowed on the Utsira Sand (red troughs denote negative reflection coefficients). Reflection energy increases rightwards from zero, peaking at layer thicknesses of about 8 m. Note velocity pushdown (~ 9 ms) at base reservoir. d) Relationship of amplitude to thickness for the three CO₂ layers. Minor amplitude variations reflect the differing thicknesses of the overlying mudstone layers, the mean tuning thickness is about 8.2 m.

The amplitude of these wavelets can be related directly to the thickness of the causative CO₂ layer (Figure 7.3), and it has been shown that CO₂ accumulations as thin as about a metre can be detected — far below the conventional seismic resolution limit of around 7 m. Even these thin accumulations cause significant, observable and measurable changes in the seismic signal, both in amplitude and in travel time. The plume is roughly 200 m high and elliptical in plan, with a major axis increasing from about 1500 m in 1999 to about 2000 m in 2001. Nine distinct layers of CO₂ have been identified on the seismic data. These can be mapped consistently on all of the repeat surveys and show systematic changes with time. It is notable that by 2002 the lower plume (Layers 1 to 4) was approaching equilibrium with only a slow rate of layer spreading (Figure 7.4), whereas the upper plume (Layers 5 to 9) continued to grow rapidly (Figure 7.5). Amplitude variations within the layers give detailed insights into CO₂ migration and plumbing in the reservoir (e.g. Chadwick et al., 2004). At a number of locations within the plume, vertical chimneys have been observed where CO₂ passes through the thin mudstone layers, including a major feature more-or-less above the injection point (Figure 7.2) that is interpreted as a major conduit for CO₂ migration upwards through the reservoir.

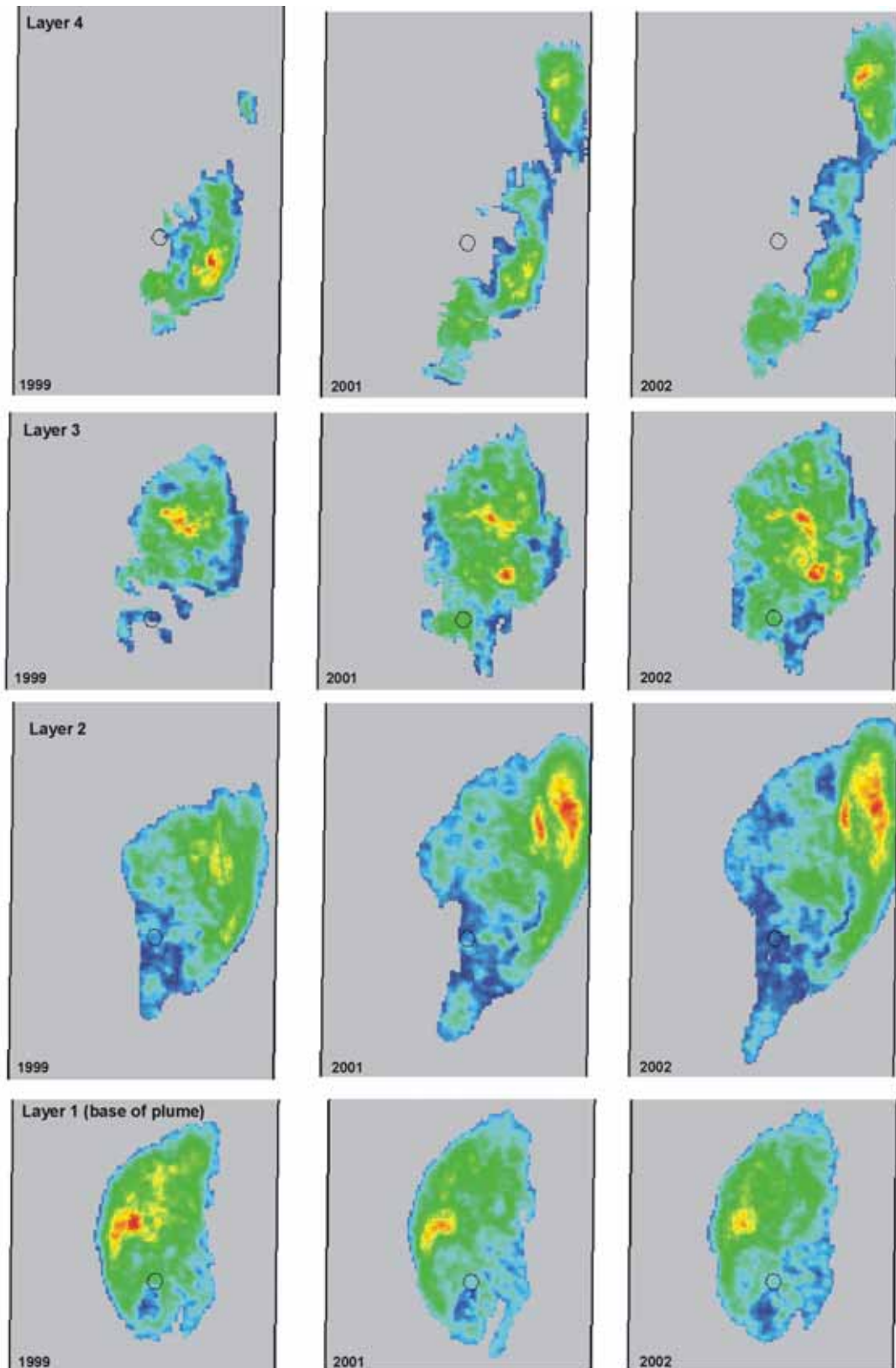


Figure 7.4 Reflection amplitude maps of the lower four layers of the Sleipner plume, showing growth from 1999 to 2002.

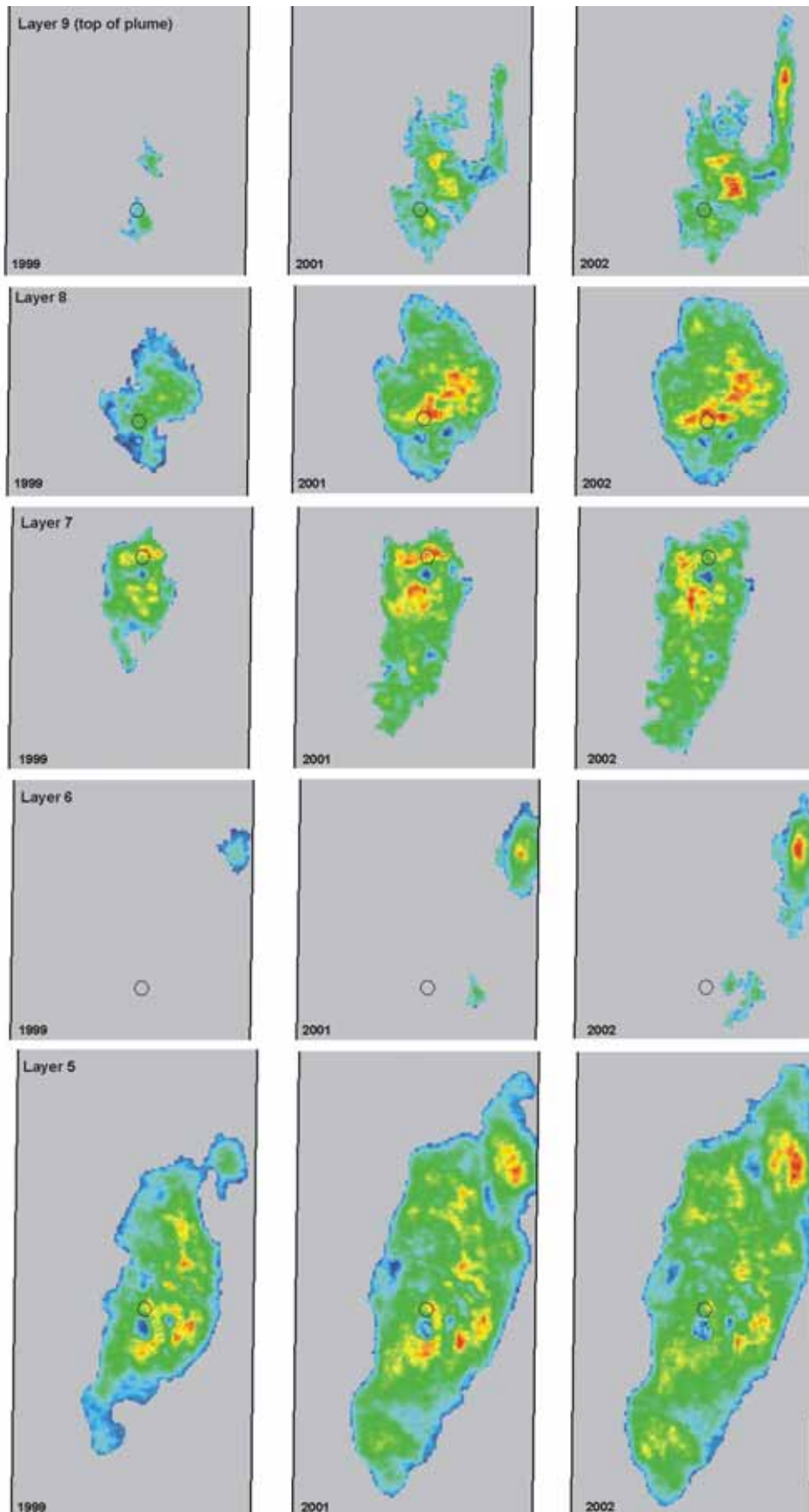


Figure 7.5 Reflection amplitude maps of the upper five layers of the Sleipner plume, showing growth from 1999 to 2002.

In addition to its reflectivity, the plume also gives rise to a prominent velocity pushdown (Figure 7.6) caused by the seismic waves travelling much more slowly through CO₂-saturated rock than through the virgin aquifer. The pushdown anomaly underlies the plume and has a similar elliptical shape to the plume itself. Maximum pushdown values have increased from > 40 ms in 1999 to perhaps >60 ms by 2002.

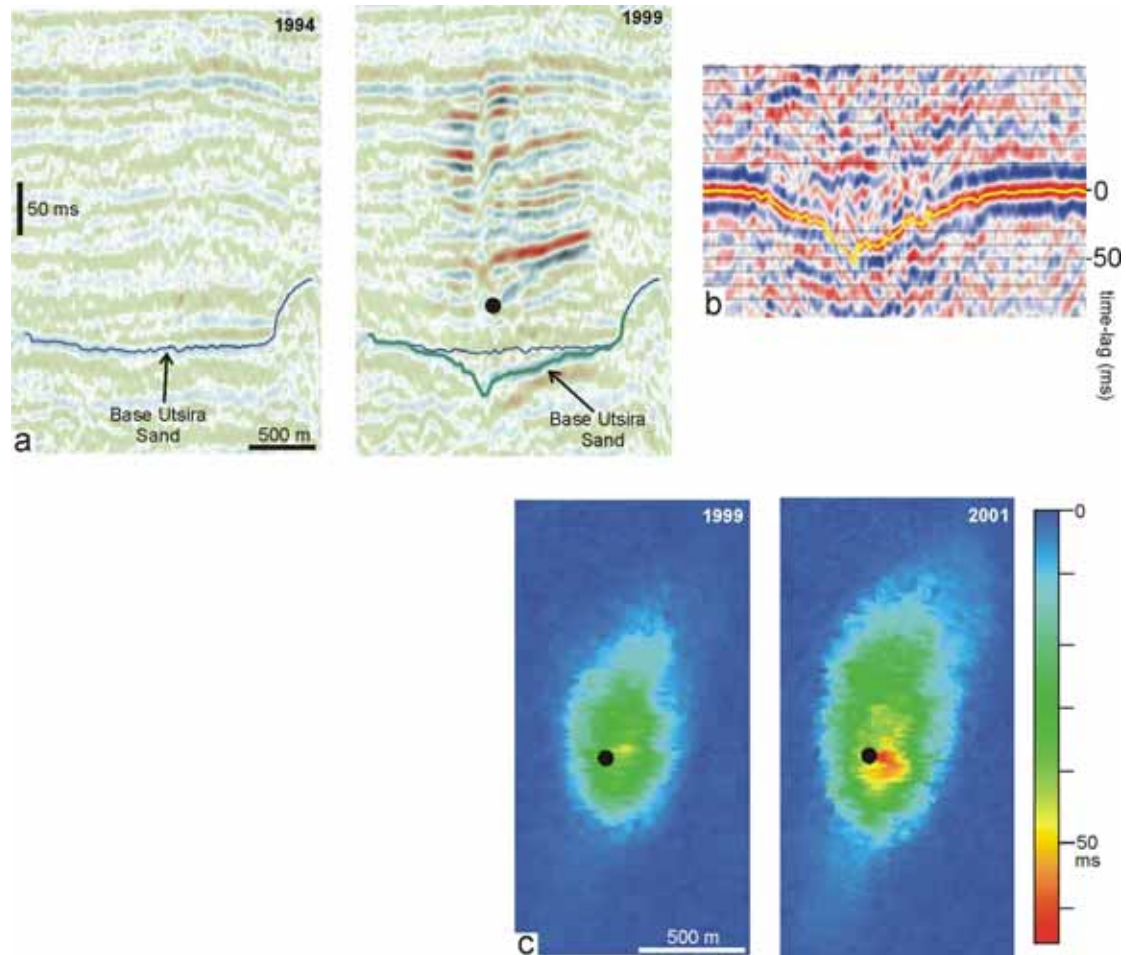


Figure 7.6 Velocity pushdown in the Sleipner plume. a) Inline through the reservoir in 1994 and 1999 showing pushdown of the Base Utsira Sand beneath the plume. b) Cross-correlogram of a reflection window beneath the central part of the 2001 plume. Pick follows the correlation peak and defines the pushdown. c) Pushdown maps in 1999 and 2001. Black disc denotes the CO₂ injection point.

The seismic data indicate that no detectable leakage of CO₂ into the caprock had occurred so far as 2002. Timeslices extracted from the seismic difference cubes (Figure 7.7) show quite random low amplitude noise associated with lack of repeatability of the surveys, but no systematic changes that would be indicative of changing reflectivity (the 2002 dataset which was not precisely matched to the earlier datasets shows different repeatability noise characteristics, consistent with its different acquisition parameters).

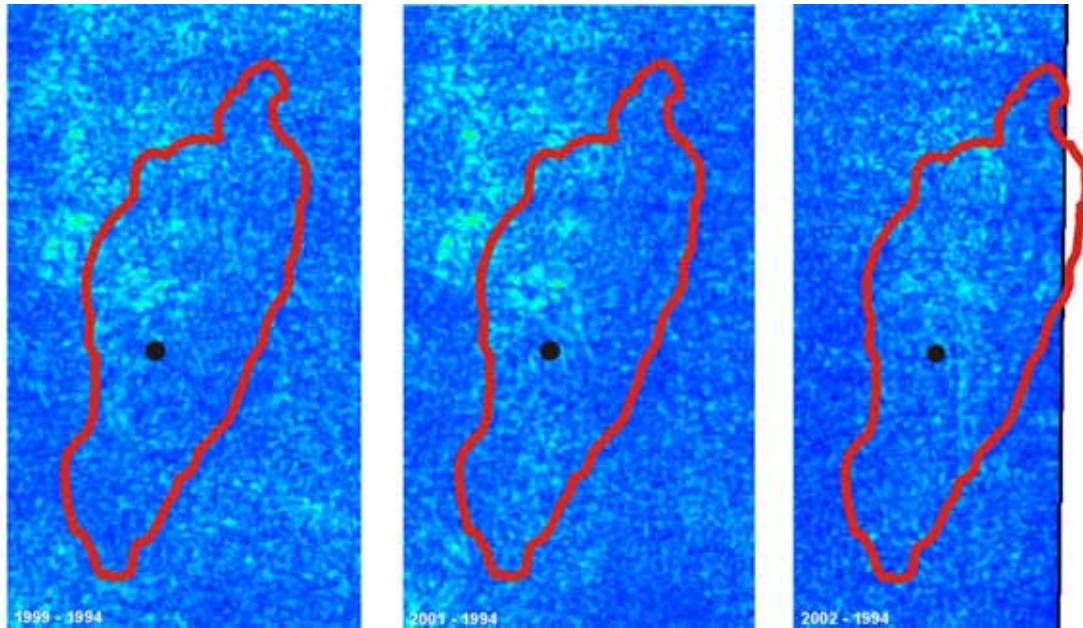


Figure 7.7 Seismic time slices taken from the caprock succession immediately above the Utsira reservoir. Difference signals show no significant changes from 1999 to 2002. Red polygon denotes lateral extent of 2002 plume.

The potential detection capability of the Sleipner data can be illustrated by examining the 1999 plume (Figure 7.8). The topmost part of the plume is marked by two small CO₂ accumulations trapped directly beneath the caprock seal. From the reflection amplitudes, the volumes of the two accumulations can be estimated at 9000 and 11 500 m³ respectively. Other seismic features on the time slice can be attributed to repeatability noise, arising from slight intrinsic mismatches between the 1999 and 1994 (baseline) surveys. It is clear that the level of repeatability noise plays a key role in determining the detectability threshold. Thus for a patch of CO₂ to be identified on the data it must be possible to discriminate between it and the largest noise peaks. Preliminary analysis suggests that accumulations larger than about 4000 m³ should fulfil this criterion. This corresponds to about 1600 tonnes of CO₂ at the top of the reservoir where, depending on the exact temperature and pressure, CO₂ may have a density as low as about 400 kgm⁻³. In the overburden, at about 500 m depth, CO₂ density would be considerably lower with a detection limit of 600 tonnes or less.

It is important to stress the need for caution in this type of analysis. Seismic detectability depends crucially on the nature of the CO₂ accumulation. Small thick accumulations in porous strata would tend to be readily detectable. Conversely, distributed leakage fluxes through low permeability strata may be difficult to detect with conventional seismic techniques. Similarly, leakage along a fault within low permeability rocks would be difficult to detect. Fluxes of CO₂ such as these may well be associated with changes in fluid pressure, in which case shear-wave seismic data is likely to prove useful as a detection tool. Saturations are also uncertain. The mass estimates given above assume quite high CO₂ saturations within the small accumulations; CO₂ at lower saturations can give comparable reflectivity, resulting in even lower detection thresholds.

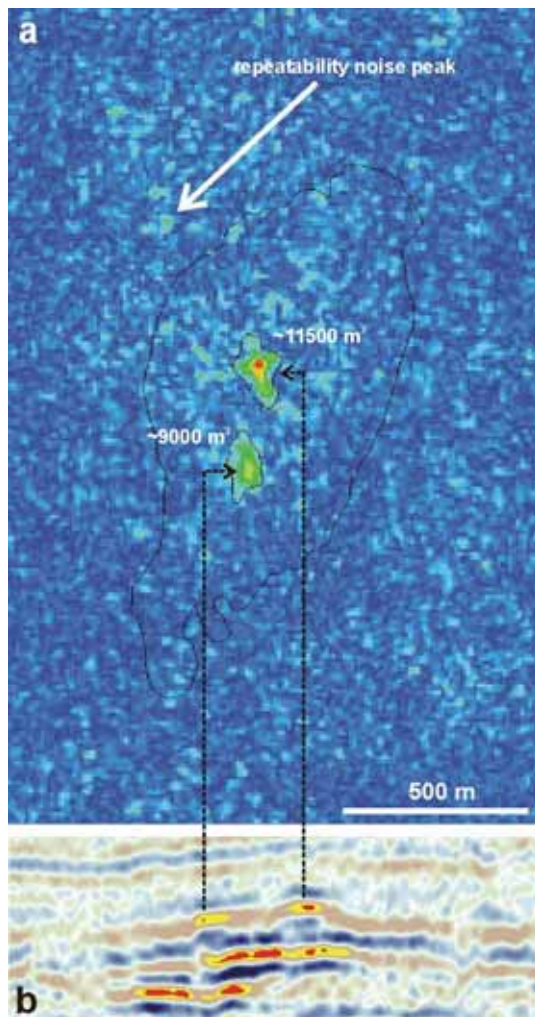


Figure 7.8 Detection limits for small amounts of CO₂ at Sleipner. a) Horizon time-slice map of the 1999–94 difference data showing integrated reflection amplitude in a 20 ms window centred on the top Utsira Sand. Note high amplitudes corresponding to the two small CO₂ accumulations. Note also scattered amplitudes due to repeatability noise. b) Seismic line showing the topmost part of the plume and the two topmost accumulations.

7.2.1.2 Quantitative assessments

Quantitative modelling aimed at verifying the in situ injected mass of CO₂ at Sleipner has utilised both inverse and forward modelling techniques.

Inverse modelling aims to quantify amounts of CO₂ by explicitly matching both the observed layer reflectivity and, simultaneously, the observed velocity pushdown (Chadwick et al., 2005). Because fluid pressures are believed to have changed very little during injection, seismic modelling is based solely on fluid saturation changes. The observed plume reflectivity most likely comprises tuned responses from thin layers of CO₂ whose thickness varies directly with reflection amplitude. Inverse modelling takes as a starting point, thin, high saturation layers of CO₂, mapped according to an amplitude-thickness tuning relationship. This is supported by structural analysis of the topmost CO₂ layer, whose thickness, estimated directly from the top reservoir topography, varies directly with reflection amplitude. In addition, in

order for the modelled CO₂ distributions to produce the observed velocity pushdown, a minor, intra-layer, component of much lower saturation (dispersed) CO₂ is required.

A measured formation temperature of 36 C is available for the Utsira reservoir, but this is poorly constrained and regional temperature patterns suggest that the reservoir may be up to 10 C warmer. At these higher temperatures, CO₂ would have markedly different physical properties, with a significantly lower density (Figure 3.1) and bulk modulus. The principal effect of lowering density would be a correspondingly larger in situ volume of CO₂, impacting crucially on any quantitative analysis. A secondary, but still important, effect of higher reservoir temperatures would be to give significantly lower seismic velocities.

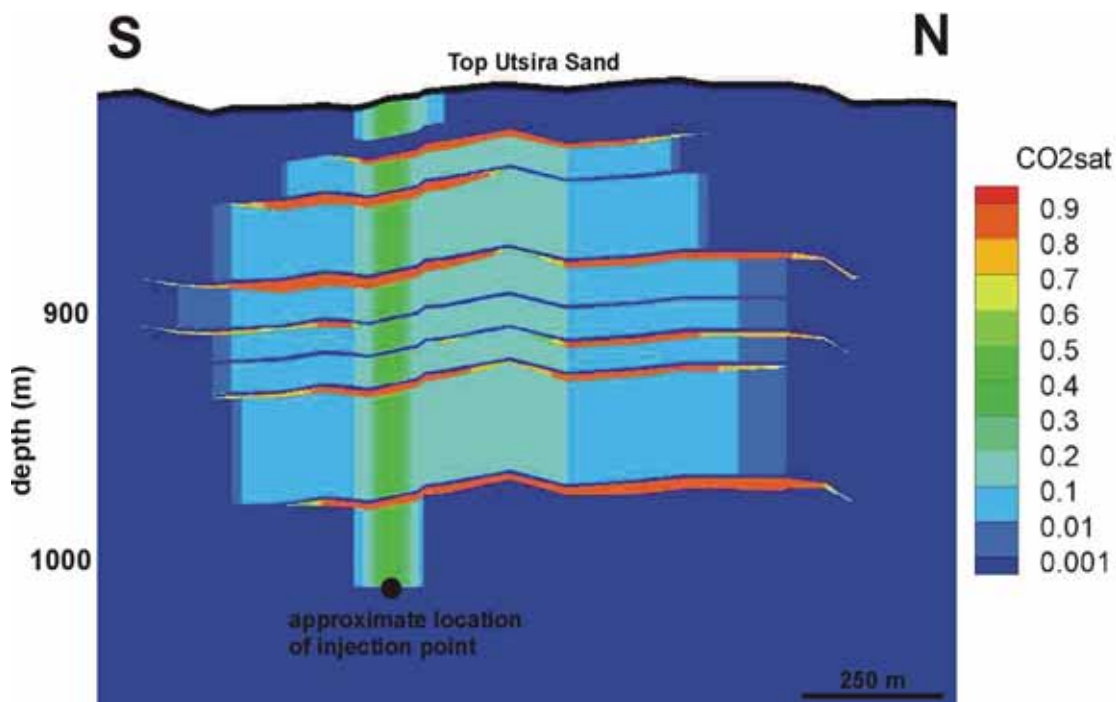


Figure 7.9 Cross-section through the 45°C (higher temperature) inverse model of the Sleipner plume with CO₂ distributions derived from analysis of reflection amplitudes and velocity pushdown.

Inverse models of CO₂ distribution in the 1999 plume have been generated, based on both the measured temperature, and a possible higher temperature scenario, the 36°C and 45°C models respectively (Figure 7.9). The distribution of CO₂ in both models is consistent with the known injected mass (allowing for parameter uncertainty) and both models can replicate the observed plume reflectivity and the observed velocity pushdown (Figure 7.10). However, the higher temperature model requires that the dispersed (low saturation) component of CO₂ has significantly higher seismic velocities than is required for the lower temperature model. This implies that the dispersed CO₂ has a somewhat patchy distribution, with heterogeneous mixing of the CO₂ and water phases (Sengupta and Mavko, 2003).

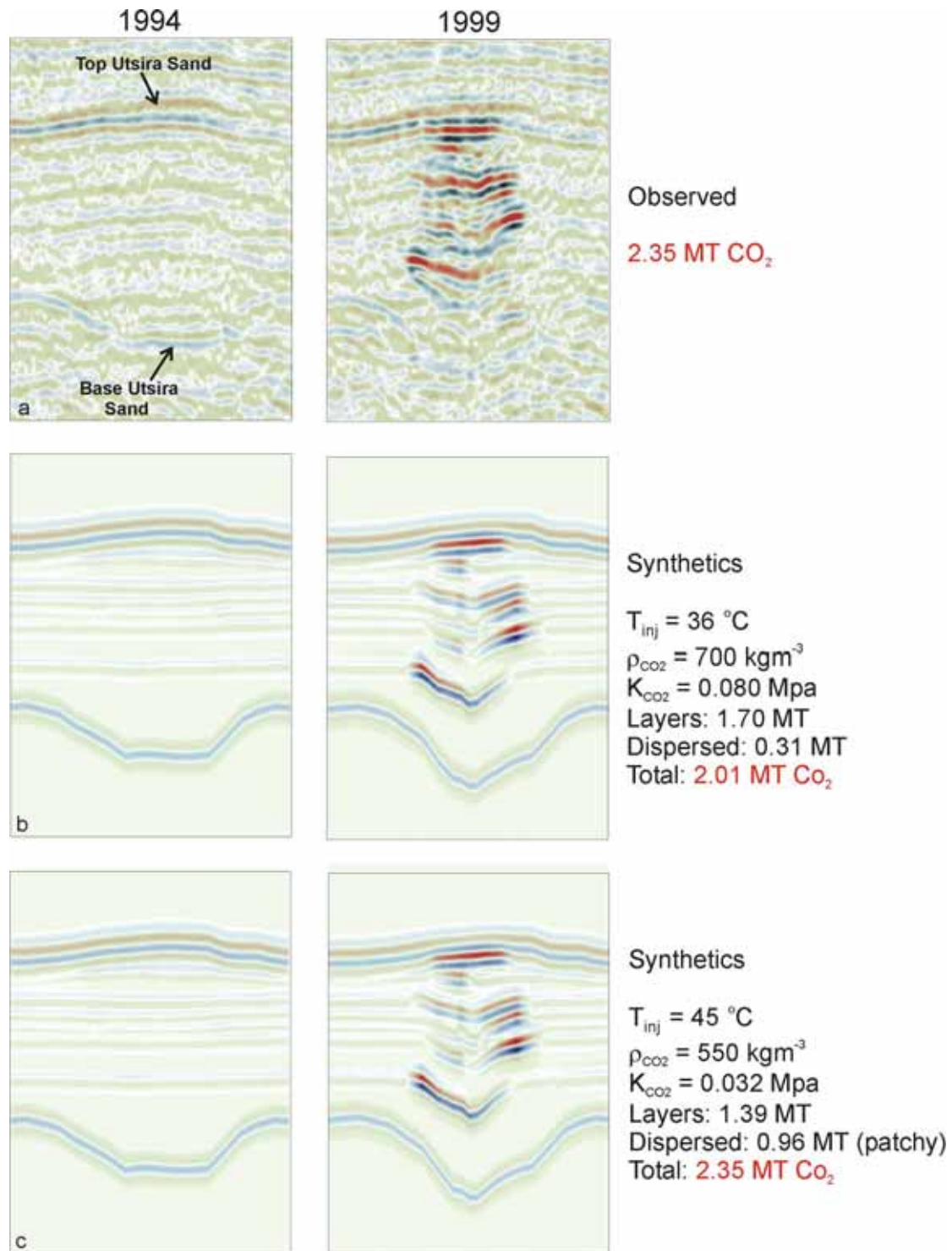


Figure 7.10 Inverse modelling of the 1999 plume and derived synthetic seismics. a) Observed data 1994 and 1999. b) Synthetic seismics 1994 and 1999 assuming lower temperature reservoir scenario with fine-scale mixing throughout. c) Synthetic seismics 1994 and 1999 assuming higher temperature reservoir scenario with patchy mixing in the intra-layer dispersed component of CO₂.

Patchy mixing on the scale of tens of centimetres gives rise to a velocity–saturation relationship (the Hills average) that is markedly different to that which arises from homogeneous or uniform mixing of the water and CO₂ phases (the Reuss average). In fact, in order to produce the observed velocity pushdown, the higher temperature inverse model requires dispersed CO₂ which has a velocity - saturation relationship

intermediate between the Reuss and Hills bounds (Figure 7.11), implying partial, but not wholly patchy mixing of the fluid phases.

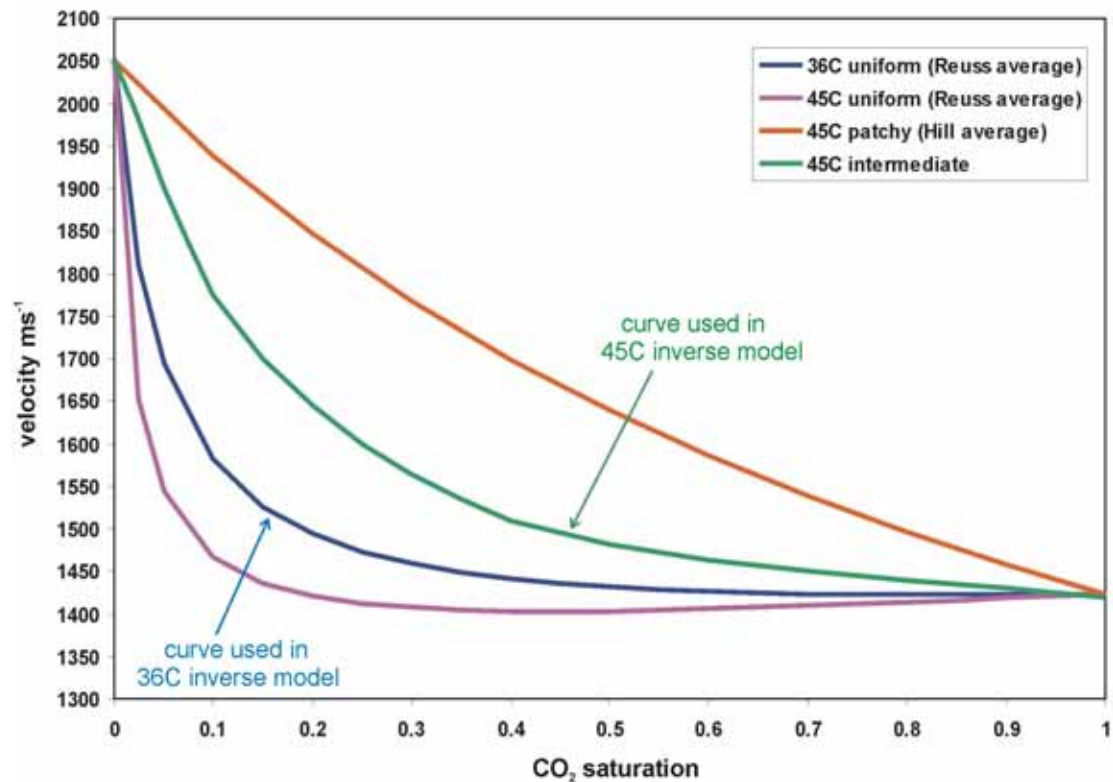


Figure 7.11 Velocity saturation plots for uniform mixing in the lower reservoir temperature scenario, and for uniform, intermediate and patchy mixing in the higher reservoir temperature scenario.

This highlights a key uncertainty in seismic quantification: the velocity behaviour of the CO₂–water–rock system, which is heavily dependent on the (poorly constrained) nature of small-scale mixing processes between the fluid phases. A limitation of the current inverse models is the fact that the CO₂ saturation model is matched to the total velocity pushdown observed beneath the base of the plume i.e vertically we integrate the total pushdown effect of the CO₂ column. Because of this, it is possible to map lateral changes in saturation in the dispersed CO₂ component, but not vertical changes. To accomplish the latter it is necessary to map the buildup of velocity pushdown within the plume itself. This is very challenging, because the pre-injection configuration of the mudstone layers is not known. Software developed within SACS has been used to map in 3D the velocity pushdown within the plume but so far this has been implemented only on incremental pushdown between repeat monitor surveys (see below).

In addition to the inverse modelling, seismic forward modelling, based on history-matched reservoir flow simulations of the CO₂ plume has been carried out (Arts et al., 2004a). A fundamental difficulty with the flow simulations is the fact that the structural geometries of the thin intra-reservoir mudstones that trap the observed CO₂ layers are not well constrained. The mudstones are effectively invisible on the 1994 baseline data and their position can only be inferred on the repeat surveys once they

are illuminated by the underlying CO₂. In particular, velocity pushdown within the plume obscures structural information, so assumptions have to be made on the shape, lateral extent and continuity of the mudstones for the reservoir simulation model. The flow simulations honour the layers of CO₂ trapped at the different depth levels and synthetic seismograms created from them produce a reasonable reflectivity match to the observed data (Figure 7.12).

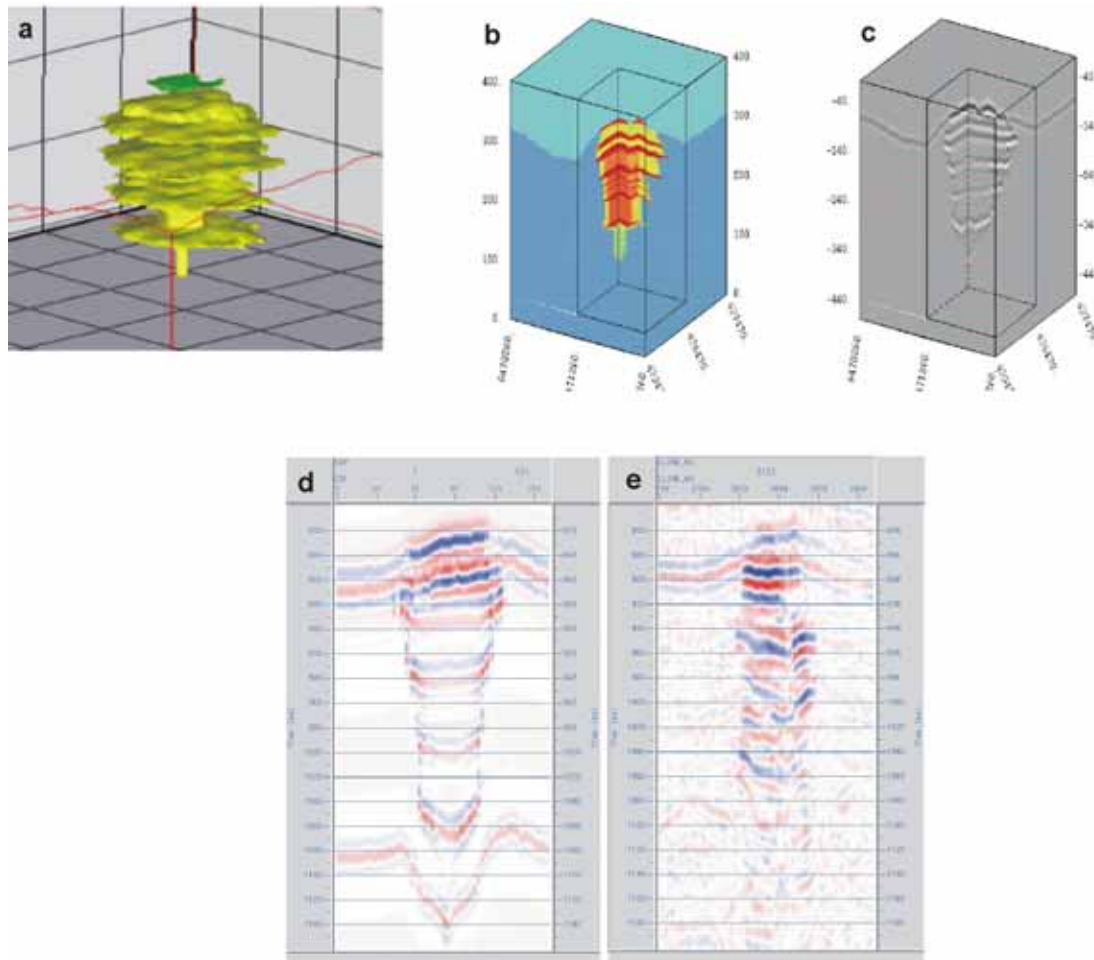


Figure 7.12 Forward modelling of the Sleipner CO₂ plume. a) 3D flow simulation of the 2001 plume. b) 3D seismic impedance model derived from the reservoir simulation of the 2001 plume. c) 3D seismic cube derived from (b). d) 2D line taken from the synthetic seismic cube. e) 2D line from the observed 2001 seismic cube.

Matching the observed velocity pushdown to the synthetic pushdown from the flow simulation raises the same issues regarding the seismic properties of the intra-layer dispersed CO₂, as did the inverse modelling. Forward modelling supports the intermediate mixing hypothesis, whereby the observed velocity pushdown lies between synthetic velocity pushdowns computed using the Hills (patchy mixing) and Reuss (uniform-mixing) averages (Figure 7.13).

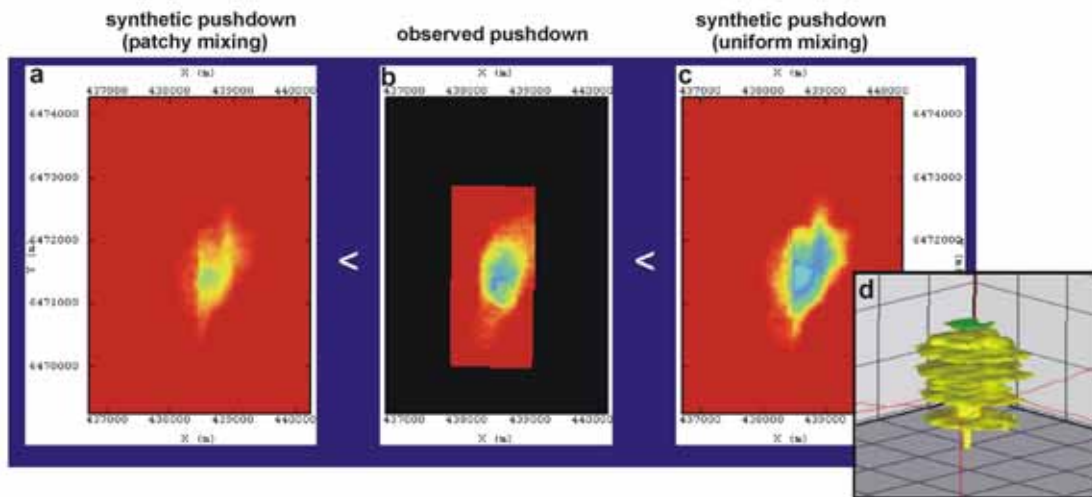


Figure 7.13 Modelling velocity pushdown at Sleipner. a) Synthetic pushdown from the 2001 flow simulation assuming patchy mixing. b) Observed velocity pushdown in 2001. c) Synthetic pushdown from the 2001 simulation assuming fine-scale mixing. d) 3D view of the 2001 flow model.

Because of these uncertainties, a unique saturation model that matches the observed seismic and the known injected amount, has not been obtained. Work on reducing modelling uncertainty is ongoing.

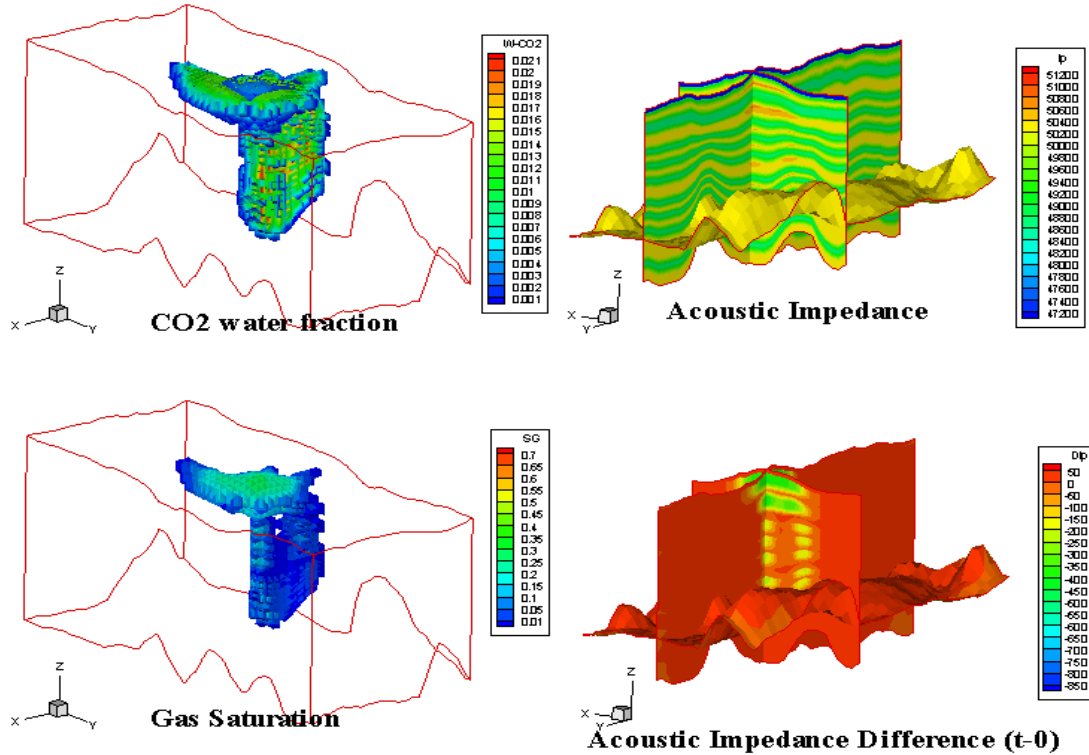


Figure 7.14 Automated modelling workflow (for 7 years of CO₂ injection) showing CO₂ mass fraction dissolved in water, gas saturation, acoustic impedance and its change.

A fully automated workflow involving 3D flow simulation and acoustic impedance calculation has been tested on a storage scenario with Utsira-like properties. Using a simple Gassmann model, with simplified petrophysical properties for the sand and mudstone layers, enables simulated CO₂ distributions to be expressed in terms of acoustic impedance (Figure 7.14). It is noteworthy that although the lower six metres of the caprock showed no signs of supercritical CO₂ entry over the 25-year injection simulation (Figure 7.15), due to diffusion of CO₂ in water phase, some dissolved CO₂ was computed in the overburden. The dissolved CO₂ did not alter the acoustic impedance of the caprock however.

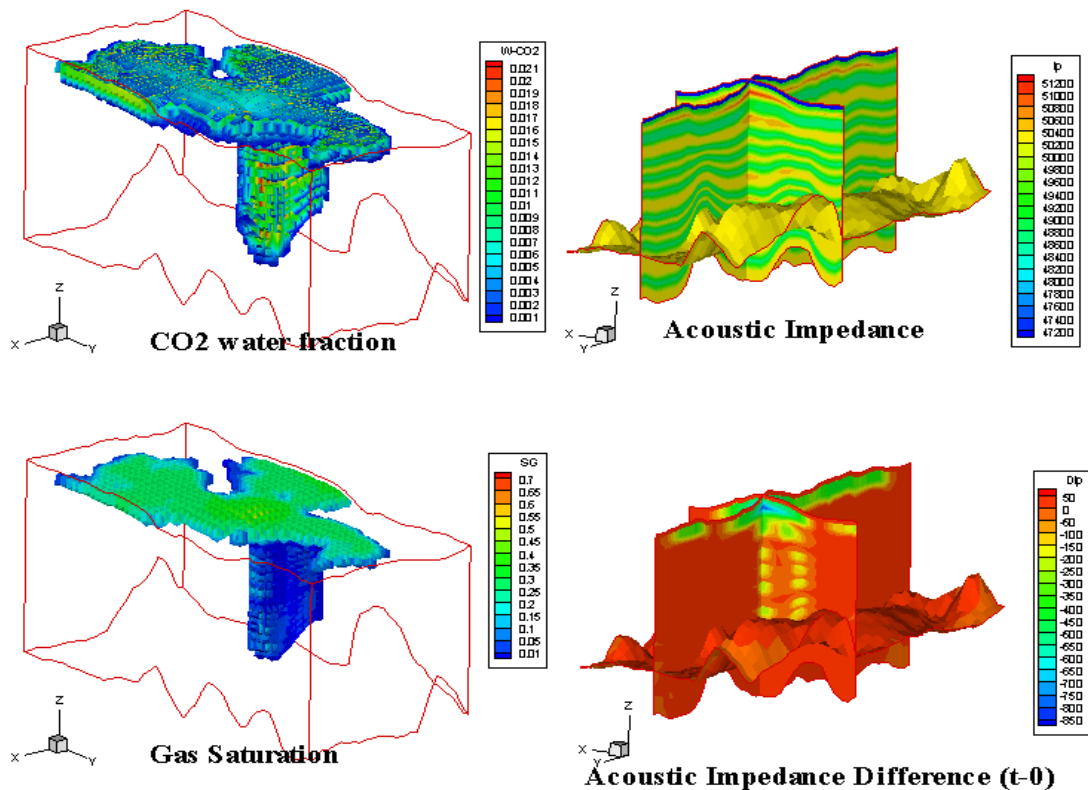


Figure 7.15 Automated modelling workflow (for 25 years of CO₂ injection) showing the CO₂ mass fraction dissolved in water, gas saturation, acoustic impedance and its change.

7.2.1.3 Other analysis

Much of the interpretation and modelling of the time-lapse seismic has concentrated on quite conventional interpretation and modelling of the post-stack datasets. In addition to this, a considerable amount of more advanced and novel analysis has been carried out, both pre- and post-stack.

Pre-stack trace inversion

Full details of the inversion methodology are given in Østmo et al. (2004). Suffice to say here that a target-oriented pre-stack inversion scheme was adopted, whereby the subsurface was divided into an upper macro model and a lower, multilayer target zone. Inversion was carried out on $-p$ transformed CMP gathers using a modified axi-symmetrical 3D radon transform. A unique feature of the method is the possibility

of accounting for multiples in the seismic data (known to be an issue at Sleipner), so as to avoid inverting sea-bottom multiple reflections into features in the derived volumes.

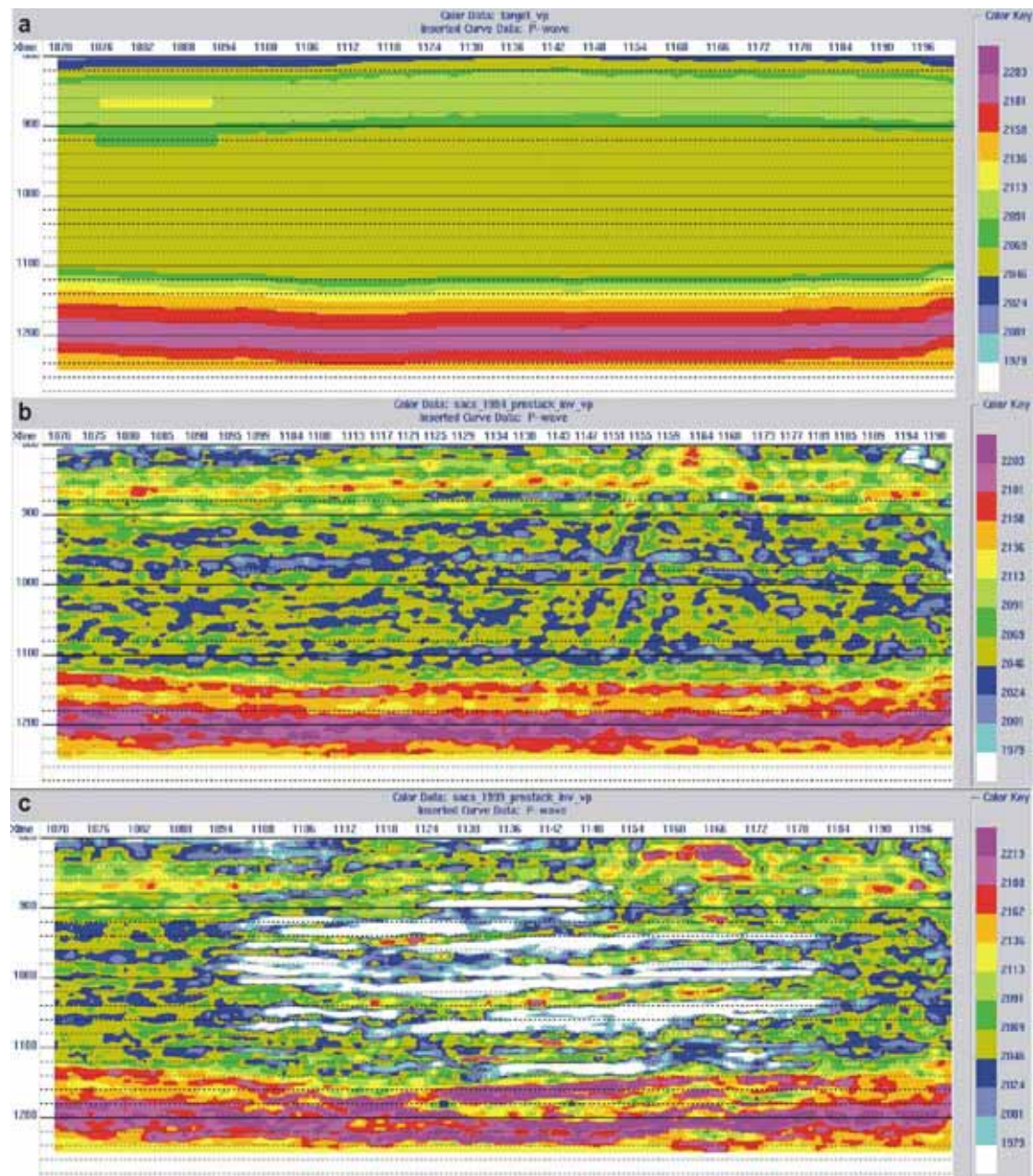


Figure 7.16 Pre-stack inversion for P-wave velocity. a) Initial model of Utsira reservoir. b) V_p (ms^{-1}) along an inline from the 1994 parameter cube. c) V_p (ms^{-1}) along an inline from the 1999 parameter cube.

Analysis was restricted to a small sub-area covering about 2 km^2 around the CO_2 plume. V_p , V_p/V_s ratio and density were computed for the 1994 and 1999 subset cubes. An inline from the middle of the inverted V_p cube (Figure 7.16) clearly shows the CO_2 layers on the 1999 dataset as low velocity lenses. Direct comparison with the observed post-stack data (Figure 7.17) shows how the inverted V_p anomalies correlate closely with the main reflection events.

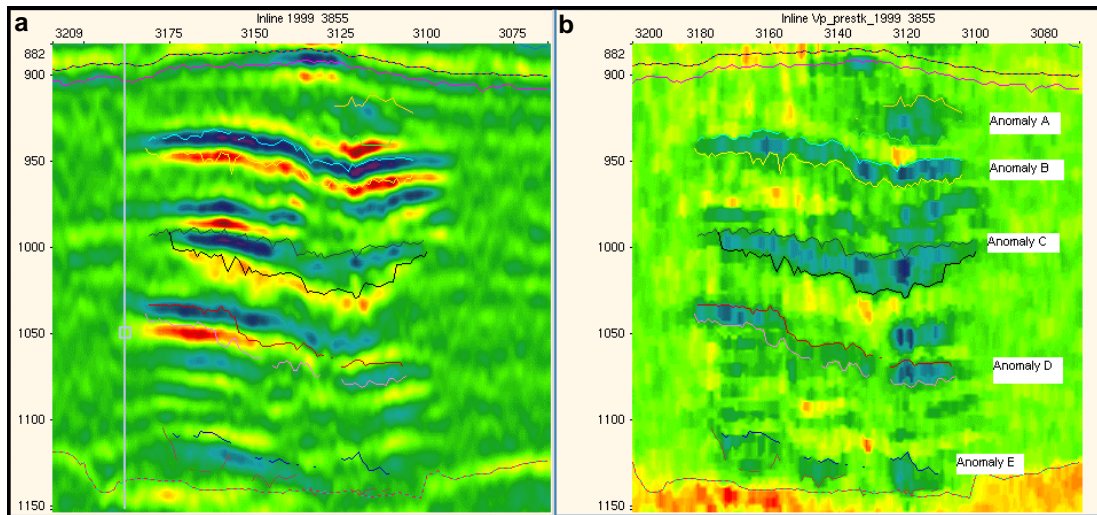


Figure 7.17 Section through the 1999 inversion cube. a) Conventional reflection section. b) Inverted Vp with polygons outlining Vp anomalies. The top and base of each polygon roughly matches the trough and peak respectively of a corresponding tuning wavelet.

However it is also notable that the thickness of the anomalies tends to track the peak to trough separation, the limit of seismic resolution. This despite the fact that the main reflections are thought to be interference composites arising from CO₂ layers only a few metres thick ($< \lambda/4$ or ~ 8 m). It is clear that the inversion is not able to account for this sub-resolution reflectivity. A corollary of overestimation of layer thickness is that the derived values for Vp are typically around 1950 m/s, compared with the approximate 1400–1500 ms⁻¹ range predicted by the Gassmann relationships (Figure 7.11).

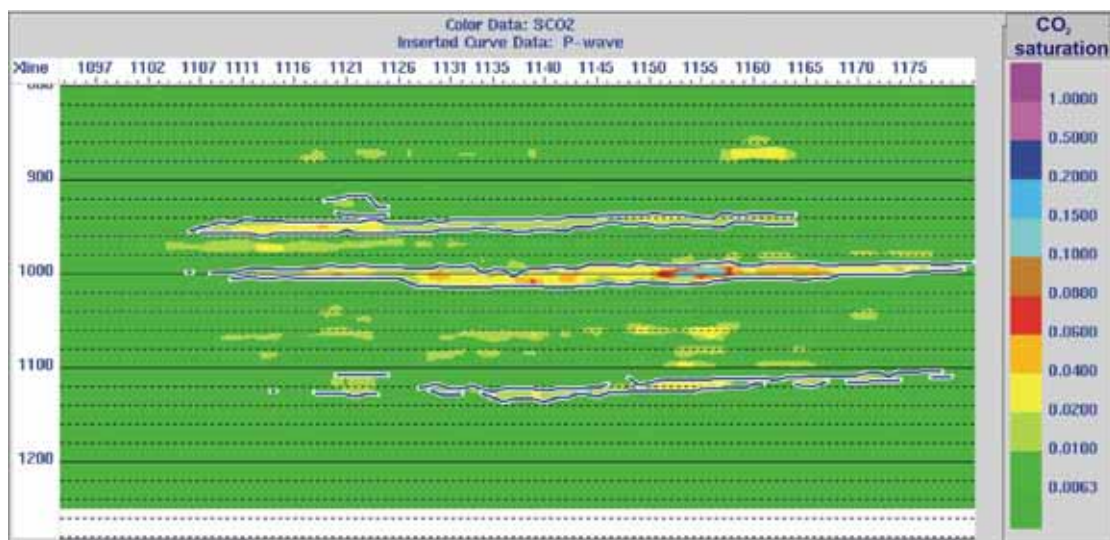


Figure 7.18 Section through the 1999 inversion cube showing CO₂ saturations derived from Vp.

The inverted Vp and inverted density cubes were used with the Gassmann relationships to derive the bulk modulus of the saturating fluid, and from this, using

the Reuss (fine-scale mixing) average, CO₂ saturations were calculated (Figure 7.18). Values of S_{CO₂} in the reflective layers are typically <0.1. These are much lower than saturations predicted from other methods, such as inverse modelling of the seismic amplitudes (Figure 7.9) and reservoir flow simulations (see below), which are typically > 0.8. This is a direct consequence of inverted V_p values being insufficiently low, exacerbated by the Reuss averaging which requires only very low CO₂ saturations to produce significant velocity reduction.

In summary, the pre-stack inversion was not able to properly resolve layers thinner than the seismic resolution. Because of this, inverted impedances and P-wave velocities will be smaller than in reality and the CO₂-rich layers consequently too thick.

Pre-stack depth migration

Inspection of CMP gathers on the Sleipner data shows a significant degree of incoherence with laterally variable timeshifts causing significantly non-hyperbolic moveout. This is mostly due to severe lateral velocity changes within the CO₂ plume.

Pre-stack depth migration (PSDM) handles lateral velocity variations much better than conventional time processing techniques, so a 3D PSDM was applied to the data. Key to the success of any PSDM is the accuracy of the velocity model. For the Sleipner data the velocity model was built via reflection tomography, with optimisation based on obtaining flat events on the common image point (CIP) gathers (Figure 7.19).

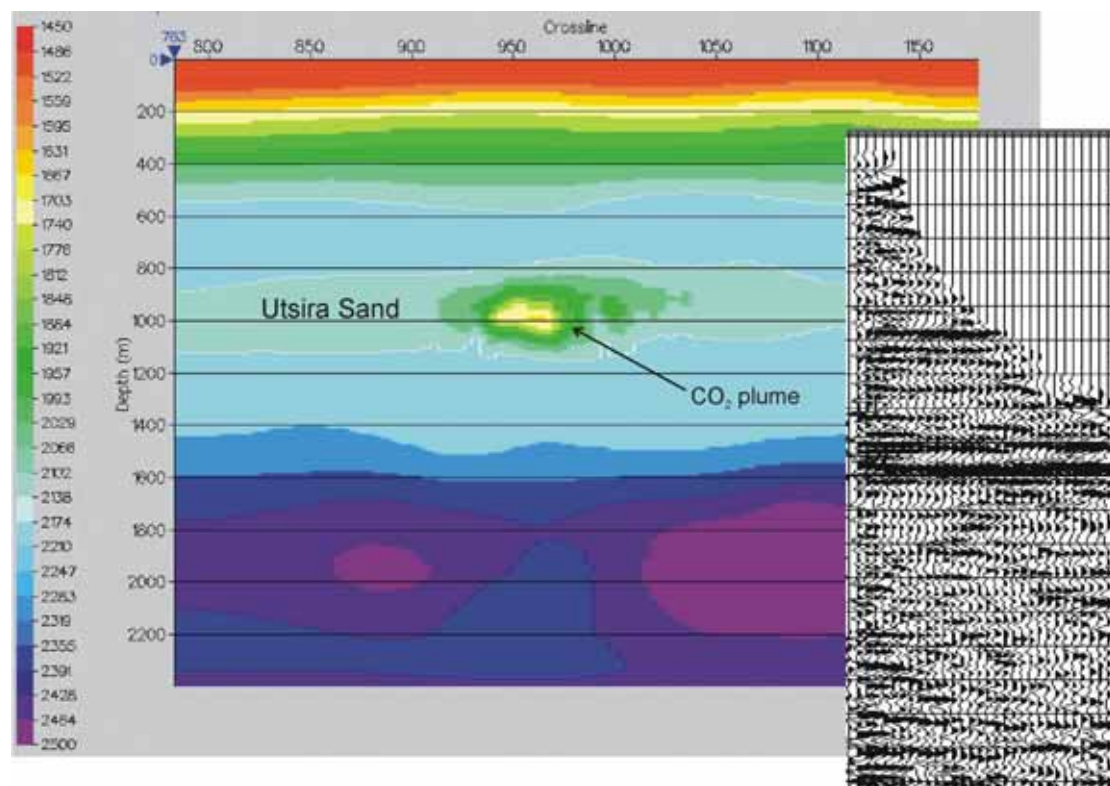


Figure 7.19 Smoothed velocity tomogram used for the prestack depth migration. Note lower velocity layer corresponding to Utsira Sand, and much lower velocity zone corresponding to the CO₂ plume. Inset shows CIP gather with flat events obtained with these velocities.

The Sleipner plume presents a particularly challenging imaging problem due its severe velocity variations, both laterally and vertically. In particular the thin, very low velocity CO₂ - rich layers cannot be explicitly resolved by the reflection tomography. The velocity model utilised therefore was a smoothed simplification of the real situation. Nevertheless, the fact that events on the CIP gathers can be satisfactorily flattened (Figure 7.19) suggests that the velocity model performed acceptably.

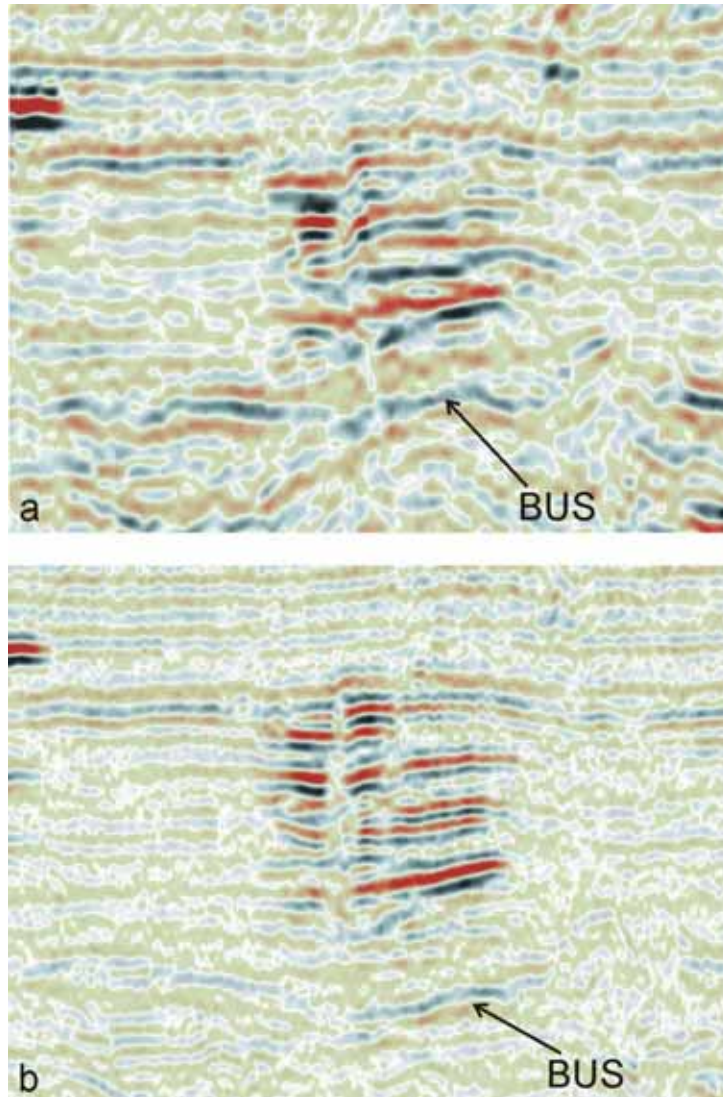


Figure 7.20 Inline through 1999 datacube. a) Pre-stack depth migration. b) Normal post-stack time migration. Velocity pushdown, evident on time section is reduced on the PSDM, but distortion remains.

Results from the PSDM (Figure 7.20) are satisfactory, with reduction of velocity pushdown in the axial parts of the plume and also beneath it. Overall though, imaging is not improved significantly. On the 1994 baseline dataset, which has no plume-induced velocity effects, the base of the Utsira Sand is quite flat (Figure 7.6), indicating that it is also quite flat in depth. It nevertheless shows significant distortion on the PSDM, indicating that significant residual velocity inaccuracies are present. This difficulty in eliminating velocity errors is probably the key limitation on image

quality. Definition of a sufficiently accurate velocity model remains a challenge. It may be that tomographic modelling with manually imposed constraints (such as very low velocity layers) would yield further improvements.

Time-shift analysis

A key observed diagnostic property of the time-lapse datasets is velocity pushdown. Measurements of total pushdown beneath the plume have been utilised in quantitative analysis (see above), but the CO₂ saturation–velocity relationship remains a major uncertainty. Measurement of the 3D buildup of velocity pushdown within the plume itself could yield greater insights into velocity distributions and how these vary with respect to, and in between, the reflective layers. This could lead to a better understanding of how velocity varies with saturation.

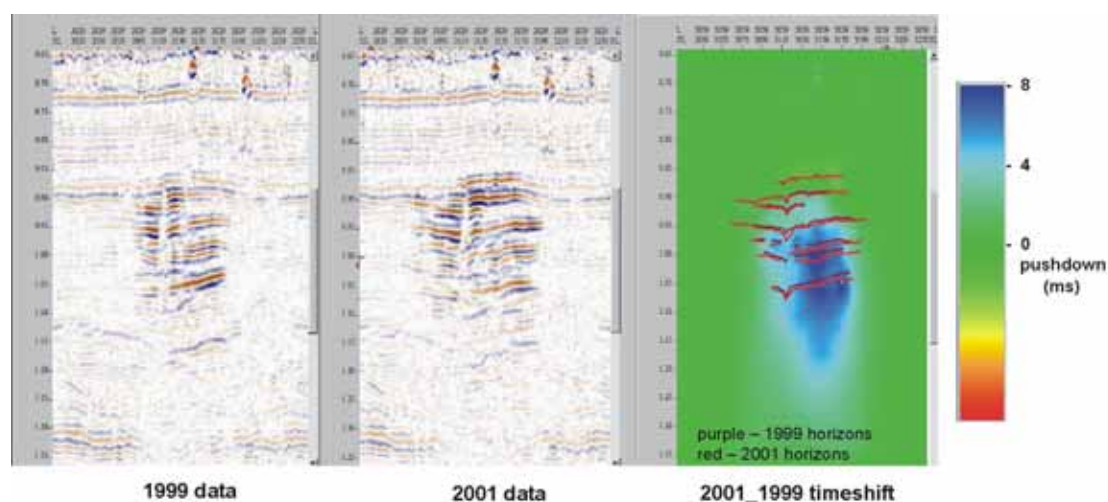


Figure 7.21 Inline from 1999 and 2001 and corresponding NRM time shifts (pushdown).

A 3D automatic estimation of the incremental pushdown from 1999 to 2001 was performed using non-rigid matching (NRM). The output from this technique is a 3D cube of velocity pushdown which can be used to better constrain velocities within the plume. A 2D section (inline) through the cube (Figure 7.21) shows that pushdown increases downwards through the plume to peak at about the level of the lowermost reflector. Comparison of measured pushdown at Layer 5 (the largest CO₂ layer in the plume), shows good correlation between the NRM-derived values and pushdown obtained by subtracting two-way travel times for the 2001 and 1999 horizon picks (Figure 7.22).

The NRM-derived pushdown field is smoother than that from the manual interpretation, but areas of greatest pushdown match well between the two maps. The NRM method seems to breakdown beneath the plume however, where reflectivity is low. One obvious drawback of the method is that, so far, it has not been able to derive the absolute pushdown relative to the pre-injection baseline. This is because it relies on comparing and matching waveforms from successive surveys and the very weak intra-reservoir reflectivity on the 1994 survey cannot be correlated with the much brighter post-injection reflections. Pushdown estimates are limited therefore to incremental values derived from the post-injection surveys.

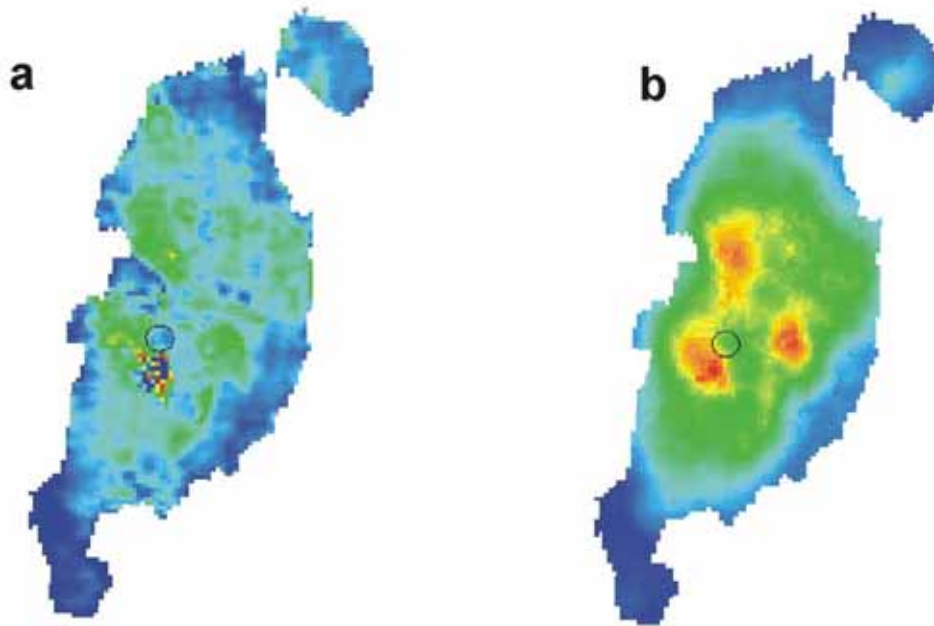


Figure 7.22 Incremental pushdown from 1999 to 2001 at the level of Layer 5.
a) Pushdown from manual interpretation of Layer 5. b) NRM calculated timeshifts.
Note correspondence of high pushdown areas.

Reflection strength analysis and advanced display options

In order to improve plume visualisation, and to introduce a measure of repeatability or objectivity, a number of alternative display options have been evaluated. The 1999 plume comprises a number of strong reflectors located above the injection point. These may be identified by traditional means such as wiggle trace or colour-amplitude displays (Figure 7.23a).

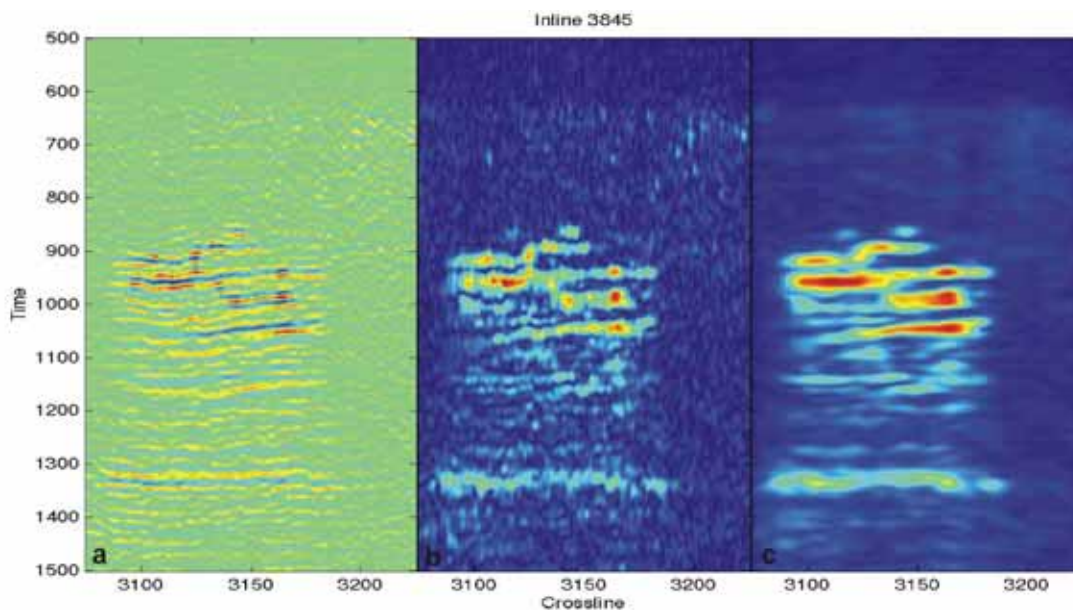


Figure 7.23 Advanced seismic amplitude displays. a) Standard colour-amplitude display. b) Amplitude envelope. c) Amplitude envelope with Gaussian spatial filter.

Alternatively the amplitude envelope of the seismic traces can be calculated (Figure 7.23b). This effectively shows the instantaneous or underlying amplitude of the signal, irrespective of phase. In order to reduce noise in the image, the envelope cube can be filtered in the horizontal directions using a Gaussian low pass filter with pass band equal to three samples in both directions (Figure 7.23c). The filtered envelope cube reveals rather clearly the different reflective layers in the seismic.

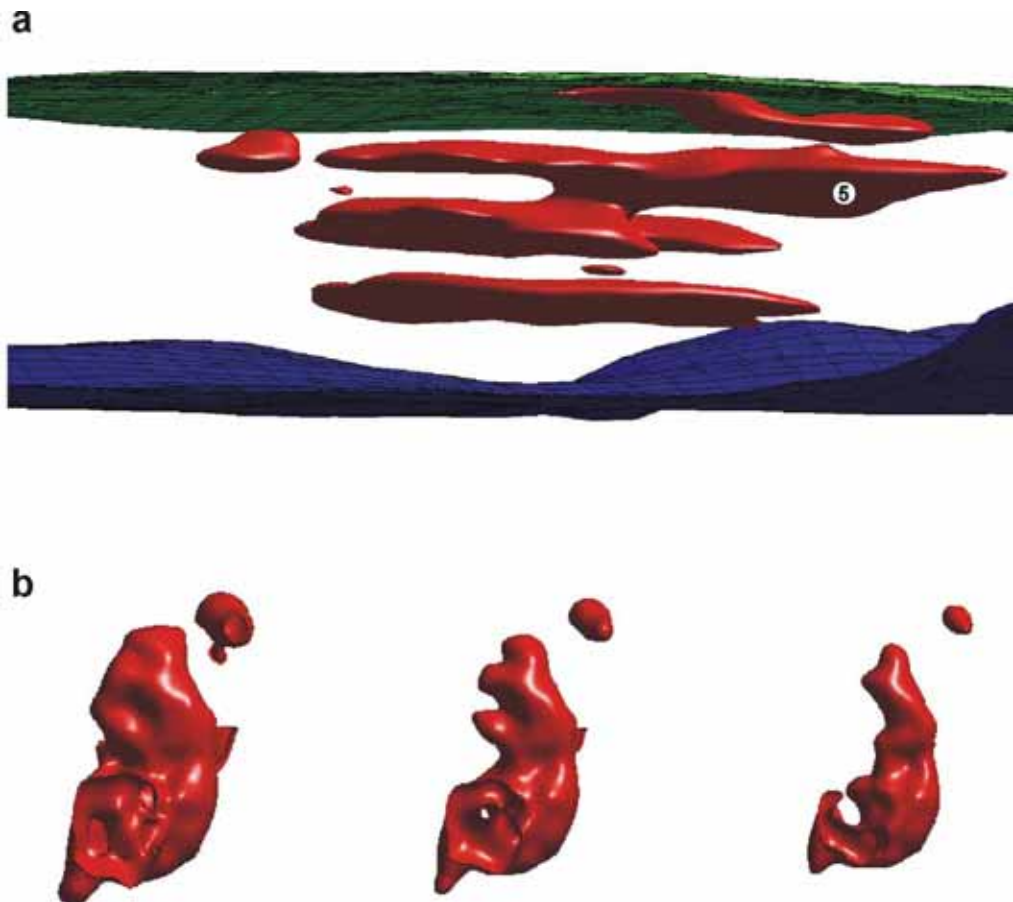


Figure 7.24 3D amplitude threshold displays of the 1999 Sleipner plume. a) Plume viewed from the side with Layer 5 labelled. b) Layer 5 viewed from above with different amplitude thresholds.

A semi-quantitative display can be based on an amplitude threshold. By normalising reflection strengths to some datum (for example initial reflection amplitude at top Utsira Sand), the envelope cube can be tuned to express changes in reflection strength caused by the CO₂. Setting the display threshold to a specific value of reflection strength can provide an impression of the spatial distribution of CO₂. A 3D iso-surface plot, corresponding to an increase in reflectivity by a factor of three (Figure 7.24a), clearly shows the layered structure of the seismic signal. The nature of the estimated CO₂ distribution depends on the value of the displayed threshold. iso-surface. This is illustrated by images of the largest individual CO₂ layer, corresponding to Layer 5 in the formal interpretation (Figure 7.5), which changes in extent depending on the selected display threshold (Figure 7.24b). Current uncertainty with regard to the relationship between increased reflectivity and CO₂ saturation renders the method qualitative rather than truly quantitative. Nevertheless, this type of

approach can complement careful manual interpretation, in particular by introducing an element of repeatability into the process.

AVO analysis and elastic inversion

McKenna (2004) performed a detailed pre-stack data analysis on the 1994 and the 1999 seismic datasets. He used a model-based seismic inversion to derive impedance data from the baseline pre-stack amplitude data. Synthetic P- and S-impedance models were generated using the interpreted horizons and the wireline logs recorded in the injection well prior to CO₂ injection. An estimate of P-wave reflectivity was derived from intercept data and S-wave reflectivity was estimated from gradient data. A statistical zero-phase wavelet extracted from the P- and S-wave reflectivity stacks was used in the inversion process. The resultant P- and S-impedance data were used to calculate the ΔV_P and ΔV_S attributes proposed by Goodway et al. (1998). Low values of these attributes have been associated with zones in the reservoir of lower porosity, and by implication, lower permeability. The interpretation remains speculative however with the postulated effects being very equivocal.

McKenna also conducted AVO analysis on the 1994 and 1999 pre-stack seismic data with the aim of estimating the state of phase of the CO₂. The analysis was limited to incident angles less than 30° to minimise the effects of seismic anisotropy. Angles of incidence for both datasets were calculated using the 1994 stacking velocities. The conclusion was that an accurate estimation of the CO₂ state-of-phase could not be achieved using the 1999 seismic data, since the analysis is hampered by tuning effects and by amplitude attenuation when the seismic signal propagates through numerous thin layers of CO₂.

Analysis of velocity anisotropy

McKenna (2004) investigated the effect of velocity anisotropy. He suggested two types of anisotropy were present at Sleipner:

Intrinsic anisotropy present in the overlying sealing Nordland shales due to the horizontal grain alignments.

Anisotropy in the Utsira Sand induced by the CO₂ injection due to the CO₂ spreading in thin low velocity layers with respect to the relatively high background velocity of the brine saturated Utsira Sand.

A comparison between the P-wave sonic log recorded in the near horizontal CO₂ injection well and the P-wave sonic logs recorded in two vertical production wells located nearby shows the horizontal P-wave velocity of the intra-Utsira mudstone layers and the overlying Nordland Shale sequence to be around 10% faster than the vertical P-wave velocity. This can significantly affect imaging below the Nordland Shale, especially when using long offset data.

By contrast, the initial P-wave anisotropy (before injection) of the Utsira Sand appears to be negligible. The elastic contrast between shale and sand will increase when the sand becomes saturated with CO₂ (after injection). A sequence of thin layers with highly contrasting elastic properties is expected to considerably increase anisotropy (vertical transverse isotropy or VTI) in the reservoir. The control on CO₂ induced anisotropy in the reservoir is whether the scale of the layering (comprising

low velocity CO₂ saturated layers typically < 8 m thick and high velocity brine saturated layers typically >10 m thick) is fine enough with respect to the seismic wavelength (typically ~ 50 m). As a rule of thumb, effective medium theory requires seismic wavelength to be a factor of 10 greater than the layering scale—a criterion that would not seem to be fulfilled in the Sleipner plume.

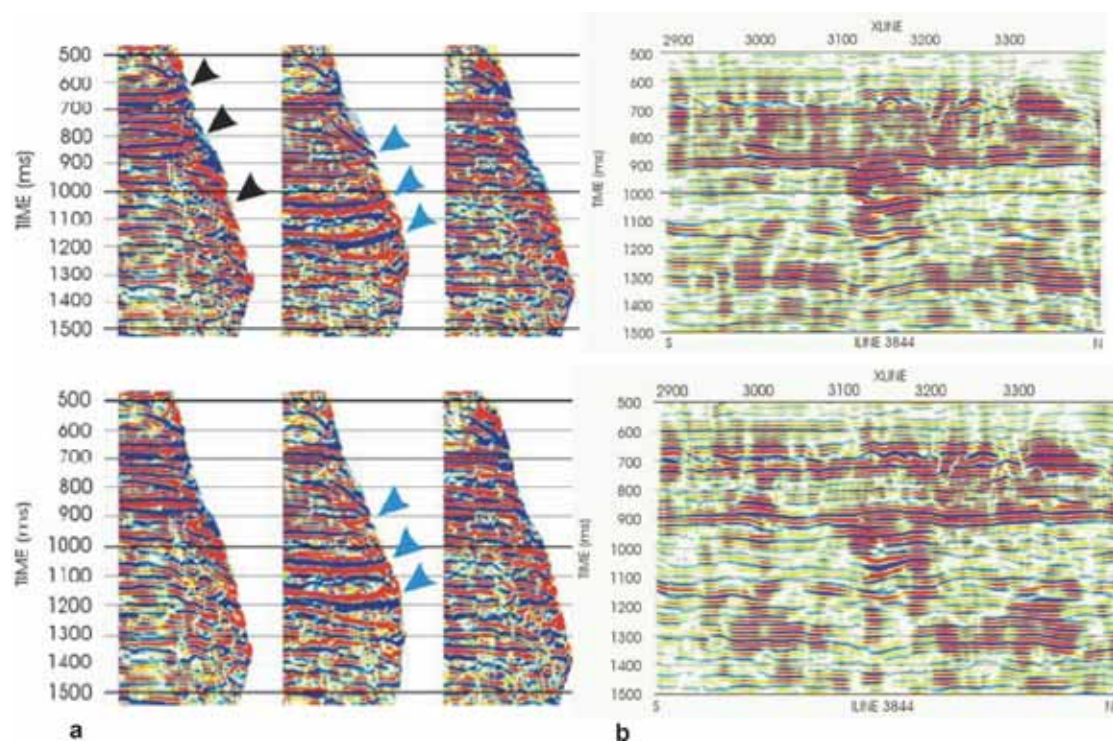


Figure 7.25 Anisotropic stacking. a) CMP gathers from the 1999 dataset with isotropic NMO applied (top) and anisotropic NMO applied (bottom). Note how the pull-ups at far offsets (black arrows) are reduced by the time-variant fourth order anisotropic NMO correction. The central gather is from within the CO₂ plume and anisotropic NMO shows marked reduction of far-offset pull-ups (blue arrows). From KcKenna (2004).

To investigate the hypothesis, 4D anisotropic velocity analysis was conducted on the 1994 and 1999 pre-stack seismic data. Initially, isotropic NMO velocities were picked on short-offset gathers for the pre-injection (1994) and post-injection (1999) seismic data. A large decrease in stacking velocity, of the order of 500 ms⁻¹, was clearly observed in the Utsira Sand after CO₂ injection. After the application of isotropic velocities, the familiar hockey stick shape of reflection events was clearly observed in the full-offset gathers (i.e. traces were misaligned at long offsets). This effect was particularly pronounced within the CO₂ plume. To correct for anisotropy, an anisotropic NMO equation (Alkhalifah and Tsvankin, 1995) was applied to the data (Figure 7.25a). The intrinsic layer anisotropy, ϵ_i , was calculated using the equation of Grechka and Tsvankin (1997). As predicted, a large increase in ϵ_i was observed in the Utsira Sand after CO₂ injection.

Though the quality (alignment) of the NMO gathers improved considerably for the long offsets, the effects on the migrated post-stack data are less evident (Figure 7.25b). One could argue for a slight improvement of the imaging within the plume for

the 1999 dataset, however this is subject to interpretation. Beneath the plume, imaging seems slightly worse.

In any case, since the NMO curve is approximated with an additional parameter in the anisotropic case, the alignment on the CMP gathers is improving. The question remains however as to whether we are really looking at anisotropy or at a laterally varying inhomogeneous medium. The answer lies in the scale of the inhomogeneities caused by the CO₂.

Super-resolution mapping of thin CO₂ accumulations

One of the challenges at Sleipner is to estimate the thickness of the thin CO₂ accumulations beneath the thin mudstones. Assuming that the reflection from the top of the CO₂ accumulation interferes with the reflection from the bottom, a so-called 'constrained deconvolution' process can be applied (Borgos and Sonneland, 2003). The number of CO₂ accumulations and the wavelet are assumed to be known (the former based on the number of mudstones proven in nearby wells). The location of the reflectors is not constrained to the maximum or minimum amplitude of the seismic signal (Figure 7.26).

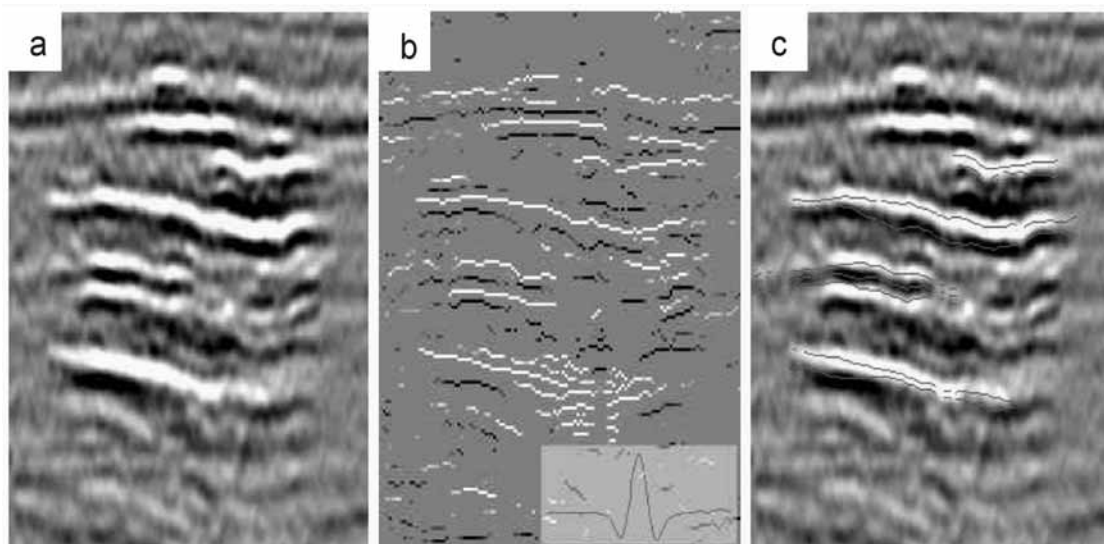


Figure 7.26 Vertical seismic section through the 1999 plume. a) Seismic data. b) Reflectivity estimates resulting from 3D blind-deconvolution, with estimated wavelet inlaid. c) Reflector positions resulting from the super-resolution algorithm, superimposed on the seismic data. From Borgos and Sonneland, 2003.

This method has been applied to map the thicknesses of the different CO₂ accumulations (Borgos and Sonneland, 2003). The reflection from the top of each mudstone layer, which is also within the interference thickness, has been considered small enough to be neglected. The results of the estimated thicknesses have been compared to the estimations derived from the amplitude inversion using the tuning relationship (Arts et al., 2004b) and with the results from the seismic AVO inversion (Østmo et al. 2004). The main conclusions are that the tuning relationship provides the most reliable analysis. The results of the two alternative methods give comparable

results, but the calibration of the thickness is extremely sensitive to the velocity model assumption (Lescoffit, 2004).

7.2.2 Time-lapse sea-bed gravimetry

The possibility of monitoring injected CO₂ with repeated gravity measurements is strongly dependent on CO₂ density and subsurface distribution. An initial study of time-lapse gravimetry at Sleipner was based on CO₂ distributions from the 1999 seismic survey (Williamson et al., 2001). Assuming uniform distribution of CO₂ within the plume envelope, a range of scenarios were modelled with CO₂ densities ranging from over 700 kgm⁻³ to less than 350 kgm⁻³. The modelling indicated that the 1999 plume, containing some 2.35 Mt of CO₂, would have produced a peak change in gravity at the seabed ranging from about about 8 to 30 Gal depending on CO₂ density (Figure 7.27), a signal that is theoretically detectable. Assuming similar subsurface distributions, it was predicted that future additions to the CO₂ plume of about 3 Mt or more, should be detectable by sea-bed gravimetry. Longer-term predictions suggested that on cessation of injection, the gravity signature of the plume would gradually decrease as it thinned by lateral migration at the reservoir top. On the other hand, if substantial amounts of CO₂ leaked to shallower levels, where it would have a lower density still, gravity changes could well exceed -100 Gal.

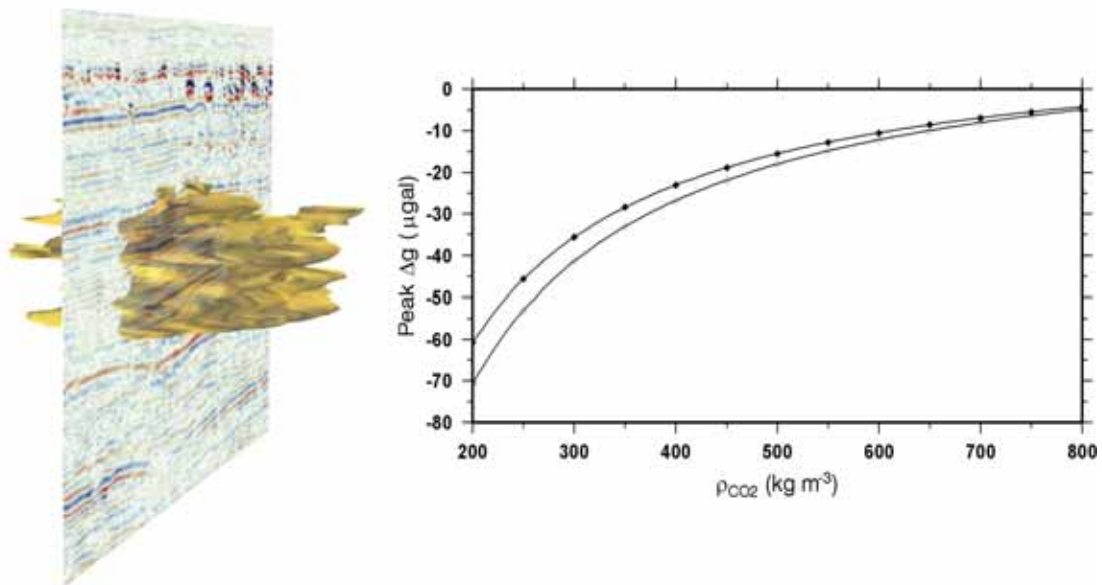


Figure 7.27 Gravity modelling of the 1999 plume. GOCAD model of the plume envelope (left) and its computed peak gravity response for a range of CO₂ densities (right). Open circles denote response at sea bed, closed circles response at sea level.

A first sea bed gravity survey was acquired at Sleipner in 2002 (Eiken et al., 2003), with 4.97 Mt of CO₂ in the plume. The survey was based around pre-positioned concrete benchmarks on the sea floor that served as reference locations for the (repeated) gravity measurements. Relative gravity and water pressure measurements

were taken at each benchmark by customised gravimetry and pressure measurement module mounted on a Remotely Operated Vehicle (Figure 7.28).



Figure 7.28 Images from the 2002 and 2005 gravimetric surveys at Sleipner. a) Survey vessel. b) ROV with gravimeter (red). c) Gravimeter located on concrete benchmark at sea bed.

Thirty benchmarked survey stations were deployed in two perpendicular lines, spanning an area some 7 km east–west and 3 km north–south and overlapping the subsurface footprint of the CO₂ plume (Figure 7.29). Each survey station was visited at least three times to better constrain instrument drift and other errors. Single station repeatability was estimated to be 4 Gal. For time-lapse measurements an additional uncertainty of 1–2 Gal is associated with the reference null level. The final detection threshold for Sleipner therefore is estimated at about 5 Gal.

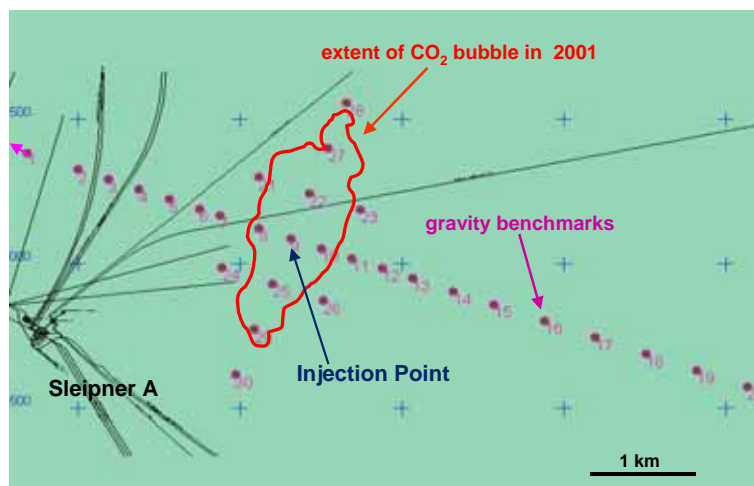


Figure 7.29 Map showing location of Sleipner gravity survey stations and CO₂ plume.

Subsequent to the 2002 gravity survey, a more detailed analysis of plume gravity signal was undertaken. This was based upon computing the gravity response of

gridded 3D plume models with detailed CO₂ distributions and densities defined by reservoir flow simulations (the latter calibrated by the seismic monitor surveys). Four model scenarios were considered, a lower temperature reservoir with and without CO₂ dissolution and a higher temperature reservoir with and without dissolution. The gravity response was computed for 2002 and for 2005 together with the changes from 2002 to 2005 (Table 7.4).

	August 2002 (4.8 Mt)			August 2005 (7.4 Mt)			Change
	Density	Dissolution	Signal	Density	Dissolution	Signal	
	kgm ³	%	μGal	kgm ³	%	μGal	μGal
Hot, no dissolution	528	0%	-31.3	523	28%	-44.3	-13.7
Hot, dissolution	531	29%	-21.1	529	0%	-29.8	-8.8
Cold, no dissolution	708	0%	-15.6	707	23%	-22.2	-6.7
Cold, dissolution	708	25%	-10.9	707	23%	-16.2	-5.4

Table 7.4 Predicted gravity changes from 2002 to 2005, for various reservoir scenarios.

Depending on temperature and dissolution, the 2002 plume has a modelled response between about -11 to -31 μGal, and the 2005 plume has a response between about -16 and -44 μGal (Figure 7.30).

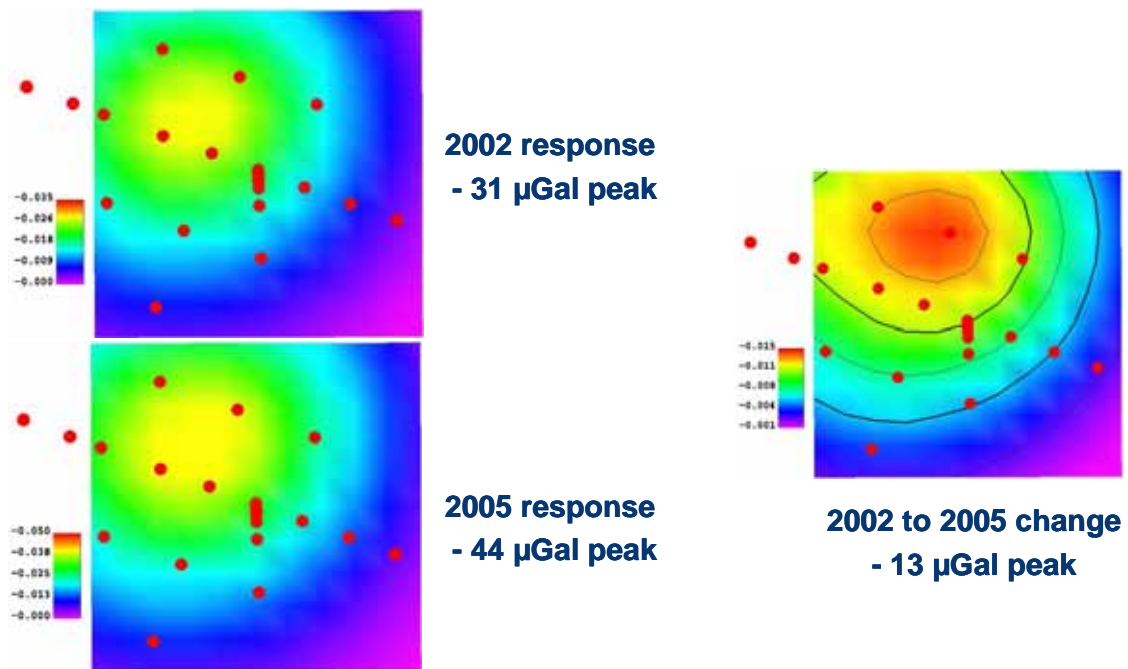


Figure 7.30 Gravity modelling based on distributions of CO₂ from flow simulations (high reservoir temperature scenario with no CO₂ dissolution). Responses calculated for the 2002 plume, the 2005 plume and for the expected change between the 2002 and 2005 surveys.

The largest signal corresponds to the higher temperature (low CO₂ density) model with no CO₂ dissolution with a predicted maximum change from 2002 to 2005 of around -13 to -14 Gal (Figure 7.30). In contrast, the lower temperature (high CO₂ density) model with CO₂ dissolution has a predicted change from 2002 to 2005 of only about -5 Gal.

The repeat gravity survey was carried out in September 2005, with around 7.75 Mt of CO₂ in the plume, an additional 2.78 Mt compared with the 2002 survey. Each station was visited at least twice. Gravity measurements were corrected for tides, instrument temperature, tilt, and drift. The uncertainty for this survey is estimated at 3.5 μ Gal.

The time-lapse gravimetric response due to CO₂ was obtained by removing the modelled gravimetric time-lapse response from the Sleipner East field (the deeper gas reservoir currently in production) from the measured gravity changes between 2002 and 2005 (Figure 7.31).

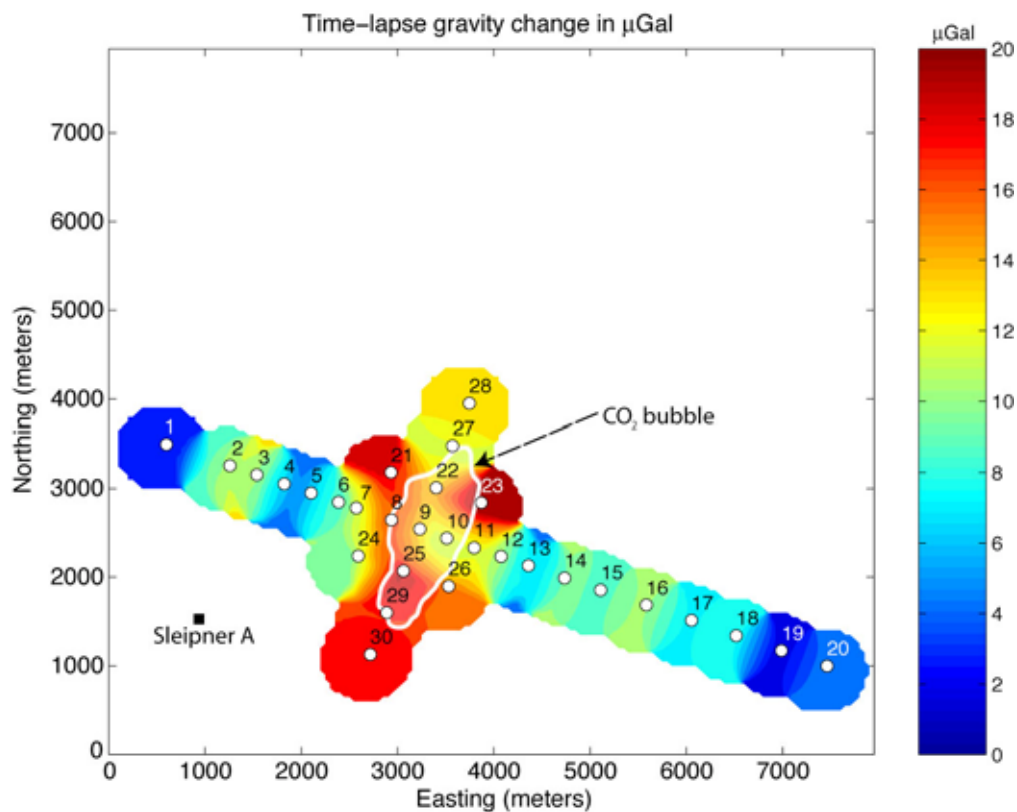


Figure 7.31 Time-lapse gravity response from 2002 to 2005. Sea-bed benchmark locations are shown by white circles with a smoothed version of the gravity changes after correcting for depth and a long wavelength trend. Note the spatially coherent gravity decrease in the central part of the survey (white polygon shows extent of the seismically imaged CO₂ plume in 2001).

Forward modelling was performed (Nooner et al., 2006, 2007) to investigate whether the gravity changes could provide an indication of the in situ CO₂ density. This was done via plume models constrained both by time-lapse seismic data (using generalised plume distributions based on the 1999 and 2001 3D surveys) and also by reservoir flow models. The best fit was obtained for the higher temperature seismically

constrained model (Figure 7.32). Statistical analysis indicates that average CO₂ density may be quite low, of the order of 530 kgm⁻³, consistent with reservoir temperatures towards the high end of the uncertainty range.

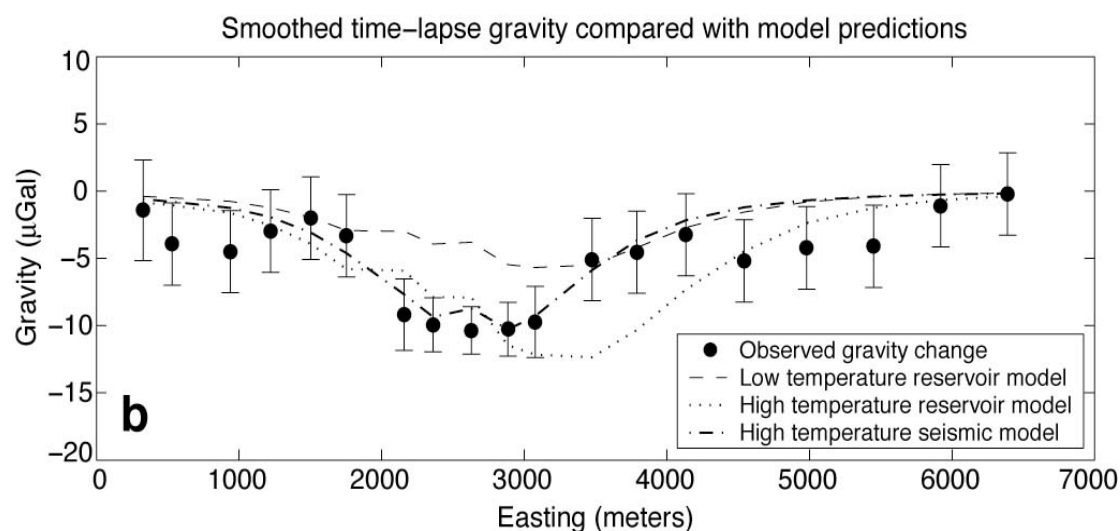


Figure 7.32 Smoothed observed time-lapse gravity change plotted with modelled gravity change for high (average CO₂ density 550 kgm⁻³) and low reservoir temperatures (average CO₂ density 700 kgm⁻³) models. Both the models and the observations have been smoothed by averaging neighbouring values. Observed gravity changes most closely match the high temperature seismic model. From Nooner et al. 2006.

Further repeat surveys in a few years' time will have a much higher gravity change to measure, with correspondingly greater confidence in the density estimates.

7.2.3 Generic findings

A key aim of site monitoring is to confirm current reservoir performance and from this to provide controlling datasets for the longer-term predictive simulations of plume behaviour. Accurate pressure and temperature information is a prerequisite. This is particularly the case for shallow storage (about 800 m depth) where conditions are near the critical point for CO₂, around which properties vary rapidly with pressure and temperature.

This highlights a key uncertainty in verification estimates; the velocity behaviour of the CO₂–water–rock system, which in addition to pressure and temperature effects, is also heavily dependent on the (poorly constrained) nature of small-scale mixing processes between the fluid phases. Detailed assessment of velocity pushdown within the plume, allied to reservoir simulations, may help cast some light on this. With only the single deviated injection well in the vicinity, Sleipner is not suitable for the deployment of well-based monitoring tools, but it is clear that the type of work being carried out at Nagaoka (Kikuta et al., 2005) and Frio (Daley et al., 2006), where well logs are being used to derive saturation-velocity relationships, tied to cross-hole seismic results and core studies, may provide the type of information needed to reduce this uncertainty.

Because of the very thin (typically < 8 m thick), very reflective CO₂ layers, tuning effects are dominant. These has been used to advantage in post-stack analysis whereby amplitudes can be related directly to thicknesses. Pre-stack techniques such as trace inversion and AVO analysis are severely hampered by this and, at Sleipner, have given misleading results. A clear lesson here is that a purely ‘black-box’ approach to data analysis will not succeed. Considerable interpretive insights are required to maximise information recovery from the data. Although specifically applicable to Sleipner this maxim could well be applicable to the general storage case. It seems quite likely, that, at least early in the injection history, thin accumulations of CO₂ could dominate plume processes and geophysical response.

As described above, forward modelling from flow simulations has been used with some success on the Sleipner datasets. As tested, a coupled workflow involving 3D flow simulation and acoustic impedance calculation where flow models can be rapidly tested in terms of their seismic response is likely to prove a powerful tool for history matching.

7.3 Flow simulations history-matched to monitoring data

A key aspect of the site operation phase is to evaluate the degree to which the site is performing compared to predictive models. Various types of monitor data can be used to history-match the observed CO₂ plume against flow simulations. The degree of matching will either validate current simulations, or indicate how modelling should be adjusted. The ultimate aim is to show that longer-term models of future plume behaviour will be robust by showing that the key modelling assumptions are supported by current observations.

7.3.1 History-matching monitoring datasets

In the SACS project, several reservoir models were built for Sleipner to address issues of short-term history-matching and longer-term prediction. Two types of models were developed for short and longer time predictions.

The short term reservoir models describe the reservoir in the immediate vicinity of the injection site. They covers an area of only a few km² and contain a large number of small grid blocks (typically 50 m across with much finer sampling in the vertical direction). The short-term models were iteratively calibrated and adjusted in the light of interpretations of the seismic images of the CO₂ accumulations from the repeated seismic surveys performed three and five years after the start of injection.

The longer term reservoir models cover a wider area (>100 km²) and are being used to predict the migration of CO₂ over a period of several thousand years under the assumption that there is no migration through the caprock seal. Due to computational constraints these flow models have to rely on a coarser grid, grid cells typically 1000 m across, with much less detail in the vertical direction.

7.3.1.1 Simulation tools used at Sleipner

Simulations have been carried out with a number of different 3D multiphase flow simulators, ECLIPSE 100 and ECLIPSE 300, SIMED II, TOUGH2 and COORES. In addition, two simulators providing coupled reaction-transport capability were also utilised: GEM and TOUGHREACT. These are summarised below:

ECLIPSE 100 is a black-oil simulator that can handle up to four flowing phases. Only the oil and gas phases were used in the SACS and CO2STORE simulations. The oil phase was given pVT and phase data corresponding to brine and the gas phase was given properties corresponding to CO₂ (pVT and solubility data and viscosities are represented in tables). This allows both solubility properties and density versus depth data to be consistently represented, as pressure variation in the model is dominated by the hydrostatic pressure gradient throughout the simulation. CO₂ densities for the pVT table were calculated by an equation-of-state developed by Span and Wagner (1996).

ECLIPSE 300 is a compositional simulator capable of handling compositional and pVT effects in a realistic way.

SIMED II is a multicomponent reservoir simulator that initially was designed for modelling the drainage of methane from coal seams (CBM). The simulator includes a gas phase density calculation using a Peng-Robinson equation of state with a Chien-Monroy correction, and viscosity by the Jossi-Thiel-Thodos method. The simulator was implemented with an option to specify depth-related temperatures for each grid block thus preserving a consistent density versus depth profile. New CO₂ solubility relationships have also been incorporated.

TOUGH2 is a general-purpose numerical simulation program for multidimensional fluid and heat flows of multiphase, multicomponent fluid mixtures in porous and fractured media. Chief application areas are in geothermal reservoir engineering, nuclear waste isolation studies, environmental assessment and remediation, and flow and transport in variably saturated media and aquifers.

COORES is a 3D, three phase compositional fluid flow simulator. COORES allows local grid refinement and dual media to better characterise the fluid flow. Fluid flow properties can be described through user-defined data or by using a governing equation such as the Peng-Robinson equation of state to compute phase density variation or the Lorehnz-Bray-Clark correlation to compute phase viscosity variation with pressure. In its current version, COORES is isothermal but handles CO₂ dissolution in water through (tabulated user-defined) equilibrium constants as well as CO₂ diffusion in the water phase. COORES has been successfully applied to model CO₂ behavior (Pruess et al., 2003; Oldenburg et al., 2003a).

GEM is a 3D, three-phase compositional fluid flow simulator. It can be used to model any type of reservoir where it is essential to model fluid composition and reactivity. An option for greenhouse gas injection (GEM-GHG) has been added to model CO₂ storage in geological formations.

The key features of the simulator are listed below.

Fluid phase equilibrium is primarily obtained through an EOS (equation of state) but gas component dissolution into the aqueous phase can alternatively be modelled with Henry's law.

Water components (ions in addition to dissolved gases) are modelled.

Chemical interactions with solid minerals are modelled through equilibrium reactions for aqueous species; mineral dissolution and precipitation rates; several activity coefficient models.

An enthalpy module to model temperature variations and take into account CO₂ injection temperature is included.

An asphaltene deposition model is used for CO₂ injection into oil reservoirs.

A robust solution method has been developed where the component convection diffusion equations, phase equilibrium equations, chemical equilibrium equations and mineral dissolution/precipitation equations are solved simultaneously.

TOUGHREACT has been developed as a comprehensive non-isothermal multi-component reactive fluid flow and geochemical transport simulator to investigate geological systems and environmental problems. A number of subsurface thermo-physical-chemical processes are considered under various thermohydrological and geochemical conditions of pressure, temperature, water saturation, and ionic strength. The simulator can be applied to one-, two- or three-dimensional porous and fractured media with physical and chemical heterogeneity. The code can accommodate any number of chemical species present in liquid, gas and solid phases. A variety of equilibrium chemical reactions are considered, such as aqueous complexation, gas dissolution/exsolution, and cation exchange. Mineral dissolution and precipitation can take place subject to either local equilibrium or kinetic controls, with coupling to changes in porosity and permeability and capillary pressure in unsaturated systems. Chemical components can also be treated by linear adsorption and radioactive decay.

7.3.1.2 Fluid and transport properties

Flow simulations assumed the lower reservoir temperature scenario (based on the measured value of 37°C at 1058 m), temperatures varying from about 29°C at the reservoir top to about 36°C at the injection point. Pressure increases downwards through the formation, but temperature and pressure have opposite effects on the density, which in practice is relatively uniform through the reservoir, at about 700 kgm⁻³ (Figure 3.1). The corresponding CO₂ viscosity is about 0.06 mPa.s.

The solubility of CO₂ in brine at Utsira reservoir conditions is about 53 kgm⁻³. Dissolved CO₂ could therefore potentially provide a significant contribution to CO₂ storage in this aquifer. To illustrate, if perfect fluid mixing could be achieved, all of the CO₂ planned to be injected at Sleipner (about 1 Mt per year for 25 years) would dissolve in a brine-filled 'cylindrical' pore volume 1300 m in radius and 200 m tall. In practice, perfect mixing will not be approached, but nevertheless as the CO₂ plume

migrates upwards through the reservoir, some water will be contacted by CO₂, particularly as it spreads laterally beneath the intra-reservoir mudstones. The mudstones tend to spread the CO₂ over a large area, increasing the surface of the CO₂ phase and increasing amounts of dissolution. In spite of this, the amount CO₂ dissolved during the injection period will be relatively limited because only a small fraction of the brine will be contacted by CO₂. Although the quantitative interpretations of the seismic are non-unique, iteration between the geophysical interpretation of the seismic reflections attributed to the injected CO₂ and the reservoir simulations showed that good matches between observed and simulated bubble areas could be achieved even if CO₂ solubility is completely neglected, at least for the low temperature reservoir scenario. From this it can be inferred that the mudstone layers do not disperse large amounts of CO₂ into many small, dissolution-prone leak streams when it is transported from layer to layer. The CO₂ transport seems rather to be concentrated at a smaller number of localised spill points or holes with relatively minor dissolution. It should be pointed however, that higher temperature reservoir scenarios would require greater volumes of CO₂ in the plume and significant dissolution even in the short-term.

7.3.1.3 Flow modelling

The Sleipner simulations illustrate well how repeated 3D seismic surveys can be used to calibrate a local reservoir model. Data from pre-injection seismic, well logs and petrophysical data obtained from laboratory experiments and core analysis were used to build the original local reservoir model of the Utsira Sand near the injection point. However, because the injection well is near-horizontal (Figure 1.2) it did not provide good information on the nature of the reservoir succession above the injection point. Furthermore there are no other wells in the immediate vicinity of the injection site. Most of the data used to construct the reservoir model was obtained from wells that passed beneath, or very close to, the Sleipner A platform, some 3 km away. With the exception of the 5-metre mudstone (Figure 4.7), the pre-injection seismic reflection data was unable to image the thin intra-reservoir mudstones. As a consequence of this, although it was predicted that these would be present, their exact number, depth and structural disposition is not known.

Initial reservoir models made certain assumptions about the geometry of the mudstones. Horizontal layering was the simplest configuration, subsequently refined to a model in which mudstone topography followed that of the 5-metre mudstone, gradually diminishing downwards. The number and relative spacing of the mudstones was based on the observed reflectivity of the 1999 time-lapse seismic data where the major seismic reflectors were interpreted as CO₂ accumulations trapped beneath the mudstones.

In the simulations, CO₂ was injected close to the base of the reservoir according to the documented injection history (Table 7.1). The mudstone layers were set up to impede its vertical migration and cause the entrapment of the CO₂ in large, near-horizontal layers within the porous medium of the sand. The mudstones were specified to be either semi-permeable (Figure 7.33), or impermeable with localised spill areas (holes) that allow migration of CO₂ to the consecutive barrier layers above (Figure 7.34). Discontinuity and heterogeneity of these mudstone layers are thought to cause the

CO₂, at least locally, to be transported in distinct chimney-like columns that are imaged on the repeat seismic surveys (Figure 7.2).

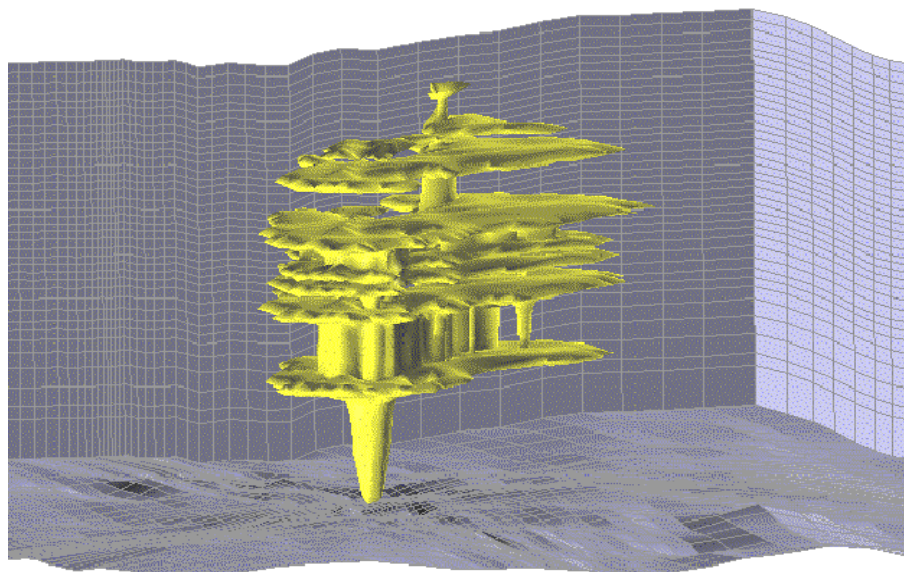


Figure 7.33 SIMED 3D flow simulation of the 1999 Sleipner plume.

Reservoir simulation incorporates the predominant driving mechanisms that control the migration of CO₂. Model predictions are sensitive to relative permeability characterisation through critical and trapped gas saturation, curve shape (Van Genuchten versus Corey) and hysteresis effects which strongly affect the plume migration (see below). In addition, the pore entry pressure of each shale formation must be accurately determined to enable correct flow computation. The model is calibrated by modifying various parameters to achieve history matching and the history-matched model is ultimately adopted to make future predictions. The transmissibility of each mudstone and the chimney-creating conduits were obtained by adjusting the transmissibility multipliers so that the resulting accumulations under the layers became similar in size to the corresponding seismic reflector (Figure 7.34). This is an iterative process that is still continuing with the 2001 and 2002 surveys. An intrinsic uncertainty in the history matching is the extent to which the thickness and shape of the CO₂ layers is controlled by mudstone topography, mudstone transmissivity, or lateral permeability variations in the reservoir sand.

The best constrained CO₂ layer is the topmost one, trapped directly beneath the caprock. Because it collects the entire flux of CO₂ through the plume, this layer is a very good ‘barometer’ of reservoir flow performance. Recent and ongoing work in CO₂STORE is focussing on accurate quantitative evaluation and modelling of this topmost layer to see how reservoir performance may be changing with time (Chadwick et al., 2006).

Thus the SACS/CO₂STORE local reservoir model has demonstrated that even without a wellbore very close to the injection site, if good quality 4D seismic data is available, the reservoir simulation can still be iteratively history matched to the seismic interpretation and predictively useful results may be obtained.

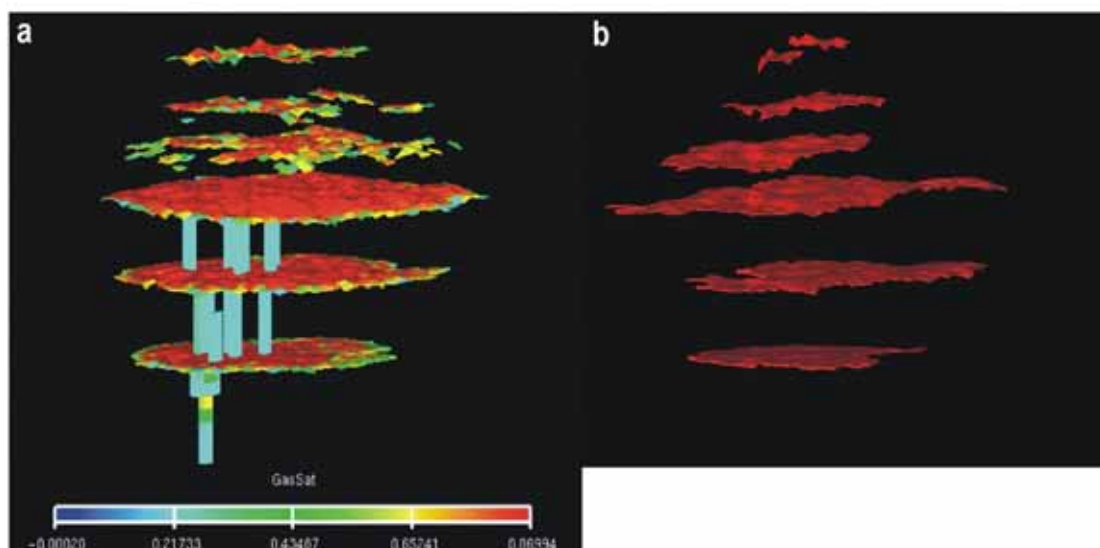


Figure 7.34 3D flow simulation of the 1999 plume (ECLIPSE 100 simulator), with detailed matching of simulated layers to observed seismic. a) CO₂ distributions in simulated layers. b) Observed layers from seismic (simplified 6 layer plume interpretation).

7.3.1.4 Simulation of the long-term fate of CO₂ in a large-scale model

One of the main objectives of reservoir simulation in a geological CO₂ storage project is to make long-term predictions of the fate of the injected CO₂. The reservoir model constructed for this purpose should include the major features of the local model that control transport of CO₂ on the relevant timescale. The fluid model of CO₂ and brine must feature correct volumetric data (densities), phase behaviour (solubility) and transport properties (viscosities and diffusion coefficient).

For the Sleipner injection case, information from the calibrated local model was extrapolated to build a 3D reservoir model covering an area of 128 km² to predict the fate of CO₂ over a time period of thousands of years. Capillary pressure and relative permeability describing the interaction between the porous media and the fluids were measured in laboratory experiments on Utsira Sand core material. Computational constraints limited the number of grid blocks in the model to less than one million to achieve acceptable computation times. This represents a substantial coarsening of the grid compared to the local model. Preserving the physical consistency of the major transport phenomena in the new grid was a major challenge. In the model the caprock mudstones are assumed to provide a capillary seal for the CO₂ phase preventing upward migration, but allowing molecular diffusion of CO₂ through the overlying strata (as for the geochemical modelling described in Chapter 4).

The results of the simulations show that most of the CO₂ accumulates in one layer under the reservoir topseal a few years after cessation of injection. The CO₂ bubble spreads laterally on top of the brine column, migration being controlled mainly by the topography of the reservoir caprock (Figure 7.35). This simulation does not incorporate dissolution of CO₂ into the formation brine, so the model is intrinsically conservative in that real plume extents will be smaller than in the model.

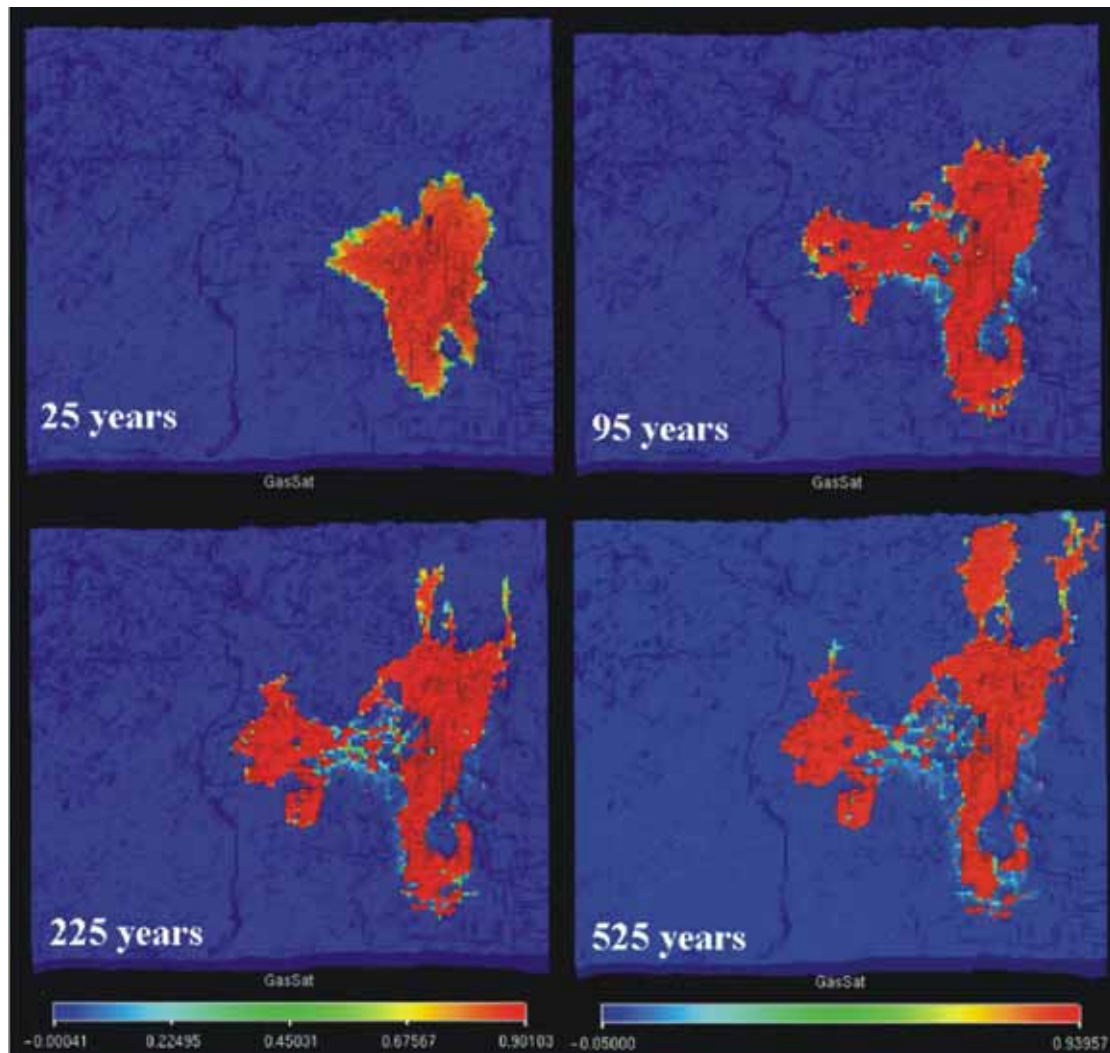


Figure 7.35 Maps illustrating simulated migration beneath the topseal of the topmost CO₂ layer (assuming no dissolution). After 500 years CO₂ reaches the boundaries of the model and starts to migrate out of the model.

Molecular diffusion is driven by concentration gradients and can usually be neglected in reservoir simulations as it is very slow compared to other transport processes. It is attenuated due to diminishing concentration gradients, which is a result of the diffusion process itself. In the longer term however, diffusion of CO₂ from the gas cap into the underlying brine column will have a more pronounced effect. The brine on top of the column, which becomes progressively enriched in CO₂, is denser than the brine below due to the specific volumetric properties of the CO₂ – brine system. This creates an instability that sets up convection cells (Figure 7.36). A consequence of this is to maintain large concentration gradients at the CO₂ – brine interface, enhancing further dissolution processes.

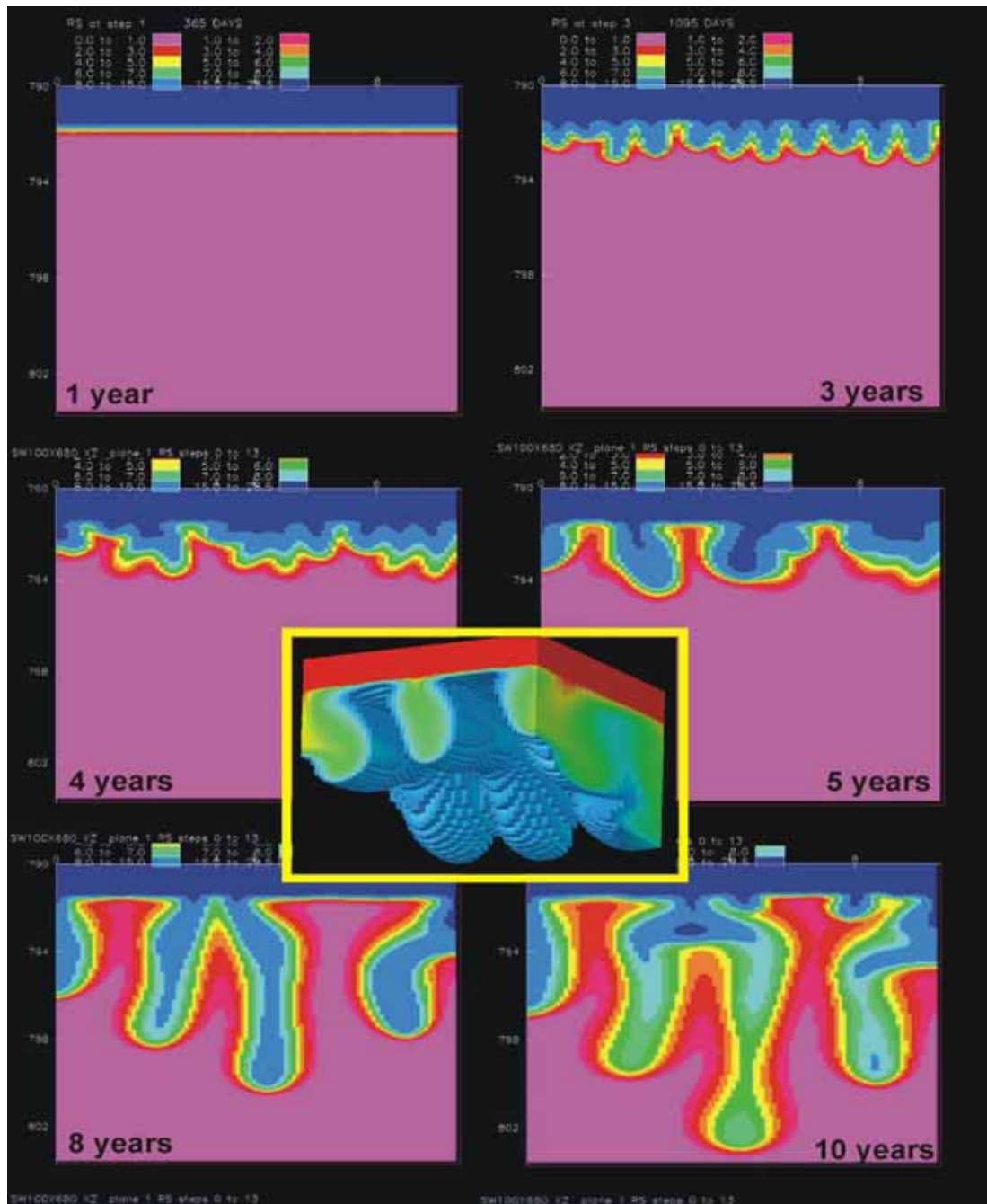


Figure 7.36 Sleipner dissolution in 10 years showing concentration profiles in a 10 x 13.6 m segment just beneath the CO₂ brine contact. From a metastable diffusion front (upper left) convectional plumes gradually develop. This process significantly enhances dissolution.

In the absence of dissolution, migration of the gas cap beneath the reservoir topseal would continue, by progressive spreading and thinning, for several hundred years (Figure 7.35). If however the effects of dissolution are included, the volume of the gas cap will gradually diminish, such that it will reach its maximum areal extent at perhaps less than 300 years. The migration and gradual dissolution of the free CO₂ cap for the first 250 years after cessation of injection are illustrated in Figure 7.37.

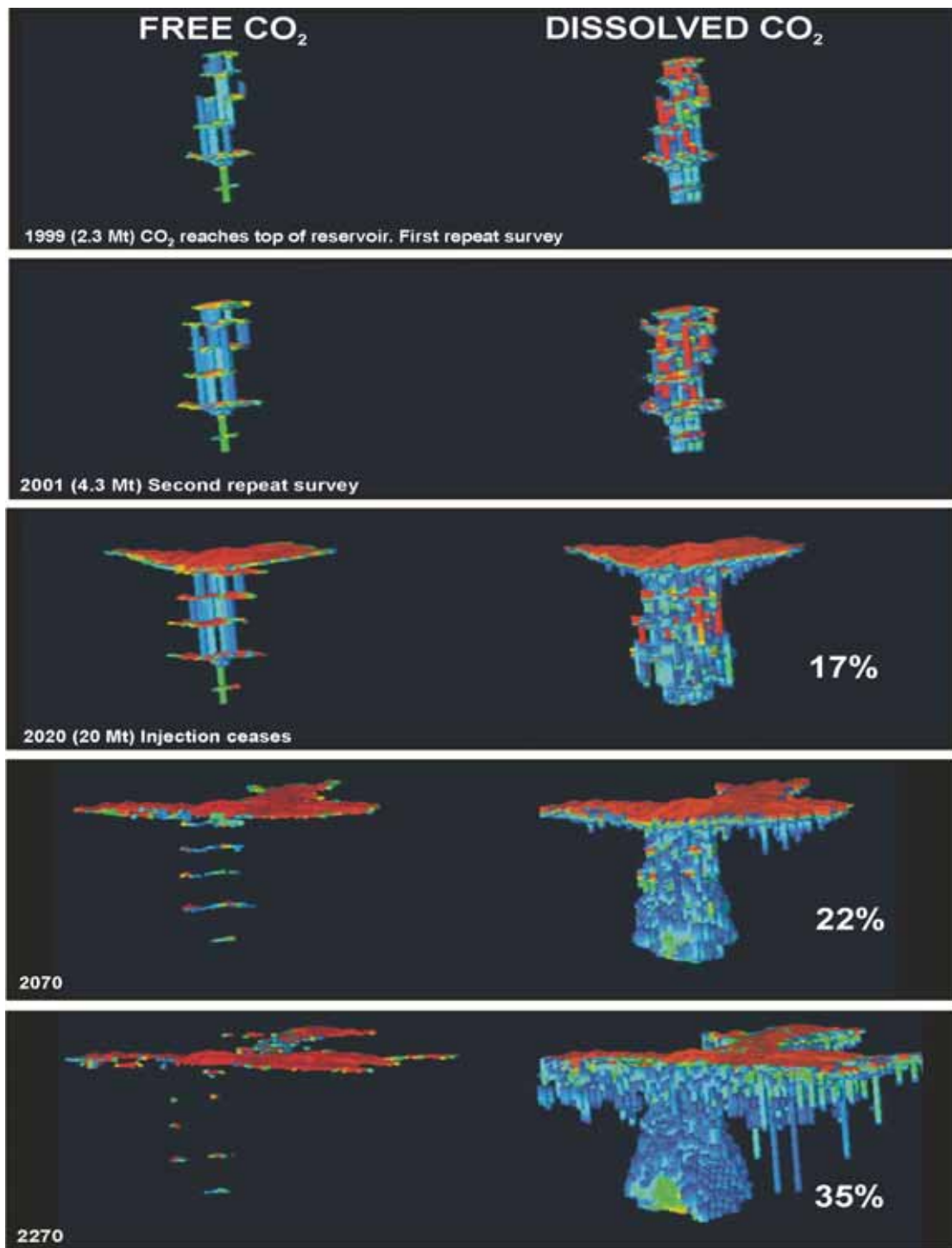


Figure 7.37 Simulation of the medium-term fate of the CO₂ plume at Sleipner. Free CO₂ (left) rises to the reservoir topseal where it migrates laterally. CO₂-saturated pore-waters (right) sink in the reservoir, the dissolution plume expanding as the cap of free CO₂ spreads (percentage of dissolved CO₂ given).

On even longer timescales, in the order of thousands of years, dissolution will become a dominant influence in constraining and ultimately halting the lateral spread of free CO₂ (Figure 7.38).

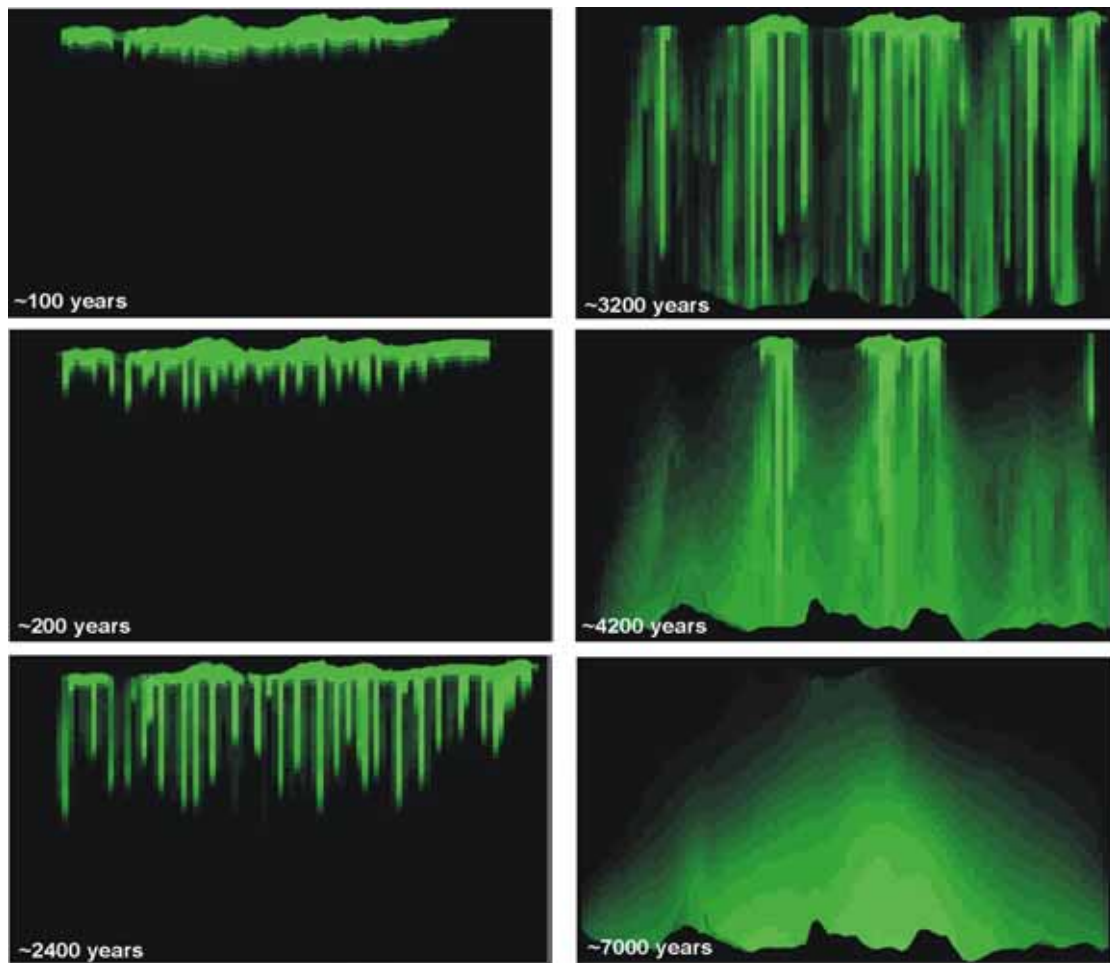


Figure 7.38 Simulation of the long-term fate of the CO₂ plume at Sleipner. Free CO₂ trapped at reservoir top progressively dissolves, as CO₂ in solution sinks towards base of reservoir. After about 5000 years all free CO₂ has dissolved.

Amounts of CO₂ in the free phase will gradually diminish (Figure 7.39), and are predicted to disappear completely after 5000 years or so (depending on the reservoir parameters). Beyond 5000 years, a plume of saline pore-waters with dissolved CO₂ will gradually sink to the bottom of the reservoir (Figure 7.38). Similar studies by Ennis-King and Paterson (2003) into dissolution in generic aquifers supports these conclusions. It is likely therefore that in the long term (> 50 years) the phase behaviour (solubility and density dependence of composition) of the CO₂–water system will become the controlling fluid parameters at Sleipner. On this timescale it may that geochemical effects will also start to have a significant impact (Section 4.3).

A potential factor in the dissolution process is the strength of natural groundwater flow in the reservoir. The stronger the flow, the more CO₂ is exposed to unsaturated water, and the greater the rate of dissolution. Pressure measurements from the Utsira Sand are close to hydrostatic with little evidence of flow. Basin modelling carried out in SACS (Kristensen and Bidstrup, 2001; SACS, 2003) suggest the possibility of natural flow velocities in the range 2–4 m per year, but these represent a maximum limit. Such velocities, acting over hundreds of years, would however slightly aid the dissolution process.

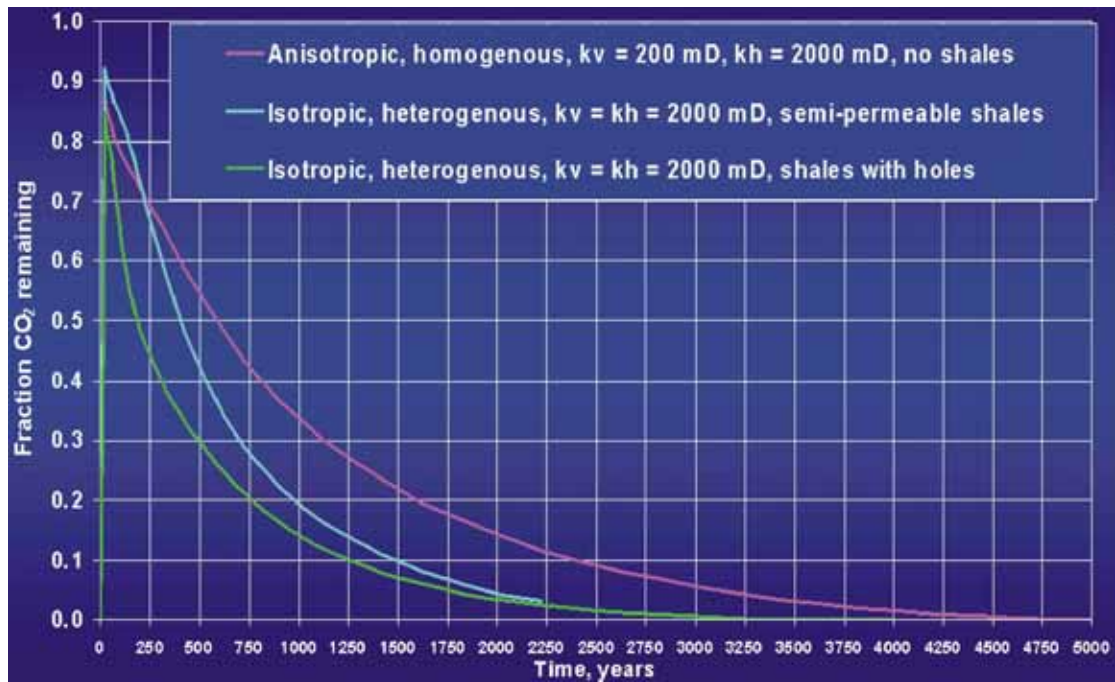


Figure 7.39 Simulated long-term CO₂ dissolution for an Utsira-like saline aquifer with various permeability characteristics.

Residual phase trapping

An additional process, which has not been considered in detail in the SACS and CO₂STORE projects, is that of residual phase (capillary) trapping caused by relative permeability hysteresis. This occurs when, for a given gas (CO₂) saturation, relative permeabilities are lower during imbibition than during the initial drainage phase.

Residual phase trapping is potentially very significant in improving the long-term storage efficacy of reservoirs (Section 3.1) by changing the migration behaviour of the plume. Strong relative permeability hysteresis leads to so-called ‘sticky’ plumes that leave behind relatively high amounts (perhaps up to 30% or more) of trapped residual CO₂. Weak relative permeability hysteresis leads to ‘slippery’ plumes that leave behind only small amounts of residual CO₂.

A Sleipner-like case was simulated (Figure 7.40) to illustrate the potential effects of residual phase trapping (note the actual degree of relative permeability hysteresis at Sleipner is not known). At the front of the CO₂ plume, a drainage process takes place in the reservoir as CO₂ displaces the pore water. At the trailing edge of the migrating plume, imbibition occurs as pore waters seek to re-occupy the pore-spaces. Due to relative permeability hysteresis, CO₂ at low saturations becomes trapped at the trailing-edge as an immobile phase. This leads to a different CO₂ distribution at the end of a 1000-year storage simulation (Figure 7.40). The main effect of residual gas trapping is to restrict lateral spreading of the plume and to increase dissolution (the immobile CO₂ residues are very effectively exposed to pore-waters during re-imbibition). Both of these effects stabilise and concentrate CO₂ within the plume envelope and are beneficial to storage.

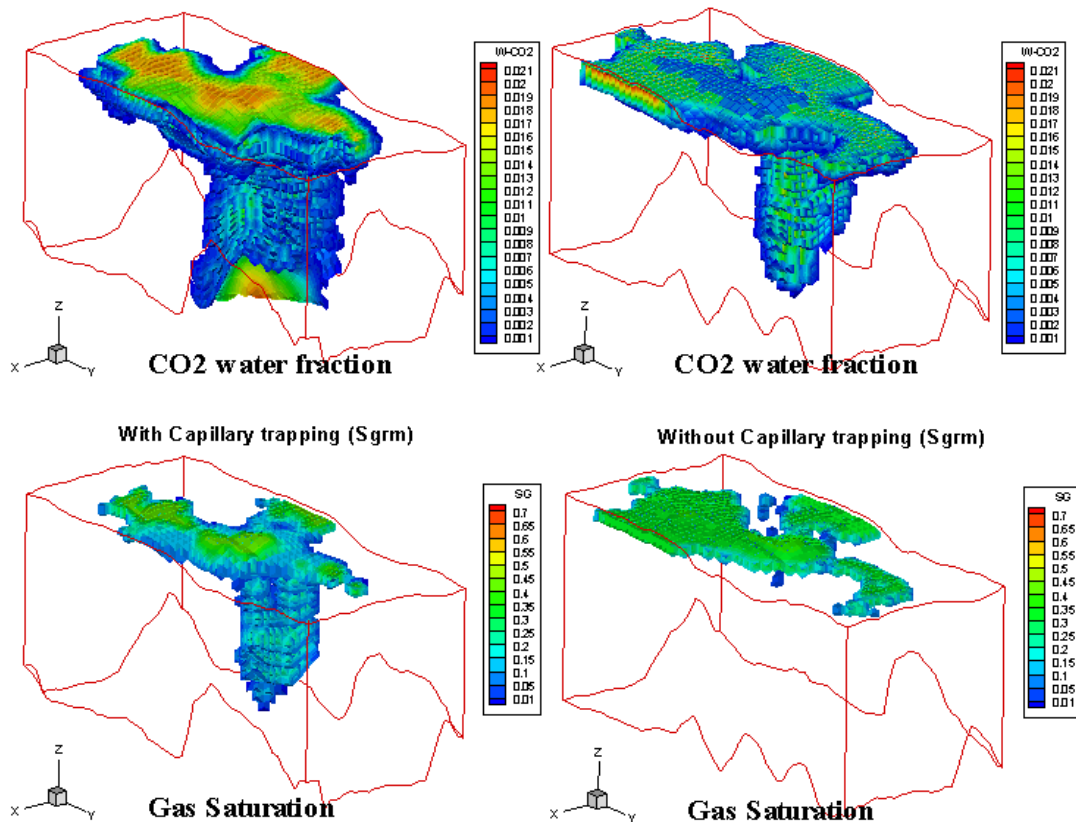


Figure 7.40 Influence of residual (capillary) phase trapping (S_{grm}). CO₂ mass fraction dissolved in water (top), and free CO₂ (gas) saturation (bottom) after 1000 years (25-year CO₂ injection and 975-year storage).

Upward molecular diffusion of CO₂ through the water-saturated overlying caprock mudstones can potentially represent an escape path for CO₂ into the atmosphere. With this process however, injected CO₂ will not reach the sea floor until several hundred thousand years after the end of injection. This escape mechanism can in practice be neglected.

Coupled reaction–transport modelling

Within CO2STORE, coupled reaction and transport modelling has been carried out for the Utsira reservoir. Results indicate that solubility trapping will be dominant over mineral trapping, and that mineral dissolution interactions are likely to be dominated by carbonates. The importance of reservoir heterogeneity in general, and for the Sleipner case in particular, is illustrated by the modelling performed using the TOUGHREACT software (Audigane et al., 2005).

The first objective of coupling flow and reactivity in the storage reservoir is to locate which areas of the reservoir are acidified, and for how long. This will provide input to site integrity evaluations (caprock sealing efficiency and well-bore alteration studies).

The second objective is to evaluate the long-term fate of the CO₂ in the storage reservoir, by identifying the dominant mode of CO₂ trapping (physical vs. solubility

vs. ionic vs. mineral trapping) at various times (hundreds or thousands of years). This can help in predicting the long-term status of the reservoir (rock mineralogy, formation water pH, free CO₂) after injection operations have ceased.

To tackle these issues, two different modelling strategies (3D and 2D) were investigated.

Firstly, the GEM-GHG 3D reaction-transport software was utilised. This combines two-phase flow simulation with a simplified geochemistry based on carbonate mineralogy (Frangeul et al., 2004). The Utsira 3D model comprised a 6 km × 7 km horizontal extent with an average 200 m reservoir thickness, and contained 48 000 cells with a simplified geochemistry to model the CO₂ reactivity. Geochemical coupling incorporated only a limited chemical dataset of carbonate minerals (Table 7.5).

9 aqueous species	Na ⁺ , Cl ⁻ , CO _{2(aq)} , H ⁺ , Ca ⁺⁺ , Mg ⁺⁺ , OH ⁻ , HCO ₃ ⁻ , CO ₃ ²⁻
2 minerals	Calcite, Dolomite
Aqueous reaction 1	H ₂ O = H ⁺ + OH ⁻
Aqueous reaction 2	CO _{2(aq)} + H ₂ O = H ⁺ + HCO ₃ ²⁻
Aqueous reaction 3	HCO ₃ ²⁻ = H ⁺ + CO ₃ ⁻
Mineral reaction 1	Calcite + H ⁺ = Ca ⁺⁺ + HCO ₃ ⁻
Mineral reaction 2	Dolomite + 2×H ⁺ = Ca ⁺⁺ + Mg ⁺⁺ + 2×HCO ₃ ⁻

Table 7.5 Aqueous species, minerals and reactions modelled in the GEM-GHG 3D model.

This modelling allowed assessment of a number of processes on timescales up to 10 000 years including:

migration of free CO₂ in a dense phase that is primarily controlled by the topography at the top of the Utsira reservoir

dissolution of CO₂ into the formation water due to molecular diffusion

initiation of gravity convection cells in the reservoir. When CO₂ dissolves, pore-waters become denser and sink to the bottom of the reservoir. This process displaces non-CO₂ charged pore waters to the top of the reservoir and these in turn dissolve more CO₂

speciation of the dissolved CO₂ into bicarbonate ions

impact of the bicarbonate ions and the water acidification on the carbonate minerals in the Utsira sand, leading primarily to their dissolution.

After 10 000 years of simulated time, additional carbon is released into the brine (due to the dissolution of carbonate minerals) while all injected CO₂ is trapped through solubility trapping. A cross-section of dolomite changes (Figure 7.41) shows cells (blue colour) where all the dolomite has dissolved. This takes place at the temporary CO₂ plume location and where acidified formation water has circulated towards the

bottom of the reservoir. The impact on porosity and permeability is limited due to the high initial porosity and the low dolomite content of the Utsira Sand.

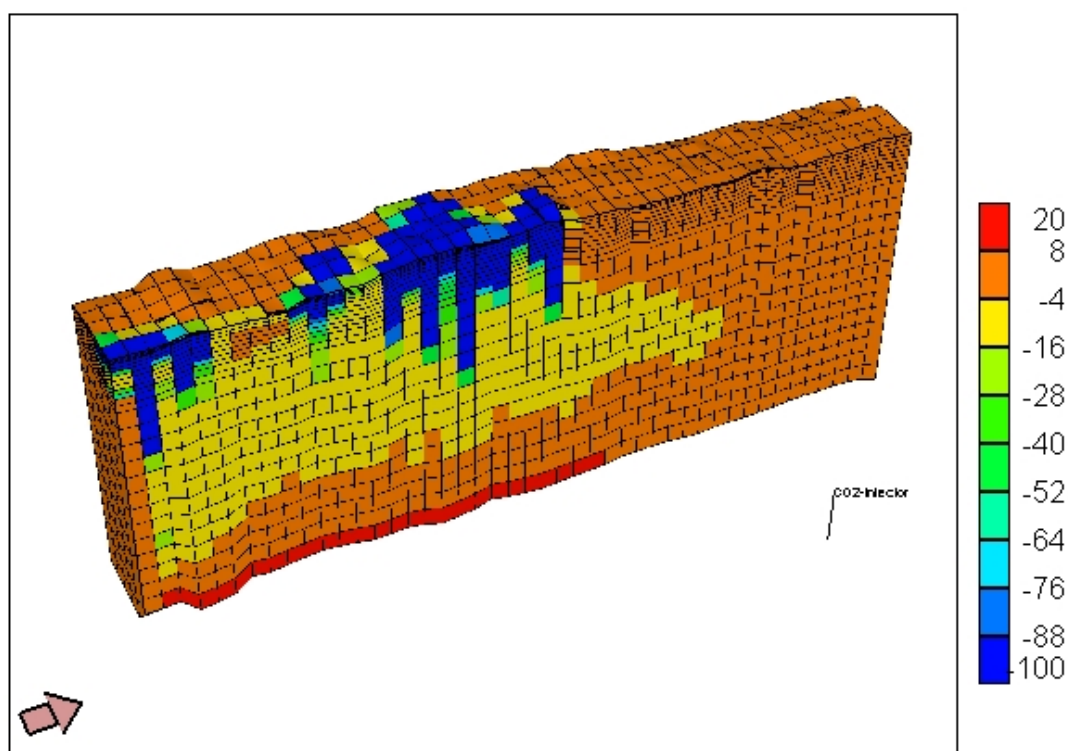


Figure 7.41 Vertical cross-section of the Utsira Sand showing percentage (by volume) of dolomite dissolved or precipitated. After 9500 years, dolomite has been completely dissolved (in blue) in the top of the reservoir (formerly the CO₂ plume location), and in sinking fingers (where denser acid formation water has circulated).

It should be emphasised that this simulation was limited to modelling carbonate reactivity. The lack of Mg⁺⁺ ion donors (coming from the dissolution of other minerals) restricted the possibility of precipitating dolomite. Further work is necessary to model more complex reaction pathways using this approach.

The second modelling strategy utilised 2D (axisymmetric or cylindrical) model geometry but with a detailed geochemical calculator. A 2D two-phase flow model was built around a vertical cylindrical geometrical mesh centred on the injection point using the TOUGHREACT code. CO₂ was injected from a point source located 152 m below the top of the Utsira reservoir (total thickness estimated at 184 m). Interactions with all the minerals (including aluminosilicates) were taken into account. The reservoir sand was assumed to contain four mudstone layers with a lower permeability and porosity. Injection of the CO₂ as a dense phase was modelled for a simulated period of 25 years, with subsequent plume dissolution and migration modelled for a further simulated 10 000 years. The upward migration of free CO₂ affected by the intra-reservoir mudstones and trapped at the top reservoir is well modelled, as is the downward migration of (denser) formation waters with dissolved CO₂ (Figure 7.42).

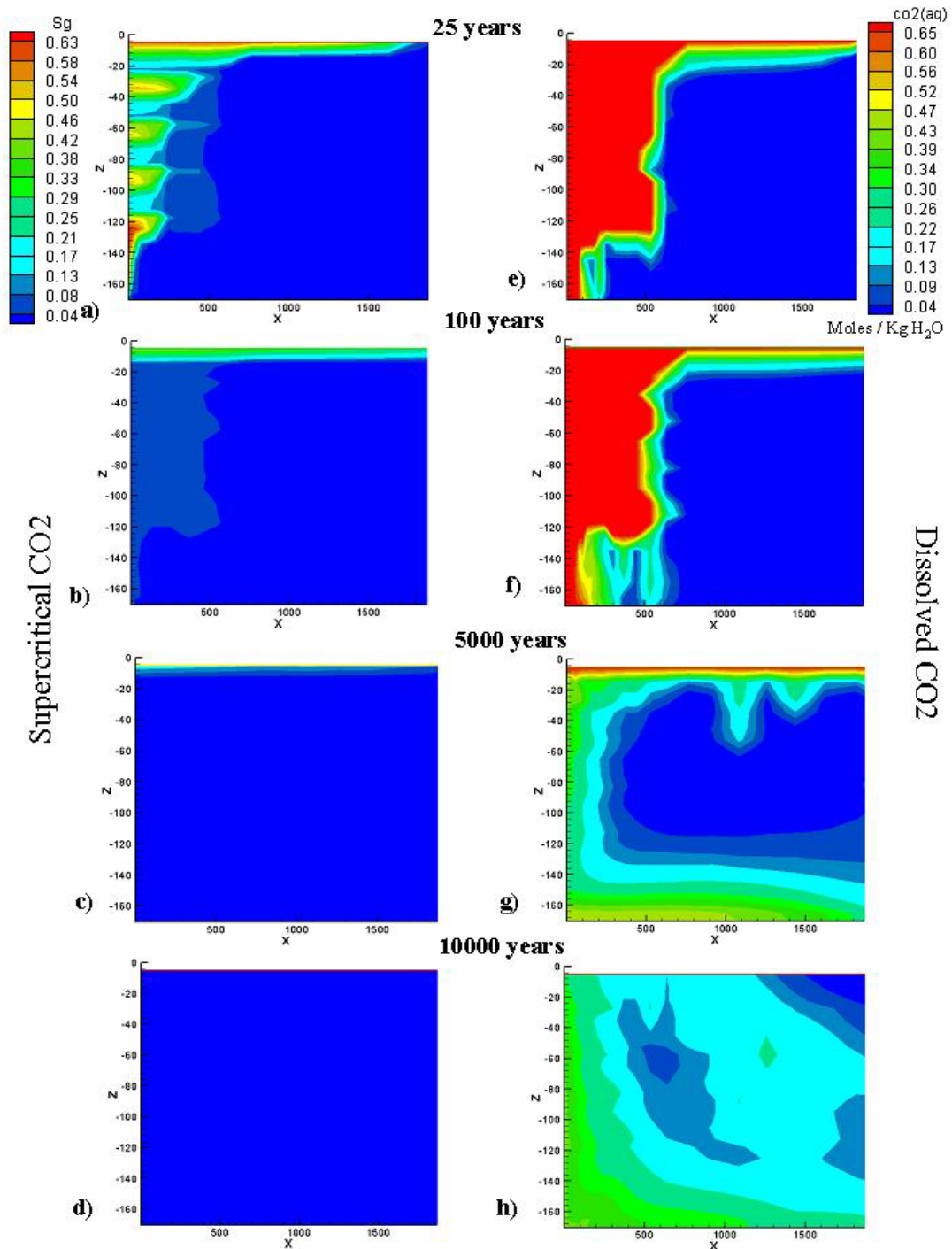


Figure 7.42 Predicted long-term dissolution in the Sleipner plume showing free CO₂ saturations (left) and dissolved CO₂ concentrations (right). Axes are annotated in metres.

Geochemical effects are predicted to be relatively minor in the Utsira reservoir, but nonetheless after 10 000 years the effects of CO₂ dissolution and migration, on pH and on the dissolution of carbonates (calcite) and feldspar can be predicted (Figure 7.43).

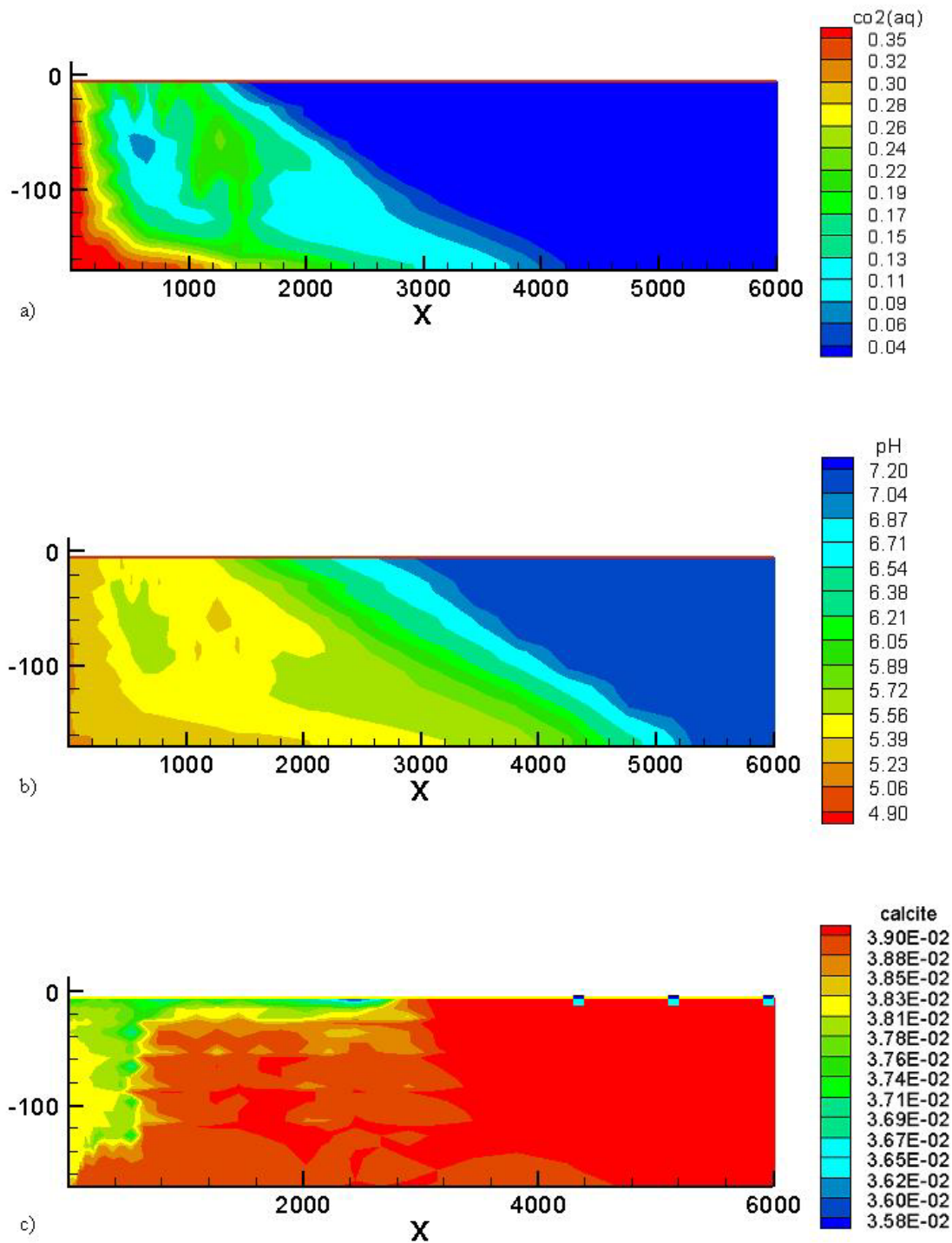


Figure 7. 43 Sleipner plume reactions over 10 000 years. Numerical simulations of a) dissolved CO₂ (in mol per kg H₂O) b) pH decrease c) calcite dissolution (in volume fraction). Axes are annotated in metres.

It is concluded from the reaction-transport modelling that geochemical reactivity will produce only minor mineralogical changes at Sleipner. Most of the changes relate to dissolution of carbonates, which are minor minerals in the Utsira reservoir, so impacts on porosity or permeability would not be very significant.

The overall modelling strategy was a trade-off between 3D modelling capability to account for gravity convection cells and predict realistic spatial localisation of events, and 2D cylindrical models that were able to incorporate silicate mineral reactions as well as the presence of clay layers in the reservoir. With current technology, optimal modelling approaches would probably involve the use of both techniques in a complementary manner.

7.3.1.5 Generic findings

Generalised results from the SACS/CO2STORE simulations are listed below.

Temperature and pressure are very important parameters that have to be known if fluid properties are to be modelled correctly. Thus we recommend that careful temperature and pressure measurements be made in the reservoir in future CO₂-injection projects.

It has been possible to generate reservoir flow models that are qualitatively consistent with a CO₂ plume imaged by the time-lapse seismics.

It has been possible to incorporate complex processes (dissolution, chemical reactions, molecular diffusion) into long-term models for the case studies.

Factors such as residual CO₂ saturation, reservoir heterogeneity, rates of dissolution and fault transport properties are key parameters controlling the long-term migration of CO₂, but are difficult to quantify.

For all timescales the density difference between brine and CO₂ and the viscosities are the dominating fluid parameters. In the long term (> 50 years) the phase behaviour (solubility and density dependence of composition) will become the controlling fluid parameters.

In highly permeable reservoirs where the heterogeneities are dominated by horizontal permeability barriers rather than faults, the heterogeneities will be a controlling parameter only on short timescales (< 25 years) even if the CO₂ is injected deep in the reservoir.

The topography and quality of the reservoir topseal will be the controlling geological parameter on migration of free CO₂ in long-term simulations. Following large-scale dissolution of CO₂, the topography of the base of the reservoir controls migration of dense CO₂-saturated brines.

7.4 Laboratory experiments on well-bore materials

As a first step to assessing well-bore integrity, a laboratory study of well-bore materials from Sleipner was undertaken using techniques based upon those used in previous CO₂ storage projects (e.g. Holloway, 1996; Czernichowski-Lauriol et al., 1996), and during the SACS project (Rochelle et al., 2002a,b; 2004). Use of similar techniques will hopefully allow for better comparison between the various studies.

The experiments utilised realistic borehole materials (samples of casing steel and cement provided by Statoil), and synthetic formation waters based upon measured compositions of nearby fluid samples (Rochelle et al., 2006). The experimental conditions chosen for the investigation were representative of in situ conditions within the lowest part of the Sleipner caprock (30°C, 8 MPa). Experiments were pressurised with either nitrogen (N₂) or CO₂, the former to provide a ‘non reacting’ reference point from which to compare the more reactive CO₂ experiments. However, it is hoped that they will also help to provide increased confidence in estimates of in situ porewater compositions within the Utsira caprock.

Borehole liner experiments involved small billets of steel and ran for two months. All experiments showed some evidence of relatively minor surface oxidation. However, the experiments pressurised with CO₂ produced significant dissolution of the steel in immediate contact with the water phase. Most of this dissolution was concentrated along grain boundaries (Figure 7.44). However, siderite was also observed as a later-stage carbonation reaction product.

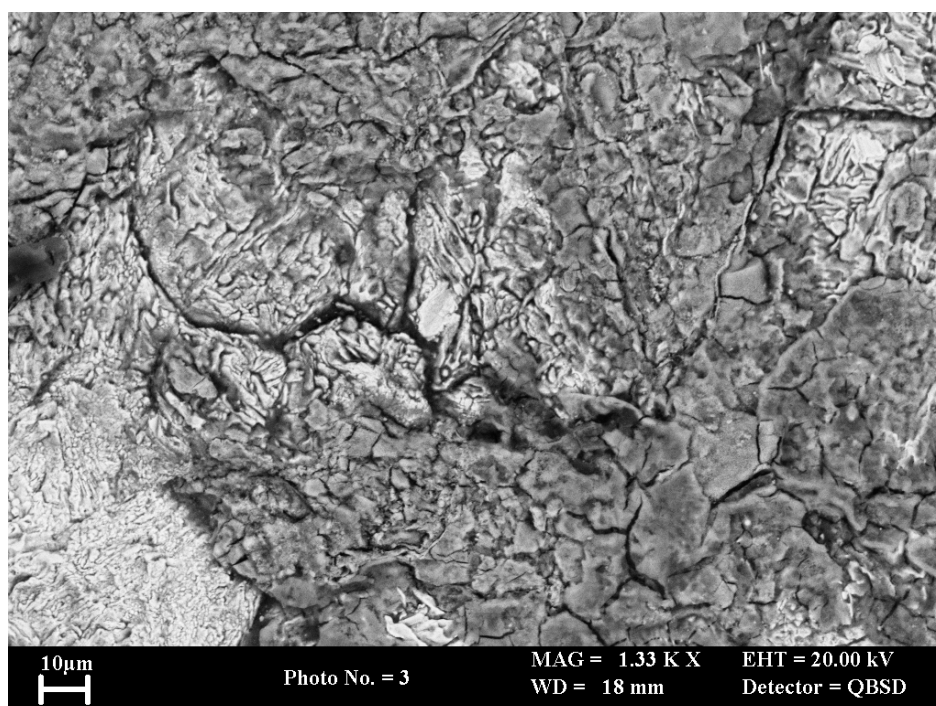


Figure 7.44 BSEM photomicrograph of corroded steel surface showing etched metal surface (bright) with particularly deep etching along intergranular boundaries. Within aqueous phase, CO₂-pressurised experiment Run 1150.

Borehole cement experiments utilised small discs of cement and ran for two months. They produced the greatest reaction seen in this study. The presence of CO₂ initiated significant carbonation reactions on and within the cement samples. These reactions involved the breakdown of portlandite and CSH phases—the two main components of cement. These were replaced by silica gel and calcium carbonate (Figure 7.45), both calcite and vaterite were identified by XRD. Petrographic analysis showed that calcite precipitated on the *surface* of the cement, whilst vaterite and calcite are both probably present as alteration products in the cement matrix. However, significantly enhanced

porosity was found in the very outer parts of the cement, suggesting that overall leaching dominated in these regions. An unexpected observation was the formation of calcium aluminium oxide chloride hydrate (typically $\text{Ca}_4\text{Al}_2\text{H}_{0.34}\text{O}_{6.34}\text{Cl}_{1.67}$), which formed in both N_2 - and CO_2 -pressurised experiments, though it was more common in the latter. It would appear that this phase was the main sink for Al in these experiments—sourced from the dissolution of cement minerals or unhydrated clinker phases. It appears to have formed in preference to dawsonite, as none of the latter was detected.

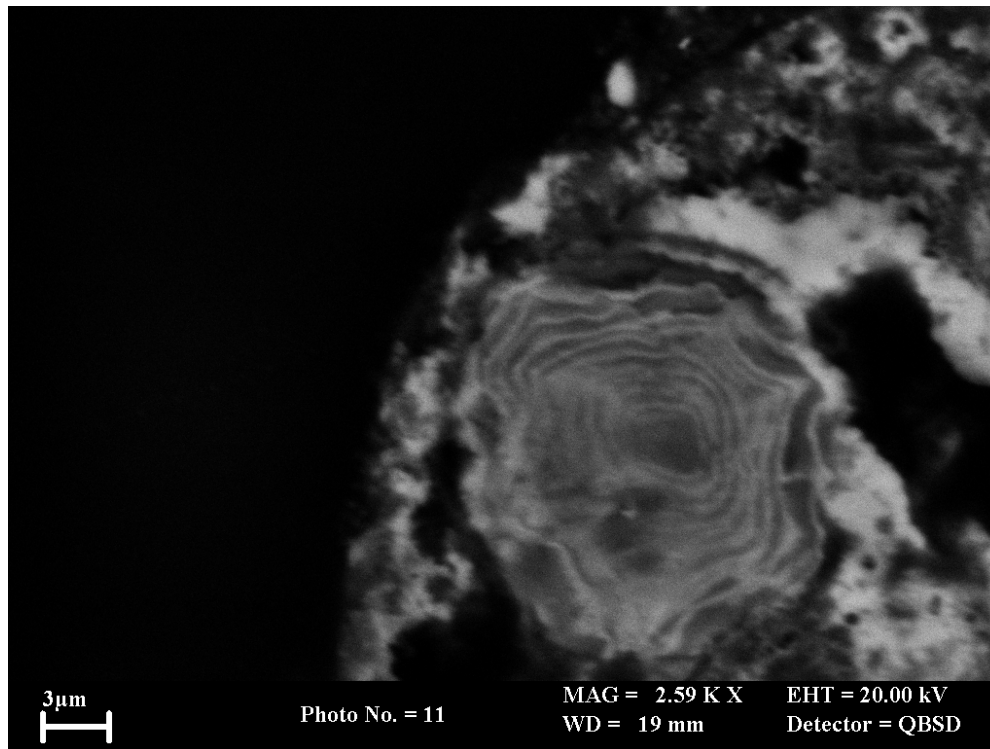


Figure 7.45 BSEM photomicrograph of outer edge of altered cement disk showing dissolution cavities lined by calcium carbonate (light grey) and partially filled by concentrically-banded amorphous silica (dark grey) and low-Ca CSH gel (mid/dull grey). CO_2 -pressurised experiment.

The experiments summarised here ran for up to 15 months. As of late 2007, similar but longer-duration experiments are running. These will be terminated and analysed in the future after they have reacted for several years, hopefully to provide better insights into these slow-acting processes.

8 CLOSURE

The closure phase of a CO₂ storage project forms part of the planned project evolution described in this document. It corresponds simply to the post-injection phase, when planned injection has ceased. This section focuses on the closure and also the post-closure stages and describes some of the issues that may need to be addressed.

For this discussion it is assumed that the project has been undertaken within a regulatory process that includes applications for licences at key stages, which are awarded to the operator by the designated competent national authority, and reflect the major decision points within the project development (e.g. Pearce et al., 2005). The closure phase will be a planned part of the licensing and regulatory process and, to a certain extent, will have been predetermined before injection started. The application to inject CO₂ is likely to have defined the amount of CO₂ to be injected and the predicted time that the injection will finish. Once injection has finished the operator will prepare to close the site. This will include continuation of a number of activities from the injection phase plus others specific to the closure stage. Ongoing activities will include continued monitoring and history matching (see Sections 4.5 and 7.3), and revisions of performance assessment (see Section 7.4) and remediation plans (see Section 4.5).

The closure and post-closure stages are, in some ways, the least well defined in terms of duration and expected activities. This part of the process has not been performed before for CO₂ storage and, though some examples of best practice can be exploited, it is not clear if the approaches taken in other industries (notably for oil and gas activities, radioactive waste, US underground liquid waste disposal or Canadian acid gas injection) are appropriate for CO₂ storage. During the post-injection stage the safety case for the post-closure phase will be revised and finalised, so that any residual liability can be minimised and transferred from the operator to the designated national authority. The duration of the post-closure period is discussed in Section 8.6.

The safety case for the post-closure period should not be based on the prerequisite need for a monitoring regime to guarantee the safety of future generations, since this may be construed as placing an unethical burden on future generations to continue monitoring. Rather, the safety of the site should be based on its inherent qualities established during site selection and characterisation, and confirmed by monitoring during injection. These qualities include the caprock integrity, well-bore abandonment techniques, sealing features such as faults and fractures and operational history (injection pressures, volumes, injection point etc.). Therefore, monitoring should not be needed in the post-closure period. However, it should also be emphasised that monitoring should not be precluded if future generations considered this was worthwhile.

8.1 Closure application

As part of a regulatory process it is likely that an operator will have to apply for permission to close a site. Decommissioning regulations within the oil and gas industry provide examples of how this might be undertaken and the scope of such a closure application. In addition to these requirements, the specific nature of the long-

term secure storage of CO₂ requires careful consideration of certain issues, which include record keeping, data transfer and archiving, decommissioning (see Section 8.3) and performance assessments (see Section 8.2).

The long-term nature of CO₂ storage and the transfer of liability to the state after site closure (Section 8.5) means that very high standards of record keeping are required throughout the project. This is explored further in Stenhouse et al. (2004). An operational log should be maintained throughout the project to comprehensively document the project history. This log and other records should be transferred to the regulator when the site is closed.

The records could include, *inter alia*, the following:

- volumes stored

- project history including:

 - site characterisation

 - application for licence to inject, including environmental impact statements

 - site development

 - injection history

- maps of all surface workings, including remaining infrastructure (pipelines, wellheads, footings, anchor points and concrete pads) and monitoring points (gravity survey markers, soil gas monitoring points)

- infrastructure removal and markers for any remaining infrastructure

- well completion and abandonment histories

- environmental impact statement

- performance assessment

 - review of initial baseline conditions – may be necessary to repeat all or most of the baseline monitoring for EIA

 - latest plume location

 - history matching with injection

 - future site performance

 - assessment to identify risks and their potential impacts.

8.2 Criteria for safe site closure

Key criteria for safe site closure are intimately linked to activities described previously in this report i.e. monitoring, risk assessment, performance assessment and remediation. In this section, issues are discussed that pertain directly to the closure and post-closure periods, making reference to additional discussion elsewhere in the document.

At a generic level, safety criteria can be considered to comprise those of a global nature and those of a local, site-specific nature. Global criteria may be defined by the average global leakage rates, global volumes of CO₂ injected, targets for stabilising atmospheric CO₂ concentration and predicted responses to those atmospheric levels. Several authors have discussed such global criteria (Hepple and Benson, 2005; Dooley and Wise 2003; Lindeberg, 2004), which are summarised in Section 8.6. Leakage rates of less than 0.01% of the volume stored per year seem to be needed in order to ensure that storage meets the fundamental aim of mitigating climate change, with retention times on the order of several thousand to 10 000 years. Note that at Sleipner, reservoir modelling indicates that after about 5000 years, the CO₂ gas cap will have completely dissolved into the brine, the CO₂-saturated pore water then sinking as its density is greater than unsaturated pore water (Section 7.3).

Site-specific criteria are defined by the potential environmental impacts of a leak from a specific site and are discussed in Section 4.5. A leakage rate of 0.01% per year at Sleipner would amount to 2000 tonnes in the first year (assuming a leak occurred after 20 Mt was injected) and decrease yearly after that. It should be emphasised that this is a purely arbitrary rate selected for hypothetical discussion, based on global estimates of minimum leakage rates required to mitigate climate change, and in no way represents a prediction of potential leakage at Sleipner. Such a leakage rate may not have a significant effect on global climate change but may have an impact on the local ecosystem, especially if this leak was concentrated over a small area of the sea bed. Therefore it is likely that local safety criteria are likely to be more stringent than global criteria. More research is needed to establish the likely scale of potential impacts, if any, on a variety of ecosystems (e.g. West et al., 2005).

Two principal aims of performance assessment, described in detail in Section 7.4, are to demonstrate that the total system relevant to CO₂ storage is understood in a sufficiently detailed way that its future potential evolution can be adequately assessed, and to establish under what circumstances leaks may occur and if such leaks pose a risk to humans or ecosystems. Predictions of future site behaviour will have been made prior to injection, based on the geological model derived during initial site characterisation and acquisition of baseline monitoring data. During the injection period the performance assessment is likely to evolve to reflect the greater understanding of the system, obtained through history matching with monitoring data acquired during injection. These predictions will extend to include the post-injection and post-closure periods. Monitoring will continue after injection has finished to validate these predictive models as reservoir pressures decrease and the CO₂ plume migrates. At some point a decision will be made that there is sufficient confidence in the models to predict acceptable future site performance, and monitoring will no longer be needed to validate the safety case. This may be considered a suitable point in time for the operator to close the site and transfer liability back to the national authority. How that point may be reached is discussed below.

8.2.1 Monitoring requirements in the post-injection and post-closure periods

Monitoring aims within the post-injection period can be summarised as follows. Further discussion of the rationale behind monitoring programmes within the post-

closure period are provided in Stenhouse et al. (2004); Pearce et al. (2005) and Pearce et al. (2006). The aims are:

- to verify the mass that continues to be stored
- to determine the mass if any, that is seeping back to the ocean or atmosphere
- to meet local health, safety and environmental (HSE) performance criteria
- to confirm, or otherwise, accuracy of predictive models
- to provide stakeholder confidence, especially during early projects
- to provide evidence that the system will behave as predicted so that the site may be abandoned.

Therefore a key aim of the monitoring programme in the post-injection, pre-closure period will be to provide data to help validate or refine the predictive models once injection has stopped. Expert judgement will be required to decide when sufficient monitoring data has been acquired to enable future site performance to be predicted with confidence, such that the risks to, and their potential impacts on, future generations have been assessed. The design of the monitoring programme, including selection of techniques, monitoring frequency and duration should specifically address the aims. For example, the operator and regulator would need confidence that the data obtained during a post-closure monitoring programme could provide confirmation of reservoir modelling predictions with the least possible ambiguity.

The frequency of monitoring is likely to decrease with time during the post-injection period as confidence in models increases. Clearly, if the system does not behave as predicted, such as if unexpected migration occurs or leaks develop, then the frequency and types of monitoring may increase. This is discussed further in section 8.4.

8.2.1.1 Types of monitoring

Where the storage system is meeting expected performance, the types of monitoring are likely to include (i) CO₂ plume movement, (ii) surface monitoring, (iii) reservoir pressure and (iv) monitoring well integrity following abandonment.

CO₂ plume movement

Monitoring of the CO₂ plume will continue during the post-injection phase, largely to confirm reservoir modelling and the rates of processes such as CO₂ solution and residual trapping. The frequency of this monitoring may decrease with time, reflecting an approach to a steady state and the increasing confirmation of reservoir simulations. For example, typical monitoring intervals during injection at Sleipner have been 4–5 years, and this may continue for a few surveys after injection but then frequencies will decrease perhaps to 10 years or greater between surveys. The location of the monitoring may also change with time as the CO₂ plume migrates and this would be reflected in defining the aerial extent of baseline datasets.

Surface monitoring

Surface monitoring is likely to be required, to demonstrate that operational practices and subsequent decommissioning have complied with the environmental impact statements made during initial application for a site licence and also to provide public confidence in the safety of a site. The surface monitoring may also provide a new baseline with which to compare future site performance, if this were deemed necessary. The types of surface monitoring will depend on the location of the site and specific regulations. For example, onshore surface monitoring is likely to include soil gas surveys which could be focussed on the high risk areas such as around wells or known potential seepage points identified during baseline surveys (Oldenburg et al., 2003b). Data will be compared to baseline data, and where anomalous results are identified these can be investigated further with more detailed sampling or using different analytical techniques.

Reservoir pressure

Monitoring of reservoir pressures could also continue during the post-injection phase, to determine the rate of CO₂ solution and/or migration. Fluid samples could also be analysed to support this. However, it should be noted that changes may occur over very long time periods and the design of any monitoring programme would have to be capable of detecting potentially very subtle changes over long periods of time.

Well integrity

A key activity of the site closure period will be the decommissioning of infrastructure and wells, and subsequent demonstration that the well plugging has been completed successfully. In hydrocarbon fields, wells used for CO₂ injection, as well as abandoned wells, producers, injectors, water-supply boreholes (onshore only), wells passing through reservoir, wells above the reservoir and monitoring wells could be checked for leakage before site closure.

8.2.2 Remediation planning

Remediation options have been discussed in Section 4.4. In the closure period, the operator will be responsible for monitoring site performance and remediating any leaks that occur above predetermined thresholds. The remediation plan could involve increased monitoring, delayed well abandonment, well workovers, new water injection wells and/or retrieving some of the CO₂ from the reservoir. Benson and Hepple (2005) provide a brief overview of some potential approaches to leak remediation, though the economic and technical practicalities of some of the techniques remain to be tested.

When the site is closed, liability for any required remedial actions will be with the designated national authority. It has yet to be decided how remediation in the post-closure period will be funded, several financial mechanisms, based on models in other industries, have been proposed.

A key part of a remediation plan will be to define key trigger events or thresholds, above which remedial plans will be invoked. These trigger events could include pressure thresholds, CO₂ concentration thresholds, or CO₂ migration pathways departing from predicted model expectations above predefined tolerances. These

thresholds could be defined differently for different parts of the system, such as the wells, reservoir, overlying aquifers, sea-bed surface or soil.

8.3 Transfer of liability from operator to national authority

8.3.1 Decommissioning

Current decommissioning practices for UK oil and gas infrastructure are described in guidelines published on the UK DTI (now DBERR) website:

www.og.dti.gov.uk/regulation/guidance/decommission.htm

It is likely that CO₂ injection facilities could follow similar practices, which is to remove almost all of the infrastructure associated with oil and gas production. Any remaining structures on the sea bed are then clearly marked and the regulator informed of their locations as part of the decommissioning approval.

The well abandonment plans are likely to have been agreed with the regulator in advance and would focus on the choice of cements, intervals to be plugged, and subsequent verification. The following section is taken from the UK DTI decommissioning guide notes:

‘Duties set out in the Offshore Installations and Wells (Design and Construction etc) Regulations 1996 also cover the abandonment of wells. These require that wells are suspended and abandoned in a way that ensures there can be no unplanned escape of fluids from a well and that the risks to the health and safety of persons from the well, anything in it, or the strata to which it is connected, are as low as reasonably practicable.’

Note that at Sleipner the risks for CO₂ migration and potential leakage along the injection well are minimised by the strongly deviated, sub-horizontal well, injection close to the base of the Utsira Sand and the topography of the reservoir top, all of which allow CO₂ to migrate away from the injection and production infrastructure.

In some cases permanent monitoring instrumentation and markers may be installed or left following decommissioning. In wells, examples of permanent instrumentation may include geophone arrays for VSP, pressure sensors or even fluid sampling systems. At the surface, pads for gravity surveys, or markers for other key surveys may be retained, so that specific future surveys, if needed, can be made at accurately located points to ensure better constrained comparisons with previous datasets. Such installations allow future generations to continue monitoring, although they should only be considered where their presence does not compromise the long-term integrity of the storage system.

As in natural-gas storage facilities, specifically designed monitoring wells may be considered in some storage projects and may have been drilled and instrumented during the injection phase. In natural-gas storage facilities these wells are terminated in the ‘top aquifer’ immediately above the storage reservoir. The choice of location will be made on the basis of site characterisation and reservoir modelling, both of

which will include inherent uncertainties. Therefore, locating the monitoring well in the correct place and deciding on the correct depth(s) to detect CO₂ migration or leakage, especially over the long-term, is unlikely to be without a degree of uncertainty. Furthermore, the presence of the well, especially if instrumented and connected to the surface, may represent a significant leakage pathway itself.

Although assuming that monitoring would not be required in the post-closure period (see below), Benson et al. (2004) estimated costs for their 'basic' monitoring package over a 1000 year timescale. This 'basic' package involved repeat seismic surveys every ten years. Using an intergenerational discount rate of 1%, monitoring costs only increased by about 10%. For example, for saline aquifer storage, costs rose to \$0.059 per tonne of CO₂ stored, indicating that cost alone would not preclude monitoring being undertaken over such a long period.

The project endpoint is defined by the end of the post-closure period, when the operator transfers site ownership to the state's designated national authority. Due to uncertainties over the long-term existence of operator companies, it is generally assumed that at this point, the state, through the designated national authority, will accept the associated liability for future site performance. Clearly, therefore, the national authority is only likely to accept that liability if the operator can demonstrate that it is as low as possible, and certainly within the terms of the injection and closure licences.

For the purposes of safety assessments it can be assumed that the post-closure period, when the state retains liability for the site, will be divided into a period of active institutional control lasting 100–300 years, reverting thereafter to 'passive' control (Stenhouse et al., 2004).

How long is the site closure period and when will transfer of liability to the state take place? There are several potential ways of approaching this, all of which have their limitations. Pearce et al. (2005) arbitrarily suggested the closure period for a generic project to be up to 100 years, approximately twice the injection period. Other technical reasons can be put forward that may, on a site-specific basis, provide an indication of the appropriate length of time for which post-injection monitoring may be continued. These could include:

The post-injection period could continue until 'equilibrium' or steady-state is reached. The definition of 'equilibrium' is likely to be open to debate and will depend on site-specific conditions such as the degree and rate of CO₂ solution into porewaters, the rate and amount of mineral trapping, of plume migration and of residual trapping. However, such processes could take several thousands of years to reach a steady-state, which would be impractical for monitoring. At Sleipner, reservoir modelling predicts (Section 7.3.1.4) that most of the CO₂ will accumulate in a single layer beneath the topseal within a few decades and that after about 250 years, geochemical processes will dominate over lateral buoyance-driven migration beneath the caprock. Indeed, long-term predictions indicate that within 5000 years or so, the CO₂ plume at Sleipner will completely dissolve in the Utsira formation waters.

The post-injection period could last until reservoir pressures decline to a certain point, after which time the reservoir is secure against geomechanical failure due to internal forces. Chalaturnyk and Gunter (2005) indicate that the timeframe for this is of the order of 100 years. At Weyburn, ambient pressures are reached after approximately 1000 years, though reservoir pressures decline from when injection is stopped (Zhou et al., 2005).

Post-injection monitoring could continue until a predicted event occurs e.g. in the Valleys case, CO₂ was predicted to migrate to the St George's fault, the transmissivity of which is poorly-constrained. It may be decided that site closure and liability transfer would not take place until after CO₂ had reached the fault and it could be shown that no leakage was occurring or likely to occur.

A minimum arbitrary, generic timeframe could be defined, such as twice the injection period. However, this seems difficult to justify from a safety or practical viewpoint.

Similarly, defining the post-injection monitoring period on the time taken for CO₂ to dissolve also seems impractical and lacking a sound basis.

The post-injection period could continue until operators and regulators are sufficiently confident that models used in predicting future site performance have been validated by history matching to monitoring data. This time could vary significantly depending on specific site characteristics and required tolerances in matching models and monitoring data.

8.4 Post-closure issues

The duration of the post-closure phase is defined by the estimated retention time of CO₂ within the reservoir or reservoirs and its ultimate fate (solution, residual trapping, mineral trapping and/or structural trapping). The minimum required duration of CO₂ retention within the reservoir is likely to have been defined or estimated during earlier stages of the licence approval process. Currently this remains an unresolved issue and as such presents some difficult challenges to overcome at international, regional and national levels. Prescribed or estimated minimum retention times may vary between regions depending on local regulations and site-specific geology. However, it is worth noting that although a minimum retention time may be stipulated as part of the licensing process, in a successful storage site CO₂ could remain trapped as a buoyant fluid for up to millions of years, similar to some naturally-occurring fields (e.g. Pearce et al., 2004; Ballentine et al., 2001).

Several authors have approached this problem by assuming that any leaks occurring at any time, which contribute to future climate change, are to be avoided. Hepple and Benson (2005) compared potential global storage volumes to extrapolated versions of the IPCC marker emission scenarios and defined acceptable seepage rates through comparison with allowable global emissions to stabilise atmospheric CO₂ at various concentrations. Assuming a seepage rate of 0.01% of total stored per year, at least 90% of the CO₂ would remain trapped for 1000 years. By simulating various fracture or well-bore leakage scenarios, and comparing them with selected, published

atmospheric CO₂ concentration targets, Lindeberg (2003) estimated that storage durations of between 4000 and 10 000 years will be needed to avoid significant future climate change.

It is important to emphasise that the above leakage criteria are not based on any geological considerations. Current understanding of geological containment, suggests that a properly selected, characterised and operated site should retain stored CO₂ indefinitely.

REFERENCES

- AKERVOLL, I, ZWEIGEL, P, and LINDEBERG, E. 2006. CO₂ storage in open, dipping aquifers. Extended abstract, 8th Conference on Greenhouse Gas Control Technologies (GHGT-8), June 2006, Trondheim. 6pp.
- ALKHALIFAH, T, and TSVANKIN, I. 1995. Velocity analysis for transversely isotropic media. *Geophysics*, Vol. 60, 1550–1566.
- ARTS, R, BREVIK, I, EIKEN, O, SOLLIE, R, CAUSSE, E, and VAN DER MEER, B. 2000. Geophysical methods for monitoring marine aquifer CO₂ storage - Sleipner experiences. 366–371 in WILLIAMS, D J, ET AL. (editors). *Greenhouse Gas Control Technologies*. (Collingwood, Australia: CSIRO Publishing.)
- ARTS, R, EIKEN, O, CHADWICK, R A, ZWEIGEL, P, VAN DER MEER, L, and ZINSZNER, B. 2004a. Monitoring of CO₂ injected at Sleipner using time-lapse seismic data. *Energy*, Vol. 29, 1383–1393. (Oxford: Elsevier Science Ltd.)
- ARTS, R, EIKEN, O, CHADWICK, R A, ZWEIGEL, P, VAN DER MEER, L, and KIRBY, G A. 2004b. Seismic monitoring at the Sleipner underground CO₂ storage site (North Sea). 181–191 in BAINES, S, GALE, J, and WORDEN, R J (editors). *Geological Storage for CO₂ emissions reduction. Special Publication of the Geological Society of London*, No. 233.
- AUDIGANE, P, GAUS, I, PRUESS, K, and XU, T. 2005. Reactive transport modeling using TOUGHREACT of the long term CO₂ storage at Sleipner, North Sea. Proceedings of the Fourth Annual Conference on Carbon Sequestration, Alexandria (Virginia).
- BACHU, S, GUNTER, W D, and PERKINS, E H. 1994. Aquifer disposal of CO₂: hydrodynamic and mineral trapping. *Energy Conversion and Management*, Vol. 35, 269–279.
- BACHU, S, and SHAW, J. 2003. Evaluation of the CO₂ Sequestration Capacity in Alberta's Oil and Gas Reservoirs at Depletion and the Effect of Underlying Aquifers. *Canadian Journal of Petroleum Technology*, Vol. 42(9), 51–61.
- BAKLID, A, KORBUL, R, and OWREN, G. 1996. Sleipner Vest CO₂ disposal, CO₂ injection into a shallow underground aquifer. SPE paper 36600, presented at 1996 SPE Annual Technical Conference and Exhibition, Denver Colorado, USA, 6–9 October 1996.
- BALLENTINE, C J, SCHOELL, M, COLEMAN, D, and CAIN, M A. 2001. 300-Myr-old magmatic CO₂ in natural gas reservoirs of the west Texas Permian basin. *Nature*, Vol. 409 (6818), 327–331.
- BATEMAN, K, TURNER, G, PEARCE, J M, NOY, D J, BIRCHALL, D, and ROCHELLE, C A. 2005. Large-scale column experiment: Study of CO₂, pore water, rock reactions and model test case. Oil and Gas Science and Technology – Revue de l'IFP (Proceedings of International Conference on Gas-Water-Rock Interactions Induced by Reservoir Exploration, CO₂ Sequestration and Other Geological Storage, held at IFP, Paris, France, 18–20 November 2003). 60, (1), 161–175.
- BAUMANN, M, CZYCHOWSKI, M, ESTENFELDER, P, HECHT, G, HÖLTING, B, KAIMER, MICHEL, G, MODEL, J, PATZKE, B, ROTTKE, A, SCHLOZ, W, ULRICH, W, WENGER, W, and SCHERLER, C. 1998. Richtlinien für Heilquellenschutzgebiete. LAWA, Länderarbeitsgemeinschaft Wasser, 27 S, Berlin (Kulturbuch).
- BECH, N, and LARSEN, P. 2003. Simulation of CO₂ storage in the Havnsø aquifer. *Danmarks og Grønlands Geologiske Undersøgelse Rapport 2003/46*, 17 pp.
- BECH, N, and LARSEN, P. 2005. Storage of CO₂ in the Havnsø aquifer – a simulation study. *Danmarks og Grønlands Geologiske Undersøgelse Rapport 2005/9*, 33 pp.

- BENSON, S M, HEPPLE, R, APPS, J, TSANG, C F, and LIPPMANN, M. 2002. Lessons learned from natural and industrial analogues for storage of carbon dioxide in deep geological formations. Report nr. LBNL-51170, Lawrence Berkeley National Laboratory, Berkeley, USA.
- BENSON, S M, GASPERKOVA, E, and HOVERSTEN, G M. 2004. Overview of monitoring techniques and protocols for geologic storage projects. IEAGHG R & D Report No. PH4/29, 89pp.
- BENSON, S M, and HEPPLE, R. 2005. Detection and options for remediation of leakage from underground CO₂ storage projects. 1329–1335 in WILSON, M, MORRIS, T, GALE, J, and THAMBIMUTHU, K (editors). Proceedings of the Greenhouse Gas Control Technologies Conference (GHGT7), Vancouver, September 2004. Vol II.
- BERTELTSEN, F. 1980. Lithostratigraphy and depositional history of the Danish Triassic. *Geological Survey of Denmark*. Series B 4, 59 pp.
- BLYSTAD, P, BREKKE, H, FÆRSETH, RH, LARSEN, B T, SKOGSEID, J, and TØRUBAKKEN, B. 1995. Structural elements of the Norwegian continental shelf, Part II: The Norwegian Sea Region. *Norwegian Petroleum Directorate Bulletin*, No. 8, 45pp.
- BØE, R, MAGNUS, C, OSMUNDSEN, P T, and RINDSTAD, B I. 2002. CO₂ point sources and subsurface storage capacities for CO₂ in aquifers in Norway. NGU Report 2002. 010, 132pp.
- BORGOS, H G, and SONNELAND, L. 2003. Super-resolution mapping of thin gas pockets. EAGE 65th Conference and Exhibition, Stavanger, Norway, 2–5 June 2003.
- BREKKE, H, SJULSTAD, H I, MAGNUS, C, and WILLIAMS, R W. 2001. Sedimentary environments offshore Norway – an overview. 7–37 in MARTINSEN, O J, and DREYER, T (editors). Sedimentary environments offshore Norway – Palaeozoic to Recent. *NPF Special Publication*, No. 10. (Amsterdam: Elsevier.)
- BREVIK, I, EIKEN, O, ARTS, R J, LINDEBERG, E, and CAUSSE, E. 2000. Expectations and results from seismic monitoring of CO₂ injection into a marine aquifer. 62nd EAGE meeting, Glasgow, paper B-21.
- BROOKS, M, TRAYNER, P M, and TRIMBLE, T J. 1988. Mesozoic reactivation of Variscan thrusting in the Bristol Channel area, UK. *Journal of the Geological Society of London*, Vol. 145, 439–444.
- BUGGE, T, KNARUD, R, and MØRK, A. 1984. Bedrock geology on the mid-Norwegian continental margin. 271–283 in Norwegian Petroleum Society. *Petroleum geology of the North European Margin*. (Graham and Trotman.)
- CARLSEN, I M, MMJAALAND, S, and NYHAVN, F. 2001. SACS2: Work Package 4—Monitoring well scenarios. *SINTEF Petroleum Research Report*, 32.1021.00/01/01. 43pp.
- CHADWICK, R A, ARTS, R, EIKEN, O, KIRBY, G A, LINDEBERG, E, and ZWEIGEL, P. 2004. 4D seismic imaging of an injected CO₂ bubble at the Sleipner Field, central North Sea. 305–314 in *3D Seismic Technology: Application to the Exploration of Sedimentary Basins*. DAVIES, R J, CARTWRIGHT, J A, STEWART, S A, LAPPIN, M, and UNDERHILL, J R (editors). *Memoir of the Geological Society of London*, No. 29.
- CHADWICK, R A, ZWEIGEL, P, GREGERSEN, U, KIRBY, G A, JOHANNESSEN, P N, and HOLLOWAY, S. 2004. Characterisation of a CO₂ storage site: The Utsira Sand, Sleipner, northern North Sea. *Energy*, Vol. 29, 1371–1381.
- CHADWICK, R A, ARTS, R, and EIKEN, O. 2005. 4D seismic quantification of a growing CO₂ plume at Sleipner, North Sea. 1385–1399 in *Petroleum Geology: North West Europe and Global Perspectives*. DORE, A G, and VINING, B (editors). Proceedings of the 6th Petroleum Geology Conference. Petroleum Geology Conferences Ltd. Geological Society, London.

- CHADWICK, R A, NOY, D, LINDEBERG, E, ARTS, R, EIKEN, O, and WILLIAMS, G. 2006. Calibrating reservoir performance with time-lapse seismic monitoring and flow simulations of the Sleipner CO₂ plume. *Proceedings of the 8th International Conference on Greenhouse Gas Control Technologies*, Trondheim, Norway, 19–22 June, 2006. ISBN 0 08 046407 6. Elsevier, published on CD.
- CHALATURNYK, R, ZHOU, W, STENHOUSE, M, SHEPPARD, M, and WALTON, F. 2004. Theme 4: Long-term risk assessment of the storage site. In *IEA Weyburn CO₂ monitoring and storage project, Summary report 2000–2004*. WILSON, M, and MONEA, M. Petroleum Technology Research Centre.
- CHALATURNYK, R, and GUNTER, W D. 2005. Geological storage of CO₂: time frames, monitoring and verification. 623–631 in *Proceedings of the Greenhouse Gas Control Technologies Conference (GHGT7)*, Vancouver. RUBIN, E S, KEITH, D, and GILBOY, C F (editors). September 2004. Volume I.
- CHRISTENSEN, N P, and HOLLOWAY, S (compilers). 2004. Geological Storage of CO₂ from Combustion of Fossil Fuel, Summary Report of the European Union Fifth Framework Programme for Research and Development, Project No. ENK6-CT-1999-00010. Geological Survey of Denmark and Greenland, Copenhagen.
- CZERNICHOWSKI-LAURIOL, I, SANJUAN, B, ROCHELLE, C, BATEMAN, K, PEARCE, J, and BLACKWELL, P. 1996a. Analysis of the geochemical aspects of the underground disposal of CO₂: scientific and engineering aspects. 565–583 in *Deep Injection disposal of hazardous and industrial waste*. APPS, J A, and TSANG, C (editors). (Academic Press.)
- CZERNICHOWSKI-LAURIOL, I, SANJUAN, B, ROCHELLE, C, BATEMAN, K, PEARCE, J, and BLACKWELL, P. 1996b. Inorganic geochemistry. 183–276 in *The Underground Disposal of Carbon Dioxide*. Final report of the Joule II project No. CT92-0031. HOLLOWAY, S (editor). (Nottingham : British Geological Survey.)
- DALEY, T M, MYER, L R, HOVERSTEN, G M, PETERSON, J E, and KORNEEV, V A. 2006. Borehole seismic monitoring of injected CO₂ at the Frio site. Extended abstract, 8th Conference on Greenhouse Gas Control Technologies (GHGT-8), June 2006, Trondheim. 6pp.
- DALLAND, A, WORSLEY, D, and OFSTAD, K. 1988. A lithostratigraphic scheme for the Mesozoic and Cenozoic succession offshore mid- and northern Norway. NPD-Bulletin no 4, 65pp.
- DOOLEY, J J, and WISE, M A. 2003. Retention of CO₂ in geologic sequestration formations: Desirable levels, economic considerations and the implications for sequestration R & D. 273–278 in *Greenhouse Gas Control Technologies*. GALE, J, and KAYA, Y (editors). Proceedings of the 6th International Conference on Greenhouse Gas Control Technologies, Kyoto, Japan, October 2002, Vol. 1. (Oxford, UK: Pergamon.)
- DURST, P, and GAUS, I. 2005. Geochemical modelling of the CO₂ impact on the Schwarze Pumpe caprock and reservoir. CO2STORE Task 1.3. BRGM Report BRGM/RP-53987-FR.
- EIKEN, O, BREVIK, I, ARTS, R, LINDEBERG, E, and FAGERVIK, K. 2000. Seismic monitoring of CO₂ injected into a marine aquifer. SEG Calgary 2000 International conference and 70th Annual meeting, Calgary, paper RC-8.2.
- EIKEN, O, STENVOLD, T, ZUMBERGE, M, and NOONER, S. 2003. Gravity monitoring at Sleipner CO₂ injection site: Report on 2002 baseline survey. Statoil Technical Report, 22pp.
- ENNIS-KING, J, and PATERSON, L. 2003. Rate of dissolution due to convective mixing in the underground storage of carbon dioxide. 507–510 in *Greenhouse Gas Control Technologies*. GALE, J, and KAYA, Y (editors). Proceedings of the 6th International Conference on Greenhouse Gas Control Technologies, Kyoto, Japan, October 2002, Vol. 1. (Oxford, UK: Pergamon.)
- EVANS, D J, WILLIAMS, G, VINCENT, C, HOLLOWAY, S, and CHADWICK, R A. 2004. An Appraisal of Offshore CO₂ Repositories for a Planned CGCCS Power Plant in South Wales. *British Geological Survey Commissioned Report*, CR/04/017C.

- FABRIOL, H. 2001. Feasibility study of microseismic monitoring at Sleipner (SACS Project Task 5.8). *BRGM Commissioned Report*, BRGM/RP-51293-FR (Confidential).
- FISCHER, G J. 1992. The determination of permeability and storage capacity: Pore pressure oscillation method. 187–212 in *Fault Mechanics and Transport Properties of Rocks*. EVANS, B, and WONG, T F (editors). (San Diego, California: Academic.)
- FISCHER, G J, and PATERSON, M S. 1992. Measurement of permeability and storage capacity in rocks during deformation at high temperature and pressure. 213–252 in *Fault Mechanics and Transport Properties of Rocks*. EVANS, B, and WONG, T F (editors). (San Diego, California: Academic.)
- FRANGEUL, J, NGHIEM, L, CAROLI, E, and THIBEAU, S. 2004. Sleipner/Utsira CO₂ Geological Storage Full Field Flow and Geochemical Coupling to Assess the Long Term Fate of the CO₂. AAPG Annual Meeting, Dallas USA, April 18–21, 2004.
- FREUND, P, and DAVISON, J. 2002. *General overview of costs*. Proceedings of Workshop on carbon dioxide capture and storage, Intergovernmental Panel on Climate Change, 79–94.
- GAUS, I. 2005. Geochemical modelling of the potential impact of CO₂ injection in the St George's Channel Basin (UK). CO2STORE Task 1.3. *BRGM Commissioned Report*, BRGM/RP-54057-FR.
- GAUS, I, AZAROUAL, M, and CZERNICHOWSKI-LAURIOL, I. 2005. Reactive transport modelling of the impact of CO₂ injection on the clayey caprock at Sleipner (North Sea). *Chemical Geology*, Vol. 217, 319–337.
- GEO-SEQ. 2004. *Geologic Carbon Dioxide Sequestration: Site Evaluation to Implementation*. GEO-SEQ Best Practices Manual.
- GOODWAY, B, CHEN, T, and DOWNTON, J. 1998. AVO and prestack inversion. Presented at: Annual Meeting Canadian Society of Exploration Geophysicists.
- HAMBERG, L, and NIELSEN, L H. 2000. Shingled, sharp-based shoreface sandstones and the importance of stepwise forced regression in a shallow basin, Upper Triassic Gassum Formation, Denmark. 69–89 in *Sedimentary responses to forced regressions*. HUNT, D, and GAWTHORPE, T L (editors). *Geological Society of London Special Publication*, No. 172.
- HAMBORG, M, KIRBY, G A, LOTHE, A E, and ZWEIGEL, P. 2003. Seismic mapping and simulation of CO₂ migration in the upper Utsira sand wedge east of the Sleipner injection site. *SINTEF Petroleum Research Report*, 33.5324.00/03/03, 42 pp.
- HARRINGTON, J F, NOY, D J, BIRCHALL, D J and HORSEMAN, S T. 2006. A Laboratory study of the Nordland Shale: Final Report. *British Geological Survey Commissioned Report*, CR/07/158.
- HARRINGTON, J F, NOY, D J, HORSEMAN, S T, BIRCHALL, D J, and CHADWICK, R A. (in press). Laboratory study of gas and water flow in the Nordland Shale, Sleipner, North Sea. In *Carbon Dioxide Sequestration in Geological Media*. GROBE, M, PASHIN, J, and DODGE, R (editors). *Special Publication of the American Association of Petroleum Geologists*.
- HENDRIKS, C, and EGBERTS, P. 2003. Carbon dioxide sequestration systems: economic evaluation and case studies. In *Geological Storage of CO₂ from Combustion of Fossil Fuel*. EU 5th Framework Programme. Project No. ENK6-CT-1999-00010. Summary Report (2nd Edition).
- HEPPLE, R P, and BENSON, S M. 2003. Implications of surface seepage on the effectiveness of geological storage of carbon dioxide as a climate change mitigation strategy. 261–266 in *Greenhouse Gas Control Technologies*. GALE, J, and KAYA, Y (editors). Proceedings of the 6th International Conference on Greenhouse Gas Control Technologies, Kyoto, Japan, October 2002, Vol. 1 (Oxford, UK: Pergamon.)

- HEPPLE, R P, and BENSON, S M. 2005. Geologic storage of carbon dioxide as a climate change mitigation strategy: performance requirements and the implications of surface seepage. *Environmental Geology*, Vol. 47(4), 576–585.
- HILDENBRAND, A, SCHLÖMER, S, KROOSS, B M, and LITTKE, R. 2004. Gas breakthrough experiments on pelitic rocks: comparative study with N₂, CO₂ and CH₄. *Geofluids*, Vol. 4, 61–80.
- HOEM, B (editor). 2005. *The Norwegian Emissions Inventory*. (Oslo-Kongsvinger: Statistik Sentralbyrå.)
- HOLLOWAY, S (editor). 1996. *The Underground Disposal of Carbon Dioxide*. Final report of the Joule II project No. CT92-0031. (Keyworth, Nottingham: British Geological Survey.)
- IPCC. 2005. *Carbon Dioxide Capture and Storage. Special Report of the Intergovernmental Panel on Climate Change*. (Cambridge: Cambridge University Press.) ISBN 13 978 0 521 86643 9.
- ISO/IEC. 2002. *Guide 73, Risk management – Vocabulary – Guidelines for use in standards*. (Geneva, Switzerland: ISO/IEC.)
- JAKOBSEN, K T. 2005. Anvendelse af geologisk lagring af CO₂ i Danmark. Unpublished Masters Thesis, Økonomisk Institut, Københavns Universitet.
- JOHANSEN, M, POULSEN, H, SKJÆRAN, H, STRAUME, T, and THORSPLASS, J O. 1988. Froanbassengets dannelse og Jurassiske sedimenter. Internal project report NTNU.
- KELLY, S R A. 1988. Middle Jurassic marine macrofauna from erratics in Trøndelag, Norway. Unpublished Internal NTNU report, 33 pp.
- KEMP, S J, BOUCH, J, and MURPHY, H M. 2001. Mineralogical characterisation of the Nordland Shale, UK Quadrant 16, Northern North Sea. *British Geological Survey Commissioned Report*, CR/01/136.
- KEMP, S J, PEARCE, J M, and STEADMAN, E J. 2002. Mineralogical, geochemical and petrographical characterisation of Nordland Shale cores from well 15/9-A-11, Sleipner field, northern North Sea. *British Geological Survey Commissioned Report*, CR/02/313.
- KEMP, S J, and BOUCH, J E. 2004. Mineralogical and petrographic characterisation of reservoirs and caprocks from the St George's Channel Basin, Irish Sea. *British Geological Survey Commissioned Report*, CR/04/130.
- KIKUTA, K, HONGO, S, TANASE, D, and OHSUMI, T. 2005. Field test of CO₂ injection in Nagaoka, Japan. 1367–1372 in *Greenhouse Gas Control Technologies. Volume II Contributed Papers and Panel Discussion*. RUBIN, E S, KEITH, D W, and GILBOY, C F (editors). (Oxford: Elsevier Science Ltd.)
- KOCKEL, F, and KRULL, P. 1995. Endlagerung stark wärmeentwickelnder radioaktiver Abfälle in tiefen geologischen Formationen Norddeutschlands. Untersuchung und Bewertung von Salzformationen, BGR, Berlin.
- KRANZ, R L, SALTZMAN, J S, and BLACIC, J D. 1990. Hydraulic diffusivity measurements on laboratory rock samples using an oscillating pore pressure method. *International Journal of Rock Mechanics and Mineral Science. Geomechanical*, Vol. 27, 345–352.
- KRISTENSEN, L, and BIDSTRUP, T. 2001. Determination of the natural fluid flow in the Utsira Sand reservoir using basin modelling. SACS Project: Final Technical Report of Task 1.6. GEUS Report 2001/2.
- KRUSHIN, J T. 1997. Seal capacity of nonsmectite shale. 31–47 in *Seals, Traps, and the Petroleum System*. SURDAM, R C (editor). *American Association of Petroleum Geologists*, Memoir 67.

- LARSEN, M, BECH, N, BIDSTRUP, T, CHRISTENSEN, N P, and BIEDE, O. 2007. Kalundborg case study, a feasibility study of CO₂ storage in onshore saline aquifers. *Danmarks og Gronlands Geologiske Undersogelse Rapport*, 2007/2, 79 pp.
- LESCOFFIT, S. 2004. Comparison of the CO₂ pocket thicknesses interpreted by 3 different methods on the 99 seismic dataset Sleipner. CO2STORE. *SINTEF Petroleum Research Report*, IK54527240_1 (internal).
- LINDEBERG, E. 1997. Escape of CO₂ from aquifers. *Energy Conversion and Management*, Vol. 38, Supp., S235–S240.
- LINDEBERG, E. 2003. The quality of a CO₂ repository: What is the sufficient retention time of CO₂ stored underground? 255–260 in *Greenhouse Gas Control Technologies*. GALE, J, and KAYA, Y (editors). Proceedings of the 6th International Conference on Greenhouse Gas Control Technologies, Kyoto, Japan, October 2002, Vol. 2 (Oxford, UK: Pergamon.)
- LINDEBERG, E, CAUSSE, E, and GHADERI, A. 1999. Evaluations of to what extent CO₂ accumulations in the Utsira formations are possible to quantify by seismic by August 1999. *SINTEF Petroleum Research Report*, 54.5148.00/01/99, 13pp.
- LIU, E, LI, X Y, and CHADWICK, R A. 2001. Saline Aquifer Storage: A Demonstration Project at the Sleipner Field. Work Area 5 (Geophysics) – Multi-component seismic monitoring of the CO₂ gas cloud in the Utsira Sand: a feasibility study. *British Geological Survey Commissioned Report*, CR/01/064.
- LUNDIN, E, POLAK, S, BØE, R, ZWEIGEL, P, and LINDEBERG, E. 2005. Storage potential for CO₂ in the Froan Basin area of the Trøndelag Platform, Mid- Norway. *Norges Geologiske Undersøkelse Report* 2005.027, 49 pp.
- MAUL, P, and SAVAGE, D. 2004. The IEA Weyburn CO₂ Monitoring and Storage Project: Assessment of Long-term Performance and Safety, QRS-1060, Quintessa.
- MAY, F, MÜLLER, C, and BERNSTONE, C. 2005. How much CO₂ can be stored in deep saline aquifers in Germany? VGB PowerTech 6/2005, 32–37.
- MCKENNA, J J. 2004. Seismic Response to CO₂ Storage in a Saline Aquifer. Unpublished PhD Thesis, Curtin University of Technology.
- MCKENNA, J J, GUREVICH, B, UROSEVIC, M, and EVANS, B J. 2003. Rock physics – application to geological storage of CO₂. *Australian Petroleum Production and Exploration Association Journal*, Vol. 43, 567–576.
- MICHELSSEN, O. 1975. Lower Jurassic biostratigraphy and ostracods of the Danish Embayment. *Danmarks Geologiske Undersøgelse II. Række* 104, 287 pp.
- MICHELSSEN, O. 1978. Stratigraphy and distribution of Jurassic deposits of the Norwegian–Danish Basin. *Danmarks Geologiske Undersøgelse Serie B*, 2, 28 pp.
- MICHELSSEN, O (editor). 1981. Kortlægning af potentielle geotermiske reservoirer i Danmark. *Danmarks Geologiske Undersøgelse Serie B*, 5, 28 pp.
- MICHELSSEN, O, and CLAUSEN, O R. 2002. Detailed stratigraphic subdivision and regional correlation of the southern Danish Triassic succession. *Marine and Petroleum Geology*, Vol. 19, 563–587.
- MICHELSSEN, O, NIELSEN, L H, JOHANNESSEN, P N, ANDSBJERG, J, and SURLYK, F. 2003. Jurassic lithostratigraphy and stratigraphic development onshore and offshore Denmark. 147–216 in *The Jurassic of Denmark and Greenland*. INESON, J R, and SURLYK, F (editors). *Geology of Denmark Survey Bulletin*, No. 38.
- MOUGIN, P. 2002. Excel Dynamic Library for computing density and compressibility (isothermal and isentropic) of CO₂, CH₄ mixtures. IFP Commissioned Report SACS-WP7, 4pp.

- MØRK, M B, JOHNSEN, S O, and TORSÆTER, O. 2003. Porosity and permeability examination of Jurassic samples from Froøyane. Unpublished report, 5pp.
- MOUGIN, P, RASOLOFASAON, P, and ZINSZNER, B. 2002. Petroacoustics of poorly consolidated reservoir rocks saturated with CO₂/Methane/Brine Mixtures. IFP Commissioned Report SACS-WP7, 26pp.
- NASCENT PROJECT. www.bgs.ac.uk/nascent/
- NEA WORKING GROUP. 1997. *Lessons Learnt from Ten Performance Assessment Studies, Paris, France.* (Paris: Nuclear Energy Agency.)
- NIELSEN, L H. 2003. Late Triassic – Jurassic development of the Danish Basin and the Fennoscandian Border Zone, southern Scandinavia. 459–526 in *The Jurassic of Denmark and Greenland*. INESON, J R, and SURLYK, F (editors). NIELSEN, L H, and JAPSEN, P. 1991. Deep wells in Denmark 1935–1990. Lithostratigraphic subdivision. *Geological Survey Geology of Denmark Survey Bulletin*, No. 38.
- NIELSEN, L H, LARSEN, F, and FRANDBEN, N. 1989. Upper Triassic–Lower Jurassic tidal deposits of the Gassum Formation on Sjælland, Denmark. *Geological Survey of Denmark. DGU Series A,23*, 30pp.
- NIELSEN, L H, AND JAPSEN, P. 1991. Deep wells in Denmark 1935–1990. Lithostratigraphic subdivision. *Danmarks Geologiske Undersøgelse Serie A31*, 179 pp.
- NOONER, S, ZUMBERGE, M, EIKEN, O, STENVOLD, T, and THIBEAU, S. 2006. *Constraining the density of CO₂ within the Utsira formation using time-lapse gravity measurements.* Proceedings of the 8th International conference on Greenhouse Gas Control Technologies (GHGT-8), Trondheim, Norway, June 2006.
- NOONER, S L, EIKEN, O, HERMANRUD, C, SASAGAWA, G S, STENVOLD, T, and ZUMBERGE, M A. 2007. Constraints on the in situ density of CO₂ within the Utsira formation from time-lapse seafloor gravity measurements. *International Journal of Greenhouse Gas Control*, Vol. 1, 198–214. (Oxford, UK: Elsevier.)
- NORDHAGEN, R. 1921. Fossilførende blokker fra Juratiden på Froøyene utenfor Trondheimsfjorden. *Naturen*, Vol. 45, 110–115.
- OB DAM, A, VAN DER MEER, L, MAY, F, KERVEVAN, C, BECH, N, and WILDENBORG, A. 2003. Effective CO₂ storage capacity in aquifers, gas fields, oil fields and coal fields. 339–344 in *Greenhouse Gas Control Technologies*. GALE, J, and KAYA, Y (editors). Proceedings of the 6th International Conference on Greenhouse Gas Control Technologies, Kyoto, Japan, October 2002, Vol. 1. (Oxford, UK: Pergamon.)
- OLDENBURG, C M, LAW, D H-S, LE GALLO, Y, and WHITE, S P. 2003a. Mixing of CO₂ and CH₄ in gas reservoirs: code comparison studies. 443–448 in *Greenhouse Gas Control Technologies*. GALE, J, and KAYA, Y (editors). Proceedings of the 6th International Conference on Greenhouse Gas Control Technologies, Kyoto, Japan, October 2002, Vol. 1. (Oxford, UK: Pergamon.)
- OLDENBURG, C M, LEWICKI, J L, and HEPPLER, R P. 2003b. Near-surface monitoring strategies for geologic carbon dioxide verification. Lawrence Berkeley National Laboratory Report, LBNL-54089, 54 pp.
- ØSTMO, S. 2004. Pre-stack inversion of seismic time-lapse data (1994 and 1999 vintages) in the Saline Aquifer CO₂ Storage (SACS) project. *SINTEF Petroleum Research Report*, 33.5324.00/07/04.
- PEARCE, J M, CZERNICHOWSKI-LAURIOL, I, LOMBARDI, S, BRUNE, S, NADOR, A, BAKER, J, PAUWELS, H, HATZIYANNIS, G, BEABIEN, S, and FABER, E A. 2004. A review of natural CO₂ accumulations in Europe as analogues for geological sequestration. 29–41 in *Geological Storage of Carbon Dioxide*. BAINES, S J, and WORDEN, R H (editors). *Geological Society of London Special Publication*, No. 233.

- PEARCE, J M, CHADWICK, R A, BENTHAM, M, HOLLOWAY, S, and KIRBY, G A. 2005. Monitoring technologies for the geological storage of CO₂. UK Department of Trade and Industry Technology Status Review Report, DTI/Pub URN 05/1033, 98pp.
- PEARCE, J, CHADWICK, R A, HOLLOWAY, S, and KIRBY, G A. 2006. *The objectives and design of monitoring protocols for CO₂ storage*. Proceedings of the 8th International Conference (GHGT-8) on Greenhouse Gas Control Technologies, Trondheim, Norway. 6pp.
- PENN, I E, CHADWICK, R A, HOLLOWAY, S, ROBERTS, G, PHARAOH, T C, ALLSOP, J M, HULBERT, A G, and BURNS, I M. 1987. Principal features of the hydrocarbon prospectivity of the Wessex–Channel Basin, U.K. 109–118 in *Petroleum Geology of North West Europe*. BROOKS, J, and GLENNIE, K (editors). (London, UK: Graham and Trotman.)
- PILLITTERI, A, CERASI, P, STAVRUM, J, ZWEIGEL, P, and BØE, R. 2003. Rock mechanical tests of shale samples from the caprock of the Utsira Sand in well 15/9-A11 – A contribution to the Saline Aquifer CO₂ Storage (SACS) project. *SINTEF Petroleum Research Report*, 33.5324.00/06/03, 28 pp.
- POLAK, S, LUNDIN, E, BØE, R, LINDEBERG, E, OLESEN, O, and ZWEIGEL, P. 2004a. Storage potential for CO₂ in the Beitstadfjord Basin, Mid-Norway. Norges Geologiske Undersøkelse Report, 2004.036; *SINTEF Petroleum Research Report*, 54.5272.00/01/04, 51 pp., Trondheim.
- POLAK, S, LUNDIN, E, ZWEIGEL, P, BØE, R, LINDEBERG, E, and OLESEN, O. 2004b. Storage potential for CO₂ in the Frohavet Basin, Mid-Norway. Norges Geologiske Undersøkelse Report, 2004.049; *SINTEF Petroleum Research Report*, 54.5272.00/02/04, 57 pp., Trondheim.
- PRUESS, K, BIELINSKI, A, ENNIS-KING, J, LE GALLO, Y, GARCIA, J, JESSEN, K, KOVSCEK, T, LAW, D H-S, LICHTNER, P, OLDENBURG, C, PAWAR, R., RUTQVIST, J, STEEFEL, C, TRAVIS, B, CHIN-FU TSANG, WHITE, S, and TIANFU XU. 2003. Code intercomparison builds confidence in numerical models for geologic disposal of CO₂. 463–468 in *Greenhouse Gas Control Technologies*. GALE, J, and KAYA, Y (editors). Proceedings of the 6th International Conference on Greenhouse Gas Control Technologies, Kyoto, Japan, October 2002, Vol. 1 (Oxford, UK: Pergamon.)
- QUINTESSA. 2006. Website: <http://www.quintessa.org/consultancy/index.html?geostorage.html>
- ROCHELLE, C A, BATEMAN, K, and PEARCE, J M. 2002. Geochemical interactions between supercritical CO₂ and the Utsira formation: an experimental study. *British Geological Survey Commissioned Report*, CR/02/060.
- ROCHELLE, C A, CZERNICHOWSKI-LAURIOL, I, and MILODOWSKI, A E. 2004. The impact of chemical reactions on CO₂ storage in geological formations: a brief review. 87–106 in *Geological Storage of Carbon Dioxide*. BAINES, S J, and WORDEN, R H (editors). Geological Storage of Carbon Dioxide. *Geological Society of London Special Publication*, No. 233.
- ROCHELLE, C A, BATEMAN, K, MILODOWSKI, A E, KEMP, S J, and BIRCHALL, D. 2006. Geochemical interactions between CO₂ and seals above the Utsira Formation: An experimental study. *British Geological Survey Commissioned Report*, CR/06/069.
- SALINE AQUIFER CO₂ STORAGE PROJECT. 2003. Saline Aquifer CO₂ Storage project (SACS) - Best Practice Manual - IEA Greenhouse Gas R&D Programme, Report PH4/21, 53pp. [online available at: [http://www.co2store.org/TEK/FOT/SVG03178.nsf/Attachments/SACSBestPractiseManual.pdf/\\$FILE/SACSBestPractiseManual.pdf](http://www.co2store.org/TEK/FOT/SVG03178.nsf/Attachments/SACSBestPractiseManual.pdf/$FILE/SACSBestPractiseManual.pdf)]
- SARIPALLI, K P, COOK, E M, and MAHASANAN, N. 2003. Risk and hazard assessment for projects involving the geological sequestration of CO₂. 511–516 in *Greenhouse Gas Control Technologies*. GALE, J, and KAYA, Y (editors). Proceedings of the 6th International Conference on Greenhouse Gas Control Technologies, Kyoto, Japan, October 2002, Vol. 1. (Oxford, UK: Pergamon.)
- SCHLÖMER, S, and KROOSS, B M. 1997. Experimental characterisation of the hydrocarbon sealing efficiency of caprocks. *Marine and Petroleum Geology*, Vol. 14 (5), 565–580.

- SCHULZ, R, and RÖHLING, H-G. 2000. Geothermische Ressourcen in Nordwestdeutschland. *Zeitschrift für angewandte Geologie*, Vol 46, 122–129.
- SENGUPTA, M, and MAVKO, G. 2003. Impact of flow-simulation parameters on saturation scales and seismic velocity. *Geophysics*, Vol. 68, 1267–1280.
- SNEIDER, R M, SNEIDER, J S, BOLGER, G W, and NEASHAM, J W. 1997. Comparison of seal capacity determinations: conventional cores vs. cuttings. 1–12 in *Seals, traps, and the petroleum system* SURDAM, R C (editor). *American Association of Petroleum Geologists*, Memoir 67.
- SOMMARUGA, A, and BØE, R. 2002. Geometry and subcrop maps of shallow Jurassic basins along the Mid-Norway coast. *Marine and Petroleum Geology*, Vol. 19, 1029–1042.
- SØRENSEN, K, NIELSEN, L H, MATHIESEN, A, and SPRINGER, N. 1998. Geotermi i Danmark: Geologi og ressourcer. *Danmarks og Grønlands Geologiske Undersøgelse Rapport*, 1998/123, 24 pp.
- SPAN, R, and WAGNER, W. 1996. A New Equation of State for Carbon Dioxide Covering the Fluid Region from the Triple-Point Temperature to 100 K at Pressures up to 800 MPa. *Journal of Physical Chemistry Reference Data*, Vol. 25 (6), 1509–1596.
- SPRINGER, N, LINGREEN, H, and FRIES, K. 2005. Saline Aquifer CO₂ Storage Project, SACS, Phase II. Caprock seal capacity test: An evaluation of the transport and sealing properties of Nordland Shale core samples from well 15/9-A11, Sleipner field. *Geological Survey of Denmark and Greenland*, Report No. 58.
- STENHOUSE, M, WILSON, M, HERZOG, H, CASSIDY, B, KOZAK, M, and ZHOU, W. 2004. Regulatory issues associated with the long-term storage of CO₂. International Energy Agency Greenhouse Gas R&D Programme Report, PH4/35, 108 pp.
- SVENSSON R, BERNSTONE C, ERIKSSON S, KREFT E, ARTS R, OBDAM A, and MEYER, R. 2005. Safety Assessment of Structure Schweinrich. Part of CO2STORE case study Schwarze Pumpe. Internal unpublished CO2STORE report, 93 pp.
- TAPPIN, D, CHADWICK, R A, JACKSON, A A, WINGFIELD, R T R, and SMITH, N J P. 1994. *United Kingdom Offshore Regional Report: the Geology of Cardigan Bay and the Bristol Channel*. (London: HMSO for the British Geological Survey.)
- TORP, T A, and BROWN, K R. 2005. CO₂ underground storage costs as experienced at Sleipner and Weyburn. 531–538 in *Greenhouse Gas Control Technologies*. RUBIN, E S, KEITH, D W, and GILBOY, C F (editors). Proceedings of the 7th International Conference on Greenhouse Gas Control Technologies, 5–9 September 2004, Vancouver, Canada, Volume I. Peer reviewed papers and overviews. (Oxford: Elsevier.)
- UK DTI. 2005. Monitoring Technologies for the Geological Storage of CO₂. DTI Technology Status Report TSR025. DTI/Pub URN 05/1032. 28pp.
- UK DTI. 2006. CO2STORE: The Valleys case study on CO₂ capture, transport and storage. DTI Report COAL R302 DTI/Pub URN 06/755, 54pp.
- VAN DER MEER, L G H. 1995. The CO₂ storage efficiency of aquifers. *Energy Conversion and Management*, Vol. 36, No. 6–9, 513–518.
- VAN EIJS, R M H E, MULDER, F M M, NEPVEU, M, KENTER, C J, and SCHEFFERS, B C. 2006. Correlation between hydrocarbon reservoir properties and induced seismicity in the Netherlands. *Engineering Geology*, Vol. 84 (3–4), 99–111.
- WEST, J M, PEARCE, J M, BENTHAM, M, and MAUL, P. 2005. Issue Profile: Environmental Issues and the Geological Storage of CO₂. *European Environment*, Vol. 15, 250–259.
- WILDENBORG, A F B, LEIJNSE A L, KREFT E, NEPVEU M N, OBDAM A N M, ORLIC B, WIPFLER E L, GRIFT, B VAN DER, KESTEREN VAN W, GAUS I, CZERNICHOWSKI-LAURIOL I, TORFS P, and WOJCIK, R.

2005. Risk assessment methodology for CO₂ storage – the scenario approach. 1293–1316 in *The CO₂ Capture and Storage Project (CCP) for carbon dioxide storage in deep geologic formations for climate change mitigation, Vol. 2: Geologic Storage of Carbon Dioxide with Monitoring and Verification*. BENSON, S M (editor). (Oxford, UK: Elsevier Publishing.)

WILLIAMSON, J P, CHADWICK, R A, ROWLEY, W J, and EIKEN, O. 2001. Gravity monitoring of the CO₂ bubble at Sleipner. *British Geological Survey Commissioned Report*, CR/01/063.

WILSON, E J, JOHNSON, T L, and KEITH, D W. 2003. Regulating the ultimate sink: Managing the risks of geologic CO₂ storage. *Environmental Science & Technology*, Vol. 37(16), 3476–3483.

WILSON, M, and MONEA, M. 2004. IEA GHG Weyburn CO₂ Monitoring & Storage Operation Summary Report 2000–2004. (Regina: Petroleum Technology Research Centre.)

ZHOU, W, STENHOUSE, M J, ARTHUR, R, WHITTAKER, S, LAW, D H-S, CHALATURNYK, R, and JAZRAWI, W. 2005. The IEA Weyburn CO₂ monitoring and storage project – modelling of the long-term migration of CO₂ from Weyburn. 721–729 in *Greenhouse Gas Control Technologies*. RUBIN, E S, KEITH, D W, and GILBOY, C F (editors). Proceedings of the 7th International Conference on Greenhouse Gas Control Technologies, 5–9 September 2004, Vancouver, Canada, Volume I. Peer reviewed papers and overviews. (Oxford: Elsevier.)

ZWEIGEL, P, HAMBORG, M, ARTS, R, LOTHE A, and TØMMERÅS, A. 2000. Prediction of migration of CO₂ injected into an underground depository: Reservoir geology and migration modelling in the Sleipner case (North Sea). 360–365 in *Greenhouse Gas Control Technologies*. WILLIAMS, D J et al. (editors). (Collingwood, Australia: CSIRO Publishing.)

ZWEIGEL, P, and HEILL, L K. 2003. Studies on the likelihood for caprock fracturing in the Sleipner CO₂ injection case – A contribution to the Saline Aquifer CO₂ Storage (SACS) project. *SINTEF petroleum Research Report*, 33.5324.00/02/03, 27pp.

ZWEIGEL, P, ARTS, R, LOTHE, A E, and LINDEBERG, E. 2004. Reservoir geology of the Utsira Formation at the first industrial-scale underground CO₂ storage site (Sleipner area, North Sea). 165–180 in *Geological Storage of Carbon Dioxide for Emissions Reduction*. BAINES, S, GALE, J, and WORDEN, R (editors). *Geological Society of London Special Publications*, No. 233.

SACS AND CO2STORE BIBLIOGRAPHY

Listed below are reports and papers arising from the SACS and CO2STORE projects, the list is not fully complete as some work is still in progress.

- ARTS, R. 2000. CO₂-volume calculations based on time-lapse seismic data. Report (ppt presentation), 14pp. [www.iku.sintef.no/projects/IK23430000/other_reports/Volume_calculation.pdf]
- ARTS, R. 2000. Ppt-presentation of seismic / time-lapse seismic interpretation results. Report (ppt presentation), 26pp. & 5pp. [www.iku.sintef.no/projects/IK23430000/other_reports/Arts_ppt_Oct_00_ldsc.pdf]
www.iku.sintef.no/projects/IK23430000/other_reports/Arts_ppt_Oct_00_portr.pdf]
- ARTS, R. 2001. Note on seismic data. - NITG-TNO report NITG 00-237-B. 18 p. [available online at: [www.iku.sintef.no/projects/IK23430000/other_reports/Note_on_seismic_data_\(TNO_Oct00\).pdf](http://www.iku.sintef.no/projects/IK23430000/other_reports/Note_on_seismic_data_(TNO_Oct00).pdf)]
- ARTS, R, BREVIK, I, EIKEN, O, SOLLIE, R, CAUSSE, E, and VAN DER MEER, B. 2000. Geophysical methods for monitoring marine aquifer CO₂ storage - Sleipner experiences. 366–37 in *Proceedings of the 5th International Conference on Greenhouse Gas Control Technologies, Cairns, Australia*. WILLIAMS, D, DURIE, B, McMULLAN, P, PAULSON, C, and SMITH, A (editors). (Collingwood, Victoria: CSIRO Publishing.) [www.iku.sintef.no/projects/IK23430000/Publications/Arts_et_al_GHGT5.pdf]
- ARTS, R J, ZWEIGEL, P, and LOTHE, A E. 2000. Reservoir geology of the Utsira Sand in the Southern Viking Graben area – a site for potential CO₂ storage. 62nd EAGE meeting, Glasgow, paper B-20. [www.iku.sintef.no/projects/IK23430000/Publications/Arts_et_al_EAGE00.pdf]
- ARTS, R, EIKEN, O, CHADWICK, A, ZWEIGEL, P, VAN DER MEER, L, and ZINSZNER, B. 2003. Monitoring of CO₂ Injected at Sleipner Using Time Lapse Seismic Data. 347–352 in *Greenhouse Gas Control Technologies*. GALE, J, and KAYA, Y (editors). Proceedings of the 6th International Conference on Greenhouse Gas Control Technologies, Kyoto, Japan, October 2002, Vol. 1. (Oxford, UK: Pergamon.)
- ARTS, R, CHADWICK, A, EIKEN, O, and ZWEIGEL, P. 2003. Interpretation of the 1999 and 2001 time-lapse seismic data (WP 5.4). TNO report NITG 03-064-B, 32pp. [www.iku.sintef.no/projects/IK23430000/formal_reports/SACS2_WP5_4_Final_Report_2002.pdf]
- ARTS, R, ELSAYED, R, VAN DER MEER, L, EIKEN, O, ØSTMO, S, CHADWICK, A, KIRBY, G, and ZINSZNER, B. 2002. Estimation of the mass of injected CO₂ at Sleipner using time-lapse seismic data. EAGE, Annual meeting 2002, Florence, Italy. [www.iku.sintef.no/projects/IK23430000/Publications/Arts_et_al_EAGE_2002_2.pdf]
- ARTS, R, EIKEN, O, CHADWICK, A, ZWEIGEL, P, VAN DER MEER, B, and KIRBY, G. 2004. Seismic monitoring at the Sleipner underground CO₂ storage site (North Sea). 181–191 in *Geological Storage of Carbon Dioxide for Emissions Reduction*. BAINES, S, GALE, J, and WORDEN, R (editors). *Geological Society of London, Special Publication*, No. 233.
- ARTS, R, EIKEN, O, CHADWICK, A, ZWEIGEL, P, VAN DER MEER, B, and ZINSZNER, B. 2004. Monitoring of CO₂ injected at Sleipner using time lapse seismic data. *Energy*, Vol. 29, 1383–1392.
- ARTS, R, CHADWICK, A, and EIKEN, O. 2005. Recent time-lapse seismic data show no indication of leakage at the Sleipner CO₂-injection site. 653–660 in *Greenhouse Gas Control Technologies*. RUBIN, E S, KEITH, D W, and GILBOY, C F (editors). Proceedings of the 7th International Conference on Greenhouse Gas Control Technologies, 5–9 September 2004, Vancouver, Canada, Volume I - Peer reviewed papers and overviews. (Oxford: Elsevier.)
- AUDIGANE, P, GAUS, I, PRUESS, K, and XU, T. 2005. Reactive transport modeling using Toughreact of the long term CO₂ storage at Sleipner, North Sea. Abstracts of the 4th Annual Conference on Carbon Sequestration, 1–5 May 2005, Alexandria, VA, US.
- AUDIGANE, P, GAUS, I, PRUESS, K, and XU, T. 2006. A Long-Term 2D Vertical Modeling of the CO₂ Storage at Sleipner (North Sea) Using TOUGHREACT. TOUGH Symposium 2006, 15–17 May 2006, LBNL. [www-esd.lbl.gov/TOUGHsymposium/pdf/Audigane_Sleipner.pdf]

- BICKLE, M, CHADWICK, R A, HUPPERT, H E, HALLWORTH, M, and LYLE, S. In press. Modelling Carbon-Dioxide Accumulation at Sleipner: Implications for Underground Carbon Storage. *Earth & Planetary Science Letters*.
- BORGOS, H G, RANDEN, T, and SØNNELAND, L. 2003. Super-resolution mapping of thin gas pockets. Extended Abstracts of EAGE Annual Meeting, Stavanger, June 2003.
- BREVIK, I, EIKEN, O, ARTS, R J, LINDEBERG, E, and CAUSSE E. 2000. Expectations and results from seismic monitoring of CO₂ injection into a marine aquifer. 62nd EAGE meeting, Glasgow, paper B-21.
- BØE, R, AND ZWEIGEL, P. 2001. Characterisation of the Nordland Shale by XRD analysis. A contribution to the Saline Aquifer CO₂ Storage (SACS) project. SINTEF Petroleum Research Report, 33.0764.00/01/01, 23 pp.
[www.iku.sintef.no/projects/IK23430000/other_reports/Boe&Zweigel_2000_XRD_Sleipnerarea.pdf]
- CARLSEN, I M, MJAALAND, S, and NYHAVN, F. 2001. SACS2, work package 4. Monitoring well scenarios. *SINTEF Petroleum Research Report*, 32.1021.00/01/01, 43 p., 2 app.
[www.iku.sintef.no/projects/IK23430000/formal_reports/SACS2_WA4_Finalreport.pdf]
- CHADWICK, R A, HOLLOWAY, S, KIRBY, G A, GREGERSEN, U, and JOHANNESSEN, P N. 2000. The Utsira Sand, Central North Sea - An assessment of its potential for regional CO₂ disposal. 349–354 in *Proceedings of the 5th International Conference on Greenhouse Gas Control Technologies, Cairns, Australia*. WILLIAMS, D, DURIE, B, MCMULLAN, P, PAULSON, C, and SMITH, A (editors). (Collingwood, Victoria: CSIRO Publishing.)
[www.iku.sintef.no/projects/IK23430000/Publications/Chadwick_et_al_GHGT5.pdf]
- CHADWICK, R A, HOLLOWAY, S, and RILEY, N. 2001. Deep subsurface CO₂ sequestration - a viable greenhouse mitigation strategy. *Geoscientist*, Vol. 11, No. 2, Feb 2001, 4–5.
[www.iku.sintef.no/projects/IK23430000/Publications/Chadwick_etal_2001_Geoscientist.pdf]
- CHADWICK, R A, KIRBY, G, HOLLOWAY, S, ZWEIGEL, P, and ARTS, R. 2001. The case for underground carbon dioxide sequestration in Northern Europe. European Union of Geosciences, XI meeting, April 2001, Strasbourg, Abstract volume, p. 172.
- CHADWICK, R A, WILLIAMSON, P, ZWEIGEL, P, ARTS, R, and EIKEN, O. 2001. Time-lapse geophysical monitoring of a subsurface CO₂ bubble in the Utsira Sand, Sleipner, northern North Sea. *3D Seismic Data: Advances in the Understanding of Stratigraphic and Structural Architecture* Conference at the Geological Society of London, Burlington House, 14–16 November 2001.
[www.iku.sintef.no/projects/IK23430000/Publications/Chadwick_etal_2001_London.pdf]
- CHADWICK, R A, KIRBY, G A, HOLLOWAY, S, GREGERSEN, U, JOHANNESSEN, P, ZWEIGEL, P, and ARTS, R. 2002. Saline Aquifer CO₂ Storage (SACS2). Final report: Geological Characterisation of the Utsira Sand reservoir and caprocks (Work Area 1). *British Geological Survey Commissioned Report*, CR/02/153 [Text part:
www.iku.sintef.no/projects/IK23430000/formal_reports/SACS2_WA1_FINAL_REPORT_V_final.pdf
Figures:
www.iku.sintef.no/projects/IK23430000/formal_reports/SACS2_WA1_Final_report_figures.pdf]
- CHADWICK, R A, ZWEIGEL, P, GREGERSEN, U, KIRBY, G, and JOHANNESSEN, P. 2003. Geological Characterisation of CO₂ Storage Sites: Lessons from the Sleipner, Northern North Sea. 321–326 in *Greenhouse Gas Control Technologies*. GALE, J, and KAYA, Y (editors). Proceedings of the 6th International Conference on Greenhouse Gas Control Technologies, Kyoto, Japan, October 2002, Vol. 1 (Oxford, UK: Pergamon.)
[www.iku.sintef.no/projects/IK23430000/Publications/Chadwick_etal_GHGT6_Sleipner_geology.pdf]
- CHADWICK, R A, ARTS, R, EIKEN, O, KIRBY, G A, LINDEBERG, E, and ZWEIGEL, P. 2004. 4D seismic imaging of an injected CO₂ plume at the Sleipner Field, central North Sea. 311–320 in *3D Seismic Technology: Application to the Exploration of Sedimentary Basins*. DAVIES, R J, CARTWRIGHT, J A, STEWART, S A, LAPPIN, M, and UNDERHILL, J R (editors). *Geological Society of London Memoir*, No. 29.
- CHADWICK, R A, HOLLOWAY, S, BROOK, M S, and KIRBY, G A. 2004. The case for underground CO₂ sequestration in northern Europe. 17–28 in *Geological Storage of Carbon Dioxide for Emissions Reduction*. BAINES, S, GALE, J, and WORDEN, R (editors). *Geological Society of London Special Publication*, No. 233.

- CHADWICK, R A, ZWEIGEL, P, GREGERSEN, U, KIRBY, G A, HOLLOWAY, S, and JOHANNESSEN, P N. 2004. Geological reservoir characterization of a CO₂ storage site: The Utsira Sand, Sleipner, northern North Sea. *Energy*, Vol. 29, 1371–1381.
- CHADWICK, R A, ARTS, R, and EIKEN, O. 2005. 4D seismic quantification of a growing CO₂ plume at Sleipner, North Sea. 1385–1399 in *Petroleum Geology: North West Europe and Global Perspectives*. DORE, A G, and VINING, B (editors). Proceedings of the 6th Petroleum Geology Conference. (London: Geological Society of London.)
- CHADWICK, R A, ARTS, R, EIKEN, O, WILLIAMSON, P, and WILLIAMS, G. 2005. Geophysical Monitoring of the CO₂ plume at Sleipner, North Sea. 303–314 in *Advances in the Geological Storage of Carbon Dioxide*. LOMBARDI, S, ALTUNA, L K, and BEAUBIEN, S E (editors). *NATO Science Series, IV. Earth and Environmental Sciences*, Vol. 65. (Dordrecht: Springer.)
- CHADWICK, R A, NOY, D, LINDEBERG, E, ARTS, R, EIKEN, O, and WILLIAMS, G. 2006. Calibrating reservoir performance with time-lapse seismic monitoring and flow simulations of the Sleipner CO₂ plume. *Proceedings of the 8th International Conference on Greenhouse Gas Control Technologies*, Trondheim, Norway, 19–22 June, 2006, ISBN: 0-08-046407-6. Elsevier, published on CD. [www.events.adm.ntnu.no/ei/viewpdf.esp?id=24&file=d%3A%5CAmlink%5CEVENTWIN%5Cdocs%5Cpdf%5C950Final00170%2Epdf].
- CZERNICHOWSKI-LAURIOL, I, ROCHELLE, C A, BROSSE, E, SPRINGER, N, PEARCE, J M, BATEMAN, K A, SANJUAN, B, and KERVÉVAN, C. 2001. Disposal of CO₂ in deep aquifers: geochemical investigations of water-rock- CO₂ interactions at Sleipner (North Sea) as part of the SACS project. European Union of Geosciences, XI meeting, April 2001, Strasbourg, Abstract volume, 172.
- CZERNICHOWSKI-LAURIOL, I, SANJUAN, B, KERVEVAN, C, SERRA, H, ROCHELLE, C A, BATEMAN, K A, PEARCE, J M, MOORE, Y A, SPRINGER, N, HØIER, C, LINDGREN, H, BROSSE, E, and PORTIER, S. 2002. Summary report SACS2 Work area 3 - Geochemistry. Technical report, 14pp. [www.iku.sintef.no/projects/IK23430000/formal_reports/SACS2_WA3_Finalreport.pdf]
- CZERNICHOWSKI-LAURIOL, I, ROCHELLE, C A, BROSSE, E, SPRINGER, E, BATEMAN, K, KERVEVAN, C, PEARCE, J M, and SANJUAN B. 2003. Reactivity of injected CO₂ with the Utsira Sand reservoir at Sleipner. 1617–1620 in *Greenhouse Gas Control Technologies*. GALE, J, and KAYA, Y (editors). Proceedings of the 6th International Conference on Greenhouse Gas Control Technologies, Kyoto, Japan, October 2002, Vol. 2. (Oxford, UK: Pergamon.)
- EIKEN, O, BREVIK, I, ARTS, R, LINDEBERG, E, and FAGERVIK, K. 2000. Seismic monitoring of CO₂ injected into a marine aquifer. SEG Calgary 2000 International conference and 70th Annual meeting, Calgary. [www.iku.sintef.no/projects/IK23430000/Publications/Eiken_et_al_2000_GHGT5.pdf]
- EIKEN, O, BREVIK, I, ART, R, LINDEBERG, E, and FAGERVIK, K. 2001. Seismic monitoring of CO₂ injected into a marine aquifer. American Association of Petroleum Geologists, Annual Meeting, June 2001, Denver, abstract volume.
- EVANS, B, and MCKENNA, J. 2002. Physical modelling study of Sleipner West CO₂ sequestration stage 1, modelling the Sleipner West overburden. Minerals and Energy Research Institute of Western Australia, Perth, Western Australia. Report No.224 (1 disc).
- FABRIOL, H. 2001. Saline Aquifer CO₂ Storage (SACS). Feasibility study of microseismic monitoring (Task 5.8). BRGM report BRGM/RP-51293, 61pp. [www.iku.sintef.no/projects/IK23430000/other_reports/Fabriol_2002_MicroSeismicMonitoring_feasibility.pdf]
- FRANGEUL, J, NGHIEM, L, CAROLI, E, and THIBEAU, S. 2004. Sleipner/Utsira CO₂ Geological Storage Full Field Flow and Geochemical Coupling to Assess the Long Term Fate of the CO₂. *Bulletin of the American Association of Petroleum Geologists*, Vol. 88, No. 13 (Supplement). Presentation given at AAPG Annual Meeting, Dallas USA, April 18–21, 2004 [www.searchanddiscovery.com/documents/abstracts/annual2004/Dallas/Frangeu.htm]
- GALE, J, CHRISTENSEN, N P, CUTLER, A, and TORP, T A. 2001. Demonstrating the Potential for Geological Storage of CO₂: The Sleipner and GESTCO Projects. *Environmental Geosciences*, Vol. 8 (3), 160–165.

- GARCIA, J E. 2003. Fluid dynamics of carbon dioxide disposal into saline aquifers. Unpublished PhD thesis, University of California, Berkeley. 136pp. [www.osti.gov/energycitations/servlets/purl/821335-QqO4VQ/native/821335.pdf]
- GAUS, I. 2005. Reactive transport modelling of the impact of CO₂ injection on the clayey caprock at Sleipner (North Sea). *Chemical Geology*, Vol. 217, 319–337.
- GAUS, I. 2005. Long term geochemical modelling of the CO₂ impact on the Sleipner caprock and reservoir. CO2STORE Task 2.1.2. BRGM Report BRGM/RC-53664-FR, 50pp.
- GAUS, I, AZAROUAL, M, and CZERNICHOWSKI-LAURIOL, I. 2002. Preliminary modelling of the geochemical impact of CO₂ injection on the caprock at Sleipner. BRGM report BRGM/RP-52081, 43pp. [www.iku.sintef.no/projects/IK23430000/other_reports/Gaus_et_al_BRGM_SACS2_WA3_geochemistry_caprock.pdf]
- GAUS, I, AZAROUNAL, M, and CZERNICHOWSKI-LAURIOL, I. 2003. Reactive transport modeling of dissolved CO₂ in the caprock base during CO₂ sequestration (Sleipner site, North Sea). Abstracts of the 2nd Annual Conference on Carbon Sequestration, 5–8 May 2003, Alexandria, VA, US. [www.iku.sintef.no/projects/IK23430000/Publications/Gaus_et_al_CarbonSeqIIConf.pdf]
- GHADERI, A, and LANDRØ, M. 2005. Pre-stack estimation of time-lapse seismic velocity changes –an example from the Sleipner CO₂-sequestration project. 633–641 in *Greenhouse Gas Control Technologies*. RUBIN, E S, KEITH, D W, and GILBOY, C F (editors). Proceedings of the 7th International Conference on Greenhouse Gas Control Technologies, 5–9 September 2004, Vancouver, Canada, Volume I, Peer reviewed papers and overviews. (Oxford: Elsevier.)
- GREGERSEN, U, JOHANNESSEN, P N, MØLLER, J J, KRISTENSEN, L, CHRISTENSEN, N P, HOLLOWAY, S, CHADWICK, R A, KIRBY, G, LINDEBERG, E, and ZWEIGEL, P. 1998. Saline Aquifer CO₂ Storage S.A.C.S Phase Zero 1998. Internal report. GEUS Internal Report.
- GREGERSEN, U, JOHANNESSEN, P N, CHADWICK, R A, HOLLOWAY, S, and KIRBY, G A. 2000. Regional study of the Neogene deposits in the southern Viking Graben area – a site for potential CO₂ storage. 62nd EAGE meeting, Glasgow. [www.iku.sintef.no/projects/IK23430000/Publications/Gregersen_et_al_EAGE2000.pdf]
- GREGERSEN, U, and JOHANNESSEN, P N. 2001. The Neogene Utsira Sand and its seal in the Viking Graben area, North Sea. GEUS rapport 2001/100, 29pp. [www.iku.sintef.no/projects/IK23430000/other_reports/Gregersen&Johann2001_Utsira&caprock_regional.pdf]
- HAMBORG, M, KIRBY, G, LOTHE, A E, and ZWEIGEL, P. 2003. Seismic mapping and simulation of CO₂ migration in the upper Utsira sand wedge east of the Sleipner injection site. A contribution to the Saline Aquifer CO₂ Storage (SACS) project. *SINTEF Petroleum Research Report*, 33.5324.00/03/03, 42pp. [www.iku.sintef.no/projects/IK23430000/other_reports/Hamborg_et_al_Sand_wedge_seismic_and_migration_report.pdf]
- HANSEN, H, EIKEN O, and AASUM, T O. 2005. Tracing the path of carbon dioxide from a gas-condensate reservoir, through an amine plant and back into a subsurface aquifer. Case study: The Sleipner area, Norwegian North Sea. SPE paper 96742, 15pp. Presented at Offshore Europe 2005 conference, Aberdeen.
- HARRINGTON, J F, NOY, D J, BIRCHALL, D J, and HORSEMAN, S T. 2006. A Laboratory study of the Nordland Shale: Final Report. *British Geological Survey Commissioned Report*, CR/07/158.
- HARRINGTON, J F, NOY, D J, HORSEMAN, S T, BIRCHALL, D J, and CHADWICK, R A. (in press). Laboratory study of gas and water flow in the Nordland Shale, Sleipner, North Sea. In *Carbon Dioxide Sequestration in Geological Media*. GROBE, M, PASHIN, J, and DODGE, R (editors). *Special Publication of the American Association of Petroleum Geologists*.
- HEAD, M J, RIDING, J B, EIDVIN, T, and CHADWICK, R A. 2004. Palynological and foraminiferal biostratigraphy of (Upper Pliocene) Nordland Group mudstones at Sleipner, northern North Sea. *Marine and Petroleum Geology*, Vol. 21, 277–297.

- KEMP, S J, BOUCH, J, and MURPHY, H M. 2001. Mineralogical characterisation of the Nordland Shale, UK Quadrant 16, northern North Sea. *British Geological Survey Commissioned Report*, CR/01/136. [www.iku.sintef.no/projects/IK23430000/other_reports/caprock_seal_capacity_uk.pdf]
- KEMP, S J, PEARCE, J M, and STEADMAN, E J. 2002. Mineralogical, geochemical and petrographical characterisation of Nordland Shale cores from well 15/9-A11, Sleipner field, northern North Sea. *British Geological Survey Commissioned Report*, CR/02/313. [www.iku.sintef.no/projects/IK23430000/other_reports/Kemp_etal_2002_Core_charact_seal_well15_9_A11.pdf]
- KEMP, S J, and BOUCH, J E. 2004. Mineralogical and petrographic characterisation of reservoirs and caprocks from the St George's Channel Basin, Irish Sea. *British Geological Survey Commissioned Report*, CR/04/130.
- KIRBY, G A, CHADWICK, R A, and HOLLOWAY, S. 2001. Depth mapping and characterisation of the Utsira Sand Saline Aquifer, Northern North Sea. *British Geological Survey Commissioned Report*, CR/01/218. [www.iku.sintef.no/projects/IK23430000/other_reports/Kirby_etal_2001_UtsiraSand_Mapping.pdf]
- KONGSJORDEN, H, KÅRSTAD, O, and TORP, T A. 1998. Saline aquifer storage of carbon dioxide in the Sleipner project. *Waste Management*, Vol. 17, 303–308 .
- KRISTENSEN, B, and BIDSTRUP, T. 2000. Determination of the natural fluid flow in the Utsira Sand reservoir using basin modelling. SACS Project: Final Technical Report of Task 1.6. GEUS Report 2001/2. [iku.sintef.no/projects/IK23430000/other_reports/Kristensen%20&%20Bidstrup_2000_report.pdf]
- LARSEN, M, BECH, N, BIDSTRUP, T, CHRISTENSEN, N P, and BIEDE, O. 2007. Kalundborg case study, a feasibility study of CO₂ storage in onshore saline aquifers. *Danmarks og Gronlands Geologiske Undersogelse Rapport*, 2007/2, 79 pp.
- LESCOFFIT, S, and ZWEIGEL, P. 2006. Interpretation of the pre-stack inversion results of seismic time-lapse data (1999 vintage) in the Saline Aquifer CO₂ Storage (SACS) project. *SINTEF Petroleum Research Report*, 20 pp.
- LINDEBERG, E, CAUSSE, E, and GHADERI, A. 1999. Evaluation of to what extent CO₂ accumulations in the Utsira formations are possible to quantify by seismic by August 1999. *SINTEF Petroleum Research Report*, 54.5148.00/01/99, 13p. [www.iku.sintef.no/projects/IK23430000/other_reports/Lindeberg_et_al_1999.pdf]
- LINDEBERG, E, ZWEIGEL, P, BERGMO, P, GHADERI, A, and LOTHE, A. 2000. Prediction of CO₂ dispersal pattern improved by geology and reservoir simulation and verified by time lapse seismic. 372–377 in *Proceedings of the 5th International Conference on Greenhouse Gas Control Technologies, Cairns, Australia*. WILLIAMS, D, DURIE, B, MCMULLAN, P, PAULSON, C, and SMITH, A (editors). (Collingwood, Victoria: CSIRO Publishing.) [www.iku.sintef.no/projects/IK23430000/Publications/Lindeberg_et_al_GHGT5.pdf]
- LINDEBERG, E, BERGMO, P, and MOEN, A. 2002. The long-term fate of CO₂ injected into an aquifer. Abstracts of the 6th International conference on Greenhouse Gas Control Technology (GHGT-6), Kyoto, Japan, 1–4 October 2002. [www.iku.sintef.no/projects/IK23430000/Publications/Lindeberg&Bergmo_2002_GHGT6_longterm_fate.pdf]
- LINDGREN, H, FRIES, K, and SPRINGER, N. 2002. SACS, Task 1.4: Evaluation of caprock sealing the reservoir. Clay mineralogy investigation of core and cuttings from the Ekofisk and Sleipner areas. GEUS rapport 2002/3, 10pp. [www.iku.sintef.no/projects/IK23430000/other_reports/Lindgren_etal_2002_GEUS_Caprock_evaluation.pdf]
- LIU, E, LI, X Y, and CHADWICK, R A. 2001. Multi-component seismic monitoring of CO₂ gas cloud in the Utsira Sand: A feasibility study (Report Work Area 5.6). *British Geological Survey Commissioned Report*, CR/01/064. [www.iku.sintef.no/projects/IK23430000/other_reports/Liu_etal_2001_Multi_comp_seis_study.pdf]

- LOTHE, A E, AND ZWEIGEL, P. 1999. Saline Aquifer CO₂ Storage (SACS). Informal annual report 1999 of SINTEF Petroleum Research's results in work area 1 'Reservoir Geology'. *SINTEF Petroleum Research Report*, 23.4300.00/03/99, 54 pp.
[www.iku.sintef.no/projects/IK23430000/other_reports/Lothe&Zweigel_99report.pdf]
- LYGREN, M, LINDEBERG, E, BERGMO, P, DAHL, G V, HALVORSEN, K A, RANDEN, T, and SONNELAND, L. 2002. History matching of CO₂ flow models using seismic modelling and time-lapse data. Society of Exploraiton Geophysicists Annual Meeting, Salt Lake City, October 2002, extended abstracts, 4pp.
- LYGREN, M, LINDEBERG, E, BERGMO, P, DAHL, G V, HALVORSEN, K, RANDEN, T, and SØNNELAND, L. 2005. A Method for Ranking CO₂ Flow Models Using Seismic Modeling and Time-Lapse Data. 405–417 in *Mathematical Methods and Modelling in Hydrocarbon Exploration and Production*. ISKE, A, and RANDEN, T (editors). (Berlin/Heidelberg: Springer Verlag.)
- MCKENNA, J J. 2004. Seismic Response to CO₂ Storage in a Saline Aquifer. Unpublished PhD thesis, Curtin University of Technology.
- MOUGIN, P, RASOLOFOSON, P, and ZINSZNER, B. 2002. Petroacoustics of poorly consolidated reservoir rocks saturated with CO₂/methane/brine mixtures. Technical report, IFP, 27pp.
[iku.sintef.no/projects/IK23430000/other_reports/Mougin_et_al_2002_IFP_Final_Report_WP7.pdf]
- NOONER, S L. 2005. Gravity changes associated with underground injection of CO₂ at the Sleipner storage reservoir in the North Sea, and other marine geodetic studies. Unpublished PhD thesis, University of California at San Diego, La Jolla.
- NOONER, S, ZUMBERGE, M, EIKEN, O, STENVOLD, T, and THIBEAU, S. 2006. Constraining the density of CO₂ within the Utsira formation using time-lapse gravity measurements. Abstract (3p) and paper (6p) of the 8th International conference on Greenhouse Gas Control Technologies (GHGT-8), Trondheim, Norway, June 2006.
[https://events.adm.ntnu.no/ei/viewpdf.esp?id=24&file=d%3A%5CAmlink%5CEVENTWIN%5Cdocs%5Cpdf%5C950Final00296%2Epdf]
- NOONER, S L, EIKEN, O, HERMANRUD, C, SASAGAWA, G S, STENVOLD, T, and ZUMBERGE, M A. 2007. Constraints on the in situ density of CO₂ within the Utsira formation from time-lapse seafloor gravity measurements. *International Journal of Greenhouse Gas Control*, Vol. 1, 198–214. (Oxford, UK: Elsevier.)
- ØSTMO, S. 2004. Pre-stack inversion of seismic-time lapse data (1994 and 1999 vintages) in the Saline Aquifer CO₂ Storage (SACS) project. *SINTEF Petroleum Research Report*, 33.5324.00/07/04, 12 pp.
- PEARCE, J M, KEMP, S J, and WETTON, P D. 1999. Mineralogical and petrographical characterisation of a 1 m core from the Utsira Formation, Central North Sea. *BGS Technical Report, Mineralogy & Petrology Series*, Report WG/99/24C, 26pp. + 3 plates.
[www.iku.sintef.no/projects/IK23430000/other_reports/Pearce_et_al_1999.zip]
- PEARCE, J M, CZERNICHOWSKI-LAURIOL, I, ROCHELLE, C A, SPRINGER, N, BROSE, E, SANJUAN, B, BATEMAN, K, and LANINI, S. 2000. How will reservoir and caprock react with injected CO₂ at Sleipner? Preliminary evidence from experimental investigations. 355–359 in *Proceedings of the 5th International Conference on Greenhouse Gas Control Technologies, Cairns, Australia*. WILLIAMS, D, DURIE, B, McMULLAN, P, PAULSON, C, and SMITH, A (editors). (Collingwood, Victoria: CSIRO Publishing.)
- PIASECKI, S, GREGERSEN, U, and JOHANNESSEN, P N. 2002. Lower Pliocene dinoflagellate cysts from cored Utsira Formation in the Viking Graben, northern North Sea. *Marine and Petroleum Geology*, Vol. 19, 55–67 .
- PILLITTERI, A, CERASI, P, STAVRUM, J, ZWEIGEL, P, and BØE, R. 2003. Rock mechanical tests of shale samples from the caprock of the Utsira Sand in well 15/9-A11. A contribution to the Saline Aquifer CO₂ Storage (SACS) project. *SINTEF Petroleum Research Report*, 33.5324.00/06/03, 28pp.
[www.iku.sintef.no/projects/IK23430000/other_reports/Pillitteri_et_al_2003_Caprock_shale_rockmecht ests_report.pdf]
- PORTIER, S, and ROCHELLE, C. 2005. Modelling CO₂ solubility in pure water and NaCl-type waters from 0 to 300 °C and from 1 to 300 bar: Application to the Utsira Formation at Sleipner. *Chemical Geology*, Vol. 217, 187–199 .

- RANDEN, T, BORGOS, H G, DALH, G V, HALVORSEN, K Å, IVERSEN, T, LYGREN, M, NICKEL, M, SKOV, T, and TJØSTHEIM, B A. 2002. SACS2 Final report by GECO [Work areas 8– 11]. Technical report, 53pp. [[www.iku.sintef.no/projects/IK23430000/formal_reports/SACS2_WA8ff_MS CO₂_Final_report.pdf](http://www.iku.sintef.no/projects/IK23430000/formal_reports/SACS2_WA8ff_MS_CO2_Final_report.pdf)]
- RIDING, J B. 2002. A palynological study of the lowermost Nordland Shale Formation in Norwegian Well 15/9-A11 at 906.00 m. *British Geological Survey Commissioned Report*, CR/03/001. [www.iku.sintef.no/projects/IK23430000/other_reports/Riding_palynology_seal_well15_9_A11.pdf]
- ROCHELLE, C A. 2002. Geochemical interactions between supercritical CO₂ and the Utsira caprock. I: Introduction to fluid–rock interaction experiments. *British Geological Survey Commissioned Report*, CR/02/238.
- ROCHELLE, C A, BATEMAN, K, and PEARCE, J M. 2002. Geochemical interactions between supercritical CO₂ and the Utsira Formation: an experimental study. *British Geological Survey Commissioned Report*, CR/02/060. [www.iku.sintef.no/projects/IK23430000/other_reports/BGS_WA3_Utsira_geochem_expts.pdf]
- ROCHELLE, C A, and MOORE, Y A. 2002. The solubility of supercritical CO₂ into pure water and synthetic Utsira porewater. *British Geological Survey Commissioned Report*, CR/02/052. [[www.iku.sintef.no/projects/IK23430000/other_reports/BGS_WA3_CO₂_%20solubility_expts.pdf](http://www.iku.sintef.no/projects/IK23430000/other_reports/BGS_WA3_CO2_%20solubility_expts.pdf)]
- SALINE AQUIFER CO₂ STORAGE PROJECT. 2000. Final technical report to EU. Technical report, 34pp. [www.iku.sintef.no/projects/IK23430000/formal_reports/SACS1_Finalreport.pdf]
- SALINE AQUIFER CO₂ STORAGE PROJECT. 2000. Final technical report SACS1, Work area 1 (Geology). Technical report, 29pp. [www.iku.sintef.no/projects/IK23430000/formal_reports/SACS1_WA1_Finalreport_long.pdf]
- SALINE AQUIFER CO₂ STORAGE PROJECT. 2000. Final technical report SACS1, Work area 2 (Reservoir). - Technical report, 42pp. [www.iku.sintef.no/projects/IK23430000/formal_reports/SACS1_WA2_Finalreport_longNew.pdf]
- SALINE AQUIFER CO₂ STORAGE PROJECT. 2000. Final technical report SACS1, Work area 3 (Geochemistry). Technical report, 36pp. [www.iku.sintef.no/projects/IK23430000/formal_reports/SACS1_WA3_Finalreport_long.pdf]
- SALINE AQUIFER CO₂ STORAGE PROJECT. 2000. Final technical report SACS1, Work area 5 (Geophysical Monitoring) Tasks 5.3 & 5.8. Technical report, 3pp. [www.iku.sintef.no/projects/IK23430000/formal_reports/SACS1_WA5_Finalreport_long.pdf]
- SALINE AQUIFER CO₂ STORAGE PROJECT. 2003. Saline Aquifer CO₂ Storage project (SACS). Best Practice Manual. IEA Greenhouse Gas R&D Programme, Report PH4/21, 53pp. [[www.co2store.org/TEK/FOT/SVG03178.nsf/Attachments/SACSBestPractiseManual.pdf/\\$FILE/SACSBestPractiseManual.pdf](http://www.co2store.org/TEK/FOT/SVG03178.nsf/Attachments/SACSBestPractiseManual.pdf/$FILE/SACSBestPractiseManual.pdf)]
- SKOV, T, BORGOS, H G, HALVORSEN, K A, RANDEN, T, SONNELAND, L, ARTS, R, and CHADWICK, R A. 2002. Monitoring and characterization of a CO₂ storage site. *SEG Annual Meeting Expanded Technical Program Abstracts with Biographies*, Vol. 72 , 1669–1672.
- SPRINGER, N, HØIER, C, and LINDGREN, H. 2002. Saline Aquifer CO₂ Storage Project, SACS, Phase II - Task 3.2: Geochemical laboratory experiments. GEUS rapport 2002/42, 27pp. [[www.iku.sintef.no/projects/IK23430000/other_reports/Springer_etal_2002_Geochem_lab_experiment s.pdf](http://www.iku.sintef.no/projects/IK23430000/other_reports/Springer_etal_2002_Geochem_lab_experiment_s.pdf)]
- SPRINGER, N, LINDGREEN, H, and FRIES, K. 2005. Caprock seal capacity test: an evaluation of the transport and sealing properties of Nordland Shale core samples from well 15/9-A11, Sleipner Field. GEUS rapport 2005/58, 37pp.
- SPRINGER, N, and LINDGREEN, H. 2006. Caprock properties of the Nordland Shale recovered from the 15/9-A11 well, the Sleipner area. Abstract (3p) and paper (6p) of the 8th International conference on Greenhouse Gas Control Technologies (GHGT-8), Trondheim, Norway, June 2006. [<https://events.adm.ntnu.no/ei/viewpdf.esp?id=24&file=d%3A%5CAmlink%5CEVENTWIN%5Cdocs%5Cpdf%5C950Final00262%2Epdf>]
- TORP, T A, and GALE, J. 2002. Demonstrating Storage of CO₂ in Geological Reservoirs: The Sleipner and Sacs Projects. Abstracts of the 6th International conference on Greenhouse Gas Control

- Technology (GHGT-6), Kyoto, Japan, 1-4 October 2002.
[www.iku.sintef.no/projects/IK23430000/Publications/Torp_and_Gale_GHGT6_SACS_overview.pdf]
- TORP, T A, and BROWN, K R. 2005. *CO₂ underground storage costs as experienced at Sleipner and Weyburn*. 531–538 in *Greenhouse Gas Control Technologies*. RUBIN, E S, KEITH, D W, and GILBOY, C F (editors). Proceedings of the 7th International Conference on Greenhouse Gas Control Technologies, 5–9 September 2004, Vancouver, Canada, Volume I. Peer reviewed papers and overviews. (Elsevier.)
- UK DTI. 2005. *Monitoring Technologies for the Geological Storage of CO₂*. DTI Technology Status Report TSR025. DTI/Pub URN 05/1032. 28pp. and UK DTI website:
[www.og.dti.gov.uk/regulation/guidance/decommission.htm]
- UK DTI. 2006. *CO₂STORE: The Valleys case study on CO₂ capture, transport and storage*. DTI Report COAL R302 DTI/Pub URN 06/755, 54pp.
- VAN DER MEER, L G H, ARTS, R A, and PATERSON, L. 2000. Prediction of migration of CO₂ after injection in a saline aquifer: reservoir history matching of a 4D seismic image with a compositional gas/water model. 378–384 in *Proceedings of the 5th International Conference on Greenhouse Gas Control Technologies, Cairns, Australia*. WILLIAMS, D, DURIE, B, MCMULLAN, P, PAULSON, C, and SMITH, A (editors). (Collingwood, Victoria: CSIRO Publishing.)
- WILKINSON, I P. 1999. The biostratigraphical and palaeo-ecological application of calcareous microfaunas from the Utsira Formation in Norwegian Well 15/9-A-23. *BGS Technical Report, Stratigraphy Series*, WH/99/124R.
[www.iku.sintef.no/projects/IK23430000/other_reports/Wilkinson_1999.pdf]
- WILLIAMSON, J P, CHADWICK, R A, ROWLEY, W J, and EIKEN, O. 2001. Work Area 5 – Gravity monitoring of the CO₂ bubble. *British Geological Survey Commissioned Report*, CR/01/063.
[www.iku.sintef.no/projects/IK23430000/other_reports/Williamson_et_al_2001_gravity_report.pdf]
- ZWEIGEL, P. 2000. Seismic anomaly maps. Report (ppt presentation), 9pp.
[[iku.sintef.no/projects/IK23430000/other_reports/Seismic_anomaly_maps_\(SINTEF_Nov00\).pdf](http://iku.sintef.no/projects/IK23430000/other_reports/Seismic_anomaly_maps_(SINTEF_Nov00).pdf)]
- ZWEIGEL, P. 2001. The Tertiary uplift and subsidence pattern of Fennoscandia and the adjacent offshore areas (Literature survey report). *SINTEF Petroleum Research Report*, 33.5324.10/01/01, 34p. [www.iku.sintef.no/projects/IK23430000/other_reports/Zweigel_2001_Literature_report.pdf]
- ZWEIGEL, P, LOTHE, A E, and LINDEBERG, E. 1999. Offshore underground CO₂-disposal – 'Reservoir geology' of the Neogene Utsira Formation, Sleipner Field, North Sea. American Association of Petroleum Geologists, International Conference and Exhibition, Birmingham 1999, Abstract in: *Bulletin of the American Association of Petroleum Geologists*, Vol. 83, 1346–1347.
- ZWEIGEL, P, HAMBORG, M, ARTS, R, LOTHE A, and TØMMERÅS, A. 2000. Prediction of migration of CO₂ injected into an underground depository: Reservoir geology and migration modelling in the Sleipner case (North Sea). 360–365 in *Proceedings of the 5th International Conference on Greenhouse Gas Control Technologies, Cairns, Australia*. WILLIAMS, D, DURIE, B, MCMULLAN, P, PAULSON, C, and SMITH, A (editors). (Collingwood, Victoria: CSIRO Publishing.)
- ZWEIGEL, P, HAMBORG, M, ARTS, R, LOTHE, A E, SYLTA, Ø, TØMMERÅS, A, and CAUSSE, E. 2000. Simulation of migration of injected CO₂ in the Sleipner case by means of a secondary migration modelling tool – a contribution to the Saline Aquifer CO₂ Storage project (SACS). *SINTEF Petroleum Research Report (CD)*, 23.4285.00/01/00, 63 p., 6 app.
[www.iku.sintef.no/projects/IK23430000/other_reports/Zweigel_et_al_2000_migr-report.zip]
- ZWEIGEL, P, LINDEBERG, E, and EIKEN O. 2000. Underjordisk lagret klimagassen CO₂ har blitt monitort med seismikk. *GEO* (norwegian popular-geoscientific journal), 2000/6, 16–18.
- ZWEIGEL, P, LOTHE, A, ARTS, R, and HAMBORG, M. 2000. Reservoir geology of the storage units in the Sleipner CO₂-injection case – a contribution to the Saline Aquifer CO₂ Storage (SACS) project. *SINTEF Petroleum Research Report (CD)*, 23.4285.00/02/00, 79 p., 3 app.
[www.iku.sintef.no/projects/IK23430000/other_reports/Zweigeletal_2000_reservoirreport_text.pdf]
(main report only)
www.iku.sintef.no/projects/IK23430000/other_reports/Zweigeletal_2000b_reservoirgeology.zip (incl. attachments)]

- ZWEIGEL, P, ARTS, R, BIDSTRUP, T, CHADWICK, R A, EIKEN, O, GREGERSEN, U, HAMBORG, M, JOHANESSEN, P, KIRBY, G, KRISTENSEN, L, and LINDEBERG, E. 2001. Results and experiences from the first industrial-scale underground CO₂ sequestration case (Sleipner Field, North Sea). American Association of Petroleum Geologists, Annual Meeting, June 2001, Denver, abstract volume (CD) 6p. [www.iku.sintef.no/projects/IK23430000/Publications/Zweigeletal_2001_AAPG_extabstr.pdf]
- ZWEIGEL, P, and GALE, J. 2001. Storing CO₂ underground shows promising results. *EOS, Transactions, of the American Geophysical Union*, Vol. 81 (45), 529 & 534. (Reprinted with added figure in *Earth in Space*, Vol. 13 (6), 8–9.)
- ZWEIGEL, P, and HAMBORG, M. 2002. The effect of time-depth conversion procedure on key seismic horizons relevant for underground CO₂ storage in the Sleipner field (North Sea). *SINTEF Petroleum Research Report*, 33.5324.00/01/02, 48pp. [www.iku.sintef.no/projects/IK23430000/other_reports/Zweigel&Hamborg_2002_TD_conversion.pdf]
- ZWEIGEL, P, and HEILL, L K. 2003. Studies on the likelihood for caprock fracturing in the Sleipner CO₂ injection case – a contribution to the Saline Aquifer CO₂ Storage (SACS) project. *SINTEF Petroleum Research Report*, 33.5324.00/02/03, 27pp. [www.iku.sintef.no/projects/IK23430000/other_reports/Zweigel_and_Heill_Caprock_fracturing_likelihood_report.pdf]
- ZWEIGEL, P, ARTS, R, LOTHE, A E, and LINDEBERG, E. 2004. Reservoir geology of the Utsira Formation at the first industrial-scale underground CO₂ storage site (Sleipner area, North Sea). 165–180 in *Geological Storage of Carbon Dioxide for Emissions Reduction*. BAINES, S, GALE, J, and WORDEN, R (editors). *Geological Society of London Special Publication*, No. 233.